BRITISH COLUMBIA

Ministry of Energy and Mines
Mining and Minerals Division

Geological Fieldwork 2003

A Summary of Field Activities and Current Research

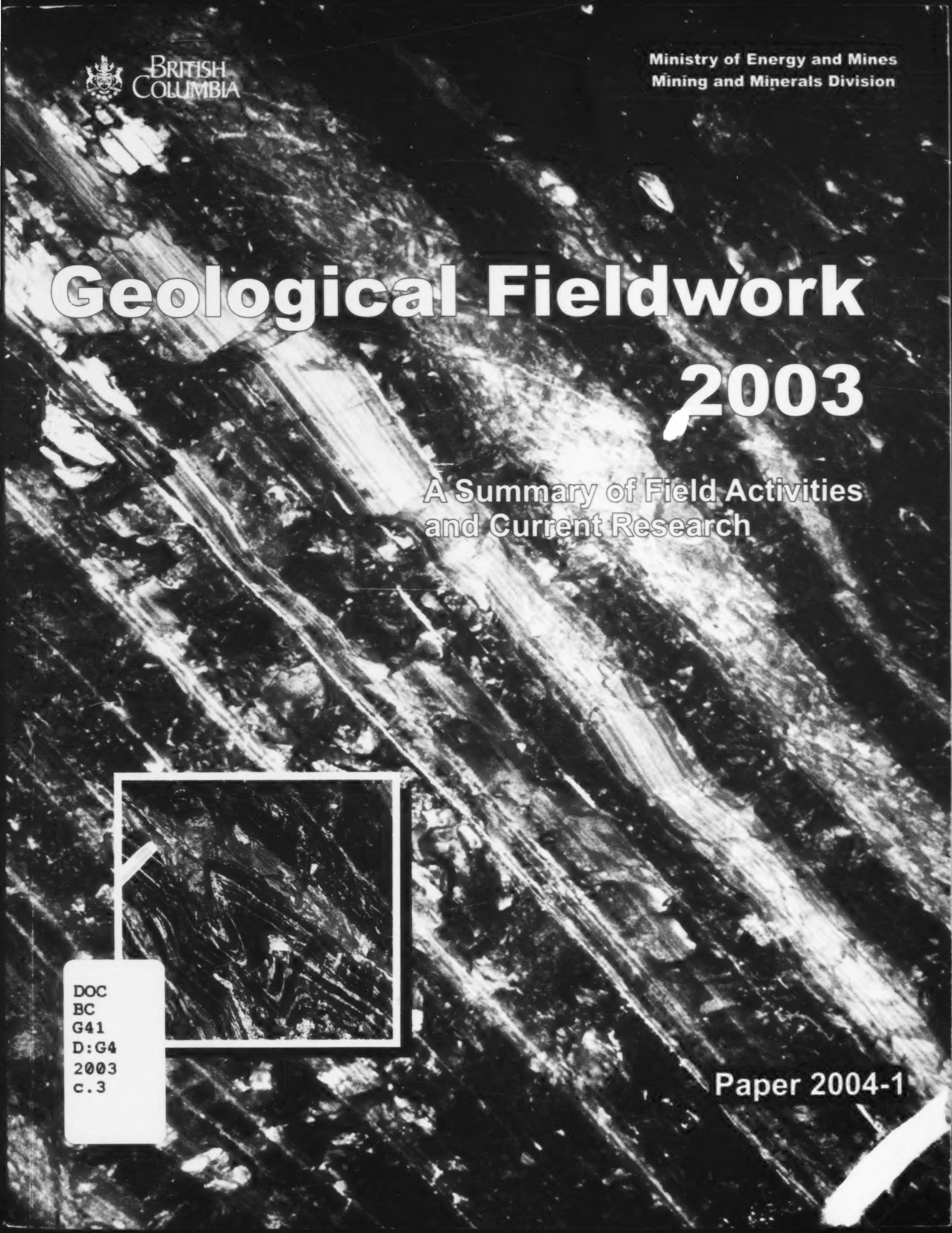

Paper 2004-1

DOC
BC
G41
D:G4
2003
c.3

LEGISLATIVE LIBRARY OF BRITISH COLUMBIA
3 3298 00283 8366

BRITISH
COLUMBIA
Ministry of Energy and Mines
Geosciences, Research and Development Branch

GEOLOGICAL FIELDWORK 2003

A Summary of Field Activities and Current Research

Paper 2004-1

LEGISLATIVE LIBRARY JAN 2 7 2004

Mines and Minerals Division
Geosciences, Research and Development Branch

Parts of this publication may be quoted or reproduced if source and authorship is acknowledged. The following is the recommended format for referencing individual works contained in this publication:

Alldrick, D.J., Stewart, M.L., Nelson, J.L. and Simpson, K.A. (2004): Tracking the Eskay Rift through northern British Columbia - Geology and Mineral Occurrences of the upper Iskut River area; *in* Geological Fieldwork 2003, *British Columbia Ministry of Energy and Mines*, Paper 2004-1, p 1-13.

This publication is also available for free, as colour, digital files in
Adobe Acrobat PDF format from the BC Ministry of Energy and Mines internet website at:

http://www.em.gov.bc.ca/Mining/Geolsurv/Publications/catalog/catfldwk.htm

COVER PHOTO: ***Eskay Creek - 21B Ore Zone*** - Black mudstones, siltstones and sandstones of Contact Mudstone host rock (dark bands), interbedded with graded clastic sulphide and sulphosalt beds (light bands) exposed in the west wall of the 865 crosscut of the 21B ore zone, Eskay Creek gold-silver mine. Stratigraphic tops toward upper right; scale bar shows 1-inch intervals in inset photo. Driven in September, 1990, the 865 crosscut offered the first opportunity to view this blind orebody in place, and provided the original bulk sample for smelter and pilot mill tests. Despite dilution from the unmineralized mudstone intervals, the 21B Zone averaged 66 g/t gold and 2,930 g/t silver. The stratiform, tabular 21B Zone is 900 metres long, up to 200 metres wide and up to 20 metres thick. - *photo by Dani Alldrick*

British Columbia Cataloguing in Publication Data
Main entry under title:
Geological Fieldwork: - 1974 -

Annual.
Issuing body varies
Vols. For 1978-1996 issued in series: Paper / British Columbia. Ministry of Energy, Mines and Petroleum Resources; vols for 1997- 1998, Paper / British Columbia. Ministry of Employment and Investment; vols for 1999- , Paper / British Columbia Ministry of Energy and Mines.

Includes Bibliographical references.
ISSN 0381-243X=Geological Fieldwork

1. Geology - British Columbia - Periodicals. 2. Mines and mineral resources - British Columbia - Periodicals. 3. Geology - Fieldwork - Periodicals. 4. Geology, Economic - British Columbia - Periodicals. 5. British Columbia. Geological Survey Branch - Periodicals. I. British Columbia. Geological Division. II. British Columbia. Geological Survey Branch. III. British Columbia. Geological Survey Branch. IV. British Columbia. Dept. of Mines and Petroleum Resources. V. British Columbia. Ministry of Energy, Mines and Petroleum Resources. VI. British Columbia. Ministry of Employment and Investment. VII. British Columbia Ministry of Energy and Mines. VIII. Series: Paper (British Columbia. Ministry of Energy, Mines and Petroleum Resources). IX. Series: Paper (British Columbia. Ministry of Employment and Investment). X. Series: Paper (British Columbia Ministry of Energy and Mines).

QE187.46 622.1'09711 C76-083084-3 (Rev.)

VICTORIA
BRITISH COLUMBIA
CANADA

JANUARY 2004

FOREWORD

The British Columbia Ministry of Energy and Mines presents the results of provincial geoscience surveys in the twenty-ninth edition of ***Geological Fieldwork: A Summary of Fieldwork and Current Research***. Most articles are contributions from staff of the Geological Survey Branch, now called the Geosciences, Research and Development Branch. As in previous years, the volume also publishes studies by university and industry authors.

This past year the Branch's field program was delivered largely through partnerships with government, industry and universities. Virtually all operating funds for field projects were provided by partners, due to government budget shortfalls; the number of projects also declined, which reflects the reduced staffing available to the Branch.

The Geological Survey of Canada was a strong partner in field surveys and collaborative geoscience studies, through their Targeted Geoscience Initiatives Program and involvement in the Atlin, Iskut and Toodoggone field projects. Articles in this volume include reports on regional mapping in the Joss'alun region south of Atlin and in the Iskut Rift north of the Eskay Creek gold mine. The discovery of a number of new mineral occurrences in both areas highlights the potential for success of prospecting and mineral exploration. A major, integrated geology and geophysics project in the Toodoggone mining camp was funded not only by the two government surveys, but also by five industry partners. The Toodoggone has proven to be one of the more active exploration regions in the province in 2003, and companies have already been staking additional claims in anticipation of the early release of new survey data.

Industry partnerships were also a significant component of the Atlin and Foremore field projects. In the latter case, interpretations of possible regional volcanic massive sulphide horizons for northwestern British Columbia are being advanced, based on work focused on the host stratigraphy of the new mineral occurrences on the property.

This volume also includes a collection of articles derived from projects funded, at least in part, by the British Columbia and Yukon Chamber of Mines through their ***Rocks to Riches*** program. Industry, university and BC Geological Survey staff have written these articles. Several projects have used the province's extensive regional geochemical survey database to identify anomalies warranting consideration and possible exploration follow-up. Three articles report on preliminary investigations into the province's emerald and diamond potential - topics of considerable interest as these gemstones have now been found in nearby Yukon and Alberta respectively. An investigation of platinum group element mineralization in the Afton copper-gold porphyry deposit provides quality analyses, which highlight a significant palladium component to this well-known BC deposit.

The Oil and Gas Division of the Ministry of Energy and Mines has had another very successful year with numerous initiatives to enhance the energy sector, including a number of geoscience-related projects. The results from these programs are being published by the Ministry in a volume entitled, ***Summary of Activities*** being published by the Energy-Resource Development and Geoscience Branch.

Over the past year the Branch published 9 Open Files, 3 Geoscience Maps, 24 GeoFiles, 1 Paper, 6 Information Circulars and Geological Fieldwork 2002, as well as improving web access to information. These, and all past publications, are posted to the Ministry of Energy and Mines website. MapPlace, one of the world's premier internet- map systems, continues to improve with the addition of new tools and data layers. The site is expected to exceed two million hits in 2003.

This volume reflects the hard work and expertise of numerous authors who have earned our thanks for their contributions. The articles have been improved by peer and supervisor review. Many of the manuscripts in the volume were formatted by George Owsiacki and Garry Payie, or individual authors. Again for yet another year, Brian Grant earns special commendation for coordinating the organization and publication of the volume.

D.V. Lefebure
Director – Chief Geologist
Geosciences, Research and Development Branch

104-02311/

TABLE OF CONTENTS

MAPPING

Alldrick, D.J., Stewart, M.L., Nelson, J.L. and Simpson, K.A.: Tracking the Eskay Rift through Northern British Columbia - Geology and Mineral Occurrences of the Upper Iskut River area 1

Canil, D., Mihalynuk, M.G., Mackenzie, J.M, Johnston, S.T., Ferreira, L. and Grant, B.: Heavy Mineral Sampling of Stream Sediments for Diamond and other Indicator Minerals in the Atlin-Nakina Area 19

Diakow, L.J. and Shives, R.B.K.: Geoscience Partnerships in the Toodoggone River and McConnell Creek Map Areas, North-Central BC 27

Laberge, J.D., Pattison, D.R.M. and Simony, P.S.: Geology of the Granby Fault, an Eocene Extensional Fault in Southeast BC 33

Larson, K.P. and Price, R.A.: Stratigraphy and Structure of the Wild Horse River Area, Southeastern BC 49

Mihalynuk, M.G, Ferreira, L. Robertson, S., Devine, F.A.M. and Cordey, F.: Geology and New Mineralization in the Joss'alun Belt, Atlin Area 61

Schiarizza, P.: Geology and Mineral Occurrences of Quesnel Terrane, Kliyul Creek to Johanson Lake 83

ECONOMIC GEOLOGY

Breitsprecher, K. and Mortensen, J.K.: Digital Compilation of Isotopic Ages for British Columbia: BCAge 2003 . 101

Logan, J.: Preliminary Lithogeochemistry and Polymetallic VHMS Mineralization in Early Devonian and(?) Early Carboniferous Volcanic Rocks, Foremore Property . . 105

MacIntyre, D.G , Massey, N.W.D. and Kilby, W.E.: The BC Mineral Potential Project - New Level 2 Mineral Resource Assessment Methodology and Results 125

Mihalynuk, M.G. and Lett. R.: Composition of Logtung Beryl (Aquamarine) by ICPES/MS: A Comparison with Beryl Worldwide 141

Sacks, P. and Mihalynuk, M.G.: Proximal Gold-Cassiterite Nuggets and Composition of the Feather Creek Placer Gravels: Clues to a Lode Source near Atlin, BC. 147

ROCKS TO RICHES

Alldrick, D.J., Jackaman, W. and Lett, R.E.W.: Compilation and Analysis of Regional Geochemical Surveys around the Bowser Basin 163

Brown, J.A.: Mineralogy and Geochemistry of Beryl and Rare-Metalbearing Granitic Pegmatites in the Kootenay Region of Southeastern BC 167

Cathro, M.S., Lane, R.A., Shives, R.B.K. and McCandless, P.M.: Airborne Multisensor Geophysical Surveys in the Central Quesnel Mineral Belt 185

Deyell, C.L., Ebert, S. and Tosdal, R.M.: Sulfur Isotopic Zonation in Alkalic Porphyry Cu-Au Systems: Applications to Mineral Exploration in BC 189

Höy, T., Jackaman, W., Terry, D. and Grant, B.: St. Mary Map-Sheet, Purcell Supergroup, Southeastern BC . . . 191

Jackaman, W. and Höy, T.: Gold Exploration, Rossland-Nelson Area, Southeastern BC 195

Lett, R. and Jackaman, W.: Iskut River - Telegraph Creek: New Exploration Opportunities in the BC Regional Geochemical Survey Database 199

Kilby, W.E., Kliparchuk, K. and McIntosh, A.: Image Analysis Toolbox and Enhanced Satellite Imagery Integrated into The Mapplace 209

Kilby, W.E., Jones L.D., and Desjardins, P.J.: MapPlace Client-Mapping Tools 217

Legun, A.: The Potential For Emeralds in B.C. - A Preliminary Overview 219

MacIntyre, D.G., McMillan, R.H. and Villeneuve, M.E.: The Mid-Cretaceous Rocky Ridge Formation – Important Host Rocks for VMS and Related Deposits in Central BC 231

Mortensen, J.K., Gordee, S.M., Mahoney, J.B. and Tosdal, R.M.: Regional Studies of Eskay Creek-Type and other VMS Mineralization in the Upper Hazelton Group in Stikinia: Preliminary Results 249

Nixon, G.T. : Platinum-Group-Elements in the Afton Cu-Au Porphyry Deposit, Southern British Columbia 263

Simandl, G.: Diamond Potential in British Columbia - Progress Report. 291

Smyth, C.P.: British Columbia Regional Geochemical Cluster Anomalies and Best Matches to Mineral Deposit Types 295

TRACKING THE ESKAY RIFT THROUGH NORTHERN BRITISH COLUMBIA - GEOLOGY AND MINERAL OCCURRENCES OF THE UPPER ISKUT RIVER AREA

(TELEGRAPH CREEK NTS 104G/1, 2, 7, 8, 9, 10)

By D.J. Alldrick[1], M.L. Stewart[1], J.L. Nelson[1] and K.A. Simpson[2]

KEYWORDS: Targeted Geoscience Initiative-II (TGI-II), Bedrock mapping, Eskay Creek, Eskay Rift, Hazelton Group, Stuhini Group, Mineral deposits

INTRODUCTION

The Eskay Creek gold-silver mine, located in northwest British Columbia, is an unusually high-grade ore deposit. The mining industry continues to spend more than $2 million each year on exploration for similar deposits in the area. The geologic setting at the minesite is well studied, but large tracts in north-central British Columbia require more detailed surveys to determine if favourable sites exist for formation and preservation of additional deposits. The British Columbia Geological Survey and the Geological Survey of Canada have launched a two-year mapping program to delineate the critical ore horizon through the region north of the mine and to assess potential for additional Eskay Creek type deposits. This horizon lies within Lower to Middle Jurassic, arc-related, rift sequence rocks along the northwest perimeter of the Bowser Basin, a large (48,000 km^2), Middle to Upper Jurassic sedimentary basin (Figure 1).

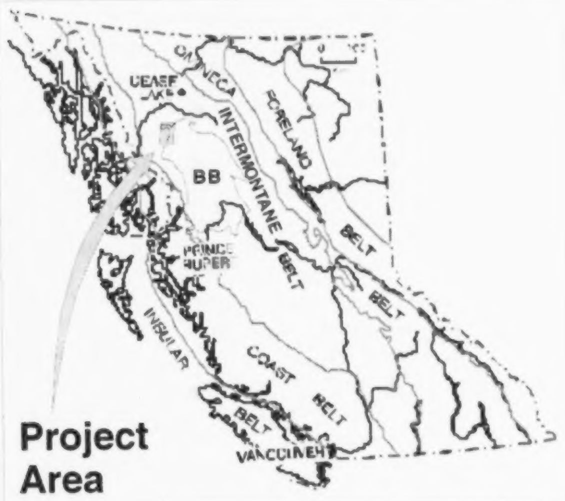

Figure 1. Project location map and Bowser Basin (BB). Modified from Logan (2000).

The two-year study will cover 6,250 km^2, extending 125 km north from the Eskay Creek mine to the Spectrum porphyry copper-gold deposit (Figure 2). The paved Stewart-Cassiar Highway (Highway 37) runs northward through the eastern part of the map area. In 2003, the first field season, an eight-person team mapped 70 km along the rift sequence between Kinaskan Lake and More Creek, west of the highway (Figure 2).

The project area straddles the eastern edge of the Coast Mountains and the broad valley of the upper Iskut River. This area lies within the Tahltan First Nation traditional area and they participated directly in this project. Topography varys from rounded glacial valleys along the upper Iskut River, to the extensive Spatsizi Plateau, to high serrated ridges and peaks that are being actively glaciated. Elevations range from 250 metres above sea level at the confluence of Iskut River and Forrest Kerr Creek, up to 2,662 metres at the summit of Hankin Peak in the west-central region of the field area. Mount Edziza can be seen rising to 2780 meters near the northern boundary of the study area. Vegetation comprises boreal spruce-pine-fir forest at low-elevation. Timberline is at 1400 metres elevation with subalpine fir and meadow areas above.

Regional-scale geology maps and reports for this area include: Operation Stikine (1957), Souther (1972), Read (1989), Evenchick (1991), Logan *et al.* (1990, 1992, 1993, 1997, 2000), Gunning (1996) and Ash *et al.* (1995, 1996, 1997a, 1997b) (Figure 2). Detailed geological maps are available in theses by Schmitt (1977) and Kaip (1997) and in many company assessment reports cited in ARIS and MINFILE. The most recent and most comprehensive study of the Eskay Creek orebodies is the Ph.D. thesis by Tina Roth (October, 2002) which offers an extensive bibliography of all previous reports on the deposit, including many progress reports and final reports that were part of the Iskut Metallogeny Project of the Mineral Deposits Research Unit at the University of British Columbia (Macdonald *et al.*, 1996).

Anderson (1993) interpreted the present study area as the northern extension of a large fault-bounded belt or rift. Sections of this area have been mapped at 1:50,000 scale

---

[1] *British Columbia Ministry of Energy and Mines*
[2] *Geological Survey of Canada, Vancouver*

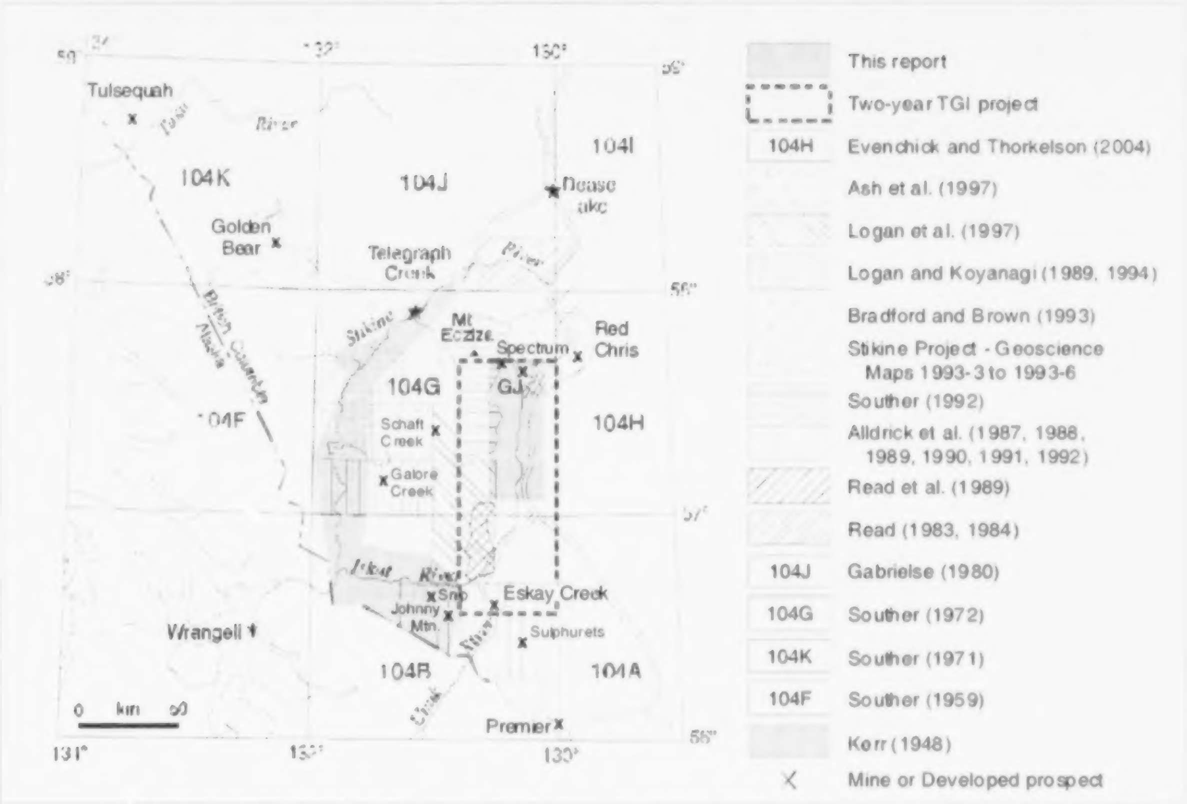
59°
134°
132°
130°
59°
Tulsequah
Taku
River
104K
104J
104I
Dease
Lake
Golden
Bear
Telegraph
Creek
River
58°
58°
Stikine
Mt
Edziza
Red
Chris
Spectrum
GJ
British Columbia
Alaska
104G
104F
Schaft
Creek
Galore
Creek
104H
57°
Iskut
River
Snip
Eskay Creek
Johnny
Mtn.
Unuk
River
Sulphurets
Wrangell
104B
104A
0 km 50
Premier
56°
131°
132°
130°
This report
Two-year TGI project
104H
Evenchick and Thorkelson (2004)
Ash et al. (1997)
Logan et al. (1997)
Logan and Koyanagi (1989, 1994)
Bradford and Brown (1993)
Stikine Project - Geoscience Maps 1993-3 to 1993-6
Souther (1992)
Alldrick et al. (1987, 1988, 1989, 1990, 1991, 1992)
Read et al. (1989)
Read (1983, 1984)
104J
Gabrielse (1980)
104G
Souther (1972)
104K
Souther (1971)
104F
Souther (1959)
Kerr (1948)
Mine or Developed prospect

Figure 2. Previous geological mapping and current project outline. Modified from Logan (2000).

by Read (1991), Logan *et al.* (1990, 1992, 1993) and Ash *et al.* (1997b). The current project will complete 1:50,000-scale coverage between these earlier mapping projects, with more detailed mapping of the strata of the upper Hazelton Group, and detailed stratigraphic investigations within the Eskay Rift (e.g. Simpson and Nelson, 2004). The federal and provincial governments have jointly funded this study as part of the "Bowser Basin Energy and Mineral Resource Potential Targeted Geoscience Initiative".

REGIONAL GEOLOGIC SETTING

The project area lies on the western edge of the Intermontane tectonic belt, within Stikine terrane, and is bounded to the east by the Bowser sedimentary basin (Figure 1). It straddles the tectonic elements of the Bowser structural basin and the Stikine Arch to the northwest.

Souther (1972) and Logan *et al.* (2000) describe the geological history of the area as a series of five mid-Paleozoic to mid-Mesozoic volcanic arcs developed in sediment-poor and sediment-rich marine settings. Lulls in volcanism at the Triassic-Jurassic boundary and in the uppermost Lower Jurassic were marked by tectonic uplift, deformation and erosion, termed the Inklinian and Nassian orogenies, respectively (Souther, 1972).

Strata range in age from Devonian through to Holocene (Figure 3). The major stratigraphic components of the project area are the Stikine Assemblage, Stuhini Group, Hazelton Group, Bowser Lake Group and Mount Edziza Complex. The Stikine Assemblage was defined by a Geological Survey of Canada team (Operation Stikine, 1957) and has most recently been described by Logan *et al.* (2000). The Stikine Assemblage consists of Early Devonian to mid-Permian volcanic and sedimentary strata, which culminate in a thick carbonate succession. The Upper Triassic Stuhini Group is characterized by pyroxene porphyritic basalt flows and breccias with intercalated clastic sedimentary rocks and minor carbonate units. The Early to Middle Jurassic Hazelton Group is an island arc succession consisting of a lower package of intermediate volcanic rocks and derived clastic sedimentary units; a middle interval of thin, but widely distributed felsic volcanic rocks; and an upper unit of fine clastic sedimentary rocks with local bimodal volcanic rocks dominated by basalt. Carbonate units are rare or absent in Hazelton Group strata. The Middle to Late Jurassic Bowser Lake Group is a thick, clastic marine sedimentary succession. Miocene to Recent

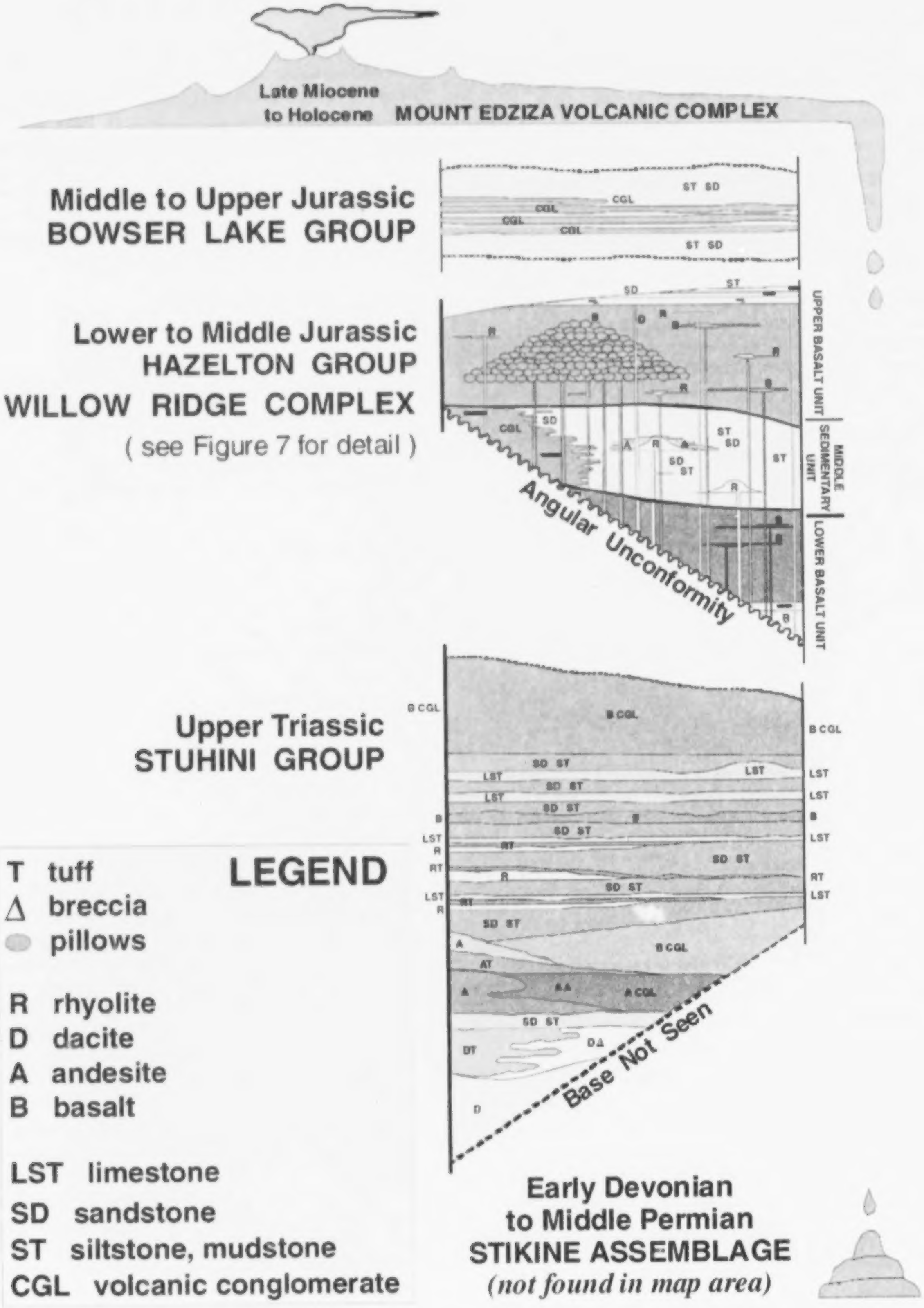
Late Miocene to Holocene
MOUNT EDZIZA VOLCANIC COMPLEX
Middle to Upper Jurassic
BOWSER LAKE GROUP
CGL
ST SD
Lower to Middle Jurassic
HAZELTON GROUP
WILLOW RIDGE COMPLEX
(see Figure 7 for detail)
UPPER BASALT UNIT
MIDDLE SEDIMENTARY UNIT
LOWER BASALT UNIT
Angular Unconformity
R
D
B
A
Upper Triassic
STUHINI GROUP
B CGL
SD ST
LST
B
RT
R
AT
A CGL
DT
DΔ
D
Base Not Seen
LEGEND
T tuff
Δ breccia
pillows
R rhyolite
D dacite
A andesite
B basalt
LST limestone
SD sandstone
ST siltstone, mudstone
CGL volcanic conglomerate
Early Devonian to Middle Permian
STIKINE ASSEMBLAGE
(not found in map area)

Figure 3. Schematic regional stratigraphy.

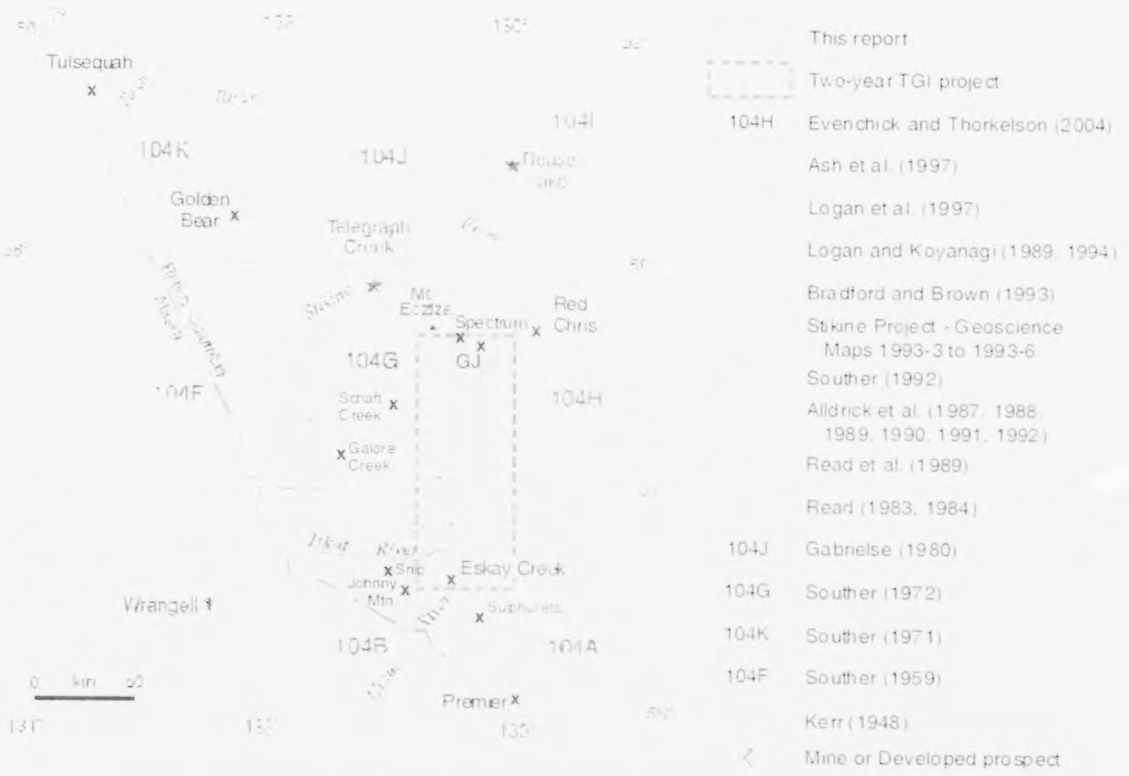
Tulsequah
104K
104J
104I
Golden Bear
Telegraph Creek
Mt Edziza
Spectrum
Red Chris
GJ
104G
104F
Schaft Creek
Galore Creek
104H
Eskay Creek
Snip
Johnny Mtn
Wrangell
Sulphurets
104B
104A
Premier
0 km 50
This report
Two-year TGI project
104H Evenchick and Thorkelson (2004)
Ash et al. (1997)
Logan et al. (1997)
Logan and Koyanagi (1989, 1994)
Bradford and Brown (1993)
Stikine Project - Geoscience Maps 1993-3 to 1993-6
Souther (1992)
Alldrick et al. (1987, 1988, 1989, 1990, 1991, 1992)
Read et al. (1989)
Read (1983, 1984)
104J Gabrielse (1980)
104G Souther (1972)
104K Souther (1971)
104F Souther (1959)
Kerr (1948)
Mine or Developed prospect

Figure 2. Previous geological mapping and current project outline. Modified from Logan (2000).

by Read (1991), Logan *et al.* (1990, 1992, 1993) and Ash *et al.* (1997b). The current project will complete 1:50,000-scale coverage between these earlier mapping projects, with more detailed mapping of the strata of the upper Hazelton Group, and detailed stratigraphic investigations within the Eskay Rift (e.g. Simpson and Nelson, 2004). The federal and provincial governments have jointly funded this study as part of the "Bowser Basin Energy and Mineral Resource Potential Targeted Geoscience Initiative".

REGIONAL GEOLOGIC SETTING

The project area lies on the western edge of the Intermontane tectonic belt, within Stikine terrane, and is bounded to the east by the Bowser sedimentary basin (Figure 1). It straddles the tectonic elements of the Bowser structural basin and the Stikine Arch to the northwest.

Souther (1972) and Logan *et al.* (2000) describe the geological history of the area as a series of five mid-Paleozoic to mid-Mesozoic volcanic arcs developed in sediment-poor and sediment-rich marine settings. Lulls in volcanism at the Triassic-Jurassic boundary and in the uppermost Lower Jurassic were marked by tectonic uplift, deformation and erosion, termed the Inklinian and Nassian orogenies, respectively (Souther, 1972).

Strata range in age from Devonian through to Holocene (Figure 3). The major stratigraphic components of the project area are the Stikine Assemblage, Stuhini Group, Hazelton Group, Bowser Lake Group and Mount Edziza Complex. The Stikine Assemblage was defined by a Geological Survey of Canada team (Operation Stikine, 1957) and has most recently been described by Logan *et al.* (2000). The Stikine Assemblage consists of Early Devonian to mid-Permian volcanic and sedimentary strata, which culminate in a thick carbonate succession. The Upper Triassic Stuhini Group is characterized by pyroxene porphyritic basalt flows and breccias with intercalated clastic sedimentary rocks and minor carbonate units. The Early to Middle Jurassic Hazelton Group is an island arc succession consisting of a lower package of intermediate volcanic rocks and derived clastic sedimentary units; a middle interval of thin, but widely distributed felsic volcanic rocks; and an upper unit of fine clastic sedimentary rocks with local bimodal volcanic rocks dominated by basalt. Carbonate units are rare or absent in Hazelton Group strata. The Middle to Late Jurassic Bowser Lake Group is a thick, clastic marine sedimentary succession. Miocene to Recent

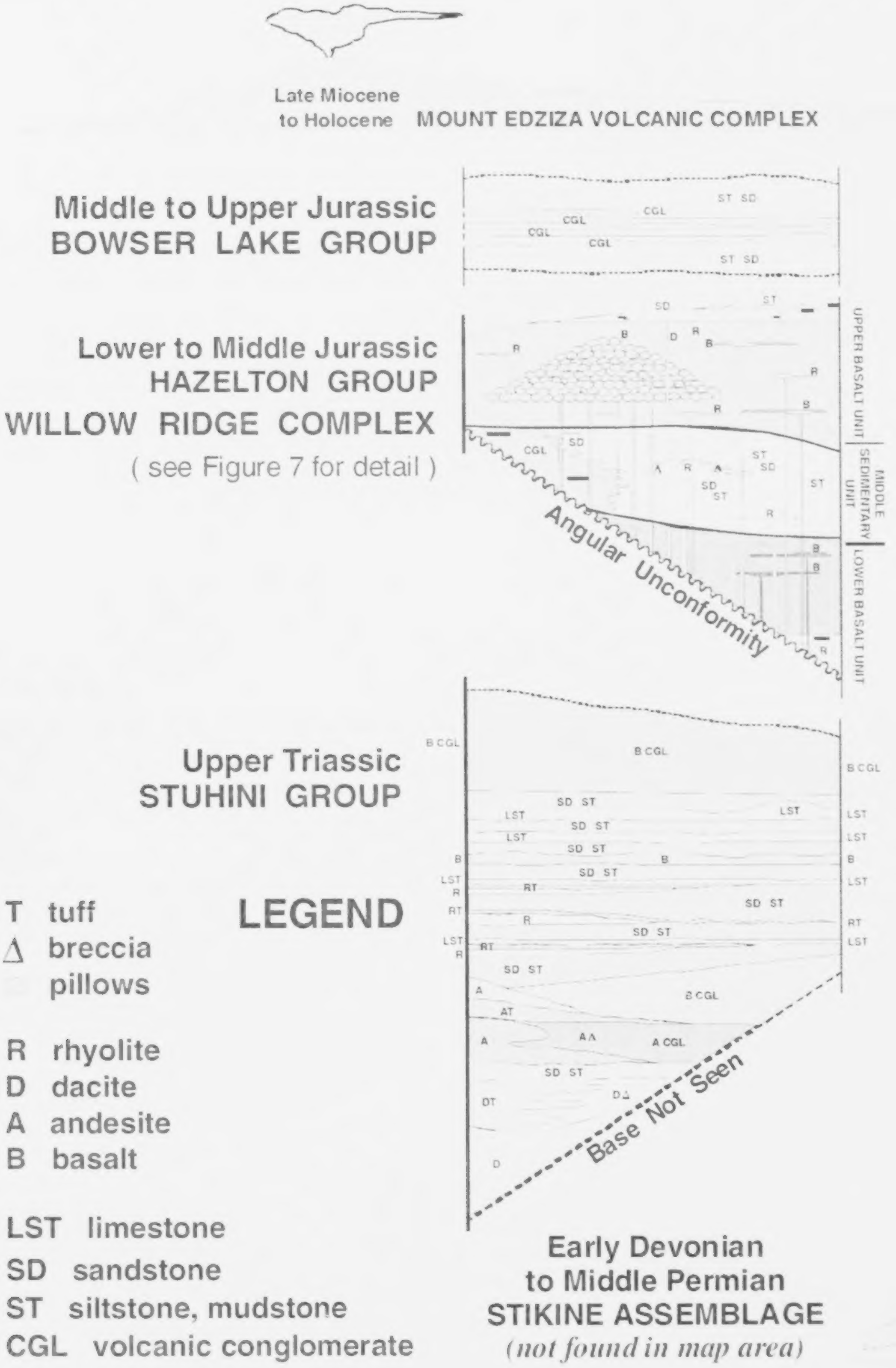
Late Miocene
to Holocene
MOUNT EDZIZA VOLCANIC COMPLEX
Middle to Upper Jurassic
BOWSER LAKE GROUP
CGL
ST SD
Lower to Middle Jurassic
HAZELTON GROUP
WILLOW RIDGE COMPLEX
(see Figure 7 for detail)
UPPER BASALT UNIT
MIDDLE SEDIMENTARY UNIT
LOWER BASALT UNIT
Angular Unconformity
Upper Triassic
STUHINI GROUP
B CGL
LST
SD ST
RT
AT
A CGL
DT
D
Base Not Seen
Early Devonian
to Middle Permian
STIKINE ASSEMBLAGE
(not found in map area)
LEGEND
T tuff
Δ breccia
pillows
R rhyolite
D dacite
A andesite
B basalt
LST limestone
SD sandstone
ST siltstone, mudstone
CGL volcanic conglomerate

Figure 3. Schematic regional stratigraphy.

volcanic strata from the Mount Edziza Volcanic Complex blanket the northwest section of the project area.

Regional-scale unconformities within the study area include a Late Permian - Early Triassic disconformity, a Late Triassic - Early Jurassic angular unconformity and nonconformity, and an Early Jurassic angular unconformity.

Logan *et al.* (2000) describes five plutonic episodes in the area. The three youngest plutonic episodes have important mineral deposits associated with them.

To the south, mid-Cretaceous regional metamorphism reached a maximum grade of lower greenschist facies (Alldrick, 1993). In the current field area chlorite is rare to absent, thus the regional metamorphic grade is interpreted as sub-greenschist, probably mid-prehnite-pumpellyite facies (Figure 4).

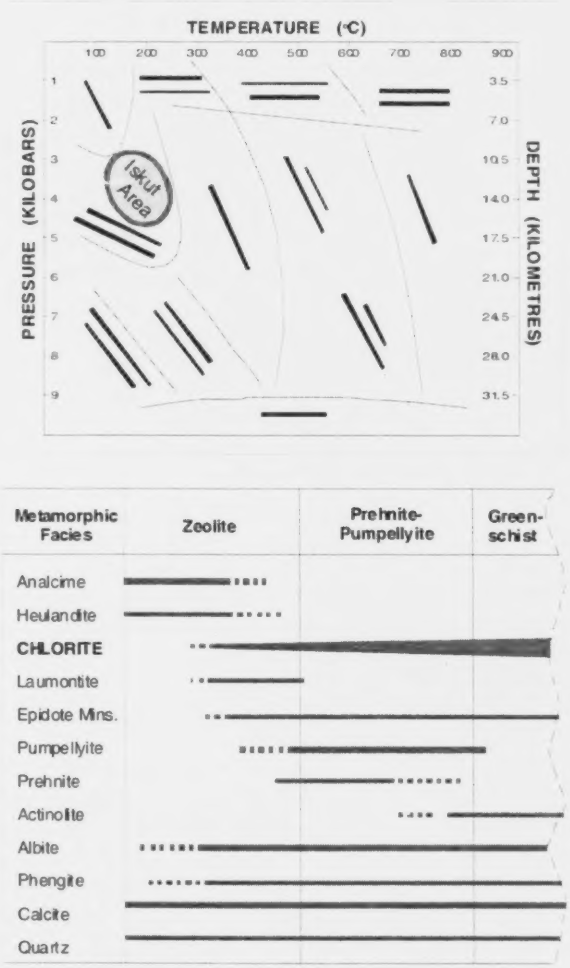

Figure 4. Regional metamorphic grade.

GEOLOGY OF THE MAP AREA

Mapping in the 2003 field season covered Upper Triassic to Middle Jurassic strata at the northern end of the two-year project area (Figure 2). Several topographic features in this year's map area have been informally named to simplify description of locations (Figure 5). Simplified geology of the 2003 map area is presented in Figure 6. Age control is provided by fossil collections from Souther (1972) and Evenchick *et al.* (2001), and by isotopic age dates tabulated in the new BCAge database (Breitsprecher and Mortensen, 2004).

STRATIFIED ROCKS

STIKINE ASSEMBLAGE (MIDDLE TO UPPER PALEOZOIC)

Carbonate-dominated Permian strata of the upper Stikine Assemblage have not been mapped in this year's survey.

STUHINI GROUP (UPPER TRIASSIC)

In the map area, the Stuhini Group consists of a lower volcanic package with lesser intercalated sedimentary rocks, overlain by a thick upper sedimentary package with lesser interlayered volcanic rocks. Locally, augite(-plagioclase)-phyric basaltic volcaniclastic rocks lie above the sedimentary succession. Upper Triassic strata extend uninterrupted from More Creek northward to the western cliffs of Table Mountain (Figure 6). On the upper plateau of Table Mountain, younger rocks of the Hazelton Group, herein defined as Willow Creek Complex, overlie the Stuhini Group. Stuhini Group strata also crop out 35 kilometres northeast of Table Mountain, on the ridgetops on either side of Kinaskan Lake (Ash *et al.*, 1997b).

The base of the Stuhini Group and its contact with underlying Paleozoic units has not been observed in the map area. The top of the Stuhini group is an angular unconformity, overlain by Hazelton Group strata. Unconformable upper contacts were observed at three localities: east of Kinaskan Lake, at Table Mountain and near the Hank deposit (Figure 6). Total thickness of Stuhini Group strata cannot be determined due to this truncation, but minimum thickness is 3,000 metres.

The lower volcanic package of the Stuhini Group has been mapped in three locations and is also described at the Hank epithermal gold deposit (Kaip, 1997). These rocks, although lithologically similar to the lower Hazelton Group, are constrained as part of the Upper Triassic succession by fossils within the overlying sedimentary units. The stratigraphically lowest recognised lithology is dacitic volcanic rocks that display both proximal and intermediate facies relationships. The proximal facies is a thick (>100 metres) accumulation of

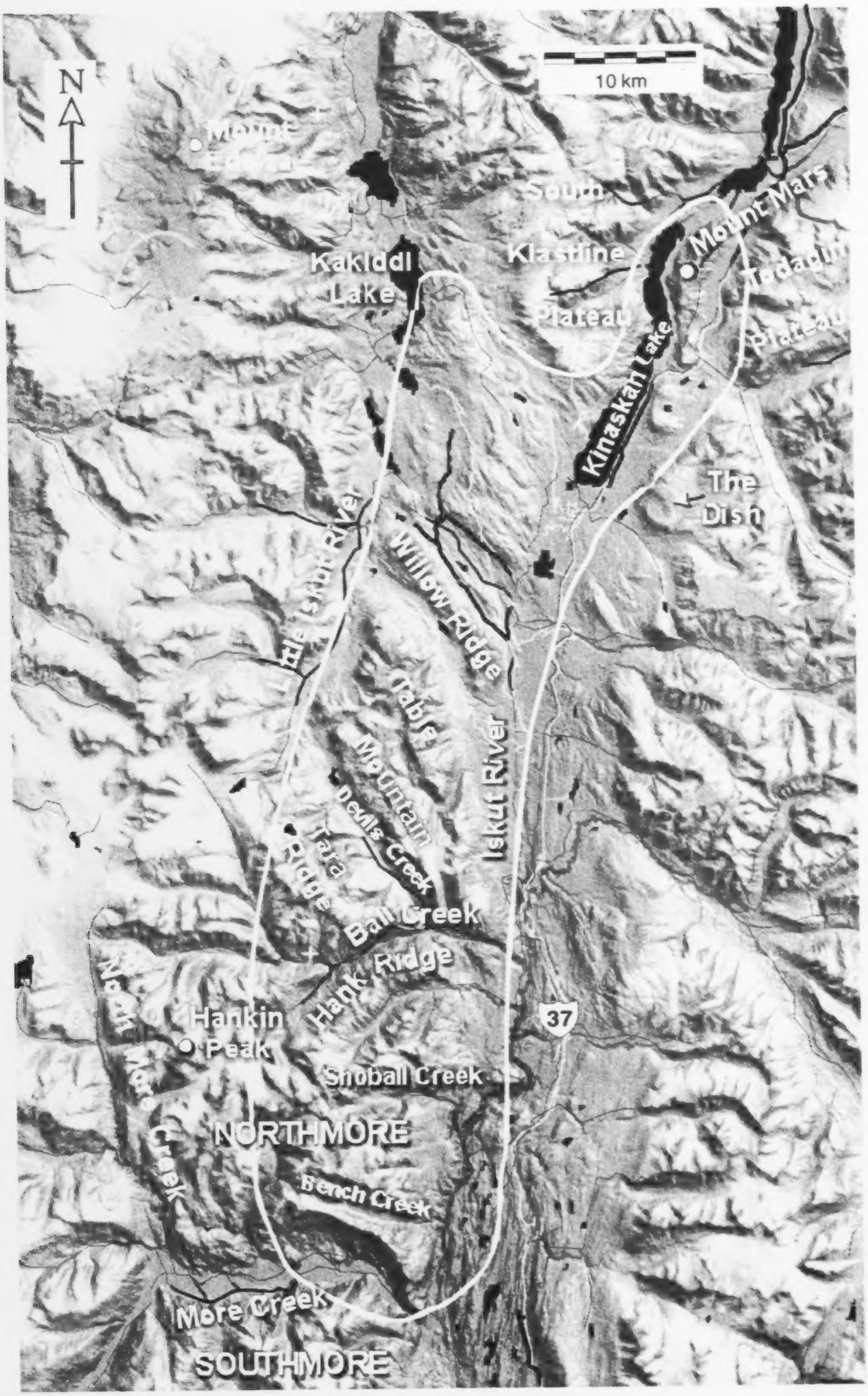
N
10 km
Mount Edziza
South
Mount Mars
Kakiddi Lake
Klastline
Todagin
Plateau
Plateau
Kinaskan Lake
The Dish
Little Iskut River
Willow Ridge
Table
Mountain
Iskut River
Devils Creek
Tara Ridge
Ball Creek
Hank Ridge
North More Creek
Hankin Peak
37
Shoball Creek
NORTHMORE
Bench Creek
More Creek
SOUTHMORE

Figure 5. Shaded DEM map showing major topographic features and outline of the area mapped during the 2003 fieldseason.

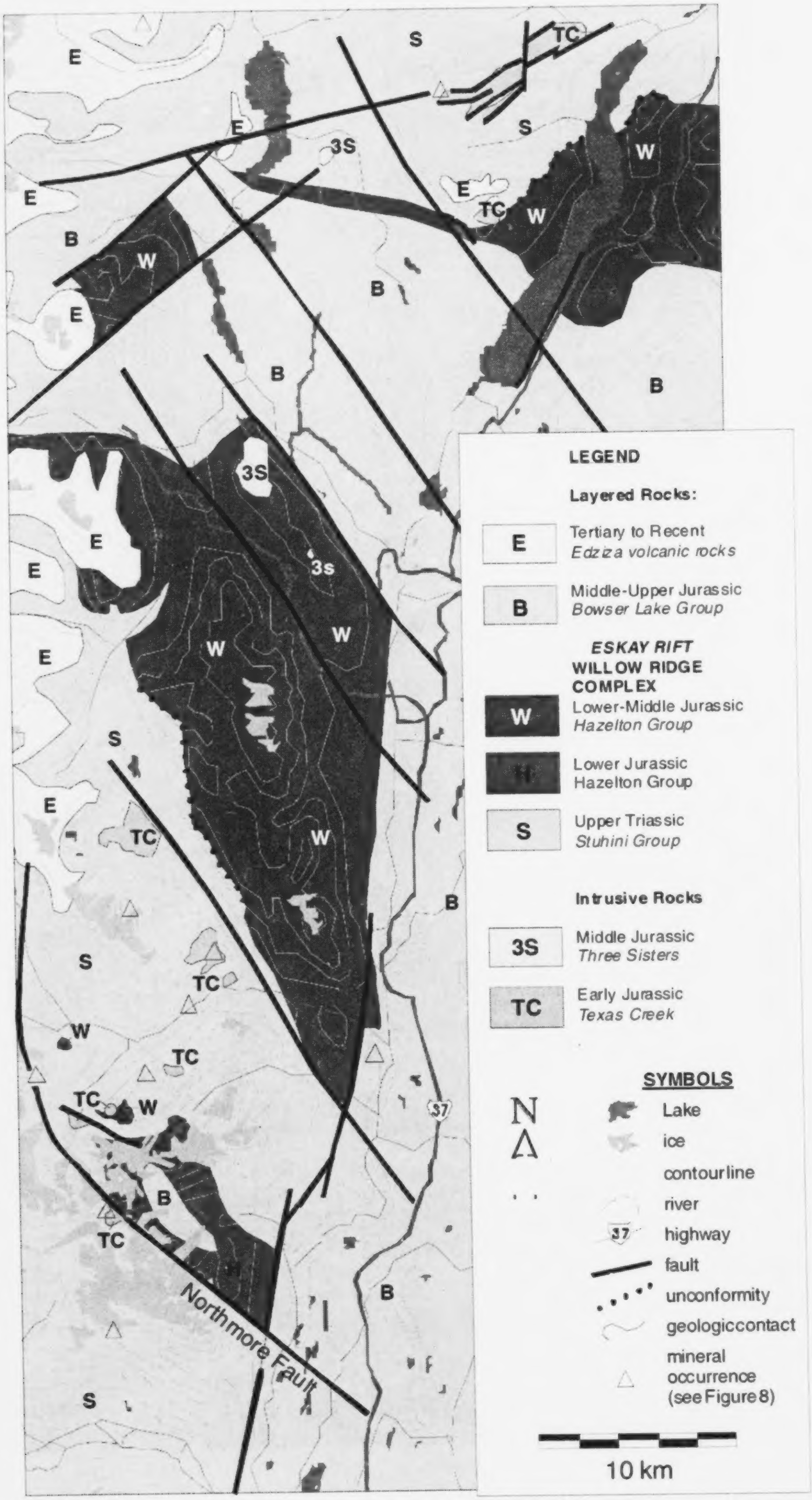
LEGEND
Layered Rocks:
E
Tertiary to Recent
Edziza volcanic rocks
B
Middle-Upper Jurassic
Bowser Lake Group
ESKAY RIFT
WILLOW RIDGE COMPLEX
W
Lower-Middle Jurassic
Hazelton Group
H
Lower Jurassic
Hazelton Group
S
Upper Triassic
Stuhini Group
Intrusive Rocks
3S
Middle Jurassic
Three Sisters
TC
Early Jurassic
Texas Creek
SYMBOLS
N
Lake
ice
contourline
river
37
highway
fault
unconformity
geologiccontact
mineral occurrence (see Figure 8)
10 km
Northmore Fault
E
B
W
S
3S
3s
TC
H
37

Figure 6. Simplified geology of the More Creek - Kinaskan Lake area (see Figure 8 for mineral occurrence names).

massive, fine-grained, light grey, aphanitic dacite overlain by a thick (150 metres) succession of light greenish grey, medium-bedded, rhythmically-bedded ash tuffs. Laterally equivalent units are preserved as coarse, massive dacite breccias and crudely bedded dacite conglomerates. Clasts are lapilli to cobble size and commonly display distinct flow banding. The dacitic units are overlain by 50 to 80 metres of fine to coarse volcanic sandstone, which is overlain in turn by an andesite sequence. The andesite sequence consists of several facies throughout the map area. Near Bench Creek in the south, the andesite sequence is a series of lava flows with varying porphyritic textures. Fine to medium grained plagioclase phenocrysts range in abundance from sparse to crowded. Minor units of tuff separate the massive andesite flows. The lateral facies equivalent to these proximal flows is a thick (>1,000 metres) succession of coarse plagioclase-phyric andesite fragmental rocks with rare sandstone interbeds. These andesitic fragmental facies are the host rock to both the Hank epithermal gold deposit and the Mary porphyry copper-molybdenum deposit. Andesitic rocks of the lower volcanic package are overlain by the upper sedimentary package of the Stuhini Group.

The upper sedimentary package consists of a fine to medium grained mixed clastic succession of siltstones, sandstones, rare pebble conglomerates and distinctive minor limestone and volcanic members. The sandstones and conglomerates are characterized by buff-orange weathering carbonate cement. Multiple horizons of massive light grey limestone and limestone conglomerates, basalt flows and breccias, and black to white rhyolite flows with associated bright apple green, massive to bedded rhyolite ash tuffs are preserved in most sections. Local thin flows of andesite and dacite have been noted, but are not evident in all areas mapped. This distinctive rock package is well exposed around the Bench and Rainbow prospects (Figures 6 and 8).

Carbonate-cemented clastic sedimentary rocks weather rapidly and generate a moderate to intense buff-orange weathered appearance to the slopes of cascading scree that can be confused with gossans from a distance. Basalt or basaltic andesite units are preserved as massive flows, which undulate in thickness along strike, and as substantial thicknesses (>200 metres) of coarse basalt volcaniclastics. These rocks are variably porphyritic with fine to coarse pyroxene phenocrysts. Minor lenses of poorly sorted, polymictic volcaniclastic layers and rare limestone layers are preserved within the thick accumulations of basaltic conglomerate.

Several thin rhyolite flows are preserved within the upper sedimentary package of the Stuhini Group. Rhyolite occurs as black, aphanitic to fine-grained, massive to flow-banded units with glassy lustre. Associated flow-banded black rhyolite dikes crosscut the underlying clastic sedimentary rocks and limestone beds. Black rhyolite flows are directly overlain by bright apple green fine-grained ash tuffs and faintly bedded tuffs. At the Rainbow prospect near the centre of Tara Ridge, rhyolite dikes have fine-grained yellow, orange and red mineral encrustations developed along hairline fractures. Analysis of these brightly coloured, vuggy dikes show elevated values of mercury, antimony and arsenic. The limestone units pinch and swell; local thick resistant limestone lenses form prominent cliffs and spires. An exceptional example is the "Easter Island Limestone", a limestone member that crops out as a series of adjacent resistant limestone pinnacles on the western slopes of Tara Ridge. Near the Bench prospect, a massive limestone unit is overlain by a conglomerate containing cobble to boulder size rounded limestone clasts in a dark brown sandy matrix.

The uppermost, clinopyroxene-bearing volcaniclastic unit occurs in two localities, at the eastern end of the ridge between More Creek and Bench Creek, and at the western edge of Tara Ridge. North of More Creek, coarse, poorly bedded augite(-plagioclase) volcanic breccia overlies a thin fossiliferous limestone to limy siltstone bed that contains corals, belemnites, ammonites and pelecypods. The volcanic breccia has incorporated limestone olistoliths, preserved as irregular bodies up to a kilometer long. On Tara Ridge, well-bedded clinopyroxene-phyric basalt conglomerate forms the top of the exposed Upper Triassic section.

The Stuhini Group in the map area is interpreted as a subaqueous accumulation of dacite, andesite and bimodal basalt-rhyolite volcanic rocks in a setting characterized by a progressively increasing accumulation of volcaniclastic sedimentary rocks with carbonate cement. The sedimentary succession is overlain by locally derived volcaniclastics from a second mafic volcanic pile. Interruptions in the deposition of clastic sedimentary units permitted the deposition and preservation of multiple carbonate units. Volcanic facies in the vicinity of the Bench prospect are proximal, facies preserved at the Hank deposit are intermediate, other locations have a mix of proximal and distal facies among the different units within the succession.

HAZELTON GROUP (LOWER TO MIDDLE JURASSIC)

The lower strata of the Hazelton Group have only been recognised in the northeast corner of the map area (Ash *et al.*, 1997b). In addition to the units recognized as lower Hazelton Group (Ash *et al.*, 1997b), we suggest that part of his unit lJme east of Kinaskan Lake also be included in the lower Hazelton Group. These rocks consist of polymictic, volcanic conglomerate, sandstone and grit. The conglomerate is dominated by plagioclase-phyric andesite clasts, but also includes sparse limestone fragments. The depositional relationship of this unit to the nearby-outcropping Upper Triassic volcanic strata is not known. These distinctive Lower Jurassic plagioclase-phyric, andesite- and dacite-dominated volcanic and sedimentary strata have not been identified in the south end of the project area, indicating that they were never deposited or have been eroded away.

Anderson and Thorkelson (1990) defined the uppermost division of the Hazelton Group as the "Eskay Creek Facies" of the Salmon River Formation. The MDRU Iskut Metallogeny Project (Macdonald *et al*, 1996) studied many features of this rock package in the Eskay Creek mine area. The key volcanic units of the Eskay Creek Facies are now recognized to extend even further to the north and south (Evenchick and McNicoll, 2002).

Willow Ridge Complex

Extensive exposures of bimodal volcanic rocks of the Eskay Creek Facies have been mapped in detail as part of this study. Based on this work and previous studies (Souther, 1972; Anderson, 1989, 1993; Anderson and Thorkelson, 1990; Evenchick, 1991), we define this sequence of bimodal volcanic rocks, and their related intrusive rocks and intercalated sedimentary rocks, as the Willow Ridge Complex (WRC). The type area for this distinctive bimodal volcanic assemblage is a long, low ridge of extensive outcrop west of the upper Iskut River between the Willow Creek Forest Access Road to the north and the old Telegraph trail to the south. The entire ridge is accessible on foot from the nearby forest service road. A second broad area of excellent exposure is Table Mountain, a high, flat-topped ridge immediately southwest of Willow Ridge.

The WRC is a thick package of basalt lava flows and feeder dikes, minor interlayered dacite and rhyolite lava flows, breccias, feeder dikes and lava domes, and intercalated volcaniclastic sedimentary rocks. A composite schematic section of this sequence is presented in Figure 7. Extensions of the WRC crop out further north

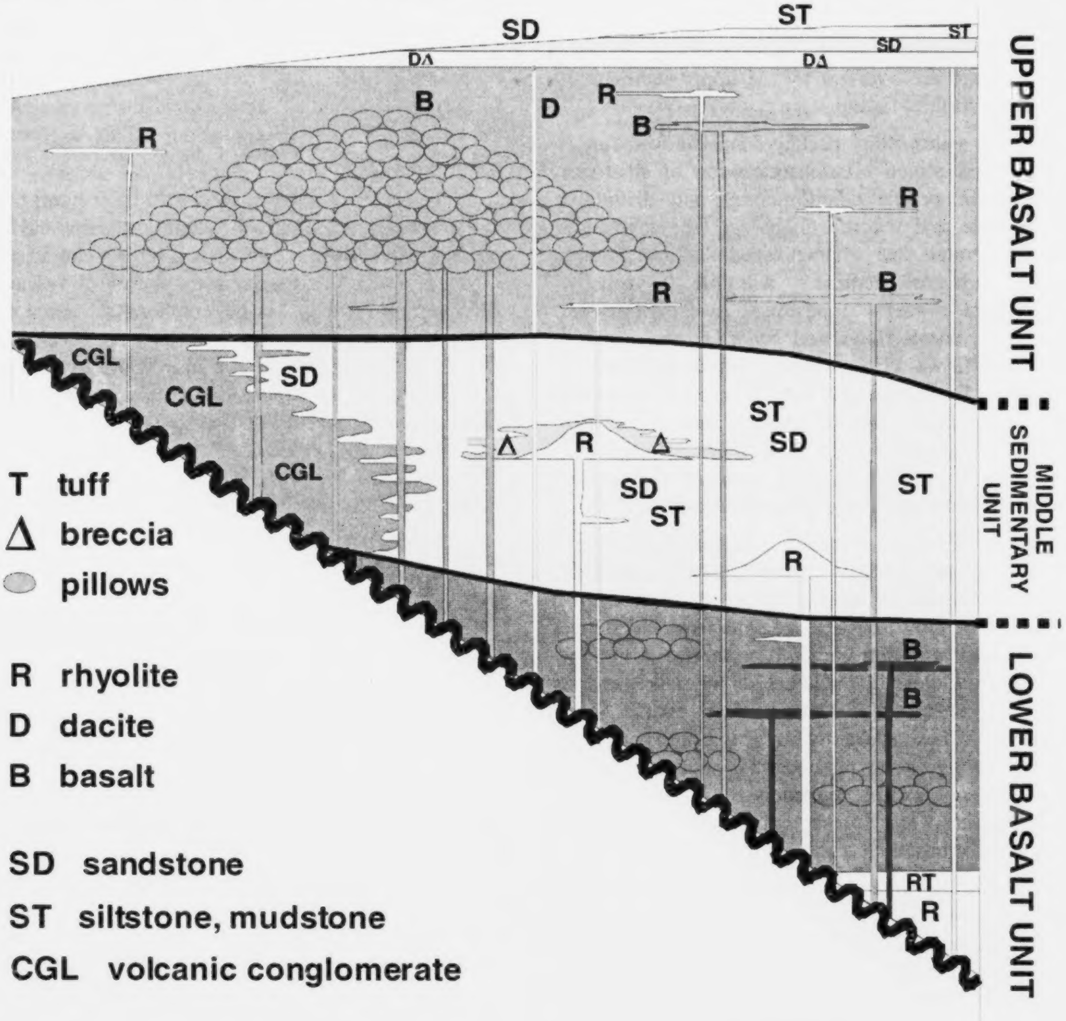
SD
ST
DΔ
SD
ST
DΔ
B
D
R
B
R
R
R
B
UPPER BASALT UNIT
CGL
CGL
SD
CGL
Δ
R
Δ
ST
SD
SD
ST
ST
R
MIDDLE SEDIMENTARY UNIT
B
B
RT
R
LOWER BASALT UNIT
T tuff
Δ breccia
pillows
R rhyolite
D dacite
B basalt
SD sandstone
ST siltstone, mudstone
CGL volcanic conglomerate

Figure 7. Schematic section of the Willow Ridge Complex, Upper Hazelton Group.

between Kakiddi Lake and Kinaskan Lake, and east and southeast of Kinaskan Lake (Figure 6). However, WRC rocks have not been recognised in mapping south of Ball Creek where distinctly different contemporaneous strata have been documented (see Snoball Creek descriptions below).

The complex is at least four kilometres thick on Table Mountain, where it consists of two distinct basalt units separated by a clastic sedimentary member. This thickness is the same order of magnitude as Pillow Basalt Ridge northwest of the Eskay Creek mine (2,000 metres, Read, 1989). On Table Mountain the base of the WRC is an angular unconformity above Upper Triassic volcaniclastic rocks; six kilometres to the northeast, the upper part of the WRC strata is eroded away.

The WRC succession exposed on Table Mountain and Willow Ridge consists of three units: a Lower Basalt Unit with intercalated rhyolite flows, sills and dikes; a Middle Sedimentary Unit with interlayered basalt and rhyolite flows, fissure dikes and several discrete felsic domes; and an Upper Basalt Unit with feeder dikes and rare intercalated sedimentary rocks and rhyolite, dacite and their feeder dikes (Figure 7; see also Simpson and Nelson, 2004). Along the western side of Table Mountain the base of the WRC lies along an angular unconformity where polymictic conglomerate, massive and pillow basalt, basalt hyaloclastite, and minor rhyolite flows and ash flow tuffs lap up against the underlying Upper Triassic andesitic volcaniclastics (Figure 7).

The lowermost section of the WRC on southwestern Table Mountain preserves thick (20-40m) altered and brecciated rhyolite and overlying ash tuffs at the base of the Lower Basalt Unit. The lower contact of these rhyolites and basalts is not exposed at this location, but is assumed to unconformably overlie Upper Triassic stratigraphy to the west. Basalts within the Lower Basalt Unit are dark green to olive green massive, pillowed or brecciated, with rare deposits of agglutinate spatter and brecciated scoria. The uppermost flows of the Lower Basalt Unit are pillow breccias and hydrothermal breccias with vugs and fractures containing agate and bladed calcite. Fine-grained volcaniclastic strata or local conglomerates of the Middle Sedimentary Unit conformably overlie the Lower Basalt Unit.

To the northwest, the Lower Basalt Unit wedges out along the unconformity and heterolithic, volcanic-dominated conglomerate with interlayered basalt hyaloclastite lies above the unconformity. The conglomerate forms an eastward-tapering lens in the centre of Table Mountain, interfingering with thin-bedded sandstones and mudstones to the east; all these lithologies form part of the Middle Sedimentary Unit. The heterolithic conglomerate incorporates clasts of the underlying Upper Triassic andesitic conglomerate lithologies near its base. Higher in the section, it contains clasts of rhyolite, basalt, mudstone, and pyritic rhyolite all derived from within the WRC. Belemnites, ammonites, pelecypods and fragments of petrified wood occur at numerous localities. Preliminary macrofossil identification from the conglomerate includes dicoelitid belemnites ranging from the Toarcian to Middle Bajocian (~184-170 Ma; J. Haggart pers. comm., 2004). Within the mudstones, aphanitic white rhyolite bodies form a northwest-trending line of lava domes and cryptodomes. These consist of massive to brecciated rhyolite, that in some cases grade outwards into carapaces of mixed rhyolite-sedimentary breccia. A few thin basalt hyaloclastite units occur within the sedimentary sequence. Interbedded spherulitic dacite and clastic sedimentary lenses indicate that the Middle Sedimentary Unit is undeformed and dips shallowly to the east.

On central Table Mountain, coarse clastic sedimentary rocks and multiple felsic eruptive centres characterize the Middle Sedimentary Member, and indicate a high-energy environment of deposition. At the northwestern and southeastern ends of Table Mountain, the Middle Sedimentary Member is preserved as a finer-grained sequence of sandstones, siltstones, mudstones and limestones and rare, thin interbedded volcanic units, suggesting a comparatively quiescent depositional environment. These latter areas of distal sediment accumulation and minor volcanism may be more favourable for the accumulation and preservation of exhalative sulphides, demonstrated by the Griz and Zinc Moss prospects described below.

The Upper Basalt Unit is extensively exposed on the eastern side of Table Mountain and on Willow Ridge. It is at least 2000 metres thick and consists of massive basalt flows, pillowed basalt flows, pillow and angular clast basalt breccia, and small bodies of rhyolite and dacite. Basalt dikes and sills are abundant; the prevalence of these intrusive equivalents within the upper basalt unit compared with their general absence in the underlying Middle Sedimentary Unit suggests that the upper basalt flows and breccias were sourced locally, and represent accumulation directly above a restricted feeder zone.

On Willow Ridge, the uppermost strata of the Upper Basalt Unit progress from massive basalt and basaltic hyaloclastite to a 100-metre-thick section of fragmental dacitic lithologies capped by thin-bedded pyritic siltstone and shale. The pyritic sedimentary unit may record the end of volcanism or it may represent a sedimentary interval within a thicker, unexposed volcanic section. The dacitic units consist of fine-grained ash tuff; fine lapilli tuff including two thin fragment-rich layers; a coarser dacite lapilli tuff with distinctive armoured clasts and columnar-jointed clasts; and a heterolithic fragmental unit with scattered pyritic clasts (interpreted as a subaqueous mass flow deposit).

The age of the WRC is constrained by previous fossil collections from the Middle Sedimentary Unit on Table Mountain. Souther (1972) reported on four ammonoid collections of Upper Toarcian (probable) and Middle Bajocian ages (GSC Nos. 37109, 85097, 85099, 85117). Evenchick *et al.* (2001) report one Middle Jurassic ammonite (GSC No. 177824) and one radiolarian collection of Bajocian or younger age (GSC No. 177823).

Lithologies and textures preserved throughout the Willow Ridge Complex indicate rapid accumulation of volcanic and sedimentary rocks in a deep-water marine setting. Feeder dikes to felsic lava flows trend northward. Feeder dikes to mafic lava flows trend eastward. Correlation with similar rock successions at the same stratigraphic position elsewhere in the region (Ash *et al.*, 1997b, Logan *et al*, 2000; Roth, 2002) suggests that these rocks span the Toarcian-Aalenian boundary (Lower Jurassic - Middle Jurassic) and are age-equivalent to the host rocks of the Eskay Creek gold mine. WRC strata constrain the age of a large diorite intrusion that cuts the Upper Basalt Unit at the northwest end of Willow Ridge (Figure 6). First mapped by Souther (1972), this stock is interpreted as part of the Middle Jurassic Three Sisters Suite (179-176 Ma).

Sulphide mineralisation within the WRC is most typically pyritic sandstones, pyritic rhyolite flows and pyritic felsic clasts in pebble to cobble conglomerates. A significant mineralized horizon of pyritic black mudstones was identified at the Griz prospect on south-central Table Mountain by M. Stewart (see below).

Hazelton Group Strata near Kinaskan Lake

Strata of the upper Hazelton Group have been reconnaissance mapped along both sides of central Kinaskan Lake in the northern part of the map area, in order to integrate mapping by Ash *et al.* (1997b) with the present project. These strata rest unconformably above maroon clinopyroxene-phyric, monolithologic volcanic breccia assigned to the Upper Triassic Stuhini Group by Ash *et al.* (1997b), and above unit lJme (described previously). Near the lake, the unconformity surface strikes northeast and dips moderately southeastwards (Figure 6). Overlying layered units, including rhyolite flows, rhyolite breccia and aphyric andesite hyaloclastite, parallel the surface of the unconformity. On the ridge on the east side of the lake, these units are subsequently overlain by an eastward-thickening (to 500-1000 m) sequence of interbedded, bimodal andesite-rhyolite volcanic rocks, volcaniclastic rocks and polymictic conglomerates, in which bedding attitudes flatten up-section. Lithologies include andesite lava flows with variable grey to green to maroon colouring, and related pillow breccias. The uppermost unit in this ridge is a distinctive shallowly dipping, multicoloured clast-rich pebble conglomerate that onlaps both the mixed sequence and locally, the unconformity surface itself. This conglomerate is polymictic, containing a mixture of bright turquoise to apple green clasts of rhyolite (similar to rhyolites flows, breccias and dikes preserved in bimodal sequences around Kinaskan Lake), aphyric basalt and andesite, and, within a few metres of the unconformity, clasts of the underlying maroon clinopyroxene-phyric volcanic rocks. This unit also contains fossil fragments of belemnites and pelecypod shells. A U-Pb analysis of rhyolite from the bimodal sequence overlying the unconformity at Kinaskan Lake yields a 183 Ma age (Toarcian; see Ash *et al.*, 1997b), contemporaneous with the lower units of the Willow Ridge Complex and probably representing related strata.

Basal Conglomerate on the Hank Property

At the Hank property, Lower Jurassic or younger sedimentary units unconformably overlie Upper Triassic volcanic rocks of the Stuhini Group. These sedimentary units are characterized by a coarsening-up sequence of siltstone through sandstone to cobble conglomerate. The dominant lithologies are interbedded siltstone, sandstone and pebbly sandstone. Pebbly sandstone is composed of subrounded lithic grains, and subrounded to well-rounded equant pebbles. Overlying cobble conglomerates display volcanic clasts with minor chert and mudstone clasts and syenite clasts similar to the felsic intrusions cutting the underlying stratigraphy. These carbonate-cemented sedimentary rocks are poorly consolidated and friable. Sedimentary structures are dominated by crude cross-bedding with shallow but variable orientations. This unit appears to fill topographic lows on underlying Upper Triassic stratigraphy. The lowermost lithology is siliceous siltstone and mudstone containing well-preserved carbonaceous leaf fossils including conifer and long bladed leaf varieties. This package is unaltered by, and may onlap onto, the eroded cap of the 184 Ma Hank porphyry dated by Kaip (1997). This sedimentary unit is correlated with Jurassic sandstones mapped six kilometres to the northwest by Logan *et al.* (1997) and with the basal conglomerates mapped above unconformities on the west side of Table Mountain and east of Kinaskan Lake.

Upper Hazelton Group strata at Snoball Creek

A section of fine-grained clastic sedimentary strata occupies the core of a tight, northwest-trending syncline exposed on three ridges between Ball Creek and More Creek. Strata consist of grey to black siltstone to mudstone, fine sandstone, limy siltstone, and sedimentary breccia with angular black mudstone intraclasts. In general this unit weathers recessively, with resistant ribs corresponding to the sandstone beds. In places thick, lumpy beds represent the sedimentary breccias and possibly olistostromes. The sedimentary strata overlie a thick section of volcaniclastic strata on a sharp but apparently conformable contact. Near the contact, bedding is parallel in both units. West of the fine-grained clastics, the volcaniclastic section forms a tight anticline. On the western limb of this fold, the uppermost volcanic unit is a thick maroon andesite flow and flow breccia that is not repeated in the fold limb below the clastic section to the east. It may have been removed by erosion prior to deposition of the overlying sedimentary strata.

This volcaniclastic sequence is dominated by resistant, ribby-outcropping, well-bedded, coarse volcanic debris flows. Most beds are monolithologic. In polymictic beds, clasts are andesite, dacite and basalt(?). Many fragments are plagioclase-phyric. Colors vary from green to dark maroon. Coarse units are interbedded with finer grained equivalents - volcanic sandstone, siltstone and tuff. A turbidite origin for the sequence is suggested by the coarse and fine sediment interbedding, by sedimentary textures such as graded bedding, load casts and flame structures, and by synsedimentary deformation features. Tabular rhyolite bodies form part of the uppermost 100 metres of section, immediately below the base of the overlying clastic sequence. Rhyolites are creamy white to grey to bright turquoise green, commonly pyritic, and show a textural variation from massive to flow-banded to brecciated to peperitic (angular to irregular, green rhyolite fragments with black mudstone infillings) to tuffaceous.

The age of the fine-grained clastic sequence is constrained by two macrofossil collections of ammonites that give Pliensbachian ages (Souther, 1972; GSC Nos. 32773 and 32802). However, two radiolarian collections of Bajocian or younger age have been obtained from the same sedimentary units (Evenchick et al., 2001; GSC Nos. 177838 and 177840). These ages would imply, respectively, correlation with the lower and upper Hazelton Group. The age of the underlying volcanic and volcaniclastic section is unknown and it is included here within the Stuhini Group (Figure 6). A sample of rhyolite within the volcaniclastic strata has been submitted for U-Pb age determination.

BOWSER LAKE GROUP

Strata of the Middle to Upper Jurassic Bowser Lake Group overlap the older volcanic sequences along the eastern part of the study area and have been most recently mapped by Evenchick (1991) and Ricketts and Evenchick (1991). To the east, stratigraphy and nomenclature for the Bowser Lake Group in the Spatsizi River mapsheet (NTS 104H) have been wholly revised and updated (Evenchick and Thorkelson, 2004).

Regionally, the basal contact of the Bowser Lake Group grades upward from the upper sedimentary strata of the Salmon River Formation (Spatsizi Formation) of the underlying Hazelton Group. The Middle Jurassic boundary between these similar sedimentary packages roughly coincides with the Bajocian-Bathonian transition at 166 Ma.

Anderson (1993) describes the lowest units within the Bowser Lake Group as thin to thick-bedded, fine to coarse-grained siliciclastic rocks including turbiditic shale, siltstone, greywacke, fine to medium grained sandstone and rare conglomerate. Anderson cautions that these units are indistinguishable in the field from similar lithologies at the top of the underlying Salmon River Formation of the Hazelton Group.

Evenchick (1991), mapping in the current study area, correlated black siltstone, fine grained sandstone and minor to large proportions of chert pebble conglomerate with the Ashman Formation of the Bowser Lake Group. Evenchick and Thorkelson (2004) note that the Hazelton Group - Bowser Lake Group contact is gradational, however, they place the boundary where thin, white-weathering tuffaceous laminae, typical of the upper Spatsizi Formation (Salmon River Formation), are no longer present in black siltstones.

Bowser Lake Group strata are well exposed along and around the road network of the Willow Creek Forest Access Road and along a low ridge which trends northward between Willow Ridge and Kakiddi Lake. Strata are notably flat lying to shallowly southeast dipping over much of this area, suggesting that the sedimentary cover over underlying volcanic strata of the Hazelton Group is relatively thin. Chert pebble conglomerate is the most resistant lithology and consequently the most prominent rock unit; black mudstone and well-sorted sandstone are less extensively exposed. Pebble conglomerate cropping out along the Willow Creek road displays distinctive multicolored pebbles including red jasper, green rhyolite or chert, pyritic volcanic rock, and black and white chert.

MOUNT EDZIZA VOLCANIC COMPLEX

The Late Cenozoic Mount Edziza Volcanic Complex blankets 1000 km^2, including part of the northwest corner of the map area. The complex is comprehensively described and illustrated in Geological Survey of Canada Memoir 420 (Souther, 1992). Volcanic rocks range in age from 7.5 Ma to 2,000 B.P. The complex comprises alkaline basalt and hawaiite with lesser intermediate and felsic volcanic flows, and it records five major cycles of magmatic activity.

INTRUSIVE ROCKS

COPPER MOUNTAIN PLUTONIC SUITE

A small pyroxenite plug first mapped by Souther (1972) crops out in central Northmore Ridge, south of the Hank prospect and near the head of Snoball Creek. Cut by a minor fault, this stock intrudes Upper Triassic sedimentary strata. It is correlated here with the similar small ultramafic stocks of the Late Triassic to Early Jurassic Copper Mountain Suite (Logan *et al.* 2000).

TEXAS CREEK PLUTONIC SUITE

A variety of fine to medium grained, commonly porphyritic, leucocratic intrusive rocks found in the map area are correlated with the Early Jurassic Texas Creek Suite (Logan *et al.* 2000). The intrusions appear as simple stocks or as clusters of anastomosing dikes. A string of small plugs and dikes are distributed along the trend of the Hank, ME and Mary mineral prospects. Intrusions of this suite are important regional loci for porphyry copper-gold, transitional gold and epithermal gold-silver deposits. In the study area, they are associated with the Hank epithermal gold, and the ME, Mary, Spectrum, GJ, Groat and Red Chris porphyry copper-gold prospects.

THREE SISTERS PLUTONIC SUITE

Fine to medium grained equigranular diorite stocks and a small medium grained gabbro plug cut Lower to Middle Jurassic strata of the Willow Creek Complex in the northern map area. These plutons are assigned to the Middle Jurassic (179-176 Ma) Three Sisters Suite defined by Anderson (1983).

HYDER PLUTONIC SUITE

The Eocene Hyder Suite forms the eastern margin of the Coast Crystalline Belt to the west of the study area. This continental-scale magmatic event is recorded within the map area by a series of north-trending, fine-grained to aphanitic rhyolite dikes first identified by Souther (1972). These intrusions are likely feeders to overlying felsic flows that have been subsequently eroded.

STRUCTURE

The dominant northwest structural grain through the central and southern map area is due to a set of northwest-trending faults that divide the region into a series of elongate, fault-parallel blocks of intact stratigraphy. Differential uplift between blocks, followed by erosion down to the common elevation of the Spatsizi Plateau, results in adjacent blocks displaying different stratigraphic levels in the regional stratigraphy (Figure 6). Minor warps and gentle folds mapped within the Upper Triassic stratigraphy are also developed along northwest-trending fold axes, suggesting minor buckling accompanying the faulting and differential uplift of blocks of intact strata.

The Northmore Fault (Figure 6) is a map-scale feature with significant sinistral offset. This fault is the locus for a string of small plutons and appears to be syn-intrusive. Strata near the fault are also more intensely folded than equivalent strata elsewhere in the region.

Anderson (1993) first described the north-trending, fault-bounded belt that hosts the "Eskay facies" strata of the Salmon River Formation. Smaller-scale, north-trending growth faults were intersected in drillholes testing Eskay facies strata near the mine workings; these faults may be important fluid pathways responsible for localizing mineralisation (Anderson, 1993).

In the present project, two lines of evidence for the northerly orientation of the Eskay Rift are the north-trending unconformity exposed along the western cliffs of Table Mountain and prominent north- to northwest-trending rhyolite and dacite feeder dikes and strings of felsic domes exposed in the central and northern areas of Table Mountain (Figure 6; see also Simpson and Nelson, 2004, Figure 2). The rhyolite dike and dome relationships are similar to those described for the Eskay Creek mine area (Bartsch, 1993).

On Willow Ridge, southwest of Kinaskan Lake, the edge of the Eskay Rift is not exposed, but the western edge of the Eskay Rift is well-exposed on the southern Klastline Plateau, on the west side of Kinaskan Lake, as a prominent northeast-trending rhyolite dike (unit lJFve of Ash *et al.*, 1997b). The western edge of the Eskay Rift crops out again on the slopes of Mount Mars on the east side of Kinaskan Lake as a distinct erosional unconformity (described above). South of the project area, similar abrupt increases in the thickness of bimodal volcanic strata correlated with the Willow Ridge Complex are evident in two east-west transects: from the toe of Bruce Glacier to the Eskay Creek minesite; and south of Sulphurets Creek from the HSOV prospect to Mount Madge.

MINERAL DEPOSITS

Northwestern BC hosts a variety of mineral deposit types characteristic of magmatic arc environments ,including calc-alkaline porphyry copper-gold deposits (Figure 1 in Schroeter and Pardy, 2004); Eskay Creek-type subaqueous hotspring deposits (Massey, 1999a); Kuroko-type VMS deposits (Massey, 1999b); and low-sulphidation epithermal deposits (Figure 1 in Schroeter and Pardy, 2004). Near the current study area, intrusive-related Cu-Ni deposits (Lefebure and Fournier, 2000) and Besshi-type VMS deposits (Massey, 1999b) are hosted in rock units that may also be present within the map area. Sedimentary strata of the Bowser Lake Group host coal deposits and have elevated concentrations of molybdenum and nickel (Alldrick *et al.*, this volume). Recent study of the Bowser Lake Group has shown potential for the generation and accumulation of petroleum (Evenchick *et al.*, 2002).

Figure 8 shows the distribution of mineral deposits and prospects in the study area. These occurrences are concentrated in the volcanic strata that pre-date deposition of the Bowser Lake Group. This distribution is reflected in metal concentrations detected in the Regional Geochemical Surveys (see Figures 5 and 7 in Lett and Jackaman, this volume). This metals-rich region lies west of Highway 37 and corresponds to the eastern edge of the Coast Mountains. Bowser Lake Group sedimentary strata, with its coal, petroleum and sediment-hosted metal potential, generally lies east of Highway 37.

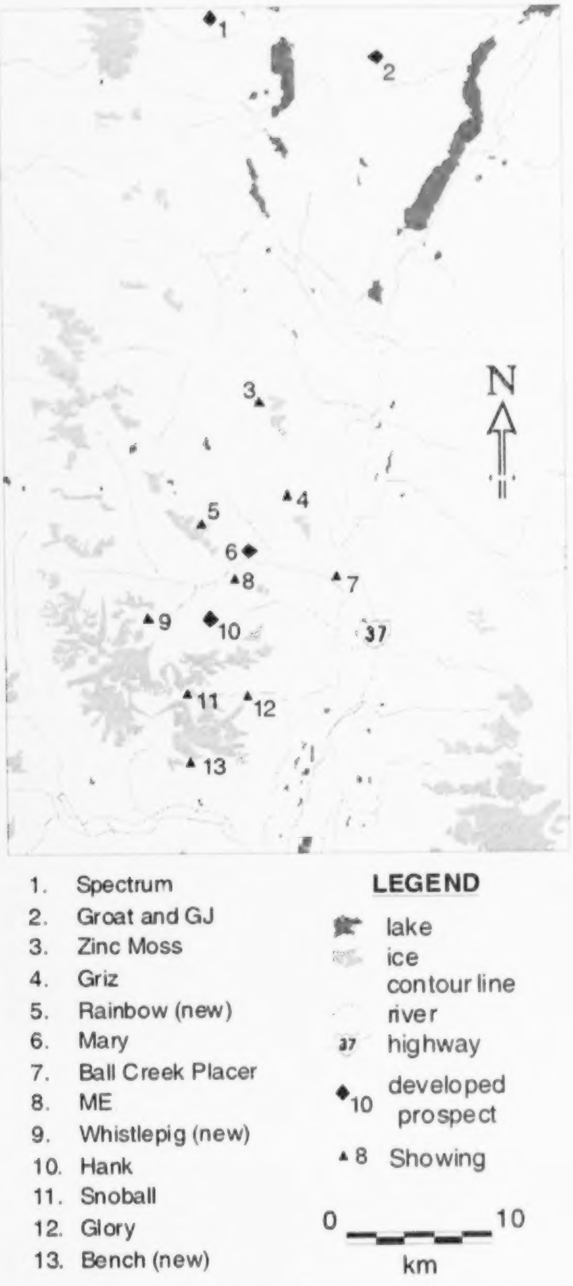

Figure 8. Mineral deposits and prospects in map area.

Intrusion-related deposit types in or near the study area include porphyry copper-gold deposits, which are particularly common in this region (Schroeter and Pardy, 2004); intrusion-related low-sulphidation epithermal deposits; and magmatic copper-nickel deposits. Volcanic-hosted deposits include some of the Eskay Creek deposits and some low-sulphidation epithermal veins (Massey, 1999a). Stratiform or stratabound deposit types include sediment-hosted molybdenum and nickel, Besshi-type sediment-hosted massive sulphide deposits, as well as volcanic-hosted VMS deposits (Massey, 1999b). Limestone units are favourable host rocks for gold-rich skarn deposits (e.g. McLymont Creek).

During the 2003 mapping program, three new mineral showings were located by government geologists on the Targeted Geoscience Inititative project. As these crews focus on mapping, not prospecting, this is a surprisingly high number of new mineral occurrences. It reflects both the high mineral potential of the region and the limited exploration work to date. More exploration work is justified in this area based on these discoveries and the presence of the "Eskay Facies" strata.

GRIZ

(UTM 09/0417580E/6354153N)

Thin-bedded black mudstones of the Middle Sedimentary Unit of the Lower to Middle Jurassic Willow Ridge Complex host thin laminae (2-8 mm) of fine-grained, pale pyrite (Figure 9). The Griz prospect is exposed where a creek cuts down through siltstone and pyritic mudstone beds (Figure 10), which conformably overlie pillow basalt and basalt breccia hosting disseminated sulphides. This recessive-weathering, poorly exposed horizon lies along strike with several gossanous exposures that extend one kilometre due south of the mudstone exposure. Gossanous units are reworked volcanic breccias, and include basalt clasts cut by pyrite veins. The prospect was explored in 1990 and 1991 by Noranda Inc. (Campbell *et al.*, 1990). Of six samples collected in 2003 along these exposures, a sample of the laminated sulphide and mudstone unit in the creekbed (Figure 9) at the north end returned the highest assay values: 0.6 ppb Au, 765 ppb Ag, 56 ppm Cu, 23 ppm Pb, 794 ppm Zn, 31 ppm As, 348 ppb Hg, 9 ppm Sb.

ZINC MOSS

(UTM 09/0415282E/6361706N)

At this location, pyritic clastic sedimentary beds in the Middle Sedimentary Unit of the Lower to Middle Jurassic Willow Ridge Complex are interbedded with thin flows of pyritic massive basalt. The basalt and adjacent sandstones, siltstones, grits, granule conglomerates and rare pebble conglomerate and limestone at the Zinc Moss prospect are strongly pyritic and well exposed over an extensive area of outcrop near the head of Compass Creek on northern Table Mountain. The prospect was explored in 1990 and 1991 by Noranda Inc. (Campbell *et al.*, 1990). Pyrite occurs as disseminations in the sedimentary rocks and as fine-grained seams and irregular pods and zones of fine-grained pyrite replacement within the basalt flows. From four samples collected for assay, the best results were obtained from a sample of pyritic pebble conglomerate: 13 ppm Cu, 11 ppm Pb, 120 ppm Zn, 1 ppb Au, 126 ppb Ag, 50 ppm As, 6 ppm Sb, 262 ppb Hg.

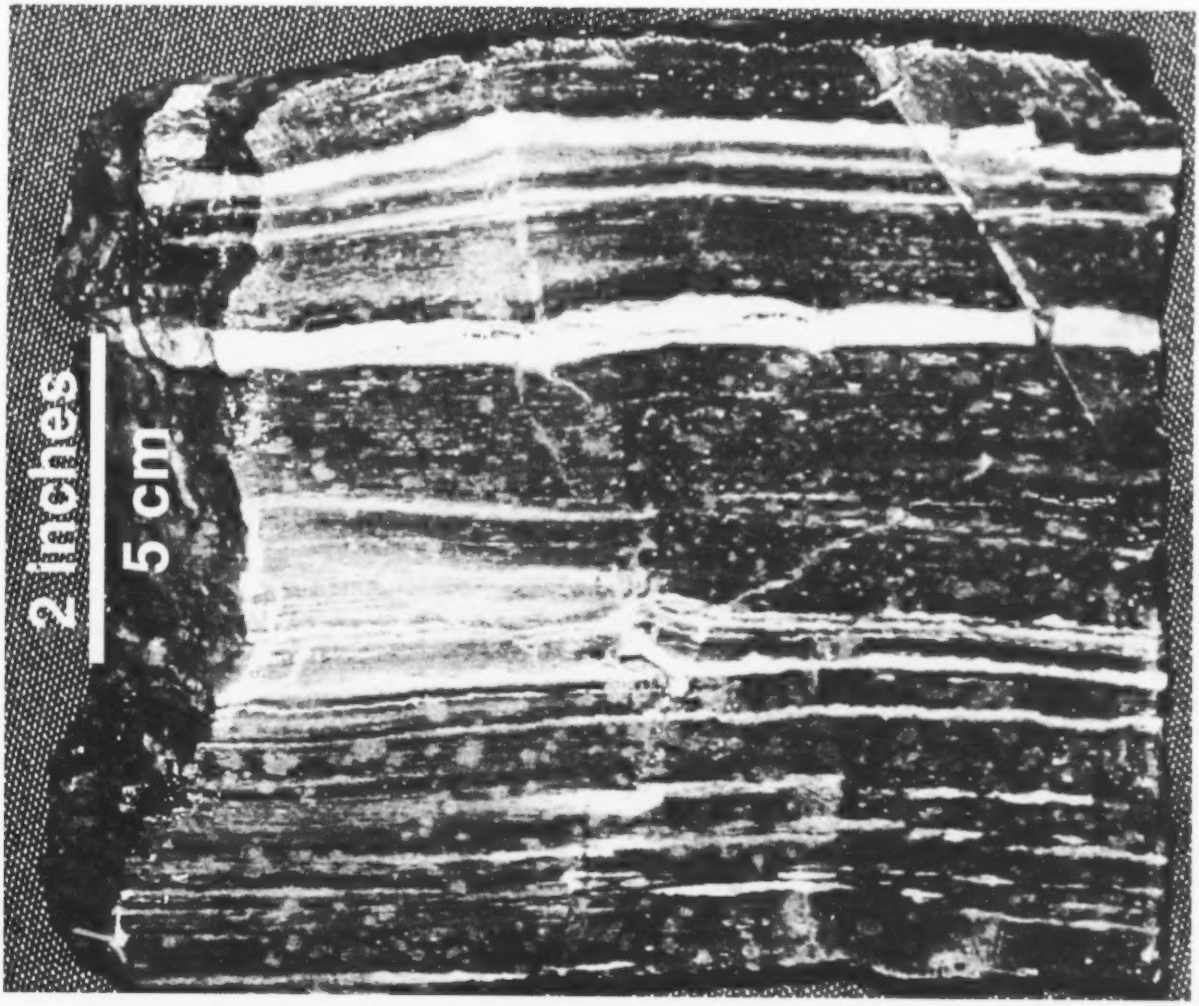
2 inches
5 cm

Figure 9. Sample of laminated pyrite and mudstone, Griz prospect.

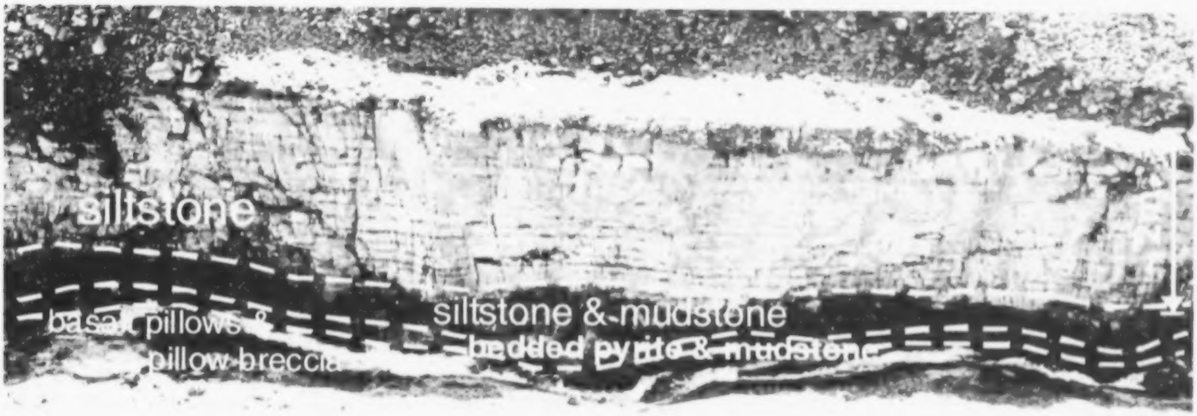
siltstone
basalt pillows &
pillow breccia
siltstone & mudstone
bedded pyrite & mudstone

Figure 10. Outcrop exposure of Griz prospect.

WHISTLEPIG (new prospect)

(UTM 09/0406808E/6342298N)

A fault zone cutting Upper Triassic siltstones host mineralization exposed along a southwestern tributary of Ball Creek, two kilometres west of the Hank deposit. Siliceous siltstones are grey to white, massive and weakly colour-banded. The Whistlepig mineralization occurs as semi-massive sulphides in fault-hosted, quartz-calcite veins. The fault is part of a regionally extensive zone of faults called the Northmore fault zone, which ranges up to 100 metres wide. This shear zone is a steeply inclined, sinistral, transverse fault, easily traced for up to several kilometers by fractures and gossanous weathering of disseminated sulphides found throughout the fault system. The veins were sampled in two locations, the best assay yielded 732 ppb Au, 2867 ppb Ag, 1001 ppm Cu, 11 ppm Pb, 24 ppm Zn, 2 ppm As, 32 ppb Hg, 1 ppm Sb.

BENCH (new prospect)

(UTM 09/0409490E/6330105N)

A band of massive to semi-massive, fine-grained, bright pyrite crops out at the base of a high cliff of black rhyolite near the head of Bench Creek. The upper part of the cliff is massive to faintly banded, black to charcoal rhyolite. Throughout the lower five metres along the base of the cliff, the rhyolite is transected by many fine hairline cracks filled with pyrite. Along most of the length of the cliff, a talus pile of coarse blocks and boulders is piled up against the basal rhyolite layer with the pyritic fractures. At one location near the upstream end of the cliff, the top of the talus pile is lower and exposes two feet of massive, fine-grained granular pyrite and semi-massive granular pyrite disseminated in white, fine-grained quartz. The significance of this small showing is its stratabound character and the high probability that this mineralisation extends laterally under the blocky talus cover.

RAINBOW (new prospect)

(UTM 09/0409426E/6349633N)

Several black, flow-banded rhyolite flows and dikes are exposed within a one-kilometre radius of the Rainbow prospect. At this location the outcropping rhyolite dike has abundant encrustations of very fine-grained, bright yellow and orange minerals developed along many hairline fractures within the dike. The country rock is massive light grey Upper Triassic limestone, but other rhyolite exposures nearby lie within limy sandstones, grits and pebble conglomerates. The best assay from this dike rock is 70 ppm Cu, 114 ppm Pb, 283 ppm Zn, 76 ppb Au, 5325 ppb Ag, 688 ppm As, 24 ppm Sb, 418 ppb Hg. These results are significant because of the elevated gold, silver, mercury, arsenic and antimony values, and the several nearby isolated outcrops and semi-continuous exposures of dikes and flows of black rhyolite with glassy lustre.

Spectrum-Red Dog (104G 036) is a porphyry copper-gold deposit with reserves of 504,800 tonnes grading 9.6 grams per tonne Au. Moderate copper grades are patchy and highest grades are obtained in areas of chalcopyrite-magnetite mineralisation in skarn. Adjacent to Spectrum, the **Hawk** (104G 005) gold-silver prospect is a series of sulphide-rich, quartz-calcite veins cutting across Upper Triassic sedimentary and volcanic rocks around the perimeter of diorite and granodiorite intrusions. These two prospects resemble other porphyry copper-gold systems in the region which feature peripheral high grade precious metal mineralisation (e.g. Red Bluff/Snip/Johnny Mountain; Kerr/Sulphurets; Snowdrift/Tanzilla)

The **GJ** (104G 034) deposit is an Upper Triassic copper-gold porphyry system hosted by the Groat granodiorite stock (205.1 +/- 0.8 Ma;) and it's Upper Triassic sedimentary country rocks. The stock is contemporaneous with the stock hosting the Red-Chris porphyry Cu-Au deposit (203.8 +/- 1.3 Ma; Friedman and Ash, 1997) 25 km to the east.

The **Mary** (104G 018) occurrence is a porphyry copper-gold-silver-molybdenum prospect hosted in coarse mafic volcaniclastic rocks cut by several large parallel to anastomosing monzonite dikes and plugs (Panteleyev, 1975). The deposit has been interpreted as an Upper Triassic porphyry system developed in coeval Upper Norian volcanic, volcaniclastic and sedimentary strata, based on a 218 +/- 24 Ma sericite K-Ar date, but it is interpreted here as an Early Jurassic stock, contemporaneous with similar intrusions on the Hank property to the southwest.

The **ME** (104G 042) showing is a series of large gossans cropping out on the south side of Ball Creek, between the Mary and Hank deposits. Copper-molybdenum mineralisation occurs as disseminations in silicified alteration zones, in quartz veins, and with galena and sphalerite in carbonate veins.

The confluence of Ball Creek and Devil's Creek was the site of the **Ball Creek** (104G 072) placer gold operation between 1936 and 1940.

The Hank (104G 107) deposit is interpreted as a bulk-tonnage, low-grade epithermal system. The deposit occurs where stratabound alteration 'blankets' extend out from Early Jurassic granodiorite stocks into permeable Upper Triassic andesitic volcaniclastic country rock. A drill-indicated geological resource of 507,500 tonnes grading 3.43 gm/tonne gold has been established in three zones on the property (Kaip, 1997). The geometry of the planar stratabound alteration envelopes surrounding the central Early Jurassic stock resembles the geometry of the Tanzilla (104I 022) gold prospect 135 kilometres to the northeast.

The **Snoball** (104G 143) property is located where Upper Triassic Stuhini Group siltstones and andesites are intruded by a diorite stock. Gold-silver mineralisation occurs as sulphide disseminations and pods within silicified hornfels or as quartz-sulphide veins cutting unaltered siltstones. Vein sulphides are arsenopyrite, pyrite, sphalerite and galena.

The **Glory** prospect was discovered in 1990 by Keewatin Engineering Inc. (Bobyn, 1991) on the south side on Snoball Creek. Massive pyrite veins and lenses up to 1.0 m wide and 60 m long are developed along intrusive contacts where fine clastic sedimentary rocks are cut by felsic dikes and sills. Mineralisation is concordant with bedding, and the felsic intrusive rocks also contain thin lenses (10 cm by 30 cm) of massive pyrite. An assay of the massive pyrite returned 2,000 ppb Ag, 1 ppb Au, 8 ppm Cu, 13 ppm Pb, 28 ppm Zn, 60 ppm As, 1 ppm Sb, 1670 ppb Hg.

METALLOGENY

In the map area and in the surrounding region, Upper Triassic mineralisation includes large porphyry copper-gold systems (GJ, Galore Creek), Besshi-type VMS deposits (Rock and Roll), Kuroko-type VMS prospects (Bench) and vuggy rhyolite dikes and flows with elevated Au, Ag, Hg, Sb, As (Rainbow). Lower Jurassic mineralisation that predates the erosional interval marked by Nassian uplift is represented by large porphyry copper-molybdenum systems (Mary, Red-Chris), stratabound bulk-tonnage epithermal mineralisation (Hank), and precious metal rich skarn deposits (McLymont). Lower to Middle Jurassic mineralisation that post-dates the Nassian uplift includes the Griz prospect and many areas of pyritic felsic volcanic units and derived volcaniclastic sedimentary rocks (e.g. Figure 4 in Simpson and Nelson, 2004), plus the Eskay Creek gold mine and numerous nearby prospects (Lulu, 22 Zone, HSOV).

EXPLORATION POTENTIAL

In this region, where mineral deposit types are characteristic of their host strata, deposit-specific exploration programs can target particular stratigraphic intervals. Due to the highly dissected terrain, geochemical stream sediment sampling has proven to be a particularly successful and cost-effective tool for assessing the potential of larger areas (Lett and Jackaman, this volume), and should be equally powerful as a second phase follow-up technique. Discovery of a number of small prospects during this season's regional mapping program indicate that the potential of this area has not yet been thoroughly assessed.

The Middle Sedimentary Unit of the Willow Creek Complex and the many minor sedimentary members within the Lower and Upper Basalt Units of the Willow Creek Complex are all favourable sites for the deposition and preservation of exhalative sulphides and should be selectively prospected. Areas of quiescent, distal sedimentation will be more conducive to the accumulation and preservation of exhalative sulphides (e.g. Griz and Zinc Moss prospects).

DISCUSSION AND CONCLUSIONS

This project has provided important new detailed geological surveys of the northern Eskay Rift rocks within the Telegraph Creek map area. Tracts of "Eskay equivalent" strata crop out on Table Mountain, Willow Ridge and on ridges east and west of Kinaskan Lake. These exposures are defined here as the Willow Ridge Complex, a thick accumulation of basalt and lesser rhyolite, accompanied by fine to coarse-grained clastic sedimentary strata. Throughout the map area, WRC strata lie unconformably above Upper Triassic Stuhini Group volcanic rocks. The Kinaskan Lake bimodal sequence may in part unconformably overlie Lower Jurassic strata as well. Sub-Middle Jurassic unconformities also occur on the Hank property, where a petrified-log-bearing conglomerate overlies both Stuhini Group rocks and a 184-Ma pluton; six kilometres to the northwest of the Hank deposit, Logan *et al.* (1997) mapped gently dipping plant-bearing Lower Jurassic sandstones above Upper Triassic strata.

It is important to establish the exact age of these mapped unconformities since Souther (1972) recognised two separate unconformities within Early Jurassic time, the Inklinian uplift at the Triassic-Jurassic boundary, and the late Early Jurassic Nassian uplift. For unconformities mapped in this year's study area, evidence so far favors a correlation with the late Early Jurassic Nassian uplift. Near Kinaskan Lake, the overlying unit is, in part, of Toarcian age (183 Ma). Toarcian-Bajocian fossils occur in conglomerate near the unconformity at the base of the Willow Ridge Complex on Table Mountain. On the Hank property, the youngest underlying unit is a 184 Ma pluton. However, more radiometric and fossil data from both underlying and overlying units is required to verify this hypothesis. It is possible that both Triassic-Jurassic and late Early Jurassic unconformities exist in the area.

The Table Mountain and Kinaskan Lake unconformities show significant similarities and differences. Both are overlain by polymictic conglomerates that are similar in clast and fossil contents, which attest to coarse, proximal sedimentation unusual elsewhere in the sequences. Both dip moderately to steeply towards the overlying successions: east in the case of the Table Mountain unconformity, and south to southeast east of Kinaskan Lake. The Table Mountain unconformity is interpreted as a fossil rift margin (Simpson and Nelson, 2004). On the east side of Kinaskan Lake, based on basinward dips and the upward shallowing of unit dips above the unconformity, a similar rift-margin origin can be proposed. West of Kinaskan Lake, a prominent rhyolite sill intrudes the same unconformity (Ash *et al.*, 1997b). The principal difference between the two localities is their strike: at Table Mountain, the western edge of the WRC strikes north, whereas near Kinaskan Lake the edge of the WRC strikes northeast. This could be due to later folding, alternatively the initial faults bounding the rift may shift from northerly trends near Table Mountain to northeasterly near Kinaskan Lake.

SUMMARY

Mapping has refined the stratigraphic and structural picture of the More Creek - Kinaskan Lake area. Important contributions include the recognition of the near absence of strata representing the lower Hazelton Group, and recognition of regional-scale unconformities that form irregular boundaries between major stratigraphic packages.

The Eskay Rift and "Eskay Facies" extend north to Kinaskan Lake. The newly defined Willow Ridge Complex comprises bimodal volcanic lithologies and related sedimentary strata correlative with strata that host the Eskay Creek orebodies to the south. The margin and base of the Willow Creek Complex is a readily recognised angular unconformity that sharply delineates these strata most favourable for the formation and preservation of similar deposits.

Previously documented mineral occurrences in the area are sparse; however, this must in part reflect limited exploration coverage as three new showings were found during this season's mapping program.

ACKNOWLEDGEMENTS

Faye Nelson, Tony Wass, Rob Dennis, Lester Dennis and Brent Dennis provided capable and cheerful assistance. We thank Adam Travis, David Mehner and Don Coolidge for valuable discussions in the field. We appreciate the cooperation and kind hospitality of Don Coolidge, who accommodated the 2003 field program at his ranch. Jim and Sharon Reed at Pacific Western Helicopters provided safe, swift and reliable helicopter support.

REFERENCES

Alldrick, D.J. (1993): Geology and metallogeny of the Stewart Mining Camp, northwestern British Columbia; British Columbia Ministry of Energy and Mines, Bulletin 85, 105p

Alldrick, D.J., Jackaman, W. and Lett, R.E.W. (2004): Compilation and Analysis of Regional Geochemical Surveys around the Bowser Basin; British Columbia Ministry of Energy and Mines, Geological Fieldwork 2003, Paper 2004-1

Alldrick, D.J., Stewart, M.L., Nelson, J.L. and Simpson, K.A. (2004): Geology of the More Creek - Kinaskan Lake area, northwestern British Columbia; British Columbia Ministry of Energy and Mines, Open File Map 2004-2, Scale 1:50 000

Anderson, R.G. (1983): The geology of the Hotailuh Batholith and surrounding volcanic and sedimentary rocks, North-central British Columbia; Carleton University, Ph.D. thesis

Anderson, R.G. (1989): A stratigraphic, plutonic and structural framework for the Iskut Map area, northwestern British Columbia; Current Research, Part E, Geological Survey of Canada, Paper 89-1 E, p.145-154

Anderson, R.G. (1993): A Mesozoic stratigraphic and plutonic framework for northwestern Stikinia, northwestern British Columbia, Canada; in Dunne, G., and McDougall, K., editors, Mesozoic Paleogeography of the western United States-II, Pacific Section SEPM, vol. 71, p.477-494

Anderson, R.G. and Thorkelson, D.J. (1990): Mesozoic stratigraphy and setting for some mineral deposits in Iskut River map area, Northwestern British Columbia, in Current Research, Part E, Geological Survey of Canada, Paper 90-1 E, p.131-139

Ash, C.H., Fraser, T.M., Branchflower, J.D. and Thurston, B.Q. (1995): Tatogga Lake Project, Northwestern British Columbia (104H/11, 12); in Geological Fieldwork 1994, Grant, B. and Newell, J.M., Editors, British Columbia Ministry of Energy, Mines and Petroleum Resources, Paper 1995-1, p.343-358

Ash, C.H., Stinson, P.K. and Macdonald, R.W.J. (1996); Geology of the Todagin Plateau and Kinaskan Lake Area (104H/12, 104G/9); in Geological Fieldwork 1995, Grant, B. and Newell, J.M., Editors, British Columbia Ministry of Energy, Mines and Petroleum Resources, Paper 1996-1, p.155-174

Ash, C.H., Macdonald, R.W.J. and Friedman, P.M. (1997a); Stratigraphy of the Tatogga Lake Area, Northwestern British Columbia (104G/9,16); in Geological Fieldwork 1996, Lefebure, D.V., McMillan, W.J. and McArthur, J.G., Editors, British Columbia Ministry of Employment and Investment, Paper 1997-1, p.283-297

Ash, C.H., Macdonald, R.W.J., Stinson, P.K., Fraser, T.M., Read, P.R., Pustka, J.F., Nelson, K.J., Ardan, K.M., Friedman, R.M. and Lefebure, D.V. (1997b): Geology and Mineral Occurrences of the Tatogga Lake Area, Northwestern British Columbia (104G/9E&16SE, 104H/12NW&13SW); British Columbia Ministry of Energy and Mines, Open File Map 1997-3, scale 1:50 000

Bartsch, R.D. (1993): A rhyolite flow dome in the upper Hazelton Group, Eskay Creek area; Geological Fieldwork 1992, British Columbia Ministry of Energy, Mines and Petroleum Resources, Geological Fieldwork 1992, Paper 1993-1, p.331-334

Bobyn, M.G. (1991): Summary report on geological mapping, prospecting, and geochemistry of the Cal 1-4 Claim Group; British Columbia Ministry of Energy and Mines, Assessment Report 20,998, 10p

Breitsprecher, K. and Mortensen, J.K. (2004): BCAge 2004 - a database of isotopic age determinations for rock units in British Columbia; British Columbia Ministry of Energy and Mines, Geological Survey, Open File 2004-3

Campbell, T., Savell, M. and Wong, T. (1990): Geological geochemical and geophysical report on the Ball Creek property; British Columbia Minstry of Energy and Mines, Assessment Report 20,617, 15p

Evenchick, C.A. (1991): Jurassic stratigraphy of east Telegraph Creek and west Spatsizi map areas, British Columbia; in Current Research, Part A, Geological Survey of Canada, Paper 91-1A, p.155-162

Evenchick, C.A., Poulton, T.P., Tipper, H.W. and Braidek, I. (2001): Fossils and facies of the northern two-thirds of the Bowser Basin, British Columbia; Geological Survey of Canada, Open File Report 3956, 103p

Evenchick, C.A., Hayes, M.C., Buddell, K.A. and Osadetz, K.G. (2002): Vitrinite and bitumen reflectance data and preliminary organic maturity model for the northern two thirds of the Bowser and Sustut basins, north-central British Columbia; Geological Survey of Canada, Open File Map 4343, scale 1:250,000

Evenchick, C.A. and McNicoll, V.J. (2002): Stratigraphy, structure, and geochronology pf the Anyox Pendant, Northwest British Columbia, and implications for mineral exploration; Canadian Journal of Earth Sciences, 39: p.1313-1332

Evenchick, C.A. and Thorkelson, D.J. (in press): Geology of the Spatsizi River map area, North-central British Columbia; Geological Survey of Canada, Bulletin 577

Friedman, R.M. and Ash, C.A. (1997): U-Pb age of intrusions related to Porphyry Cu-Au mineralisation in the Tatogga Lake area; British Columbia Ministry of Employment and Investment, Geological Fieldwork 1996, Paper 1997-1, p.291-297

Gunning, M.H. (1996): Definition and interpretation of Paleozoic volcanic domains, Northwestern Stikinia, Iskut River area, British Columbia; University of Western Ontario, Ph.D. thesis, 388p

Kaip, A.W. (1997): Geology, alteration and mineralization on the Hank property, Northwestern British Columbia: a near-surface, low-sulfidation epithermal system; University of British Columbia, M.Sc. Thesis, 198p

Lefebure, D.V. and Fournier, M.A. (2000): Platinum group element mineral occurrences in British Columbia; British Columbia Ministry of Energy and Mines, Geofile Map 2000-2, scale 1:2,000,000

Lett, R. and Jackaman, W. (2004): New exploration opportunities in the B.C. regional geochemical survey database; British Columbia Ministry of Energy and Mines, Geological Fieldwork 2003, Paper 2004-1

Logan, J.M., Koyanagi, V.M. and Drobe, J.R (1990): Geology and Mineral Occurrences of the Forrest Kerr – Iskut River Area (104B/15); British Columbia Ministry of Energy Mines and Petroleum Resources, Open File Map 1990-2, scale 1:50,000

Logan, J.M., Drobe, J.R. and Elsby, D.C. (1992): Geology, Geochemistry and Mineral Occurrences of the More Creek Area, Northwestern British Columbia (104G/2): British Columbia Ministry of Energy, Mines and Petroleum Resources, Open File 1992-5

Logan, J.M. and Drobe, J.R. (1993): Geology of the Mess Lake Area, Northwestern British Columbia (104G/7W); British Columbia Ministry of Energy, Mines and Petroleum Resources, Open File 1993-6

Logan, J.M., Drobe, J.R., Koyanagi, V.M. and Elsby, D.C. (1997): Geology of the Forest Kerr - Mess Creek Area, Northwestern British Columbia (104B/10,15 & 104G/2 & 7W), British Columbia Ministry of Employment and Investment, Geoscience Map 1997-3, scale 1:100 000

Logan, J.M., Drobe, J.R. and McClelland, W.C. (2000): Geology of the Forest Kerr - Mess Creek Area, Northwestern British Columbia (104B/10,15 & 104G/2 & 7W); British Columbia Ministry of Energy and Mines, Bulletin 104, 164p

MacDonald, J.A., Lewis, P.D., Thompson, J.F.H., Nadaraju, G., Bartsch, R.D., Bridge, D.J., Rhys, D.A., Roth, T., Kaip, A., Godwin, C.I. and Sinclair, A.J. (1996): Metallogeny of an early to middle Jurassic Arc, Iskut River area, Northwestern British Columbia; Economic Geology, 91:6, p.1098-1114

Massey, N.W.D. (1999a): Potential for subaqueous hot-spring (Eskay Creek) deposits in British Columbia; British Columbia Ministry of Energy and Mines, Open File Map 1999-14, scale 1:2,000,000

Massey, N.W.D. (1999b): Volcanogenic massive sulphide deposits in British Columbia; British Columbia Ministry of Energy and Mines, Open File Map 1999-2, scale 1:2,000,000

Operation Stikine (1957): Stikine River area, British Columbia (104A, B, G, H, I, J). Map 9-1957

Panteleyev, A. (1975): Mary; in Geology in British Columbia, British Columbia Ministry of Mines and Petroleum Resources, p.G81-G85

Read, P.B., Brown, R.L., Psutka, J.F., Moore, J.M., Journeay, M., Lane, L.S. and Orchard, M.J. (1989): Geology, More and Forest Kerr Creeks (parts of 104B/10,15,16 & 104G/1, 2), Northwestern British Columbia; Geological Survey of Canada, Open File 2094

Ricketts, B.D. and Evenchick, C.A. (1991): Analysis of the middle to upper Jurassic Bowser Basin, Northern British Columbia; in Current Research, Part A, Geological Survey of Canada, Paper 91-1A, p.65-73

Roth, T. (2002): Physical and chemical constraints on mineralization in the Eskay Creek deposit, northwestern British Columbia: evidence from petrography, mineral chemistry, and sulfur isotopes; University of British Columbia, Ph.D. Thesis, 401p

Schmitt, H.R. (1977): Triassic - Jurassic granodiorite monzodiorite pluton southeast of Telegraph Creek, B.C. University of British Columbia, B.Sc. thesis, 79p

Schroeter, T.G. and Pardy, J.W. (2004): Lode gold production and resources in British Columbia; British Columbia Ministry of Energy and Mines, Open File 2004-1

Simpson, K.A. and Nelson, J.L. (2004): Preliminary interpretations of mid-Jurassic volcanic and sedimentary facies in the East Telegraph Creek map area; Geological Survey of Canada, Current Research 2004-A1, 8p

Souther, J.G., 1972: Telegraph Creek map-area, British Columbia; Geological Survey of Canada, Paper 71-44

Heavy Mineral Sampling of Stream Sediments for Diamond and Other Indicator Minerals in the Atlin-Nakina Area (NTS 104N and 104K)

by D. Canil[1], M. Mihalynuk[2], J.M. MacKenzie[1], S.T. Johnston[1], L. Ferreira[1] and B. Grant[2]

KEYWORDS: Atlin, diamond, heavy mineral indicator, kimberlite, eclogite, placer, ophiolite, Cache Creek, subduction, mantle tectonite.

INTRODUCTION

Kimberlite and lamproite magmas sample diamonds deep in the mantle and depending on the rapidity of ascent and emplacement, bring them to the surface in various states of preservation. Economic diamond deposits are usually hosted in primary kimberlite and lamproite diatremes that intrude Archean crustal provinces. Placer deposits of diamonds that are sourced in kimberlite from Archean crustal provinces are also well known.

Diamond occurrences have also been documented in more non-traditional settings. For example, some placer diamonds appear to have a source in orogenic belts that border Precambrian crustal provinces (van Roermund et al, 2002; Griffin et al, 2000; Barrows et al, 1996; Walker 1994). Increasing recognition of diamonds in metapelitic metamorphic rocks in recent years has clearly demonstrated the burial of rocks to hundreds of kilometres depth during collisional orogenesis. Although reported decades earlier in ophiolite and 'Alpine" ultramafic rocks in orogenic settings, such occurrences of diamond have met with greater skepticism and controversy. This is due to the lack of evidence for the high pressures required to stabilize diamond in the mineral assemblages typical of ophiolites, for which far lower temperature (T) and pressure (P) conditions are commonly envisioned for origin, exhumation and emplacement.

There are several reports and rumours of 'anomalous' alluvial diamonds in streams and gravels from southeastern Alaska, southwestern Yukon and northwestern British Columbia (Black, 1951, 1953; Casselman & Harris 2002). The source of such diamonds is not obvious. There are no known Archean crustal provinces in these regions and no evidence of diamond-bearing alkaline igneous rocks, which could have been eroded to produce detrital diamond. Alluvial transport is unlikely because drainage patterns in the region are not obviously sourced in any Precambrian crustal province to the east. Glacial transport is unlikely because some regions in southwestern Yukon north of the Denali fault are reported to contain alluvial diamonds, yet they have not been glaciated.

The recognition of microdiamond in harzburgite tectonite from ophiolite elsewhere (van Roermund et al, 2002) begs the question whether diamond occurrences in southeastern Alaska, southwestern Yukon and northwestern British Columbia are sourced in ophiolites or in high pressure-low temperature metamorphic rocks (blueschists and eclogites) in accretionary margins associated with ophiolites. Large mantle tectonite sections of ophiolite have been recognized and documented in greater detail in these regions, and blueschist and eclogitè occur in several parts of Yukon, and in the Cache Creek Terrane of British Columbia. To address this question, and ultimately to explain the source of anomalous diamond occurrences in the northern Cordillera, we carried out a comprehensive study of heavy minerals in sediments sampled from streams, which drain ophiolite bedrock in the Atlin-Nakina area of northwestern British Columbia. The Atlin area is known historically for its placer gold mining operations, where one such anomalous diamond occurrence has been reported in Wilson Creek (Casselman and Harris, 2002). We wished to test if other diamonds could be found, by investigating stream sediments for diamonds or minerals, which may be indicative of bedrock that is associated with a high pressures origin and thus could be linked with the occurrence of diamond.

METHODS

Fifteen stream locations were sampled in map areas NTS 104N and 104K. Streams were chosen that drain bedrock of mantle tectonite in ophiolite. Two samples were also collected from commercial placer operations on Wilson and Feather creeks, from the tailings of clean-up sluices. Control samples were also collected from below the placer workings in these two creeks. A sample was collected from McKee Creek, off the sluice box end during active mining within a pay streak.

Stream sediment samples were taken in stream flow gradients that would efficiently concentrate heavy minerals in the bedload. Stream sediments were sieved on site to grain sizes less than 2 mm. The resultant sieved samples (4 to 8 kg) were processed for heavy minerals at Vancouver

---

[1] *School of Earth and Ocean Sciences, University of Victoria, Victoria, B.C., V8W 3P6*

[2] *Geoscience, Research and Development Branch, Ministry of Energy and Mines, Victoria, BC*

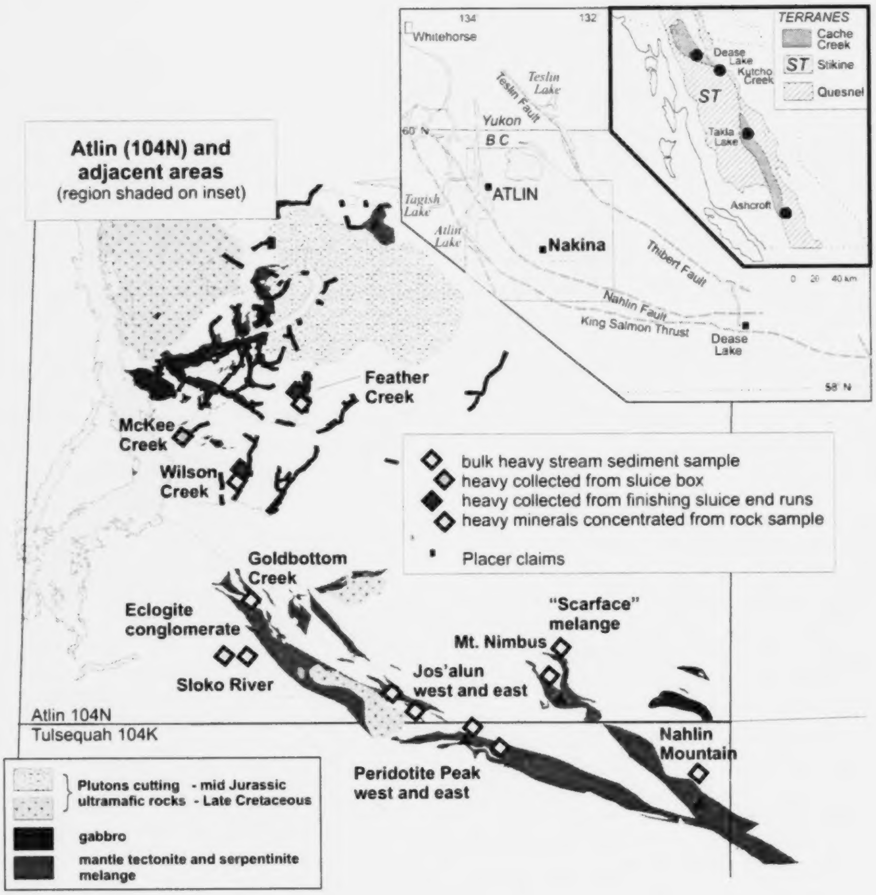
Atlin (104N) and adjacent areas
(region shaded on inset)
Whitehorse
134
132
Teslin Lake
Teslin Fault
Yukon
BC
60° N
Tagish Lake
Atlin Lake
ATLIN
Nakina
Thibert Fault
Nahlin Fault
King Salmon Thrust
Dease Lake
58° N
TERRANES
Cache Creek
ST Stikine
Quesnel
Dease Lake
Kutcho Creek
Takla Lake
Ashcroft
0 20 40 km
Feather Creek
McKee Creek
Wilson Creek
Goldbottom Creek
Eclogite conglomerate
Sloko River
"Scarface" melange
Mt. Nimbus
Jos'alun west and east
Peridotite Peak west and east
Nahlin Mountain
Atlin 104N
Tulsequah 104K
bulk heavy stream sediment sample
heavy collected from sluice box
heavy collected from finishing sluice end runs
heavy minerals concentrated from rock sample
Placer claims
Plutons cutting ultramafic rocks - mid Jurassic - Late Cretaceous
gabbro
mantle tectonite and serpentinite melange

Fig. 1 - Bedrock geology highlighting ultrmafic rocks of the Atlin-Nakina area (after Mihalynuk *et al* 2003) and showing location of heavy mineral samples used in this study.

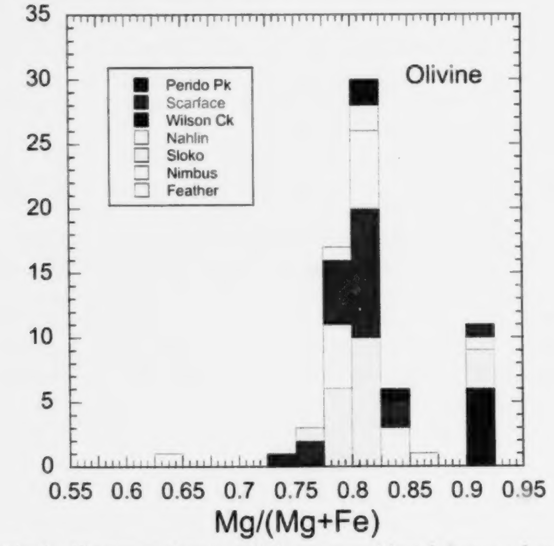

Fig. 2 – Histogram showing olivine compositions in heavy mineral samples at each locality.

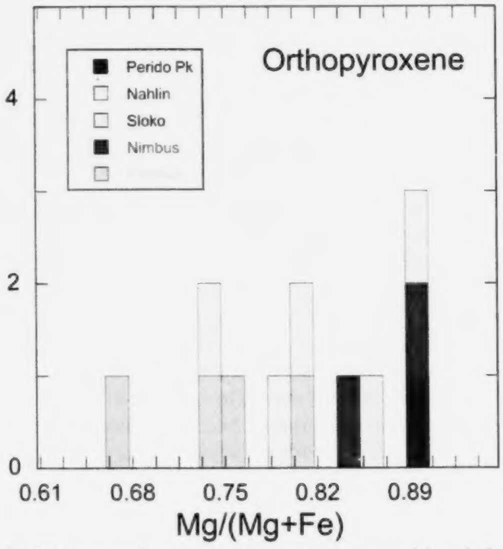

Fig. 3 - Histogram showing orthopyroxene compositions in heavy mineral samples at each locality.

Indicator Processors Inc. Samples were wet screened to less than 0.25 mm fraction, passed through a magnetic separator operating at 2.1 Tesla, and underwent two steps of heavy liquid separation to specific gravities greater than 3.33.

The non-magnetic heavy mineral fractions were picked for diamond and gold by I & M Morrison Geological Services. Magnetic heavy mineral fractions were hand-picked at the University of Victoria. In each sample, 20-30 grains of each mineral were picked, mounted in epoxy, and polished. Major element compositions of the grains in eight of the fifteen samples were determined by electron microprobe analysis at the University of British Columbia. Operating procedures and data reduction methods for this instrument are similar to those described in MacKenzie and Canil, 1999.

RESULTS

NON-MAGNETIC FRACTION

No diamonds were found in any of the non-magnetic heavy mineral fractions. Gold grains up to 1 mm in size were recognized in sediments from north of Hard Luck Peaks, Mt. Nimbus and in Feather Creek. Lack of gold in the McKee Creek sample may be an indication of an efficient placer operation.

MAGNETIC FRACTION

Table 1 lists the major minerals identified in the magnetic heavy mineral fraction from each sample studied. The subdivision into different groups of the same mineral was based in part on optical examination, but mainly on mineral chemical observations that are described in more detail below.

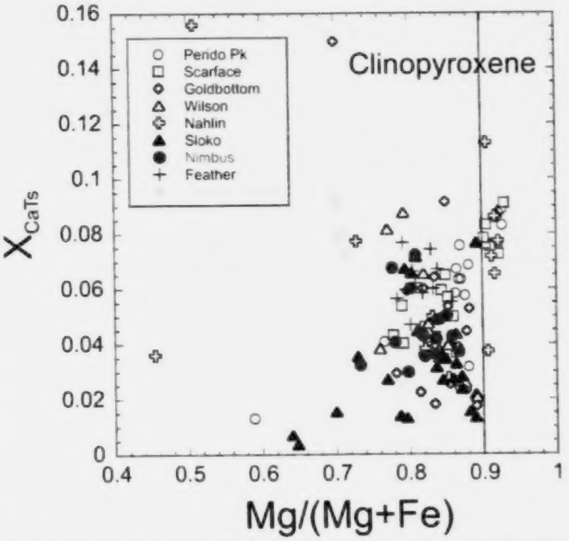

Fig. 4. Plot of Mg# in clinopyoxene in heavy mineral samples versus its Al-content expressed as the mole fraction of its CaTschermaks (CaTs) component ($CaAl_2SiO_6$). Clinopyroxenes from mantle tectonites plot right of the vertical line at Mg# = 0.9.

OLIVINE

Olivine was identified optically in heavy fractions by its light green colour and conchoidal fracture. In some cases, olivine preserved exceptionally well-defined crystal habit and faceted faces, indicative of an igneous origin, and little abrasion during transport from proximal source rock.

Olivine from mantle tectonite in ophiolite has a distinctly high Mg/(Mg+Fe) (Mg# > 0.89) and lower CaO content when compared to olivine from cumulate plutonic rocks, or from phenocrysts in volcanic rocks. This is due to the distinctly higher Mg# and lower Ca content of the bulk

TABLE 1. SUMMARY OF MINERALS IN THE ATLIN-NAKINA HEAVY MINERAL CONCENTRATE SAMPLES

		Gold	Olivine		Clinopyroxene			Garnet		Cr-Spinel	Spinel
Sample #	Location	Grains	Mantle	Cumulate	Mantle	Cumulate	Eclogitic	Eclogitic	Skarn	Mantle	Cumulate
15-4 BB	**Scarface**		*	*	*	*	*	*	*	*	*
24-4b*	Feather Ck. sluice end run	*									
24-1	Feather Ck.	*		*		*		*			*
16-4 BW	**Goldbottom Ck.**					*				*	*
16-3 BW	Hardluck Peaks North	*									
7-1 WB	Hard Luck Peaks East										
16-2*	Laberge Gp. coarse wacke						*	*			
18-1 WW	McKee Ck Sluice box run-off										
18-7 BW	**Mt. Nimbus North**	*		*		*				*	*
18-4 BW	**Nahlin Mtn. North**		*	*	*	*				*	*
11-14 BB	**Peridotite Peak North**		*		*	*		*		*	*
18-5 BW	Peridotite Peak East										
18-6 BW	**Sloko River**		*		*	*	*	*		*	*
18-3 WW	**Wilson Ck.**			*		*		*		*	*
18-2 WW	Wilson Ck. sluice end run										

samples in bold face analysed by EMP

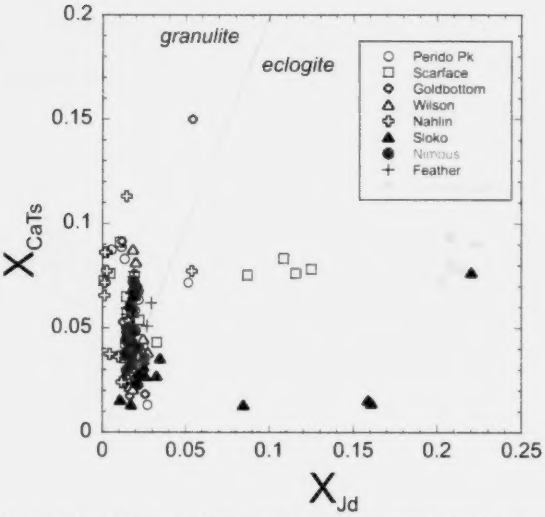

Fig. 5 – Plot of the mole fraction of CaTschermaks (CaTs) component (CaAl$_2$SiO$_6$) vs its jadeite (NaAlSi$_2$O$_6$) component in clinopyroxenes from heavy mineral samples and in eclogite clasts in coarse wacke from the Laberge Group. The line dividing the fields of eclogite and granulite pyroxenes is from White (1964).

compositions of mantle tectonites, which represent lithosphere formed as a residue of basalt extraction. Olivine with Mg# greater than 0.89 and low in CaO content (<0.1 wt%) typical of mantle tectonites was sampled at Sloko, Peridotite Peak, Scarface and Nahlin (Fig. 2). Most of the olivines sampled in this study were distinctly lower in Mg# than typical mantle olivine and were likely derived from cumulate rocks which form the basal lower crustal section above mantle tectonite in ophiolite.

ORTHOPYROXENE

Orthopyroxene was identified optically as light green or brown grains. In many cases, what was identified optically as orthopyroxene was later found to be clinopyroxene by electron microprobe analysis. Orthopyroxene was thus poorly represented in the heavy mineral fraction sampled. In what was sampled, orthopyroxene was present at five locations. The Kd$_{Fe\text{-}Mg}$ ol-opx is near unity so orthopyroxene has the same Mg# of olivine in which it is in equilibrium. Orthopyroxene with typical Mg# of mantle tectonites was found only at Peridotite Peak, Nimbus and Nahlin Mountain (Fig. 3). All other orthopyroxenes lower in Mg# appear to be derived from cumulate rocks.

CLINOPYROXENE

Clinopyroxene was identified as grains with either bright emerald green or dark green colour, usually showing well-developed cleavage and a prismatic grain shape. The emerald green colour in many clinopyroxenes is due to the presence of significant Cr^{3+}. Clinopyroxene forms in several igneous and metamorphic environments and its protolith can be difficult to distinguish for grains out of their coexisting mineral paragenesis. Clinopyroxene from mantle tectonite is rich in Cr and Al, and poor in Na, and has a high Mg#. It is often referred to as 'chrome diopside'. The Kd$_{Fe\text{-}Mg}$ ol-cpx is greater than one such that clinopyroxene from mantle tectonite should have an Mg# greater than 0.9. Clinopyroxenes from mantle residues of basalt extraction are also rich in Cr$_2$O$_3$ (> 0.5 wt%) and poor in Na, which is an incompatible element during melting.

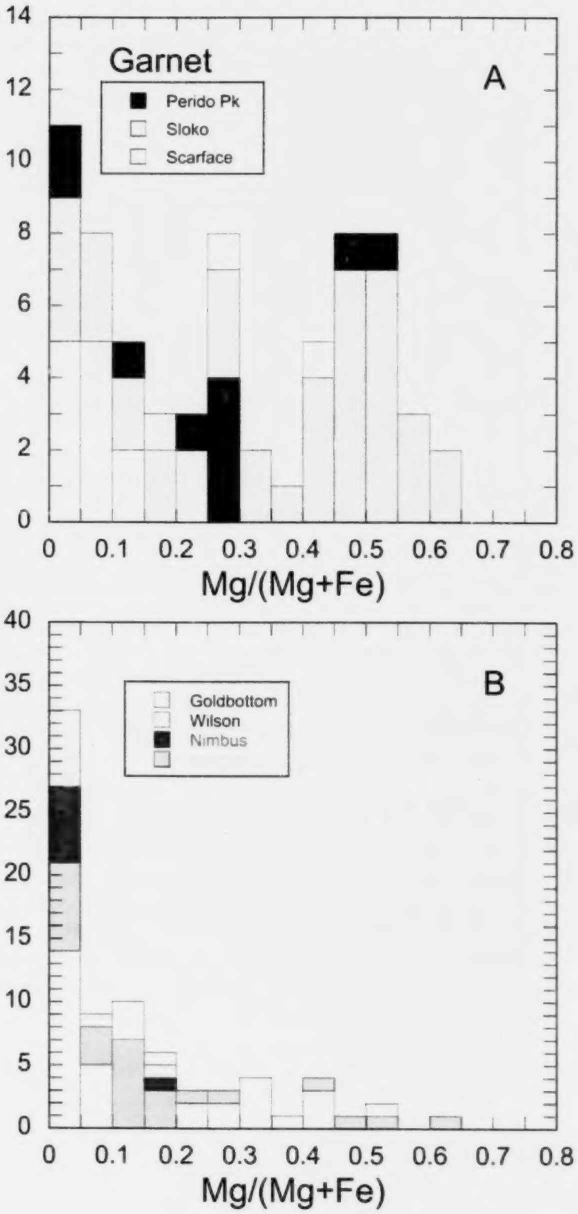

Fig. 6 - Histogram showing mole fraction of pyrope (XPyr) component (Mg$_3$Al2Si$_3$O$_{12}$) in garnets from heavy mineral samples at each locality. Arrow shows the compositions of garnet in eclogite clasts in coarse wacke from the Laberge Group. Note the abundance of more pyrope-rich eclogitic garnets in localities in (a) compared to those in (b).

Clinopyroxene with Mg# greater than 0.9, and rich in Al as a Ca-Tschermaks (CaTs - $CaAl_2SiO_6$) component is represented only at Nahlin, Scarface and Peridotite Peak (Fig. 4). Clinopyroxenes with lower Mg# and Cr contents at other sample locations must have been eroded from other sources. Many of these grains have high CaTs and so could be derived from cumulate rocks (Fig. 5) but a few of these clinopyroxenes in the Scarface and Sloko samples are distinctly rich in jadeite (Jd - $NaAlSi_2O_6$) component indicative of an eclogitic paragenesis. Clinopyroxenes from the latter locations are almost certainly derived from eclogite source rock, because clasts of this rock type with identical Jd-rich clinopyroxene compositions are recognized in a distinct ridge of garnetiferous wacke within the Laberge group to the west. This source rock is also supported in the chemistry of garnets described below.

GARNET

Garnets were recognized by their pink, purplish pink or orange colour, and in some cases well-developed dodecahedral crystal faces. The dominant garnet in all samples is a pink variety, poor in pyrope (X_{Pyr}<0.05) and rich in almandine component (Fig. 6a). These are likely crustal garnets derived from metapelitic protoliths. Thermal-metamorphic aureoles around Middle Jurassic and younger plutons in the Atlin area are known to contain garnet. Garnets preserved in Early Jurassic strata, however, are too old to be attributed to contact metamorphism around these plutons. A source of older garnets is not known within the study area.

A significant proportion of garnets rich in pyrope component (X_{Pyr} = 0.1 to 0.6) are recognized at Peridotite Peak, Black Caps and Sloko River (Fig. 6b). Many of these garnets are red-orange in color and are identical to the garnets in eclogite clasts from garnetiferous wacke within the Laberge group to the west. Their compositions would correspond to Group C and B (crustal) eclogites according to the classification scheme of Coleman *et al.* Red-orange eclogitic garnets are also found in smaller numbers at Feather and Wilson Creeks.

A notable population of light green garnets with nearly 100% andradite component is common at Scarface and also at Goldbottom and Nimbus. The andradite grains are likely sourced from skarns in areas where limestone units are in contact with felsic intrusive rocks or from meta-rhodingite blocks that are locally abundant within serpentinite melange.

SPINEL

Spinels occur as shiny black conchoidally fractured grains or as euhedral octahedrons and cubes. Most spinel is well–preserved but some grains are rounded with a frosted dull grey sheen. The majority of the spinels in the population are Cr-rich spinel, and at each location show a positive correlation between Cr/(Cr+Al) (Cr#) and Fe/(Fe+Mg) (Fe#) (Fig. 7). The trends for spinels on the latter diagram reflect the interplay of cation exchange equilibrium between spinel and olivine as a function of temperature. The Cr# vs Fe# diagram (Fig. 7) is also useful to distinguish magnetite and 'ferrit-chromit' (an alteration product of Cr-spinel) from Cr-spinels; the former plot along the right hand side of this diagram.

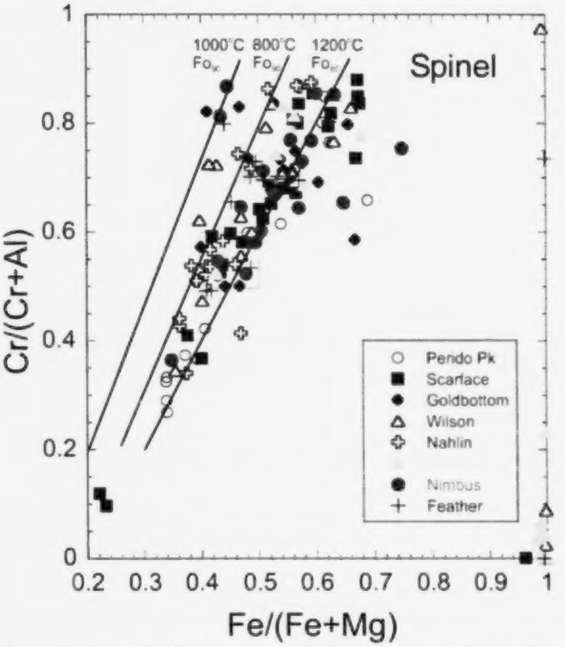

Fig. 7. Plot of Cr# (Cr/Cr+Al) versus Fe# (Fe/Fe+Mg) for spinel grains from heavy mineral concentrates. The lines show trends expected for spinel in equilibrium with various olivine compositions at different temperatures (after Roeder, 1994). Also shown is a field (box) that encompasses the compositions of 40 spinel grains from two harzburgite tectonite samples in outcrop north of Hard Luck Peaks, which equilibrated at 850 to 700°C as determined by olivine-spinel Fe-Mg exchange thermometry . Note the abundance of spinel compositions that could not be in equilibrium with mantle tectonite olivine (Fo_{90}) at those temperatures of equilibration.

The spectrum of spinel compositions in the heavy mineral samples is compared with trends for spinel in equilibrium at various temperatures with olivine having compositions that encompass the range expected in mantle tectonites (Mg# > 0.89) and that typical of cumulate rocks from ophiolites and layered intrusions (Mg# 0.80). Also shown for comparison is the range of spinel compositions in forty grains from two harzburgite samples from mantle tectonite in outcrop north of Hard Luck Peaks. Application of Fe-Mg exchange thermometry applied to coexisting olivine and spinel in these two samples show they last equilibrated between 700 and 850°C.

Almost all locations contain some proportion of Cr-spinel that could have been in equilibrium with mantle olivine (Mg# ~ 0.9) at temperatures measured using olivine-spinel geothermometry for the harzburgite samples (Fig. 7). The majority of the spinel grains at each location, however, occur along an array that is indicative of equilibrium with olivine that has a far lower Mg# than typical mantle olivine. The majority of these spinels are apparently derived from rocks in equilibrium with olivine having a Mg# between 0.9 and 0.8, likely in cumulate rocks. The latter interpretation is borne out by the abundance of olivine compositions having Mg# between 0.86 and 0.75 in most samples (Fig. 2), as well as the euhedral nature of many spinel grains, which is expected for magmatic spinel in plutonic ultramafic rocks, but not for spinel recrystallized at high temperature in mantle tectonites.

TITANITE

Titanites were recognized as equant red-brown grains. All of the titanites are low in Al_2O_3 (< 2 wt%) indicative of protoliths from low P environments likely as accessory phases in felsic plutonic rocks.

DISCUSSION AND CONCLUSIONS

The Mg-rich compositions of olivine, clinopyroxene and spinel in samples from Peridotite Peak, Scarface and Sloko suggest a mantle tectonite source for heavy minerals in the samples. Several large masses of mantle tectonite crop out throughout the study area, and sample sites were chosen in the drainages of these regions to examine them as potential sources for diamond (Fig. 1). Ironically, there are many sample sites containing large proportions of olivine and spinel that are not sourced in mantle tectonite. Indeed, somewhat perplexing is the preponderance of olivine, clinopyroxene, spinel and orthopyroxene having mineral compositions with lower Mg# more indicative of cumulate rocks from the crustal section of ophiolites. Although peridotite cumulates are known from the lower crustal section of some ophiolites, they are not as well represented proportionately in outcrops of the Atlin-Nakina area. Only a small section less than 100 m thick of peridotite cumulate is recognized just north of Hard Luck Peaks. Gabbro in the same lower crustal section is very poor in olivine (< 5%). Larger tracts of 104 N/1 are underlain by gabbro, but these are not obviously rich in olivine. Thus, the source for cumulate olivine, spinel and clinopyroxene in the heavy minerals from most of the samples remains puzzling. One possibility is that a large proportion of the serpentinite melange throughout the Atlin-Nakina is an alteration product of cumulate peridotite, rather than mantle tectonite. The melange units, being less competent and easily eroded, could contribute more to stream sediments. If so, it remains unclear how fresh igneous olivine and spinel grains would have been preserved in melange that is heavily altered to serpentine and magnetite.

The presence of eclogitic garnet and clinopyroxene in several heavy mineral samples is also significant. Exposures of this rock type are sporadic in the Cordillera, but known at one locality on the eastern margin of Cache Creek Terrane in British Columbia and further north in Yukon Tanana Terrane of Yukon. The results of this study are intriguing in that they show widespread occurrence of this rock as a source for the heavy minerals from at least five locations, some as far east as Peridotite Peak, yet no eclogite has been recognized in outcrop in the Atlin-Nakina area. Clasts of eclogite have only been recently documented (in the past field season) in a coarse garnetiferous wacke of the Laberge Group to the west. These rare clasts are less than 1 cm, but are likely the source of much of the garnet within this particular unit of the Laberge Group, as evidenced by the great abundance of eclogitic minerals in heavy mineral concentrate from a stream draining this region.

The Laberge Group coarse wacke is the only known bedrock containing eclogitic garnets and pyroxenes in the Atlin region, but is an unlikely source for these heavy minerals throughout the entire study area. The Laberge wacke crops out only in the western portion of the study area west of the Nahlin fault. Ice flow during the last glaciation in the Atlin area was west to east. Glacial transport could explain the presence of eclogitic grains in stream sediments proximal to the Sloko site, such as at Wilson and Feather Creeks. Outside and further south of the Atlin area, however, the orientation of mega-rat-tail features on air photos suggests ice directions were southward, and yet eclogitic garnets are recognized over 100 km to the east near Black Caps Mountain, and Peridotite Peak. These occurrences require a more proximal source for eclogite in outcrop than units of the Laberge Group. Such a source is not obvious, but may lie within the melange units that are widespread in the Atlin-Nakina area. Eclogite blocks are common in the classic Franciscan mélange , and may also be present yet unrecognized in large areas of mélange throughout the Nakina area. As is the case with the source rock for cumulate olivine and spinels, the melange units are easily eroded, and could contribute their eclogitic material to stream sediments.

The source of eclogite clasts, Mg-rich mantle olivine and Cr-spinel in the garnetiferous wacke unit in the Laberge Group is likely to be ophiolite and associated melange that was part of Cache Creek Terrane to the east. Erosion of uplifted ophiolite and eclogite in mélange from the Cache Creek Terrane would have shed detritus into the basin accumulating proximal to the structures along which the ophiolite and melange were exhumed. Similar detritus is present in flysch deposits proximal to many ophiolites, such as the Bay of Islands, Newfoundland and Labrador, and is interpreted to have accumulated after convergence, uplift and collapse. An outstanding problem is that no eclogite units have been found in outcrop in the mélange. Further stream sediment sampling and processing of the remaining seven samples of this study may aid in identifying its location. Future study of the eclogite-bearing conglomerate should include careful paleocurrent study to test whether or not simple turbidity currents could have carried the clasts from the adjacent Cache Creek rocks.

A diamond in the Atlin area was originally reported over 10 years ago by Marvin Sherman in a placer operation on Wilson Creek. The yellowish white diamond was ~6 mm in diameter with a rough rounded shape. None of the heavy mineral samples from this study, including one on Wilson Creek, produced any diamonds. This study shows that the Wilson Creek diamond, if real, was not obviously sourced in mantle tectonite from ophiolite. The Wilson Creek occurrence, as well as those to the north in Yukon, remains enigmatic.

ACKNOWLEDGMENTS

We sincerely thank Norm Graham of Discovery Helicopters in Atlin for getting us to where we wished to go, and Ryan Rhodes for mineral picking. This study was carried out under the Atlin Targeted Geoscience Initiative. Olmer Brown and John Harvey provided access to placer workings at McKee Creek. Dale Halstead provided access to the Feather Creek placer workings and clean-up heavy minerals. Peter Burjowski provided access to placer workings on Wilson Creek and clean-up heavy minerals, and shared local diamond lore.

REFERENCES

Ash, C. (1994): Origin and tectonic setting of the ophiolitic ultramafic and related rocks in the Atlin area, British Columbia (NTS 104N). *B.C. Ministry of Energy, and Mines,*. Bulletin 94, 48 p.

Bai, W.-J., Zhou, M.-F. and Robinson, P.T. (1993): Possibly diamond-bearing mantle peridotites and podiform chromitites in the Luobusa and Donqiao ophiolites, Tibet. *Canadian Journal of Earth Sciences*., 30: 1650-1659.

Ballhaus, C., Berry, R.F. and Green, D.H. (1991): High pressure experimental calibration of the olivine-orthopyroxene-spinel oxygen barometer: implications for the oxidation state of the upper mantle. *Contrib. Mineral. Petrol.*, 107: 27-40.

Barrows, L.M., Lishmunwg, R., Oakes, M, Barron, B.J. and Sutherland, F.L. (1996): Subduction model for the origin of some diamons i the Phanerozoic of eastern New South Wales; Australian Journal of Earth Sciences, vol 43, pp 257-267.

Black, J.M. (1951): Atlin placer camp; *BC Ministry of Energy and Mines,* Vertical File 2470 C1, page gl 2 and page bl 14.

Black, J.M. (1953): Report on the Atlin placer camp; *BC Ministry of Energy and Mines,* Miscellaneous report, 70 pages.

Brey, G., Köhler, T. and Nickel, K.G. (1990): Geothermobarometry in four-phase lherzolites I. Experimental results from 10 to 60 kb. J Petrol, 31: 1313-1352.

Canil, D. and Johnston, S.T. (2002): Harzburgite Peak: A large mantle tectonite in ophiolite from southwestern Yukon. *Yukon Geology and Exploration*, 2002-1: 1-10.

Casselman, S. and Harris, W. (2002): Yukon diamond rumour map and notes; *Yukon Geology*.

Cawood, P.A. and Suhr, G. (1992): Generation and obduction of ophiolites: Constraints from the Bay of Islands complex, western Newfoundland. *Tectonics*, 11: 884-897.

Coleman, R.G., Lee, D.E., Beatty, L.B. and Brannock, W.W. (1965): Eclogites and eclogites: Their simularities and differences. *Geological Society of America* Bulletin 76: 483-508.

Erdmer, P., Ghent, E.D., Archibald, D.A. and Stout, M.Z., (1998): Paleozoic and Mesozoic high-pressure metamorphism at the margin of ancestral North America in central Yukon. *Geological Society of America* Bulletin 110: 615-629.

Foster, H.L., Keith, T.E.C. and Menzie, W.D. (1994): Geology of the Yukon-Tanana area of east-central Alaska. In: G. Pflacker and H.C. Berg (Editors), The Geology of North America. *Geological Society of America*, Boulder, pp. 205-240.

Franz, G. and Spear, F.S. (1985): Aluminous titanite (sphene) from the eclogite zone, south-central Tauern window, Austria. *Chem. Geol.*, 50: 33-46.

Griffin, W.L., O'Reilly, S.Y and Davies, R.M. (2000): Subduction-related diamond deposits?: Constraints, Possibilities and new data from Eastern Australia. Reviews in Economic Geology. Chap 11, pp291-310.

Helmstaedt, H.H. and Gurney, J.J. (1994): Geotectonic controls on the formation of diamonds and their kimberlitic and lamproitic host rocks: Applications to diamond exploration. *Proc. 5th Int. Kimb. Conf.*, 2: 236-250.

Irvine, T.N. (1965): Chromian spinel as a petrogenetic indicator. I. Theory. *Can. J. Earth Sci.*, 2: 648-672.

Kaminsky, F.V. and Vaganov, V.I. (1977): Petrological conditions for diamond occurrences in Alpine-type ultrabasic rocks. *Inter. Geol. Rev.*, 19: 1151-1162.

LeCheminant, A.N. and Bedard, J.H. (1995): Diamonds associated with ultramafic complexes and derived placers. In: A.N. LeCheminant, D.G. Richardson, R.N.W. DiLabio and K.A. Richardson (Editors), Searching for Diamonds In Canada. *Geol. Surv. Can.*, Ottawa, pp. 171-177.

LeCheminant, A.N. and Kjarsgaard, B.A. (1995) Introduction. In: A.N. LeCheminant, D.G. Richardson, R.N.W. DiLabio and K.A. Richardson (Editors), Searching for Diamonds In Canada. *Geol. Surv. Can.*, Ottawa, pp. 5-11.

Levson, V.M. (1992): Quaternary geology o fthe Atlin area (104N/11W, 12E). *in* Geological Fieldwork 1991: *B.C. Ministry of Energy and Mines,* p375-385.

Lowe, C. et al. (2003): Overview of the Atlin Integrated Geosceicen Project, northwestern British Columbia, year three. *Geol. Surv. Can.* Current Research., 2003-A11: 1-10.

MacKenzie, J.M. and Canil, D. (1999): Composition and thermal evolution of cratonic mantle beneath the central Archean Slave Province, NWT, Canada. *Contributions to Mineralogy and Petrology*, 134: 313-324.

Mercier, J.C. and Nicolas, A. (1975): Textures and fabrics of upper mantle peridotites as illustrated by xenoliths from basalts. *J. Petrol.*, 20: 727-741.

Mihalynuk, M.G. et al. (2003): Atlin TGI, Part III: Regional geology and mineralization of the Nakina area (NTS 104N/2W and 3). *in* Geological Fieldwork 2002: *B.C. Ministry of Energy and Mines,* pp 9-15.

Moores, E.M. (1982): Origin and emplacement of ophiolites. *Rev. Geophys.*, 20: 735-760.

Moores, E.M. and Jackson, E.D. (1974): Ophiolites and oceanic crust. *Nature*, 228: 837-842.

Proudlock, P.J. and Proudlock W.M. (1976): Stratigraphy of the placers in the Atlin placer mining camp, British Columbia; *BC Ministry of Energy and Mines*, Miscellaneous Report, 71 pages.

Roeder, P.L. (1994): Chromite: from the fiery rain of chondrules to the Kilauea Iki lava lake. *Can. Mineral.*, 32: 729-746.

Roeder, P.L. and Campbell, I.H. (1985): The effect of post-cumulus reactions on composition of chrome spinels from the Jimberlana intrusion. *J. Petrol.*, 26: 763-786.

Shellnutt, J.G., Canil, D. and Johnston, S.T. (2001): Preliminary results of a petrological study of ultramafic rocks of the northern Cordillera. *Yukon Geology and Exploration*, 2001: 229-237.

Stevens, R.K., (1970): Cambro-Ordovician flysch sedimentation and tectonics in west Newfoundland and their possible bearing on a proto-Atlantic ocean. *Geol. Soc. Can. Spec. Pap.*, 7: 165-177.

van-Roermund, H.L.M, Carswell, D.A., Drury, M.R. and Heijboer, T.C. (2002): Microdiamonds in a megacrystic garnet websterite pod from Bardane on the island of Fjortoft, western Norway; evidence for diamond formation in mantle rocks during deep continental subduction; Geological Society of America,

van Roermund, H.L.M., Carswell, D.A., Drury, M.R. and Heijboer, T.C. (2002): Micro-diamonds in a megacrystic garnet websterite pod from Bardane on the island of Fjortoft, western Norway: evidence for diamond formation in mantle rocks during deep continental subduction. *Geology*, 30(11), 959-962.

von Seckendorff, V. and O'Neill, H.S. (1993): An experimental study of Fe-Mg partitioning between olivine and orthopyroxene at 1173, 1273 and 1423 K and 1.6 GPa. *Contrib Mineral Petrol.*, 113: 196-207.

Walker, R.T. (1994): Diamond potential in southeast British Columbia; *Northwest Geology*, Proceedings Volume, from joint meeting of British Columbia Geological Survey Branch, Geological Survey of Canada, East Kootenay Chamber of Mines, Consolidated Ramrod and Tobacco Root Geological Society, vol 23, pp 77-79.

White, A.J. (1964): Clinopyroxenes from eclogites and basic granulites. *Am. Mineral.*, 49: 883-888.

GEOSCIENCE PARTNERSHIPS IN THE TOODOGGONE RIVER AND MCCONNELL CREEK MAP AREAS, NORTH-CENTRAL BRITISH COLUMBIA[1]

(PARTS OF TOODOGGONE RIVER NTS 094E/2, 3, 6, 7, 10, 11 AND MCCONNELL CREEK NTS 94D/8,9,15)

By L.J. Diakow[2] and R.B.K Shives[3]

KEYWORDS: : P3, Public Private Partnership, Targeted Geoscience Initiative-II (TGI-II), Bedrock Mapping, Airborne Magnetic Survey, Gamma-Ray Spectrometric Survey, Toodoggone River, Finlay River.

INTRODUCTION

The Toodoggone geoscience partners are investigating the magmatic and structural evolution [of the Toodoggone mining camp] and the intertwined development of hydrothermal systems associated with epithermal, porphyry and skarn mineralization. This partnership involves a consortium of five mining exploration companies - Stealth Minerals Ltd., Northgate Exploration Ltd., Finlay Minerals Ltd., Bishop Resources Inc. and Sable Resources Ltd., in addition to the B.C. Geological Survey (BCGS), the Geological Survey of Canada (GSC), and The University of British Columbia.

In 2003, government programs comprised 1:20 000 bedrock mapping and an airborne multiparameter geophysics survey, both using operating funding derived from the Federal-Provincial Targeted Geoscience Initiative-II (2003-2005) and mining company participants. Regional mapping conducted by the B.C. Geological Survey focussed on two regions, the northerly of these surveys located between the Finlay and Toodoggone rivers in the central Toodoggone River map area **(Figure 1).** The southern survey area, near Johanson Lake in the McConnell Creek map area, was mapped by Schiarizza and is reported upon separately (2004, this volume). This brief report introduces the components of field programs conducted in the Toodoggone River area.

The Toodoggone River area is currently the focus of some of the most active mineral exploration in British Columbia. The region hosts several gold-enriched porphyry copper deposits (including Kemess North and Kemess South) and past-producing, low sulphidation epithermal gold mines (Chappelle-Baker, Lawyers, Shasta and Al). The premier deposit in the Toodoggone area is Kemess South, an open-pit mine with proven reserves of 109.4 million tonnes (Mt) of ore grading 0.71 grams gold and 0.23% copper, or 2.5 million contained ounces (oz) of gold. Approximately 6 km to the north is the Kemess North porphyry deposit, which has an estimated 4 million oz gold resource contained in 369 Mt of material grading 0.34 grams per tonne gold and 0.18% copper.

BEDROCK MAPPING

The emphasis of bedrock mapping in the Toodoggone region is on Early Jurassic volcanic and plutonic rocks, since they are the predominant host rocks for past gold production from high-level epithermal systems (Lawyers, Shasta, and Bonanza-Al), and current production from deeper porphyry deposits, as at Kemess South. Over the past several years mining exploration has shifted east and north beyond areas where the BCGS established a geological framework for gold-enriched porphyry and epithermal prospects (Diakow *et. al.*, 1993 and 2001). This adjacent, poorly understood area has large gossans and a number of potential exploration targets highlighted by a B.C. Regional Geochemical Survey (Jackaman, 1997). Grassroots prospecting has been an important component of recent exploration programs, leading to new epithermal and porphyry discoveries in this frontier area by Stealth Minerals Limited and other companies.

The enhanced exploration activity has provided added impetus for additional regional mapping. During the past summer, the BCGS embarked on a two-year initiative to complete detailed mapping within a region covering roughly 1000 km^2 (Figure 1). This region is considered to be highly prospective in terms of mineral potential, but lacks the geologic context and timing constraints established through detailed mapping and geochronometry elsewhere in the Toodoggone region.

Fieldwork in 2003 resulted in 1:20 000 map coverage of approximately 215 km^2 in the Swannell Mountains between the Finlay and Toodoggone Rivers. The Shasta

---

[1] *Contribution of the Federal-Provincial Targeted Geoscience Initiative-II (TGI-II)*

[2] *B.C. Geoscience Research and Development Branch, Victoria*

[3] *Geological Survey of Canada, Ottawa*

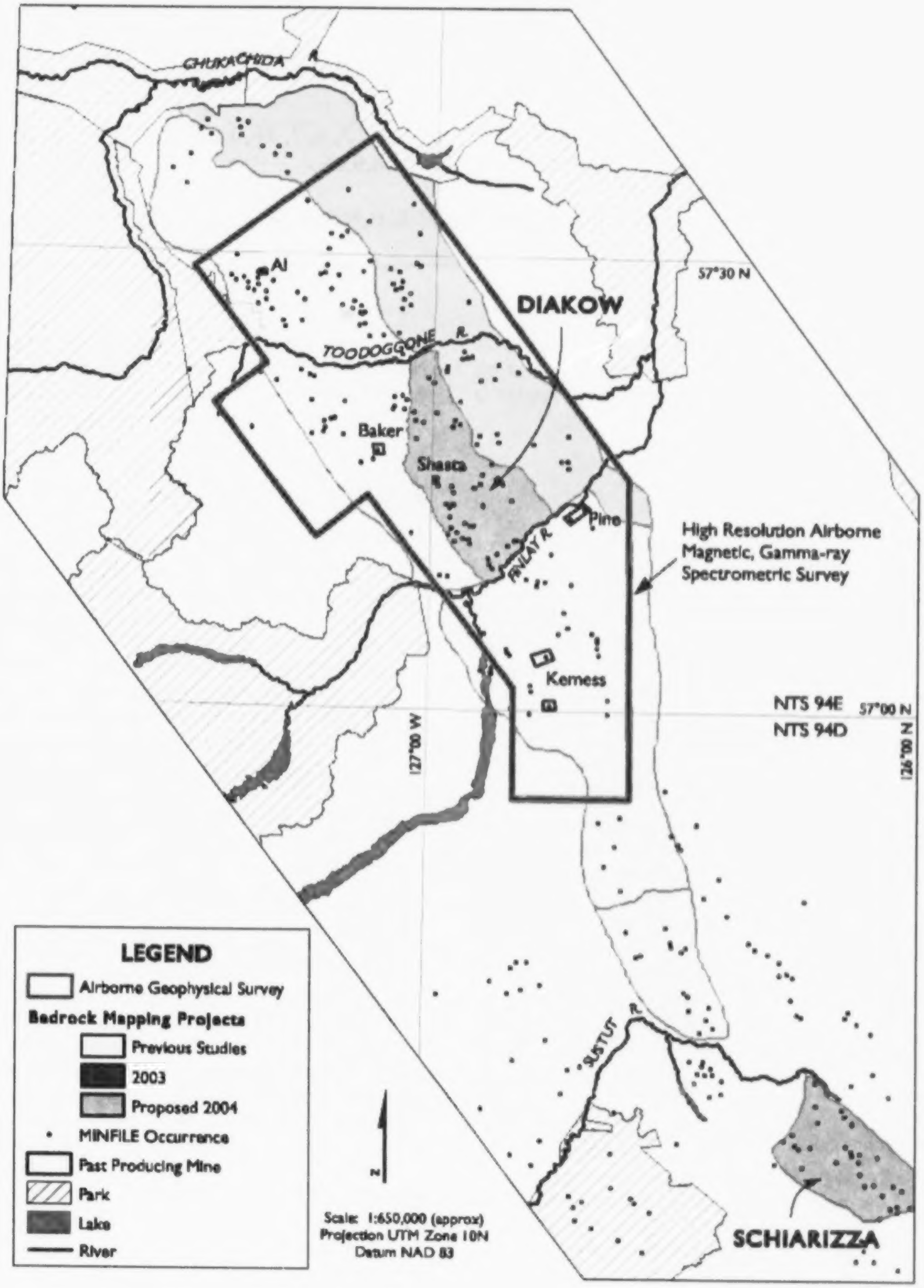
CHUKACHIDA R.
Al
DIAKOW
TOODOGGONE R.
57°30 N
Baker
Shasta
Pine
FINLAY R.
High Resolution Airborne Magnetic, Gamma-ray Spectrometric Survey
Kemess
NTS 94E
57°00 N
NTS 94D
127°00 W
126°00 W
LEGEND
Airborne Geophysical Survey
Bedrock Mapping Projects
Previous Studies
2003
Proposed 2004
MINFILE Occurrence
Past Producing Mine
Park
Lake
River
SUSTUT R.
N
Scale: 1:650,000 (approx)
Projection UTM Zone 10N
Datum NAD 83
SCHIARIZZA

Figure 1. Location of government-mining company funded bedrock mapping and airborne gamma-ray spectrometric and magnetic total field surveys in the Toodoggone River (parts of NTS 094E/2,6,7) and McConnell Creek (parts of NTS 094D/8,9) map areas. The airborne survey covers over 2200 km^2 of Early Jurassic rocks that contain the majority of mineral prospects (shown as dots) and mines in the Toodoggone mining camp. Northgate Exploration Ltd funded an extension to the original survey, south of the Kemess South mine.

and Baker gold vein deposits are situated near the western boundary of the project area, and the porphyry prospects Brenda and Pil North, situated along the eastern boundary. Part of this region has been previously mapped at reconnaissance scale (Diakow *et. al*, 1985). The current study will produce a map, and upgrade the regional stratigraphy and structural interpretation, and provide additional timing constraints for magmatic and mineralizing events.

GEOLOGICAL HIGHLIGHTS

- Three major stratigraphic units exposed between the Finlay and Toodoggone rivers are consistent with those mapped in adjacent areas of the Toodoggone magmatic [illegible]. Listed from oldest to youngest, they consist of: the Asitka Group, the Takla Group and the Toodoggone Formation of the Hazelton Group. In the study area, distribution of the oldest rocks, assigned to the Late Carboniferous to Early Permian Asitka Group, and the overlying Late Triassic Takla Group, reflect uplift associated with high-level emplacement of the Early Jurassic Duncan pluton. In general these rocks occupy differentially uplifted blocks, presently dislocated by faults oriented subparallel to the northwest-trending margin of the Duncan pluton, and they crop out as relatively thin pendants resting directly on the pluton. The Asitka Group is subdivided into a lower unit composed of subaerial pyroclastic rocks of andesite to dacite composition, and an upper unit composed of recrystallized limestone, with or without relatively thin mudstone, siltstone and sandstone sections. Skarns carrying primarily chalcopyrite and magnetite, and occasionally anomalous gold concentrations, are common in the vicinity of Drybrough Peak within contact metamorphosed pendants in calcareous rocks of the Asitka Group. Notable examples are those being explored at the VIP and Dry Pond prospects. The Late Triassic Takla Group overlies the Asitka Group above a non-erosive contact. The Takla Group is generally composed of thick, monotonous augite-phyric and comparatively rare, bladed plagioclase porphyritic basalts and basaltic andesites. Pyroxene-rich sandstones and siltstone, evidently derived from the mafic flows are scattered in the low-lying terrain adjacent to the Finlay River. In the Toodoggone region, limestone is rarely observed within the Takla Group, however, several kilometres southeast of Black Lake, it occurs as discrete lenses, between 0.5 and 5 metres thick, enclosed by volcanic rocks. These limestones provide evidence for restricted basins within the predominately subaerial volcanic pile, which comprises most of the Takla Group.

  The Early Jurassic Toodoggone Formation is the sole stratigraphic subdivision of the Hazelton Group in the Toodoggone River map area. It depositionally overlies Triassic volcanic rocks above an erosional unconformity, which in the 2003 study area is marked by deposits of conglomerate. This conglomerate is exposed at four main localities with the unconformable contact traceable intermittently over a distance of 7 kilometres. Without exception, all localities are characterized by crudely bedded cobble conglomerate dominated by rounded clasts of fine-grained "crowded" hornblende-plagioclase porphyritic andesite and interlayered locally with lesser sandstone. The clast lithology is unlike any observed rocks found locally in the underlying Takla Group. The conglomerate is therefore interpreted to represent some of the earliest extrusive products of the Toodoggone Formation eroded a short time after eruption.

  The Toodoggone Formation is a compositionally uniform, subaerial volcanic succession composed of quartz, biotite, hornblende and titanite-bearing high-silica andesite to dacite pyroclastic rocks and lesser trachyandesite lava flows (Diakow *et. al.*, 1993). Map units, composed predominantly of pyroclastic rocks exposed throughout much of the 2003 study area, are believed to be representative of those mapped near the bottom and top of the formation in adjacent areas. Trachyandesite lava flows predominate in the southeast part of the area. They correlate with rocks stratigraphically lower in the Toodoggone succession.

- Stocks and smaller plutons of the Early Jurassic Black Lake suite are temporally and probably genetically related to extrusive rocks of the Toodoggone Formation. Typical Black Lake intrusions consist mainly of biotite, hornblende and titanite-bearing granodiorite with a medium to coarse-grained equigranular texture. These plutons differ compositionally from those associated with gold-copper porphyry mineralization at the Kemess deposits, where they are more mafic and consist of monzodiorites and medium to coarse grained monzonite porphyries. These "mafic" plutons also have a distinctly tabular geometry, and in the case of the Maple Leaf pluton at Kemess South, emplacement appears to be at a sub-volcanic crustal level. A new finding this summer is that the Black Lake monzonite intrusions also are related to mineralization in the present study area. For example, at the "Pil North" porphyry prospect, widespread propylitic and argillic alteration zones are centred over monzonite porphyry that is flanked by an older biotite-hornblende granodiorite. Nearby at the "Brenda" porphyry target, a swarm of monzonite dikes are interpreted to be the near surface expression of a deeply seated pluton. Additionally, recently discovered vein mineralization at the "10 K" prospect adjacent to the Finlay River, and gold-bearing copper-magnetite skarn at "Dry Pond" near Drybrough Peak are both related to monzonitic dike emplacement. The association of copper-gold mineralization with hypabyssal monzonitic bodies is observed at multiple localities in the Toodoggone region, and the distinctiveness of these plutons and their field relationships suggest they represent a distinct magmatic pulse(s) in the Black Lake suite.

- Regional geological and metallogenic studies of the Toodoggone River map area conducted over the past 20 years, mainly by the BCGS, demonstrate that the porphyry and epithermal styles of mineralization formed 200 to 190 million years ago. This mineralizing epoch coincides in space and time with a suite of earliest Jurassic granitoids shallowly emplaced within a contemporaneous subaerial volcanic succession. Their distribution is confined to an elongate syn-volcanic extensional trough.
- Unravelling the history of magmatic and mineralizing events is a key objective of the Toodoggone program. Presently, age dating of 20 samples is in progress to determine ages for various mineralized monzonites, and to directly date alteration associated with epithermal and porphyry mineralization.

HELICOPTER-BORNE NATGAM SURVEY (GAMMA-RAY SPECTROMETRIC AND MAGNETIC TOTAL FIELD)

In late summer, a combined, high-resolution airborne gamma-ray spectrometric and magnetic survey was completed in the Toodoggone region (Figure 1). This survey provides new public domain gamma ray data and higher resolution aeromagnetic data for the entire Toodoggone mining camp, within a broader GSC-industry funded aeromagnetic survey published in 1999. The principal objective of the new survey is to provide a consistent geophysical and geochemical (via radioactive elements: K, U,Th) framework to supplement regional bedrock mapping by the B.C. Geological Survey and ongoing property-scale exploration. The surveyed region has clear economic potential, demonstrated by the Kemess South Mine, the gold-copper porphyry deposit at Kemess North, several past-producing mines and numerous gold epithermal prospects. Hydrothermal alteration minerals associated with porphyry and epithermal mineralization in the Toodoggone are known to respond well to these airborne techniques, and have been shown to respond to ground gamma ray surveys in the Shasta deposit area (Shives, unpublished data).

Gamma ray spectrometry (surface geochemical information) and magnetic total field measurements (deeper-looking geophysical information) are complementary, as features with low magnetic response are commonly enriched in radioactive elements, and vice versa. Excellent bedrock exposure throughout most of the survey area will optimize detection of known and new mineral prospects, broad zones of hydrothermally altered rocks, bedrock lithologic contrasts and structures.

AIRBORNE SURVEY

The survey boundaries were designed by theBCGS in consultation with industry partners and the GSC. Funding was provided, in part, by Stealth Minerals Ltd., Northgate Explorations Ltd., Finlay Minerals Ltd., Bishop Resources Inc. and Sable Resources Ltd. The GSC provided contract preparation, tendering, evaluation and, on July 24th, awarded the contract through Public Works and Government Services Canada to Fugro Airborne Surveys of Mississauga, Ontario.

The GSC (Radiation Geophysics Section and Regional Geophysics Section) is responsible for overall quality control, including system calibrations, conducted in Ottawa prior to mobilization, and field checks to ensure specifications and procedures adhere to well-established NATGAM national standards.

The survey overlies a topographic transition from eastern Spatsizi Plateau into relatively subdued mountains of the Swannell Ranges. The mountainous terrain required a helicopter survey to maintain a nominal terrain clearance of 135 m, with no more than 30 m difference between traverse line and magnetic control line elevations. The helicopter used was a Eurocopter AS350B2. Flight speed averaged 120 kph. A total of 6214 line kilometres were flown, covering 2214 km^2, with flight lines oriented 055°, spaced at 400 m intervals and magnetic control lines oriented at 321°, spaced at 4000m intervals.

Gamma ray spectrometric measurements were made using an Exploranium GR820 spectrometer to record 256 channel spectra every second, from 33.6 liters of downward-looking and 4.2 liters of upward-looking sodium iodide detectors. The detector boxes were carried inside the helicopter and in a cage mounted outside **(Figure 2)**. Prior to mobilization, system-specific correction factors were determined using GSC portable

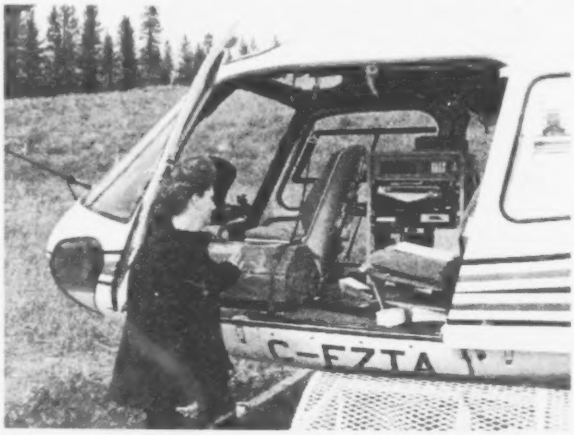

Figure 2. Gamma-ray spectrometric system includes two sodium iodide detector boxes mounted inside (orange box) and outside (in white cage, lower right) the helicopter, linked to spectrometer console in the system rack, behind pilot.

calibration pads at Ottawa airport and the GSC calibration test strip in Breckenridge, Quebec. In the field, daily calibration checks were completed using Cs^{137} and Tl^{208} sources and a test line was established and flown daily to monitor reproducibility of all measured variables.

Standard energy windows were used to record the gamma ray counts. These are 1370-1570 keV for potassium, 1660-1860 keV for uranium, 2410-2810 keV for thorium and 400-2810 keV for total radioactivity. Several corrections are applied to the raw window counts prior to conversion to standard concentration units, including: system dead time; background activity from cosmic radiation, the aircraft and atmospheric radon decay products; spectral scattering in the ground, air and detectors; deviations of altitude from the planned terrain clearance; temperature and pressure variations.

Magnetic total field measurements were made using a cesium split-beam sensor sampling at 10Hz, with an in-flight sensitivity of 0.01 nT, housed in a bird towed 30 m below the helicopter (**Figure 3**).

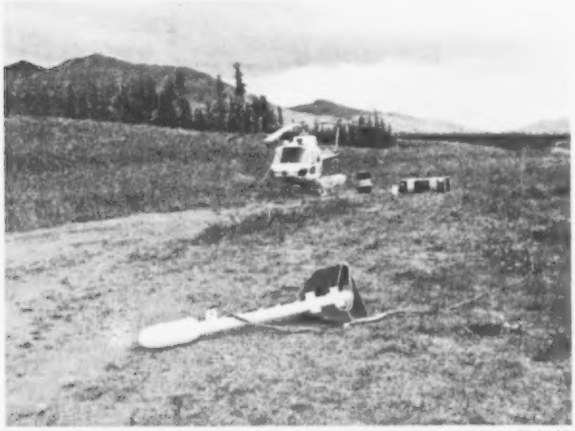

Figure 3. Cesium split-beam magnetometer is housed in a "bird" (foreground), towed 30 m below the helicopter.

The system was calibrated using the Bourget, Ontario magnetic test range prior to mobilization, to determine heading effects and lag on the magnetic measurements. In the survey area, ground magnetometer stations continuously recorded diurnal magnetic variations to monitor variation in the earth's magnetic field.

Positional information was provided by a dual frequency Ashtech differential GPS system, monitoring up to twelve satellites, and yielding a positional accuracy of approximately 2-3 m after post-flight differential correction.

AIRBORNE SURVEY STATUS

The Toodoggone survey commenced August 19, 2003 and was completed on September 17. The preliminary data covering mineral claims owned by the respective industry partners was distributed on December 1, 2003, after Fugro had completed preliminary corrections to the raw magnetic and radiometric data, and subdivided the data into property blocks. Additional corrections will be applied and final digital data and colour maps for the entire survey will be delivered to the GSC by mid-February. The geophysical data for all areas covered by claims held by other companies or individuals or available for staking will be realeased to the public along with the company partner information in late March 2004.

2004 TOODOGGONE TGI PROGRAM

Next year is anticipated to be an active one for mineral exploration in the Toodoggone region, and the GSB will continue to aid this work by providing a geological framework at a scale of 1:20 000. Mapping completed this season in the Swannell Mountains will be expanded to the east, thereby completing geologic coverage between the Finlay and Toodoggone rivers and the mapping in the Johannsen Lake area expanded (see 2004 mapping in Figure 1). The new Griz-Sickle epithermal vein system, discovered by Stealth Minerals Ltd. in 2003, is near the centre of the northern mapping area for 2004. This program will then shift north westward into remote terrain bridging the Toodoggone and Chukachida rivers, a region containing the north easternmost extent of prospective Early Jurassic rocks in the Stikine Terrane.

Initiation of several detailed mineral deposit studies involving graduate students from the Department of Earth and Ocean Sciences at The University of British Columbia, under the guidance of Dr. Steve Rowins, are planned with mining company partners in 2004. These studies will focus on aspects of porphyry copper-gold and epithermal gold styles of mineralization, and although the timing of these projects will carry on beyond the duration of TGI-II, the results will ultimately be integrated with those of the regional bedrock program leading to a better understanding of the metallogeny of the Toodoggone mining camp.

ACKNOWLEDGMENTS

We express our gratitude to the group of mining companies involved in the first year of the Toodoggone TGI-Public-Private Partnership; namely, Bishop Resources Inc., Finlay Minerals Ltd., Northgate Exploration Ltd., Sable Resources Ltd. and Stealth Minerals Ltd. Our partners openly shared confidential information and are also thanked for their generous financial and logistical support. In particular, we acknowledge the dedication of company field personnel for leading the way to new discoveries. We thank Phu Van Bui for being an excellent assistant. We benefited from his enterprising spirit and keenness throughout the program. Thanks are extended to Ben Kerr for constructing the location figure. Any errors or omissions are the sole responsibility of the principal author.

REFERENCES

Diakow, L.J. (2001): Geology of the Southern Toodoggone River and Northern McConnell Creek Map Areas, North-central British Columbia (Parts of NTS 94E/2, 94D/15 and 16a); *B.C. Ministry of Energy and Mines*, Geoscience Map 2001-1, 1:50,000 scale.

Diakow, L.J., Panteleyev, A and Schroeter, T.G. (1993): Geology of the Early Jurassic Toodoggone Formation and Gold-Silver Deposits in the Toodoggone River Map Area, Northern British Columbia; *B.C. Ministry of Energy, Mines and Petroleum Resources*, Bulletin 86, 72 pages with maps at 1:100,000 scale.

Diakow, L.J., Panteleyev, A and Schroeter, T.G. (1985): Geology of the Toodoggone River Area, NTS 94E; *B.C. Ministry of Energy, Mines and Petroleum Resources*, Preliminary Map 61, 1:50,000 scale.

Jackaman, W. (1997): British Columbia Regional Geochemical Survey NTS 94E-Toodoggone River, Stream Sediment and Water Geochemical Data; *B.C. Ministry of Employment and Investment*, BC RGS 46.

Jackaman, W. (1997): British Columbia Regional Geochemical Survey NTS 94D-McConnell Creek, Stream Sediment and Water Geochemical Data; *B.C. Ministry of Employment and Investment*, BC RGS 45.

GSC (1999): Aeromagnetic Residual Total Field Survey of Toodoggone River (NTS 94E) and Ware (NTS 94F); *Geological Survey of Canada*, Open File 3495, 8 sheets at 1:100,000 scale.

GEOLOGY OF THE GRANBY FAULT, AN EOCENE EXTENSIONAL FAULT IN SOUTHEAST BRITISH COLUMBIA

By J.D. Laberge[1], D.R.M. Pattison[1] and P.S. Simony[1]

KEYWORDS: Southern Omineca Belt, Eocene extension, metamorphic core complex, Grand Forks Group, Granby fault, Knob Hill Group, Brooklyn Formation.

INTRODUCTION

The Grand Forks complex, northern equivalent to the Kettle dome in the United States (e.g, Cheney, 1977; Cheney, 1980; Rhodes and Cheney, 1981), is one of many exposures of high-grade metamorphic rocks of North American miogeoclinal affinity in the southern Omineca Belt (Figure 1). These structural culminations bounded by Tertiary normal faults, often collectively referred to as the Shuswap complex, were rapidly exhumed by tectonic uplift during post-Laramide crustal extension in the Eocene (e.g. Lorencak *et al.*, 2001; Parrish *et al.*, 1988; Vanderhaeghe *et al.*, 1999). The western margin of the Grand Forks complex is the west-dipping Granby fault, which juxtaposes low-grade rocks of Quesnel Terrane to the west against the high-grade gneisses of the complex.

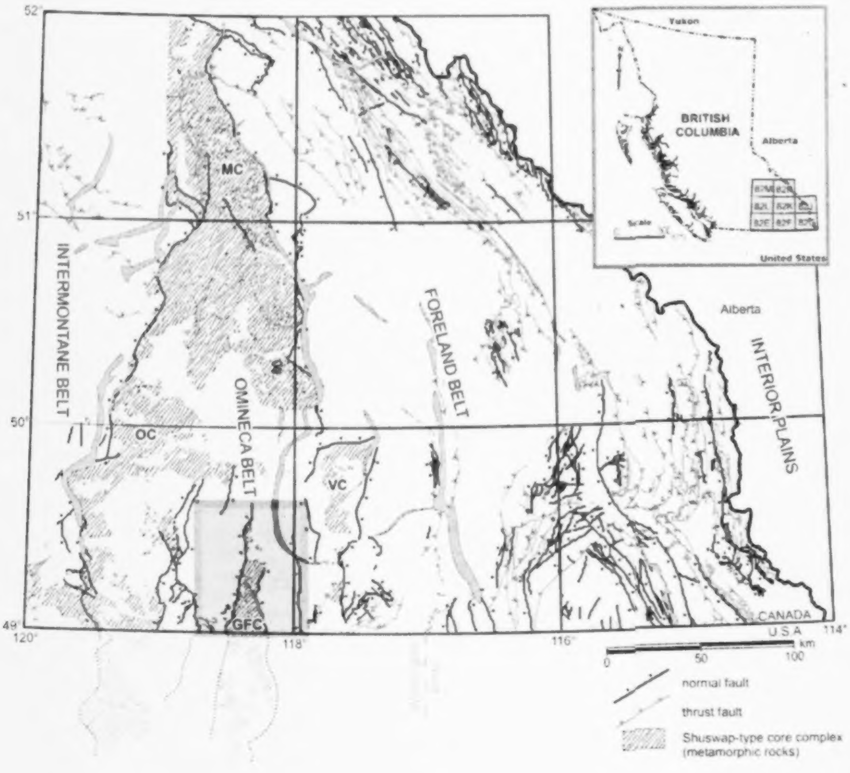
52°
51°
50°
49°
120°
118°
116°
114°
MC
OC
VC
GFC
INTERMONTANE BELT
OMINECA BELT
FORELAND BELT
INTERIOR PLAINS
Alberta
CANADA
U.S.A
Yukon
BRITISH COLUMBIA
Alberta
Scale
United States
0
50
100
km
normal fault
thrust fault
Shuswap-type core complex (metamorphic rocks)

Figure 1: Map of the southeastern British Colombia showing the occurrence of the Shuswap-type metamorphic core complexes in the southern Omineca Belt. MC-Monashee Comlpex; OC-Okanagan Complex; GFC-Grand Forks Complex; VC-Valhalla Complex. Shaded box shows location of figure 2.

---

[1] Department of Geology and Geophysics, University of Calgary

This report describes the geology along 7 km of the Granby fault in the Volcanic Creek area, approximately 12 km north of the city of Grand Forks (Figure 2). The results presented here are based on one season of mapping and a limited amount of petrography and mineral chemistry. This study is part of an on-going tectono-petrological study on the significance of the Granby fault in the denudation history of the southern Omineca Belt.

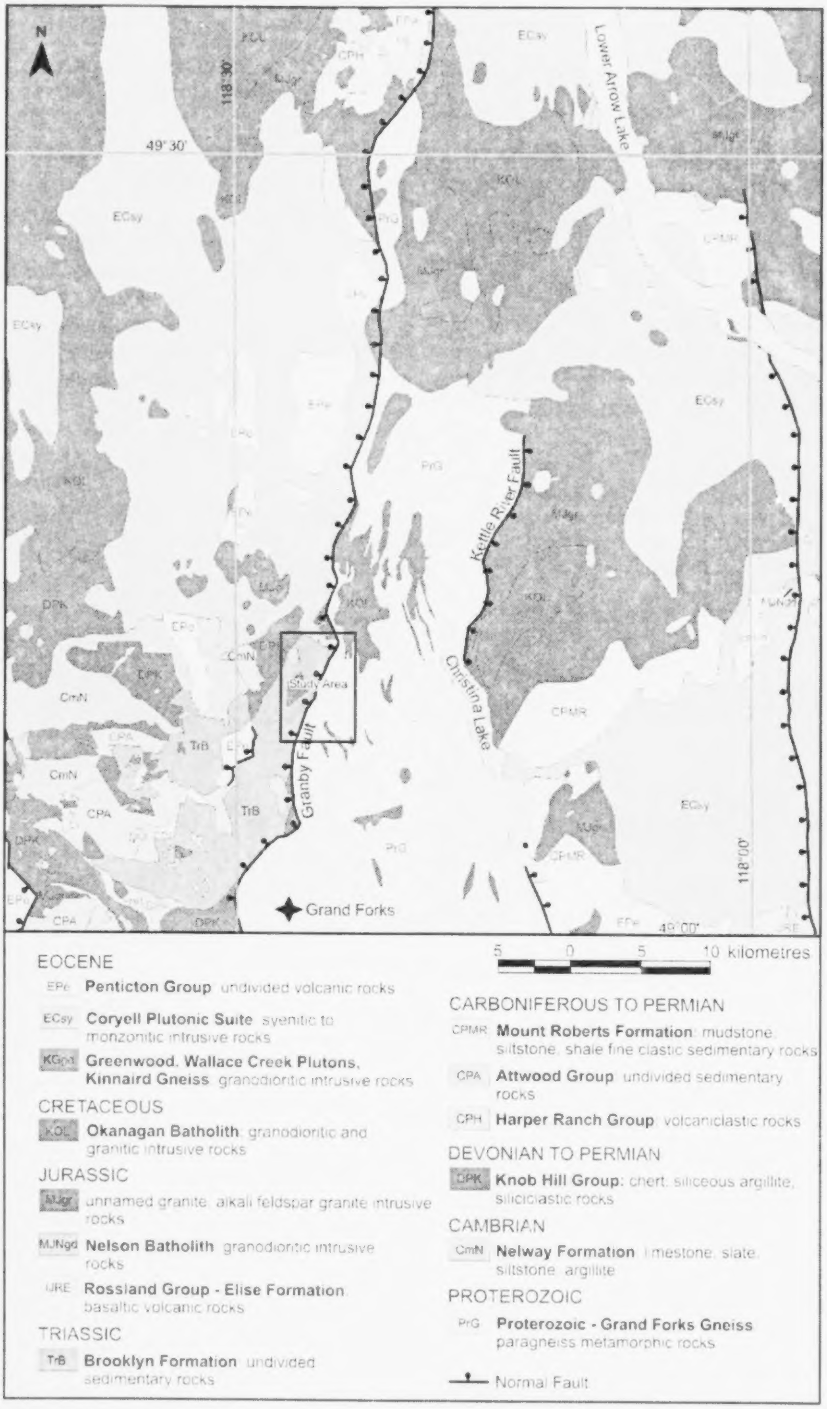
N
118°30'
49°30'
ECsy
KOL
CPH
MJgr
PrG
DPK
EPe
CmN
CPA
TrB
Study Area
Granby Fault
Kettle River Fault
Christina Lake
Lower Arrow Lake
CPMR
Grand Forks
118°00'
49°00'
5 0 5 10 kilometres
EOCENE
EPe Penticton Group: undivided volcanic rocks
ECsy Coryell Plutonic Suite: syenitic to monzonitic intrusive rocks
KGgd Greenwood, Wallace Creek Plutons, Kinnaird Gneiss: granodioritic intrusive rocks
CRETACEOUS
KOL Okanagan Batholith: granodioritic and granitic intrusive rocks
JURASSIC
MJgr unnamed granite: alkali feldspar granite intrusive rocks
MJNgd Nelson Batholith: granodioritic intrusive rocks
JRE Rossland Group - Elise Formation: basaltic volcanic rocks
TRIASSIC
TrB Brooklyn Formation: undivided sedimentary rocks
CARBONIFEROUS TO PERMIAN
CPMR Mount Roberts Formation: mudstone, siltstone, shale fine clastic sedimentary rocks
CPA Attwood Group: undivided sedimentary rocks
CPH Harper Ranch Group: volcaniclastic rocks
DEVONIAN TO PERMIAN
DPK Knob Hill Group: chert, siliceous argillite, siliciclastic rocks
CAMBRIAN
CmN Nelway Formation: limestone, slate, siltstone, argillite
PROTEROZOIC
PrG Proterozoic - Grand Forks Gneiss: paragneiss metamorphic rocks
Normal Fault

Figure 2: Regional geological map around the Grand Forks complex showing Paleozoic to Early Mesozoic units of the accreted Quesnel Terrane, and younger plutonic and volcanic suite (modified from Massey *et al.*, 2003).

This report describes the geology along 7 km of the Granby fault in the Volcanic Creek area, approximately 12 km north of the city of Grand Forks (Figure 2). The results presented here are based on one season of mapping and a limited amount of petrography and mineral chemistry. This study is part of an on-going tectono-petrological study on the significance of the Granby fault in the denudation history of the southern Omineca Belt.

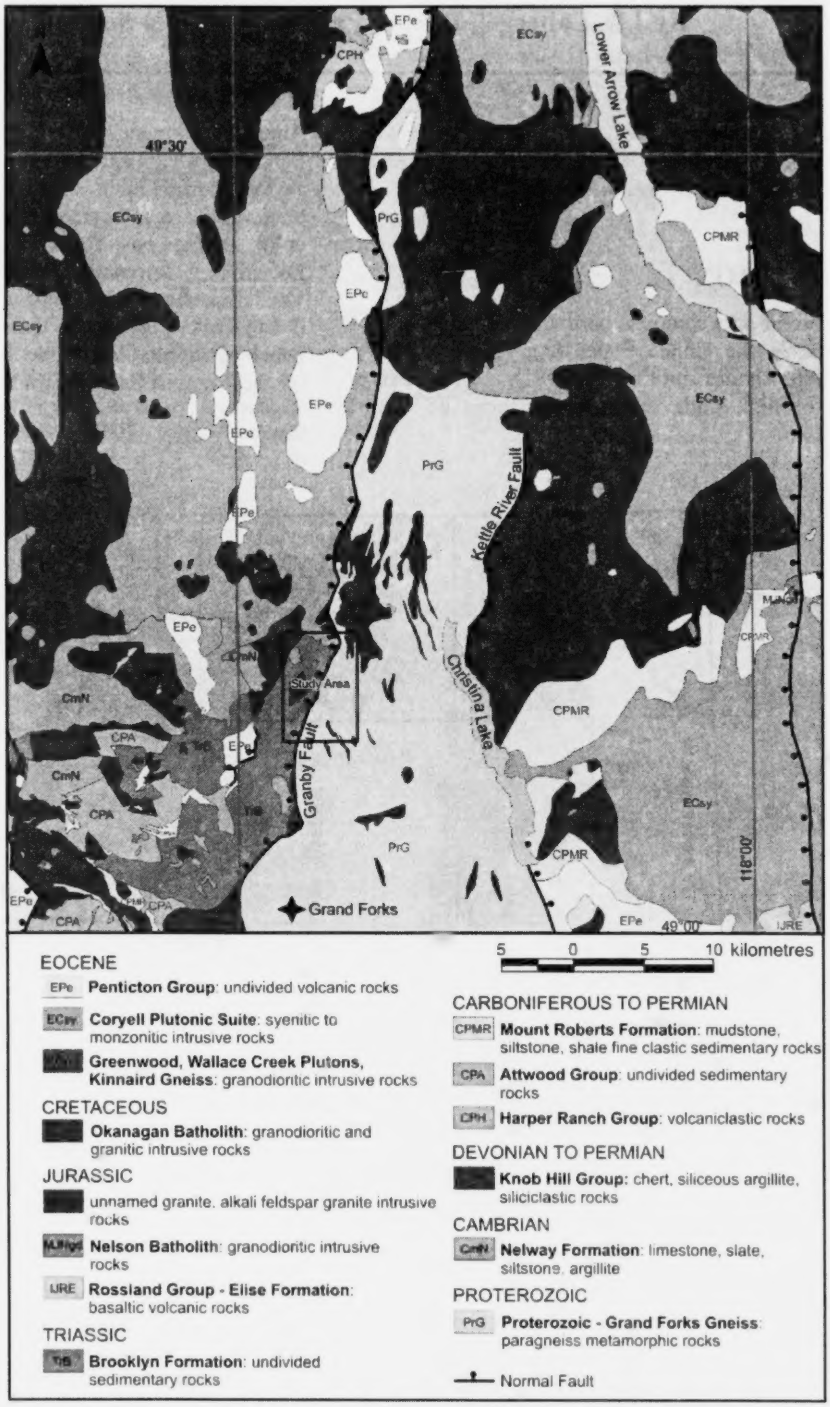
EPe
CPH
ECsy
Lower Arrow Lake
49°30'
PrG
CPMR
Kettle River Fault
Study Area
CmN
CPA
Christina Lake
Granby Fault
Grand Forks
49°00'
118°00'
IJRE
5 0 5 10 kilometres
EOCENE
EPe Penticton Group: undivided volcanic rocks
ECsy Coryell Plutonic Suite: syenitic to monzonitic intrusive rocks
Greenwood, Wallace Creek Plutons, Kinnaird Gneiss: granodioritic intrusive rocks
CRETACEOUS
Okanagan Batholith: granodioritic and granitic intrusive rocks
JURASSIC
unnamed granite. alkali feldspar granite intrusive rocks
MJNgd Nelson Batholith: granodioritic intrusive rocks
IJRE Rossland Group - Elise Formation: basaltic volcanic rocks
TRIASSIC
TrB Brooklyn Formation: undivided sedimentary rocks
CARBONIFEROUS TO PERMIAN
CPMR Mount Roberts Formation: mudstone, siltstone, shale fine clastic sedimentary rocks
CPA Attwood Group: undivided sedimentary rocks
CPH Harper Ranch Group: volcaniclastic rocks
DEVONIAN TO PERMIAN
Knob Hill Group: chert, siliceous argillite, siliciclastic rocks
CAMBRIAN
CmN Nelway Formation: limestone, slate, siltstone, argillite
PROTEROZOIC
PrG Proterozoic - Grand Forks Gneiss: paragneiss metamorphic rocks
Normal Fault

Figure 2: Regional geological map around the Grand Forks complex showing Paleozoic to Early Mesozoic units of the accreted Quesnel Terrane, and younger plutonic and volcanic suite (modified from Massey *et al.*, 2003).

REGIONAL GEOLOGY

The Grand Forks complex is bounded by outward dipping Eocene normal faults: the Granby fault to the west and the Kettle River fault to the east (Figure 2). In the hanging-wall of the Granby fault are sedimentary and volcanic assemblages of Quesnel Terrane, cross-cut by younger intrusions. Quesnel Terrane is generally interpreted as a package of allochthonous rocks accreted to the western margin of North America, characterized by Paleozoic to Mesozoic island-arc assemblages and associated intrusions (e.g. Acton *et al.*, 2002; Gabrielse *et al.*, 1991). The island-arc assemblage in the Grand Forks region consists of sedimentary and volcaniclastic rocks deposited during the Cambrian to the Triassic, with rare Jurassic volcanic rocks (Figure 2). Jurassic to Cretaceous plutons of granitic to granodioritic composition are also widespread within Quesnellia. Eocene plutonic rocks of the Coryell Suite and Eocene volcanic rocks of the Penticton Group are the youngest units in the area.

LITHOLOGICAL UNITS

Footwall: High-grade metamorphic rocks of the Grand Forks Core Complex

The Grand Forks complex is mainly composed of a high-grade meta-sedimentary succession described and mapped as the Grand Forks Group, occurring as paragneiss, schist, quartzite and marble (Preto, 1970a). Amphibolite, pegmatite, orthogneiss and granitoids are also present within the complex, as well as late, cross-cutting, north trending syenitic to monzonitic dikes.

Armstrong *et al.* (1991) dated the sillimanite-paragneiss (described below) from whole-rock Rb-Sr, whole-rock Sm-Nd and U-Pb in zircon. They obtained rather inconsistent results, with ages ranging from 1.6 to 2.0 Ga, concluding that the sillimanite-paragneiss is Early Proterozoic in age, with a strong Mesozoic to Early Cenozoic metamorphic overprint. Detrital zircons in this unit are interpreted as being derived from the North American craton to the east (Parrish *et al.*, 1989). Detrital zircons in the quartzite directly overlying the sillimanite-paragneiss have been dated as 650 ±15 Ma (Ross and Parrish, 1991), implying a major Proterozoic unconformity between the two units. The age of the high-grade metamorphism in the complex is still unknown.

Paleogene cooling ages of 50 to 67 Ma from K-Ar analysis in biotite and hornblende, respectively, have been obtained from the Kettle gneiss (Engels *et al.*, 1976), suggesting exhumation of the Grand Forks complex from moderate depths in the Paleogene.

MIDDLE PROTEROZOIC

Sillimanite-paragneiss (I)

Coarse-grained sillimanite-paragneiss represents the structurally lowest meta-sedimentary unit of the complex exposed in the map area (Figure 3). It is the most widespread and thickest map unit. The unit contains more than 35% white leucogranitic pegmatite to very coarse leucogranite, inter-layered with the paragneiss.

The pelitic gneiss is migmatitic and stromatic (Photo 1). The mineral assemblages include some or all of K-feldspar, sillimanite, biotite, cordierite, garnet, quartz and plagioclase. Compositional banding is defined by thin, dark bands enriched in sillimanite, altered cordierite, biotite, Fe-oxide and locally garnet, alternating with coarse-grained leucosomes of plagioclase, K-feldspar and quartz. Sillimanite is acicular and is typically closely associated with cordierite. Samples rich in biotite contain rare sillimanite and vice versa. With the exception of one locality, cordierite is completely altered. Where present, garnet is anhedral and typically occurs within the altered cordierite.

The pegmatite bands and sills have apparent thicknesses of less than 15 metres, and are commonly ~5 metres thick. They are more resistant to weathering than the associated gneiss, and commonly form ridges oriented parallel to the gneissosity. They have a leucocratic granitic composition with biotite and rare sillimanite, garnet and tourmaline.

Photo 1: Migmatitic texture in sillimanite-paragneiss.

LATE PROTEROZOIC TO CAMBRIAN

Quartzite (II)

A quartzite unit ~200-300 metres thick occurs unconformably (on the basis of previously mentioned geochronological data) above the sillimanite-paragneiss. It is mainly composed of coarse-grained quartz, with up to

5% coarse white K-feldspar crystals, which are rounded and elongated within the gneissosity. Compositional banding is defined by modal variations in feldspar. Sillimanite rarely occurs within the unit. Some thin granitic pegmatite bands are locally inter-layered with the quartzite.

Marble (IIa)

Coarse white marble forms a thin (~100 m) lens within the quartzite. It is mainly composed of 3-5 mm crystals of calcite with euhedral black spinel, anhedral diopside and euhedral phlogopite as accessory metamorphic minerals.

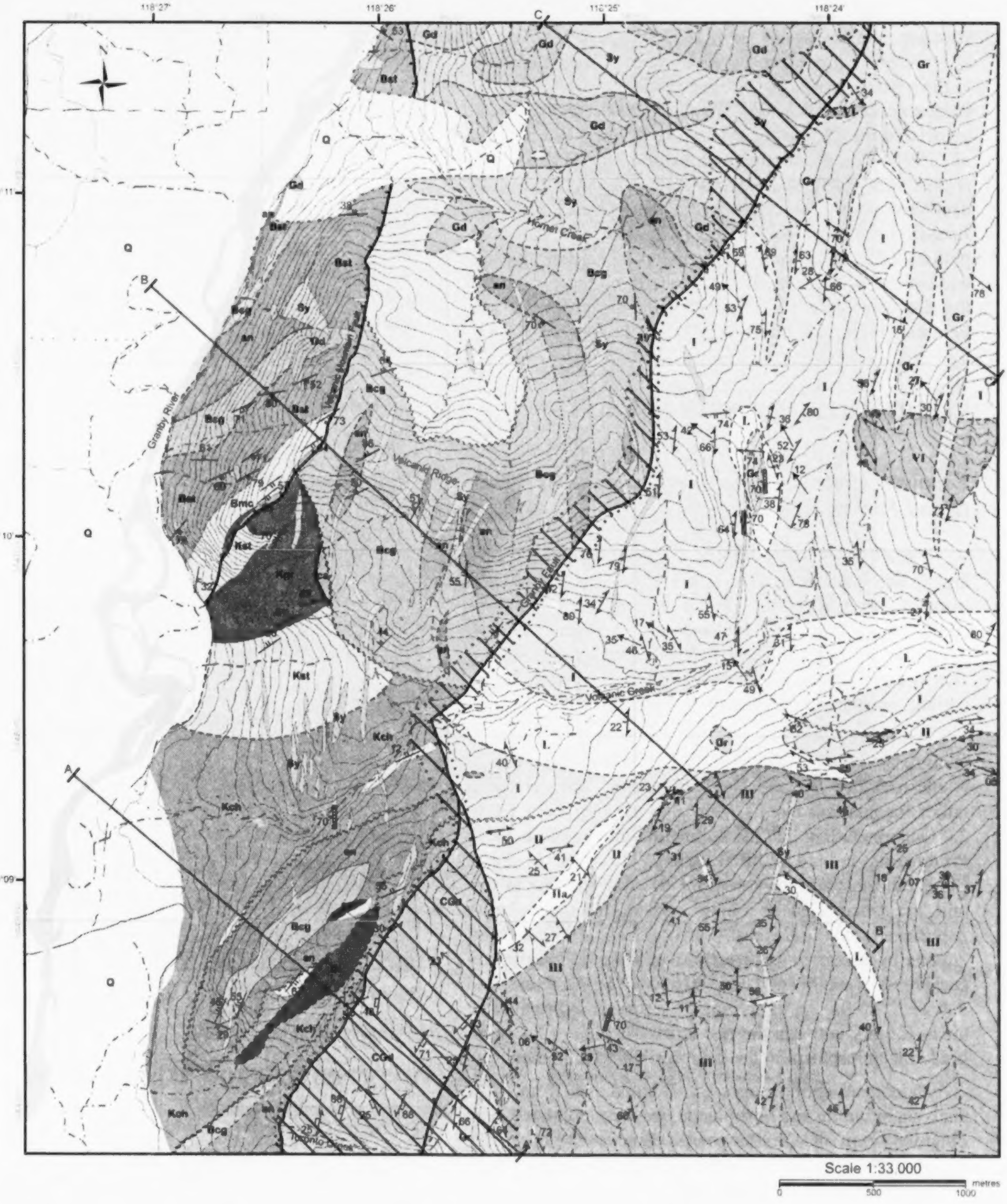

118°27'
118°26'
118°25'
118°24'
49°11'
49°10'
49°09'
A
B
C
B'
C'
Q
Gd
Sy
Gr
Bst
Bcg
Bmc
Kst
Kch
CGd
an
I
II
IIa
III
VI
Granby River
Homer Creek
Volcanic Ridge
Volcanic Creek
Granby Fault
Toronto Creek
Scale 1:33 000
0
500
1000
metres

Figure 3a: Geological map of the western margin of the Grand Forks complex and bounding Granby fault, in the Volcanic Creek area. Universal Transverse Mercator Grid: Zone 11, NAD83; 20 metre contour intervals.

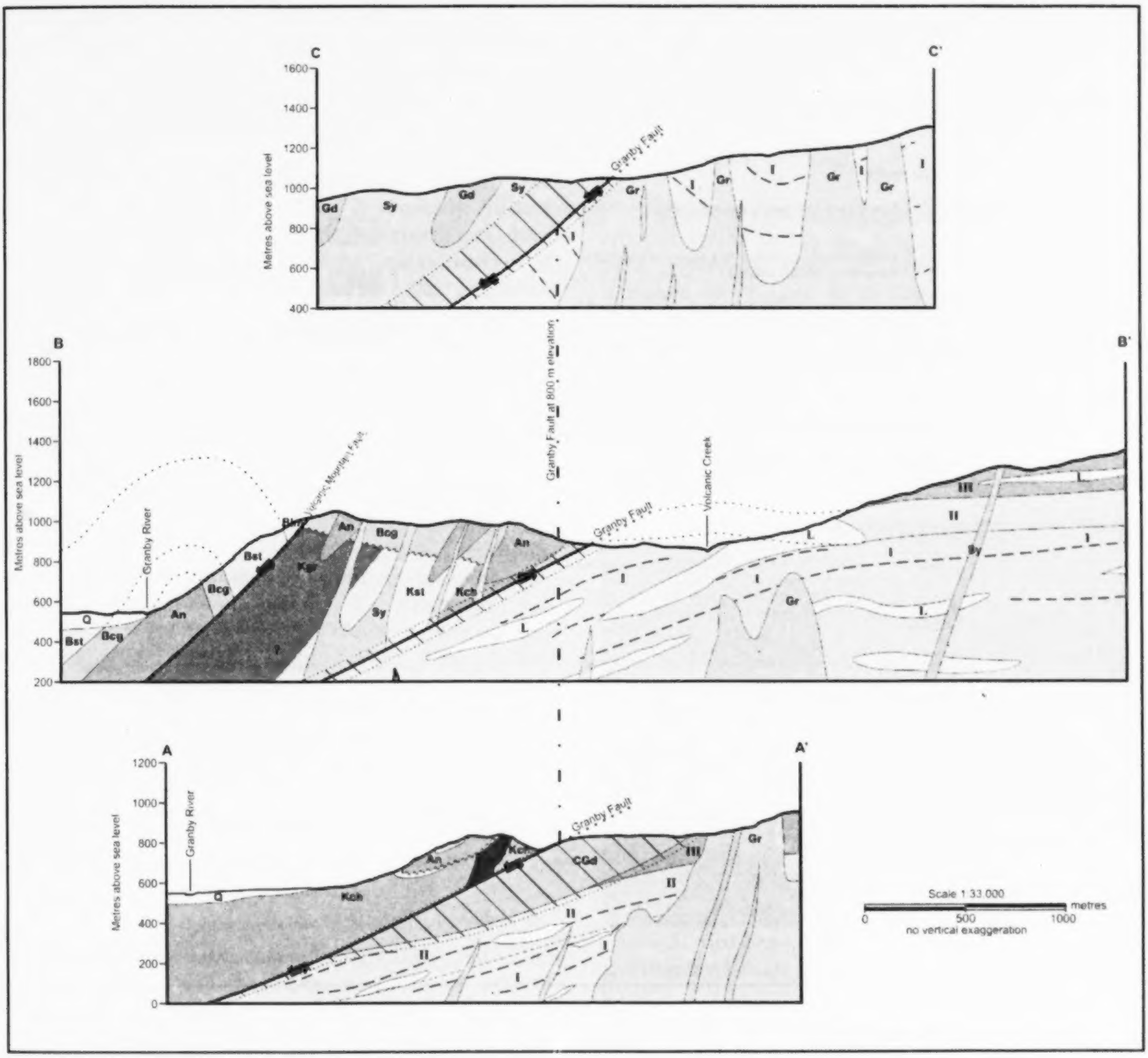
C
C'
1600
1400
1200
1000
800
600
400
Metres above sea level
Granby Fault
Gd
Sy
Gd
Sy
Gr
I
Gr
Gr
I
Gr
I
B
B'
1800
1600
1400
1200
1000
800
600
400
200
Metres above sea level
Granby River
Volcanic Mountain Fault
Granby Fault at 800 m elevation
Volcanic Creek
Granby Fault
Bst
An
Bcg
An
Bst
Bcg
Kst
Kch
Sy
Q
Bst
Bcg
An
?
L
I
Gr
III
II
L
I
Sy
A
A'
1200
1000
800
600
400
200
0
Metres above sea level
Granby River
Granby Fault
An
Kch
CGd
III
Gr
Q
Kch
II
II
I
II
I
Scale 1:33 000
metres
0
500
1000
no vertical exaggeration

Figure 3b: Cross-section across the Granby fault, accompanying Figure 3. Geological boundaries, although assumed, are not dashed for clarity.

Biotite-paragneiss (III)

Biotite-paragneiss represents the structurally highest unit within the metamorphic core complex. It is widespread within the map area, but its thickness is unknown, as the unit is truncated by the erosional surface. The paragneiss is migmatitic with alternating biotite-rich layers and quartzo-feldspathic leucosomes defining the gneissic banding (Photo 2). Biotite, plagioclase and quartz (minor) are the main constituents while garnet and/or sillimanite are locally present but generally not abundant. Clinopyroxene has been observed in one outcrop only (garnet- and sillimanite-free), on the northwest-facing slope south of Volcanic Creek. The mineral composition is suggestive of a semi-pelitic to psammitic protolith. Quartzo-feldspathic leucosomes a few millimetres to centimetres thick are common within the unit and locally contain garnet and sillimanite. The biotite-gneiss is interlayered with abundant pegmatite in a similar fashion to the sillimanite-paragneiss unit. The amount of coarse to pegmatitic leucogranite ranges up to 40% of the unit. Rare thin layers of quartzite (quartz + K-feldspar ± sillimanite) also occur within this gneiss.

5% coarse white K-feldspar crystals, which are rounded and elongated within the gneissosity. Compositional banding is defined by modal variations in feldspar. Sillimanite rarely occurs within the unit. Some thin granitic pegmatite bands are locally inter-layered with the quartzite.

Marble (IIa)

Coarse white marble forms a thin (~100 m) ler within the quartzite. It is mainly composed of 3-5 m crystals of calcite with euhedral black spinel, anhedra diopside and euhedral phlogopite as accessor metamorphic minerals.

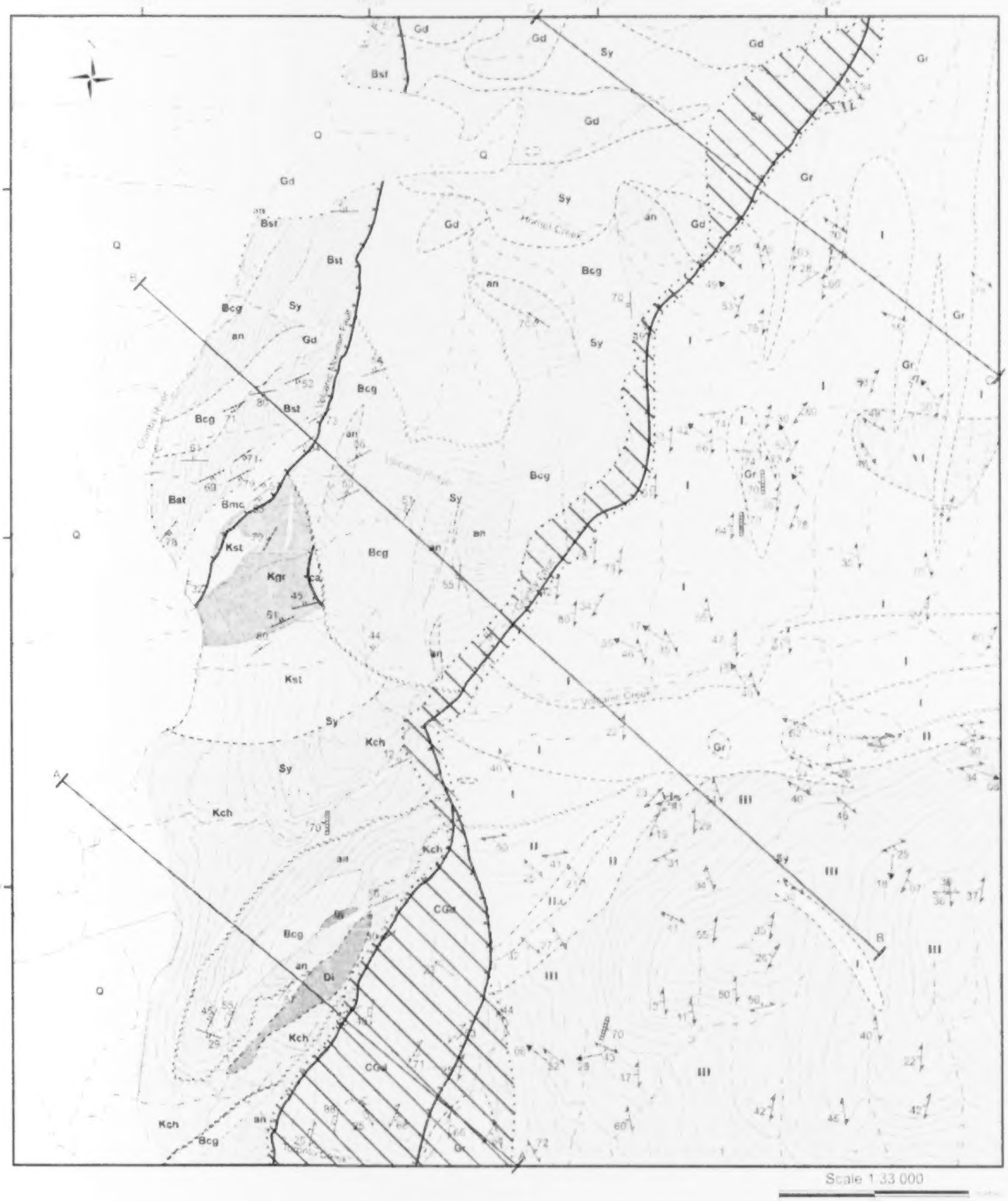

Gd
Sy
Gr
Bst
Q
Bcg
an
Bat
Bmc
Kst
Kgr
ca
Kch
CGd
Di
I
II
III
IIa
A
B
C
Volcanic Creek
Scale 1:33 000

Figure 3a: Geological map of the western margin of the Grand Forks complex and bounding Granby fault, in the Volcan Creek area. Universal Transverse Mercator Grid: Zone 11, NAD83; 20 metre contour intervals.

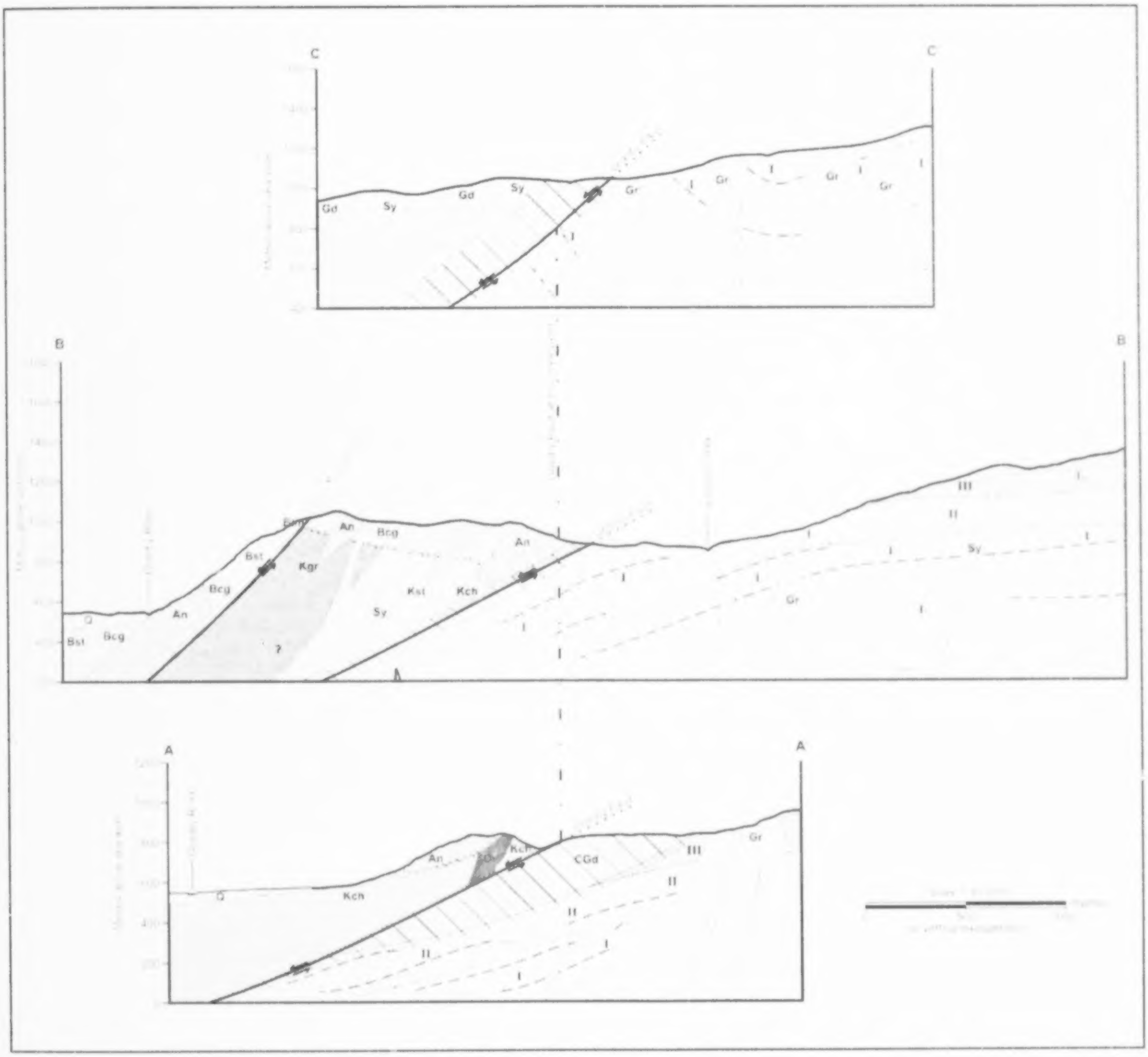

Figure 3b: Cross-section across the Granby fault, accompanying Figure 3. Geological boundaries, although assumed, are not dashed for clarity.

Biotite-paragneiss (III)

Biotite-paragneiss represents the structurally highest unit within the metamorphic core complex. It is widespread within the map area, but its thickness is unknown, as the unit is truncated by the erosional surface. The paragneiss is migmatitic with alternating biotite-rich layers and quartzo-feldspathic leucosomes defining the gneissic banding (Photo 2). Biotite, plagioclase and quartz (minor) are the main constituents while garnet and/or sillimanite are locally present but generally not abundant. Clinopyroxene has been observed in one outcrop only (garnet- and sillimanite-free), on the northwest-facing slope south of Volcanic Creek. The mineral composition is suggestive of a semi-pelitic to psammitic protolith. Quartzo-feldspathic leucosomes a few millimetres to centimetres thick are common within the unit and locally contain garnet and sillimanite. The biotite-gneiss is interlayered with abundant pegmatite in a similar fashion to the sillimanite-paragneiss unit. The amount of coarse to pegmatitic leucogranite ranges up to 40% of the unit. Rare thin layers of quartzite (quartz + K-feldspar ± sillimanite) also occur within this gneiss.

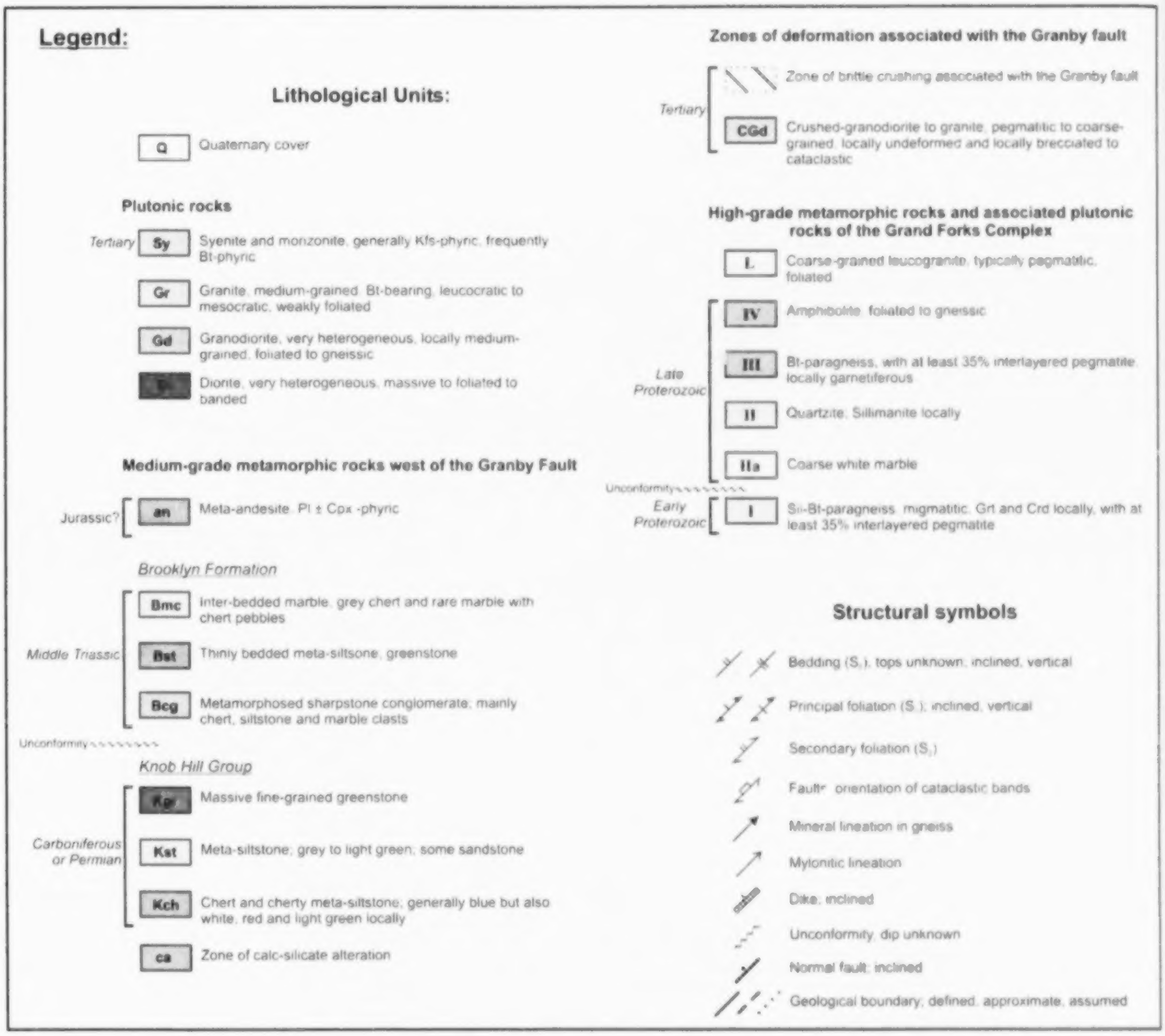
Legend:
Lithological Units:
Q Quaternary cover
Plutonic rocks
Tertiary
Sy Syenite and monzonite, generally Kfs-phyric, frequently Bt-phyric
Gr Granite, medium-grained, Bt-bearing, leucocratic to mesocratic, weakly foliated
Gd Granodiorite, very heterogeneous, locally medium-grained, foliated to gneissic
Diorite, very heterogeneous, massive to foliated to banded
Medium-grade metamorphic rocks west of the Granby Fault
Jurassic?
an Meta-andesite, Pl ± Cpx -phyric
Brooklyn Formation
Middle Triassic
Bmc Inter-bedded marble, grey chert and rare marble with chert pebbles
Bst Thinly bedded meta-siltsone, greenstone
Bcg Metamorphosed sharpstone conglomerate; mainly chert, siltstone and marble clasts
Unconformity
Knob Hill Group
Carboniferous or Permian
Kg Massive fine-grained greenstone
Kst Meta-siltstone; grey to light green; some sandstone
Kch Chert and cherty meta-siltstone; generally blue but also white, red and light green locally
ca Zone of calc-silicate alteration
Zones of deformation associated with the Granby fault
Tertiary
Zone of brittle crushing associated with the Granby fault
CGd Crushed-granodiorite to granite, pegmatitic to coarse-grained, locally undeformed and locally brecciated to cataclastic
High-grade metamorphic rocks and associated plutonic rocks of the Grand Forks Complex
L Coarse-grained leucogranite, typically pegmatitic, foliated
Late Proterozoic
IV Amphibolite, foliated to gneissic
III Bt-paragneiss, with at least 35% interlayered pegmatite, locally garnetiferous
II Quartzite; Sillimanite locally
IIa Coarse white marble
Unconformity
Early Proterozoic
I Sil-Bt-paragneiss, migmatitic, Grt and Crd locally, with at least 35% interlayered pegmatite
Structural symbols
Bedding (S.), tops unknown; inclined, vertical
Principal foliation (S.); inclined, vertical
Secondary foliation (S.)
Faults: orientation of cataclastic bands
Mineral lineation in gneiss
Mylonitic lineation
Dike; inclined
Unconformity, dip unknown
Normal fault; inclined
Geological boundary; defined, approximate, assumed

Figure 3c: Legend accompanying Figures 3 and 4.

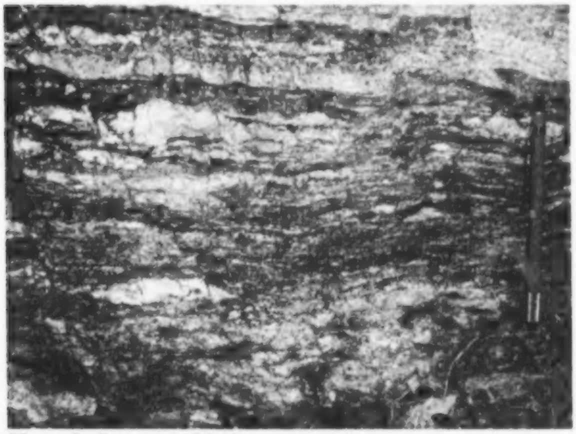

Photo 2: Stromatic biotite-paragneiss.

Amphibolite (IV)

Amphibolite is present throughout the metamorphic complex, generally occurring in small, discrete outcrops too small to be mapped individually. However, zones containing abundant amphibolite have been mapped (Figure 3a). The amphibolite is composed of hornblende, plagioclase, biotite, minor quartz, and rare clinopyroxene, and has a coarse-grained, foliated to gneissic texture. Alternating amphibole-rich and leucocratic bands are usually 1-4 millimetres thick. The amphibolite has been interpreted, on the basis of geochemistry, as metamorphosed Na-rich mafic plutons and dikes intruded into the meta-sedimentary sequence (Preto, 1970b).

Coarse to pegmatitic leucogranite (L)

Pegmatitic to very coarse-grained leucogranite is inter-layered within all meta-sedimentary units of the core complex but individual bodies are generally too thin (<10 metres) to be mapped. The map unit shown in Figure 3 therefore only represents the mappable portions of pegmatitic leucogranite. The leucogranite is white, with some biotite and rare sillimanite and garnet. The leucogranite appears massive, but is distinctly foliated when biotite is present. The textural continuum from leucosomes to pegmatite sills, and the local occurrence of sillimanite and garnet, suggest that the pegmatite represents leucogranitic melt locally derived from *in-situ* partial melting of the meta-pelitic to meta-psammitic rocks.

Hanging-wall: Low grade metamorphic rocks of Quesnel Terrane

The supracrustal rocks exposed west of the Granby fault include metamorphosed argillite, siltstone, sandstone, polymictic sharpstone-conglomerate, limestone and porphyritic andesite. The stratigraphy and inferred ages are based on the regional mapping and correlations of Little and Thorpe (1965), Preto (1970a) and Little (1983). These rocks range in age from Devonian to Jurassic and are part of Quesnel Terrane (Wheeler and McFeely, 1991). The exact age of the low-grade regional metamorphism is unknown.

KNOB HILL GROUP (CARBONIFEROUS OR PERMIAN)

Chert (Kch)

Massive chert represents a thick (>200m) unit in the southern half of the map area. It is almost entirely composed of microcrystalline quartz and varies in colour from dark blue to white, red and light green, and is locally silty. Near its upper contact, chert is inter-bedded within siltstone.

Meta-siltstone (Kst)

Grey to greenish-grey meta-siltstone is generally quartz-rich, and contains the metamorphic minerals biotite, amphibole, plagioclase, quartz, epidote, muscovite and locally, small (<1 mm) euhedral garnet. It is generally massive to poorly-bedded and locally contains up to 5% sand-size clasts. Up to 15% of the unit is composed of medium-grained meta-sandstone. Pyrite and rare chalcopyrite occur in discrete zones throughout this unit, associated with minor faults. Mineralization is generally disseminated, with local centimetre-scale lenses of massive pyrite, that are generally associated with silicification of the host rock.

Greenstone (Kgr)

Greenstone exposed on the west-facing slope next to the Granby River is massive, light green and aphanitic.

BROOKLYN FORMATION (MIDDLE TRIASSIC)

Meta-conglomerate (Bcg)

Metamorphosed conglomerate and epiclastic breccias are widespread within the hanging-wall of the Granby fault (Figure 3a). They are physically and chemically immature, as revealed by angular to sub-rounded clasts and up to cobble-size sub-angular carbonate clasts. Clasts are polygenetic, consisting of chert, fine-grained quartzite, siltstone, marble and intermediate to mafic volcanic rocks (Photo 3). The metamorphosed matrix is relatively mafic, consisting mainly of biotite, actinolite, hornblende and secondary chlorite, giving the rock a greenish colour.

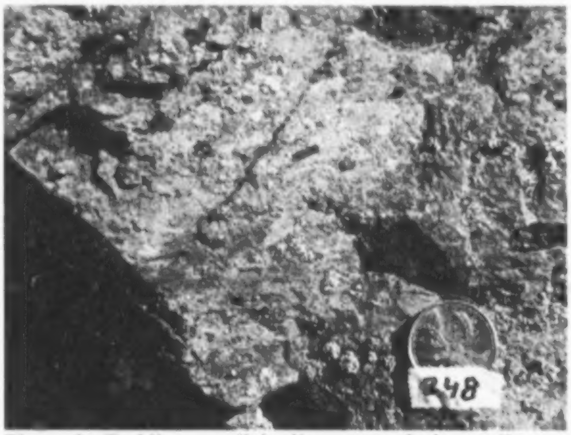

Photo 3: Bedding-parallel alignment of chert, siltstone and limestone clasts in meta-conglomerate.

Thinly bedded meta-siltstone (Bst)

Overlying the sharpstone-conglomerate in the northwest is a laminated greenish siltstone, locally massive and grey. The transition between the two units is gradational as conglomerate and siltstone are inter-bedded at the contact. Most of the meta-siltstone is thinly bedded, with beds ranging from 2 to 15 mm, with slight compositional variations. Dark to light green beds are likely derived, at least partly, from greenstone or other volcanogenic sources. Grey to bluish-grey beds are silty to cherty. The south end of the unit (Figure 3) is in conformable contact with metamorphosed limestone and chert (Bmc).

Inter-bedded marble and chert (Bmc)

This thin unit is composed of closely associated fine-grained light-grey marble and dark-grey chert. The unit is well exposed on the west-facing slope north of Volcanic Creek, east of the Granby River. There it consists of thinly inter-bedded marble and chert, with beds ~10-20 cm thick, that are concentrically folded (Photo 4). Locally the unit occurs as marble with pods of chert and some beds with rounded chert pebbles (2 to 6 mm) in a carbonate matrix (Photo 5).

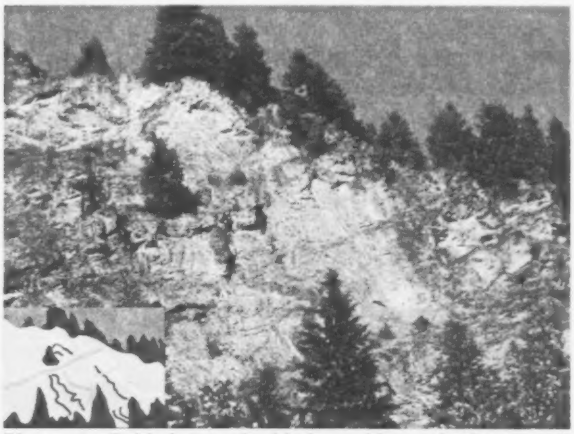

Photo 4: Folded inter-bedded marble and chert, with cross-cutting dikes and contact with meta-siltstone to the right.

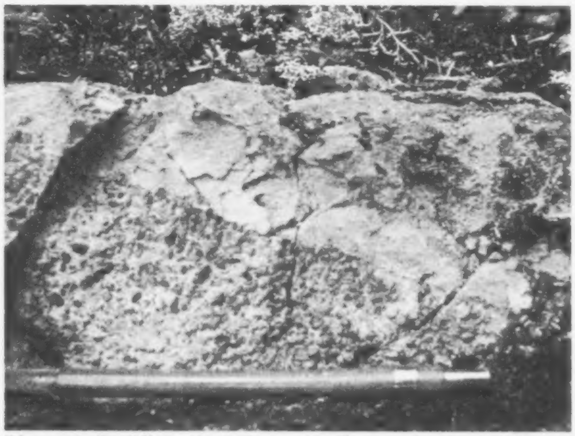

Photo 5: Bedding plane between fine-grained marble and chert-wackestone (conglomerate) within the inter-bedded marble and chert unit (pen for scale).

Calc-silicates, skarn (ca)

Calc-silicate alteration of meta-sedimentary rocks occurs in two lenses within the hanging-wall, both associated with normal faults (Figure 3a). The northern one, in contact with the marble unit is a reddish brown siliceous rock (siltstone?) containing anhedral garnet. The other zone of calc-silicate replacement is observed within the meta-conglomerate at its contact with the underlying greenstone, and is marked by the development of garnet, diopside and calcite in the matrix.

UNCONFORMITY BETWEEN THE KNOB HILL GROUP AND THE BROOKLYN FORMATION

Strata within the Knob Hill Group and Brooklyn Formation appear to be internally conformable. However, a stratigraphic or structural break must be present between the meta-conglomerate of the Brooklyn Formation and the underlying metamorphosed chert, siltstone and greenstone of the Knob Hill Group. The high angle between bedding in the Knob Hill Group and the contact between the Knob Hill Group and the Brooklyn Formation, combined with the observation that clasts in the very immature conglomerate/epiclastic breccia appear to be directly derived from underlying units, suggest that the stratigraphic break is an unconformity. This interpretation is consistent with the unconformable relationship between the Brooklyn Formation and Knob Hill Group in the Greenwood area (Little, 1983). On the western slope of Volcanic Ridge, marble and chert in higher levels of the Brooklyn Formation are also in contact with greenstone from the Knob Hill Group, but here the contact is represented by a northwest-dipping normal fault, which is interpreted to truncate the unconformity.

TRIASSIC TO JURASSIC?

Meta-andesite (an)

Meta-andesite is fine-grained and generally porphyritic, containing small (<2 mm) plagioclase phenocrysts and locally large (2-6 mm) hornblende-actinolite pseudomorphs after clinopyroxene penocrysts. Primary plagioclase laths are preserved in the matrix, along with metamorphic actinolite, hornblende, epidote, calcite and minor quartz as metamorphic minerals. Locally the composition appears to be more dacitic, as a few rounded quartz grains have been observed. These intermediate igneous rocks were likely emplaced as shallow dikes and sills within the sedimentary package, but because of limited exposure, the geometry of theses bodies and their relationship with the surrounding rocks is poorly understood. The meta-andesite is closely associated with the Brooklyn meta-conglomerate. In the south of the map area, the meta-andesite underlying the conglomerate lens is interpreted here as being a volcanic flow, unconformably deposited on the Knob Hill Group. Some small intermediate to mafic dikes (<3 m thick) are also observed within the meta-siltstone and the inter-bedded marble units of the Brooklyn Formation. In the Greenwood area to the west, the only observed porphyritic andesites are interpreted to be of possible Jurassic age (Little, 1983).

Plutonic Rocks

JURASSIC?

Hanging-wall granodiorite (Gd)

A texturally heterogeneous biotite-granodiorite is exposed in the north of the map area, in the low-grade rocks west of the Granby Fault. It is generally medium-grained, foliated to gneissic and locally coarse-grained and massive, and varies in composition from leucocratic to mesocratic. This unit is older than the Coryell syenite as enclaves of granodiorite occur within the syenite.

CRETACEOUS-PALEOGENE?

Footwall granite (Gr)

A granitic body occurs in the footwall in the northern end of the map area, and gradually branches off and disappears to the south. Small bodies of similar-looking granite have been mapped elsewhere within the footwall. The massive to weakly foliated biotite-granite is medium-grained, leucocratic to mesocratic.

EOCENE

Syenite and monzonite of the Coryell Suite (Sy)

The syenite of the Coryell suite is mainly exposed as a pluton more than 2 km wide in the hanging-wall of the Granby Fault at the northern end of the map area. There, it occurs as a pink, coarse-grained, K-feldspar + biotite ± amphibole- phyric syenite, that may grade into a massive K-feldspar megacrystic (~1 cm) syenite. In the rest of the map area, the Coryell suite plutonic rocks occur as discrete dikes of monzonite and syenite, in both the hanging-wall and footwall of the Granby fault. They generally range from 5 to 20 metres in thickness and are limited to a few hundred metres in length, resulting in lens-shaped bodies. They are usually steeply dipping to the west but sometimes to the east. They frequently display dark, fine-grained chilled margins.

The dikes vary in texture across the fault. Within the hanging-wall, they are typically either very coarse-grained, or K-feldspar ± biotite ± amphibole- phyric in a fine-grained grey matrix (Photo 6). In contrast, within the footwall, the dikes tend to be massive and medium-grained, and frequently contain rounded grey enclaves of similar material with a higher mafic content.

These dikes represent the youngest unit in the map area. However, at least some of them are older than the latest movement on the Granby fault because the Granby fault cuts some of the dikes (Figure 3), and they are locally sheared and brecciated within the fault zone. On the other hand, the degree of cataclastic deformation in the dikes in the vicinity of the fault is much less than that of the host rocks, suggesting emplacement late in the fault history. Emplacement of the dikes therefore may have been, at least in part, synchronous with the movement on the Granby fault, consistent with their trend sub-parallel to the fault zone and the variable amount of deformation in dikes close to the fault. A sample of the Coryell syenite collected 10.5 km north of the northwest corner of the map area yielded a zircon U-Pb age of 51.1 ± 0.5 Ma (Carr and Parkinson, 1989). Movement on the Granby fault therefore both predates and postdates this age.

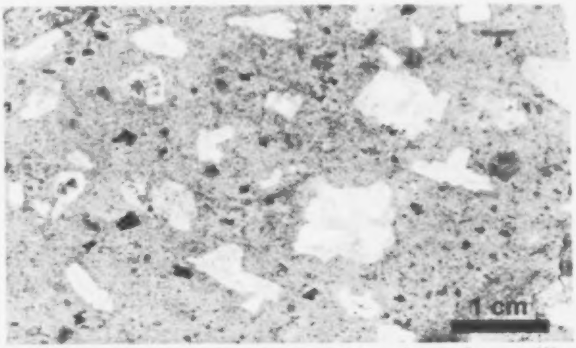

Photo 6: Slab of porphyritic syenite (trachyte) from a dike within the hanging-wall. Phenocrysts are K-feldspar, biotite and hornblende.

AGE UNKNOWN

Sheared and crushed granodiorite along the Granby Fault (CGd)

A medium- to very coarse-grained granodiorite occurs within the fault zone in the southern end of the map-area, near Toronto Creek. It is mesocratic (hornblende-biotite), locally with very coarse-grained leucocratic granitic fractions. The unit is sheared and highly fractured. Ductile shearing is expressed as an irregular foliation and lineation. Brittle brecciation of the unit occurs as thin chloritized zones (1-10 mm thick) containing crushed crystals. Light green outcrops of completely crushed fine-grained cataclasite occur locally on the western margin of the unit, near and along the Granby fault. Discrete mylonites occur within this unit but lack lateral as well as longitudinal continuity, suggesting that they have been reworked by subsequent brittle deformation. The intrusion occurs as a 300 m thick lens, with its long axis parallel to the fault trend. The overall shape and orientation of the body may suggest that it may have been intruded along the fault zone, and subsequently deformed brittly.

Hanging-wall diorite (Di)

A coarse-grained, deformed and fractured hornblende-diorite is exposed just north of Toronto Creek. It is very heterogeneous, massive to foliated to compositionally banded. The diorite occurs as two thin lenses with long axes of 240 and 1100 m, oriented roughly parallel to the Granby Fault. The observed foliation and shearing within this unit suggest that it may have been intruded during a deformation event. Because of textural similarity and comparable shape and orientation of the two units, the diorite (Di) could be genetically associated with the sheared granodiorite (CGd).

STRUCTURAL GEOLOGY

Footwall

Gneisses and other high-grade metamorphic rocks of the Grand Forks complex display a penetrative planar fabric represented by mineral foliation, leucosomes and gneissosity. This foliation is here termed S_1. Primary layering S_0, defined by the contacts between the various meta-sedimentary units, appears to be conformable with the regional foliation and gneissic layering, suggesting that it was transposed along the S_1 surface. The S_1 gneissosity within the western margin of the complex generally strikes north-south, with shallow dips to the west. This regional fabric controls the orientation of pegmatite sills and of larger bodies of coarse leucogranite.

The variation of the S_1 foliation through the map area is presented on an equal-area stereographic projection (Figure 4). The distribution of the poles to gneissosity indicates an overall gentle dip-direction to the west and southwest, with a calculated mean S_1 surface oriented 166/34W.

Small-scale folding of the S_1 surface is observed throughout the complex. The style of the minor folds is variable, even within the same unit. They can range from similar to parallel, from tight to open. Wavelengths vary from a few centimetres to metres. Folding is typically cylindrical, with straight fold axes at the outcrop scale. The observed axial surfaces are parallel to the surrounding S_1 surfaces (outside the hinge zone).

A mineral lineation defined by the alignment of sillimanite crystals can be observed in the gneisses. This lineation is also expressed by small crenulations in biotite-rich layers. The lineations are consistently parallel to the fold axis of the previously described minor folds. Since these lineations are always developed on the (locally crenulated) S_1 surface, they are here termed L_2. The measured mineral lineations tend to be gently plunging (<45°), and generally trend to the northwest (Figure 4). The mean lineation, calculated from 13 relatively invariant measurements, is 310-41.

Although brittle deformation features are observed in the rocks close to the Granby fault (see below), the ductile fabrics noted above show no changes in the vicinity of the fault zone, suggesting that they represent deformation events that predate the Granby fault. Whether the structural features within the Grand Forks complex in the study area are the result of two distinct tectono-thermal events, responsible respectively for the S_1 foliation, an the L_2 lineation and minor folds, or represent complexitie in one main tectono-thermal event, cannot be determine at present. The gently west-dipping structures (i.e. S_1, L are part of an overall dome-shaped structure of the Gran Forks complex (1970a) and Kettle dome (Cheney, 1980) in which the foliation and lineation gently dips toward th eastern and western margins of the complex, defining large-scale antiform. Such doming could result fro isostatic uplift of the core complex following it exhumation during crustal extension. Therefore, domin driven by Eocene normal faulting, which denuded th Grand Forks complex (Parrish *et al.*, 1988), could hav led to the shallow tilting to the west (in the order of 30 or dip of the mean S_1) of the structural fabrics in th northwestern margin of the complex, assuming sub-horizontal S_1 before faulting.

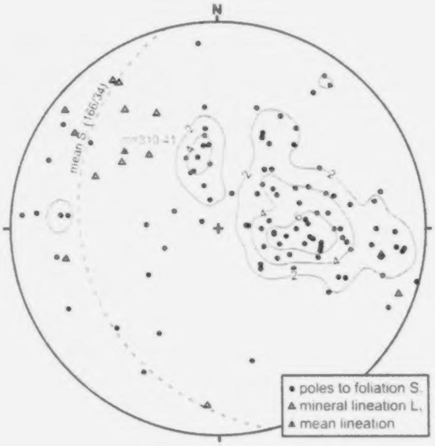

Figure 4: Equal-area stereographic projection of poles t foliation S_1 (gneissosity) in the Grand Forks complex, an mineral lineation L_1. Calculations are based on 103 S_1 an 13 L_1 measurements. Contours for poles to foliation i percent, based on a spherical Gaussian grid with weighting factor k=100 (1% area equivalent) and Gaussian minimum value of 0.05. The great circl represents the calculated mean foliation.

Hanging-wall

Structural data in the hanging-wall of the Granb fault is limited by poor exposure and by the massiv nature of most units. Scarce primary bedding o geological contacts (S_0) were measured, but foliations o other penetrative fabric were not observed. Hanging-wal rocks are highly fractured, but the complexity and lack o consistency of the fracture sets has so far defied analysis.

Minor faults are present throughout the hanging-wal but are rarely clearly exposed. A hanging-wall fault o significant extent is however mapped in the northern hal of the map area, and is herein named Volcanic Mountai fault (Figure 3). It is a normal fault striking north

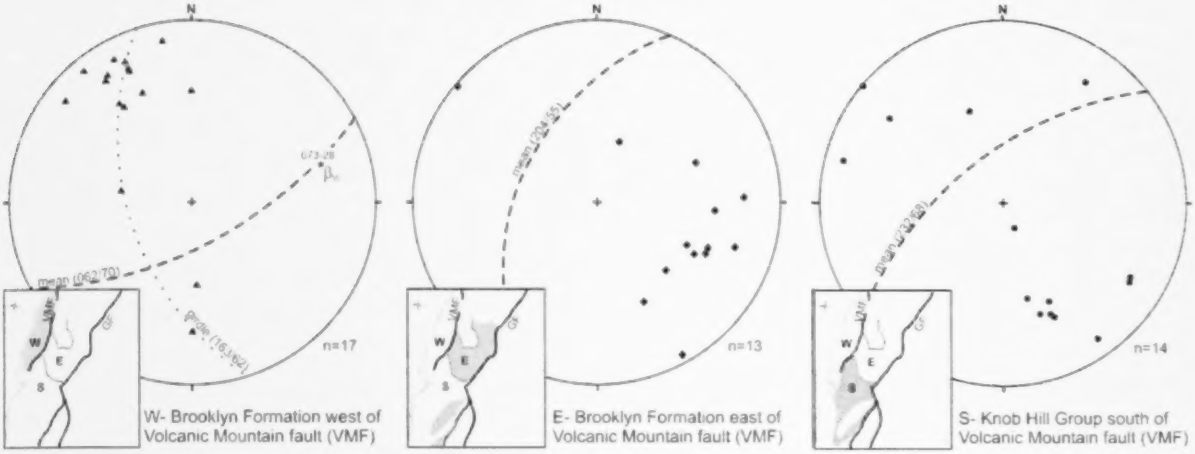

W- Brooklyn Formation west of Volcanic Mountain fault (VMF)

E- Brooklyn Formation east of Volcanic Mountain fault (VMF)

S- Knob Hill Group south of Volcanic Mountain fault (VMF)

Figure 5: Equal-area stereographic projection of poles to bedding S_0 west of the Granby fault (GF). Data has been separated in 3 structural domains bounded by the Volcanic Mountain fault (VMF) and the unconformity between the Knob Hill Group and the Brooklyn Formation. Granby Fault.

northeast and dipping 40° to 50° to the west, according to its trend across the topography. It is extended towards the north based on regional work by Fyles (1990). The fault's orientation suggests that it could be related to the Granby fault.

Ductile deformation in the hanging-wall of the Granby fault is rarely seen, with the exception of folding within one unit. Extensive parallel folding with wavelengths of a metre to tens of metres is displayed within the inter-bedded marble and chert unit on the steep west-facing slope next to the Granby River (Photo 4). The meso-scale folding in this unit is perhaps due to the favorable rheological properties (i.e. ductility) of the inter-bedded marble and chert compared to other units. Macro-scale folding is seen in a small overturned synform in the south of the map area, with meta-conglomerate in its core, and in a possible antiformal structure associated with the meta-conglomerate in the northwest.

Equal-area stereographic projections of poles to bedding are plotted in Figure 5. Three structural domains are defined: (1) a western domain within the Brooklyn Formation, west of the Volcanic Mountain fault, (2) an eastern domain within the Brooklyn Formation, east of the Volcanic Mountain fault, and (3) a southern domain within the Knob Hill Group. Each domain yields different overall bedding orientation, although in all domains there is a generally northeast-southwest strike. In the western domain, where folding has been observed at the outcrop-scale (Photo 4), poles to bedding suggest a fold axis gently plunging to the north-northeast, consistent with outcrop measurement of a fold axis of 075-25. Although separated by an unconformity, the mean bedding plane in the eastern and southern domains have similar orientations.

Granby Fault

The Granby fault separates low-grade metamorphic rocks of the hanging-wall (west of fault) from high-grade rocks of the Grand-Forks Complex in the footwall (east of fault). The trace of the Granby fault crosses the map area from south-southwest to north-northeast. The fault zone is characterized by a zone of brittle deformation (cataclasis) in which both hanging-wall and footwall rocks are brecciated and crushed. Fault zone rocks are cohesive breccias and cataclasites, suggesting recrystallization at moderate depths. Breccias are characterized by anastomosing shear zones up to a few millimetres in thickness, containing small angular crushed crystal fragments ± chlorite, which cut through existing larger crystals (e.g. quartz and feldspars in pegmatite; clasts in conglomerate). Cataclasites are fine-grained, green, cohesive rocks, composed in part by recrystallized chlorite + quartz ± fluorite, and locally containing remnant subrounded crystal fragments (usually quartz).

The zone of cataclasis and brecciation varies in thickness through the map area. In the central part, between Volcanic and Hornet Creek, the zone of brittle deformation is on average ~100 metres thick and affects both hanging-wall and footwall rocks. In the North, the crush zone is up to ~230 metres thick and is largely restricted to the syenite unit (Sy) in the hanging-wall. In the South, near Toronto Creek, the zone of brittle deformation is up to ~300 metres in thickness, and is largely restricted to the crushed granodiorite unit (CGd) and some gneisses and pegmatite of the footwall.

The orientation of the fault in three dimensions can be estimated from its map trace. The Granby fault strikes south to south-southwest, and from its trace across topography, appears to dip ~35° to the west. Some outcrop surfaces of cataclasites and breccias observed along or near the fault plane display a similar orientation (parallel to the fault plane?), although others do not display any consistent planar fabric.

The latest displacement on the Granby fault is interpreted to be younger than 51.1 Ma, the age of the Coryell syenite, owing to deformation of syenite dikes in the fault zone. Accepting the biotite and hornblende K-Ar data for cooling of the Kettle gneiss (50-67 Ma, Engels *et al.*, 1976), displacement on the fault may have occurred over a period of tens of millions of years.

METAMORPHISM

Footwall – Grand Forks complex

The presence of garnet + cordierite + K-feldspar in the pelitic gneiss combined with the absence of orthopyroxene in the amphibolite (metabasite) implies that the core complex is in the transitional zone between upper amphibolite and granulite facies (Figure 6). Regional metamorphism affecting these rocks is therefore low to medium pressure (<7.5kbar) and moderately high temperature, between ca. 700 and 850°C.

The peak mineral assemblage of the metapelite is Sil +Crd +Grt +Bt +Kfs +Pl +Qtz +leucosome, the latter inferred to be partial melt (mineral abbreviations of Kretz, 1983). This assemblage lies on the model KFMASH univariant reaction Sil +Bt +Qtz +Pl = Crd +Grt +Kfs +L (Figure 6). The Fe/(Fe+Mg) ratio in the core of the garnet, assumed to preserve peak metamorphic conditions, is ~0.85 (see appendix), corresponding to a P-T condition of ~ 4 kbar at ~740°C (Figure 5 of Spear *et al.*, 1999). Assuming an averaged density for a mixed crust of 2.85 $g\cdot cm^{-3}$, or 3.6 km/kbar, this indicates a perturbed geothermal gradient of ~58°C/km (Figure 6).

Hanging-wall – Knob Hill Group and Brooklyn Formation

The metamorphosed sedimentary and volcanic rocks in the hanging-wall of the Granby fault display a markedly lower grade of metamorphism than in the footwall. The presence of hornblende in meta-volcanic rocks (see appendix) combined with the occurrence of garnet in some meta-sediments, is an indication of lower amphibolite facies metamorphism.

Coexistence of actinolite with hornblende (Figure 7, see appendix) suggests that these rocks are close to the greenschist-amphibolite transition. The occurrence of Hbl + Act + Andesine puts this assemblage above the incoming of hornblende and oligoclase, and below the terminal stability of actinolite (Bégin, 1992, Figure7). The occurrence of garnet and biotite in the meta-siltstone provides a further, albeit loose, constraint (Figure 6).

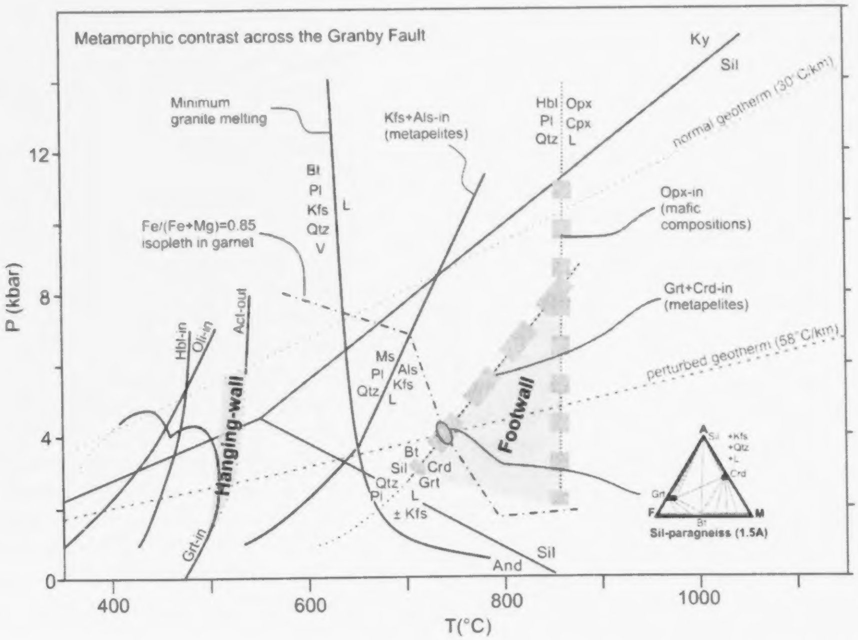

Figure 6: Pressure-temperature diagram showing the contrast in metamorphism across the Granby fault. Selected high-grade reactions are from Pattison *et al.* (2003). The Fe/(Fe+Mg) isopleth in garnet is from Spear *et al.* (1999). Mineral isograds for hornblende (Hbl), Oligoclase (Oli) and Actinolite (Act) in metabasites are from Bégin (1992). Grt-in isograd is from Tinkham *et al.* (2001). See text for discussion.

Combining the above constraints, the approximate stability zone for mineral assemblages in the hanging-wall of the Granby fault in the Volcanic Creek area is plotted in Figure 6. A maximum temperature of ~530° is indicated, with pressure largely unconstrained. Further petrological work will be undertaken to improve these constraints.

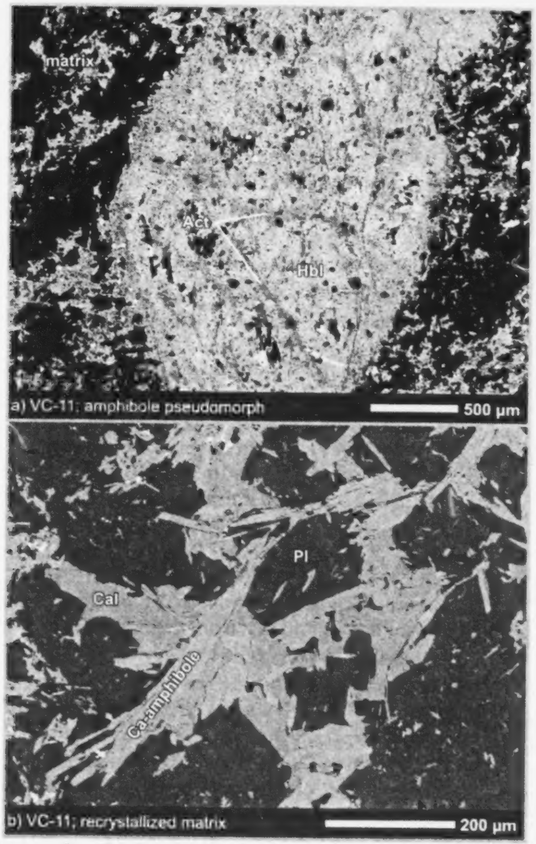
matrix
Act
Hbl
a) VC-11; amphibole pseudomorph
500 µm
Pl
Cal
Ca-amphibole
b) VC-11; recrystallized matrix
200 µm

Figure 7: Back-scattered electron image of textural relationships and occurrences of amphiboles in the meta-andesite. a) Relict clinopyroxene phenocryst recrystallized as hornblende + actinolite; b) Recrystallized matrix with acicular amphiboles, calcite and plagioclase.

P-T contrast across the Granby fault, and tectonic implications

The above constraints indicate a minimum peak temperature difference of ~200°C across the Granby fault, with pressure difference unknown at present (Figure 6). The timing of peak metamorphism on either side of the Granby fault has yet to be determined, so that the observed P-T contrast may or may not constrain the extent of movement on the fault. If it is assumed that peak metamorphism was synchronous in the hanging-wall and footwall, and that the rocks lay on the same geothermal gradient, a tentative estimate of the depth contrast across the fault can be made. Using the estimated geothermal gradient for the footwall paragneiss of 58°C/km, a minimum temperature contrast of 200°C represents a minimum depth difference of ~4 km. With a dip of 35°, the Granby fault could have therefore accommodated 7 km or more of horizontal displacement during Tertiary extensional events.

A composite cross-section drawn by Fyles (1995) suggests that the west side of the Granby fault consists of a succession, some 4-6 km thick, of thrust slices repeating the Knob Hill Group and overlying Brooklyn Formation. This would require at least 4-6 km west-side-down slip on the Granby fault near Grand Forks, supporting the estimated displacement suggested by the metamorphic contrast.

CONCLUSIONS

The west-dipping Granby normal fault juxtaposes lowermost amphibolite facies rocks of Quesnel Terrane in its hanging-wall against transitional upper-amphibolite to granulite facies metamorphic rocks of the Grand Forks core complex in its footwall. The Grand Forks complex in the Volcanic Creek area consists of metapelitic gneiss, quartzite, marble and amphibolite, with significant volumes of granitic pegmatite interpreted to be due to *in-situ* anatectic melting. The rocks of the Quesnel Terrane consist of chert, siltstone and greenstone of the Knob Hill Group, overlain unconformably by sharpstone-conglomerate and related units of the Brooklyn Formation.

The Granby fault is a zone of brittle deformation tens to hundreds of metres wide, which dips gently (~35°) to the west. Normal displacement along the fault appears to be synchronous, at least in part, with the emplacement of dikes related to the 51.1 Ma Coryell plutonic suite.

The peak metamorphic temperature contrast across the fault is at least 200°C, with pressure unconstrained. The age of metamorphism on either side of the fault is unknown. Assuming synchronous metamorphism and similar geothermal gradient across the fault, the Granby fault could have accommodated a minimum of 4 km of vertical displacement, or 7 km or more horizontally. Further P-T work and thermochronometry is required to better constrain the evolution of the Granby fault.

ACKNOWLEDGMENTS

Financial support for fieldwork was provided by Natural Sciences and Engineering Research Council Grant 0037233 to D.R.M. Pattison. J.D. Laberge would like to acknowledge financial support from the Department of Geology and Geophysics at the University of Calgary. Scott McLaren provided efficient assistance and great company in the field. Critical review by Rob Brady helped improved this document.

REFERENCES

Acton, S. L., Simony, P. S. and Heaman, L. M. (2002): Nature of the basement to Quesnel Terrane near Christina Lake, southeastern British Columbia. *Canadian Journal of Earth Sciences*, 39(1), p. 65-78.

Armstrong, R. L., Parrish, R. R., van, d. H. P., Scott, K., Runkle, D. and Brown, R. L. (1991): Early Proterozoic basement exposures in the southern Canadian Cordillera; core gneiss of Frenchman Cap, Unit I of the Grand Forks Gneiss, and the Vaseaux Formation. *Canadian Journal of Earth Sciences*, 28, p. 1169-1201.

Bégin, N. J. (1992): Contrasting mineral isograd sequences in metabasites of the Cape Smith Belt, northern Québec, Canada: three new bathograds for mafic rocks. *Journal of Metamorphic Geology*, 10, p. 685-704.

Carr, S. D. and Parkinson, D. L. (1989): Eocene stratigraphy, age of the Coryell Batholith, and extensional faults in the Granby Valley, southern British Columbia. *Geological Survey of Canada Paper 89-1E*, p. 79-87.

Cheney, E. S. (1977): The Kettle Dome; the southern extension of the Shuswap terrane into Washington. *Abstracts with Programs - Geological Society of America*, 9(7), p. 926.

Cheney, E. S. (1980): Kettle dome and related structures of northeastern Washington. In: *Cordilleran metamorphic core complexes* (eds Crittenden, M. D., Coney, P. J. and Davis, G. H) *GSA Memoir 153*, p. 463-483.

DePaoli, G. R. and Pattison, D. R. M. (1995): Constraints on temperature-pressure conditions and fluid composition during metamorphism of the Sullivan orebody, Kimberley, British Columbia, from silicate-carbonate equilibria. *Canadian Journal of Earth Sciences*, 32, p. 1937-1949.

Engels, J. C., Tabor, R. W., Miller, F. K. and Obradovich, J. D. (1976): Summary of K-Ar, Rb-Sr, U-Pb, Pbalpha , and fission-track ages of rocks from Washington State prior to 1975 (exclusive of Columbia Plateau basalts*). USGS Miscellaneous Field Studies Map*, MF-0710.

Fyles, J. T. (1995): Knob Hill Group, Attwood Formation and Brooklyn Formation. In: Roback, R., Schiarizza, P., Nelson, J., Fyles, J., Ferri, F., Hoy, T., Ash, C. and Danner W.R.: Late Paleozoic Arc and Oceanic Terranes and their Exernal Relationships, Southern Quesnellia. *Geological Association of Canada, Field Trip Guidebook*, Victoria '95, p. 40-43.

Fyles, J. T. (1990): Geology of the Greenwood-Grand Forks area, British Columbia; NTS 82E/ 1,2. *British Columbia Ministry of Energy, Mines and Petroleum Resources*, Open File, 19 p.

Gabrielse, H., Monger, J. W. H., Wheeler, J. O. and Yorath, C. J. (1991): Morphogeological belts, tectonic assemblages, and terranes, Chapter 2, part A. In: *Geology of the Cordilleran Orogen in Canada* (eds Gabrielse, H. and Yorath, C. J.) *Geology of Canada*, p. 13-59.

Kretz, R. (1983): Symbols for rock-forming minerals. *American Mineralogist*, 68, p. 277-279.

Leake, B. E., Woolley, A. R., Arps, C. E. S., Birch, W. D., Gilbert, M. C., Grice, J. D., Hawthorne, F. C., Kato, A., Kisch, H. J., Krivovichev, V. G., Linthout, K., Laird, J., Mandarino, J. A., Maresch, W. V., Nickel, E. H., Rock, N. M. S., Schumacher, J. C., Smith, D. C., Stephenson, N. C. N., Ungaretti, L., Whittaker, E. J. W. and Guo, Y. (1997): Nomenclature of amphiboles; report of the subcommittee on amphiboles of the International Mineralogical Association, Commission on New Minerals and Mineral Names. *The Canadian Mineralogist*, 35 (1), p. 219-246.

Little, H. W. (1983): Geology of the Greenwood map-area, British Columbia, *Geological Survey of Canada*, Paper 79-29, 37 p.

Little, H. W. and Thorpe, R. I. (1965): Greenwood map-area, British Columbia. *Geological Survey of Canada*, Paper 65-1, p. 55-60.

Lorencak, M., Seward, D., Vanderhaeghe, O., Teyssier, C. and Burg, J. P. (2001): Low-temperature cooling history of the Shuswap metamorphic core complex, British Columbia; constraints from apatite and zircon fission-track ages. *Canadian Journal of Earth Sciences*, 38(11), p. 1615-1625.

Massey, N. W. D., MacIntyre, D. G. and Desjardins, P. J. (2003): Digital Map of British Columbia: Tile NM11 Southeast B.C., *British Columbia Ministry of Energy and Mines*, Geofile 2003-2.

Parrish, R. R., Carr, S. D. and Parkinson, D. L. (1988): Eocene extensional tectonics and geochronology of the southern Omineca Belt, British Columbia and Washington. *Tectonics*, 7(2), p. 181-212.

Parrish, R. R., Ross, G., Carr, S. D., Coleman, V. and Journeay, J. M. (1989): Single grain U-Pb provenance ages of detrital zircons from metaquartzites of the southern Omineca Belt, British Columbia. *Abstracts with Programs - Geological Society of America*, p. 127-128.

Pattison, D. R. M., Chacko, T., Farquhar, J. and McFarlane, C. R. M. (2003): Temperatures of granulite-facies metamorphism: constraints from experimental phase equilibria and thermobarometry corrected for retrograde exchange. *Journal of Petrology*, 44(5), p. 867-901.

Preto, V. A. (1970a): Structure and petrology of the Grand Forks Group, British Columbia, *Geological Survey of Canada*, Paper 69-22, 80 p.

Preto, V. A. G. (1970b): Amphibolites from the Grand Forks Quadrangle of British Columbia, Canada. *Geological Society of America Bulletin*, 81(3), p. 763-782.

Rhodes, B. P. and Cheney, E. S. (1981): Low-angle faulting and the origin of Kettle Dome, a metamorphic core complex in northeastern Washington. *Geology*, 9(8), p. 366-369.

Ross, G. M. and Parrish, R. R. (1991): Detrital zircon geochronology of metasedimentary rocks in the southern Omineca Belt, Canadian Cordillera. *Canadian Journal of Earth Sciences*, 28(8), p. 1254-1270.

Spear, F. S., Kohn, M. J. and Cheney, J. T. (1999): P-T paths from anatectic pelites. *Contributions to Mineralogy and Petrology*, 134(1), p. 17-32.

Vanderhaeghe, O., Teyssier, C. and Wysoczanski, R. (1999): Structural and geochronological constraints on the role of partial melting during the formation of the Shuswap metamorphic core complex at the latitude of the Thor-Odin Dome, British Columbia. *Canadian Journal of Earth Sciences*, 36(6), p. 917-943.

Wheeler, J. O. and McFeely, P. (1991): Tectonic Assemblage Map of the Canadian Cordillera and adjacent parts of the United States of America. *Geological Survey of Canada*, Map 1712A.

APPENDIX

Mineral compositions were acquired using wavelength-dispersive analysis on the JEOL JXA-8200 electron microprobe at the University of Calgary, using standard operating conditions (15 kV; 10 nA; focused beam) and a range of well-characterized natural and synthetic standards (e.g. DePaoli and Pattison, 1995). Quantitative analyses were subjected to matrix corrections based on the ZAF method. Results of analyses of garnet of the footwall and amphiboles of the hanging-wall are presented in tables 1 and 2, respectively. Estimates of Fe^{3+}/Fe^{2+} in amphiboles is the average between maximum and minimum estimates based on the method outlined by Schumacher (appendix 2 in Leake *et al.*, 1997). Amphibole names are based on the IMA nomenclature of amphiboles (Leake *et al.*, 1997).

Table 1: Average analyses of garnet in Sil-paragneiss (gran 1.5A). The numbers of cations calculated for the structural formulae are based on 12 oxygens.

	core	rim
SiO_2	37.01	37.66
Al_2O_3	20.95	20.78
FeO	28.58	28.78
MnO	7.72	9.04
MgO	2.91	2.24
CaO	2.34	2.12
Total	99.51	100.63
Cations based on 12 oxygens:		
Si	2.99	3.02
Al	2.00	1.97
Fe^{2+}	1.93	1.93
Mg	0.35	0.27
Mn	0.53	0.62
Ca	0.20	0.18
X Alm	0.64	0.64
X Prp	0.12	0.09
X Sps	0.18	0.21
X Grs	0.07	0.06
Fe/(Fe+Mg)	0.85	0.88

Table 2: Averaged representative analyses of amphiboles. The numbers of cations calculated for the structural formulae are based on 23 oxygen equivalents (O-F,Cl,OH).

	Meta-conglomerate (gran 6B)	Relict phenocryst in meta-andesite (VC-11)		Matrix amphibole in meta-andesite (VC-11)	
SiO2	44.88	50.79	47.27	51.88	48.37
TiO2	0.22	0.07	0.28	0.25	0.21
Al2O3	9.68	4.5	8.14	3.45	6.06
FeO	16.7	13.53	15.84	13.04	14.73
MnO	0.81	0.52	0.53	0.56	0.5
MgO	10.92	14.51	12.12	15.22	14.47
CaO	12.14	13.36	12.07	12.25	11.51
Na2O	0.85	0.42	0.97	0.44	0.52
K2O	0.41	0.16	0.27	0.08	0.16
F	0.04	ND	ND	0.02	ND
total	96.65	97.86	97.49	97.19	96.53
Cations based on 23 oxygens :					
Si	6.69	7.36	6.94	7.50	7.04
Al	1.70	0.77	1.41	0.59	1.04
Ti	0.03	0.01	0.03	0.03	0.02
Fe2+	1.47	1.36	1.51	1.25	0.85
Fe3+	0.61	0.28	0.43	0.32	0.88
Mg	2.43	3.13	2.65	3.28	3.14
Mn	0.10	0.06	0.07	0.07	0.06
Ca	1.94	2.00	1.90	1.90	1.80
Fe	0.00	0.00	0.01	0.01	0.07
Na	0.25	0.12	0.28	0.12	0.15
K	0.08	0.03	0.05	0.02	0.03
F	0.02	0.00	0.00	0.01	0.00
OH	1.98	2.00	2.00	1.99	2.00
cat. SUM	15.29	15.19	15.27	15.08	15.07
Fe/(Fe+Mg)	0.46	0.34	0.42	0.33	0.36
Mineral species	Magnesio-hornblende	Actinolite	Magnesio-hornblende	Actinolite	Magnesio-hornblende

STRATIGRAPHY AND STRUCTURE OF THE WILD HORSE RIVER AREA, SOUTHEASTERN BRITISH COLUMBIA

By Kyle P. Larson[1] and Raymond A. Price[1]

KEYWORDS: Regional geology, Fernie map-area, Southern Canadian Cordillera thrust and fold belt, Paleozoic sediments and volcanics, mid-Cretaceous plutons.

INTRODUCTION

The Wild Horse River area is situated in an anomalous part of the western Main Ranges of the Rocky Mountains near Cranbrook, B.C. (Figure 1). It lies immediately north of the transverse NE-trending Boulder Creek fault which is part of the Crowsnest Pass Cross Strike Disconintuity (CPCSD; Price, 1994, 2000), a major structural and stratigraphic discontinuity in the Southern Cordillera that coincides with a 220 km right hand offset in the margin of the Cordilleran miogeocline. The anomalous features of the Wild Horse River area include: conspicuous variations in Cambrian stratigraphy, the occurrence of anomalous mafic volcanics within Cambrian and Ordovician miogeoclinal strata, several small mid Cretaceous (?) plutons, and the enigmatic steep northeast-trending Boulder Creek transverse fault. This critical segment of the western Main Ranges has the potential to provide important new insights on the tectonic evolution of the Cordilleran miogeocline and the Cordilleran foreland thrust and fold belt in the vicinity of the CPCSD.

The stratigraphic succession in the Wild

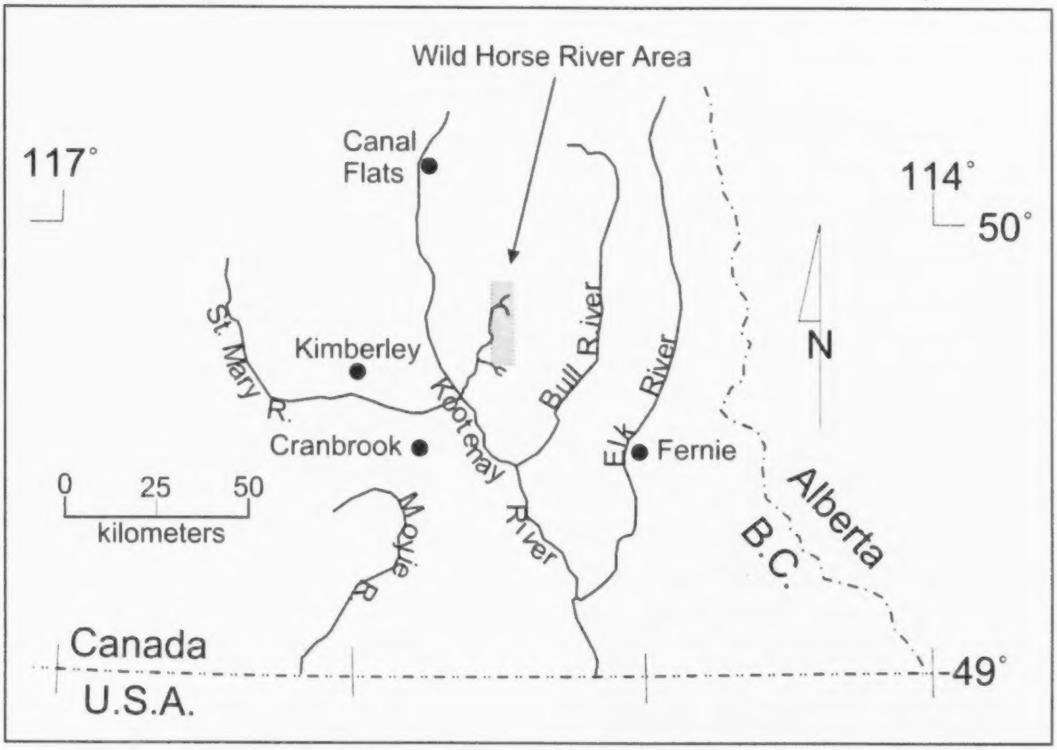
Wild Horse River Area
117°
114°
50°
49°
Canal Flats
Kimberley
Cranbrook
Fernie
St Mary R.
Kootenay River
Bull River
Elk River
Moyie R.
N
0 25 50
kilometers
Alberta
B.C.
Canada
U.S.A.

Figure 1. Location map of the Wild Horse River area (outlined in grey).

---

[1] Queen's University, Kingston, ON

Horse River area comprises Cambrian and Ordovician miogeoclinal carbonate rocks, shales and sandstones that unconformably overlie Mesoproterozoic sedimentary rocks of the Purcell Supergroup (Schofield 1922; Rice, 1937; Leech, 1958; Welbon and Price, 1992a, 1992b, 1993). The geological structure of the Wild Horse River area is complex, comprising, west-verging back thrusting and folding along the western flank of the Porcupine Creek fans structure, and superposed east-verging structures associated with the Lussier River thrust fault, which underlies the eastern limb of the Purcell anticlinorium. At least part of the displacement on the anomalous transverse, northeast trending Boulder Creek fault, may be related to the much younger (Tertiary) normal faulting that produced the Southern Rocky Mountain Trench. Detailed structural mapping in the Wild Horse River area has outlined the relationships between east and west verging structures, and has elucidated the enigmatic stratigraphy, and timing relationships between thrusting and folding and the mid-Cretaceous plutons.

PREVIOUS WORK

The initial systematic outline of the regional geology of the Cranbrook region was based on reconnaissance geological mapping by J.S. Schofield (1922). Subsequently H.M.A. Rice (1937) published a more detailed map (1 inch = 1 mile) and description of the regional bedrock geology of the Cranbrook map area, which includes the southwest corner of the Wild Horse River area. In the late 1950's G.B. Leech (1958, 1960) produced a 1 inch = 2 miles map of the Fernie map area, west half, that encompassed all of the Wild Horse River area and he also defined the regional geological setting upon which later more detailed studies have been based. More recently, H y (1982, 1985) and McMechan (1979) have produced more detailed maps (1:50,000) of the Mesoproterozoic rocks; Welbon and Price (1992a, 1992b, 1993) produced more detailed maps of the relationships between the Mesoproterozoic and Cambrian rocks of the Hughes Range; Norford and Cecile (1994a, 1994b) have described the complex stratigraphic and structural relationships of Ordovician and Upper Cambrian sedimentary and volcanic rocks in the Wild Horse River area, and Stretch (1997) has outlined detailed structure and anomalous stratigraphy in the area adjacent to and southeast of the Wild Horse River area.

STRATIGRAPHY

The Wild Horse River area includes parts of two distinct fault-separated tectonostratigraphic domains (Figure 2) each characterized by a distinctive Lower Paleozoic stratigraphy and structural style. In the Hughes Range a relatively thin Lower Cambrian platformal shallow-water succession unconformably overlies Mesoproterozoic sedimentary rocks of the Purcell Supergroup. In the Tanglefoot domain the Purcell Supergroup is overlain by a thick succession of Cambrian and Ordovician shale and shaley carbonate miogeoclinal rocks, including deep water and slope deposits.

The Cranbrook Formation

The Lower Cambrian Cranbrook Formation (Schofield, 1922), which unconformably overlies Mesoprotererozoic Purcell Supergroup sediments in the Cranbrook area, typically consists of massive coarse-grained, white, pale red and grayish purple quartz arenites (locally conglomeratic) in beds up to 1 m thick; crossbedding is common (Rice, 1937; Leech, 1958; Stretch, 1997).

In the Wild Horse River area (Figure 3) the Cranbrook Formation comprises up to 100 m of coarse to medium grained, white to grayish purple, blocky weathering quartz arenite. Conglomeratic sandstones, which are common locally, contain pebbles of quartz and quartzite. The Cranbrook Formation varies locally throughout the map area. In the Boulder Creek area, in the hanging-wall of the Lussier River Thrust it occurs as a fine grained dark brown to black weathering sandy siltstone interbedded with thin (<0.5m) lenses of buff to light brown weathering quartz arenite. The variability of the Cranbrook Formation may be due in part to stratigraphic on-lap of local structures produced by Cambrian block faulting (Welbon and Price, 1993).

The Eager Formation

The Lower Cambrian Eager Formation (Schofield, 1922) consists of a thick succession of dark grey, commonly rusty weathering argillite (Rice, 1937) with minor interbedded dark brown shales, siltstone and limestone (Leech, 1958). The contact with the underlying

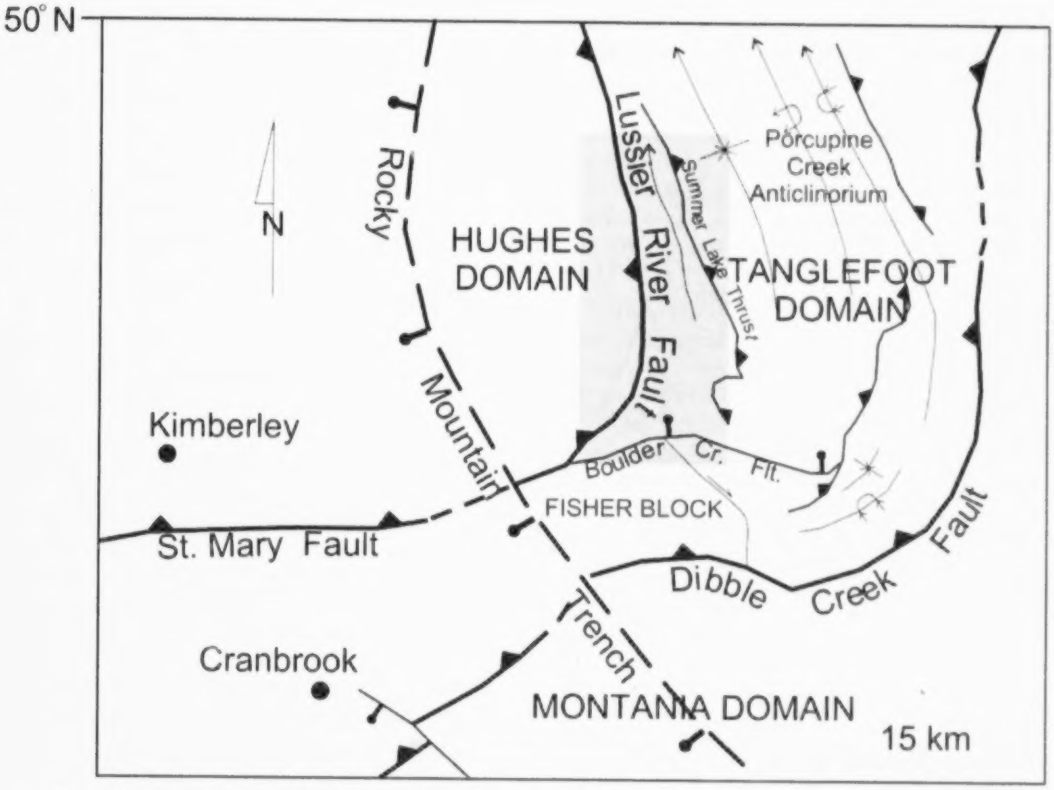

Figure 2. Tectonostratigraphic domains of the Wild Horse River area (shown in grey) and the surrounding region. The Fisher block within the Tanglefoot domain comprises an east-northeast facing panel of Mesoproterozoic rocks beneath a décollement in the Eager Formation. Modified from Stretch (1997).

Cranbrook Formation is conformable (Leech, 1958; Stretch, 1997), characterized by transitional interbedded fine sands and argillite (Schofield, 1922), however, some studies have suggested local disconformity at the base of the Eager Formation (Rice, 1937).

The Eager Formation in the Wild Horse River area occurs as two separate and distinct successions: 1) "thin" Eager within the Hughes Range domain and 2) the "thick" Eager in the Tanglefoot domain. The "thin" Eager, which is missing locally because of erosion beneath the unconformably overlying Jubilee Formation, is a thin veneer of shale and/or shallow-water limestone on top of the Cranbrook Formation (Leech, 1958). The "thick" Eager of the Tanglefoot domain comprises up to 2000 m (Rice, 1937) of dark grey, brown to black weathering, structurally incompetent argillite with minor dark to medium grey weathering argillite and minor shale (Leech, 1958; Stretch, 1997). Beds (where discernable) are about 1 cm thick commonly with micaceous partings. In the Wild Horse River area, Middle Cambrian deep-water, resedimented carbonate deposits of the "Tanglefoot Unit" overlie the "thick" Eager Formation with apparent conformity.

Jubilee Formation

The Middle (?) to Upper Cambrian Jubilee Formation (Evans, 1933; Henderson, 1954; Leech, 1954, 1958, 1960) occurs in the Hughes Range domain. It is a cliff-forming succession of platformal dolostone that is about 1200 m thick (Leech, 1954). A lower division consists of finely laminated, medium bedded, light grey and white, cream to dark grey weathering dolostone (Leech, 1954); an upper division comprises poorly bedded, dominantly massive, locally coarsely crystalline medium grey dolostone (Leech, 1954). The Jubilee Formation overlies the "thin" Eager and Cranbrook Formations and locally the Mesoproterozoic strata of the Purcell Supergroup unconformably (Leech, 1954, 1958, 1960; Welbon and Price 1992a, 1992b, 1993), however, Leech (1958) noted the contact between the Jubilee Formation and underlying Lower Cambrian rocks may locally be transitional. Upper Cambrian rocks of the basal unit of the McKay Group

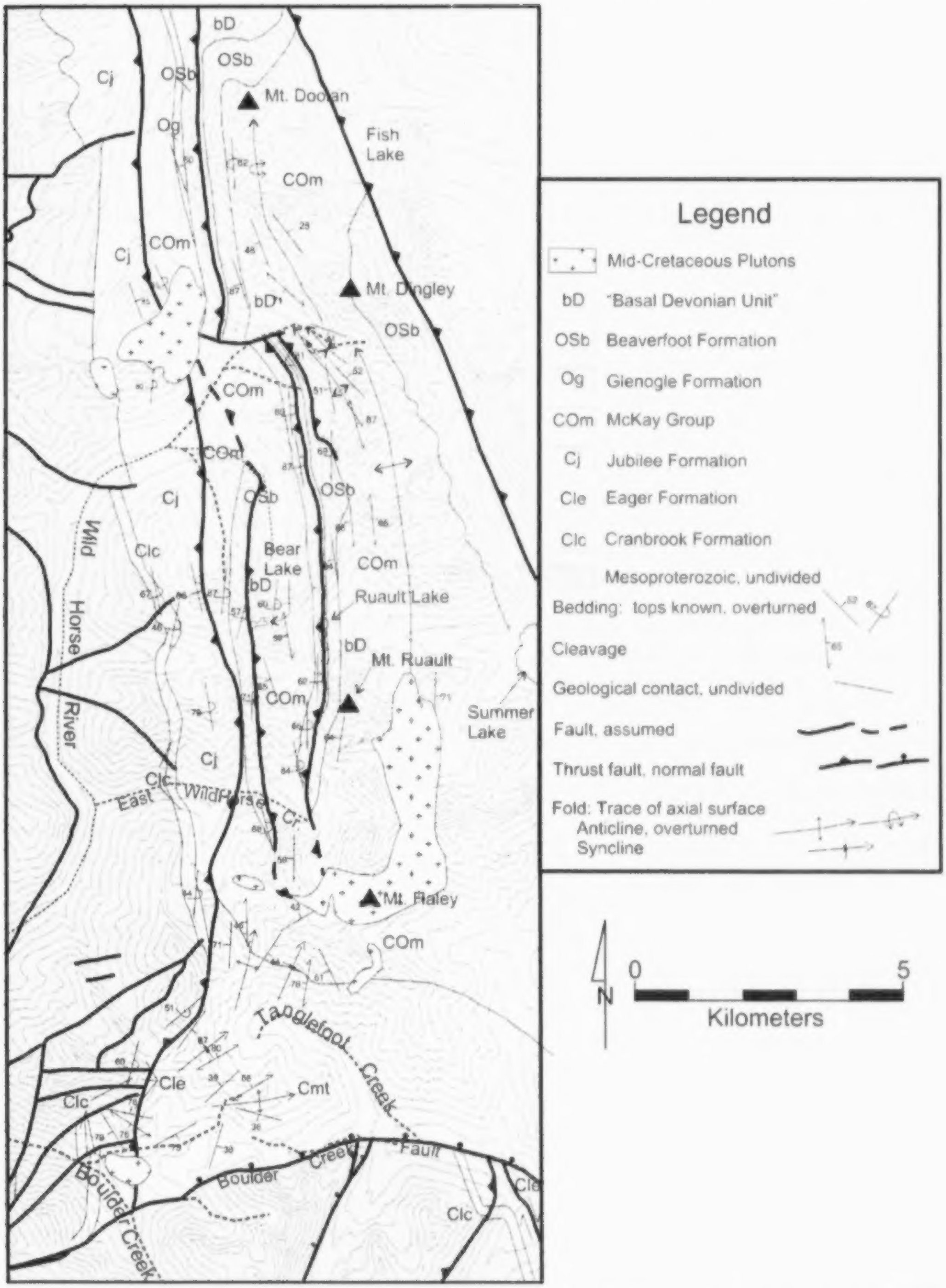
bD
OSb
Cj
Og
Mt. Doolan
Fish Lake
COm
Mt. Dingley
bD
Bear Lake
Ruault Lake
Mt. Ruault
Summer Lake
Wild Horse River
Clc
East Wildhorse Cr.
Mt. Haley
Tanglefoot Creek
Cle
Cmt
Boulder Creek Fault
Boulder Creek
Legend
Mid-Cretaceous Plutons
bD "Basal Devonian Unit"
OSb Beaverfoot Formation
Og Glenogle Formation
COm McKay Group
Cj Jubilee Formation
Cle Eager Formation
Clc Cranbrook Formation
Mesoproterozoic, undivided
Bedding: tops known, overturned
Cleavage
Geological contact, undivided
Fault, assumed
Thrust fault, normal fault
Fold: Trace of axial surface
Anticline, overturned
Syncline
N
0
5
Kilometers

Figure 3. Geological map of the Wild Horse River area. See text for unit descriptions. The data are from 2003 field work plus Leech (1958, 1960), Welbon and Price (1993), and Stretch (1997).

conformably overlie the Jubilee Formation.

"Tanglefoot Unit"

The Middle Cambrian "Tanglefoot unit"(Leech, 1958, 1960; Thompson, 1962; Stretch, 1997) occurs in the Tanglefoot domain, where it conformably overlies the Eager Formation. It consists of banded, medium to dark grey and brown weathering, medium to dark grey argillaceous allodapic limestone, mudstone, wackestone and packstone, carbonate breccia, with minor dolostone and shale (Stretch, 1997). In the Boulder Creek area the "Tanglefoot unit" locally contains intercalated andesitic extrusive volcanics. The "Tanglefoot unit" which is unique to the southern end of the western Main Ranges of the Canadian Rocky Mountains, resembles parts of the Chancellor Formation of the Kickinghorse Pass area. In the Wild Horse River area it appears to be conformably gradational into the overlying McKay Group, which is underlain by the Ottertail Limestone in the Kickinghorse Pass area. The upper part of the "Tanglefoot unit", at least, occupies the same stratigraphic position as the Jubilee Formation and thus the two units may be lateral equivalents. The Jubilee Formation and the "Tanglefoot unit" have not been observed in stratigraphic contact.

McKay Group

The Upper Cambrian and Lower Ordovician McKay Group (Evans, 1933; Leech 1958; Aitken and Norford, 1967) is a widespread 1-1.5 kilometer thick succession of thin-bedded light coloured shales and limestones. The McKay Group is separable into two main lithologic divisions: a lower recessive shale dominated division with minor nodular shaley limestones, and a more resistant cliff-forming upper division comprising thinly bedded grey limestones with minor intercalated shale (Leech, 1958).

In the Wild Horse River Area the McKay Group is characterized by an upper division dominated by light to medium grey weathering, medium grey fresh, thin to medium bedded limestone, argillaceous limestone and minor dolomite, and a lower succession of dark grey to rusty brown weathering, medium grey fresh limey shales, nodular limestone and minor thinly bedded limestone. McKay Group rocks conformably overly the Jubilee Formation in the Hughes Range domain and the "Tanglefoot unit" in the Tanglefoot domain. They are locally conformably overlain by the Glenogle Formation, but most commonly are found unconformably below the Beaverfoot Formation. The sub-Beaverfoot unconformity cuts down section to the south, removing most, if not all of the Ordovician McKay Group strata (Norford and Cecile, 1994a).

The McKay Group in the Wild Horse River area is enigmatic because it contains abundant intercalated volcanic rocks (Norford and Cecile 1994a, 1994b). These are mainly volcanic agglomerates consisting of coarse sand to cobble sized clasts of orange weathering dolostone and dark green-grey volcanic clasts, but amygdular, intermediate to mafic volcanic flows are also common. The volcanic rocks within the McKay Group are not widespread; they occur mainly within one thin (<1km) north-south trending thrust-fault sheet.

Glenogle Formation

The Middle Ordovician Glenogle Formation (Burling, 1922; Henderson, 1954; Leech 1954, 1958) typically comprises < 300 meters of black, locally calcareous graphitic shale and dark grey laminated silty shale. It conformably and gradationally overlies Cambro-Ordovician limestones and shales of the McKay Group, and is unconformably overlain by either the Ordovician Mount Wilson Formation (Norford, 1964) or the Ordovician and Silurian Beaverfoot Formation.

The Glenogle Formation is only present at the extreme northern edge of the Wild Horse River Area, where it forms a thin (<100 m) south-tapering wedge beneath the sub-Beaverfoot unconformity. It comprises dark brown to black, laminated mudstone and quartz wackestone overlain by black limestone containing 2-3 mm euhedral pyrite crystals.

Beaverfoot Formation

The Upper Ordovician and Lower Silurian Beaverfoot Formation (McConnell, 1887; Burling, 1922; Evans, 1933; Leech, 1958; Norford, 1962) consists of thickly bedded, medium to buff grey mottled weathering, cliff forming dolostone with minor intercalated limestone and cherty limestone. The Beaverfoot Formation, which is widespread in the Southern Canadian Rocky Mountains, records a transgressive carbonate shelf that developed above a regional unconformity.

In the Wild Horse River Area, the Beaverfoot Formation consists of ~ 250 m of mottled medium to very light grey weathering, thickly bedded (up to 1 m) medium grey, finely to medium crystalline dolostone. The Beaverfoot Formation is locally fossiliferous (corals, cephalopods, gastropods, and crinoids) and sporadically interbedded with thin (up to 20 cm), rusty red to brown weathering quartz arenite. The base of the Beaverfoot Formation in the Wild Horse River area commonly contains a 5-10 meter thick volcaniclastic unit possibly related to volcanics in the underlying McKay Group or to the Mt. Dingley diatreme, which formed after deposition of the McKay Group, but before the deposition of the Beaverfoot Formation (Norford and Cecile, 1994a).

"Basal Devonian Unit"

The "Basal Devonian unit" of the Wild Horse River area is a midden of rubbly weathering, variably bedded pale yellowish orange, grayish yellow, red, grayish purple and medium gray weathering dolostone, sandy dolostone, dolostone breccia with a limestone matrix, limestone and local mixed lithology cobble conglomerates. The "Basal Devonian unit" unconformably overlies the Beaverfoot Formation and at one locality contains clasts of the underlying Beaverfoot Formation. In the Wild Horse River area the "Basal Devonian Unit" is found between two opposing panels of the Beaverfoot Formation, where it is structurally complicated, and difficult to characterize, however, it is thought to represent parts of the Cedared (Belyea and Norford, 1967) and/or Burnais Formations (Shepard, 1926; Evans, 1933; Henderson, 1954; Leech, 1954,1958)

Mid-Cretaceous Plutons

The Wild Horse River differs from other parts of the southern Canadian Rocky Mountains in that it contains several small leucocratic mid-Cretaceous "granitic" plutons (Leech, 1958; Welbon and Price, 1992a, 1992b). These vary somewhat in composition, but commonly comprise coarse, to very coarse grained monzonite or quartz monzonite, with up to 15% hornblende. The largest pluton in the area, the Mt. Haley stock, has been dated ($^{40}Ar/^{39}Ar$ on hornblende) at ~108 Ma (Stretch, 1997). The age of these plutons is highly significant because it provides a minimum age for the faulting and folding within the Wild Horse River area

STRUCTURE

The Wild Horse River area straddles two distinctive structural subprovinces within the Southern Canadian Rocky Mountains: The Western Ranges and the Western Main Ranges subprovinces of North and Henderson (1954). The Western Ranges subprovince coincides with the Hughes Range tectonostratigraphic domain; the Western Main Ranges subprovince coincides with the Tanglefoot domain (Figure 2). There area conspicuous changes in structural style and in physiographic expression between the two subprovinces. Each structural subprovince/tectonostratigraphic domain will be discussed separately.

Hughes Range domain (Western Ranges subprovince)

The Hughes Range domain comprises a steeply dipping to overturned east-facing panel of Mesoproterozoic Purcell Supergroup sedimentary rocks and unconformably overlying Lower Paleozoic strata that are separated from the main Purcell anticlinorium by an west-dipping Tertiary listric normal fault that follows the east side of the Rocky Mountain Trench (Figure 2). The eastern boundary of the Hughes Range domain is marked by the Lussier River Fault, a listric, west-dipping, east-verging, out-of-sequence thrust that separates east-verging structures associated with the Purcell anticlinorium from the west-verging structures in the western flank of the Porcupine Creek fan structure (Leech, 1958, 1960; Welbon and Price, 1992a, 1992b, 1993). Deformation within the Hughes Range domain is dominated by faults. Many of these are steeply dipping northeast-trending transverse faults, some with normal separation, and others with reverse separation. Variations in preservation of underlying formations along unconformities beneath the Cranbrook Formation and the Jubilee Formation indicate that these faults were active as normal faults during the Proterozoic and the Cambrian and were reactivated during Mesozoic thrusting and folding (Welbon and Price, 1992a, 1992b, 1993).

Tanglefoot domain (Western Main Ranges subprovince)

The Tanglefoot domain is underlain by the Porcupine Creek anticlinorium (Balkwill, 1972), a broad, north-trending fan structure with east-verging folds and thrusts in the east flank, west-verging folds and thrust in the west flank, and in the Wild Horse River area, an intervening broad, open syncline (the Top of the World syncline) that extends across the fan axis (Figure 2). The west-verging "Mt. Doolan anticline", which dominates the western flank of the fan structure, plunges gently northward, and locally is overturned. It changes along strike from a broad, open fold, in the south, near Tanglefoot Creek to a close fold northeast of Ruault Lake, and to a moderately inclined tight fold, overturned to the west at Mt. Doolan (Figure 3).

A west-verging, east-dipping thrust fault ("Summer Lake thrust") imbricates the upper part of the McKay Group and the lower part of the Beaverfoot Formation in the east limb of the "Mt. Doolan anticline". Strata in the hanging wall of the "Summer Lake thrust", dip gently to the east beneath the broad, shallowly north-plunging Top of the World syncline.

A principal focus of this thesis/study has been the elucidation of the enigmatic structure that occurs between the western limb of the "Mt. Doolan anticline" and the Lussier River fault. This structure comprises steeply dipping inward-facing panels of McKay and Beaverfoot strata and an intervening thick succession of shaley strata with abundant intercalated dark green volcanic rocks. This structure initially was mapped by Leech (1958, 1960) and by Welbon and Price (1992a, 1993) as a syncline with volcanogenic Silurian(?) or Middle Devonian(?) strata in the core and Ordovician and Cambrian Beaverfoot and McKay strata in the limbs. The eastern limb of this supposed syncline is the west limb of the Mount Doolan anticline; the western limb is a steeply dipping, east-facing panel of Beaverfoot and McKay strata that is truncated southward against the footwall of the Lussier River fault. New biostratigraphic data and mapping by by Norford and Cecile (1994a) have shown that the volcanic rocks in the core of the supposed syncline belong to the Cambrian and Lower Ordovician McKay Group, that these McKay strata are in fault above the top of the east-facing McKay and Beaverfoot Formations in the west limb of the supposed syncline, and that the Beaverfoot Formation in the east limb of the supposed "syncline" actually comprises two separate inward-facing panels of Beaverfoot Formation, one forming the west-facing west limb of the Mount Doolan anticline, and the other forming the top of an east-facing structural panel that extends downward into a the McKay succession within which the volcanogenic rocks are interbedded. Both of the inward-facing panels of Beaverfoot Formation are capped by a thin (~50 m) interval of basal Devonian Cedared Formation. Overlying gypsum of the Middle Devonian Burnais Formation is not exposed; and if present, is very thin. Norford and Cecile (1994a) concluded that the two inward-facing panels of McKay, Beaverfoot, and Cedared strata at Ruault lake (Figure 3) form the limbs of a "very tight" (essentially isoclinal) syncline. Noting that the fault that juxtaposes the volcanic-rich succession of McKay strata with the Beaverfoot Formation at Bear Lake (Figure 3) is more or less parallel with the strata on either side of it, and that the Cedared Formation is preserved locally beneath the McKay Group along this fault (Figure 3), they concluded that this fault is an east-verging thrust fault that was rotated into a near vertical to overturned orientation during subsequent folding the formations in which it is embedded.

In the present study we have attempted to trace these structures along strike to the north and to the south, and to determine where the vertical to overturned east-verging thrust fault might emerge eastward and, in particular, whether the two inward-facing panels of Beaverfoot Formation and overlying Cedared Formation are connected by a fold hinge, or separated by this east-verging thrust fault.

The contact between the two inward-facing panels of Beaverfoot Formation and overlying Cedared Formation is exposed at several localities between Mount Ruault and the upper headwaters of Wildhorse River (Figure 3). Locally, as on the east-west ridge north of Ruault Lake, near vertical and subparallel, inward-facing panels of Cedared Formation are separated by a bedding-parallel thrust or detachment fault that may follow the gypsum of the Burnais Formation. Elsewhere to the south and to the north, various stratigraphic levels within the Beaverfoot Formation, on the west, are in fault contact with Cedared Formation, on the east. This relationship is indicative of an east-verging thrust fault that juxtaposes a hanging wall ramp, along which the fault cuts up-section in the direction of fault displacement, over a footwall "flat", along which the fault follows a bedding-parallel detachment. Southward from Ruault Lake to Mount Ruault, this thrust fault, which we will refer to as the "Ruault Lake fault" is parallel with the Cedared Formation in the over-ridden ("footwall") panel but cuts down-section in the over-riding ("hanging wall") panel cutting out the Beaverfoot Formation completely south of Mount Ruault. Southward from Mount Ruault, the Ruault Lake thrust also cuts down-section in the over-ridden ("footwall") panel toward the valley of the headwaters of East Wild Horse Creek. There bedrock is concealed by extensive glacial overburden and the location of the fault is uncertain. Farther south, in the vicinity of the Mount Hayley stock, where the Beaverfoot Formation appears to have been cut out on both sides of the Ruault Lake fault and McKay Group strata apparently occur on both sides, the location of the fault has been inferred by extrapolation (Figure 3). Between Mount Ruault and the upper headwaters of the Wild Horse River, the Ruault Lake fault follows an extensive bedding detachment above the Cedared Formation (probably in the gypsum of the Burnais Formation) along the footwall of the Ruault Lake fault. We have interpreted the extensive bedding detachment beneath the Ruault Lake fault as the emergent eastern equivalent of the east-verging thrust in the western part of the Wild Horse River area that separates the McKay Group strata with intercalated volcanics rocks from the Beaverfoot Formation (Figure 4). This fault also is sub parallel with Cedared-Beaverfoot contact along its footwall. This suggests that it probably also follows a footwall detachment in Middle Devonian gypsum here. South of East Wild Horse Creek the fault cuts down-section in its footwall toward the Mount Haley stock (Figure 3). In the vicinity of the stock the location of this east-dipping fault has been inferred by interpolation to connect with the west-dipping part of the Ruault Lake fault around the hinge of a north-plunging synform. The implication is that the Ruault Lake fault has been folded, along with the beds above and below it, to form a tight, north-trending synform. This overall structure, will be referred to below at the "Upper Wild Horse River (UWHR) structure".

Along the east branch of upper Wild Horse River, the Beaverfoot Formation is cut out northward along a footwall ramp on the Ruault Lake fault; farther north the fault has McKay Group on both sides and it is difficult to locate.

There is an abrupt 1.5 km left-hand offset of the entire UWHR structure along a concealed east-west fault beneath the glacial drift of the upper Wild Horse River west of Mount Dingley (Figure 3). This fault offset coincides with an equivalent left-hand deflection of the hinge zone of the Mount Doolan anticline; but there is no deflection of the east limb of the Mount Doolan anticline or of the Summer Lake thrust, which imbricates the McKay and Beaverfoot strata within the east limb of the anticline. Further work is planned for the elucidation of the nature and significance of this left-hand transverse structure.

Boulder Creek Fault

The Boulder Creek Fault is an enigmatic east-west trending transverse structure with a left-hand strike separation and apparent downthrow to the north (Leech, 1958). It forms part of the Crowsnest Pass cross-strike discontinuity (Price, 1994, 2000); and is aligned with the St Mary fault, which follows the locus of an older structure that was active during the deposition of the Neoproterozoic Windermere Supergroup of the western Purcell Mountains (Lis and Price, 1976). The Boulder Creek fault also is aligned with a conspicuous deflection of the Porcupine Creek anticlinorium, which changes from north-trending north of the Boulder Creek fault to east-northeast-trending south of it. The Boulder Creek fault either truncates or has reactivated the regional d collement in the Lower Cambrian Eager Formation that forms the base of the Porcupine Creek anticlinorium in the Tanglefoot area (Stretch, 1997). The present left-hand separation with apparent downthrow to the north may be associated with reactivation of the Boulder Creek fault as a normal fault during the Tertiary crustal extension that produced the southern Rocky Mountain trench.

The Boulder Creek fault evidently has had a complex displacement history, with stratigraphic

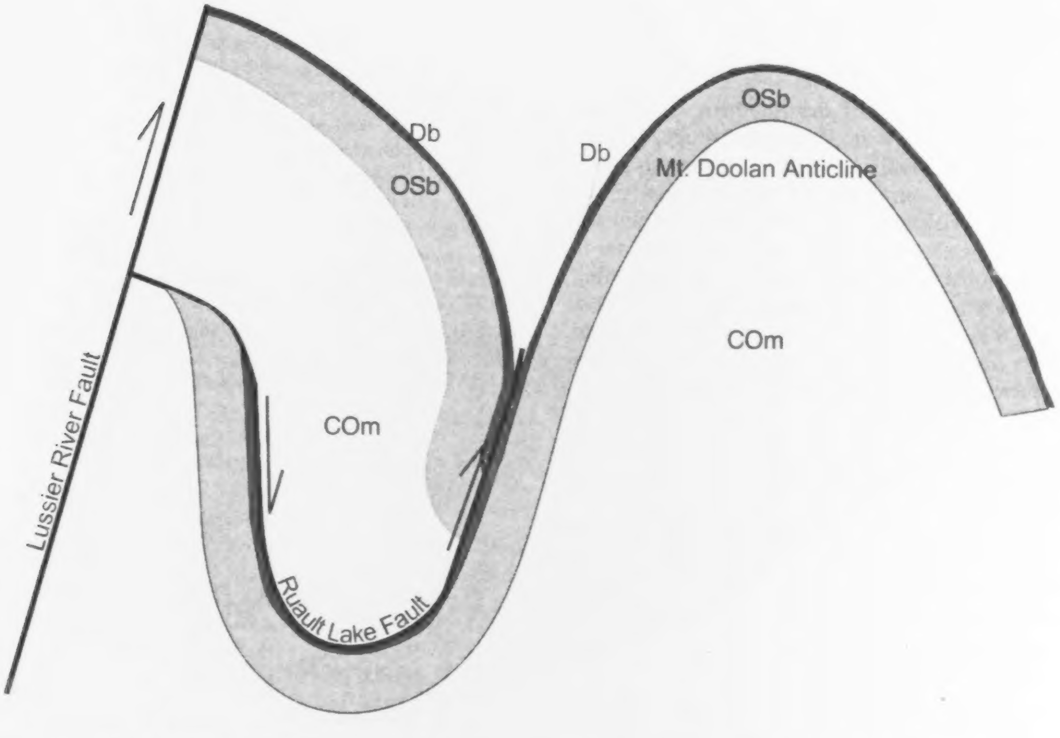

Figure 4. A skematic cross-section through the Upper Wild Horse River structure showing fault juxtaposed, inward facing panels of Beaverfoot Formation and a folded Ruault Lake fault. The Upper Wild Horse River structure is cut out to the west by the out-of-sequence Lussier River Fault.

evidence suggesting it was a Stratigraphic evidence indicates down-to-the-south displacement during deposition of Mesoprotoreozoic rocks of the Aldridge Formation (H y. 1993) and during deposition of the Lower Cambrian Eager and Tanglefoot Formations. Structural evidence suggests the fault was reactivated as a right-handed reverse fault in the Cretaceous related to deflection in the axis of the Porcupine Creek anticlinorium, and the Lussier River fault. As indicated above, it may also have been reactivated during Tertiary extensional deformation.

Three distinct sets of minor faults can be distinguished in fabric data collected along the north side of the Boulder Creek fault, however, they do not provide an unequivocal indication of the kinematics of the fault. The first set, observed ~1.5 km north of the Boulder Creek fault, consists of small faults that tend to dip steeply to the north with tectonic lineations plunging shallowly (20-30°) to the east. A second set, observed less than 500 meters north of the fault consists of moderately steeply (60-70°) south-dipping faults with lineations plunging shallowly (~30°) to the west. The third set of minor faults, observed at both localities, consists of shallowly south- and north-dipping (30°) faults with down dip lineations.

Timing of Thrust and Fold Deformation

The timing of thrusting and folding in the Wild Horse River area is constrained by small crosscutting plutons one of which has been dated at ~108 Ma (Stretch, 1997). An unnamed monzonite pluton near the headwaters of the Wild Horse River postdates motion on the Lussier River Fault; the 108 Ma Mt. Haley stock intrudes the core of the Mt. Doolan anticline near Mt. Ruault truncating the structures in the folded rocks. These crosscutting relationships show that deformation related to the development of the Porcupine Creek Anticlinorium and displacement along the Lussier River Fault occurred prior to ~108 Ma.

CONCLUSIONS

The Wild Horse River area is a geologically complex segment of the Southern Cordilleran Thrust and Fold Belt. Enigmatic abrupt contrasts in Cambrian stratigraphy are due to juxtaposition of different stratigraphic domains by thrust faulting. Volcanic rocks intercalated within the Cambro-Ordovician strata are local phenomena that probably due to diatremes. Cross-cutting Mid-Cretaceous granitic plutons show that thrust and fold deformation in the Wild Horse River area occurred prior to ~108 Ma. The Boulder Creek fault has a complex displacement history

AKNOWLEDGMENTS

Thanks to Kyl Chhatwal for able and jovial field assistance. D. Terry and the British Columbia Geological Survey Branch are also to be thanked for contributions to this project. Funding for this study was provided by a Natural Sciences and Engineering Research Council Operating Grant #0092417-01 to R.A. Price.

REFERENCES

Aitken, J. D. and B. S. Norford (1967): Lower Ordovician Survey Peak and Outram formations, southern Rocky Mountains of Alberta; *Bulletin of Canadian Petroleum Geology* 15(2), pages 150-207.

Balkwill, H. R. (1972): Structural geology, lower Kicking Horse River region, Rocky Mountains, British Columbia; *Bulletin of Canadian Petroleum Geology* 20(3), pages 608-633.

Belyea, H. R. and B. S. Norford (1967): The Devonian Cedared and Harrogate Formations in the Beaverfoot, Brisco, and Stanford Ranges, southeast British Columbia; *Geological Survey of Canada, Bulletin* 146, 64p.

Burling, L. (1922): A Cambro-Ordovician section in the Beaverfoot Range near Golden, British Columbia; *Geological Magazine*, 59p.

Evans, C. S. (1933): Brisco-Dogtooth map-area, British Columbia; *Geological Survey of Canada, Summary Report 1932*, part AII, pages 106-176.

Henderson, G. G. L. (1954): Geology of the Stanford Range of the Rocky Mountains, Kootenay District, Britsh Columbia; *British Columbia Department of Mines*, Bulletin 35.

Höy, T. (1982): The Purcell Supergroup in southeastern British Columbia: sedimentation, tectonics, and stratigraphy from lead-zinc deposits; *in* Precambrian sulphide deposits, *Geological Association of Canada*, Special Paper 25, pages 127-147.

Höy, T. (1985): The Purcell Supergroup, Fernie west-half, southeastern British Columbia, part A. Stratigraphy – measured sections; *B.C. Ministry of Energy, Mines and Petroleum Resources*, Bulletin 76, 79p.

Höy, T. (1993): Geology of the Purcell Supergroup in the Fernie west-half map area, southeastern British Columbia; *Ministry of Energy, Mines and Petroleum Resources*, Bulletin 84, 157p.

Leech, G. B. (1954): Canal Flats, British Columbia (map and preliminary account); *Geological Survey of Canada*, Paper 54(7), 31p.

Leech, G. B. (1958): Fernie map-area, west half, British Columbia; *Geological Survey of Canada*, Paper 58(10), 40p.

Leech, G. B. (1960): Geology of the Fernie map-area (West Half) Kootenay District, British Columbia, *Geological Survey of Canada*, Map 11-1960.

Lis, M. G. and R. A. Price (1976): Large-scale block faulting during deposition of the Windermere Supergrouop (Hadrynian) in southeastern British Columbia. *Report of Activities, Part A, Geological Survey of Canada*, Paper 76-1A, pages 135-136.

McConnell, R. G. (1887): Report on the geological features of a portion of the Rocky Mountains, accompanied by a section measured near the 51st parallel; *Geological Survey of Canada, Annual Report for 1886* 2(D), pages 1-41.

McMechan, M. E. (1979): Geology of the Mt. Fisher-Sand Creek area; *British Columbia Ministry of Energy, Mines and Petroleum Resources*, Preliminary Map 34.

Norford, B. S. (1962): The Beaverfoot-Brisco Formation in the Stanford Range, British Columbia; *Journal of the Alberta Society of Petroleum Geologists*, 10(7), pages 443-453.

Norford, B. S. (1964): Ordovician-Silurian, Part 2 (Chap. 4). Geological history of western Canada. R. G. McCrossan and R. P. Glaister, Alberta Society of Petroleum Geologists, pages 42-48.

Norford, B. S. and M. P. Cecile (1994a): Cambrian and Ordovician volcanic rocks in the McKay Group and Beaverfoot Formation, western ranges of the Rocky Mountains, southeastern British Columbia; *Current Research - Geological Survey of Canada* Paper 94(1B), pages 83-90.

Norford, B. S. and M. P. Cecile (1994b): Ordovician emplacement of the Mount Dingley Diatreme, western ranges of the Rocky Mountains, southeastern British Columbia; *Canadian Journal of Earth Sciences* 31(10), pages 1491-1500.

North, F. K. and G. L. Henderson (1954): Summary of the geology of the Southern Rocky Mountains of Canada; Guidebook, Fourth annual field conference, *Alberta Society of Petroleum Geologists*, pages 15-81.

Rice, H. M. A. (1937): Cranbrook map area, British Columbia; *Geological Survey of Canada*, Memoir 207, 67p.

Price, R. A. (1994): A 200-km right-hand offset in the cratonic margin at the Crowsnest Pass cross-strike discontinuity: Tectonic heredity with Late, Middle, and Early Proterozoic antecedents; *Exploration Update '94, CSEG & CSPG Joint National Convention, Calgary*, Program, Expanded Abstracts and Biographies, page 315.

Price, R. A. (2000): The southern Canadian Rockies: Evolution of a foreland thrust and fold belt; *Calgary, Alberta, GeoCanada 2000*, Field Trip Guidebook No. 13, 244 p.

Schofield, S. J. (1922): Relationship of the Precambrian (Beltian) terrain to the lower Cambrian strata of southeastern British Columbia; *Geological Survey of Canada* Bulletin 35, 15p.

Shepard, F. P. (1926): Further investigations of the Rocky Mountain Trench; *Journal of Geology* 34, pages 634-641.

Stretch, G. W. (1997): The Southern Termination of the Main Ranges and Western Ranges of the Southern Canadian Rocky Mountains: Stratigraphy, structural geology, and tectonic implications; *Queen's Univeristy*, M.Sc. Thesis, 114p.

Thompson, T. L. (1962): Stratigraphy, tectonics, structure, and gravity in the Rocky Mountain Trench area, southeastern British Columbia, Canada; *Standford University*, Ph.D. Thesis, 166p.

Welbon, A. I. and R. A. Price (1992a): Geology of the Central Hughes Range British Columbia, NTS 82G/11, 12, 13, 14; *Ministry of Energy, Mines and Petroleum Resources*, Open File Map no. 1992-17.

Welbon, A. I. and R. A. Price (1992b): Stratigraphic dating of fault systems of the central Hughes Range, Southeast British Columbia (82G/12); *in*: Geological Fieldwork; B. Grant and J. M. E. Newell, eds., *British Columbia Ministry of Energy, Mines and Petroleum Resources*, Paper 1991-1, pages 21-26.

Welbon, A. I. and R.A.Price (1993): Geology of the Wild Horse River-Lussier River area, S.E. British Columbia, NTS 82G/11,12,13,14; *British Columbia Ministry of Energy, Mines and Petroleum Resources*, Open File Map no. 1993-7.

Geology and New Mineralization in the Joss'alun belt, Atlin Area

Mitch Mihalynuk[1], Lee Ferreira[2], Steve Robertson[3], Fionnuala A.M. Devine[4] and Fabrice Cordey[5]

Introduction

In 2002, Ministry of Energy and Mines personnel discovered copper mineralization approximately 75 km south southeast of Atlin while conducting a regional geological mapping program as part of the federal and provincially funded Targeted Geoscience Initiative. Following a press release (Mihalynuk, 2002), several parties staked ground in the belt. Subsequently, Imperial Metals Corporation consolidated interests and is now the key operator and tenure-holder in the area. The claim group is referred to as the NAK property and the principal mineralized zone is the Joss'alun massive sulphide occurrence.

As part of a public-private partnership agreement with Imperial Metals Corporation (henceforth referred to as "Imperial"), approximately three weeks of field mapping was conducted in 2003 in the belt of rocks containing the mineralization to clarify geological relationships. An additional 1.5 weeks on reconnaissance geological mapping was aimed at outlining more regional exploration targets. Operational funding was provided by Imperial.

This report is based upon the results of mapping conducted on the claim blocks owned or optioned by Imperial (NIC, KNACK, WACK, Dark and D1 to D12). In addition, we report here on results of mapping and sampling outside of the claim blocks, and a brief synopsis of drill results and property exploration. Highlights include:

- discovery of new mineralizaton within the belt of rocks containing the Joss'alun occurrence, extending the mineralized belt about 2.5 km northwest and 5 km southeast of the Joss'alun;
- intersections in two drill holes at the Joss'alun that assayed 0.94% copper over 17.75 metres and 0.34% copper over 53.45 metres;
- lithogeochmical data that points to a forearc or back-arc setting for the unit hosting mineralization;
- recognition of Paleozoic-Mesozoic stratigraphy that appears to have regional application, including an extensive ferruginous chert horizon, locally copper stained, that is probably of Early Permian age; and
- synthesis of a regionally applicable structural history that includes an episode of extension, possibly back arc basin extension, with implications for volcanogenic and sedimentary-exhalative (VMS/SEDEX) mineralization.

Access and Previous Work

Access to the NAK property is most effectively achieved using a helicopter charter based out of Atlin, 75 kilometres to the north-northwest. One large lake about 7.5 km north northwest of the Joss'alun occurrence, informally known as Windy Lake, is large enough to accommodate a floatplane - so long as loaded departures are not required. There are no all-season roads within the area. One rough, fire abatement road extends to Kuthai Lake, about a 2.5-hour drive from Atlin, and about 30 km northwest of the NAK property. It is suitable for four wheel drive or all-terrain vehicles and requires fording the O'Donnel River and Dixie Lake outflow. Around the NAK property, travel by foot is relatively easy, except for some steep mountainsides around Hardluck Peaks. The proposed access road to the Tulsequah Chief mine is, at its closest point, 22 km from the NAK property.

Previous regional map coverage of the NAK area is of early to mid 1950s vintage (Aitken, 1959), pre-dating the advent of plate tectonics. Thematic revision mapping in the mid to late 1960's by Monger (1969, 1975) covered much of the carbonate-dominated rocks north and east of the NAK property. Monger (1975) pieced together a biostratigraphy and used igneous geochemistry, map relationships, and the recognition of a disrupted ophiolitic succession to show that the Atlin area is composed largely of relict ocean basin crust and oceanic islands. Terry (1977) confirmed this assertion and suggested an analogue in the Pindos ophiolites of Greece. Ash (1994) drew similar conclusions from the ophiolitic ultramafic rocks near the town site of Atlin. A more extensive geochemical and petrogenetic study by English *et al.* (2002) shows that the most common mafic volcanic rocks in the region formed within a primitive island arc setting.

---

[1] *Geoscience, Research and Development Branch, Ministry of Energy and Mines, Victoria, BC*

[2] *University of Victoria, Victoria, BC*

[3] *Imperial Metals Corporation, Vancouver, BC*

[4] *Imperial Metals Corporation. Current affiliation: Department of Earth Sciences, Carleton University, Ottawa, ON*

[5] *PaléoEnvironnements & PaléobioSphere, Université Claude Bernard, Lyon, France*

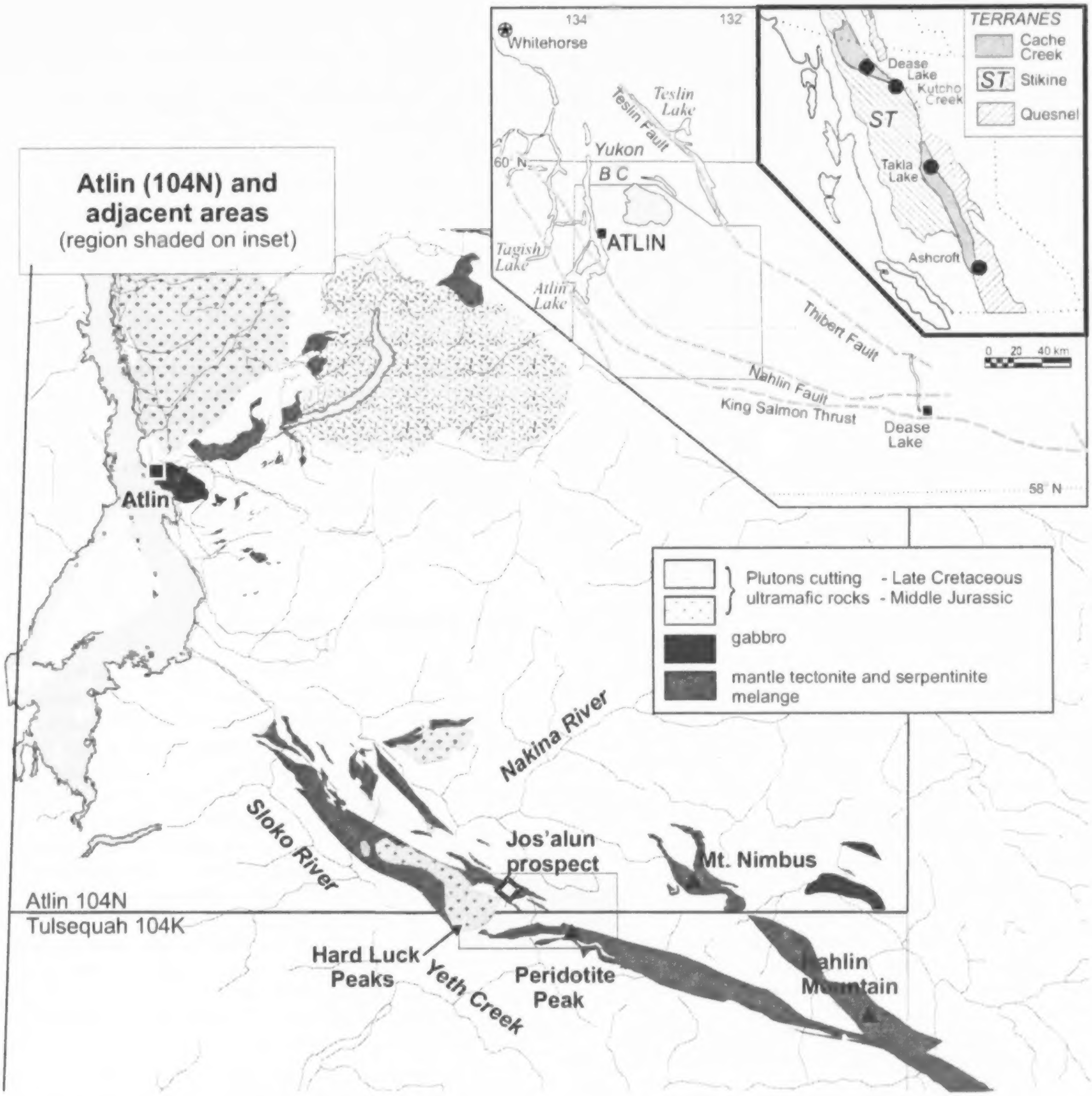
Atlin (104N) and adjacent areas
(region shaded on inset)
134
132
Whitehorse
Teslin Lake
Teslin Fault
Yukon
BC
60° N
Tagish Lake
ATLIN
Atlin Lake
Thibert Fault
Nahlin Fault
King Salmon Thrust
Dease Lake
58° N
TERRANES
Cache Creek
ST Stikine
Quesnel
Dease Lake
Kutcho Creek
ST
Takla Lake
Ashcroft
0 20 40 km
Atlin
Plutons cutting ultramafic rocks - Late Cretaceous - Middle Jurassic
gabbro
mantle tectonite and serpentinite melange
Nakina River
Sloko River
Jos'alun prospect
Mt. Nimbus
Atlin 104N
Tulsequah 104K
Hard Luck Peaks
Yeth Creek
Peridotite Peak
Nahlin Mountain

Figure 1. Location of the NAK property. Geology after Mihalynuk *et al.* (1996, 2003a, b) shows the Nahlin ultramafic body and other mantle rocks, and major intrusive bodies. Location of Figure 2 is shaded on the map. The region covered by the map is shown shaded on the inset figure of British Columbia.

In 1996, a compilation of Atlin geology was completed as part of a provincial mineral potential evaluation (Mihalynuk *et al.*, 1996). This map has been corrected and recompiled by Massey *et al.* (2003); it is available for viewing or download at http://www.em.gov.bc.ca/Mining/Geolsurv/Publications/. In 1978 a Regional Geochemical Survey (RGS) was conducted over the entire Atlin 1:250 000 sheet (BCMEM, 1978). Archival stream sediment samples were reanalysed for a broader range of elements, including gold, and published in 2000 (Jackaman, 2000; available for download at www.em.gov.bc.ca/Mining/Geolsurv/rgs/sheets/104n .htm). In the same year, a regional aeromagnetic survey of the entire Atlin map sheet, about 14 000 square kilometers, was conducted (e.g. Dumont *et al.*, 2001). Mapping at 1:50 000 scale across a transect of the southern Atlin mapsheet (104N/1, 2 & 3) was begun in 2001 as part of the two-year, Federal and Provincially-funded Targeted Geoscience Initiative (TGI). Results of TGI mapping have been published by Mihalynuk *et al.* (2002, 2003a and references therein). Three 1:50 000

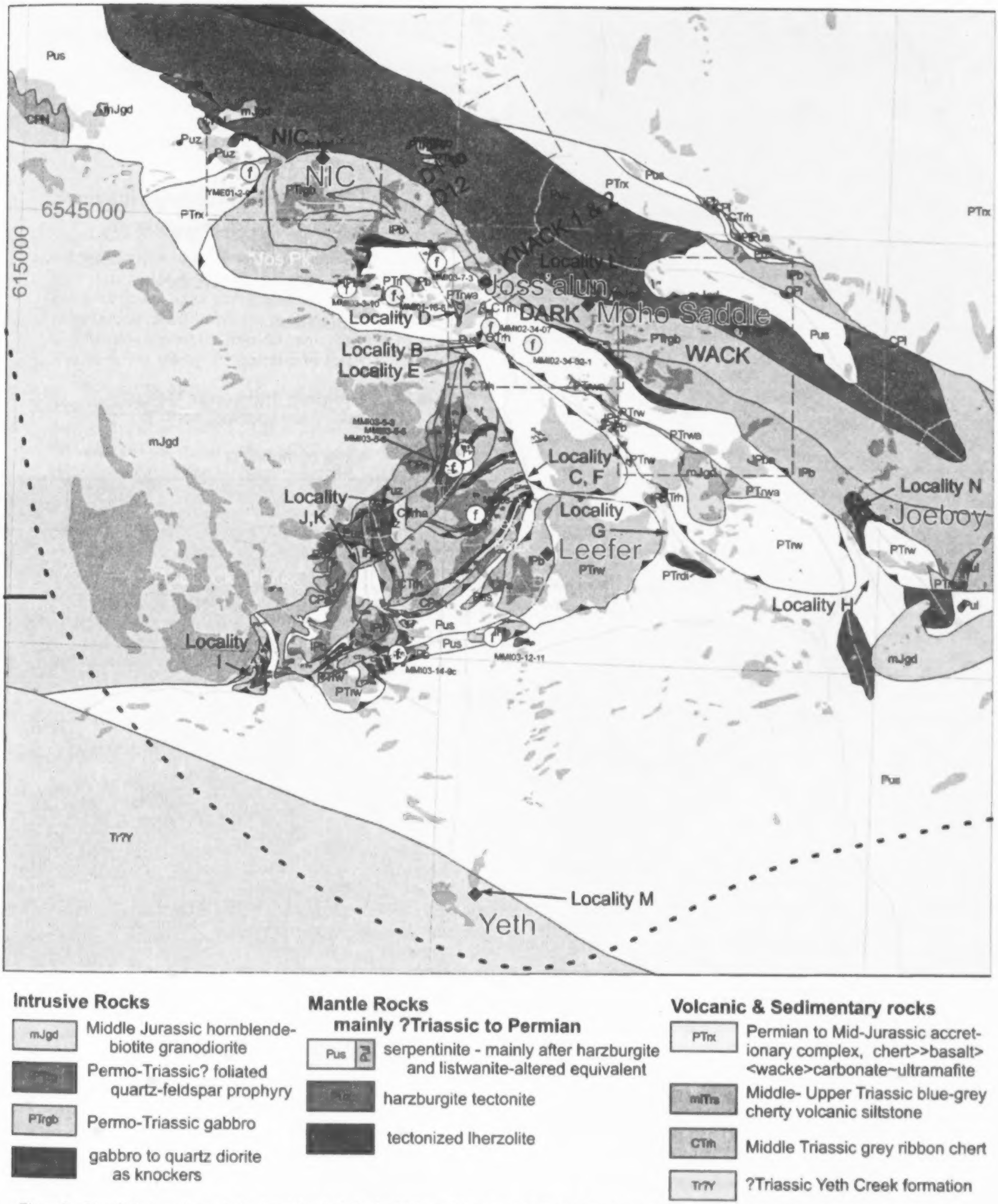
Pus
mJgd
CPN
Puz
NIC
PTrgb
DT
D12
PTrx
Pus
CTrh
6545000
615000
KNACK 1 & 2
Locality L
Joss'alun
DARK
Mpho Saddle
Locality D
Locality B
Locality E
PTrwa
PTrw
WACK
CPl
IPb
Locality C, F
Locality G
Leefer
PTrdi
Locality N
Joeboy
Locality H
Locality J,K
Locality I
PTrw
mJgd
Tr?Y
Locality M
Yeth
Pus
Intrusive Rocks
mJgd Middle Jurassic hornblende-biotite granodiorite
Permo-Triassic? foliated quartz-feldspar prophyry
PTrgb Permo-Triassic gabbro
gabbro to quartz diorite as knockers
Mantle Rocks mainly ?Triassic to Permian
Pus Pul serpentinite - mainly after harzburgite and listwanite-altered equivalent
harzburgite tectonite
tectonized lherzolite
Volcanic & Sedimentary rocks
PTrx Permian to Mid-Jurassic accretionary complex, chert>>basalt><wacke>carbonate~ultramafite
mTrs Middle- Upper Triassic blue-grey cherty volcanic siltstone
CTrh Middle Triassic grey ribbon chert
Tr?Y ?Triassic Yeth Creek formation

Figure2. Simplified geology of the Joss'alun belt in the Nakina River area (BC Geographic Survey sheets 104K.096N, 097N and 104N.006S, 007S. Geology is based upon published mapping by Mihalynuk et al. (2002, 2003a, b) and regional geology of Aitken (1959) and Souther (1971).

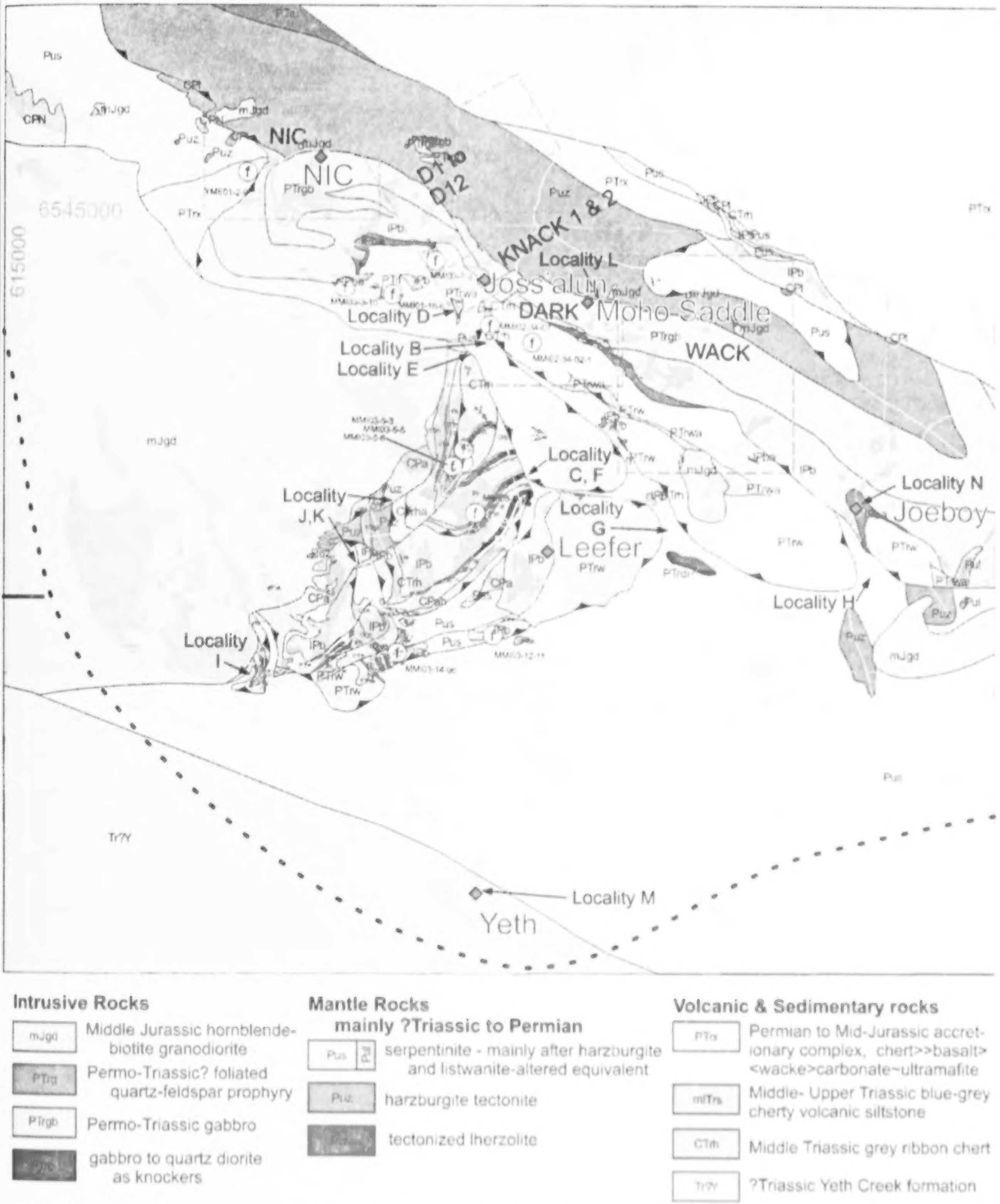
NIC
D11 to D12
KNACK 1 & 2
Locality L
Joss'alun
DARK
Moho-Saddle
WACK
Locality D
Locality B
Locality E
Locality C, F
Locality G
Leefer
Locality J,K
Locality I
Locality N
Joeboy
Locality H
Locality M
Yeth
6545000
615000
Pus
CPN
mJgd
PTrgb
PTrx
Puz
IPb
CTrh
PTrw
PTrwa
CPa
Tr?Y
Intrusive Rocks
mJgd
Middle Jurassic hornblende-biotite granodiorite
PTrg
Permo-Triassic? foliated quartz-feldspar prophyry
PTrgb
Permo-Triassic gabbro
gabbro to quartz diorite as knockers
Mantle Rocks mainly ?Triassic to Permian
Pus
serpentinite - mainly after harzburgite and listwanite-altered equivalent
Puz
harzburgite tectonite
tectonized lherzolite
Volcanic & Sedimentary rocks
PTrx
Permian to Mid-Jurassic accretionary complex, chert>>basalt><wacke>carbonate~ultramafite
mlTrs
Middle- Upper Triassic blue-grey cherty volcanic siltstone
CTrh
Middle Triassic grey ribbon chert
Tr?Y
?Triassic Yeth Creek formation

Figure2. Simplified geology of the Joss'alun belt in the Nakina River area (BC Geographic Survey sheets 104K 096N, 097N and 104N 006S, 007S. Geology is based upon published mapping by Mihalynuk et al. (2002, 2003a, b) and regional geology of Aitken (1959) and Souther (1971).

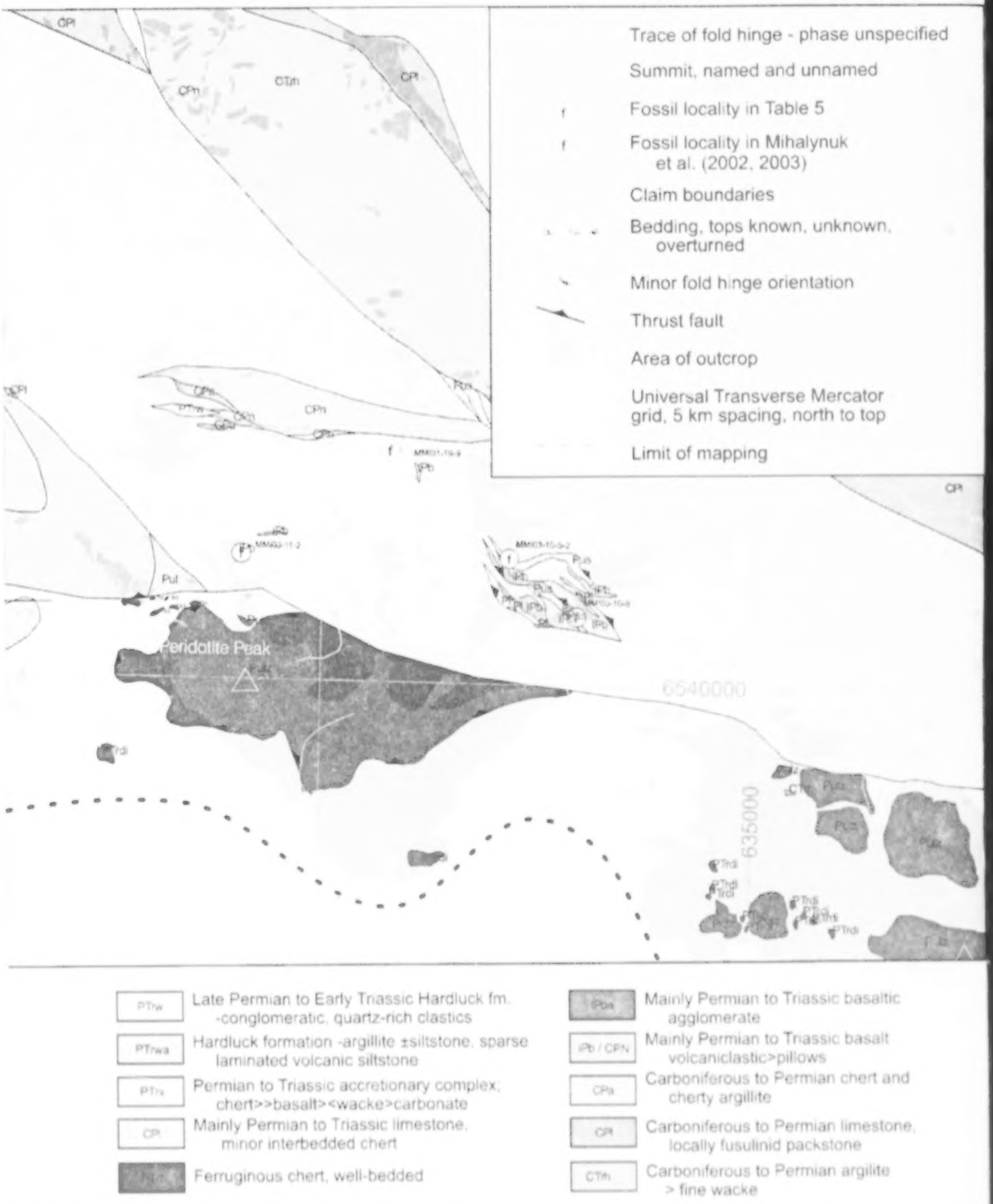
Trace of fold hinge - phase unspecified
Summit, named and unnamed
Fossil locality in Table 5
Fossil locality in Mihalynuk et al. (2002, 2003)
Claim boundaries
Bedding, tops known, unknown, overturned
Minor fold hinge orientation
Thrust fault
Area of outcrop
Universal Transverse Mercator grid, 5 km spacing, north to top
Limit of mapping
CPl
CTfh
CPh
Pul
PTrw
MM01-19-9
MM03-11-2
MM03-10-9-2
IPb
Peridotite Peak
6540000
635000
PTrdi
PTrw
Late Permian to Early Triassic Hardluck fm. -conglomeratic, quartz-rich clastics
PTrwa
Hardluck formation -argillite ±siltstone, sparse laminated volcanic siltstone
PTrx
Permian to Triassic accretionary complex; chert>>basalt><wacke>carbonate
CPl
Mainly Permian to Triassic limestone, minor interbedded chert
Ferruginous chert, well-bedded
IPba
Mainly Permian to Triassic basaltic agglomerate
IPb / CPN
Mainly Permian to Triassic basalt volcaniclastic>pillows
CPa
Carboniferous to Permian chert and cherty argillite
CPl
Carboniferous to Permian limestone, locally fusulinid packstone
CTfh
Carboniferous to Permian argilite > fine wacke

Unpublished mapping by Canil and Johnston (2004) is presented in the southeastern corner (Peridotite Peak and ultramafic rocks to the southeast)

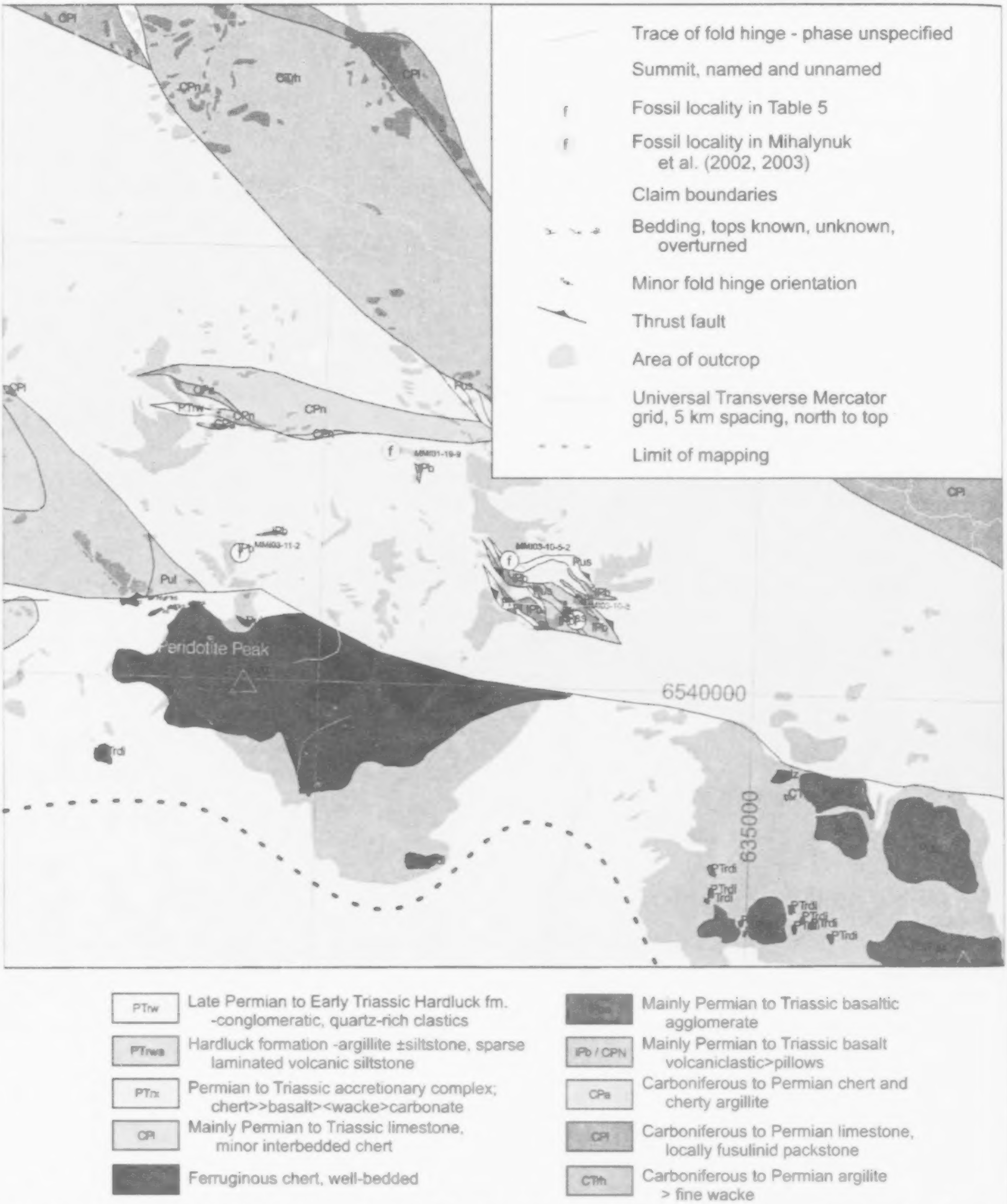
Trace of fold hinge - phase unspecified
Summit, named and unnamed
f Fossil locality in Table 5
f Fossil locality in Mihalynuk et al. (2002, 2003)
Claim boundaries
Bedding, tops known, unknown, overturned
Minor fold hinge orientation
Thrust fault
Area of outcrop
Universal Transverse Mercator grid, 5 km spacing, north to top
Limit of mapping
CPl
CPn
CTrh
CPl
Pus
PTrw
CPn
CPn
MMI01-19-9
IPb
MMI03-11-2
MMI03-10-5-2
Pus
Pul
Peridotite Peak
6540000
635000
Trdi
PTrdi
CPl
PTrw Late Permian to Early Triassic Hardluck fm. -conglomeratic, quartz-rich clastics
PTrwa Hardluck formation -argillite ±siltstone, sparse laminated volcanic siltstone
PTrx Permian to Triassic accretionary complex; chert>>basalt><wacke>carbonate
CPl Mainly Permian to Triassic limestone, minor interbedded chert
Ferruginous chert, well-bedded
Mainly Permian to Triassic basaltic agglomerate
IPb / CPN Mainly Permian to Triassic basalt volcaniclastic>pillows
CPa Carboniferous to Permian chert and cherty argillite
CPl Carboniferous to Permian limestone, locally fusulinid packstone
CTrh Carboniferous to Permian argilite > fine wacke

Unpublished mapping by Canil and Johnston (2004) is presented in the southeastern corner (Peridotite Peak and ultramafic rocks to the southeast).

scale geological maps that cover the transect area will be published in the near future.

Mineral exploration work around the Joss'alun discovery has been carried out by Imperial Metals Corporation, included geophysical and geochemical surveys, culminating in a diamond drill program which was concluded in the autumn of 2003.

Regional Geological Setting

Rocks comprising the belt that hosts the Joss'alun occurrence can be broadly separated into three distinct packages. From oldest to youngest they are: Mississippian to Early Jurassic Cache Creek oceanic rocks; coarse, quartz-rich clastic strata of probable Late Permian to Triassic age; and Middle Jurassic, post-tectonic intrusions, like the Nakina River stock.

Southwest of the NAK property, the Cache Creek rocks are bounded by the crustal-scale Nahlin fault that marks the contact with Lower to Middle Jurassic strata of the Laberge Group. All rocks older than the ~172 Ma Jurassic plutons have been folded and faulted, most recently by southwest-verging folds and thrusts, that formed between 174 and 172 Ma (Mihalynuk *et al.*, 2004). Discreet high angle faults cut plutons south of the map area that are as young as Eocene (Mihalynuk *et al.*, 1995).

Nak Stratigraphy

In a gross sense, a mantle to supracrustal architecture can be recognized in the NAK area, and the mantle/crustal components (harzburgite/gabbro) can be treated as stratigraphic elements, originally located beneath the supracrustal strata. A description of the mantle to supracrustal components follows.

MANTLE

Mantle rocks are best exposed within the Atlin area north of the Joss'alun occurrence, where they comprise part of the Nahlin ultramafic body, a coherent 1.5 x 15 km, dun-weathering body, best exposed south of the Nakina River. At that locality, the mantle rocks are bound to the west by gabbro, which passes upwards into submarine basalt, host to massive sulphide mineralization at the Joss'alun occurrence. Mantle rocks are comprised almost entirely of harzburgite (olivine, orthopyroxene and chrome spinel), with minor dunite (olivine). To the southeast, at Peridotite Peak, lherzolite containing up to 25% bright green chromian diopside, is exposed together with the harzburgite (see Canil *et al.*, this volume). Harzburgite commonly displays a high temperature tectonite fabric (Photo 1), which results in quasiductile elongation of the pyroxene grains (e.g. both harzburgite and dunite have been subjected to varying degrees of serpentinization). Typically, only relicts of olivine persist within a serpentine matrix. Other alteration minerals include quartz-magnesite-mariposite (listwanite alteration assemblage), and chrysotile (typically as veinlets less than 5 mm thick).

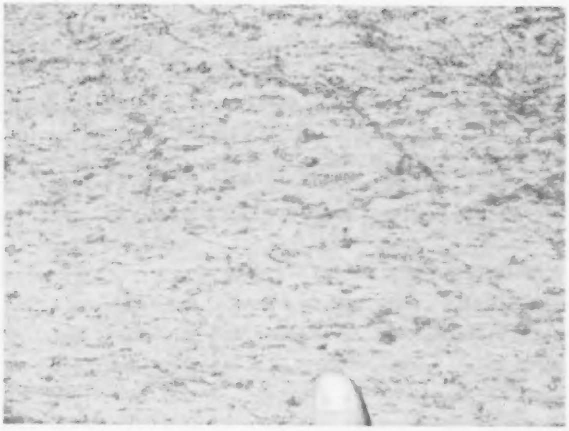

Photo 1. A high temperature mantle tectonite fabric is developed in the harzburgite west of "Jos Creek".

GABBRO

Gabbro forms a relatively continuous outcrop belt along the eastern margin of the mantle section. It is composed mainly of clinopyroxene orthopyroxene, with pyroxene subequal in abundance to plagioclase. It is typically medium-grained; although locally pegmatitic, such as in the saddle northeast of the NAK camp. A conspicuous feature of the gabbro is the presence of a reticulate vein network. Petrographic work conducted on gabbro throughout the Cache Creek terrane shows these veins to be comprised mainly of prehnite quartz and calcite. In two outcrops northwest of the NAK camp, gabbro shows an intrusive contact relationship with the mantle rocks. In at least three other localities, an intrusive relationship between gabbro and the overlying mafic and hypabyssal volcanic rocks is preserved.

BASALT

Basalt exposed within the NAK area is typically green-grey, blocky-weathering and dark green on fresh surfaces. It is a relatively resistant unit and caps several ridges south and east of the Joss'alun occurrence. Three lithologies are recognized: pillowed flows, agglomerate (herein defined as a monomict volcanic unit with large lapilli or breccia-sized fragments that are commonly rounded), and varitextured tuffaceous strata that may include hyaloclastite, flow breccia, tuffite and dense flows (a grab bag of basaltic lithologies not included in the first two units).

Pillowed flows are well displayed at the Joss'alun and on the peak at the western head of "Jos valley" ("Sleeper Peak", Photo 2). Pillow basalts are fine grained, rarely containing medium-grained feldspar laths comprising up to 10% of the rock. Pillows are typically vesicular and may display zones of varying vesicle size. Rims are chilled and chlorite altered. Pillows range from 15 to 150 cm across and appropriately oriented sections may show flow tubes and clear indications of flow tops. Interpillow lime mud or, less

TABLE 1. RESULTS OF INDUCTIVELY COUPLED PLASMA MASS SPECTROSCOPY (ICPMS) ANALYSIS

Element	Mo	Cu	Pb	Zn	Ag	Ni	Co	Mn	Fe	A	U	Au	Th	Sr	Cd	Sb	Bi	V
Units	ppm	ppm	ppm	ppm	ppb	ppm	ppm	ppm	%	ppm	ppm	ppb	ppm	ppm	ppm	ppm	ppm	ppm
Detection Limit	0.01	0.01	0.01	0.1	2	0.1	0.1	1	0.01	0.1	0.1	1	0.1	0.5	0.01	0.02	0.02	2
Station Number																		
LFE03-4-1	0.05	1562.18	0.19	7.6	171	102.1	11.3	167	0.99	0.6	b.d.	490.9	b.d.	46.8	0.06	0.02	b.d.	7
LFE03-17-4	0.85	2224.89	1.35	33.3	761	29.4	35.1	444	9.52	16.8	0.1	16.2	b.d	45.7	0.14	0.14	0.17	68
LFE-03-17-7	8.02	121.14	5.29	568.9	124	3.1	17.4	1153	6.97	15.3	b.d.	6.6	b.d.	4.4	1.85	0.38	0.55	94
STD GSB Till 99	0.78	154.01	181.02	320.2	1233	192	40.9	1259	6.17	48.2	0.4	34	3	15.7	0.62	7.76	0.21	91
MMI03-12-2	8.09	8818.62	1.59	39.7	618	10.8	126.3	879	13.29	11.1	b.d.	13.8	b.d.	2.6	0.12	0.11	0.61	144
MMI03-12-2-3	1.74	323.14	0.37	59.1	40	9.4	27.3	608	6.05	3.9	b.d.	1.1	0.1	2.6	0.09	0.12	0.09	131
MMI03-12-2-4	2.09	33008.09	1.26	36.5	1901	11.3	99.8	267	10.73	2.4	b.d.	15.8	b.d.	1.4	0.58	0.09	0.12	77
MMI03-12-2-5	0.05	13.34	0.05	17.8	7	1481.1	72	873	4.13	29.7	b.d.	10	b.d.	238.8	0.01	0.23	b.d.	18
MMI03-12-5	0.3	11.14	0.19	15.8	6	1464.6	53.8	584	3.1	48.1	b.d.	0.6	b.d.	111.5	0.01	0.9	b.d.	3
MMI03-2-11	10.78	1157.96	0.93	2283.7	251	3.5	27.7	1813	8.68	8.4	0.1	18.5	b.d.	1.8	6.63	0.11	0.55	180
Acme QC	0.09	25.46	1.11	65.7	42	23.5	13.3	797	3.91	15.9	0.1	0.3	0.3	104.8	0.14	0.14	0.02	66
MMI03-25-14	2.14	526.91	36.3	1383.3	4189	10.9	26.4	833	6.37	25	0.4	114.8	b.d.	4.6	5.79	0.85	b.d.	238
Std. GSB Till 99	0.83	161.36	186.49	333.7	1209	204.2	43.8	1317	6.43	51.8	0.4	23.2	3.1	16.3	0.65	7.42	0.22	97
MMI03-25-15b	19	480.4	316.34	733.5	2054	20.1	11.4	653	2.7	9.7	b.d.	607.5	b.d.	2.4	4.55	0.4	0.03	70
MMI03-25-5	0.17	61.54	0.28	44.4	14	61.1	25.7	618	5.21	4.3	b.d.	0.2	b.d.	4.1	0.02	0.02	b.d.	336
MMI03-25-7	0.75	177.92	13.89	241.5	584	67.8	43.8	1014	8.2	8.2	0.1	30.5	b.d.	8.5	0.76	0.1	0.05	227
MMI03-2-7	25.79	30133.98	1.66	300.4	248	29.8	317.3	1029	11.48	31.3	0.4	57.2	b.d.	0.9	0.37	0.95	0.16	137
MMI03-31-10a	0.04	33900.84	0.42	124.4	3429	163.4	62.2	502	3.22	2.6	b.d.	33.8	b.d.	2.5	0.29	b.d.	0.11	15
MMI03-31-10b	0.02	10637.51	0.79	75.3	246	84.7	63.5	447	3.27	4.1	b.d.	1	0.1	16.1	0.44	0.02	0.06	36
MMI03-31-10c	0.04	38746.7	2.86	79.2	1775	229.2	66.9	672	5.17	2.1	b.d.	1.7	b.d.	6.9	2.36	0.08	0.18	16
MMI03-31-10d	0.03	45994.16	0.81	109.4	135	322.6	108.7	1069	8.3	0.6	b.d.	2.2	b.d.	11	3.13	0.03	0.25	27
MMI03-31-12a	0.07	73665.82	1.56	61.5	4204	89.9	40.3	223	8.04	10.5	b.d	29.9	b.d.	27.4	3.35	0.18	0.13	3
Acme QC	13.19	138.19	25.51	130.1	281	24.5	11.7	762	2.91	19.3	6.1	44.9	2.9	48	5.64	3.67	6.67	58
MMI03-31-12b	0.05	34.88	0.14	12.9	8	834.3	43.8	667	2.26	1	b.d.	b.d.	b.d.	5	0.01	b.d.	b.d.	4
MMI03-31-12c	0.05	60397.96	1.64	40.3	3192	54.3	16.9	169	6.68	1.8	b.d.	14.4	b.d.	23.3	2.44	0.11	0.05	8
MMI03-5-19-1	2.82	14981.71	3.67	87.7	6419	10.8	35.8	113	4.27	32.6	b.d	76.4	b.d.	25.9	2.98	0.23	0.09	38
MMI03-5-19-2	0.9	9804.62	0.8	25.6	2204	5.2	8	113	1.77	4.2	b.d.	16.5	b.d.	21.2	9.25	0.04	0.03	25
MMI03-5-6	0.18	370.5	5.08	55.1	10	106.3	11	3653	1.7	0.7	0.4	0.6	1.1	20.6	0.08	0.29	0.28	15
MMI03-6-2-2	0.02	17.66	0.06	7	5	329	5.3	591	2.07	2.1	b.d.	0.2	b.d.	63	0.02	b.d.	b.d.	14
MMI03-6-5	0.86	27.16	1.89	60.3	52	5.8	8.2	505	2.47	3.5	0.1	0.6	0.1	8.1	0.09	0.6	0.06	39
MMI03-7-2	0.06	32.34	0.33	24.7	52	18.8	11.4	273	1.55	2	b.d.	b.d.	b.d.	45.1	0.03	0.05	b.d.	80
MMI03-8-7	0.13	20.56	0.38	60.3	9	13.4	16.8	767	4.14	1.7	0.2	b.d.	0.1	12	0.14	0.03	b.d.	108
MMI03-8-8	14.69	13578.54	0.75	62.7	1554	25.2	59	1128	13.97	5.6	0.1	9.9	b.d.	5.4	0.32	0.03	0.12	145
Acme QC	4.1	63.44	7.57	161.4	219	20.4	16.1	420	3.86	13.6	0.4	2.7	0.4	13.4	0.9	0.21	0.09	63
Silica blank	0.15	5.27	0.53	1.6	6	4.5	0.6	17	0.24	2.8	0.1	0.4	0.4	0.8	0.01	0.03	b.d.	7
BGR-1-001	1.56	25.02	1.48	51.4	86	26.5	60.1	559	9.01	16.9	b.d	20.4	b.d.	10.7	0.04	0.04	0.08	59
Acme QC	12.28	137.06	23.14	128.5	264	23.3	11.5	739	2.83	18.8	5.7	39.7	2.7	45.4	5.29	3.7	5.93	57
STD GSB Till 99	0.78	154.01	181.02	320.2	1233	192	40.9	1259	6.17	48.2	0.4	34	3	15.7	0.62	7.76	0.21	91
Std. GSB Till 99	0.83	161.36	186.49	333.7	1209	204.2	43.8	1317	6.43	51.8	0.4	23.2	3.1	16.3	0.65	7.42	0.22	97
	0.805	157.685	183.755	326.95	1221	198.1	42.35	1288	6.3	50	0.4	28.6	3.05	16	0.635	7.59	0.215	94
	0.04	5.2	3.9	9.5	17.0	8.6	2.1	41.0	0.2	2.5	0.0	7.6	0.1	0.4	0.0	0.2	0.0	4.2
	4.4	3.3	2.1	2.9	1.4	4.4	4.8	3.2	2.9	5.1	0.0	26.7	2.3	2.7	3.3	3.2	3.3	4.5

Note: see Table 2 for sample locations

TABLE 1. ICPMS ANALYSES CONTINUED.

Element	Ca	P	La	Cr	Mg	Ba	Ti	B	Al	Na	K	W	Sc	Tl	S	Hg	Se	Te	Ga
Units	%	%	ppm	ppm	%	ppm	%	ppm	%	%	%	ppm	ppm	ppm	%	ppb	ppm	ppm	ppm
Detection Limit	0.01	0.001	0.5	0.5	0.01	0.5	0.001	1	0.01	0.001	0.01	0.2		0.02	0.02	5	0.1	0.02	0.02
Station Number																			
LFE03-4-1	3.9	b.d.	b.d.	113.9	1.6	93.5	0.003	2	2.89	0.016	0.01	b.d.	2.4	b.d.	0.08	b.d.	2.7	0.08	3.4
LFE03-17-4	0.83	0.019	0.5	107.2	1.16	11.8	0.175	1	1.5	0.001	0.02	b.d.	5.4	b.d.	9.46	168	13.4	0.56	5.8
LFE-03-17-7	0.57	0.031	1.1	30.6	2.02	4.5	0.128	3	2.17	0.043	0.03	b.d.	8.2	0.11	5.12	33	2.4	0.42	7.9
STD GSB Till 99	0.32	0.101	13.6	237.4	2.43	227.8	0.085	1	2.64	0.004	0.04	b.d.	14.4	0.09	b.d.	292	0.3	0.25	8.2
MMI03-12-2	0.87	0.022	1.4	59.4	2.34	1.5	0.005	2	2.24	0.004	b.d.	b.d.	8	0.17	8.82	263	25.4	1.01	10.6
MMI03-12-2-3	0.43	0.059	1.5	28.7	2.17	1.4	0.007	4	2.04	0.027	0.01	b.d.	10.4	0.23	3.31	398	1.7	0.16	9.5
MMI03-12-2-4	0.05	0.014	0.6	98.8	1.11	1.6	0.012	2	1.23	0.009	0.01	b.d.	5.3	0.09	6.49	406	46.5	0.21	6.4
MMI03-12-2-5	12.95	0.002	b.d.	441.1	9.37	34.8	b.d.	9	0.11	0.007	0.01	0.4	6.3	0.08	b.d.	4032	b.d.	0.05	0.3
MMI03-12-5	3.85	0.001	b.d.	122.8	7.17	17.7	0.002	35	0.02	0.011	b.d.	0.4	2.2	0.24	b.d.	608	b.d.	0.02	0.2
MMI03-2-11	0.21	0.045	1.6	37	1.34	2.5	0.09	1	1.91	0.026	0.02	b.d.	9.6	0.03	6.53	118	8.3	0.31	8.8
Acme QC	3.75	0.052	2.8	67.9	1.81	76.8	0.012	2	2.56	0.036	0.11	b.d.	4.9	0.02	0.12	6	b.d.	0.04	7.4
MMI03-25-14	1.17	0.033	0.6	17.5	3.67	6.2	0.383	3	3.33	0.038	0.04	b.d.	14.4	1.08	2.67	411	0.9	3.01	11.3
Std. GSB Till 99	0.34	0.107	14.4	247.6	2.55	239.4	0.09	b.d.	2.77	0.005	0.04	b.d.	14.7	0.1	b.d.	305	0.4	0.25	8.6
MMI03-25-15b	0.28	0.013	0.5	108.6	1.41	6.3	0.122	b.d.	1.21	0.025	0.05	b.d.	5.2	0.04	1.07	211	0.5	0.03	4
MMI03-25-5	1.58	0.017	b.d.	132.7	2.14	5.1	0.288	3	2.9	0.029	0.01	b.d.	5.8	b.d.	0.2	10	0.2	b.d.	9.2
MMI03-25-7	1.28	0.039	1.3	143.3	4.24	16.9	0.34	3	3.59	0.017	0.02	b.d.	16.9	0.03	2.56	415	1.4	0.03	12.5
MMI03-2-7	0.09	0.028	b.d.	47.5	2.33	2.4	0.053	1	3.61	0.003	0.02	b.d.	9.7	0.04	2.78	159	43.7	2.42	11.6
MMI03-31-10a	2.69	0.001	b.d.	159	3.13	0.9	0.012	1	3.47	0.003	0.01	b.d.	2.7	b.d.	0.89	5	30.1	1.48	4.4
MMI03-31-10b	3.4	0.019	0.9	186.5	2.46	9.7	0.044	2	3.38	0.016	0.01	b.d.	3.2	b.d.	0.34	b.d.	4.9	0.17	6
MMI03-31-10c	4.32	0.001	b.d.	296.7	2.84	1.1	0.009	1	1.87	0.007	0.01	b.d.	3.2	b.d.	2.53	8	16.4	0.41	3.6
MMI03-31-10d	5.71	0.001	b.d.	569.4	4.11	0.7	0.015	2	2.59	0.005	b.d.	b.d.	2.6	b.d.	3.6	b.d.	20.3	0.24	5.4
MMI03-31-12a	1.26	0.004	b.d.	43.5	1.11	1	0.006	1	1.31	0.002	b.d.	b.d.	0.6	b.d.	4.49	22	98.4	0.47	2
Acme QC	0.73	0.097	12.3	185.6	0.66	135.7	0.094	18	2.02	0.034	0.13	5.2	3.5	1.09	b.d.	173	4.4	0.83	6.5
MMI03-31-12b	5.64	0.001	b.d.	312.2	7.09	2.6	0.004	3	0.13	0.001	b.d.	b.d.	3.2	0.02	0.07	b.d.	0.1	b.d.	0.3
MMI03-31-12c	0.85	0.005	b.d.	63.1	1.06	0.6	0.016	b.d.	1.16	0.003	b.d.	b.d.	1	b.d.	3.3	24	74.6	0.51	1.8
MMI03-5-19-1	0.72	0.007	b.d	88.3	0.09	0.5	0.139	1	0.47	0.001	b.d.	b.d.	2.5	0.03	3.05	467	8.4	0.23	2
MMI03-5-19-2	2.08	0.002	b.d.	79.9	0.08	b.d.	0.056	b.d.	0.4	0.001	b.d.	b.d.	1.5	b.d.	1.27	224	6.3	0.05	1.8
MMI03-5-6	2.06	0.101	7.6	84.9	0.56	2195.2	0.066	1	0.6	0.007	0.36	0.9	3.1	0.13	0.03	6	b.d.	0.14	4.6
MMI03-6-2-2	6.82	0.001	b.d.	38.8	17.66	17	0.004	2	0.01	0.003	b.d.	b.d.	3.1	b.d.	0.06	b.d.	0.2	b.d.	0.1
MMI03-6-5	0.53	0.021	1.2	86.8	0.94	13.3	0.16	4	1.15	0.065	0.07	b.d.	6.6	0.02	0.63	12	0.2	0.04	5
MMI03-7-2	1.25	0.015	0.5	53.8	0.84	3.9	0.219	4	1.26	0.015	0.01	b.d.	4.4	b.d.	0.02	b.d.	b.d	b.d.	3.7
MMI03-8-7	3.65	0.037	1.2	10.9	1.44	5.2	0.2	3	1.68	0.094	0.05	b.d.	1.6	b.d.	0.01	b.d.	b.d.	b.d.	6.9
MMI03-8-8	0.27	0.016	0.6	33.3	2.63	1.5	0.077	1	2.75	0.006	b.d.	b.d.	9	b.d.	0.11	22	20.9	0.09	10.1
Acme QC	0.64	0.088	2.4	42.2	0.97	25.4	0.172	1	1.3	0.05	0.11	0.2	5.9	0.04	1.47	b.d.	3.7	0.08	4.2
Silica blank	0.01	0.001	2.3	182.3	0.01	15.9	0.004	1	0.04	0.002	0.02	b.d.	0.1	b.d.	0.03	b.d.	b.d.	b.d.	0.1
BGR-1-001	0.82	0.012	b.d.	88.9	1.72	0.8	0.108	1	1.55	0.002	b.d.	b.d.	6.4	b.d.	7.04	35	7.1	0.22	4.9
Acme QC	0.7	0.092	11.2	183.1	0.64	134.6	0.087	17	1.99	0.032	0.13	4.8	3.4	0.98	0.03	170	4.5	0.82	6.5

STD GSB Till 99	0.32	0.101	13.6	237.4	2.43	227.8	0.085	1	2.64	0.004	0.04	b.d.	14.4	0.09	b.d.	292	0.3	0.25	8.2
Std. GSB Till 99	0.34	0.107	14.4	247.6	2.55	239.4	0.09	b.d.	2.77	0.005	0.04	b.d.	14.7	0.1	b.d.	305	0.4	0.25	8.6
	0.33	0.104	14	242.5	2.49	233.6	0.0875	1	2.705	0.0045	0.04	b.d.	14.55	0.095	b.d.	298.5	0.35	0.25	8.4
	0.0	0.0	0.6	7.2	0.1	8.2	0.0		0.1	0.0	0.0		0.2	0.0		9.2	0.1	0.0	0.3
	4.3	4.1	4.0	3.0	3.4	3.5	4.0		3.4	15.7	0.0		1.5	7.4		3.1	20.2	0.0	3.4

Note: see Table 2 for sample locations

TABLE 2. RESULTS OF INDUCED NEUTRON ACTIVATION ANALYSES (INAA)

		Element	Au	As	Ba	Ca	Co	Cr	Fe	Hf	Mo
		Units	ppb	ppm	ppm	%	ppm	ppm	%	ppm	ppm
		Detection Limit	2	0.5	50	1	1	5	0.02	1	1
Station Number	**Easting**	**Northing**									
LFE03-4-1	620020	6542337	1480	1.3	160	14	24	719	2.51	b.d.	b.d.
LFE03-17-4	624689	6541846	20	18	b.d.	7	34	196	13.5	1	b.d.
LFE-03-17-7	622472	6543267	4	15.9	b.d.	2	18	70	7.51	2	8
STD GSB Till 99			26	61.4	960	2	45	368	7.71	3	b.d.
MMI03-12-2	620487	6537407	20	11.9	85	b.d.	114	126	13.6	1	b.d.
MMI03-12-2-3	620487	6537407	b.d.	3.6	b.d.	b.d.	25	51	6.33	4	b.d.
MMI03-12-2-4	620487	6537407	26	2.5	b.d.	b.d.	88	190	11.1	b.d.	b.d.
MMI03-12-2-5	620487	6537407	5	28	b.d.	14	69	1800	4.18	b.d.	b.d.
MMI03-12-5	620463	6537537	b.d.	55.1	b.d.	4	63	2540	3.45	b.d.	b.d.
MMI03-2-11	620373	6544373	25	9.2	b.d.	b.d.	25	73	8.42	2	11
MMI03-25-14	623445	6542687	137	27.7	b.d.	1	26	35	7.08	2	b.d.
Std. GSB Till 99			36	60.4	930	b.d.	45	368	7.78	3	b.d.
MMI03-25-15b	623544	6542801	584	9.6	b.d.	b.d.	12	176	3	b.d.	21
MMI03-25-5	625137	6542383	b.d.	b.d.	b.d.	7	41	175	8.63	1	b.d.
MMI03-25-7	624802	6542092	43	6.7	b.d.	3	47	237	10.3	2	b.d.
MMI03-2-7	620314	6544344	76	31.5	b.d.	b.d.	302	98	12.4	2	18
MMI03-31-10a	618326	6545686	543	1.7	b.d.	14	75	480	5.06	b.d.	b.d.
MMI03-31-10b	618326	6545686	b.d.	2.8	430	12	78	525	6.61	b.d.	b.d.
MMI03-31-10c	618326	6545686	31	3	b.d.	14	71	1300	7.11	b.d.	b.d.
MMI03-31-10d	618326	6545686	b.d.	3.2	b.d.	11	125	1130	11.8	b.d.	b.d.
MMI03-31-12a	618432	6545725	48	13	b.d.	10	45	156	12.7	b.d.	b.d.
MMI03-31-12b	618432	6545725	b.d.	2.2	b.d.	7	44	1380	2.61	b.d.	b.d.
MMI03-31-12c	618432	6545725	29	3.4	b.d.	10	33	300	10.3	b.d.	b.d.
MMI03-5-19-1	621005	6541401	110	35.3	b.d.	5	33	196	6.73	b.d.	b.d.
MMI03-5-19-2	621005	6541401	39	5	b.d.	6	7	180	4.2	b.d.	b.d.
MMI03-5-6	620072	6542193	b.d.	3.7	24000	2	12	176	2.37	3	b.d.
MMI03-6-2-2	621633	6544264	b.d.	1.7	b.d.	7	6	49	2.06	b.d.	b.d.
MMI03-6-5	621933	6544290	b.d.	4.6	120	b.d.	8	151	2.53	2	b.d.
MMI03-7-2	619753	6544718	4	b.d.	b.d.	7	11	101	5.05	1	b.d.
MMI03-8-7	621232	6541095	5	b.d.	b.d.	9	29	29	7.22	2	b.d.
MMI03-8-8	621102	6540832	17	5.7	b.d.	2	59	69	16.6	b.d.	8
Silica blank			b.d.	1.8	b.d.	b.d.	1	359	0.33	b.d.	b.d.
BGR-1-001	621083	6541361	23	15.8	100	3	58	165	10.8	1	b.d.
QC											
STD GSB Till 99			26	61.4	960	2	45	368	7.71	3	b.d.
Std. GSB Till 99			36	60.4	930	b.d.	45	368	7.78	3	b.d.
Mean			31	60.9	945	2	45	368	7.75	3	b.d.
SD			7.07	0.71	21.21		0	0	0.05	0	
%RSD			22.8	1.16	2.245		0	0	0.64	0	
Silica blank			b.d.	1.8	b.d.	b.d.	1	359	0.33	b.d.	b.d.

TABLE 2. INAA RESULTS CONTINUED

Element	Na	Ni	Sb	Sc	Se	Th	Zn	La	Ce	Nd	Sm	Eu	Yb	Lu	Mass
Units	%	ppm	ppm	ppm	ppm	ppm	ppm	ppm	ppm	ppm	ppm	ppm	ppm	ppm	g
Detection Limit	0.01	20	0.1	0.1	3	0.5	50	0.1	3	5	0.1	0.2	0.2	0.05	0.1
Station Number															
LFE03-4-1	0.26	b.d.	b.d.	26.4	b.d.	b.d.	b.d.	b.d.	b.d.	b.d.	0.2	b.d.	0.5	0.07	28.09
LFE03-17-4	0.03	b.d.	0.7	17.2	13	0.5	b.d.	3.4	8	b.d.	1.9	1.3	1.9	0.28	28.05
LFE-03-17-7	1.85	b.d.	0.7	18.1	b.d.	b.d.	638	2.3	5	7	1.9	0.7	3.1	0.46	28.56
STD GSB Till 99	1.75	244	13.8	27.6	b.d.	5.6	399	29.4	54	24	5.7	2.1	2.8	0.42	20.51
MMI03-12-2	0.34	b.d.	b.d.	11.4	21	b.d.	88	2.1	7	b.d.	1.2	0.6	1.3	0.22	31.46
MMI03-12-2-3	2.67	b.d.	b.d.	19.1	b.d.	b.d.	92	2.9	9	8	2.5	0.9	5.5	0.85	30.41
MMI03-12-2-4	0.26	b.d.	b.d.	7.5	40	b.d.	b.d.	1.4	b.d.	b.d.	0.8	0.4	1	0.15	29.06
MMI03-12-2-5	0.03	1050	1.9	6.4	b.d.	b.d.	55	b.d.	b.d.	b.d.	b.d.	b.d.	b.d.	b.d.	37.06
MMI03-12-5	0.04	1070	8.1	2.5	b.d.	b.d.	b.d.	b.d.	b.d.	b.d.	b.d.	b.d.	b.d.	b.d.	31.44
MMI03-2-11	2.26	b.d.	0.3	17.5	4	0.4	2250	2.7	10	7	2.1	0.8	3.4	0.51	33.39
MMI03-25-14	2.48	b.d.	1.8	32.8	b.d.	b.d.	1550	2.2	11	7	2.1	0.8	3	0.48	30.38
Std. GSB Till 99	1.77	241	13.4	28.8	b.d.	5.8	431	30.1	54	23	5.8	2.2	3	0.46	23.58
MMI03-25-15b	1.08	b.d.	0.6	13	b.d.	b.d.	832	0.9	3	b.d.	0.7	0.4	1.1	0.16	25.41
MMI03-25-5	2.13	170	0.2	45.2	b.d.	0.4	155	1.7	5	b.d.	1.8	0.6	2.7	0.41	31.78
MMI03-25-7	2.47	b.d.	0.3	41.6	b.d.	b.d.	320	2.5	7	b.d.	2.5	1.2	3.2	0.47	31.6
MMI03-2-7	0.15	b.d.	2.1	16.7	53	b.d.	375	1.7	5	b.d.	1.4	0.2	2.2	0.35	29.25
MMI03-31-10a	0.08	130	b.d.	24.7	35	b.d.	178	0.6	3	b.d.	0.3	b.d.	0.4	0.06	31.71
MMI03-31-10b	0.46	74	b.d.	29.5	b.d.	b.d.	184	2.7	7	b.d.	1.1	0.6	0.9	0.14	31.2
MMI03-31-10c	0.11	290	0.8	37	17	b.d.	164	0.6	b.d.	b.d.	0.3	b.d.	0.6	0.09	36.49
MMI03-31-10d	0.08	327	0.2	27.2	26	b.d.	180	0.6	b.d.	b.d.	0.2	b.d.	b.d.	b.d.	29.51
MMI03-31-12a	0.05	b.d.	0.2	7.1	119	b.d.	76	0.6	b.d.	b.d.	0.2	0.7	b.d.	b.d.	30.1
MMI03-31-12b	0.03	741	0.3	3.6	b.d.	b.d.	b.d.	0.7	b.d.	b.d.	b.d.	b.d.	b.d.	b.d.	26.59
MMI03-31-12c	0.06	b.d.	b.d.	21.2	74	b.d.	111	0.9	3	b.d.	0.4	0.5	0.6	0.09	34.1
MMI03-5-19-1	0.02	b.d.	b.d.	11	7	b.d.	82	1.6	4	b.d.	1	0.5	1.5	0.23	29.45
MMI03-5-19-2	0.02	b.d.	b.d.	6.4	7	0.2	b.d.	0.9	b.d.	b.d.	0.5	0.5	0.7	0.11	33.32
MMI03-5-6	0.1	79	0.8	8.8	b.d.	1.6	78	18.9	16	13	3.4	0.8	2.3	0.36	30.43
MMI03-6-2-2	0.03	272	b.d.	3.5	b.d.	b.d.	b.d.	b.d.	b.d.	b.d.	b.d.	b.d.	b.d.	b.d.	30.92
MMI03-6-5	2.6	b.d.	0.8	11.9	b.d.	0.4	76	3.2	9	7	2.2	0.7	3.6	0.54	30.17
MMI03-7-2	0.73	109	b.d.	18.5	b.d.	b.d.	b.d.	2.1	5	b.d.	1.5	0.7	2.1	0.31	38.02
MMI03-8-7	2.54	b.d.	b.d.	34.8	b.d.	b.d.	b.d.	2.7	8	b.d.	2.2	0.8	3.3	0.5	30.24
MMI03-8-8	0.28	b.d.	b.d.	19.8	22	b.d.	113	4.6	11	b.d.	2.8	1.9	1.9	0.3	34.59
Silica blank	0.04	b.d.	0.1	0.5	b.d.	0.7	b.d.	4.5	7	b.d.	0.4	b.d.	b.d.	b.d.	28.88
BGR-1-001	0.16	196	b.d.	18.4	b.d.	b.d.	78	1.3	b.d.	b.d.	0.9	0.2	1.5	0.23	37.35
QC															
STD GSB Till 99	1.75	244	13.8	27.6	b.d.	5.6	399	29.4	54	24	5.7	2.1	2.8	0.42	20.51
Std. GSB Till 99	1.77	241	13.4	28.8	b.d.	5.8	431	30.1	54	23	5.8	2.2	3	0.46	23.58
Mean	1.76	243	13.6	28.2	b.d.	5.7	415	29.8	54	23.5	5.75	2.15	2.9	0.44	22.05
SD	0.01	2.12	0.28	0.85		0.14	22.6	0.49	0	0.71	0.07	0.07	0.14	0.028	2.171
%RSD	0.8	0.87	2.08	3.01		2.48	5.45	1.66	0	3.01	1.23	3.29	4.88	6.428	9.847
Silica blank	0.04	b.d.	0.1	0.5	b.d.	0.7	b.d.	4.5	7	b.d.	0.4	b.d.	b.d.	b.d.	28.88

Photo 2. Pillowed basalt flows are very well developed on "Sleeper Peak" immediately west of "Black Goat Peak".

commonly, chert are locally preserved and present opportunities for age dating via microfossils, either conodonts or radiolaria. Interpillow or interflow hyaloclastite is recognizable in well preserved sections.

Agglomerate is exposed at the structural top of the pillowed section hosting the Joss'alun mineralization. The definition of "agglomerate" used herein is: a monomict volcanic breccia composed primarily of rounded clasts (bombs, not erosional).

On the eastern side of "Jos valley" the agglomerate grades into basalt breccia with a cherty ferrugenous maroon matrix (Photo 3), which in turn, grades into ferruginous chert from which "Permian" radiolaria were extracted (Mihalynuk *et al.*, 2003b). The same stratigraphic relationship is seen on the west side of "Jos Peak", suggesting a regionally correlatable succession (see also "Ferruginous chert" below).

Sections of basalt exposed within the NAK area probably span a range of ages, but no field criteria that permit basalts of varying ages to be distinguished from one another have yet been recognized.

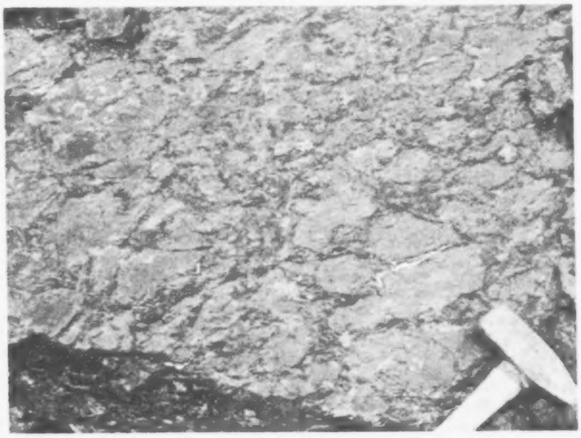

Photo 3. Volcanic breccia near the top of the mafic volcanic section commonly displays a maroon, cherty ash matrix. Locally this unit grades into ferruginous chert.

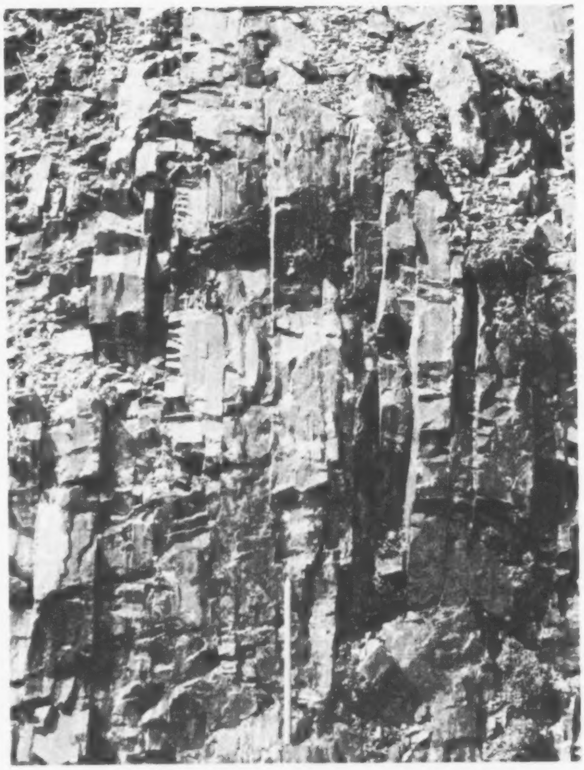

Photo 4. A typical exposure of ferruginous chert. Layer thickness of 1-5 centimetres and ruler straight beds are typical, but not displayed in all occurrences.

Geochemistry

We collected 5 samples of basalt from the belt of mafic volcanic rocks and probable correlatives within the Joss'alun belt and analyzed major, trace and rare earth elements in order to test the tectonic affinity of the parent magma(s). The data are given in Table 3 and plotted in Figure 6.

Figure 6A is a plot of alkalis versus silica with the alkaline-subalkaline fields of Irvine and Baragar (1971); all samples are subalkaline. Figure 6Bshows rock classification fields of Cox *et al.* (1979), all of the samples are basalt or basltic andesite. Alkalis and silica can be mobile in metamorphosed rocks. However, the samples plot in corresponding fields based on their immobile elements composition (Fig. 6C, D; Winchester and Floyd, 1977), confirming the rock type assignment made on the basis of major oxides.

Descrimination of modern petrogenetic environments can be shown by plotting elemental abundances in basalts. Composition of ancient basalts can be compared with modern environments in order to resolve the tectonic environment in which they formed. The Th-Hf/3-Ta descriminat-ion plot of Wood (1980) separates the geochemical fields of basalts generated at a destructive plate margin (arc) from

TABLE 3. RESULTS OF MAJOR OXIDE X-RAY FLUORESCENCE (XRF) ANALYSES

Field Number	Description	SiO2	TiO2	Al2O3	Fe2O3	MnO	MgO	CaO	Na2O	K2O	P2O5	Xba	LOI	Total	XRb	XSr	XBa	XNb	XZr	XHf
MMI03-5-6	"Sleeper Peak" chert	79.26	0.15	2.43	3.35	0.47	1.07	3.00	0.23	0.75	0.15	2.56	3.04	96.46	26	76	25594	12	56	4
MMI03-3-2-1	Gabbro S of Joss'alun, intrudes 3-2-2	46.95	0.27	7.09	8.18	0.14	18.79	13.35	0.25	0.01	0.01	0.01	4.28	99.33	5	20	24	3	17	<3
MMI03-3-2-2	Ultramafite intruded by 3-2-1	40.56	0.10	3.54	14.39	0.14	28.64	2.34	0.07	0.01	0.01	0.01	9.89	99.70	<3	<3	35	5	16	<3
MMI03-3-8*2	Jos - S pillow breccia atop clastics	49.15	1.05	14.38	10.05	0.18	6.42	9.10	2.18	1.15	0.10	0.01	5.92	99.69	12	128	64	<3	77	<3
MMI03-4-2	Hardluck Pks agglomerate	49.40	1.41	14.81	10.32	0.25	5.67	9.61	2.36	0.66	0.15	0.01	5.00	99.65	16	118	57	4	89	<3
MMI03-5-2*2	"Sleeper Pk." mafic fragmental	49.68	1.07	14.84	9.73	0.17	8.06	10.07	2.94	0.50	0.07	0.35	1.99	99.47	11	262	3502	4	63	3
MMI03-5-11-2	"Sleeper Pk." pillow basalt	50.09	1.50	15.25	11.75	0.15	5.94	10.06	3.40	0.20	0.18	0.01	1.29	99.82	6	134	67	6	97	4
MMI03-10-6-2	Pillow basalt NE Peridotite Pk	48.84	0.99	13.19	11.32	0.15	7.19	11.97	2.00	0.02	0.09	0.01	4.07	99.84	3	51	136	5	58	<3
MMI03-12-1	Yeth Ck volcs	48.22	0.43	13.35	8.02	0.14	10.47	9.85	1.97	2.01	0.10	0.01	4.59	99.16	23	173	145	<3	40	<3
MMI03-28-11	Dense basalt -McCallum Pk	52.11	1.47	17.05	10.17	0.14	3.50	4.48	5.59	1.90	0.38	0.15	2.53	99.47	43	721	1482	6	149	4
MMI03-25-5	Altd gabbro + cpy flecks -Unnamed Ck	47.97	1.49	14.68	11.39	0.14	7.63	9.55	2.64	0.03	0.07	0.01	4.05	99.65	6	45	37	<3	51	<3
MMI03-25-7	Basalt Ck between Peridotite and Hardluck	52.74	0.80	14.64	8.97	0.09	7.55	6.80	2.46	0.02	0.09	0.01	5.48	99.65	5	33	53	<3	58	<3
MMI03-27-2	Massive tuff - Peninsula Mtn.	56.63	0.75	17.45	7.36	0.11	2.72	6.28	2.51	2.14	0.20	0.15	3.02	99.32	67	709	1499	4	128	3
MMI03-25-15a	Massive basalt flows - Unnamed Ck.	49.45	0.93	15.10	9.77	0.18	8.26	4.53	3.73	0.17	0.07	0.01	7.23	99.43	<3	72	83	<3	67	<3
MMI03-14-6	Foliated Granodiorite U-Pb S Hardluck	59.29	0.57	16.71	5.76	0.10	3.28	6.59	2.80	1.05	0.10	0.11	3.21	99.57	31	569	1066	3	91	3
STD FER-3		53.52	0.01	0.07	44.43	0.07	1.00	0.83	0.01	0.01	0.09	0.01	-0.19	99.86	<3	29	20	<3	<3	<3
Std. CANMET SY-4		49.81	0.28	20.65	6.21	0.10	0.52	8.03	7.03	1.62	0.12	0.03	4.80	99.20	53	1214	349	14	504	12
Std. CANMET SY-4		49.81	0.28	20.65	6.21	0.10	0.52	8.03	7.03	1.62	0.12	0.03	4.80	99.20	53	1214	349	14	504	12
SY-4 standard		49.90	0.29	20.69	6.21	0.11	0.54	8.05	7.10	1.66	0.13	0.03	4.56	99.27	55	1191	340	13	517	11

TABLE 4. RESULTS OF TRACE ELEMENT ANALYSES (ICPMS)

Stn No	Y	Zr	Nb	Ba	La	Ce	Pr	Nd	Sm	Eu	Gd^{160}	Tb	Dy	Ho	Er	Tm	Yb	Lu	Hf	Ta	Th	Nb_{Rerun}
MMI03-5-6	15.284	50.84	7.14	26304	18.33	14.64	4.309	17.88	4.00	1.13	3.72	0.588	3.54	0.687	2.01	0.304	2.09	0.35	0.99	0.19	1.81	3.54
MMI03-3-2-1	7.023	5.42	3.75	31	0.15	0.58	0.143	1.04	0.56	0.25	0.97	0.193	1.44	0.297	0.97	0.125	0.82	0.12	0.23	0.02	0.01	0.23
MMI03-3-2-2	1.916	1.59	3.99	17	0.05	0.18	0.043	0.28	0.15	0.09	0.25	0.048	0.36	0.078	0.24	0.038	0.25	0.04	0.07	0.02	0.01	0.49
MMI03-3-8*2	22.402	87.39	6.09	82	3.02	8.65	1.452	7.97	2.71	0.98	3.61	0.652	4.35	0.857	2.56	0.373	2.34	0.36	2.24	0.16	0.19	1.93
MMI03-4-2	29.220	104.40	5.36	60	3.70	9.87	1.877	10.68	3.59	1.30	5.18	0.870	5.68	1.198	3.51	0.491	3.10	0.44	2.70	0.11	0.15	1.40
MMI03-5-2*2	18.212	69.49	7.27	4321	3.07	8.02	1.286	6.82	2.23	0.80	3.19	0.524	3.56	0.768	2.25	0.331	2.20	0.33	1.76	0.20	0.20	3.59
MMI03-5-11*2	24.252	112.13	11.72	51	5.11	13.68	2.149	11.24	3.37	1.16	4.55	0.741	4.80	0.977	2.85	0.404	2.66	0.38	2.70	0.37	0.36	6.97
MMI03-10-6*2	18.860	64.29	6.97	159	2.79	7.37	1.205	6.47	2.09	0.92	3.10	0.522	3.51	0.753	2.25	0.332	2.13	0.32	1.55	0.17	0.15	2.98
MMI03-12-1	11.456	32.43	3.97	181	1.37	3.44	0.583	3.23	1.10	0.42	1.58	0.271	1.92	0.416	1.31	0.195	1.35	0.20	0.88	0.04	0.10	0.79
MMI03-28-11	28.290	170.49	16.54	1836	22.03	43.83	6.105	27.24	6.08	1.73	6.33	0.909	5.42	1.082	3.03	0.430	2.80	0.41	3.77	0.52	4.03	9.58
MMI03-25-5	17.076	56.81	3.82	15	1.28	4.34	0.798	4.53	1.73	0.60	2.68	0.490	3.38	0.701	2.14	0.312	2.12	0.32	1.55	0.07	0.12	1.64
MMI03-25-7	17.211	59.72	3.02	55	2.05	5.94	1.023	5.71	1.97	0.80	2.82	0.497	3.35	0.686	2.06	0.303	2.00	0.30	1.64	0.06	0.14	0.86
MMI03-27-2	18.201	140.77	9.26	1853	21.01	39.03	4.755	19.61	4.15	1.24	4.01	0.595	3.59	0.712	2.04	0.300	1.98	0.31	3.26	0.34	5.29	6.35
MMI03-25-15a	34.174	157.59	11.02	1329	10.48	22.94	3.187	14.78	4.24	1.49	5.65	0.976	6.49	1.346	4.07	0.613	4.05	0.62	3.90	0.37	2.04	
MMI03-14-6	14.691	95.36	8.50	1295	9.15	18.13	2.263	10.04	2.35	0.80	2.66	0.455	2.95	0.592	1.83	0.274	1.87	0.29	2.33	0.37	1.92	5.84
Detect Limit	0.004	0.04	0.03	0.08	0.01	0.01	0.003	0.03	0.01	0.01	0.02	0.004	0.03	0.002	0.01	0.003	0.01	0.003	0.02	0.04	0.01	
Std. CANMET SY-4	103.94	697.51	21.49	402	56.12	114.44	14.14	57.57	12.51	1.99	14.65	2.742	19.67	4.392	14.64	2.342	15.58	2.11	12.31	0.81	1.15	16.36
CANMET Ref	119.00	517.00	13.00	340	58.00	122.00	15.00	57.00	12.70	2.00	14.00	2.600	18.20	4.300	14.20	2.300	14.80	2.10	10.60	0.90	1.40	13.00
percentDifference	13.507	29.73	49.21	17	3.30	6.40	5.924	1.00	1.51	0.45	4.51	5.316	7.74	2.117	3.06	1.810	5.15	0.43	14.95	10.53	19.69	22.89

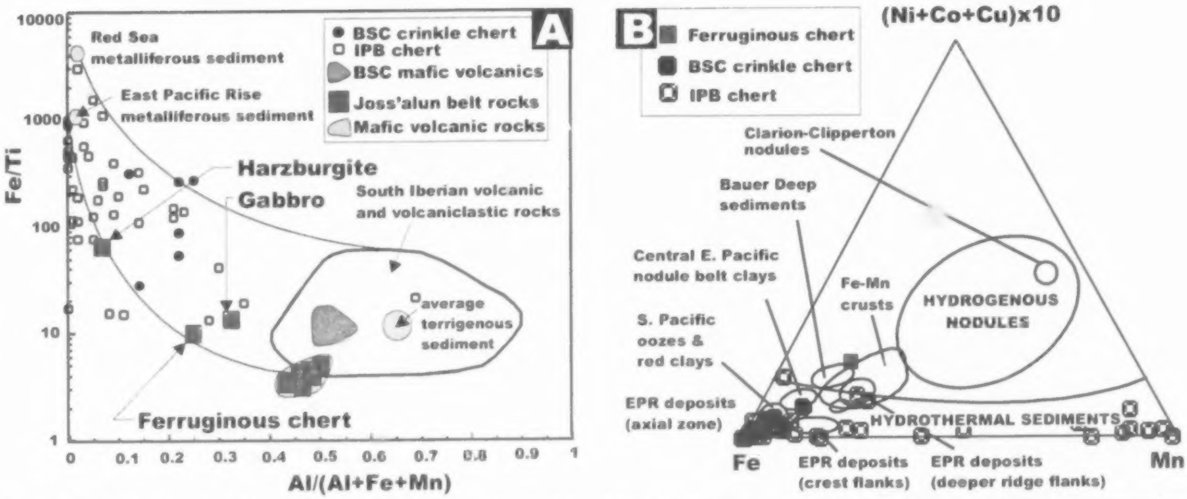

Figure 3. Chemical composition of ferruginous chertas compared on a plot of Fe/Ti versus Al/(Al+Fe+Mn) as a measure of the proportion of hydrothermal or terrigenous imputs (A). andon (B) the Ni+Co+Cu - Fe -Mn ternary diagram, to discriminate between hydrothermal and hydrogenous or biogenic sources (see Mihalynuk and Peter, 2001 for sources). Also compared are the composition of chert and volcanic rocks from the Big Salmon complex (Mihalynuk and Peter, 2001). Although theferruginous chert unit is locally copper stained, elevated copper contents are common in oceanic settings and do not necessarily indicate a hydrothermal source. Ferruginous chert chemical composition plots within between the fields of hydrothermal sediment and terrigenous sediment (A) and with deep sea sediments and Fe-Mn crusts (B).

TABLE 5. RESULTS OF RADIOLARIAN PROCESSING AND IDENTIFICATION IN 2003

Samples	Location UTM zn8 E/N	Lithology	Radiolarian Occurrence	Preser-vation	Content and radiolarian taxa	Age
MMI03-3-10	618779 6544207	red chert	+	poor	sponge spicules, recrystallized spumellarians,silica fragments	**indeterminate**
MMI03-5-3	620190 6542388	laminated grey/black siliceous argillite	?	/	silica fragments, one conodont specimen sent to M.J. Orchard, Geological Survey of Canada, Vancouver	**see M.J. Orchard**
MMI03-5-5	620090 6542240	grey siliceous argillite	+	poor	abundant recrystallized flattened radiolarians. Large triradiate Latentifistulidae	**Carboniferous-Permian**
MMI03-5-6	620070 6542195	red chert	+	very poor	recrystallized silica fragments, red clays	**indeterminate**
MMI03-5-12	620346 6541664	red chert	+	poor	sponge spicules, silica fragments, large Latentifistulidae, ?*Quinqueremis* sp.	**Carboniferous-Permian**
MMI03-7-3	619800 6544550	grey-brown siliceous argillite	+	poor	silica fragments and aggregates, rare spumellarians	**indeterminate**
MMI03-10-5-2	632156 6541448	grey chert	+	moderate	*Haploaxon* sp., *Latentifistula* sp., *Pseudoalbaillella sakmarensis*, *Quinqueremis* sp.	**Early Permian, late Asselian-Sakmarian**
MMI03-10-8	632946 6540788	black chert	+	moderate	*Entactinia* sp., *Latentibifistula* sp., *Pseudoalbaillella sakmarensis*, *Quinqueremis* sp., abundant quartz crystals	**Early Permian; late Asselian-Sakmarian**
MMI03-11-2	629051 6541445	grey chert	+	good	*Canesium lentum*, *Capnodoce* sp., *Capnuchosphaera schenki*, *Sarla* sp., *Saitoum* sp., *Triassocampe* sp.	**Late Triassic, latest Carnian-early Norian**
MMI03-12-11	620588 6540268	grey chert	+	poor	quartz crystals, sphaeromorphs, probable spumellarians	**indeterminate**
MMI03-14-9c	619500 6540030	grey chert	+	poor	silica fragments, sponge spicules, quartz and pyrite crystals, ?*Oertlispongus*, *Triassocampe* sp., recrystallized spumellarians and nasselarians	**Middle or Late Triassic**

Chemical procedure: HF 7%, 3 series of 24 hours for each sample

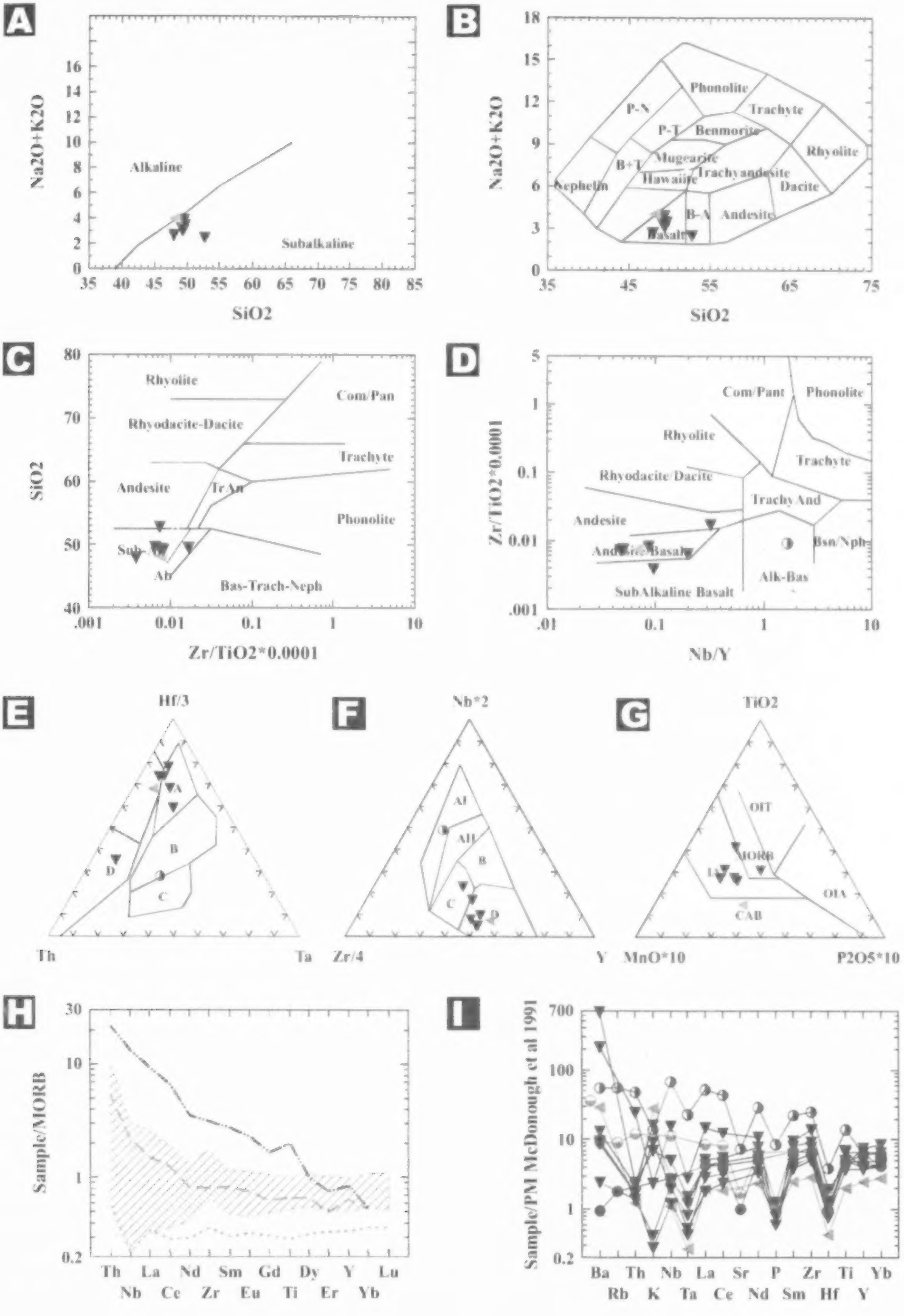
A
Na2O+K2O
SiO2
Alkaline
Subalkaline
35 40 45 50 55 60 65 70 75 80 85
0 2 4 6 8 10 12 14 16
B
Na2O+K2O
SiO2
0 3 6 9 12 15 18
35 45 55 65 75
Phonolite
P-N
Trachyte
P-T
Benmorite
Rhyolite
B+T
Mugearite
Hawaiite
Trachyandesite
Nephelin
Dacite
B-A
Andesite
Basalt
C
SiO2
Zr/TiO2*0.0001
40 50 60 70 80
.001 0.01 0.1 1 10
Rhyolite
Com/Pan
Rhyodacite-Dacite
Trachyte
Andesite
TrAn
Phonolite
Sub-Ab
Ab
Bas-Trach-Neph
D
Zr/TiO2*0.0001
Nb/Y
.001 0.01 0.1 1 5
.01 0.1 1 10
Com/Pant
Phonolite
Rhyolite
Trachyte
Rhyodacite/Dacite
TrachyAnd
Andesite
Andesite/Basalt
Bsn/Nph
Alk-Bas
SubAlkaline Basalt
E
Hf/3
Th
Ta
A
B
C
D
F
Nb*2
Zr/4
Y
AI
AII
B
C
D
G
TiO2
MnO*10
P2O5*10
OIT
MORB
IAT
OIA
CAB
H
Sample/MORB
0.2 1 10 30
Th La Nd Sm Gd Dy Y Lu
Nb Ce Zr Eu Ti Er Yb
I
Sample/PM McDonough et al 1991
0.2 1 10 100 700
Ba Th Nb La Sr P Zr Ti Yb
Rb K Ta Ce Nd Sm Hf Y

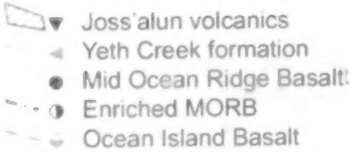

Figure 4. Geochemical plots show that the volcanic rocks in the study are are subalkaline basalt based upon major oxide analyses (A, method of Irvine and Baragar, 1971; B, methodl of Cox, 1979) and trace elements (C, D; based upon method of Winchester and Floyd, 1977). Consistency between A, B and C, D) provides a test for the reliability of the trace element analyses. Pettrogenetic environment is shown in descrimination plots E, F, G (method of Wood, 1980; Meschede, 1986; and Mullen, 1983)). Samples fall within or straddle the boundary between destructive plate margin (field D) and normal MORB (field B, field AI is wwithin-plate basalt/EMORB field) on the Th-Ta-Hf/3 plot (Figurre E). Figure F likewise shows that data straddle the boundary bertween volcanic arc basalt (fields C-D) and NMORB (field D); witthin plate alkaline basalts fall within field AI. Figure G similarly sshows that samples straddle the fields between MORB and islannd arc tholeiite (IAT); CAB is the field of calc-alkaline basalt.

Photo 5. Copper staining on argillaceous beddi ng planes at the interbedded contact between marley ferruginous chert and limestone.

Photo 6. Chert layers in recrystallized limestone are typical of the best developed limestone sections.

Photo 7. A typical exposure of well-bedded, grey ribbon chert.

those formed in other environments. Basalts from the Joss'alun belt as well as the Yeth Creek formation fall within or straddle the boundary between the volcanic arc field (VAB) and normal Mid-Ocean Ridge Basalt (N-MORB). Plotting Th-Hf/3-Nb/16 (not shown) yields nearly identical results and confirms the consistency of Nb and Ta analyses. In a plot of Zr/4-Y-Nb/2 after the method of Meschede (1986) the Joss'alun belt samples fall within the volcanic arc basalt and N-MORB fields (D); Yeth Creek formation falls in field D. The Ocean Island Basalt (OIB) and N-MORB standards fall into the expected within-plate (AI) and N- MORB (D) fields. Figure 6G shows the TiO_2-MnO-P_2O_5 plot after the method of Mullen (1983). On this plot, Joss'alun belt samples fall within the Island Arc Tholeiite and MORB fields while the Yeth Creek formation sample falls within the Calc Alkaline Basalt field.

On the variation diagrams (Fig. 6H, I) the sample compositions are plotted normalized to MORB and Primitive mantle respectively. Figure 6H shows that the file of Joss'alun belt samples overlaps MORB and E-MORB, but are more depleted (except for heavy REEs) than OIB. They also display Nb depletion, as does the Yeth Creek formation sample, which is more depleted overall than MORB. Figure 6I shows depletion of Ta, P and Hf when compared with primitive mantle composition. K is depleted in two Joss'alun belt samples, whereas the others show enhrichment of all Large Ion Lithophile (LIL) elements (Ba, Rb, K). Depletion of Nb and Ti, is typical of arc magmatism. Elevated LILs are consistent with magma generation above a subducted slab, and elevated values of both Th and Hf may indicate crustal contamination.

This small geochemical data set is most consistent with generation of Joss'alun belt magmas within an environment which has geochemical characteristics of both arc and within-plate sources. Modern environments which display similar chemical heterogeneity include back arc settings. Geochemical characteristics displayed by the Yeth Creek formation sample are most consistent with a volcanic arc setting.

FERRUGINOUS CHERT

Bright maroon ferruginous chert is a persistent unit that occurs structurally above the basalt unit at several localities in the NAK area. It has an estimated stratigraphic thickness of 5 m, although it can attain structural thicknesses in excess of 20m. Ruler straight 2-4 cm thick beds are characteristic (Photo 4), but locally beds can be bulbous and 10+ cm thick. Argillaceous interlayers are less than 1 cm. Radiolaria are common (Photo 9). At one locality the unit is malachite-stained (Photo 5). Trace element geochemical analysis of the chert unit shows that it is elevated in Cu and Ba (Tables 1 and 2), but such values fall within the range of normal hemipelagite (Figure 3).

Away from the basalt, ferruginous chert passes into limestone via increasing numbers of medium to thin limestone beds across a section typically two metres or less in thickness. Ferruginous chert above the basalt may correlate with a similar unit within the Hardluck clastic unit (see below).

Age of ferruginous chert

At one lolcality, the ferruginous chert yields Permian radiolaria (Mihalynuk *et al.*, 2003b) and one conodont element recoved from a different locality is of Carboniferous to Early Permian age (M. Orchard, written communication, 2003). A common age range of Early Permian is the assumed age of the ferruginous chert unit. This age assignment relies upon the assumption that the ferruginous chert at both localities is correlative and coeval.

LIMESTONE

Recrystallized, foliated limestone forms a layer with a maximum average structural thicknesses of 20 m, although the unit is commonly only a few metres thick or represented by brown or grey marley layers at the "upper" contact of the ferruginous chert unit (Photo 5). It is light grey to tan (dolomitic?)-weathering, with beds 2-10cm+ thick. It is commonly interbedded with dark grey, irregular chert beds of equal thickness (Photo 6). Some chert beds are laminated. Best exposures are on the western side of upper "Jos valley".

WELL-LAYERED, GREY CHERT

Chert layers abruptly increase in abundance above the limestone forming a section of light to dark grey ribbon chert. Some sections of this unit are much more than 10m thick. Chert beds are normally 2-10 cm thick, continous, and are interlayered with argillaceous beds less than 1.5 cm thick (Photo 7). Ribbons locally give way to massive laminated chert in beds a metre or more in thickness. Laminations are 1-3 mm thick and are thought to signal chert formed from a siliceous argillite progenitor. Grey chert grades rapidly into rusty chert; although the contact is commonly modified by faulting.

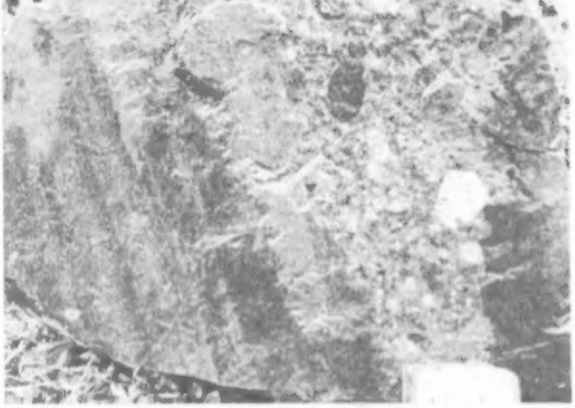

Photo 8. Granitoid clasts in ferruginous chert demonstrates consanguinity between Hardluck formation and an episode of ferruginous chert deposition.

RUSTY CHERT

Eye-catching, rusty-weathering ribbon chert has a thickness that varies dramatically from place to place, probably because it is the locus of thrust faults and subject to structural thickening and thinning. Maximum structural thickness is more than 100m. In some sections it has been cut out entirely or is present as fault-bounded lozenges a few metres thick. Ribboned chert beds are 2-10 cm thick and tan coloured on fresh surfaces. Locally it is rubbly weathering and a fresh surface can be difficult to obtain. Argillite interbeds are typically 0.5 cm thick, up to 2 cm thick, pyritic, bleached and stained by yellow jarositic clays. At several localities west of upper "Jos Creek", the unit structurally overlies basalt.

MÉLANGE

Mélange is a structural unit that is interpreted to be younger than most other units within the NAK area. Much

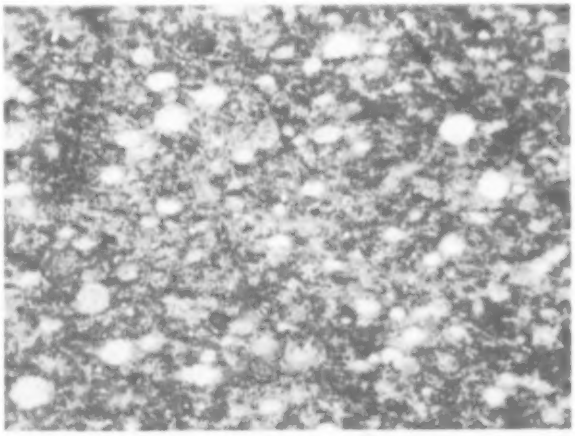

Photo 9. Photomicrograph shows recrystallized radiolaria. These are not well enough preserved to permit an age assignment.

of the low-lying areas south and east of the NAK property are underlain by serpentinite mélange. Serpentine may comprise more than 50% of areas several square kilometres in size; knockers up to a square kilometre or more are enveloped by the serpentinite. Most common knocker types are serpentinized harzburgite, chert and mafic volcanic knockers, but almost any lithology can be found within this tectonic unit, including ferruginous chert and volcanic sandstone. Knockers of coarse conglomerate belonging to the Hardluck formation (see below) are not observed, although volcanic sandstone knockers which are lithologically similar to restricted units within the Hardluck formation do occur.

A structural panel of blue-grey Middle to LateTriassic radiolarian-bearing cherty volcanic siltstone occurs between the mélange and the overlying succession that includes Permian chert (Location A, Figure 2). Blocks of similar cherty volcanic siltstone occur within the mélange unit. If the blocks are correctly correlated, the age of the mélange must extend at least into the Middle Triassic.

HARDLUCK FORMATION

Polymictic, granitoid boulder conglomerate, and quartz-rich arkosic lithic sandstone characterize a succession of very immature clastic rocks that we informally refer to as the Hardluck formation. It is widespread on the northern flanks of Hardluck Peaks. One of the most conspicuous types of clast is porphyritic granitoid boulders. These locally dominate a mix of other clasts derived from lithologies within the Cache Creek complex: chert, mafic volcanics, limestone, and ultramafite (in order of decreasing abundance). Soft sediment deformation, olistostromal deposits and basin cannibalization, result in drastic facies changes, variability of bedding, flips in facing directions and innumerable intraformational unconformities. A number of the units formed as fault scarp talus and submarine landslide debris, which contain blocks up to the size of small cabins.

Previous observations led to the suggestion that in all areas Hardluck clastic rocks rest on mafic volcaniclastic strata (Mihalynuk *et al.*, 2003a). However, observations made during the 2003 field season show that volcanic flow breccia locally rests on an angular unconformity above the clastic unit and that granitoid conglomerate lenses are intercalated with maroon chert (Photo 8) that may correlate with the ferruginous chert unit. At two localities, Hardluck conglomerate rests on (or structurally overlies) marly ferruginous chert and is intercalated with mafic tuff. The unit could be diachronous, as old as Early Permian (age of ferruginous chert), and at least as young as Earliest Triassic detrital zircons that it contains (Mihalynuk *et al.*, 2003b). Middle Triassic radiolaria have been extracted from in a cabin-sized block near the base of the unit (Location B, Figure 2), but it seems unlikely that a small, tectonically active basin could have remained active and received very coarse detritus over such a long period of time. A thrust fault mapped between the Hardluck formation and the well-exposed stratigraphy on "Sleeper Peak" is interpreted to also juxtapose the Middle Triassic chert unit with older rocks of the structurally overlying Hardluck formation.

VOLCANIC SILTSTONE/CHERT

Structural domains of blue-grey volcanic siltstone and chert are mapped across areas of less than ~1 km^2. Very fine laminations and delicate, well-preserved volcaniclastic textures characterize the unit. Bed thickness ranges from millimeters to decimeters and compositions range from light green tuff, to white, grey or black thick bedded, to thinly ribboned chert. Silty argillaceous beds are a conspicuous blue-grey colour. Where measured, folds within the unit have variable orientations, not concordant with folds of similar scale in adjacent panels. Thus, the unit appears to exist in isolated structural panels between the mélange and other coherent units. However, at one locality (Locality C on Figure 2), the unit may grade into the Hardluck clastic unit. Radiolaria extracted from this unit indicate a Middle or Late Triassic age (MMI03-14-9c, Table 5).

Nak Structure

Rocks within the NAK area have been subjected to a protracted series of deformational events that have affected different parts of the area to varying degrees. A preliminary structural history is presented here:

- an early fold and thrust event juxtaposed panels of layered units (Photo 10). A common décollement surface appears to be the rusty chert unit (Figure 2, Location C).

- an episode of extensional faulting led to formation of basins receiving Hardluck clastic detritus. Small-scale extensional structures within the Hardluck unit are common (Photo 11) and likely mimic basin-scale structures (a possible example is at Location D, Figure 2). Extensional basin formation was probably coextensive with the duration of Hardluck clastic deposition. Minor volcanism appears coeval with extension as breccia units overly local angular unconformities within the Hardluck clastic unit. Extension may have affected the entire crust, leading to exposure of the mantle rocks and their serpentinization. Within the main harzburgite body, there is no deformational fabric that post-dates emplacement of pyroxenite dikelets in a probable mantle setting, indicating that strain was highly partitioned, with the harzburgite acting as a rigid body during emplacement and subsequent deformational episodes. Strain was most likely focused at serpentinized fault boundaries.

- A second episode of contractional deformation produced open to isoclinal, mainly upright folds with variable orientations, and thrust faults that cut previously folded and thrust faulted units (e.g. Figure 2, Locations E, F; Figure 12). The old detachment faults were probably reactivated as a major décollement surface. Motion along this fault produced serpentinite mélange or increased the volume of mélange units adjacent serpentinized ultramafite. Above these units, many of the structural panels were translated. The large size of some knockers argues against entrainment of knockers as "xenoliths" during serpentine diapirism or

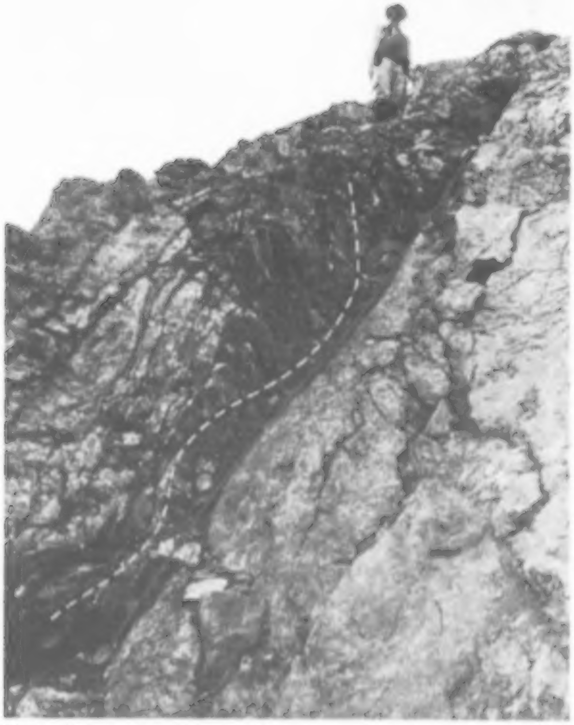

Photo 10. Layering in mafic tuffaceous rocks is cut by a thrust fault that juxtaposes them with recrystallized limestone below. Subsequent deformation has folded the thrust.

subduction zone backflow, at least when compared to modern analogues. Volcanic sandstone within mélange constrains the age of mélange formation to postdate the coarse clastic unit (if such a correlation is correct).

• A third, mainly south-verging fold and thrust event deformed earlier thrust faults; and produced a third generation of thrust faults. Deformation outlasting motion on the major décollement produced kilometre-scale, flame-like infolds of serpentinite mélange as offshoots of the main ultramafite belt (Fig. 2, locations G and H), or infolding with other units on a finer scale (Fig. 2, location I). Folds related to this event exert a fundamental control on the present day distribution of rock types within the study area as well as the Early to Middle Jurassic Laberge Group strata to the southwest. This phase of deformation is probably related to a short-lived event between 174 and 172 Ma (Mihalynuk et al., 2004) related to emplacement of the Cache Creek terrane.

• Motion along the Nahlin fault may be kinematically linked to late strike-slip and dip-slip faults that cut third-phase folds within the NAK area (e.g. Figure 2, location J, K) and local injection of serpentine between crustal blocks.

• The Nakina River stock cuts all major structures and thermally metamorphoses all deformed units. It is dated as 174.5 ±1.7 Ma (Villeneuve and Mihalynuk, unpublished).

• Relatively minor high angle faulting and reactivation of earlier-formed faults resulted in concentration of brittle deformation in a ~1m wide zone near the eastern margin of the Nakina stock. Dehydration of serpentine during and following emplacement of the stock may have resulted in dilation and minor block faulting.

• Neogene slump failure of serpentinite mélange has caused numerous landslides within the belt. Neogene extensional cracks riddle the harzburgite at Hardluck Peaks. The set of open fractures that are conspicuous from the air (Photo 12). Future failure of this unit could be catastrophic, and may result in blockage of the Nakina River.

Mineralization

Mineralization at the Joss'alun was evaluated through further surface mapping, trenching and drilling by Imperial Metals Corporation. New mineralization was discovered as part of the regional mapping in the Joss'alun belt both northwest and southeast of the Joss'alun prospect. Including these new showings, the present along-strike extent of mineral showings is now approximately 7.5 km. Mineralization was also found south of the Joss'alun, at the head of "Jos Creek", and farther south still, along the Nahlin Fault, on the south flank of Hardluck Peaks. New showings are called the "Joeboy", "NIC", "Leefer", and "Yeth" respectively (Figure 2).

JOSS'ALUN

Further work on the Joss'alun mineralization has extended the known limits of the mineralized zone at surface to at least 40 metres beyond its previously reported northwestern extent. In places the mineralization appears to be brecciated and is perhaps controlled by faulting (Photo 13). In other places, evidence points to a syngenetic origin for the most substantial sulphide lenses. Evidence for syngenesis includes:

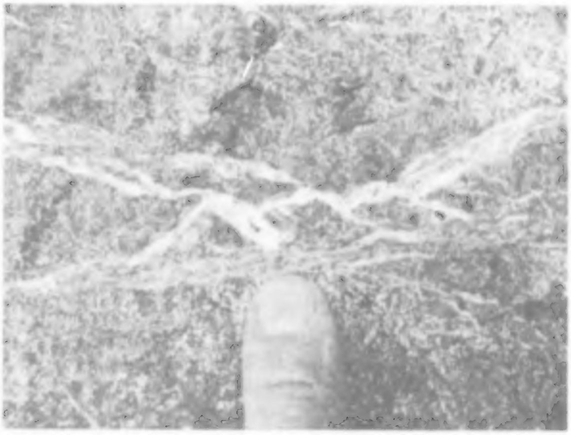

Photo 11. Evidence for extension within the Hardluck formation is widespread. An example of small-scale extensional faults is well displayed here where outlined by quartz veining.

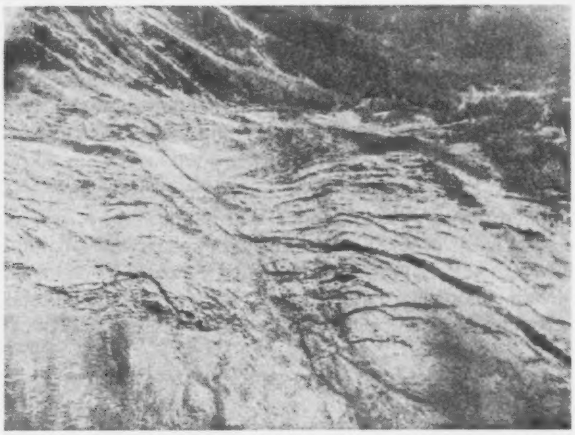

Photo 12. Aerial photograph of Neogene tension cracks within the main harzburgite body north of Hardluck Peaks. The rock mass is moving down slope, towards the Nakina River.

- near the main sulphide lenses: banding in some of the fine-grained sulphides and interlamination with silica-rich layers of possible exhalative origin (Photo 14).
- light grey, quartz-phyric felsic clasts are found in the hyaloclastite horizon above the main sulphide lens. They are an indicator synchronous felsic volcanism. Their presence raises the possibility of Kuroko-style mineral occurrences. A sample of the unit was collected for U-Pb geochronology.
- chalcopyrite mineralization is clearly focused along some of the pillow margins, suggesting extrusion of the flows onto unconsolidated sulphide mud.

A diamond drilling program was conducted on the NAK Property by Imperial to test the Joss'alun and the Jennusty showing (~ 2 km to the northwest). Nine holes, totalling 1,511 metres were completed with seven testing the Joss'alun, five of which intersected widespread copper mineralization. The mode of occurrence of copper is stringers, disseminations and pods of chalcopyrite with minor associated chalcocite.

The unit hosting the copper mineralization is comprised of a series of basaltic flows and breccias which havebeen faulted and folded, resulting of both the stacking and extension of the volcanic package. The brecciated units are heterolithic and probably reworked, containing subrounded clasts with evidence for multiple episodes of brecciation. Alteration associated with copper mineralization is most commonly quartz +/- calcite with accessory epidote and chlorite. Alteration intensity ranges from complete invasion and replacement of the host rock to flooding of the matrix or fractures, or simply amygdular infilling. Chalcopyrite can also occur in the pillow basalts as pillow rinds, hairline fracture filling or disseminations without quartz-/carbonate alteration.

The best intercepts of the drill program include hole NAK-03-05, drilled beneath the main Joss'alun showing, with 17.75 metres of 0.94% copper; and hole NAK-03-07 with 53.45 metres of 0.34% copper. The most easterly drill hole, intersected mainly tuffaceous units intermixed with basaltic flows, believed to be in the hangingwall of the pillow basalts that host the copper mineralization. Drilling results confirm that the volcanic stratigraphy on the NAK Property hosts considerable copper mineralization over a large area and is open along strike in both directions and to depth.

Cumulative evidence points to a mafic dominated VMS setting for the concordant massive sulphide lenses at the Joss'alun prospect. However, remobilized sulphide textures or discordant veins are clearly displayed, particularly in diamond drill core.

LEEFER BOULDER SHOWING (NEW)

Near the head of "Jos Creek", on the east side of the valley, is moraine that contains blocks of mafic volcanic and fine-grained diorite cut by quartz-epidote-chalcopyrite veins that occur in sheeted sets. We have named the showing the "Leefer". Boulders which are most intensely mineralized contain approximately 10% chalcopyrite as blebs within a 20cm thick quartz-epidote (+prehnite?) vein (Table 1, Sample MMI03-5-19-1, 1.5% Cu, >6 g/t Ag).

Attempts to trace this mineralization back to source were unsuccessful. Gossanous zones in the col east of "Black Goat Peak" contain 2-15% pyrite over widths of nearly a metre and several metres long, but they lack chalcopyrite. Centimetre-thick epidote-quartz veins containing chalcopyrite and pyrite were found south of "Black Goat Peak", but chalcopyrite was not nearly as abundant as in the moraine blocks. Considering the current physiography, the boulders seem most probably to have been derived from the north side of the mountain where no mineralization could be found. Considering the possible effects of continental glaciation, an alternative down-valley source is possible.

At least one period of glaciation with southward (up-valley) ice movement is suggested by extensive harzburgite boulders in the moraine that extends up the valley from the main harzburgite exposures. Up-valley transport of harzburgite erratics probably occurred during continental glaciation. Mineralized blocks may have likewise been car-

Photo 13. Fault planes above and below a rusty lens of pyrite-chalcopyrite at the Joss'alun occurrence. In contrast, many of the sulphide lenses do not show evidence of structural control.

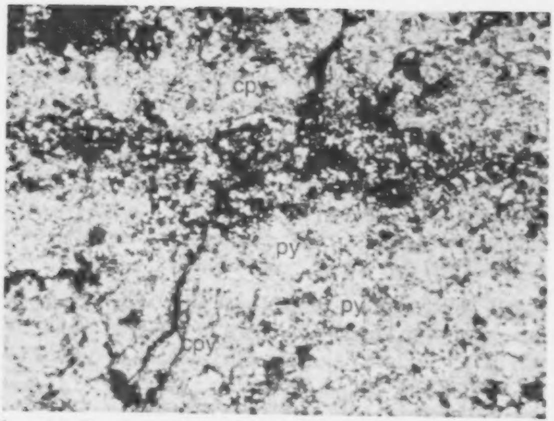

Photo 14. Banding within a sulphide lens near the discovery outcrops at the Joss'alun occurrence hints at a syngenetic origin. Photomicrograph width represents ~4mm. cpy = yellow chalcopyrite, py = white pyrite.

ried southward by continental glacier ice and then redistributed by valley glaciers at the close of the Quaternary. Similar mineralization is found in place at the NIC occurrence to the south (see below).

"MOHO SADDLE" VEINS (NEW)

Two families of veins crop out below the saddle in which the contact between harzburgite and gabbro is exposed, here called "Moho Saddle" (locality L, Figure 2). Most conspicuous is a white-weathering outcrop easily visible from across the valley. It comprises a 2 m thick vein composed of a tan to flesh-coloured, polygenetic, magnesite breccia. Much of the magnesite is probably finely intergrown with quartz, because it is unusually hard. At this locality, the vein is cut by several generations of chalcedonic and cocks-comb quartz veins, typically oriented at a high angle to the magnesite vein contact. Veins of similar character, but with thicknesses of 20 cm or less, crop out in the creek valley to the immediate north. Geochemical analyses (Tables 1 and 2) confirm visual indications of a barren vein system. Magnesite probably formed as a result of CO_2-charged fluid interacting with the adjacent Mg-rich rocks.

Immediately north of the main creek draw the mountain slope is littered with angular blocks of orange-brown-weathering gabbro cut by veins of milky white prehnite-quartz with knots of chalcopyrite up to 1.5cm in diameter. Although the blocks are not in place, they are believed to be of local derivation as they are mainly gabbro comprised of coarse orthopyroxene (4-15 mm; 30%) and altered plagioclase. Rocks cropping out in the immediate area are predominantly of this lithology. Analysis of the sample containing chalcopyrite yielded 0.15% Cu (LFE03-4-1, Table 1) and nearly 1.5 g/t Au (Table 2).

YETH OCCURRENCE (NEW)

A steep draw is cut into intensely fractured rocks along the Nahlin fault, which juxtaposes a package of unnamed volcanic strata here called the "Yeth Creek formation" with serpentinized harzburgite. Between elevations of 900 m and 1100 m the draw is a shallow slot canyon less than 3 m wide with a bedrock floor and unstable bedrock walls capped by up to ~ 80 m of glacial till. This is the only location known to the authors where it is possible to walk on exposures of the Nahlin fault (locality M, Figure 2).

Sub-vertical listwanite alteration zones along the Nahlin fault trend 125°.Cinnabar occurs as coatings on fracture surfaces near the margins of listwanite alteration zones. At the lower end of the canyon, the Yeth Creek formation contains tabular, rusty, pyrite-flooded zones up to 2 m thick. The zones are approximately vertical and trend 090°.

A ~10m by 10 m exposed area contains pyrite chalcopyrite pods 1 to 15 cm thick and up to 1 m long spaced ~ 2m apart. This is the principle exposure of the Yeth occurrence. Two sets of irregular sulphide layers are apparent with orientations clustering around 145/50° and 075/70°. Three grab samples of sulphide plus country rock were carefully collected from the unstable canyon walls. A sample of a 10 cm thick ~ 2m long vein yielded 0.88% Cu and 0.6 g/t Ag (MMI03-12-2-1, Table 1). A ~3 cm thick chalcopyrite-rich layer within one of the ~2 m wide pyritiferous zones yielded 3.3% Cu and 1.9g/t Ag (MMI03-12-2-4). Further exploration of Yeth Creek formation may be warranted, however, these rocks tend to form steep and dangerously unstable exposures.

JOEBOY SULPHIDE OCCURRENCE (NEW)

Bright red ferrugenous cherty ash and intercalated green volcanic lapilli tuff and breccia is well exposed along the steep walls of a 2 - 4 m wide, unnamed, south-flowing creek between Hardluck peaks and Peridotite Peak. Unlike ferruginous chert elsewhere, distinct bedding is not displayed, but the unit's structural thickness is estimated as tens of metres. Numerous rusty zones occur at the contact with the adjacent mafic volcanic unit. Within one rusty zone, above the exposed creek section, angular blocks of strongly pyritic mafic volcanic rock were recovered from amongst moss-covered tree roots (Figure 2, Location N). Pyrite comprises up to ~20% of decimeter-sized blocks, with accessory chalcopyrite. Analysis of one such block yielded 0.22% Cu (LFE03-17-4; Table 1). Mineralization at the Joeboy makes it noteable, but more important is the existence of chalcopyrite-pyrite mineralization 5 km along strike from the pyrite-chalcopyrite lenses at the Joss'alun occurrence.

NIC COPPER OCCURRENCE (NEW)

Serpentinized and extensively faulted gabbro is exposed immediately south of the main harzburgite body, west of the ridge that extends north from "Jos Peak". Quartz - carbonate - chalcocite - bornite and quartz-epidote-chalcopyrite-pyrite +/- bornite veins within the gabbro contain up to 3 cm thicknesses of chalcocite (in outcrop, Photo 15A) and 10 cm thicknesses of chalcopyrite (in talus

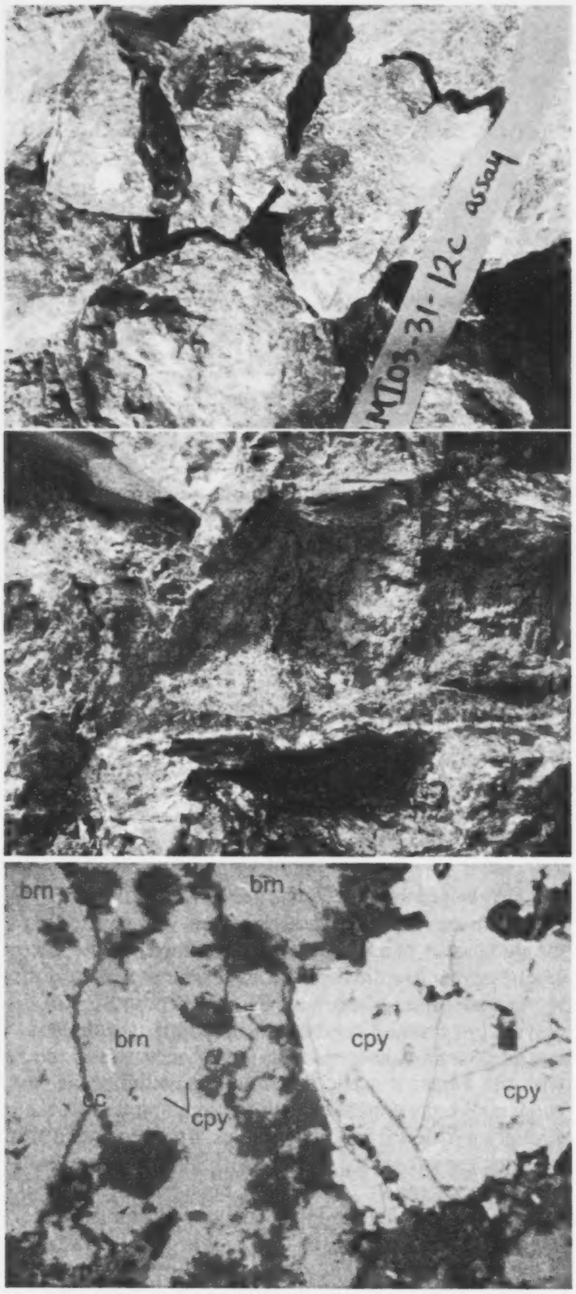

Photo 15. Mineralization at the NIC showing occurs mainly as (A, top) chalcopyrite veins up to 5 cm thick (Table 1, sample MMI03-31-10b) and (B) bornite-chalcocite/digenite veins up to 2 cm thick. Photomicrograph of chalcocite/digenite invading fracture and gangue boundaries in chalcopyrite and bornite. Also note exsolution lamellae of chalcopyrite in bornite (C, bottom). cpy = chalcopyrite, cc = chalcocite/digenite, brn = bornite (purple). Photomicrograph width represents ~ 0.1mm.

blocks, Photo 15B). Chalcopyrite-rich veins trend due west and dip steeply north (265/80). Analysis of mineralized grab samples yield values of ~3.4% Cu and 3.4 g/t Ag (2 cm chalcocite vein in outcrop, MMI03-31-10a, Table 1); 1% Cu (chalcopyrite-bornite pods in outcrop, MMI03-31-10b); 3.8 % Cu and 1.8 g/t Ag (chalcopyrite vein, MMI03-31-10c); 4.6% Cu (2 cm chalcopyrite-bornite vein in outcrop, MMI03-31-10d); 7.3% and 6.0% Cu with 4.2 and 3 g/t Ag (MMI03-31-12a, c; quartz-epidote-chalcopyrite-pyrite veins, 6 cm thick, in talus blocks). Similar quartz-epidote-chalcopyrite-pyrite veins resemble those found in moraine at the Leefer showing, about 3 km south, up "Jos Creek" valley.

Mineralization at the NIC occurrence is significant because it extends the known limits of sulphide mineralization within the Joss'alun belt an additional ~2.5 km northwest of the Joss'alun prospect.

Geological History

Oldest strata within the northern Cache Creek terrane are Early Mississippian chert (Monger, 1975) and Pennsylvanian carbonate (Mihalynuk, *et al.*, 2003a) interbedded with volcanic strata of ocean island parentage (English, *et al.*, 2002). Great thicknesses of Permian carbonate may have deposited as platforms atop oceanic plateaus, especially during the Middle Permain, when large fusulinids were important contributors to the volume of carbonate produced. A significant proportion of these organisms now found as fossils within the Cache Creek terrane, were endemic to the Tethyan realm, at the eastern margin of Pangea. In the Permian, the supercontinent extended from the south pole to within a few degrees of the north pole (Ross and Ross, 1985) resulting in extreme provinciality of low-latitude marine fauna, including fusulinids.

Permian time can also be considered the birthdate of the Cache Creek terrane. Rupture and initiation of subduction of Panthalassic ocean crust gave birth to the Cache Creek intra-oceanic arc. Oldest isotopically dated volcanic rocks attributed to this arc are ~263 Ma ignimbritic units in the French range near Dease Lake (Mihalynuk *et al.*, 2004). Oceanic strata offscraped during subduction at this arc produced an accretionary prism that comprises much of the Cache Creek terrane as we know it today. The arc component is called the Kutcho arc in northern British Columbia, where it is of particular importance because it includes the Kutcho Creek volcanogenic massive sulphide deposit. In the Atlin area, massive sulphide mineralization at the Joss'alun occurrence may be hosted by Kutcho-equivalent volcanic rocks (Mihalynuk, *et al.*, 2003b). Volcanic detritus containing zircons of only Latest Permian - earliest Triassic age accumulated to form what we have informally called the Hardluck formation. Yet the plutonic roots of the arc are nowhere in evidence near Hardluck Peaks, perhaps indicating deposition of the Hardluck formation at some distance from the arc axis, despite the proximal character of the conglomerate units with boulders reaching one metre or more in diameter. Volcaniclastic rocks intercalated with the jumbled Hardluck formation have a chemical composition that resembles MORB in some respects, but they also displays some characters of an arc tholeiite. Rocks in the Marianas basin have similarly variable chemical composition (e.g. Hawkins, *et al.*, 1990). We interpret the mafic volcanic rocks in the Joss'alun belt as deposited in an extending fore- or back-arc setting, like in the Marianas basin. Mantle rocks of the Nahlin body may have been exposed and serpentinized in this extensional environment as suggested by serpentinite pebbles in the Hardluck formation. Alternatively the Hardluck formation may have been deposited in piggy-back basins atop an accretionary complex that included minor slivers of ultramafic rocks which were eroded and redeposited.

By the Early Triassic, Pangea was beginning to break up, although it was not until the Early Jurassic that an equatorial seaway was established allowing east-west migration of fauna (e.g. Krobicki, 2003), resulting in loss of equatorial faunal provincialism. As Pangea break-up commenced, the Kutcho arc shut down. The reason for cessation of Kutcho volcanism is unknown. Perhaps the subduction zone was clogged with a carbonate-laden oceanic plateau, but it is questionable whether oceanic plateaus are buoyant enough to plug a subduction zone (e.g. Cloos, 1993), especially when the subducting lithosphere is likely to have been about 100 m.y. old (*i.e.* cold, dense and easily subducted). Lack of abundant ocean island basalt within the Cache Creek argues against plateau collision. Perhaps volcanism shut down because of a plate reconfiguration, or because of subduction zone hijacking by the neighbouring Stikine arc. Plate reconfigurations were likely during Pangea breakup, but this *ad hoc* explanation is difficult to test. Subduction zone hijacking is intriguing because a magmatic gap in the Stikine arc roughly corresponds with activity in the Kutcho arc, but the underlying cause remains at large. Whatever the cause, we tentatively ascribe a second phase of folding and thrust faulting in the accretionary complex to a local orogenic event at about this time.

Late in the Pliensbachian (late Early Jurassic ~186 Ma) Kutcho arc may have collided with the conjoined Quesnel and Stikine arcs (for a paleogeographic overview see (Mihalynuk *et al.*, 1999; Mihalynuk *et al.*, in press). The Quesnel arc was driven up onto the miogeocline (Nixon *et al.*, 1993), and coeval, very rapid uplift was recorded by adjacent parts of Stikinia (Johnston, 1995) and widespread conglomerate blankets in the Whitehorse Trough (Johannson *et al.*, 1997). We speculate that this event produced a third set of folds (second set of folds that affect structures formed by the process of accretionary prism growth).

Subduction of oceanic crust was reestablished as evidenced by the presence of Early Jurassic radiolarian-bearing units within the accretionary complex as well as 174 Ma blueschist (Mihalynuk *et al.*, 2003, in press). The major segments of the Stikine and Quesnel arcs rotated into parallelism, entrapping relicts of Panthalassa oceanic crust and the Cache Creek terrane between them. Between 174 Ma and 172 Ma the two arc segments collided and northern Cache Creek terrane was emplaced southwestward over the Stikine arc segment. Emplacement structures include the major folds that deform Whitehorse Trough and Cache Creek strata; all are cut by the ~172 Ma plutons of the Fourth of July suite (Mihalynuk, 1999).

Only relatively minor brittle adjstments have effected the upper crust since ~172 Ma. One manifestation is a northwest-trending brittle fault zone that cuts the southeastern margin of the Nakina River stock, and northeast-trending faults cut stratigraphy (Figure 2).

In Quaternary time, a lobe of continental glacier ice advanced up "Jos valley" transporting moraine that contained blocks of harzburgite as well as basalt/diorite with quartz--epidote-chalcopyrite-pyrite veins. Alpine glacier ice that persisted after retreat of the continental ice sheet were largely responsible for the present physiography as well as exhumation of copper sulphide mineralization in the upland areas, including the Joss'alun occurrence. This mineralization is now known to occur sporadically for at least 7.5 km along strike.

Conclusions

Four new copper sulphide showings within the belt of rocks containing the Joss'alun occurrence extend the limits of known mineralization to more than 7.5 km along strike. Analysis of mineralized samples of these vein occurrences, (NIC, Leefer, Moho Saddle, and Joeboy) show that some contain modest silver values, and that the sample from the Moho Saddle occurrence, contains nearly 1.5 g/t Au.

Imperial Metals Corporation carried out a diamond drill program at the Joss'alun occurrence in 2003. Two of the best intercepts were 17.75 m of 0.94% copper and 53.45 m of 0.34% copper (Robertson, 2003).

Major, minor and trace element composition of the volcanic rocks within the Joss'alun belt suggest a back- or forearc parentage, possibly analogous to the Marianas arc/back-arc system. Three phases of deformation within the belt include an episode of extension, possibly recording extension in the back- or forearc environment.

South of the Joss'alun belt, along the Nahlin fault, copper mineralization was found in a mafic volcanic unit informally named the Yeth Creek formation, and is herein called the "Yeth occurrence". These basaltic rocks have geochemical characteristics which are arc-like in many respects.

In all, five new copper showings were discovered within the area during the course of a ~ 3 weeks geological mapping program. Further prospecting and geological investigation is clearly warranted.

Acknowledgements

Operational funds for this project in 2003 were provided by Imperial Metals Corporation. Patrick McAndless, vice-president of exploration at Imperial Metals, is a major contributor to the success of this project through his unflagging and enthusiastic support. Dante Canil and Steve Johnston contributed substantially to this project by their mapping of the mantle rocks at Peridotite Peak and points southeast, and through stimulating discussions in the field. Norm Graham of Discovery Helicopters in Atlin, once again delivered flawless helicopter transportation. Able field assistance of Kyoko Nakano was made possible through the thoughtfulness of Gregg Dipple at The Univer-

sity of British Columbia. Rita Scott and Nora (Kuya) Minogue once again offered us refuge in their home in Atlin. Not least of all, thanks to the townsfolk of Atlin who continually support our field programs in many ways.

References Cited

Aitken, J.D. (1959): Atlin map-area, British Columbia; *Geological Survey of Canada*, Memoir, 307, 89 pages.

Ash, C.H. (1994): Origin and tectonic setting of ophiolitic ultramafic and related rocks in the Atlin area, British Columbia (NTS 104N); *B.C. Ministry of Energy, Mines and Petroleum Resources*, Bulletin, 94, 48 pages.

BCMEM (1978): Atlin regional geochemical survey, 882 sites plus 160 lake sites; *BC Ministry of Energy and Mines* and the *Geological Survey of Canada*, RGS 51.

Cloos, M. (1993): Lithospheric buoyancy and collisional orogenesis: Subduction of oceanic plateaus, continental margins, island arcs, spreading ridges, and seamounts; *Geological Society of America Bulletin*, Volume 105, pages 715-737.

Dumont, R., Coyle, M. and Potvin, J. (2001): Aeromagnetic total field map British Columbia: Sloko River, NTS 104N/3; *Geological Survey of Canada*, Open File, 4093.

English, J.M., Mihalynuk, M.G., Johnston, S.T. and Devine, F.A. (2002): Atlin TGI Part III: Geology and Petrochemistry of mafic rocks within the northern Cache Creek terrane and tectonic implications; *in* Geological Fieldwork 2001, *BC Ministry of Energy and Mines*, Paper 2002-1, pages 19-29.

Hawkins, J.W., Lonsdale, P.F., Macdougall, J.D. and Volpe, A.M. (1990): Petrology of the axial ridge of the Mariana Trough backarc spreading center; *Earth and Planetary Science Letters*, Volume 100, pages 226-250.

Jackaman, W. (2000): British Columbia Regional Geochemical Survey, NTS 104N/1 - Atlin; *BC Ministry of Energy and Mines*, BC RGS, 51.

Johannson, G.G., Smith, P.L. and Gordey, S.P. (1997): Early Jurassic evolution of the northern Stikinian arc; evidence from the Laberge Group, northwestern British Columbia; *Canadian Journal of Earth Sciences*, Volume 34, pages 1030-1057.

Johnston, S.T. (1995): Stikinia and the Aishihik metamorphic suite: evidence of an arc-continent collision; *in* Geological Society of America, Cordilleran Section, 91st annual meeting; *Geological Society of America*, Volume 27, page 28.

Krobicki, M. and Golonka, J. (2003): Onset of the Pangea breakup marked by the migration of Early Jurassic bivalves; *3rd Workshop of the IGCP Project 458,* Triassic/Jurassic boundary changes, Stara' Lesna', Slovakia, 28-30.

Massey, N.W.D., MacIntyre, D.G. and Desjardins, P.J. (2003): Digital map of British Columbia: Tile NO10 (Northwest BC); *BC Ministry of Energy and Mines*, Geofile 2003-17.

Mihalynuk, M.G. (1999): Geology and mineral resources of the Tagish Lake area (NTS 104M/ 8,9,10E, 15 and 104N/ 12W), northwestern British Columbia; *BC Ministry of Energy and Mines*, Bulletin 104, 217 pages.

Mihalynuk, M.G. (2002): Geological setting and style of mineralization at the Joss'alun discovery, Atlin area, British Columbia; *BC Ministry of Energy and Mines*, Geofile, GF2002-6, 4 pages (plus digital presentation).

Mihalynuk, M.G., Bellefontaine, K.A., Brown, D.A., Logan, J.M., Nelson, J.L., Legun, A.S. and Diakow, L.J. (1996): Geological compilation, northwest British Columbia (NTS 94E, L, M; 104F, G, H, I, J, K, L, M, N, O, P; 114J, O, P); *BC Ministry of Energy and Mines*, Open File 1996-11.

Mihalynuk, M.G., Erdmer, P., Ghent, E.D., Archibald, D.A., Friedman, R.M., Cordey, F., Johannson, G.G. and Beanish, J. (1999): Age constraints for emplacement of the northern Cache Creek Terrane and implications of blueschist metamorphism; *in* Geological Fieldwork, *BC Ministry of Energy, Mines and Petroleum Resources*, Paper 1999-1, pages 127-142.

Mihalynuk, M.G., Erdmer, P., Ghent, E.D., Archibald, D.A., Friedman, R.M., Cordey, F. and Johannson, G.G. (2004): Emplacement of French Range blueschist: Subduction to exhumation in less than 2.5 m.y.?; *Geological Society of America Bulletin*, in press.

Mihalynuk, M.G., Johnston, S.T., Lowe, C., Cordey, F., English, J.M., Devine, F.A.M., Larson, K. and Merran, Y. (2002): Atlin TGI Part II: Preliminary results from the Atlin Targeted Geoscience Initiative, Nakina Area, Northwest British Columbia; *in* Geological Fieldwork 2001, *BC Ministry of Energy and Mines*, Paper 2002-1, pages 5-18.

Mihalynuk, M.G., Johnston, S.T., English, J.M., Cordey, F., Villeneuve, M.J., Rui, L. and Orchard, M.J. (2003a): Atlin TGI Part II: Regional geology and mineralization of the Nakina area (NTS 104N/2W and 3); *in* Geological Fieldwork, *BC Ministry of Energy and Mines*, Paper 2003-1, pages 9-37.

Mihalynuk, M.G. and Lowe, C. (2002): Atlin TGI, Part I: An introduction to the Atlin Targeted Geoscience Initiative; *in* Geological Fieldwork 2001, *BC Ministry of Energy and Mines*, Paper 2001-1, pages XX.

Mihalynuk, M.G. and Peter, J.M. (2001): A hydrothermal origin for "crinkle chert" within the Big Salmon Complex; *in* Geological Fieldwork 2000, *BC Ministry of Energy and Mines*, Paper 2001-1, pages 83-84.

Mihalynuk, M.G., Villeneuve, M.E. and Cordey, F. (2003b): Atlin TGI, Part III: Geological setting and style of mineralization at the Joss'alun occurrence, Atlin area (NTS 104N/2SW), MINFILE 104N136; *in* Geological Fieldwork 2002, *BC Ministry of Energy and Mines*, Paper 2003-1, pages 39-49.

Monger, J.W.H. (1969): Stratigraphy and structure of Upper Paleozoic rocks, northeast Dease Lake map-area, British Columbia (104J); *Geological Survey of Canada*, Paper 68-48, 41 pages.

Monger, J. (1975): Upper Paleozoic rocks of the Atlin Terrane, northwestern British Columbia and south-central Yukon; *Geological Survey of Canada*, Paper 74-47, 63 pages.

Nixon, G.T., Archibald, D.A. and Heaman, L.M. (1993): ^{40}Ar-^{39}Ar and U-Pb geochronometry of the Polaris alaskan-type complex, British Columbia; precise timing of Quesnellia-North America interaction; *in Geological Association of Canada, Mineralogical Association of Canada*; annual meeting; program with abstracts; *Geological Association of Canada*, 1993, page 76.

Robertson, S. (2003): Nak drilling hits long interval of copper mineralization; *Imperial Metals Corporation*, News Release, October 15, 2003, Vancouver, BC, page 30.

Ross, C.A. and Ross, J.R.P. (1985): Carboniferous and Early Permian biogeography; *Geology*, Volume 13, pages 27-30.

Souther, J.G. (1971): Geology and mineral deposits of the Tulsequah map area; *Geological Survey of Canada*, Memoir 362, 76 pages.

Terry, J. (1977): Geology of the Nahlin ultramafic body, Atlin and Tulsequah map-areas, northwestern British Columbia; *in* Current Research, Part A, *Geological Survey of Canada*, pages 263-266.

GEOLOGY AND MINERAL OCCURRENCES OF QUESNEL TERRANE, KLIYUL CREEK TO JOHANSON LAKE (94D/8, 9)

By Paul Schiarizza

KEYWORDS: Quesnel Terrane, Takla Group, Triassic-Jurassic plutons, pyroxenite, diorite, tonalite, granodiorite, magnetite, gold, copper, molybdenum.

INTRODUCTION

The Johanson Lake project is a two-year bedrock mapping program initiated by the Geological Survey Branch in 2003 as part of the Toodoggone Targeted Geoscience Initiative (TGI). The project focuses on a belt of Mesozoic arc volcanic and plutonic rocks in the eastern part of the McConnell Creek (94D) map sheet. This area contains a number of gold, copper and molybdenum mineral occurrences and Regional Geochemical Survey sample sites that returned anomalously high values of gold and copper. The aim of the project is to improve the quality and detail of bedrock maps for the area and determine the setting and controls of mineral occurrences. This will help guide exploration strategies on known mineral occurrences and focus exploration for new occurrences.

This report summarizes the results from the first year's fieldwork on the Johanson Lake Project. It covers an area of about 150 square kilometres that was mapped from July 19 to August 22, 2003 (Figure 1). Operating funds were provided by the Toodoggone TGI and a private-public partnership agreement with Northgate Exploration Ltd. The project area is 350 kilometres northwest of Prince George and encompasses rugged terrain within the Omineca Mountains. Road access to Johanson Lake is provided by the Omineca Resource Access Road. Most of the 2003 fieldwork was conducted from fly camps serviced by a Canadian Helicopters base at the Kemess Mine, 60 kilometres to the north-northwest.

PREVIOUS WORK

The Johanson Lake project area is located along the eastern edge of the McConnell Creek (NTS 94D) map sheet. Systematic geologic mapping of eastern McConnell Creek sheet was undertaken by the Geological Survey of Canada (GSC) in the early to mid 1940s and published as Memoir 251 with accompanying 1:253 440-scale geological map (Lord, 1948). There was little published geological information on the area prior to that time, although Lay's (1940) descriptions of geology and mineral occurrences in selected areas in the Aiken Lake sheet (NTS 94C/E) to the east included a very small part of the present map area along the lower reaches of Croyden Creek. The mineral occurrences along Croyden Creek, together with new discoveries within the McConnell Creek sheet to the west, some of which were made during the GSC's mapping program, were described by White (1948). Systematic mapping of the Aiken Lake sheet was completed by the GSC in the late 1940s, and published as Memoir 274 with 1:253 440-scale geological map (Roots, 1954).

Church (1974, 1975) mapped portions of the McConnell Creek sheet directly west of the current project area in response to interest generated by discovery of the Sustut copper occurrence in 1971. This work overlapped with the studies of Monger (1974, 1976, 1977; Monger and Paterson, 1974), which focused on Upper Triassic volcano-sedimentary rocks in the McConnell Creek map area (Monger and Church, 1977). These studies, together with several other detailed studies of specific map units, including those of Irvine (1974, 1976) on Alaskan-type intrusions and Woodsworth (1976) on granitoid intrusions, were incorporated in an updated geologic map of the eastern McConnell Lake map area at 1:250 000-scale (Richards, 1976a, b).

In 1987 the B.C. Geological Survey Branch initiated a multi-year program designed to investigate the mineral potential of Alaskan-type ultramafic-mafic intrusions within the province (Nixon and Rublee, 1988). This project included mapping and lithogeochemical studies of the Johanson Lake, Wrede Creek and Polaris ultramafic-mafic bodies located within and adjacent to the Johanson Lake project area (Nixon *et al.*, 1990a, b; Hammack *et al.*, 1990; Nixon *et al.*, 1997)

In the late 1980s, K. Minehan (1989a, b) studied the volcanic stratigraphy and petrochemistry of the Upper Triassic Takla Group a short distance north of Johanson Lake as part of her Masters project at McGill University. A subsequent Ph.D. study by G. Zhang, also at McGill University, focused on the structural geology of a region straddling the Finlay-Ingenika fault system and encompassing the present project area (Zhang, 1994; Zhang and Hynes, 1991, 1992, 1994, 1995; Zhang *et al.*, 1996).

Areas both east and west of the Johanson Lake project area have been covered by recent 1:50 000-scale geological mapping programs by the B.C. Geological Survey Branch. The area to the east and southeast was mapped by Ferri *et al.* (1993; 2001b) as part of the Aiken Lake project, and the area around Lay and Wrede creeks,

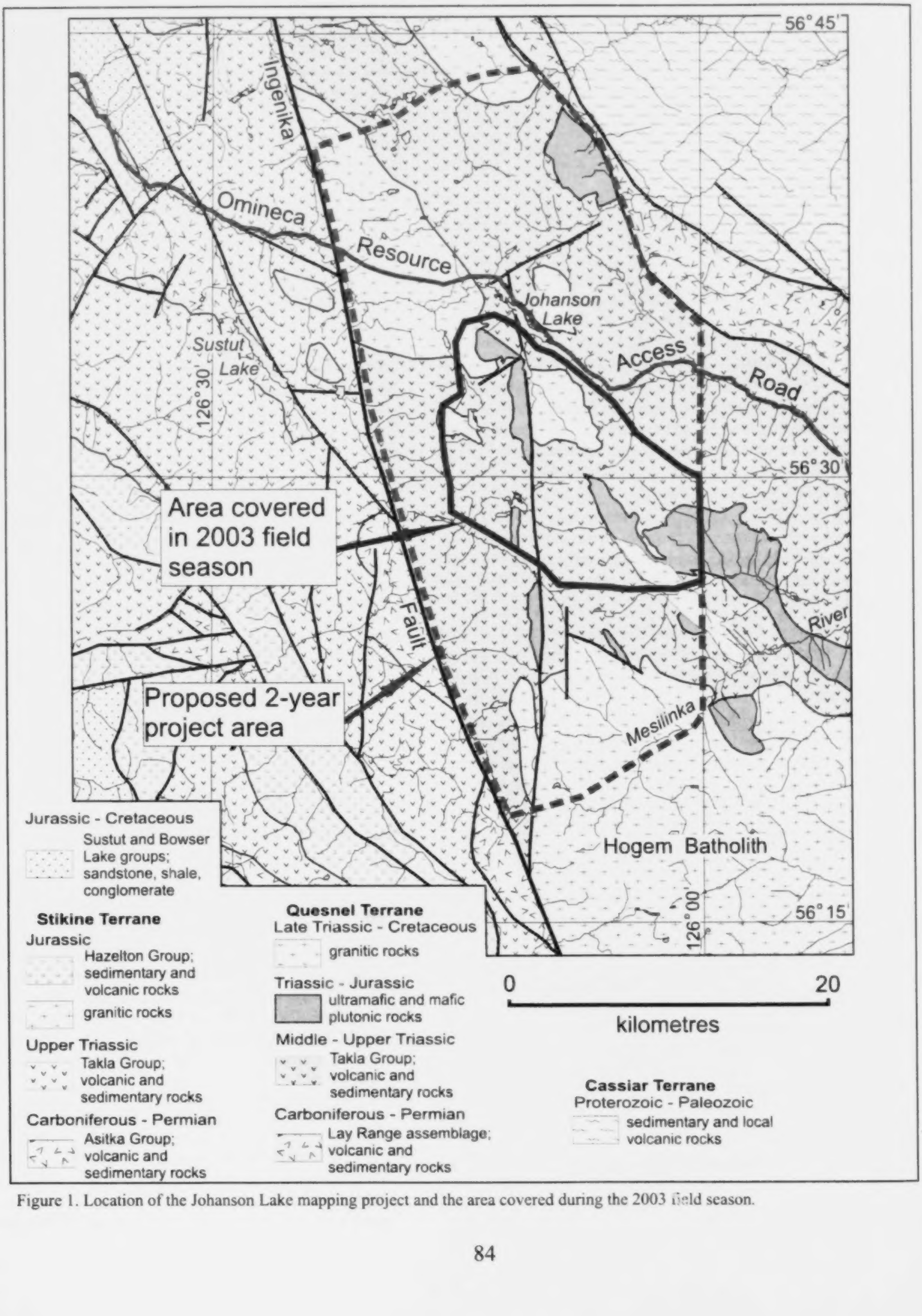
56° 45'
Ingenika
Omineca
Resource
Johanson Lake
Access
Road
Sustut Lake
126° 30'
56° 30'
Area covered in 2003 field season
Fault
River
Proposed 2-year project area
Mesilinka
Hogem Batholith
126° 00'
56° 15'
0
20
kilometres
Jurassic - Cretaceous
Sustut and Bowser Lake groups; sandstone, shale, conglomerate
Stikine Terrane
Jurassic
Hazelton Group; sedimentary and volcanic rocks
granitic rocks
Upper Triassic
Takla Group; volcanic and sedimentary rocks
Carboniferous - Permian
Asitka Group; volcanic and sedimentary rocks
Quesnel Terrane
Late Triassic - Cretaceous
granitic rocks
Triassic - Jurassic
ultramafic and mafic plutonic rocks
Middle - Upper Triassic
Takla Group; volcanic and sedimentary rocks
Carboniferous - Permian
Lay Range assemblage; volcanic and sedimentary rocks
Cassiar Terrane
Proterozoic - Paleozoic
sedimentary and local volcanic rocks

Figure 1. Location of the Johanson Lake mapping project and the area covered during the 2003 field season.

northeast of the project area, is covered by Ferri (2000a, b). The area west of Johanson Lake, underlain by the Stikine Terrane, was studied by Legun (1998, 2001a, b).

REGIONAL GEOLOGIC SETTING

The Johanson Lake project area is underlain by rocks of the Quesnel Terrane, a volcanic arc terrane that is found along most of the length of the Canadian Cordillera. The Quesnel Terrane is in large part represented by Middle and Upper Triassic volcanic and sedimentary rocks, which are assigned to the Takla Group in northern and central British Columbia and to the Nicola Group in the south. These rocks are locally overlain by Lower Jurassic volcanic and sedimentary rocks, and are cut by a several suites of Late Triassic through Early Jurassic plutons. In north-central British Columbia, older components of the Quesnel Terrane comprise arc volcanic and sedimentary rocks of the Lay Range assemblage, which are restricted to the eastern margin of the Quesnel belt (Ferri, 1997).

Late Triassic-Early Jurassic intrusive rocks are a prominent and economically important component of the Quesnel Terrane. These include both calc-alkaline and alkaline plutonic suites, as well as Alaskan-type ultramafic-mafic intrusions. Many of these plutonic suites are found within and adjacent to the Hogem Batholith (Garnet; 1978; Woodsworth, 1976; Woodsworth *et al.*, 1991) which extends from the Johanson Lake project area more than 150 kilometres south to the Nation Lakes area. In addition to Late Triassic-Early Jurassic rocks, the composite Hogem Batholith also includes younger granitic phases correlated with Early Cretaceous plutons that are common regionally and crosscut Quesnel and adjacent terranes.

At the latitude of Johanson Lake, Quesnel Terrane is contacted to the east by Proterozoic and Paleozoic carbonates and siliciclastics of the Cassiar Terrane, representing part of the ancestral North American miogeocline (Figure 2). Farther south, Quesnel and Cassiar terranes are separated by an intervening assemblage of Late Paleozoic oceanic rocks assigned to Slide Mountain Terrane. The boundary between the Quesnel and Cassiar terranes is a complex structural zone that includes late Early Jurassic east-directed thrust faults that juxtapose Quesnel Terrane above Cassiar Terrane (Ferri, 1997, 2000a; Nixon *et al.*, 1997). These east-directed faults and related folds are locally overprinted by somewhat younger west-directed structures that reverse this stacking order (Bellefontaine, 1989), as well as by dextral strike-slip and normal faults that formed in Cretaceous and early Tertiary time (Ferri, 1997; 2000a).

The Quesnel Terrane in the Johanson Lake area is juxtaposed against the similar Stikine Terrane to the west, across the Finlay - Ingenika fault system. Regionally, however, these two arc terranes are separated by the intervening, oceanic Cache Creek Terrane which, in part, includes the remnants of a Mesozoic accretion-subduction complex related to the Triassic-Jurassic Quesnel magmatic arc (Travers, 1978; Struik, 1988). This subduction may have ultimately led to collision between Stikine and Quesnel terranes, as reflected in imbricate southwest-directed thrust faults within Cache Creek Terrane (Struik *et al.*, 2001), the juxtaposition of Stikine Terrane beneath Cache Creek Terrane across northeast-dipping thrust faults (Monger *et al.*, 1978), and the record of chert-rich detritus that was shed westward from Cache Creek Terrane into the Bowser Basin, which formed above Stikine Terrane beginning in Middle Jurassic time (Ricketts *et al.*, 1992). The subsequent structural history of the area includes the development of prominent dextral strike-slip fault systems in Cretaceous and Early Tertiary time. These structures include the Finlay - Ingenika and Pinchi faults, which may have more than 100 kilometres of cumulative displacement, resulting in the omission of the Cache Creek Terrane at the latitude of the Johanson Lake area (Gabrielse, 1985).

LITHOLOGIC UNITS

The 2003 study area is underlain by Upper Triassic volcaniclastic and volcanic rocks of the Takla Group, together with abundant intrusions of ultramafic to granitic composition (Figure 3).

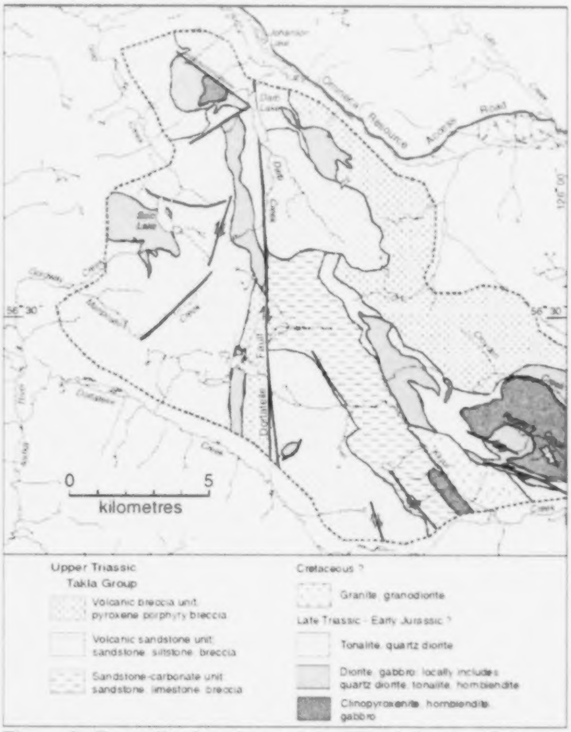
Johanson Lake
Dem Lake
Omineca Resource Access Road
Dem Creek
Fault
126°00'
56°30'
56°30'
0
5
kilometres
Upper Triassic
Takla Group
Volcanic breccia unit: pyroxene porphyry breccia
Volcanic sandstone unit: sandstone, siltstone, breccia
Sandstone-carbonate unit: sandstone, limestone, breccia
Cretaceous ?
Granite, granodiorite
Late Triassic - Early Jurassic ?
Tonalite, quartz diorite
Diorite, gabbro; locally includes quartz diorite, tonalite, hornblendite
Clinopyroxenite, hornblendite, gabbro

Figure 3. Generalized geology of the Kliyul Creek – Johanson Lake area, based on 2003 fieldwork and published reports referred to in text.

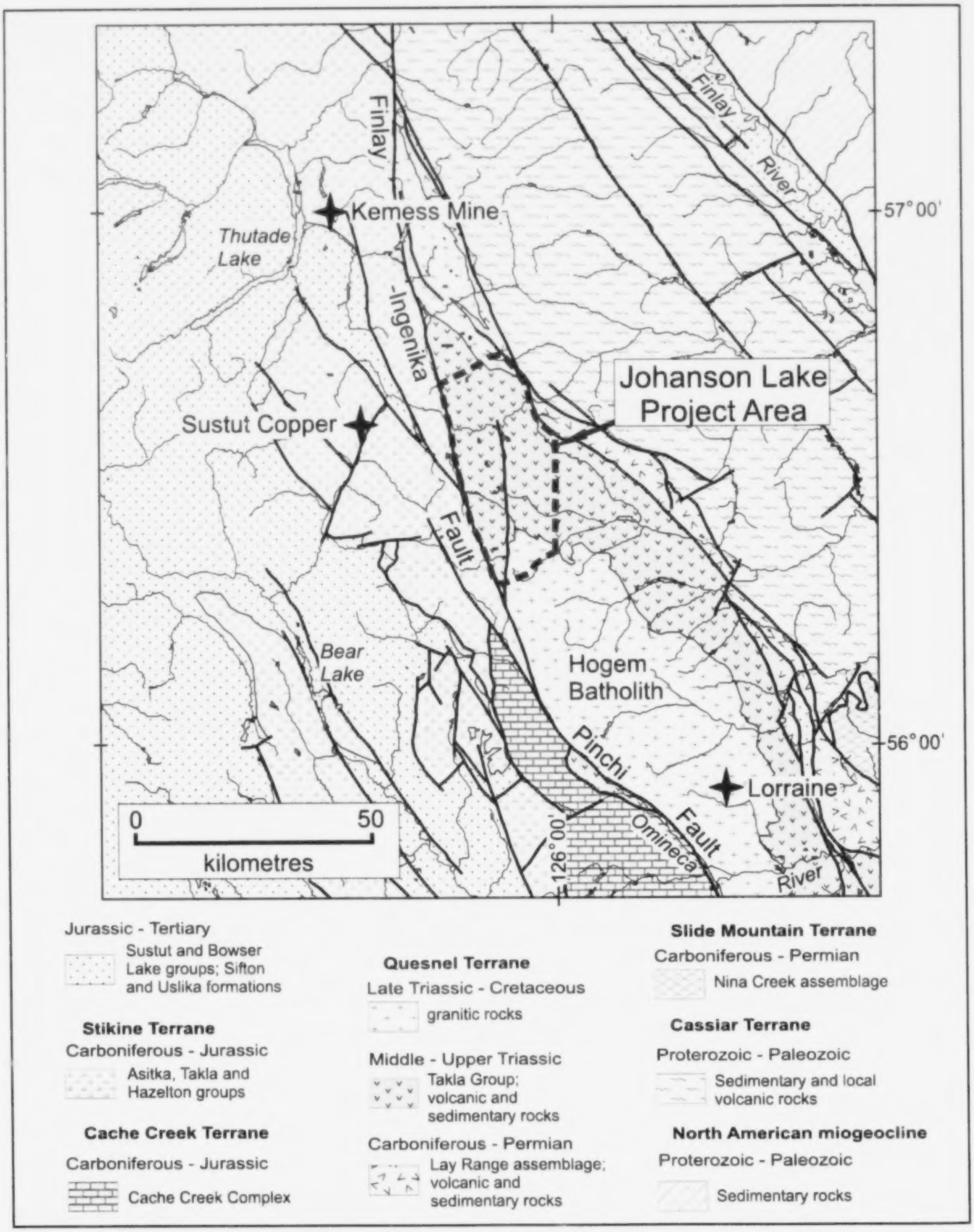
Finlay
Finlay
River
Kemess Mine
Thutade Lake
-Ingenika
Johanson Lake Project Area
Sustut Copper
Fault
Bear Lake
Hogem Batholith
Pinchi
Fault
Lorraine
Omineca
River
57° 00'
56° 00'
126° 00'
0
50
kilometres
Jurassic - Tertiary
Sustut and Bowser Lake groups; Sifton and Uslika formations
Stikine Terrane
Carboniferous - Jurassic
Asitka, Takla and Hazelton groups
Cache Creek Terrane
Carboniferous - Jurassic
Cache Creek Complex
Quesnel Terrane
Late Triassic - Cretaceous
granitic rocks
Middle - Upper Triassic
Takla Group; volcanic and sedimentary rocks
Carboniferous - Permian
Lay Range assemblage; volcanic and sedimentary rocks
Slide Mountain Terrane
Carboniferous - Permian
Nina Creek assemblage
Cassiar Terrane
Proterozoic - Paleozoic
Sedimentary and local volcanic rocks
North American miogeocline
Proterozoic - Paleozoic
Sedimentary rocks

Figure 2. Regional geologic setting of the Johanson Lake project area.

The intrusions are not well dated, but are suspected to be Late Triassic-Early Jurassic and Cretaceous in age.

Takla Group

Armstrong (1946, 1949) used the name Takla Group for occurrences of Upper Triassic and Jurassic volcanic and sedimentary rocks exposed west and southwest of the main arm of Takla Lake in the Fort St. James map area. In addition to the exposures around Takla Lake, he also included in the group a more extensive belt to the east of the Pinchi fault, which extended from Pinchi Lake north-northwestward to beyond Germansen Lake. The name Takla Group was retained for both belts of Triassic-Jurassic rocks where they were traced northward into the McConnell Creek and Aiken Lake map areas by Lord (1948) and Roots (1954), respectively. Subsequent revisions to the nomenclature of the western belt, based largely on excellent exposures in the McConnell Creek map area directly west of the present study area, restricted the name Takla Group to Triassic rocks, and included the overlying Lower to Middle Jurassic volcanic-sedimentary succession in the Hazelton Group (Tipper and Richards, 1976; Monger, 1977; Monger and Church, 1977). In this revised scheme the Upper Triassic Takla Group within the Stikine Terrane is subdivided into 3 formal formations, the Dewar, Savage Mountain and Moosevale.

The eastern Takla belt, including the exposures in the Johanson Lake map area, is part of the Quesnel Terrane. The group has recently been mapped in some detail along a continuous belt extending for almost 250 kilometres from the Nation Lakes area northward to the eastern edge of the Johanson Lake project area (Ferri and Melville, 1994; Nelson and Bellefontaine, 1996; Ferri *et al.*, 1992; 1993, 2001a, 2001b). The group has not been subdivided into formal formations within this belt, although several lithologically distinct, but partially coeval successions have been identified and named. In some of these studies the name Takla Group has been used for both Upper Triassic and Lower Jurassic rocks, as originally defined by Armstrong (1949). However, Nelson and Bellefontaine (1996) recognized that, in the Nation Lakes area, the Lower Jurassic rocks are readily distinguished from the Triassic rocks and are separated from them by an unconformity. They suggested that the term Takla Group be restricted to include only the Triassic rocks, and this recommendation is adopted here.

The Takla Group within the Johanson Lake project area is shown mainly as undivided volcanic and volcaniclastic rocks on the maps of Lord (1948), Richards (1976b) and Monger (1977). Zhang and Hynes (1991, 1992) subdivide the group into several informal units in their sketch maps of the area, some of which are reflected in the subdivisions applied here. For the purposes of this report, the Takla Group is subdivided into 2 major divisions and 3 units. The most widespread package comprises a heterogeneous assemblage of volcanic sandstones, siltstones and breccias, with local mafic volcanic flows, referred to as the volcanic sandstone unit. A subunit of this package comprises similar rocks intercalated with locally abundant limestone and limestone breccia; these rocks are assigned to the sandstone-carbonate unit. The third unit, referred to as the volcanic breccia unit, is dominated by massive breccias containing pyroxene porphyry volcanic fragments.

VOLCANIC SANDSTONE UNIT

Rocks assigned to the volcanic sandstone unit comprise most of the Takla Group west of the Dortatelle fault. The base of the unit is not seen, but it is overlain by the volcanic breccia unit in the southeastern part of this area, near the Dortatelle fault. East of the Dortatelle fault, the volcanic sandstone unit crops out as two belts that overlie, but also seem to interfinger with, an intervening belt comprised of the sandstone-carbonate unit. The western belt generally faces and dips to the southwest, and is truncated by the Dortatelle fault. The eastern belt faces and dips to the east, and is overlain by the volcanic breccia unit.

The dominant lithology within the volcanic sandstone unit is grey to green, fine to coarse-grained volcanogenic sandstone composed largely of feldspar crystals and feldspathic lithic fragments. Pyroxene grains, and lithic grains with pyroxene phenocrysts, are common in some sections but virtually absent in others. The sandstone occurs partly as well-defined, thin to thick beds (Photo 1) and partly as massive units, up to tens of metres thick, in which bedding is not apparent.

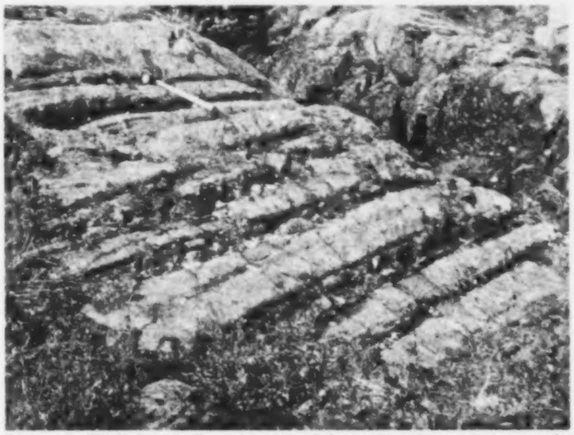

Photo 1. Well-bedded sandstone of the volcanic sandstone unit, south of west branch of Kliyul Creek.

Well-bedded intervals locally display graded bedding, scoured bases, flame structures and rip-up clasts. Locally, some sandstone units are calcareous.

Green siltstone, also probably of volcanogenic origin, is fairly common within the volcanic sandstone unit, either as thin beds intercalated with beds of coarser sandstone, or as thin-bedded to laminated intervals up to many metres thick comprised only of siltstone. Also present in places are intervals, locally more than 10 metres thick, of dark grey, rusty-weathered, thin-bedded siltstone and argillite. Thin to medium beds of dark grey limestone are also found within the unit, but are rare.

Coarse-grained intervals, ranging from pebbly volcanogenic sandstone or lapilli tuff to coarse breccias containing fragments approaching a metre in size, are not uncommon within the volcanic sandstone unit and typically form massive, resistant units many tens of metres thick. Fragments of feldspar porphyry and pyroxene-feldspar porphyry are commonly present, and clasts of hornblende-feldspar porphyry, diorite and tonalite were also observed. Also present are distinct units of very coarse breccia, one to several metres thick, that occur as single layers or a few closely spaced layers within much finer grained feldspathic sandstone intervals. These breccia units invariably contain mainly pyroxene porphyry fragments, which are supported by a matrix rich in pyroxene mineral grains. The clasts commonly range from a few centimeters to more than a metre in size, and some fragments have irregular amoeboid-like contacts and faintly chilled margins, suggesting that they were not completely cooled when they were incorporated into the breccia. These breccias probably represent mass flow deposits that tapped a different source than the much finer feldspathic sandstones with which they are intercalated.

Units of massive pyroxene porphyry and pyroxene-feldspar porphyry, probably derived from mafic flows and/or sills, are found scattered throughout the volcanic sandstone unit, but seem to be most common at higher stratigraphic levels.

SANDSTONE-CARBONATE UNIT

Rocks assigned to the sandstone-carbonate unit form a single belt that extends from the southern boundary of the map area northwestward about 10 kilometres to the Dortatelle fault and Darb Creek pluton. This belt is broadly anticlinal in nature, as the sandstone-carbonate unit is flanked by outward-facing rocks of the volcanic sandstone unit to both the northeast and southwest.

The dominant lithologies within the sandstone-carbonate unit are volcanogenic sandstones and breccias that are identical to those of the volcanic sandstone unit. Associated with these rocks however, are dark-grey limestones that are mixed with volcanogenic sandstone in lenses and layers that were probably derived from slump deposits (Photo 2). In many of these units there are subequal proportions of limestone and sandstone, and they form lenses and blocks that are intimately mixed in a chaotic fashion. In other units, one rock type predominates and appears to form a matrix containing clasts of the other. Still elsewhere, limestone occurs as discrete layers or patches, many tens of metres in size, that appear to form beds within the sandstone succession. However, some of these thick units contain laminations that are folded in a chaotic and irregular fashion suggesting soft-sediment deformation.

A very thick limestone unit exposed on the ridge south of the Darb Creek pluton, at the north end of the sandstone-carbonate belt, displays regular east dips that are concordant with bedding orientations in the overlying volcanic sandstone unit. This might be a very large slump block within the sandstone-carbonate unit, or it might mark the transition into a part of the source terrain from which the slump blocks were derived. Monger (1977) collected Late Triassic macrofossils from this unit. Limestone samples from this area and others within the sandstone-carbonate unit were collected during the 2003 field season and are being processed for conodonts. The nature of this unit indicates, however, that any conodont ages will have to be interpreted with caution.

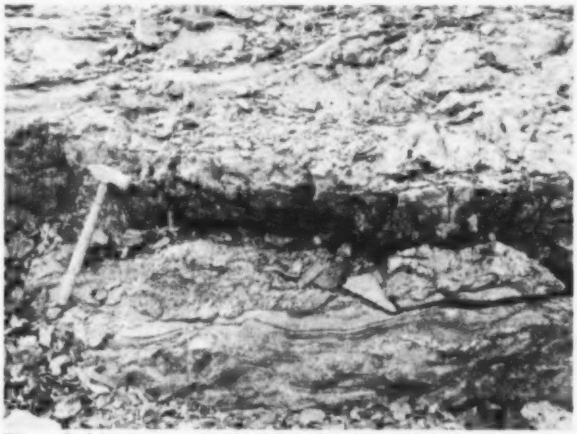

Photo 2. Limestone mixed with volcanic sandstone, sandstone-limestone unit, head of Kliyul Creek.

VOLCANIC BRECCIA UNIT

The volcanic breccia unit comprises a monotonous succession of mafic volcanic breccias dominated by clasts of pyroxene-phyric basalt (Photo 3). It locally includes narrow intervals of interbedded pyroxene-rich volcanic sandstone and siltstone, as well as massive pyroxene-phyric flows and/or sills.

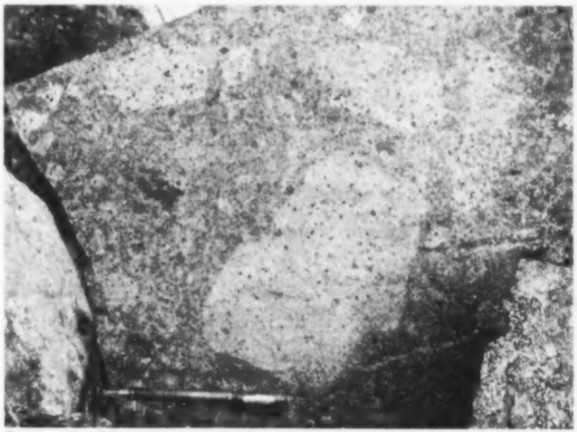

Photo 3. Pyroxene porphyry breccia, volcanic breccia unit, upper Croyden Creek.

The unit is well exposed as a series of prominent ridges in the northwestern part of the map area. It also occurs in a narrow belt directly west of the Dortatlelle fault in the southern part of the map area. In both of these exposure belts it rests structurally, and apparently stratigraphically, above finer-grained and more distinctly bedded rocks of the volcanic sandstone unit.

The rocks of the breccia unit typically form resistant, blocky, green-brown to rusty-brown weathered exposures. Stratification, or contacts between different breccia units are generally not evident. Fresh surfaces are dark green to grey-green. Breccia fragments are dominantly or exclusively pyroxene and pyroxene-feldspar-phyric basalt, although there is commonly considerable textural variation among clasts based on size and abundance of phenocrysts, as well as proportions of feldspar versus pyroxene phenocrysts. Locally, in the panel west of the Dortatelle fault, the breccia also contains fragments of hornblende-feldspar porphyry and microdiorite.

Pyroxene±feldspar porphyry fragments within the breccias are typically angular to subangular and unsorted to poorly sorted. The fragments are commonly up to 10 centimetres in size and locally range up to several tens of centimetres. The matrix typically consists of pyroxene plus or minus feldspar crystals and small, commonly pyroxene-bearing, lithic grains. In many exposures it is virtually indistinguishable from the fragments, such that the breccia texture is not readily apparent. Locally the matrix is calcareous and recessive-weathering, causing the fragments to stand out in relief.

TAKLA GROUP CORRELATIONS

The Takla Group within the 2003 map area is contiguous with Takla exposures mapped as the Upper Triassic Plughat Mountain succession to the east and southeast (Ferri *et al.*, 1993; 2001b). The Plughat Mountain succession in this area has been subdivided into two broad subdivisions; the first comprises units dominated by bedded tuffs and volcanic-derived sedimentary rocks, intercalated with local beds of argillite and limestone (units lTrP1 and lTrP2 of Ferri *et al.*, 2001b), whereas the second comprises an overlying to laterally equivalent succession dominated by coarse breccias and agglomerates containing pyroxene-phyric basalt fragments (Unit lTrP3 of Ferri et al., 2001b). The first division of the Plughat Mountain succession correlates with the volcanic sandstone and sandstone-limestone units of the Johanson Lake area, whereas the coarse breccias and agglomerates that overlie and interfinger with the finer-grained facies are correlated with the volcanic breccia unit of this study. The Plughat Mountain succession has been traced more than 100 kilometres southward to the Germansen Lake area, where it is underlain by, and interfingers with, Middle to Upper Triassic sedimentary and local volcanic rocks assigned to the Slate Creek succession (Ferri and Melville, 1994). The Slate Creek succession comprises the base of the Takla Group in this area.

Farther south, in the Nation Lakes area, the Upper Triassic volcanic-dominant component of the Takla Group is subdivided into a lower, predominately epiclastic unit, the Inzana Lake succession, and an upper unit dominated by coarse augite-phyric breccias and agglomerates referred to as the Witch Lake succession (Nelson and Bellefontaine, 1996). This two-fold subdivision resembles the volcanic sandstone versus volcanic breccia subdivision applied to the present map area, as well as the broad lower and upper subdivisions that have been applied to much of the intervening Plughat Mountain succession. Nelson and Bellefontaine point out, however, that the simple correlations suggested by these subdivisions may be misleading, since the predominantly epiclastic units appear to interfinger and overlap in age with the pyroxene-rich volcanic breccia units. Furthermore, they suggest that facies and thickness relationships in the Nation Lakes - Germansen Lake area suggest that the Takla Group accumulated in and adjacent to at least two distinct volcanic centers that may or may not have been coeval.

Plutonic Rocks

MAFIC AND ULTRAMAFIC INTRUSIVE ROCKS BETWEEN KLIYUL AND CROYDEN CREEKS

Clinopyroxenite, hornblendite, gabbro and diorite are the dominant lithologies within an intrusive complex that extends for about 4 kilometres westward from the eastern boundary of the map area, along Croyden and Porphyry creeks. These rocks form the northwestern end of a large, elongate, mafic-ultramafic complex, referred to as the Abraham Creek complex, that extends an additional 24 kilometres to the southeast (Ferri *et al.*, 1993, 2001b). Within the present study area, the Abraham Creek complex has been subdivided into a central unit of mainly clinopyroxenite, hornblendite and mafic gabbro, and a unit dominated by diorite, gabbro and microdiorite which flanks the ultramafic unit to the north and south. Xenoliths of clinopyroxenite and hornblendite are common within the diorite unit, and an intrusion breccia containing fragments of clinopyroxenite and mafic gabbro within a leucodiorite host occurs locally along the contact between the two units. These relationships suggest that the ultramafic rocks are for the most part older than the dioritic rocks. Dikes of diorite, microdiorite, diabase, pyroxene porphyry, hornblende-feldspar porphyry and monzodiorite are common within both mappable units, and are though to be an integral part of the intrusive complex.

A separate body of mainly diorite, microdiorite, monzodiorite and gabbro crops out along the slopes east of the north branch of Kliyul Creek, to the west and northwest of the Abraham Creek complex. This body is similar to the diorite unit of the Abraham Creek complex, and the intervening Takla Group is cut by numerous diorite and microdiorite dikes of similar composition. The western diorite unit is therefore thought to be related to the Abraham Creek complex; this correlation is supported by the local presence of clinopyroxenite and hornblendite at the north end of the western pluton.

An ultramafic-mafic unit described as peridotite, gabbro and diorite crops out along the southwest slopes of Kliyul Creek in the southern part of the map area (Noel, 1971b). These rocks were not examined during the present study, but apparently intrude the sandstone-carbonate unit of the Takla Group, and are themselves cut by the Kliyul Creek granodiorite pluton.

JOHANSON LAKE MAFIC-ULTRAMAFIC COMPLEX

The Johanson Lake mafic-ultramafic complex is located in the northwestern part of the study area, about 1.5 kilometres southwest of Johanson Lake. These rocks were described briefly by Irvine (1976) and were subsequently studied in more detail by Nixon *et al.* (1990b, 1997). The latter authors subdivided the complex into two units; one dominated by clinopyroxenite and hornblendite, and another, more voluminous unit consisting mainly of gabbro to diorite. The Johanson Lake complex was not remapped during the 2003 field season, but is shown on Figure 3 after Nixon *et al.* (1997).

The Johanson Lake complex intrudes the volcanic sandstone unit of the Takla Group, presumably at a relatively high stratigraphic level since it is at the north end of a fairly extensive north-dipping structural panel. Unaltered hornblende from coarse-grained hornblendite of the Johanson Lake complex has yielded a K-Ar date of 232±13 Ma (Stevens *et al.*, 1982, sample GSC 80-46). This Middle Triassic date is suspect since it suggests that the intrusive rocks are older than their Upper Triassic host.

MAFIC INTRUSIVE COMPLEXES WEST OF THE DORTATELLE FAULT

Gabbro, diorite and microdiorite, with minor amounts of quartz diorite and tonalite, form a narrow, northerly-trending unit that has been traced for about six kilometres within the volcanic sandstone unit of the Takla Group, just west of the Dortatelle fault where it follows Darb Creek. Similar rocks form a north-striking, sill-like body that marks the contact between the volcanic sandstone and volcanic breccia units a short distance to the south. These northerly-trending intrusive units are lithologically similar to the mafic portions of the Abraham Creek and Johanson Lake mafic-ultramafic complexes.

SOLO LAKE STOCK

The Solo Lake stock intrudes the volcanic sandstone unit of the Takla Group in the west-central part of the study area, along and southwest of Solo Lake. The intrusion consists mainly of light to medium grey, medium grained, equigranular hornblende quartz diorite to diorite. Melanocratic hornblende-rich diorite, locally grading to hornblendite, occurs locally, as do patches and dikes of mafic-poor tonalite. Dikes showing a similar range of composition are common within the Takla Group peripheral to the stock. The age of the stock is unknown, but a sample collected during the 2003 field season has been submitted to the UBC geochronology laboratory for U-Pb isotopic dating.

DARB CREEK PLUTON

Massive, light grey weathered, medium to coarse grained hornblende-biotite tonalite forms a pluton that is well exposed on the slopes surrounding the prominent eastern tributary of Darb Creek. Along its south margin the pluton truncates an east-dipping succession that includes all three map units of the Takla Group; where observed this contact is sharp, although the tonalite contains abundant xenoliths of country rock for a few tens of metres along its outer margin. The pluton is apparently truncated by the Dortatelle fault to the west, but this contact was not observed. Along its northeast margin the tonalite cuts an older northwest-trending stock consisting of diorite and quartz diorite. The age of the Darb Creek pluton is not known, but a sample of tonalite collected during the 2003 field season has been submitted to the UBC geochronology laboratory for U-Pb isotopic dating.

JOHANSON CREEK PLUTON

Massive, medium-grained, light-grey weathering hornblende-biotite tonalite to quartz diorite crops out in the northwestern corner of the 2003 map area, where it apparently intrudes both the Takla Group and the Johanson Lake mafic-ultramafic complex (Nixon *et al.*, 1997). These exposures represent the south end of a large, predominantly quartz diorite pluton that extends more than 10 kilometres farther north, and is referred to as the Johanson Creek stock by Richards (1976b). Biotite and hornblende separates from a sample of this pluton collected north of Johanson Creek have yielded K-Ar dates of 121±4 Ma and 142±12 Ma, respectively (Wanless *et al.*, 1979; samples GSC 78-12 and GSC 78-13).

KLIYUL CREEK PLUTON AND DAVIE CREEK STOCK

Light grey to pink weathered, medium to coarse grained biotite granodiorite crops out on the steep slopes northeast of Kliyul Creek near the southeastern corner of the 2003 map area. It intrudes the volcanic sandstone unit of the Takla Group as well as dioritic phases of the Abraham Creek mafic-ultramafic complex. A small stock of similar, but largely potassic-altered, biotite granodiorite (Davie Creek stock), measuring about 700 metres long by 300 metres wide, cuts across pyroxenite and related rocks of the Abraham Creek complex 1.5 kilometres to the northeast. This stock hosts the Davie Creek porphyry molybdenum occurrence.

The granodiorite along Kliyul Creek comprises the northwest end of a narrow pluton that extends for about 7 kilometres to the southeast. This pluton, together with several others of similar composition within and peripheral to the Hogem Batholith, are informally referred to as the Osilinka stocks by Woodsworth *et al.* (1991). They assigned the Osilinka stocks a Cretaceous age, based on their similarity to the Cassiar suite of plutons, and biotite K-Ar dates of 122±6 Ma (Wanless *et al.*, 1972, sample GSC70-11) and 120 Ma (G. Woodsworth, unpublished data) from two separate stocks within the Hogem batholith. However, one of these dated stocks has recently yielded a U-Pb zircon date of 192.3 +2.1/-4.8 Ma (Nelson *et al.*, 2003; J. Nelson, personal communication 2003), indicating that at least one of the Osilinka stocks is Early Jurassic in age. In order to determine the crystallization age of the granodiorite stocks in the present map area, a sample collected from the Davie Creek stock has been submitted to the UBC geochronology laboratory for U-Pb isotopic dating.

OTHER INTRUSIVE ROCKS

The only intrusion not previously mentioned, but sufficiently large to be portrayed on Figure 3, is a small body of chlorite-epidote-altered hornblende diorite that is exposed on the ridge north of Dortatelle Creek, a short distance east of the Dortatelle fault. This body intrudes the volcanic sandstone unit of the Takla Group along its northwest contact, but its southeastern contact is marked by a northwest-dipping chloritic shear zone that contains sigmoidal foliation domains suggesting components of reverse and sinistral movement.

Dikes are abundant in the vicinity of the mappable plutons within the study area, where they generally reflect the composition of the adjacent major intrusions. Dikes of pyroxene ±feldspar porphyry, diorite and microdiorite are common throughout the area. These dikes dip steeply and typically strike northwest, although northeast strikes were also observed. A number of northwest-striking pyroxene porphyry dikes on the ridge northeast of Croyden Creek contain common xenoliths of pyroxenite. Brown-weathering lamprophyre dikes were observed cutting the volcanic sandstone unit of the Takla Group south of upper Croyden Creek.

STRUCTURE

Mesoscopic Structure

The structure of most outcrops within the study area is characterized by brittle to brittle-ductile faults. A large proportion of these outcrop-scale faults strike northwest to north and dip steeply; some show evidence for dextral strike-slip displacement, consistent with the interpretation that these structures are related to Cretaceous-Tertiary dextral strike slip faults that are prominent regional structures (Zhang and Hynes, 1994). However, a significant number of northwest-striking, relatively ductile faults with sinistral displacement were also observed; these may relate to an earlier period of sinistral faulting that has not been well-documented in the region. Penetrative foliations are for the most part restricted to local high strain zones associated with faults. However, a weak slaty cleavage of more regional aspect is apparent locally, mainly in the southern part of the area. This cleavage is axial planar to local mesoscopic folds and, in the area west of the Dortatelle fault, is associated with larger folds with wavelengths of several hundred metres. The age of these structures is unknown; they may be related to the Cretaceous-Tertiary dextral strike slip faults that dominate the structure of much of the area (Zhang and Hynes, 1994), or might be vestiges of an older event, such as the late early Jurassic thrusting of the Quesnel Terrane over terranes to the east.

General Map-Scale Structure

The Kliyul Creek – Johanson Lake map area is separated into two domains by the north-striking Dortatelle Fault. The area east of the fault is broadly anticlinal in nature, with a poorly-defined hinge occurring within the western part of the sandstone-carbonate unit of the Takla Group. Along its northeast margin this unit dips and faces to northeast at moderate to gentle angles and is overlain by a relatively thin section of the volcanic sandstone unit, which is in turn overlain by a thick section belonging to the volcanic breccia unit. Along its southwestern margin, the sandstone-carbonate unit dips and faces southwestward at somewhat steeper angles, and is overlain by a thicker section of the volcanic sandstone unit. This western limb of the anticline is progressively truncated northward along the Dortatelle fault.

The volcanic sandstone unit in the southern part of the western domain is characterized by northerly-striking bedding that displays several dip-reversals across mainly north-plunging fold hinges. The easternmost fold limb comprises an east-dipping panel several kilometres wide that is overlain by the volcanic breccia unit adjacent to the Dortatelle fault. In the northern part of the western domain, a thick section of the volcanic sandstone unit is exposed in a more or less homoclinal panel that dips and faces to the north. This panel is separated from the folded rocks to the south by a complicated zone of faults in the vicinity of Solo Lake and upper Mariposite Creek.

Dextral Fault Systems

The structural geology of a region encompassing the current map area was studied by Zhang and Hynes (1991, 1992, 1994), who concluded that most of the deformation was related to dextral transcurrent movement on the Finlay-Ingenika fault system. They found that most faults were subvertical, and were either dextral strike-slip faults with northwest, north-northwest or north strikes, or sinistral strike-slip faults with east-northeast strikes. This suite of faults corresponds closely with the predicted orientations of structures that would form in a stress field resulting from dextral displacement along the Finlay-Ingenika fault (Tchalenko, 1970; Figure 18 of Zhang and Hynes, 1994). Zhang and Hynes also concluded, based on variations in the orientation of conjugate shear sets that formed early in the deformation history, that fault-bounded domains had rotated clockwise about subvertical axes in response to progressive displacement. Their analysis indicates rotations of up to 59 degrees adjacent to the Finlay-Ingenika fault, decreasing systematically to zero about 20 kilometres away from the main fault.

The suite of structures described by Zhang and Hynes (1994) was recognized during the 2003 mapping program, but almost exclusively at the outcrop scale. With a few exceptions, such as the Dortatelle fault, individual faults could not be traced confidently beyond a single ridge or cirque basin.

Dortatelle Fault

The Dortatelle fault was mapped by Richards (1976b), who shows it extending from the Ingenika fault northward about 40 kilometres to just beyond Johanson Lake (Figure 1). Parts of the fault were studied in detail by Zhang and Hynes (1994), who demonstrated that it was a dextral strike-slip fault on the basis of the geometric relationships between S and C surfaces and associated folds. The fault was not examined in detail during the present study, but is easily mapped on the basis of its prominent topographic expression and the apparent truncation of map units along it. Rocks adjacent to the fault, particularly on its west side, are commonly strongly foliated for several hundred metres beyond the fault trace. The foliation typically strikes north-northwest and dips steeply, consistent with the interpretation of dextral displacement along the fault.

Sinistral Faults

Faults with documented sinistral strike-slip displacement within the southeastern part of the study area are shown on Figure 4. Three of these strike east to northeast and are reasonably interpreted as conjugate riedel shears within a dextral fault system related to the Cretaceous-Tertiary Finlay-Ingenika fault (Zhang and Hynes, 1994). Most of the sinistral faults strike west-northwest to northwest, however, and probably represent a separate deformation event.

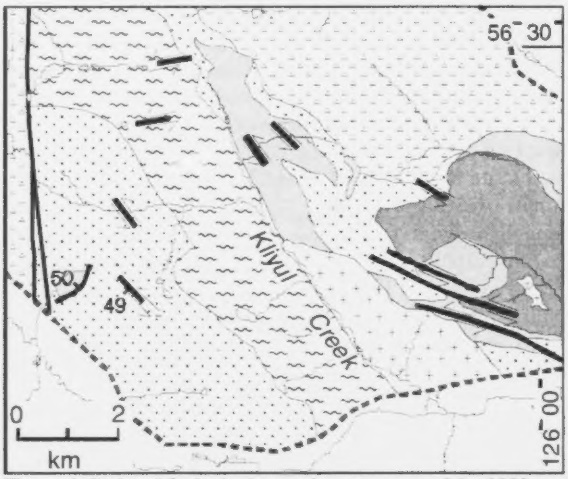

Figure 4. Sinistral faults in the southeastern part of the 2003 map area.

The sinistral faults are best represented by three structures, each traced for 2 to 3 kilometres, that form prominent topographic lineaments on the ridges and cirques between Kliyul and Porphyry creeks (Figure 4). From south to north, these are informally referred to as the South Bear Creek, North Bear Creek and Karen Creek faults (Grexton and Roberts, 1991). Sinistral offset of the mineralized layer on the Soup South occurrence by about 400 metres along the North Bear Creek fault was documented by McTaggart (1965), and sinistral displacement on all three faults was suggested by Grexton and Roberts (1991) on the basis of more equivocal evidence, consisting mainly of the apparent offsets of dikes. Sinistral movement along the South Bear Creek fault was confirmed during the present study. The fault is commonly defined by several tens of metres of sheared and foliated rock that at one place was observed to include well-developed S-C fabrics demonstrating a sinistral sense of shear.

None of the other northwest-striking sinistral faults shown on Figure 4 were traced for any substantial distance. Most comprise shear zones ranging from tens of centimetres to a few metres in width, with sinistral sense of displacement inferred from the angular relationship between the shear zone boundaries and the associated flattening foliation. Of note is the fact that these shear zones are in general more ductile than many outcrop-scale faults observed in the area, and that in two areas the shear zones were localized along pyroxene porphyry dikes. It is suspected that that sinistral faulting may have been broadly contemporaneous with the latter stages of mafic magmatism in the area.

MINERAL OCCURRENCES

Mineral occurrences within the Kliyul Creek – Johanson Lake map area are shown on Figure 5. Most contain copper and gold, and are associated with mafic-ultramafic plutons and related diorite dikes. These include pyrite-chalcopyrite in shear zones and veins within and peripheral to the ultramafic-mafic plutonic rocks; magnetite-pyrite-chalcopyrite lodes in shear zones peripheral to the plutonic rocks, and magnetite-pyrite-chalcopyrite skarn and replacement bodies where calcareous units of the Takla Group are intruded by diorite dikes. Gold-bearing quartz veins occur within shear zones in the Solo Lake stock. Veins containing gold and copper occur within a major quartz-pyrite alteration zone at the headwaters of Darb and Kliyul creeks, and within a quartz-carbonate alteration zone along Mariposite Creek. These major alteration zones underscore the area's potential for large porphyry-style copper-gold mineralizing systems. Porphyry molybdenum mineralization associated with the Davie Creek stock is suspected to be Cretaceous in age, and considerably younger than most of the copper-gold mineralization.

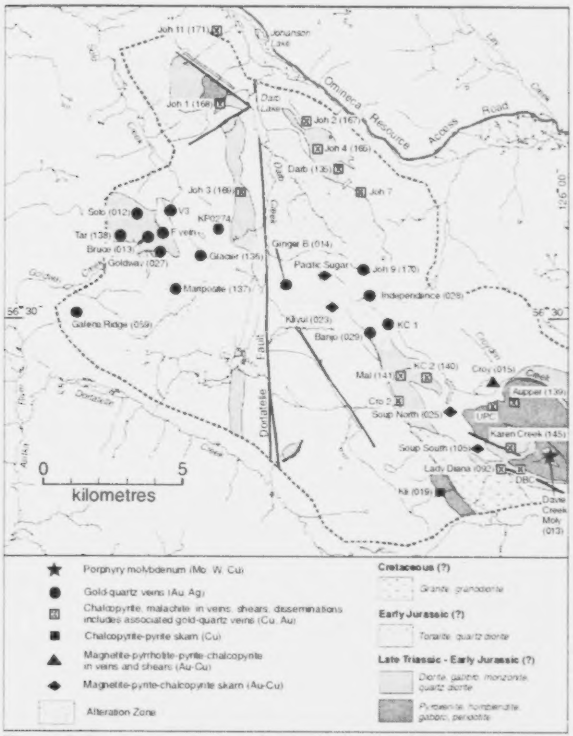
Joh 11 (171)
Johanson Lake
Joh 1 (168)
Darb Lake
Joh 2 (167)
Joh 4 (166)
Darb (135)
Joh 7
Joh 3 (169)
Omineca Resource Access Road
Darb Creek
Solo (012)
V3
KP0274
Tar (138)
F vein
Bruce (013)
Goldway (027)
Glacier (136)
Ginger B (014)
Pacific Sugar
Joh 9 (170)
Mariposite (137)
Independence (028)
Galena Ridge (059)
56°30'
126°00'
Kliyul (023)
KC 1
Banjo (029)
Fault
Dortatelle
Croydon Creek
KC 2 (140)
Mal (141)
Croy (015)
Aupper (139)
Cro 2
Soup North (025)
UPC
Karen Creek (145)
Soup South (105)
Lady Diana (092)
DBC
Kli (019)
Davie Creek Moly (013)
0
5
kilometres
Porphyry molybdenum (Mo W Cu)
Gold-quartz veins (Au Ag)
Chalcopyrite, malachite in veins, shears, disseminations includes associated gold-quartz veins (Cu, Au)
Chalcopyrite-pyrite skarn (Cu)
Magnetite-pyrrhotite-pyrite-chalcopyrite in veins and shears (Au-Cu)
Magnetite-pyrite-chalcopyrite skarn (Au-Cu)
Alteration Zone
Cretaceous (?)
Granite, granodiorite
Early Jurassic (?)
Tonalite, quartz diorite
Late Triassic - Early Jurassic (?)
Diorite, gabbro, monzonite, quartz diorite
Pyroxenite, hornblendite, gabbro, peridotite

Figure 5. Locations of mineral occurrences in the Kliyul Creek – Johanson Lake map area. Occurrences found in the MINFILE database shown with 094D MINFILE number appended in brackets.

Magnetite-Pyrrhotite-Pyrite-Chalcopyrite Shear Veins at the Croy Showing (MINFILE 094D 015)

The Croy occurrence, located on a bench southwest of Croyden Creek, was discovered in the mid 1940s and corresponds to mineralization described by White (1948) on the Shell claims. Early development work, including trenching and sampling, led to drill programs in the early 1970s and mid 1980s (Grexton and Roberts, 1991), although the results of the drilling were not filed for assessment credits. The mineralization is hosted in volcanic and volcaniclastic rocks of the Takla Group on the northwest margin of the Abraham Creek intrusive complex.

Mineralization at the Croy occurrence comprises massive to disseminated magnetite-pyrrhotite-pyrite-chalcopyrite associated with quartz-calcite-chlorite gangue. It occurs as lenses, locally arranged in en echelon fashion, within steeply dipping west-northwest to northwest trending shear zones. Mineralized areas are typically marked by abundant malachite and azurite staining. Although numerous mineralized zones have been recognized only two, traced for about 75 and 170 metres, respectively (Noel, 1971a) are known to have substantial lengths. The largest and most continuously mineralized section occurs within the longest of these zones; it is about 20 metres long and averages less than 60 centimetres wide (White, 1948). White reports assay results from two channel samples collected about 15 metres apart within this mineralized segment. One, across 46 centimetres, yielded 0.28 ounces per ton gold, 1.1 ounces per ton silver and 6.5 per cent copper. The other, across 23 centimetres, contained 0.47 ounces per ton gold, 0.6 ounces per ton silver and 12.5 per cent copper.

Mineralization Along the South Margin of the Abraham Creek Intrusive Complex

Widespread mineralization within and adjacent to the southern part of the Abraham Creek mafic-ultramafic complex is represented by the Lady Diana (MINFILE 094D 092), DBC and Karen Creek (MINFILE 094D 145) occurrences. These occurrences correspond to the mineralization described by Grexton and Roberts (1991) from South Porphyry Ridge, Davie – Bear creeks and Karen Cirque, respectively.

Mineralization at the Lady Diana showing occurs over an area of about 200 metres by 200 metres, directly south of the South Bear Creek fault. It comprises pyrite-chalcopyrite disseminations, fracture fillings and stringers within microdiorite of the Abraham Creek complex and adjacent hornfelsed volcaniclastic rocks of the Takla Group. Chalcopyrite-bearing grab samples reported by

Grexton and Roberts (1991) are all enriched in gold, with a high of 3900 ppb Au from a sample that also contained 18.5 ppm Ag and 13670 ppm Cu. They also describe a narrow quartz vein containing galena, which yielded 15500 ppb Au, 214.7 ppm Ag and 18439 ppm Pb.

The DBC showing consists of narrow quartz veins and shear zones, sparsely mineralized with pyrite and chalcopyrite, spread over a relatively small area that straddles the North Bear Creek fault zone. The highest gold value from an *in situ* sample within this cluster reported by Grexton and Roberts (1991) came from a chlorite-quartz-carbonate-altered shear zone that contains trace chalcopyrite and pyrite, along with malachite, azurite and magnetite. This sample contained 4700 ppb Au, 24.4 ppm Ag and 30648 ppm Cu. A nearby sample mineralized with pyrite, malachite and magnetite, collected during the 2003 mapping program (sample 03PSC-54), yielded 1260 ppb Au, 14.4 ppm Ag and 10871 ppm Cu, as well as 66 ppb Pt and 75 ppb Pd.

The Karen Creek showing encompasses numerous occurrences scattered over a large area that straddles the Karen Creek fault. Mineralization includes gold-bearing quartz veins sparsely mineralized with pyrite and chalcopyrite, as well as pyrite-chalcopyrite-malachite as disseminations and within shear zones. One unusual occurrence, in the central part of the cluster, a short distance north of the Karen Creek fault, comprises a pod of massive sulphides and quartz located along the intersection of two faults. The sulphides include pyrite, chalcopyrite, galena and sphalerite. A sample from this pod yielded high base metal values, as well as 25000 ppb Au, 282.2 ppm Ag, 4730 ppb Hg and 881 ppm Sb (Grexton and Roberts, 1991, sample M136).

Two samples collected during the present study confirm the general nature of mineralization at the Karen Creek showings. One (sample 03PSC-82) was from a silicified lens, heavily stained with limonite and malachite, within the Karen Creek fault zone. This sample yielded 1573 ppb Au, 16 ppb Pt, 67 ppb Pd, 11.78 ppm Ag and 4051 ppm Cu. The other sample came from a gently-dipping, white quartz vein that is exposed for more than 50 metres in a cliff face several hundred metres north of the Karen Creek fault. Where sampled, the vein is 30 centimetres wide and contains numerous rusted out pits containing traces of pyrite, as well as patches of chlorite and fragments of the dioritic wall rock. The sample (03PSC-84) yielded 20884 ppb Au, 25.620 ppm Ag and 113.5 ppm Cu. This vein was also sampled by Grexton and Roberts (1991) at three different locations, and yielded gold values ranging from 14000 ppb to 41500 ppb (samples S173, S174, S175).

Mineralization on the North Side of the Abraham Creek Intrusive Complex

Mineralization within the northern part of the Abraham Creek mafic-ultramafic complex is represented by the Aupper (MINFILE 094D 139) and UPC occurrences. These occurrences correspond to the mineralization described by Grexton and Roberts (1991) from Croyden Ridge and Upper Porphyry Creek, respectively. The mineralization in both areas comprises gold-bearing quartz veins, in part localized along shear zones, scattered throughout east-west zones about 1 kilometre long. The quartz veins commonly contain pyrite, chalcopyrite and malachite; one vein within the Aupper showing contains pyrite and galena. A sample selected from a quartz vein containing 2 to 5 per cent chalcopyrite on the Aupper occurrence yielded 2700 ppb Au, 43.5 ppm Ag and 38064 ppm Cu (Grexton and Roberts, 1991, sample A96). A grab sample from a shear vein with only a trace of pyrite on the UPC occurrence contained 25000 ppb Au and 46.1 ppm Ag (Grexton and Roberts, 1991, sample S146).

Mineralization Within the North Kliyul Creek Dioritic Stock

The dioritic stock that crops out on the slopes east of the north fork of Kliyul Creek hosts mineralization represented by the KC 2 (094D 140) and Mal (094D 141) MINFILE occurrences. The Cro 2 occurrence is along the southwest margin of the stock about 1 kilometre south of the Mal.

Mineralization at the KC 2 occurrence covers a broad area along the northeast margin of the stock and extends into the Takla country rocks. It includes quartz veins and silicified or quartz-carbonate-altered shear zones mineralized with magnetite, pyrite, chalcopyrite, malachite and azurite, and locally galena and sphalerite (Wilson, 1984; Cross, 1985). Shear zones trend northwest, north and northeast. Samples of mineralized material have yielded assay values of up to 5484 ppb Au and 14.5 ppm Ag (Cross, 1985).

The Mal occurrence comprises variably oriented quartz-carbonate veins associated with fractures and shear zones that occur over several hundred metres along a major tributary to the north fork of Kliyul Creek. Some of the veins and shears are mineralized with pyrite, galena and malachite. A sample of one rusty quartz-carbonate vein containing disseminated pyrite yielded 16200 ppb Au and 3.10 ppm Ag (Wilson, 1984).

At the Cro 2 occurrence, rocks of the Takla Group are cut by silicified, chloritized and pyritized shear zones for at least several tens of metres along the southwest margin of the diorite stock. The zone contains small quartz-pyrite veins, and a sample of one of these veins contained 294 ppb Au and 5.40 ppm Ag (Fox, 1991).

Magnetite-Pyrite-Chalcopyrite Skarn Occurrences

Mineralization on the Soup North (MINFILE 094D 025) and Soup South (MINFILE 094D 105) occurrences consists of one and locally two stratabound layers of magnetite that are exposed intermittently over a strike length of more than 2.5 kilometres (McTaggart, 1965; Williams, 1997). These layers occur within volcaniclastic rocks of the volcanic sandstone unit, which dip at low to moderate angles into the steep southwest-facing slope on which the showings occur. The Takla Group in this area is intruded by abundant dioritic to microdioritic dikes. The mineralized layers exposed on surface are 1 to 5 metres thick and comprise 60 to 100 per cent magnetite with disseminated pyrite and chalcopyrite, and gangue minerals that include epidote, tremolite, garnet and calcite. Williams (1997) reports that an oblique drill intersection of 22.71 metres across one of the magnetite layers on Soup North contains 1.09 ppm Au and greater than 3915 ppm Cu. The best gold values, up to 68 ppm, occur in the Saddle Gully zone on Soup North, where segments of stratabound magnetite mineralization and cross-cutting mineralized shears are localized along a north-northeast-striking fault zone (Smit and Meyers, 1984; Williams, 1997).

The Kliyul magnetite-pyrite-chalcopyrite occurrence (MINFILE 094D 023) is located in an area of poor bedrock exposure within the broad valley, bounded by gossanous bluffs and talus slopes, at the head of Kliyul Creek. Geology projected from the south and north suggests that the volcaniclastic rocks that host the mineralization are within the sandstone-carbonate unit of the Takla Group. The area was staked in 1970 and explored with silt, soil and geophysical surveys. Copper-gold mineralization associated with magnetite was discovered in 1974 by a drill program that tested a magnetic anomaly. Exploration by various companies subsequent to the initial discovery included diamond drilling in 1981 and reverse circulation drilling in 1993. The latter program extended the known skarn mineralization and suggested that the resource estimate of 2.5 million tons grading 0.3 per cent Cu an 0.03 ounces/ton Au from the initial drilling could be increased (Gill, 1993).

The Pacific Sugar skarn showing, located about 1 kilometre north of the Kliyul occurrence, was discovered in the mid 1990s. It is hosted by the volcanic sandstone unit of the Takla Group, which at this location includes an interval of calcareous siltstones and limestones. Exploration work to date has outlined a magnetite-pyrite-epidote-garnet skarn unit measuring 40 metres by 100 metres and 3 to 6 metres thick (Gill, 1995). Mineralization consists of massive magnetite and pyrite containing disseminations, impregnations and clots of pyrrhotite and chalcopyrite. Endoskarned diorite in the footwall of the unit is inferred to be the source of the skarn mineralization. The skarn was tested with 5 diamond drill holes, with a cumulative length of 154.8 metres, in 1996. Significant drill results include 2048 ppm Cu and 625 ppb Au over 3.97 metres (Leriche and Harrington, 1996).

Mineralization Associated with Diorite on the Northeast Margin of the Darb Creek Pluton

Numerous small occurrences of pyrite and chalcopyrite are found within and adjacent to the dioritic stock located along the northeast margin of the Darb Creek pluton. This mineralization is described by Leriche and Luckman (1991a, b) and is represented by the Joh 2 (094D 167), Joh 4 (094D 165) and Darb (094D 135) MINFILE occurrences. Similar mineralization occurs at the Joh 7 occurrence, about 1 kilometre to the south-southeast, where Takla volcanic rocks are cut by numerous diorite dikes that may be related to the mineralized stock to the northwest (Gill, 1994).

The mineralization in this area occurs within the diorite stock, associated dikes and the Takla country rocks. Pyrite and chalcopyrite occur as disseminations, as blebs and disseminations in quartz veins, and in silicified shear zones. Malachite is commonly associated with the chalcopyrite, and also occurs as fracture and joint coatings in adjacent rocks. A 25 centimetre chip sample across a zone of disseminated chalcopyrite-pyrite, within the diorite stock at the Joh 4 occurrence, returned 2000 ppb Au, 13.8 ppm Ag and 21 517 ppm Cu (Leriche and Luckman, 1991b, sample KR 14).

Gold Quartz Veins Associated with the Darb Creek – Kliyul Creek Quartz-Pyrite Alteration Zone

A series of bright red and yellow outcrop bluffs and talus slopes define an irregular zone of quartz-pyrite±sericite alteration that extends from the head of Darb Creek for about 5 kilometres southeast, to the head of the north fork of Kliyul Creek (Figure 5). This conspicuous alteration attracted early prospectors in the area, who discovered the Ginger B (MINFILE 094D 014), Independence (094D 028) and Banjo (094D 029) gold-bearing quartz vein systems within and peripheral to the zone (White, 1948). The KC 1 occurrence, northeast of the Banjo, was discovered within the alteration zone at a later date (Fox, 1982).

The quartz veins at these showings are commonly found within shear zones that strike northwest, north or east, and are mineralized with various combinations of pyrite, chalcopyrite and galena. Significant gold and silver values have been reported from all of the occurrences (White, 1948; Fox, 1982; Christopher, 1986). A sample collected from a pyrite-chalcopyrite-bearing quartz vein on the Banjo showing during the 2003 mapping program contains 2251 ppb Au and more than 100 ppm Ag (sample 03PSC-93).

Gold Quartz Veins Associated with the Solo Lake Stock

Gold-bearing quartz veins within, and along the margins of, the Solo Lake stock are among the oldest documented mineral exploration targets within the study area. The Solo (MINFILE 094 D 012), Bruce (MINFILE 094D 013) and Goldway (MINFILE 094D 027) occurrences were explored in the mid 1940s and are described by White (1948). Exploration has continued intermittently to the present time, and new vein systems have been discovered, including the F vein (Pawliuk, 1985), the V3 occurrence (V1, V2 and V3 samples of von Rosen, 1986) and the Tar occurrence (MINFILE 094D 138; L veins of Richards, 1991).

The vein systems associated with the Solo Lake stock are well described by Richards (1991). Each occurrence shown on Figure 4 comprises a number of veins, with individual veins ranging from several metres to several hundred metres in length, and from a few centimeters to several metres in width. Gold and silver ratios are commonly near one to one, and the precious metals are associated with pyrite, and locally galena and sphalerite. Visible gold has been reported from the A and C veins of the Bruce occurrence. The A vein has returned assay values up to 74.19 grams/tonne Au over 29 centimetres (Phendler, 1984).

The geometry of the vein systems is most apparent at the Solo and Bruce occurrences, where individual veins are arranged en echelon within northwest-striking zones that approach one kilometre in length. Individual veins strike more northerly than the overall system, and are inferred to occupy extensional fractures within dextral shear systems (Richards, 1991). Alteration related to the veins is minimal, and Richards (1991) suggests that the veins may be related to fault movements during the late stages of emplacement and cooling of the Solo Lake stock.

Gold Quartz Veins and Stockwork within the Mariposite Creek Alteration Zone

A zone of quartz-ankerite-pyrite alteration, marked in part by conspicuous orange-brown-weathered outcrops, extends north and south of upper Mariposite Creek for a total length of about 5 kilometres (Figure 5). Quartz veins are an integral part of this alteration, and exploration at the Glacier (MINFILE 094D 136) and Mariposite (MINFILE 094D 137) occurrences, where veins are particularly dense, has been directed towards evaluating the area's potential to host a bulk tonnage gold deposit. Gill (1996) reports that 743 rock samples collected in the area of the Mariposite and Glacier occurrences included 70 samples (9 per cent) that contained greater than or equal to 500 ppb Au. Two diamond drill holes on the Mariposite occurrence intersected high density quartz-carbonate vein and stockwork intervals, but these contained only weak gold mineralization (Gill, 1996).

Davie Creek Moly (MINFILE 094D 113)

Porphyry molybdenum mineralization is associated with the Davie Creek stock, which intrudes hornblendite and associated rocks of the Abraham Creek complex on the south side of lower Porphyry Creek. The stock and associated mineralization was discovered by Rio Tinto in 1963, and was explored by diamond drilling in 1964. Subsequent drill programs by various companies in 1979, 1981 and 1982 have demonstrated that much of the stock is mineralized (Folk, 1979a; Bowen, 1982; Norman, 1982). Molybdenite occurs in quartz veinlets with pyrite and local traces of chalcopyrite, and along dry fractures. The mineralization is commonly associated with strong K-feldspar alteration. Soil and rock sampling indicate that the molybdenum mineralization is flanked by peripheral zones of tungsten and copper enrichment (Folk, 1979b).

Other Occurrences

KLI (MINFILE 094D 019)

The Kli occurrence, on the slopes southwest of Kliyul Creek near the southern boundary of the map area, consists of small skarn zones along the sheared contact between an ultramafic-mafic plug and the sandstone-carbonate unit of the Takla Group (Noel, 1971b). Mineralization consists of irregular disseminations of chalcopyrite and pyrite within epidote-calcite-garnet-quartz-diopside(?) skarn.

GALENA RIDGE (MINFILE 094D 059)

The Galena Ridge showing comprises a northeast-striking quartz vein, up to 30 centimetres wide, within Takla volcaniclastic rocks about 1 kilometre south-southeast of the confluence of Mariposite and Goldway creeks. The vein was discovered in 1984 during an exploration program by BP Resources Canada Limited in the area between Goldway and Dortatelle creeks. The vein contains 10% pyrite, 5% galena and minor chalcopyrite. A high-grade grab sample from the vein contained 4000 ppb Au and 170.6 ppm Ag (Meyers and Smit, 1985).

JOH 1 (MINFILE 094D 168)

The Joh 1 occurrence is within diorite of the Johanson Lake mafic-ultramafic complex, about 1 kilometre west of Darb Lake. It comprises a limonite and malachite stained quartz vein, about 60 centimetres wide, containing minor blebs of chalcopyrite. A chip sample across this vein returned 3479 ppm Cu and 4200 ppb Au (Leriche and Luckman, 1991a).

JOH 3 (MINFILE 094D 169)

The Joh 3 occurrence, hosted by fractured diorite and microdiorite about 1 kilometre west of Darb Creek, consists of shear zones and quartz veins sparsely mineralized with pyrite and chalcopyrite. The showing is centred on a north-northwest striking vertical shear zone, about 3 metres wide, that contains disseminated pyrite. A one metre chip sample across this zone yielded 5900 ppb Au, 1338 ppm Cu and 1.9 ppm Ag (Leriche and Luckman, 1991b). About 200 metres south of this shear zone is a gently-dipping quartz vein, one to three metres wide, that locally contains minor amounts of pyrite, chalcopyrite and malachite. A 40 centimetre chip sample within a relatively sulphide-rich part of this vein yielded 2508 ppm Cu, 5.4 ppm Ag and 356 ppb Au.

JOH 9 (MINFILE 094D 170)

The Joh 9 occurrence consists of a rusty quartz vein containing disseminated pyrite, collected from a northwest-dipping shear zone along the southern contact of the Darb Creek pluton. A 64 centimetre chip sample across the vein contained 1100 ppb Au (Leriche and Luckman, 1991b, sample KR08).

JOH 11 (MINFILE 094D 171)

The Joh 11 occurrence refers to a grab sample of hornfelsed volcanic rock collected by a claim staker on the Joh 11 claim, a short distance west of Johanson Lake. The sample was submitted for assay and returned 2288 ppm Cu, 8.3 ppm Ag and 1200 ppb Au (Leriche and Luckman, 1991a, sample 14940).

KP0274

Grab sample KP0274 was collected from a northeast trending zone of quartz veins, about 20 centimetres wide, that cuts the Takla volcanic sandstone unit 1.5 kilometres east of Solo Lake. The sample yielded 5500 ppb Au (Gill, 1996).

SUMMARY

The Takla Group within the Kliyul Creek – Johanson Lake area has been subdivided into 2 major divisions. The lower division, represented mainly by the volcanic sandstone unit, comprises massive to well-bedded, commonly feldspar-rich, volcanic sandstones, intercalated with volcanic breccias and local mafic flows. The sandstone-carbonate unit, also included in the lower division, is made up of similar rocks, but with significant amounts of limestone that in large part occurs within slump breccias and as clasts in conglomerate. The upper division, comprising the volcanic breccia unit, consists of massive pyroxene-rich volcanic breccias and pyroxene porphyry flows. This two part subdivision of the Takla Group is similar to the lower and upper divisions that have been applied to the Plughat Mountain succession of the Takla Group to the east and southeast of the map area (Ferri *et al.*, 1992, 1993, 2001a, b).

The Takla Group is cut by numerous plutons that are tentatively subdivided into three suites. The oldest comprises clinopyroxenite, hornblendite, gabbro and diorite of the Abraham Creek and Johanson Lake mafic-ultramafic complexes, as well as several diorite stocks that are similar to the dioritic phases within those complexes. These rocks are suspected to be Late Triassic –Early Jurassic in age They are cut by tonalite and quartz diorite of the Darb Creek and Johanson Creek plutons, which must be younger and are suspected to be Early(?) Jurassic. The Kliyul Creek and Davie Creek granodiorite plutons are the youngest plutonic rocks in the area, and are suspected to be Cretaceous following Woodsworth *et al.* (1991). U-Pb dating in progress will provide some constraints with which to test these assignments.

Northwest-striking sinistral faults are recognized in the southeastern part of the map area and are thought to predated the dextral faults that dominate much of the region's structure. The sinistral faulting may have been coincident with some of the mafic magmatism, and sinistral faults appear to control some of the copper-gold mineralization in the Abraham Creek complex.

Copper and gold mineralization, occurring as veins and disseminations, magnetite-pyrite-chalcopyrite lodes in shear zones, and magnetite-pyrite-chalcopyrite skarns, is widespread within the area. It is in large part spatially associated with the mafic-ultramafic intrusive rocks, and with substantial alteration zones at Mariposite Creek and the head of Kliyul Creek. A number of the occurrences have significant gold values that warrant more investigation. Porphyry molybdenum mineralization associated with the Davie Creek stock is thought to be much younger and probably Cretaceous in age.

ACKNOWLEDGMENTS

I thank Sen-Huy Tan for his capable and enthusiastic assistance during fieldwork. I am also grateful to Carl Edmunds and Chris Rockingham of Northgate Exploration Ltd. for their interest in the area, and for entering into the partnership agreement that provided the funding necessary for fieldwork.

REFERENCES

Armstrong, J.E. (1946): Takla, Cassiar District, British Columbia, *Geological Survey of Canada*, Map 844A.

Armstrong, J.E. (1949): Fort St. James map-area, Cassiar and Coast districts, British Columbia; *Geological Survey of Canada*, Memoir 252, 210 pages.

Bellefontaine, K. (1989): Tectonic evolution of Upper Proterozoic Ingenika Group, north-central British Columbia (94C/12); *in* Geological Fieldwork 1988, *B.C. Ministry of Energy, Mines and Petroleum Resources*, Paper 1989-1, pages 221-226.

Bowen, B.K. (1982): Diamond drilling report on the Kliyul 1 group of claims, Omineca Mining Division, N.T.S. 94C/5W; 94D/8E; *B.C. Ministry of Energy, Mines and Petroleum Resources*, Assessment Report 10 009, 9 pages.

Christopher, P.A. (1986): Geological, geochemical and geophysical report on KC property (KC 1 and KC 2 claims), Omineca Mining Division, Johanson Lake area, British Columbia; *B.C. Ministry of Energy, Mines and Petroleum Resources*, Assessment Report 15583, 11 pages.

Church, B.N. (1974): Geology of the Sustut area; *in* Geology, Exploration and Mining in British Columbia, 1973, *B.C. Department of Mines and Petroleum Resources*, pages 411-416.

Church, B.N. (1975): Geology of the Sustut area; *in* Geology, Exploration and Mining in British Columbia, 1974, *B.C. Department of Mines and Petroleum Resources*, pages 305-309.

Cross, D.B. (1985): Geological, geophysical and geochemical report, KC 1 and 2 claims, Omineca Mining Division, British Columbia, N.T.S. 94D/8E, 9E; *B.C. Ministry of Energy, Mines and Petroleum Resources*, Assessment Report 14416, 18 pages.

Ferri, F. (1997): Nina Creek Group and Lay Range Assemblage, north-central British Columbia: Remnants of late Paleozoic oceanic and arc terranes; *Canadian Journal of Earth Sciences*, Volume 34, pages 854-874.

Ferri, F. (2000a): Devono-Mississippian felsic volcanism along the western edge of the Cassiar Terrane, north-central British Columbia (NTS 93N, 94C and 94D): *in* Geological Fieldwork 1999, *B.C. Ministry of Energy and Mines*, Paper 2000-1, pages 127-146.

Ferri, F. (2000b): Preliminary geology between Lay and Wrede ranges, north-central British Columbia (NTS 94C/12; 94D/9, 16): *B.C. Ministry of Energy and Mines*, Geofile 2000-1, 1:50 000-scale.

Ferri, F. and Melville, D.M. (1994): Bedrock geology of the Germansen Landing - Manson Creek area, British Columbia (94N/9, 10, 15; 94C/2); *B.C. Ministry of Energy, Mines and Petroleum Resources*, Bulletin 91, 147 pages.

Ferri, F., Dudka, S., and Rees, C. (1992): Geology of the Uslika Lake area, northern Quesnel Trough, B.C. (94C/3, 4, 6); *in* Geological Fieldwork 1991, *B.C. Ministry of Energy Mines and Petroleum Resources*, Paper 1992-1, pages 127-145.

Ferri, F., Dudka, S., Rees, C. and Meldrum, D. (1993): Geology of the Aiken Lake and Osilinka River areas, northern Quesnel Trough (94C/2, 3, 5, 6, 12); *in* Geological Fieldwork 1992, *B.C. Ministry of Energy Mines and Petroleum Resources*, Paper 1993-1, pages 109-134.

Ferri, F., Dudka, S., Rees, C., Meldrum, D and Willson, M. (2001a): Geology of the Uslika Lake area, north-central British Columbia (NTS 94C/2, 3, 4); *B.C. Ministry of Energy and Mines*, Geoscience Map 2001-4, 1:50 000-scale.

Ferri, F., Dudka, S., Rees, C. and Meldrum, D. (2001b): Geology of the Aiken Lake area, north-central British Columbia (NTS 94C/5, 6, 12); *B.C. Ministry of Energy and Mines*, Geoscience Map 2001-10, 1:50 000-scale.

Folk, P. (1979a): Diamond drill report, Kliyul claim, #1581 (12), 20 units, Omineca Mining Division, Map 94D/8E, 94C/5W; *B.C. Ministry of Energy, Mines and Petroleum Resources*, Assessment Report 7743, Part 1, 3 pages.

Folk, P. (1979b): Geochemical report, Kliyul claim, #1581 (12), 20 units, Omineca Mining Division, Map 94D/8E, 94C/5W; *B.C. Ministry of Energy, Mines and Petroleum Resources*, Assessment Report 7743, Part 2, 4 pages.

Fox, M. (1982): Geological and geochemical report, KC 1 and 2 mineral claims, N.T.S. 94D/8E and 9E, Omineca Mining Division, British Columbia; *B.C. Ministry of Energy, Mines and Petroleum Resources*, Assessment Report 10346, 14 pages.

Fox, M. (1991): Geological and geochemical exploration report, Jo 1-8 and Cro 1-5 mineral claims, N.T.S. 94D/8E and 9E, Omineca Mining Division, British Columbia; *B.C. Ministry of Energy, Mines and Petroleum Resources*, Assessment Report 21502, 18 pages.

Gabrielse, H. (1985): Major dextral transcurrent displacements along the northern Rocky Mountain Trench and related lineaments in north-central British Columbia; *Geological Society of America Bulletin*, Volume 96, pages 1-14.

Garnett, J.A. (1978): Geology and mineral occurrences of the southern Hogem Batholith; *British Columbia Ministry of Mines and Petroleum Resources*, Bulletin 70, 67 pages.

Gill, D.G. (1993): Drilling assessment report on the Kliyul property, N.T.S. 94D/8, 9; *B.C. Ministry of Energy, Mines and Petroleum Resources*, Assessment Report 23033, 12 pages.

Gill, D.G. (1994): Geological and geochemical assessment report on the Joh property, N.T.S. mapsheet 94D/9; *B.C. Ministry of Energy, Mines and Petroleum Resources*, Assessment Report 23543, 15 pages.

Gill, D.G. (1995): Geological assessment report on the Joh 3 group of claims, N.T.S. mapsheet 94D/9; *B.C. Ministry of Energy, Mines and Petroleum Resources*, Assessment Report 23842, 16 pages.

Gill, D.G. (1996): Drilling report on the Mariposite property, N.T.S. 94D/8, 9; *B.C. Ministry of Energy, Mines and Petroleum Resources*, Assessment Report 24778, 23 pages.

Hammack, J.L., Nixon, G.T., Wong, R.H. and Paterson, W.P.E. (1990): Geology and noble metal geochemistry of the Wrede Creek Ultramafic Complex, north-central British Columbia (94D/9); *in* Geological Fieldwork 1989, *B.C. Ministry of Energy, Mines and Petroleum Resources*, Paper 1990-1, pages 405-415.

Irvine, T.N. (1974): Ultramafic and gabbroic rocks in the Aiken Lake and McConnell Creek map-areas, British Columbia; *in* Report of Activities, Part A, *Geological Survey of Canada*, Paper 74-1A, pages 149-152.

Irvine, T.N. (1976): Studies of cordilleran gabbroic and ultramafic intrusions, British Columbia; *in* Report of Activities, Part A, *Geological Survey of Canada*, Paper 76-1A, pages 75-81.

Lay, D. (1940): Aiken Lake area, north-central British Columbia; *B.C. Department of Mines*, Bulletin No. 1, 32 pages.

Leriche, P.D. and Harrington, E. (1996): Diamond drilling report on the Joh property, Johanson Lake area, Omineca Mining Division, British Columbia; *B.C. Ministry of Energy, Mines and Petroleum Resources*, Assessment Report 25099, 22 pages.

Leriche, P., D. and Luckman, N. (1991a): Geological and geochemical report on the Joh property, Johanson Lake area, Omineca Mining District, British Columbia: *B.C. Ministry of Energy, Mines and Petroleum Resources*, Assessment Report 21781, 22 pages.

Leriche, P., D. and Luckman, N. (1991b): Geological and geochemical report on the Darb property, Johanson Lake area, Omineca Mining District, British Columbia; *B.C. Ministry of Energy, Mines and Petroleum Resources*, Assessment Report 21782, 23 pages.

Legun, A. (1998): Toodoggone-McConnell Project: Geology of the McConnell Range, Jensen Creek to Johanson Creek (parts of NTS 94D/9, 10, 15, 16); *in* Geological Fieldwork 1997, B.C. Ministry of Employment and Investment, pages 8b-1 - 8b-10.

Legun, A. (2001a): Geology of the area between the Sustut copper deposit and the Day porphyry copper prospect; in Geological Fieldwork 2000), *B.C. Ministry of Energy and Mines*, Paper 2001-1, pages 75-82.

Legun, A. (2001b): Geology of the southern McConnell Range and Sustut River areas, British Columbia (parts of NTS 94D/3, 7, 9, 10, 15, 16); *B.C. Ministry of Energy and Mines*, Open File Map 2001-18, 1:50 000-scale.

Lord, C.S. (1948): McConnell Creek map-area, Cassiar District, British Columbia; *Geological Survey of Canada*, Memoir 251, 72 pages.

McTaggart, K.C. (1965): Geology of the Soup Mineral claims, Omineca Mining Division; *B.C. Department of Mines and Petroleum Resources*, Assessment Report 675, 10 pages.

Minehan, K. (1989a): Takla Group volcano-sedimentary rocks, north-central British Columbia: a summary of fieldwork (94D/9); *in* Geological Fieldwork 1988, *B.C. Ministry of Energy, Mines and Petroleum Resources*, Paper 1989-1, pages 227-232.

Minehan, K. (1989b): Paleotectonic setting of Takla Group volcano-sedimentary rocks, Quesnellia, north-central British Columbia: unpublished M.Sc. thesis, *McGill University*, 102 pages.

Monger, J.W.H. (1974): The Takla Group near Dewar Peak, McConnell Creek map-area (94D) British Columbia; *in* Report of Activities, Part B, *Geological Survey of Canada*, Paper 74-1B, pages 29-30.

Monger, J.W.H. (1976): Lower Mesozoic rocks in McConnell Creek map-area (94D) British Columbia; *in* Report of Activities, Part A, *Geological Survey of Canada*, Paper 76-1A, pages 51-55.

Monger, J.W.H. (1977): The Triassic Takla Group in McConnell Creek map-area, north-central British Columbia; *Geological Survey of Canada*, Paper 76-29, 45 pages.

Monger, J.W.H. and Church, B.N. (1977): Revised stratigraphy of the Takla Group, north-central British Columbia; *Canadian Journal of Earth Sciences*, Volume 14, pages 318-326.

Monger, J.W.H. and Paterson, I.A. (1974): Upper Paleozoic and Lower Mesozoic rocks of the Omineca Mountains; *in* Report of Activities, Part A, *Geological Survey of Canada*, Paper 74-1A, pages 19-20.

Monger, J.W.H., Richards, T.A. and Paterson, I.A. (1978): The Hinterland Belt of the Canadian Cordillera: New data from northern and central British Columbia; *Canadian Journal of Earth Sciences*, Volume 15, pages 823-830.

Meyers, R.E. and Smit, H.Q. (1985): 1984 assessment report of the geological and geochemical exploration program on the Goldway 1-8 claims, Omineca Mining Division, NTS 94D/8, 9; *B.C. Ministry of Energy, Mines and Petroleum Resources*, Assessment Report 13697, 83 pages.

Nelson, J.L. and Bellefontaine, K.A. (1996): The geology and mineral deposits of north-central Quesnellia; Tezzeron Lake to Discovery Creek, central British Columbia; *B.C. Ministry of Energy, Mines and Petroleum Resources*, Bulletin 99, 112 pages.

Nelson, J., Carmichael, B. and Gray, M. (2003): Innovative gold targets in the Pinchi Fault/Hogem Batholith area: The Hawk and Axelgold properties, central British Columbia (94C/4, 94N/13): *in* Geological Fieldwork 2002, *B.C. Ministry of Energy and Mines*, Paper 2003-1, pages 97-113.

Nixon, G.T. and Rublee, V.J. (1988): Alaskan-type ultramafic rocks in British Columbia: New concepts of the structure of the Tulameen Complex; *in* Geological Fieldwork 1987, *B.C. Ministry of Energy, Mines and Petroleum Resources*, Paper 1988-1, pages 281-294.

Nixon, G.T., Hammack, J.L., Connelly, J.N., Case, G. and Paterson, W.P.E. (1990a): Geology and noble metal geochemistry of the Polaris Ultramafic Complex, north-central British Columbia (94C/5, 12); *in* Geological Fieldwork 1989, *B.C. Ministry of Energy, Mines and Petroleum Resources*, Paper 1990-1, pages 387-404.

Nixon, G.T., Hammack, J.L. and Paterson, W.P.E. (1990b): Geology and noble metal geochemistry of the Johanson Lake Mafic-Ultramafic Complex, north-central British Columbia (94D/9); *in* Geological Fieldwork 1989, *B.C. Ministry of Energy, Mines and Petroleum Resources*, Paper 1990-1, pages 417-424.

Nixon, G.T., Hammack, J.L., Ash, C.H., Cabri, L.J., Case, G., Connelly, J.N., Heaman, L.M., Laflamme, J.H. G., Nuttall, C. Paterson, W.P.E. and Wong, R.H. (1997): Geology and platinum-group-element mineralization of Alaskan-type ultramafic-mafic complexes in British Columbia; *B.C. Ministry of Employment and Investment*, Bulletin 93, 141 pages.

Noel, G.A. (1971a): Geological - geochemical report on the Croy mineral claims, Aiken Lake area; *B.C. Department of Mines and Petroleum Resources*, Assessment Report 2862, 10 pages.

Noel, G.A. (1971b): Geological - geophysical - geochemical report on the Kli mineral claims, Kliyul Creek area; *B.C. Department of Mines and Petroleum Resources*, Assessment Report 3264, 30 pages.

Norman, G.E. (1982): Diamond drilling report on the Kliyul 1 group of claims, Omineca Mining Division, N.T.S. 94C/5W; 94D/8E; *B.C. Ministry of Energy, Mines and Petroleum Resources*, Assessment Report 10730, 8 pages.

Pawliuk, D.J. (1985): Report on assessment work on the Goldway Peak property, Omineca Mining Division, Johanson Lake, British Columbia; *B.C. Ministry of Energy, Mines and Petroleum Resources*, Assessment Report 14105, 17 pages.

Phendler, R.W. (1984): Report on assessment work (sampling and assaying) on Vi 1 and Vi 2 (Record Nos. 1948 and 1949), Johanson Lake area, Omineca Mining Division, British Columbia; *B.C. Ministry of Energy, Mines and Petroleum Resources*, Assessment Report 13175, 9 pages.

Richards, T.A. (1976a): Takla Project (Reports 10-16): McConnell Creek map-area (94D, east half), British Columbia; *in* Report of Activities, Part A, *Geological Survey of Canada*, Paper 76-1A, pages 43-50.

Richards, T.A. (1976b): Geology, McConnell Creek map-area (94D/E); *Geological Survey of Canada*, Open File 342, 1:250 000-scale.

Richards, T.A. (1991): Geologic setting and sampling of vein systems, Solo Group of mineral claims, Omineca Mining Division, 94D/9; *B.C. Ministry of Energy, Mines and Petroleum Resources*, Assessment Report 21394, 39 pages.

Ricketts, B.D., Evenchick, C.A., Anderson, R.G. and Murphy, D.C. (1992): Bowser basin, northern British Columbia: Constraints on the timing of initial subsidence and Stikinia-North America terrane interactions; *Geology*, Vol. 20, p. 1119-1122.

Roots, E.F. (1954): Geology and mineral deposits of Aiken Lake map-area, British Columbia; *Geological Survey of Canada*, Memoir 274, 246 pages.

Smit, H.Q. and Meyers, R.E. (1984): Assessment report on the 1984 geological and geochemical exploration program on the Soup 8-84 claim group, Omineca Mining Division, NTS 94D/8; *B.C. Ministry of Energy, Mines and Petroleum Resources*, Assessment Report 13315, 30 pages.

Stevens, R.D., Delabio, R.N. and Lachance, G.R. (1982): Age determinations and geological studies, K-Ar isotopic ages, Report 15; Geological Survey of Canada, Paper 81-2, 56 pages.

Struik, L.C. (1988): Crustal evolution of the eastern Canadian Cordillera; *Tectonics*, Volume 7, pages 727-747.

Struik, L.C., Schiarizza, P., Orchard, M.J., Cordey, F., Sano, H., MacIntyre, D.G., Lapierre, H. and Tardy, M. (2001): Imbricate architecture of the upper Paleozoic to Jurassic oceanic Cache Creek Terrane, central British Columbia; *Canadian Journal of Earth Sciences*, Volume 38, pages 495-514.

Tchalenko, J.S. (1970): Similarities between shear zones of different magnitudes; *Geological Society of America*, Bulletin, Volume 81, pages 1625-1640.

Tipper, H.W. and Richards, T.A. (1976): Jurassic stratigraphy and history of north-central British Columbia; *Geological Survey of Canada*, Bulletin 270, 73 pages.

Travers, W.B. (1978): Overturned Nicola and Ashcroft strata and their relations to the Cache Creek Group, southwestern Intermontane Belt, British Columbia; *Canadian Journal of Earth Sciences*, Volume 15, pages 99-116.

von Rosen, G. (1986): Assessment geological report on mapping, sampling and bulk sampling program on the Good (4155) - Prospects (4147) - Much (4149) - Pro (4150) - Fit (4151) - Dar (4154) mineral claims (Gold group), Goldway Peak - Johanson Lake area, Omineca Mining Division; *B.C. Ministry of Energy, Mines and Petroleum Resources*, Assessment Report 15313, 35 pages.

Wanless, R.K., Stevens, R.D., Lachance, G.R. and Delabio, R.N. (1972): Age determinations and geological studies, K-Ar isotopic ages, Report 10; Geological Survey of Canada, Paper 71-2, 96 pages.

Wanless, R.K., Stevens, R.D., Lachance, G.R. and Delabio, R.N. (1979): Age determinations and geological studies, K-Ar isotopic ages, Report 14; Geological Survey of Canada, Paper 79-2, 67 pages.

White, W.H. (1948): Sustut-Aiken-McConnell Lake area; *in* Annual Report of the Minister of Mines for 1947, *B.C. Department of Mines*, pages A100-A111.

Williams, J.D. (1997): Report on drilling in 1997 on the Soup gold-copper property; *B.C. Ministry of Employment and Investment*, Assessment Report 25185, 25 pages.

Wilson, G.L. (1984): Geological, geochemical and geophysical report, KC 1 and 2 mineral claims, N.T.S. 94D/8E and 9E, Omineca Mining Division, British Columbia; *B.C. Ministry of Energy, Mines and Petroleum Resources*, Assessment Report 13580, 17 pages.

Woodsworth, G.J. (1976): Plutonic rocks of McConnell Creek (94D west half) and Aiken Lake (94C east half) map-areas, British Columbia; *in* Report of Activities, Part A, *Geological Survey of Canada*, Paper 76-1A, pages 69-73.

Woodsworth, G.J., Anderson, R.G. and Armstrong, R.L. (1991): Plutonic regimes, Chapter 15, *in* Geology of the Cordilleran Orogen in Canada, H. Gabrielse and C.J. Yorath, eds., *Geological Survey of Canada*, Geology of Canada, no. 4, pages 491-531; also *Geological Society of America*, The Geology of North America, v.G-2.

Zhang, G. (1994): Strike-slip faulting and block rotations in the McConnell Creek area, north-central British Columbia: structural implications for the interpretation of paleomagnetic observations; unpublished Ph.D. thesis, *McGill University*, 238 pages.

Zhang, G. and Hynes, A. (1991): Structure of the Takla Group east of the Finlay-Ingenika Fault, McConnell Creek area, north-central B.C. (94D/8, 9); *in* Geological Fieldwork 1990, *B.C. Ministry of Energy, Mines and Petroleum Resources*, Paper 1991-1, pages 121-129.

Zhang, G. and Hynes, A. (1992): Structures along Finlay-Ingenika Fault, McConnell Creek area, north-central British Columbia (94C/5; 94D/8, 9); *in* Geological Fieldwork 1991, *B.C. Ministry of Energy, Mines and Petroleum Resources*, Paper 1992-1, pages 147-154.

Zhang, G. and Hynes, A. (1994): Fabrics and kinematic indicators associated with the local structures along Finlay-Ingenika Fault, McConnell Creek area, north-central British Columbia; *Canadian Journal of Earth Sciences*, Volume 31, pages 1687-1699.

Zhang, G. and Hynes, A. (1995): Determination of position-gradient tensor from strain measurements and its implications for the displacement across a shear zone; *Journal of Structural Geology*, Volume 17, pages 1587-1599.

Zhang, G., Hynes, A. and Irving, E. (1996): Block rotations along the strike-slip Finlay-Ingenika Fault, north-central British Columbia: Implications for paleomagnetic and tectonic studies; *Tectonics*, Volume 15, pages 272-287.

DIGITAL COMPILATION OF ISOTOPIC AGES FOR BRITISH COLUMBIA: BCAGE 2003 RELEASED AS MS-ACCESS OPEN-FILE CD

By Katrin Breitsprecher and James K. Mortensen, University of British Columbia

KEYWORDS: Ar-Ar, database, geochronology, fission-track, isotopic age, K-Ar, Rb-Sr, Re-Os, Sm-Nd, U-Pb, (U-Th)-He

INTRODUCTION

Isotopic age determinations form a critical part of the geoscientific knowledge base for British Columbia. Isotopic ages were first reported for rock units in British Columbia in 1960, with the advent of the potassium-argon (K-Ar) method of dating. Subsequent decades witnessed the widespread application of additional dating methods, such as the Rb-Sr method in the mid-1970's, the U-Pb and fission-track methods in the mid-1980's, and the ^{40}Ar/^{39}Ar and Nd-Sm methods in the late 1990's. More recently, age determinations utilizing the Lu-Hf, Re-Os or (U-Th)-He systems are increasingly being reported as these dating methods are refined. Isotopic dating has been widely used in British Columbia for more than four decades, and the number of isotopic ages which have been generated from rock units within British Columbia is very large. However, because all of the data was never collated into a single database, accessing and utilizing these age determinations for geologic study has been difficult. Firstly, while it is generally known that some older age determinations are not reliable due to either revision to applicable decay constants, outdated systematics and/or analytical techniques, most users do not have the technical background required to evaluate the reliability of a reported age. Secondly, not all reported dates are properly indexed or keyworded such that they can be found by an indexing engine such as GeoRef. Finally, a great many isotopic ages are reported in "grey literature" such as unpublished theses, which are difficult and in some cases expensive to obtain, and are commonly only available in a cumbersome format such as microfiche. Theses are also usually not consistently indexed on any search engine, and contained age data must be laboriously extracted by searching each university's individual library catalogue.

BCAge 2003 was released in December of 2003, as a Micosoft-Access–based database which includes all currently available isotopic age determinations for rock units within British Columbia. The database contains almost 7,000 ages from over 4,750 different rock units in British Columbia, reported in more than 600 individual sources. The database is available as a BC Geological Survey Branch Open File in CD format. We have chosen to provide the database in Microsoft Access format because this is a very widely available and reasonably user-friendly software package, that loads easily even on lower-end personal computers. BCAge 2003 compliments its northern counterpart, YukonAge 2002, which was released in 2002. In addition to providing the public with a single queriable source for geochronologic data, BCAge provides several unique additional features which enhance the utility of the data. Firstly, a *'reliability rating'* has been assigned to each age determination in the compilation. This feature allows a user to quickly evaluate which ages returned by a query would be considered to be reliable by present-day geochronologic standards. Secondly, wherever possible, older ages have been recalculated to current (IUGS) decay constants. Many older dates, particularly in the K-Ar system, were considered unreliable because they had been calculated with since-revised (obsolete) decay constants. Thirdly, many earlier K-Ar ages were reported with 1-sigma errors; these have been standardized in the data-base to the current standard of reporting errors for age determinations at the 2-sigma level; thus reported ages and errors are comparable throughout the entire data set. Finally, a number of previously unpublished isotopic ages generated at the University of British Columbia Geochron Lab during the 1970's and 1980's have been included in BCAge.

SYSTEM REQUIREMENTS

The database is designed for use on newer PC (Windows-based) systems, using Microsoft Access 2000 or above. The database has been rigorously tested on Windows 2000, ME and XP. The product is expected to work on Mac systems running MS-Access 2000 or above, although this has not yet been tested. The database is *not* a stand-alone module; Microsoft Access must be installed before the data-base can be opened. BCAge should run on any PC which runs Microsoft Access 2000 or better; however, because of the large size of the database (over 30 Meg), it runs slowly on PII, and poorly (inoperably slowly) on Pentium-I systems.

INCLUSION CRITERIA

Post-1987 reports containing isotopic ages were identified using a 'ground-up' approach. Georef was queried for *absolute-age, geochronology, dating, Ar-Ar,* *K-Ar, Rb-Sr, U-Pb, Sm-Nd,* and *fission-track.* Each returned source was checked to see whether it reported age determinations. All BCGS Fieldwork and GSC Current Research articles, which are not fully indexed, were checked visually for isotopic age content. GSC Paper-2 series on radiogenic ages "Silverbook reports" and GSC "Summary of K-Ar and Ar-Ar Age Determination" reports were similarly checked for data pertaining to the British Columbian jurisdiction. An exhaustive thesis search was conducted, beginning with those generated at UBC, then searching library catalogues of each Canadian university with a geology department, and finally searching U.S. universities with in-house geochron facilities, or those known to have faculty involved in Cordilleran studies. All hard-rock theses were obtained for verification of geochronological content. Soft-rock studies were only obtained if it was apparent from the title or other indicators that the study included detrital mineral dating.

Some levels of reporting are considered too preliminary for inclusion in the BCAge compilation. These include: ages cited as "personal communication"; ages in abstracts which are not accompanied by either analytical data (or visual representation of data), or adequate sample information (including location); ages which are reported as a point locations on a map without supporting data or written documentation (e.g. preliminary dates plotted on open-file maps).

CONTENT

BCAge contains nearly 7,000 geo-referenced age determinations. The dataset incorporates an older data compilation (the R.L. Armstrong age database at UBC), which included ages reported to about 1987, and all ages subsequently published, including those indexed by Georef up to June 2003. Also, the database contains a number of age determinations from older theses from universities in eastern Canada and the United States, which were not in the original Armstrong database. In some cases, more than one age is available for a sample. In the case of clastic rocks for which ages of detrital minerals are reported, each grain analyzed represents a unique age determination. Over 4,750 different samples are represented by the age determinations in BCAge 2003. In the interest of maintaining a high level of data utility and flexibility, neither the BCAge interface nor the data has been encrypted.

The data-base consists of 3 linked tables: 1) a rock table, which contains one record for each sample dated; 2) an age table, containing one record for each age determination reported; and 3) a sources table, containing one record for each report containing ages. The relational nature of the database ensures that multiple age determinations from a single sample (e.g. either as replicate analysis, as ages determined using different isotopic systems, or as multiple, multi-sourced grains in a clastic sedimentary rock), are linked to that single sample, and display as such to the user. Furthermore, this structure allows for ages from a single sample which appeared in different reports (e.g. Ar-Ar ages in one publication and U-Pb ages in another) to appear simultaneously to the user, because they are linked to a single record in the "rock" table.

Data compiled in BCAge remains the ownership of the authors who produced or reported that information. All ages returned by BCAge queries are linked to a complete listing of the original source of the data and should be cited to that original report. Users who wish to cite the results of a query, however, such as "Previously reported ages for Unit X range from 85 to 115 Ma", or who wish to cite the relative reliability of individual ages, should cite the BCAge compilation as the source of that information.

Accuracy of the data returned by BCAge should be verified by the user from the original source(s). BCAge is intended as a search engine to locate reports containing original isotopic age data; the level of funding for the project did not allow for double-checking of data after input. Further, in many cases, accuracy is limited by the quality of the original reports. Of particular note is significant errors in sample locations in some original reports, which have been noted during the process of data entry. Problems include locations drawn on sketch maps with erroneous coordinates, UTM coordinates reported one digit short of a proper coordinate, and loosely constrained sample locations (the latter is particularly true for older reports, which commonly constrain locations only to the nearest 5 minutes). Where noted and where possible, such errors in original reporting have been corrected during compilation. As GIS-based mapping is becoming the new norm, even a small amount of rounding in the reported coordinates can place a sample in the wrong polygon for its lithologic type. The Geological Survey of Canada has provided extra funding on this project to conduct a comprehensive verification of data coordinates to the latest GIS map products for the 82L and 82K mapsheets in southern British Columbia. A field exists in the 'rocks' table called "checked to GIS" which, if empty (presently, all records except those on the 2 mapsheets noted above), indicates to the user that the location has not been verified to a current map. It is hoped that as new mapping projects proceed, similar verification of this data will be undertaken as part of the mapping function.

USAGE NOTES

Data may be queried using the interface provided on the basis of AGE (query the 'ages' table), LOCATION (query the 'rock' table) or SOURCE (query the 'refs' table). Each of these queries will return records meeting input criteria which the user is prompted for, in addition to linking essential information to that record from each of the other two tables. Hotlinked buttons will take the user to additional details on rock/source. Using the "search by age" function permits the user to easily export the query results in the form of an Excel (or other format) table, which can then be modified as desired by the user for insertion into a report. Alternatively, because each age is geo-referenced, the user may wish to link the exported Excel table to a spatial format (GIS) so that records are plotted graphically. Secondary filters may be applied to returned criteria. For example, a user may start by asking for all records between 85 and 115 Ma in age. This will return all records from throughout B.C. in this age range. The user may wish to see only those records occurring on a particular mapsheet: right-click on the "mapsheet" field of the records dialogue box, enter your mapsheet ID (e.g. 104B) in the "filter for" field, hit "enter" and all other records will be screened out. These types of filters may be applied to any field visible on the age-records dialogue box, and may be made repetitively, such that the query is continually refined in a series of steps (i.e. filter by lithology, then reliability rating, dating method etc.). Note that filtering is not 100% Boolean; wild-carding (*) is necessary the user wishes to short-cut the filter criteria.

Querying "by location" returns all rocks (samples) that meet the search criteria, with age(s) tied to each sample in a cascading screen. This function permits the user to easily identify cases in which more than one age has been determined from the same sample (e.g., using different isotopic methods). This is particularly useful for those many cases where such determinations are published in different reports, as is often the case due to variability in turn-around time at different labs, and for different systems of dating. Additional usage notes are provided as "read me" files on the CD.

PLANNED UPDATES

It is anticipated that BCAge will be updated on an annual basis to reflect new ages reported during the previous year.

FUTURE APPLICATIONS

In addition to regular updates of BCAge in its present format, at least 3 other applications/enhancements are planned at the time of writing. The first is the pending integration of BCAge data with MapPlace. This will permit MapPlace users to see the BCAge data plotted graphically with respect to geology, geochemistry and any other MapPlace dataset. The second application will be to integrate reliable age determinations into the North America Data Model (NADM); this is being done under the direction of M.E. Villeneuve at the Geological Survey of Canada. NADM is an Oracle-based engine which is envisioned to hold data pertaining to all aspects of geology for the entire North American continent. This project, which was initiated by the US Geological Survey and is now being carried out in conjunction with the Geological Survey of Canada, will ultimately incorporate isotopic age data from throughout the US and Canada. The Geological Survey of Canada will import portions of BCAge data which are relevant to the NADM project (e.g. exclude unreliable ages) in its own open-file for the purpose of facilitating internal data management for that project. The interested reader should note that BCAge is the product intended for use by scientists conducting local or regional Cordilleran studies, whereas the pending GSC version open-file is intended to facilitate data management, modeling and geologic study at a much larger (national to continental) scale.

The third planned application of the dataset is to create a cross-jurisdictional database. YukonAge 2002 contains approximately 1,500 ages from the Yukon Territory and is in the same format at BCAge. In addition, the US Geological Survey (Anchorage) hopes to release a geochronological compilation for Alaska at some point in the future (P. Haeussler and D.W. Bradley, personal communication, 2003). In the case of the Canadian Cordilleran (B.C. and Yukon) jurisdictions, the database products were designed at the outset for easy integration in the future. The viability of fusing with the Alaskan database is presently uncertain from a logistical perspective; there is general agreement however from all involved jurisdictions that a complete isotopic age compilation for the entire northern Cordilleran would be very desirable. Preparation of a Canadian Cordillera product (fusion of YukonAge and BCAge) will proceed imminently, and is expected to be released sometime in 2004. This product will contain updates for 2004 (newly reported ages) for both jurisdictions. Some interface improvements are also planned, including a "search by terrane" function. Finally, the authors are considering, at a conceptual level, the possibility of generating a 4D graphical product from the data as a spin-off product of the database.

ACKNOWLEDGMENTS

Financial support for the preparation of BCAge 2003 was provided jointly by the BC Geological Survey Branch and the Geological Survey of Canada, and in part by a Natural Sciences and Engineering Research Council grant to JKM. Logistical support for the project is provided by the Pacific Centre for Isotopic and Geochemical Research at the University of British Columbia. BCAge 2003 utilizes an earlier hard copy age database that was compiled by R.L. Armstrong and associates, and digitized by A. Bentzen in the late 1980's with funding from the BC Geological Survey Branch. Mike Villeneuve at the Geological Survey of Canada is thanked for his early input concerning the database design. Finally we thank Brian Grant from the BC Geological Survey Branch, Grant Abbott from the Yukon Geological Survey and Bob

Thompson from the Geological Survey of Canada for their on-going support for the project.

PRELIMINARY LITHOGEOCHEMISTRY AND POLYMETALLIC VHMS MINERALIZATION IN EARLY DEVONIAN AND(?) EARLY CARBONIFEROUS VOLCANIC ROCKS, FOREMORE PROPERTY

By James Logan

KEYWORDS: gold-enriched, polymetallic VHMS, Devono-Mississippian, Kuroko, Stikine assemblage, U-Pb dates, NWBC

INTRODUCTION

The recent discovery on the Foremore property of new VHMS mineralization that contains significant precious metal values has caused resurgence in the exploration interests of Paleozoic volcanic rocks in northern British Columbia. VHMS deposits are well documented in Devonian and Early Carboniferous volcanic sequences at the Kudz Ze Kayah and Wolverine deposits in the southern Yukon (Yukon-Tanana terrane) and at the Tulsequah Chief deposit in northern British Columbia (Stikine terrane). Devono-Mississippian rocks of the Stikine terrane also host polymetallic mineralization at the Foremore property (Fig. 1).

The Foremore project is a private-public partnership developed between the Ministry of Energy and Mines and Roca Mines Inc. The main objectives of the project are: to isolate the felsic magmatic and carbonaceous sedimentary interval(s) that are associated with the massive sulphide mineralization and identify their ages and positions within the volcanic stratigraphic on the property, establish the chemical affinity of the felsic units (extrusive and/or subvolcanic) to evaluate their prospectivity, and test the hypothesis that the different styles of mineralization (syngenetic, massive/laminated and epigenetic, carbonate replacement) represented by float boulders in the north, south and eastern parts of the property are genetically linked through a single mineralizing event or represent multiple events and finally to establish a tectonic and metallogenic model that can direct VHMS exploration to prospective strata within the remnant Paleozoic volcano-plutonic belt of rocks.

REGIONAL GEOLOGICAL SETTING

The study area straddles the boundary between the Intermontane Belt and the Coast Belt and is underlain mainly by rocks of the Stikine Terrane (Stikinia), the westernmost terrane of the Intermontane Superterrane (Fig. 1). Like other terranes of the North American Cordillera, its pre-Jurassic geological history, paleontological and paleomagnetic signatures are unique. They have been interpreted to indicate that the Stikine Terrane originated far removed from the margin of ancestral North America (Gabrielse and Yorath, 1991) and was amalgamated with the Cache Creek, Quesnel and Slide Mountain terranes prior to accretion to the North American craton (Fig. 1).

Recent studies suggest that the Stikine terrane developed adjacent to the ancestral margin of North America (McClelland, 1992; Mihalynuk et al., 1994; Gunning 1996) and that parts of the Paleozoic Stikine assemblage are correlative with and depositionally tied to Paleozoic rocks of the Yukon-Tanana Terrane. Depositional ties between the Quesnel and Yukon-Tanana terranes are also known and this together with the hook-like geometry of the 0.706 initial 87Sr/86Sr line around the northern end of Stikinia (Fig. 1) led Nelson and Mihalynuk (1993) and Mihalynuk et al. (1994) to propose a single arc model consisting of the Quesnel, Yukon Tanana, Nisling and Stikine terranes.

The distribution of Devono-Mississippian VHMS camps for British Columbia, Yukon and parts of Alaska (Fig. 1) define a similar hook-like geometry that closely follows the contact between the ancient Pacific margin terranes (Kootenay-Yukon-Tanana-Nisling) or their displaced equivalents, and the allochthonous (?) island-arc terranes (Quesnellia-Stikinia). Deposits and occurrences include Homestake, Samatosum (Eagle Bay), Kudz Ze Kayah and Wolverine (Finlayson Lake district), Bonnington and Delta districts (Alaska), Tulsequah Chief and Big Bull, Foremore and Ecstall. Deposits of Wrangellia-Alexander terranes (*i.e.* Myra Falls) are not shown. The Devono-Mississippian deposits have characteristics of the Kuroko/Noranda subclass of volcanic-hosted massive sulphide deposits (VHMS) that typically form within, or behind oceanic- or continental margin-arc settings undergoing rifting or local extension (Sawkins, 1990; Hoy, 1991; Lentz, 1998). The Kuroko/Noranda or polymetallic VHMS subclass are major producers of Cu, Zn, Ag, Au and Pb in Canada and worldwide and constitute important exploration targets in Devono-Mississippian volcanic rocks of northern British Columbia.

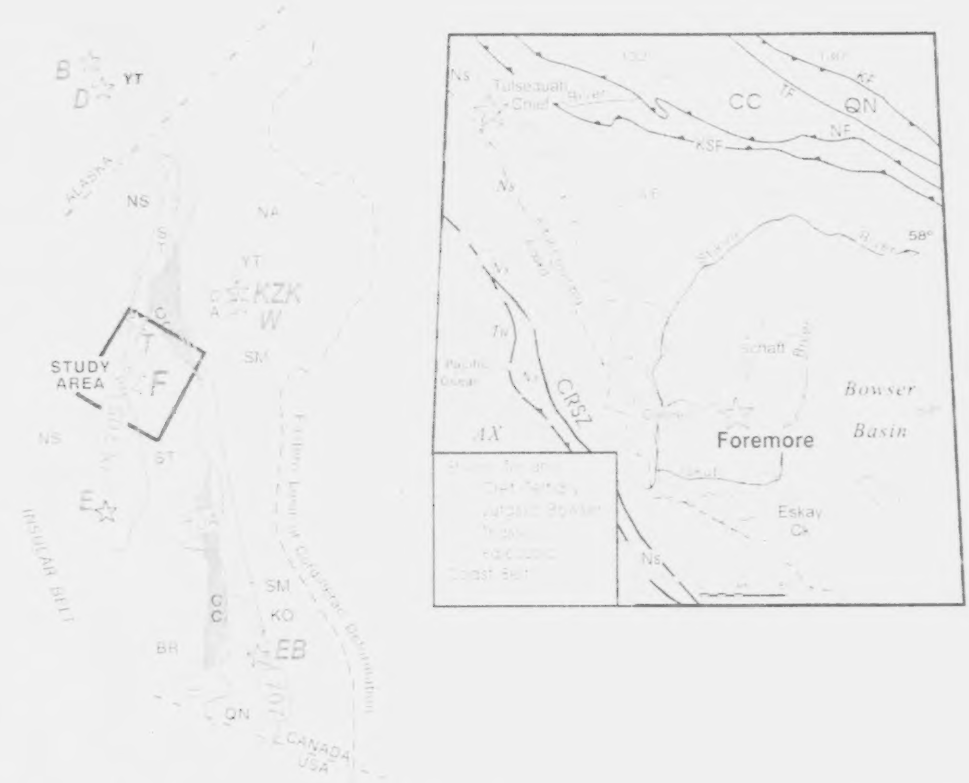

Figure 1. (a) Terrane map showing tectonostratigraphic setting of the study area and the location of Devono-Mississippian VHMS deposits. EB=Eagle Bay deposits. W=Wolverine. KZK=Kudz Ze Kayah. B=Bonnington district. D=Delta district. T=Tulsequah. F=Foremore. E=Ecstall. Mesozoic initial strontium isopleths from Armstrong (1988). NA=Ancestral North America. CA=Cassiar. NS=Nisling. KO=Kootenay. SM=Slide Mountain. QN=Quesnellia. CC=Cache Creek. ST=Stikinia. BR=Bridge River. YT=Yukon Tanana (modified from Wheeler and McFeely, 1991). (b) Inset shows location of study area relative to the major tectonostratigraphic features of the northwestern Cordillera, regional distribution of Paleozoic, Triassic, Jurassic and Cretaceous-Tertiary rocks of Stikinia and regionally significant mineral occurrences. AX=Alexander Terrane. TU=Taku Terrane. Ns=Nisling Terrane. CRSZ=Coast Range Shear Zone. KSF=King Salmon Fault. NF=Nahlin Fault. TF=Thibert Fault. KF=Klinkit Fault.

The stratigraphic and plutonic framework of northwestern Stikinia is summarized by Anderson (1993), Gunning (1996) and Logan (2000). It consists of a Paleozoic to Mesozoic sedimentary and volcano-plutonic arc assemblage that includes: the Devonian to Permian Stikine assemblage, the Late Triassic Stuhini Group and the Early Jurassic Hazelton Group. These are overlain by Middle Jurassic to early Tertiary successor-basin sediments of the Bowser Lake and Sustut Groups, Late Cretaceous to Tertiary continental volcanic rocks of the Sloko Group, and Late Tertiary to Recent bimodal shield volcanism of the Edziza and Spectrum ranges.

PALEOZOIC STIKINE ASSEMBLAGE

Rocks of the Stikine assemblage are the structurally and stratigraphically lowest supracrustal rocks observed in the study area. Stikine assemblage rocks were informally named by Monger (1977) to include all upper Paleozoic rocks (within Stikinia) that cropped out around the periphery of the Bowser Basin. The assemblage consists of Permian, Upper Carboniferous, Lower Carboniferous and Devonian age strata and plutons. The dominant lithologies are calcalkaline, mafic and bimodal flows and volcaniclastics, interbedded carbonate, minor shale and chert. The Permian carbonates and volcanics are a distinctive part of the Stikine assemblage, traceable for over 500 kilometres from the Taku River to south of Terrace, but the Devonian and Carboniferous volcanic rocks have the highest potential to host polymetallic VHMS deposits (Fig. 1).

The Late Paleozoic history of Stikinia comprises three volcanic cycles: Early Devonian, Early Carboniferous and Late Carboniferous separated by three intervening sedimentary cycles (Logan and Koyanagi, 1994; Gunning, 1996). A composite stratigraphic section of the Stikine assemblage is presented which includes five main subdivisions (Fig. 2). From the oldest to the youngest, they are: (1) an Early to Middle Devonian

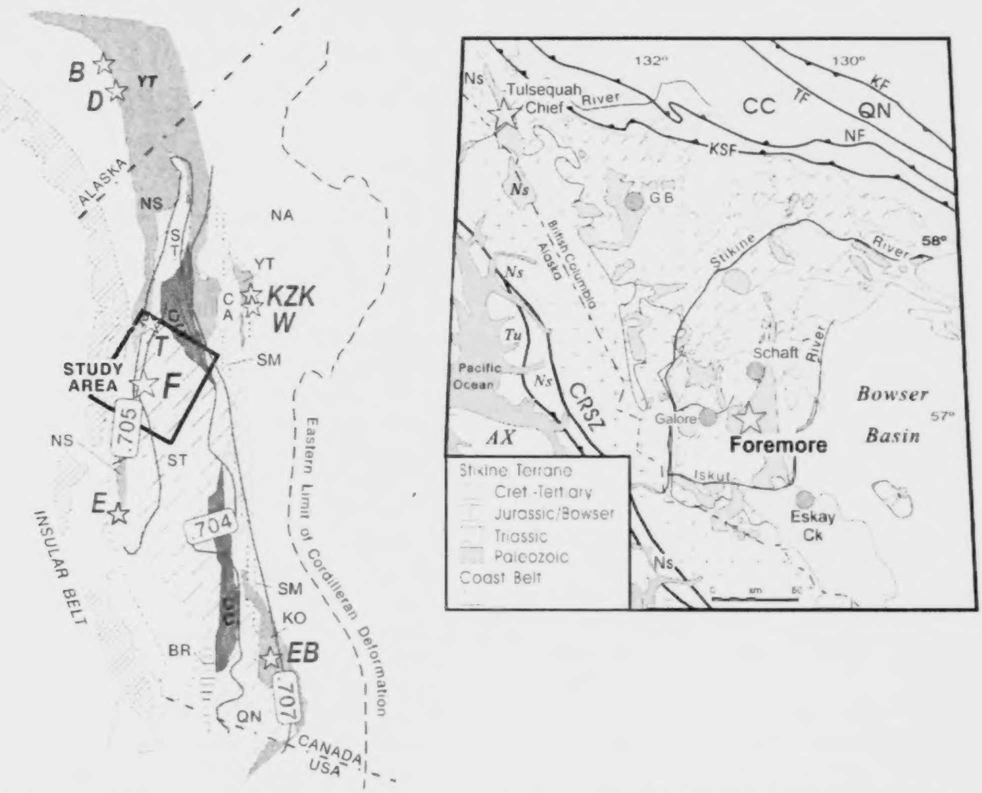
B
D
YT
ALASKA
NS
S
T
NA
YT
C
A
KZK
W
T
SM
STUDY AREA
F
705
NS
ST
E
704
INSULAR BELT
Eastern Limit of Cordilleran Deformation
SM
KO
BR
EB
707
QN
CANADA
USA
132°
130°
Ns
Tulsequah Chief
River
CC
TF
KF
QN
NF
KSF
Ns
GB
British Columbia
Alaska
Stikine
River
58°
Ns
Tu
Schaft
River
Pacific Ocean
Ns
CRSZ
Bowser Basin
57°
Galore
Foremore
AX
Iskut
Eskay Ck
Stikine Terrane
Cret.-Tertiary
Jurassic/Bowser
Triassic
Paleozoic
Coast Belt
Ns
km

Figure 1. (a) Terrane map showing tectonostratigraphic setting of the study area and the location of Devono-Mississippian VHMS deposits. EB=Eagle Bay deposits, W=Wolverine, KZK=Kudz Ze Kayah, B=Bonnington district, D=Delta district, T=Tulsequah, F=Foremore, E=Ecstall. Mesozoic initial strontium isopleths from Armstrong (1988). NA=Ancestral North America, CA=Cassiar, NS=Nisling, KO=Kootenay, SM=Slide Mountain, QN=Quesnellia, CC=Cache Creek, ST=Stikinia, BR=Bridge River, YT=Yukon Tanana (modified from Wheeler and McFeely, 1991). (b) Inset shows location of study area relative to the major tectonostratigraphic features of the northwestern Cordillera, regional distribution of Paleozoic, Triassic, Jurassic and Cretaceous-Tertiary rocks of Stikinia and regionally significant mineral occurrences. AX=Alexander Terrane, TU=Taku Terrane, Ns=Nisling Terrane, CRSZ=Coast Range Shear Zone, KSF=King Salmon Fault, NF=Nahlin Fault, TF=Thibert Fault, KF=Klinkit Fault.

The stratigraphic and plutonic framework of northwestern Stikinia is summarized by Anderson (1993), Gunning (1996) and Logan (2000). It consists of a Paleozoic to Mesozoic sedimentary and volcano-plutonic arc assemblage that includes: the Devonian to Permian Stikine assemblage, the Late Triassic Stuhini Group and the Early Jurassic Hazelton Group. These are overlain by Middle Jurassic to early Tertiary successor-basin sediments of the Bowser Lake and Sustut Groups, Late Cretaceous to Tertiary continental volcanic rocks of the Sloko Group, and Late Tertiary to Recent bimodal shield volcanism of the Edziza and Spectrum ranges.

PALEOZOIC STIKINE ASSEMBLAGE

Rocks of the Stikine assemblage are the structurally and stratigraphically lowest supracrustal rocks observed in the study area. Stikine assemblage rocks were informally named by Monger (1977) to include all upper Paleozoic rocks (within Stikinia) that cropped out around the periphery of the Bowser Basin. The assemblage consists of Permian, Upper Carboniferous, Lower Carboniferous and Devonian age strata and plutons. The dominant lithologies are calcalkaline, mafic and bimodal flows and volcaniclastics, interbedded carbonate, minor shale and chert. The Permian carbonates and volcanics are a distinctive part of the Stikine assemblage, traceable for over 500 kilometres from the Taku River to south of Terrace, but the Devonian and Carboniferous volcanic rocks have the highest potential to host polymetallic VHMS deposits (Fig. 1).

The Late Paleozoic history of Stikinia comprises three volcanic cycles: Early Devonian, Early Carboniferous and Late Carboniferous separated by three intervening sedimentary cycles (Logan and Koyanagi, 1994; Gunning, 1996). A composite stratigraphic section of the Stikine assemblage is presented which includes five main subdivisions (Fig. 2). From the oldest to the youngest, they are: (1) an Early to Middle Devonian

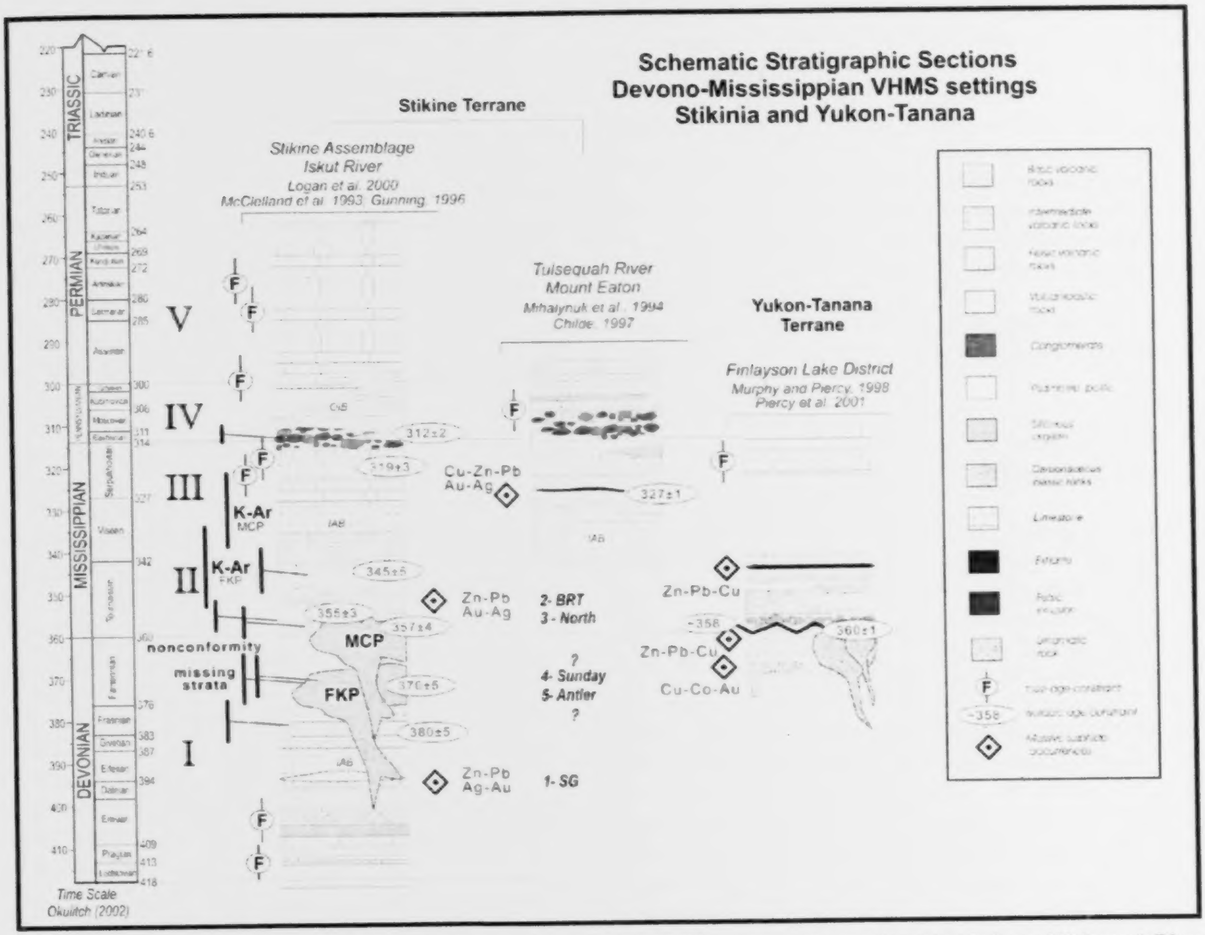
Schematic Stratigraphic Sections
Devono-Mississippian VHMS settings
Stikinia and Yukon-Tanana
Stikine Terrane
Stikine Assemblage
Iskut River
Logan et al. 2000
McClelland et al. 1993, Gunning, 1996
Tulsequah River
Mount Eaton
Mihalynuk et al. 1994
Childe 1997
Yukon-Tanana
Terrane
Finlayson Lake District
Murphy and Piercy 1998
Piercy et al. 2001
TRIASSIC
PERMIAN
MISSISSIPPIAN
DEVONIAN
V
IV
III
II
I
K-Ar
MCP
K-Ar
FKP
nonconformity
missing
strata
MCP
FKP
312±2
319±3
345±5
355±3
357±4
370±5
380±5
327±1
~358
360±1
Cu-Zn-Pb
Au-Ag
Zn-Pb
Au-Ag
Zn-Pb
Ag-Au
Zn-Pb-Cu
Zn-Pb-Cu
Cu-Co-Au
2- BRT
3 - North
?
4- Sunday
5- Antler
?
1- SG
Time Scale
Okulitch (2002)

Figure 2. Schematic Late Paleozoic Stratigraphic columns for northwest Stikine terrane: Forrest Kerr-Mess Lake and Tulsequah River areas, British Columbia and one for the Yukon-Tanana terrane: Finlayson Lake district, Yukon. Sources referenced on Figure.

package of penetratively deformed, intermediate to mafic metavolcanic tuff, flows, diorite and gabbro, recrystallized limestone, graphitic schist, rhyolite and quartz sericite schist; (II) an Early Carboniferous package of bimodal mafic and felsic volcanic flows and tuffs; (III) a mid Carboniferous echinoderm-rich limestone and cherty tuff unit, which overlies the Early Mississippian volcanic flows and clastic rocks along the northern edge of the Andrei Glacier; (IV) Late Carboniferous to Early Permian aphyric basalt, limestone and intermediate to felsic tuffs and flows and (V) thick Early Permian carbonate that forms the top of the Paleozoic section north of the study area. Early and middle Devonian macro- and microfossils from the carbonates interlayered with the sedimentary and volcanic rocks constrain ages for Division I. Missing or unrecognized from the section are Late Devonian stratified rocks, although magmatism during this period is evident from Late Devonian composite diorite-tonalite plutons. Intrusion of an Early Carboniferous (Tournaisian) 355±3Ma U/Pb zircon age from waterlain felsic tuff located above Devonian limestone (Logan *et al.*, 2000) and Early and mid Carboniferous U/Pb zircon ages (345±5 Ma and 319±3Ma, Friedman, in Gunning, 1996) from intermediate to felsic crystal tuffs sampled below and above mid-Carboniferous fossil-rich limestone (Division III) constrain the age of the second volcanic cycle (Fig. 2). Coeval, in part comagmatic intrusive episodes include the Early Mississippian More Creek plutons. The Late Carboniferous volcanic cycle is constrained by an early Late Carboniferous (Bashkirian) 312±2Ma U/Pb zircon age and Mid-Carboniferous microfossils from stratigraphically lower carbonate units and Early Permian microfossils from carbonate units which depositionally overlie the volcanic rocks (Fig. 2).

In general, the Foremore property is underlain by a primitive calcalkaline suite of volcanic rocks, and fine-grained sedimentary and carbonate rocks that range in age from Early Devonian to mid Carboniferous. It is flanked on the east and south by two synvolcanic and comagmatic plutons, the Late Devonian Forrest Kerr and Early Mississippian More Creek bodies. These composite plutons (each ~250 km^2) comprise a peraluminous felsic phase, which ranges from biotite granodiorite to biotite tonalite and trondhjemite, and an older metaluminous mafic phase of mainly hornblende monzodiorite and gabbro composition. Initial $^{87}Sr/^{86}Sr$ values from the diorite and tonalite phases range between 0.7039 to 0.7043 and suggest a relatively primitive magma source region; consistent with the juvenile Nd-isotopic signatures from the felsic phases (unpublished data) and lack of inheritance patterns in zircon. Proterozoic inheritance in zircons at Tulsequah indicate a north and westward transition from an intraoceanic-setting to one either underlain by pericratonic crust or continent-derived sediments, similar to the modern Aleutian Arc.

STRATIGRAPHY AND LITHOGEOCHEMISTRY

Three distinct episodes of mafic volcanism are recognized within the Stikine assemblage: Early Devonian, Early Carboniferous and Late Carboniferous. Representative samples of these volcanic cycles were collected during the current study. Fifteen samples collected during regional mapping in 1990-1992 (Logan et al., 2000) were re-analyzed with the current samples to augment the current database and characterize the regional volcanic stratigraphy and discriminate the tectonic setting in which they formed.

Samples were steel milled at the British Columbia Geological Survey Branch Laboratory in Victoria. Splits were shipped for analyses to: Cominco-Teck Laboratories, Vancouver for major element and trace element abundances (Ba, Rb, Sr, Nb, Zr and Y) by X-ray fluorescence (XRF); to ACME analytical Labs, Vancouver for trace element analyses using inductively coupled plasma emission spectrometry (ICP-ES); and to Memorial University, Newfoundland for trace element analyses using inductively coupled plasma mass spectrometry (ICP-MS).

Due to the highly mobile nature of the alkalis (Na, Ca and K), SiO_2 and Mg particularly during hydrothermal alteration and metamorphism much of the preliminary data set was culled and the following characterization of geochemical data relies primarily on alteration-insensitive immobile element ratios (with the exception of TiO_2 and Al_2O_3. Only select elements and ratios are presented in this paper (Tables 1, 2 and 3).

In the region around the Foremore property, lithogeochemistry indicates a mainly calcalkaline assemblage of submarine autoclastic basalt, pillowed basalt, tuff and cherty argillite (Unit 1 and 2), that is overlain disconformably by an alkaline assemblage of autoclastic basalt and pillowed basalt (Unit 3). The lithogeochemical and stratigraphic relationships between Unit 1 and 2 are equivocal and may also be separated by nonconformable relationships.

UNIT 1

Early Devonian (Lochkovian and Emsian) cherty carbonaceous argillite, fossiliferous limestone and chert pebble conglomerate are the oldest known rocks in Stikinia. This predominantly fine grained sedimentary package is characterized by dark black, green and white, well-bedded siltstone, sandstone, tuffaceous siltstone and ash tuff that form the basement to an unknown thickness of Early to middle Devonian volcanic rocks in the More Creek area. A single U/Pb zircon age of 380±5 Ma from felsic tuffs in the Forrest Kerr area indicates local volcanism. Maroon feldspar phyric volcaniclastic and epiclastic units underlie the fossiliferous Devonian limestone and much of lower portions of the Hanging valley on the Foremore property. This intermediate volcanic package is composed of a sequence of coarse-grained heterolithic volcaniclastic rocks, that vary from coarse cobble sized angular to sub-rounded, poorly sorted debris flows to fine-grained graded sandstones. Interlayered are well-bedded and commonly normal graded crystal tuffs.

In the vicinity of the SG mineralized zone the volcaniclastic rocks form the base of an upward fining and upright interpreted sequence defined by Oliver (2003) as follows: the base of the section is a thick, poorly-bedded heterolithic maroon volcaniclastic conglomerate with lesser fine-grained epiclastic units that are overlain by approximately 100m of basic flows and volcaniclastic rocks. Above the mafic volcanic rocks are approximately 100m of fine-grained phyllite, tuffite and limestone that have been intruded and inflated by basic sills and dikes. Overlying the sedimentary rocks are felsic tuffs (which host the Au-Ag-Pb-Zn±Cu mineralization) and massive felsic flows that together comprise less than 100m. A heterolithic (pyrite clast bearing) breccia unit, recognized only in float is postulated to overlie the felsic flows. The uppermost package consists of well-bedded volcanic siltite and sandstone, volcaniclastic rocks and sills that lie unconformably above the felsic volcanic rocks and are interpreted to be Triassic age (Barnes, 1989; Oliver, 2003).

Fewer lithogeochemical samples from this unit were collected due to its generally higher degree of alteration and deformation and because it is comprised primarily of heterolithic volcaniclastic units that are less desirable samples to use when characterizing rock chemistry. Rhyolite at the SG zone was sampled and is described below with Unit 2 felsic rocks

UNIT 2

Early Carboniferous volcanic rocks are well described for the More Creek area (Logan et al., 1992; Gunning, 1996; Logan et al., 2000). The base of the section (355±3 Ma waterlain felsic tuff) is located on a

Subgroup	Basalt Unit 2	Average	Basalt Unit 3	Average
Mg#	35.8-67.6	(45.9)	43.8-56.8	(51.53)
SiO2	46.98-57.54	(54.16)	43.3-57.68	(50.89)
TiO2	0.96-1.39	(1.16)	0.84-3.41	(2.4)
Na2O	2.87-6.23	(5.12)	4.12-6.11	(4.56)
K2O	0.52-1.65	(1.0)	0.55-2.51	(1.47)
La/Yb_{CN}	1.70-3.15	(2.2)	10.40-14.25	(12.5)
Zr/Y	1.82-3.83	(2.53)	7.83-11.71	(10.4)
Th/Yb	0.37-0.82	(0.58)	1.1-1.73	(1.36)
Zr	39.0-75.9	(56.6)	232-329	(269)
Nb	<3-5	(3.25)	24-75	(49.8)

CN = normalized to Chondrite values.

Table 1. Selected element concentrations and ratios for Early Carboniferous basalt and basaltic andesites (Unit 2) and Late Carboniferous basalts and trachyandesites (Unit 3). Values in brackets are average values.

Subgroup	Rhyodacite(2)	Average	Rhyolite A (1)	Average	Rhyolite B (2)	Average
SiO2	65.3-67.5	(65.5)	73.62-80.19	(76.25)	72.27-78.88	(74.05)
Na2O	4.05-8.0	(6.03)	2.25-2.64	(2.48)	2.80-6.94	(4.56)
K2O	1.51-1.96	(1.7)	1.45-3.23	(2.23)	1.26-1.64	(1.51)
La/Yb_{CN}	6.60-8.54	(7.57)	4.12-5.22	(4.69)	1.36-2.96	(2.37)
Zr/Y	2.49-3.19	(2.84)	3.07-6.58	(4.58)	2.62-3.82	(3.26)
Th/Yb	1.56-3.15	(2.36)	0.83-1.92	(1.64)	0.61-0.93	(0.76)
Zr	86-117	(102)	92-230	(145)	84-160	(121)
Eu/Eu^{*1}	0.89-0.99	(0.93)	0.37-0.75	(0.57)	0.61-0.78	(0.72)

$^{1}Eu/Eu^{*}=Eu_{N}/(Sm_{N}*Gd_{N})^{1/2}$; N = normalized to primitive mantle values;

CN = normalized to Chondrite values.

Table 2. Selected element concentrations and ratios for Early Devonian rhyolite (Unit1) and Early Carboniferous rhyodacite and rhyolite-b (Unit 2). Values in brackets are average values.

Subgroup	FKPS felsic	Average	FKPS mafic	Average
SiO2	72.19-75.44	(74.16)	48.71-64.96	(54.39)
Na2O	3.92-4.97	(4.22)	1.30-3.12	(2.33)
K2O	0.85-1.43	(1.11)	0.15-1.18	(0.69)
La/Yb_{CN}	4.56-9.0	(6.78)	1.51-2.13	(1.87)
Zr/Y	4.79-14.4	(7.78)	1.57-5.61	(3.45)
Th/Yb	2.22-2.88	(2.55)	0.31-2.49	(1.23)
Zr	89-173	(114)	31-112	(67)
Eu/Eu^{*1}	0.79-1.24	(1.02)	0.94-1.38	(1.10)

$^{1}Eu/Eu^{*}=Eu_{N}/(Sm_{N}*Gd_{N})^{1/2}$; N = normalized to primitive mantle values;

CN = normalized to Chondrite values.

Table 3. Selected element concentrations and ratios for Late Devonian to Early Carboniferous Forrest Kerr Plutonic Suite felsic rocks (tonalite and trondhjemite) and Forrest Kerr Plutonic Suite mafic rocks (hornblende diorite). Values in brackets are average values.

nunatak in More Glacier (Logan et al., 2000) and the top of the section (319±3 Ma, intermediate to felsic crystal tuffs; Friedman, in Gunning, 1996) is exposed north of Andrei Glacier where volcanics are overlain depositionally by mid-Carboniferous fossil-rich limestone. On the Foremore property the basal unit comprises a well-bedded section of pale green intermediate volcanic sandstone and siltstone, felsic lapilli tuff and black mafic ash tuff which overlie Devonian limestone on both north and south sides of Hanging Valley. Barnes (1989) and Oliver (2003) mapped these as Late Triassic Stuhinni Group rocks in part due to their unconformable relationship to the Early Devonian rocks.

Elsewhere, Unit 2 volcanic rocks are mainly basalt, dolerite, lesser intermediate andesite, dacite and rhyolite. The mafic and felsic rocks are intercalated, although Gunning (1996) recognized multiple individual small felsic eruptive centers associated with the Early to mid Carboniferous volcanic cycle. The mafic rocks comprise dark green massive to amygdaloidal flows, pillowed flows and pillow breccias, but the most common are green and purple autoclastic breccias, reworked volcaniclastic or epiclastic rocks are rare. The monolithic, scoriaceous tephra contain variably sized, non-sorted fragments of plagioclase microphenocrystic basalt in a finer matrix of similar composition. Fragments are often globular shaped, showing plastic deformation or chilled and altered margins. Hyaloclastite breccias with characteristic curvilinear fracture surfaces, quench-texture brecciation and clusters of sigmoidal to equant devitrified quenched basalt occur west and south of the Hanging valley in thick sections of autoclastic breccias. Further west (on nunataks in More Glacier) the proportions of fine-grained, planar-bedded volcanic sandstones and siltstones exceed the proportions of coarse basalt breccias and flows.

Intermediate rocks appear to be subordinate to the mafic rocks and felsic rocks based on the analyses, but again this might be an artifact of sampling. The intermediate rocks comprise andesite flows and small intrusive sills. The rocks are grey to green in colour, feldspar-rich and typically porphyritic. Light green, grey and white intermediate composition centimeter-thick, sharp-based beds with planar laminations are indicative of distal water lain tuff or resedimented tuffite.

Felsic rocks are mainly fragmentals and are localized around eruptive centres, cryptodomes. Proximal deposits include flows, breccias, agglomerates and coarse tuffs. Distal felsic deposits include well-bedded often-graded tuffs, tuffaceous siltstone and cherty tuff. Compositions range from dacite to rhyolite. Textures include complex flow banded, to massive felsite and a variety of fragmental and autobrecciated forms. Devonian rhyolite flows and proximal deposits of felsic breccias are known to occur (i.e. SG rhyolite).

The North and BRT mineralized zones are hosted in rocks with no definitive age constraints. Limestone is missing from the section and deformation has transposed the stratigraphy. The sequence is interpreted to be Early Mississippian based on lithologic characteristics and the more radiogenic Pb-isotope character of the mineralization (see section on isotopes). At the BRT-North zones Oliver (2003) divided the stratigraphy into three packages; an upper mafic volcanic flow and breccia unit (correlated with Unit 3 on the basis of lithogeochemistry), a medial package of well-bedded cherty tuffs and fine-grained siliceous sediment and a lower package of mixed volcaniclastics, mafic flows, felsic tuffs and light and dark siliciclastic rocks (correlated with Unit 2). In addition, the upper and medial units occupy the hanging wall of the North Zone Thrust fault, separating them from the structurally lower bimodal volcaniclastic and sedimentary rock package which hosts the BRT and North mineralized zones.

Major and trace element contents of rhyolites (type a) from the lower volcanic package (Unit 1) and from a wide variety of mafic to felsic volcanic rocks from the medial volcanic package (Unit 2) permit the data to be subdivided into four geochemical suites (Table 1, Fig. 3a and b).

Using the Zr/Ti - Nb/Y and SiO2 - Zr/Ti projections of Winchester and Floyd (1977) it is possible to discriminate a mafic, an intermediate and two felsic suites having basaltic to basaltic-andesite, andesitic to rhyodacite and rhyolite affinities, respectively. They have low Zr/TiO2 and Nb/Y values that suggest a subalkaline affinity (Fig. 3a). In contrast, Unit 3 alkalic basalts have moderate Nb/Y values (Table 1) that suggest alkalic affinities (see description for Unit 3).

Zr/Y, La/Yb and Th/Yb ratios have been shown to be useful in discriminating between felsic volcanic rocks associated with calc-alkaline versus tholeiitic sequences (Pearce and Norry, 1979; Lesher et al., 1986; Barrett and MacLean, 1999). Using Zr/Y ratios and the divisions suggested by Barrett and MacLean (1994), that tholeiitic sequences have lower Zr/Y (2-4.5) and calcalkaline rocks Zr/Y (>7), with a transitional group having Zr/Y (4.5 to 7); the majority of felsic volcanic rocks in the Foremore area have Zr/Y ratios between 2 and 4.5, which are compatible with the association of tholeiitic volcanic rocks (Fig. 3c). Two rhyodacites from rhyolite B have higher Zr/Y ratios (4.5 to 7) indicative of transitional affinity, while the alkaline basalts and one trachy-andesite have higher Zr/Y ratios (7-15) consistent with a calcalkaline to alkaline affinity. The felsic to intermediate Foremore lavas contain only 90-170 ppm Zr and 25-47 ppm Y, which are abundances more characteristic of calcalkaline than tholeiitic lavas (Lentz, 1998; Barrett and MacLean, 1999). La/Yb and Th/Yb ratios are more effective to determine magmatic affinity for calcalkaline lavas because La and Th typically remain incompatible with fractionation, whereas Zr and Y commonly become compatible to varying degrees (Barrett and MacLean, 1999). On the Th/Yb plot the majority of mafic volcanic

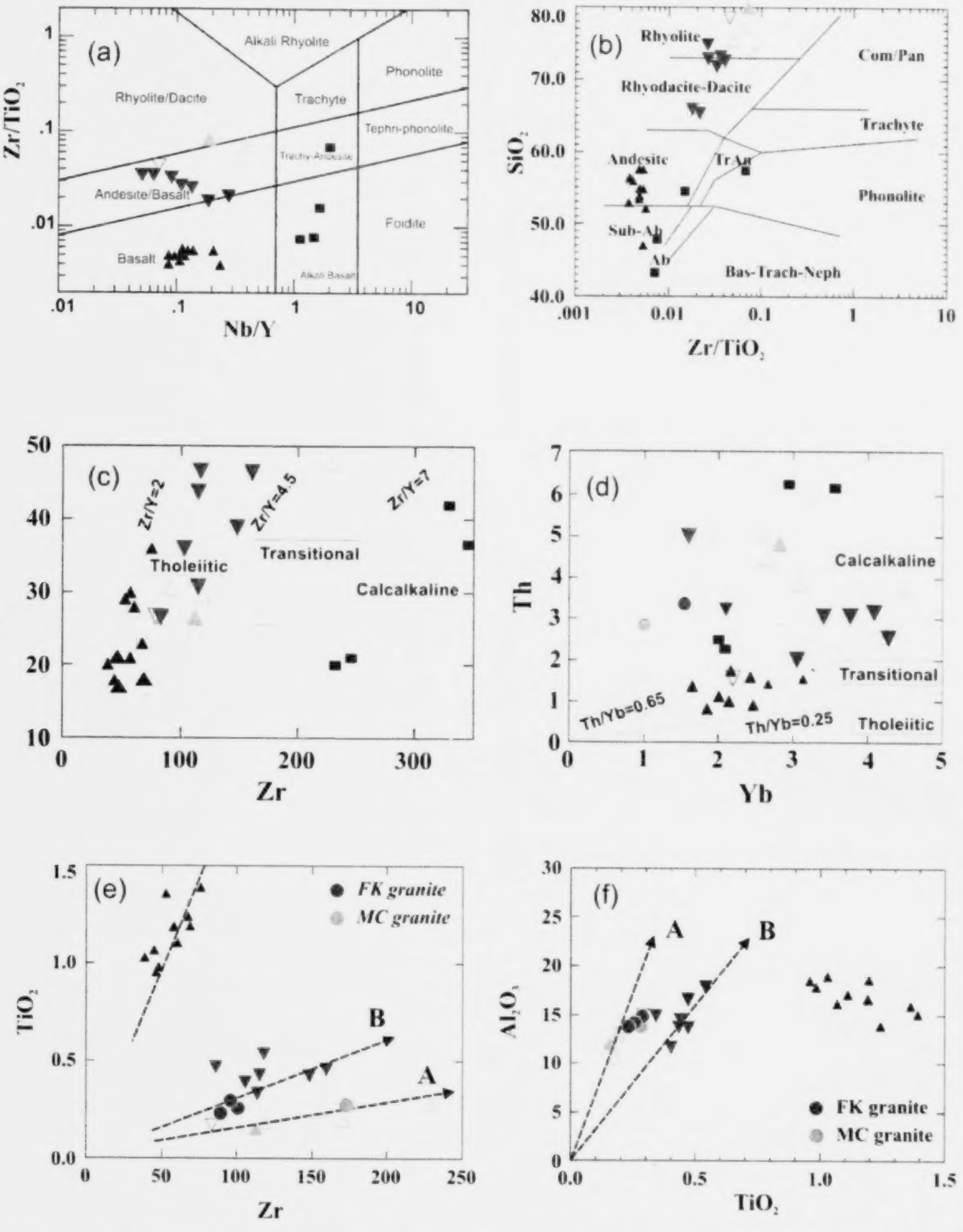

Figure 3. (a) Zr/TiO2 vs. Nb/Y diagram of Winchester and Floyd (1977), revised after Pearce (1996). (b) SiO2 vs. Zr/TiO2 diagram of Winchester and Floyd (1977). (c) Y vs. Zr plot (after Barrett and MacLean, 1984) showing Zr/Y ranges for the various magmatic affinities. (d) Th vs. Yb plot (after Barrett and MacLean, 1999) showing Th/Yb ranges for the various magmatic affinities. (e) TiO2 vs. Zr. (f) Al2O3 vs. TiO2. Symbols for Figure 3 and subsequent plots as follows: Unit 1, rhyolite A (green triangle); Unit 2, basalt (dark green-filled triangle), rhyodacite-dacite (inverted purple-filled triangle), rhyolite B (inverted pink-filled triangle), Unit 3, alkalic basalt (filled square).

FIGURE 4

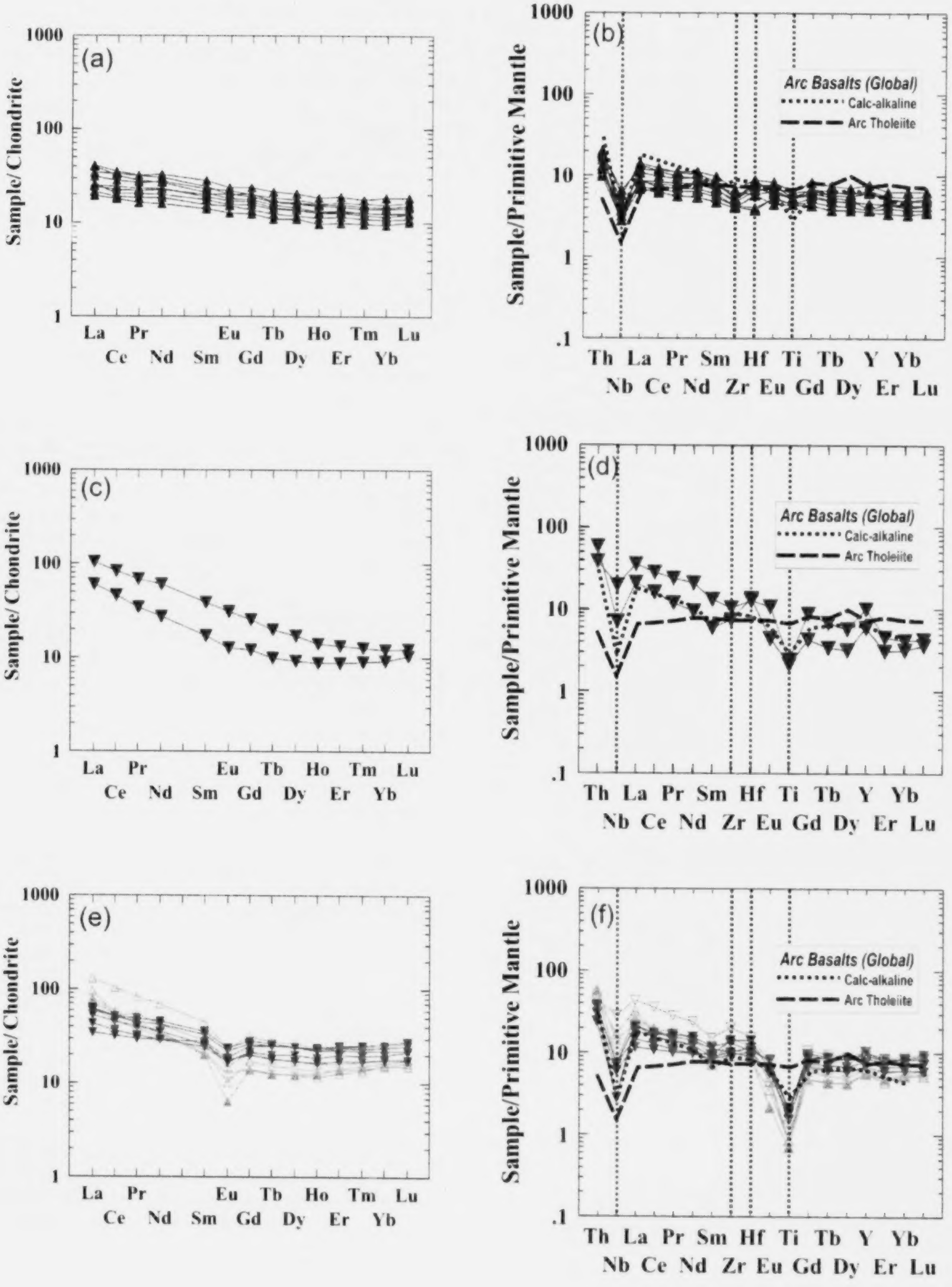
(a)
(b)
(c)
(d)
(e)
(f)
Sample/ Chondrite
Sample/Primitive Mantle
1000
100
10
1
.1
La Pr Eu Tb Ho Tm Lu
Ce Nd Sm Gd Dy Er Yb
Th La Pr Sm Hf Ti Tb Y Yb
Nb Ce Nd Zr Eu Gd Dy Er Lu
Arc Basalts (Global)
Calc-alkaline
Arc Tholeiite

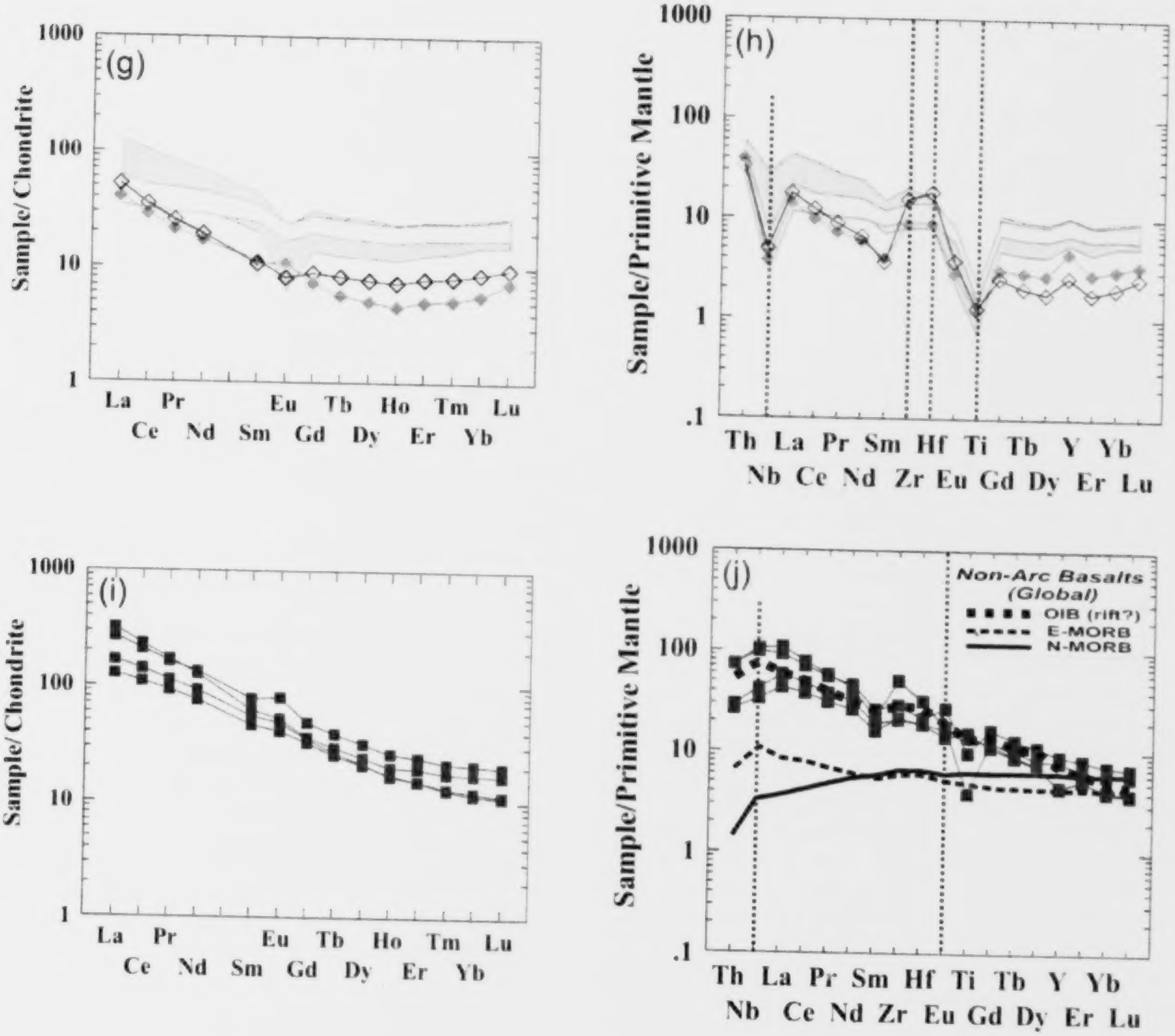

Fig. 4. Chondrite-normalized REE and primitive mantle-normalized multi-element plots for: (a and b) basalt and basaltic andesite from Early Mississippian Unit 1; (c and d) intermediate rhyodacite of Unit 1; (e and f) Rhyolite A and Rhyolite B from Unit 1; (g and h) tonalite and trondhjemite of the FKPS, shaded areas corresponds to the range of values for Rhyolite A (dark) and B (light); (i and j) alkaline basalt and trachy-andesite of Unit2. Chondrite and primitive mantle normalization values are from Sun and McDonough (1989). Primitive mantle normalized patterns for Arc basalts (global) include: a calcalkaline profile from the Sunda arc (Jenner, in Piercey, 1999) and an arc tholeiite from Valu Fa ridge in the Lau Basin (Rautenschlein et al., 1985). Primitive mantle normalized profiles for Non-Arc basalts (global) include: compilations of ocean island basalts (OIB), mid-ocean ridge basalts (MORB) of both the normal type (N-MORB) and enriched type (E-MORB) from Sun and McDonough (1989).

rocks have transitional affinities with Th/Yb ratios between 0.37 and 0.82. The intermediate and felsic suites have Th/Yb ratios >0.65 and strong calcalkaline affinities. Rhyolite B has Th/Yb ratios between 0.61 and 0.93 and averages 0.76 (Table 1). The Th/Yb ratios for rhyolite A and the alkaline suite samples average 1.64 and 1.56 respectively. There are no lavas with tholeiitic Th/Yb ratios of 0.25 to 0.1.

TiO_2 -Zr and Al_2O_3-TiO_2 relationships for the basaltic andesite, rhyodacite and rhyolite suites (from Fig 3a) are shown in Figure 3e and f, respectively. The alkaline lavas have elevated Zr and TiO_2 values which lie outside the plot. Although limited by the number of samples, a two-fold subdivision of the rhyolites (A and B) as well as basaltic andesite is apparent from their Al-Ti-Zr relationships. The covariation between TiO_2 and Zr reflects compatible behaviour of Zr at higher silica compositions (rhyolite vs. rhyodacite) and indicates both low Zr and high Zr subgroups for both. Two rhyodacite samples show affinities with rhyolite B. Also shown is data for granites of the Forrest Kerr Plutonic Suite as they may be coeval with one or the other felsic unit. It is generally possible to identify primary fractionation trends on these plots (Barrett and Maclean, 1999), however the variable ages and differing Zr/Y ratios imply that the felsic units are not related to the mafic unit(s) by fractionation.

Mafic rocks are mainly basalt and basaltic andesites. The basalts have TiO_2 contents of 1.0 to -1.4 percent and low Nb contents of <3 to 4 ppm (Table 1). The chondrite-normalized REE patterns for the Foremore basalts are characterized by LREE enrichment (La/Yb_{CN} = 1.7-3.1) and a downward sloping pattern towards the HREE elements (Fig. 4a). The HREE are essentially flat, (10-20 x's chondrite). The primitive mantle-normalized patterns of the subalkaline basalt suite is similar to the REE plot, with the exception of the negative Nb anomaly with respect to Th and La, and the negative Zr anomaly relative to Sm and Hf. Unit 2 has primitive mantle-normalized patterns (Fig.4b) that are variably depleted, but closely parallel the pattern for calcalkaline arc basalts from the Sunda arc (Jenner, in Piercey, 1999), which supports the field relationships (i.e. interlayered pillowed flows, hyaloclastite breccias and coarse to fine tuffs).

The lithogeochemical data for the intermediate to felsic volcanic rocks are presented in Table 2. Three subdivisions: an intermediate rhyodacite suite and two rhyolite suites are based on the major and trace element chemistry. The geochemical signatures for all are broadly similar and suggest affinities to a calcalkalic continental arc. Rhyolite A is associated with intermediate volcaniclastic rocks and limestone of Unit 1. The intermediate rhyodacite suite and rhyolite B are intimately interlayered with mafic volcanic rocks of unit 2 and show chemical affinities for the FKPS rocks.

Rhyolite A is characterized by higher Ti, Fe, P, and Zr than rhyolite B and a Na:K ratio of approximately 1. In contrast, the intermediate rhyodacite and rhyolite B have Na:K ratios of approximately 3:1 which are more like the Na:K ratios for the tonalites of the FKPS (Table 2 and 3).

The chondrite-normalized REE patterns for rhyolite A are characterized by relatively flat HREE patterns, moderate LREE enrichment (La/Yb_{CN} = 4.12-5.22) sloping downward towards the HREE elements and a moderate negative Eu anomaly (Eu/Eu^* = 0.37-0.75), Zr/Y (3.07-6.58) and moderate Th/Yb (1.25-1.92; Table 2; Fig. 4e and f).

The rhyodacite subunit is characterized by steep chondrite-normalized REE patterns (La/Yb_{CN} = 6.60-8.54), a slight to non-negative Eu anomaly (Eu/Eu^* = 0.89-0.99), low Zr/Y (2.49-3.19) and high Th/Yb (1.56-3.15; Table 2; Fig. 4c and d). The chondrite-normalized REE patterns for Rhyolite B show a slight LREE enrichment (La/Yb_{CN} = 1.36-2.96), a slight negative Eu anomaly (Eu/Eu^* = 0.61-0.78), low Zr/Y (2.62-3.82) and low Th/Yb (0.61-0.93; Table 2; Fig. 4e and f). The primitive mantle-normalized values for all three felsic suites have broadly similar patterns (Fig. 4d and f). All are characterized by either moderate or strong negative Nb anomalies relative to Th and La, all possess variable negative Ti anomalies and a generally downward sloping profile from LREE to HREE. Rare-earth element patterns of the rhyolites show distinct enrichment in the light REE, with relatively flat heavy REE patterns implying derivation from an undepleted mantle source (Fig. 4e and f).

Unit 2 subalkaline basalt and basaltic andesites have HFSE abundances (specifically Nb depletion) that are characteristic of volcanic arc basalts, and plot in the calcalkaline (Hf/Th ratios of less than 3) portion of the arc basalt field on Figure 5 (after Wood, 1980). On the Zr, Y, Nb tectonic discrimination diagram (after Meschende, 1986) the basalt and basaltic andesites from Unit 2 fall predominantly in the VAB field (D).

Unit 3

An extensive package of primarily mafic volcanic flows and breccias, and lesser trachyte and rhyolite occupy the structural and topographic highest positions in the northern part of the study area. This package is not constrained by isotopic dates or fossil ages in the immediate area, but to the north correlative, massive alkalic basalt and fragmental rocks are depositionally overlain by latest Late Carboniferous limestone (Logan et al., 2000).

The volcanic rocks comprise dark green and grey mafic basalt flows, flow breccias and pillowed flows, lesser purple and green lapilli tuffs and coarse volcanic conglomerate to well-bedded, fine-grained epiclastic

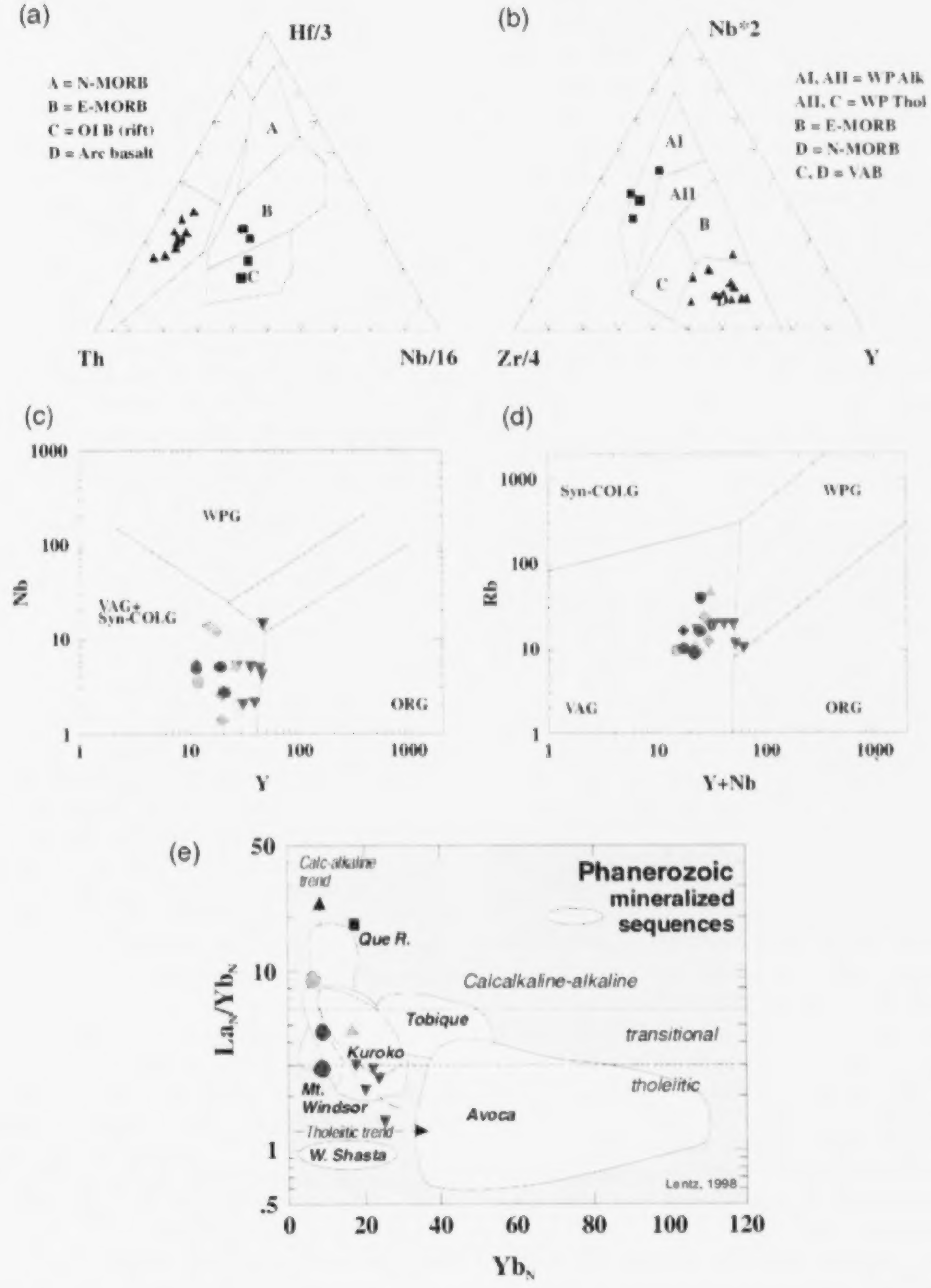

Fig. 5. (a) Tectonic discrimination diagram based on Th, Hf, Nb (after Wood, 1980) used to distinguish arc basalts (and theoretically between calcalkaline and tholeiitic arc basalts) from non-arc basalts (Nb depletion in the former). Basalt and basaltic andesite from Unit 1 fall within the calcalkaline arc basalt field (D). Unit 2 alkaline basalts and trachy-andesite plot within the OIB (rift) and E-MORB fields. (b) Tectonic discrimination diagram based on Zr, Y, Nb (after Meschende, 1986) used to distinguish non-arc basalts (Nb depletion) The diagram is also useful in deciphering within plate alkalic (AI) versus within plate tholeiitic (AII) rocks. Basalt and basaltic andesite from Unit 1 fall predominantly in the VAB field (D). Unit 2 alkaline basalts and trachy-andesite plot in the within plate alkaline basalt field (A1). (c and d) Nb *vs.* Y and Rb *vs.* Y+Nb plots (after Pearce et al., 1984) showing the majority of the intrusion and rhyolite samples lying within the I-type volcanic arc granite (VAG) field. The extension of several samples into the within-plate granite (WPG) probably reflects their high degree of fractionation. (e) La_{CN}/Yb_{CN} *vs.* Yb_{CN} plot (after Lentz, 1998) showing the fields for selected Phanerozoic felsic volcanic rocks associated with VHMS deposits and estimated tholeiitic and calcalkaline fractionation trends.

units. The pillows are well preserved, <1m oblate and pillow bud forms interlayered with amoeboid-shaped autoclasts and breccia fragments. Massive to amygdaloidal (chlorite and/or calcite) basalt flows are present throughout and comprise approximately one third of the section. The flows are characterized by fine white microphenocrysts of plagioclase and commonly <1cm long elliptical amygdules. Above the BRT/North zone (Fig 3), a distinctive monolithic purple vesicular basalt breccia with green matrix forms the lowermost unit (Oliver, 2003). Prismatic primary igneous amphibole crystals occur within some basalt flows and is a distinctive feature in some of the interflow lapilli and crystal tuffs of Unit 3. Block and lapilli-sized coarse-grained amphibolite fragments (Photo 1) are also common in Unit 3 tuffs located north and south of More Creek. These are thought to represent zenoliths of mafic cumulates incorporated and extruded during subsequent eruptions.

Photo 1. Coarse-grained amphibolite lapilli fragment in amphibole crystal-rich alkaline tuffs of Unit 3.

Correlative strata occupy the area immediately east of the headwaters of Mess Creek and north of More Creek. Gunning (1996) divided this area into a western succession of coherent and autobrecciated basalt, pillowed and pillow breccia basalt and an eastern dacite-rhyolite flow complex and speculated that the morphology and composition represented a steep-sided volcanologic dome cored by the eastern felsic complex. The author mapped and sampled a single traverse down through the western assemblage of mafic basalt breccias and flows. Close to the bottom of the valley, at the contact between volcanic rocks of Unit 3 and lapilli and cherty felsic tuff, sericite-chlorite schist and siliceous graphitic phyllite of Unit 1, the structure style changes abruptly from brittle, non-penetrative fabrics in the overlying rocks to recumbently folded and penetratively foliated fabrics within the lower finer-grained section. A similar structural discordance is evident at the lower contact of Unit 3 above the BRT zone. At this location an angular unconformity has been suggested to explain the discordant relationship between the gently dipping, 025° trending lower contact of Unit 3 basalts and the steeply-dipping, 150° to 170° striking fine-grained, well-bedded tuffaceous and siliciclastic rocks of Unit 2.

Above the BRT the estimated thickness of unit 3 is 50 to 100 m (Oliver, 2003), whereas north of More Creek, Gunning (1996) shows a combined thickness of close to 5,000 m. The composite thickness is complicated by normal faulting and includes an eastern section, which incorporates calcalkaline basalts that underlie the dacite-rhyolite complex. These might be more appropriately assigned to Unit 1 or 2 on the basis of their igneous affinity. Regardless, thickness estimates for the alkaline volcanic section located north of More Creek are impossible to estimate due to the network of normal faults (Gunning, 1996).

Chemical analyses of pillowed [illegible] flow breccia basalts are basaltic and trachy-and[illegible]e in composition (Fig. 3a and b), Gunning (1996) [illegible]o reports trachyte compositions and alkaline igneous affinity (Fig. 3a). The chondrite-normalized REE patterns for the alkaline rocks of Unit 3 are characterized by a LREE enrichment (La/Yb_{CN} = 10.40-14.25) and a steep downward sloping pattern towards the HREE elements, Zr/Y (7.83-11.71) and moderate Th/Yb (1.1-1.73); Table 2; Fig. 4i). All possess slightly positive Eu anomalies. The primitive mantle-normalized patterns for Unit 3 (Fig. 4j) are similar to the REE patterns, with steep negative slopes that closely overlap the global compilation patterns for OIB (Sun and McDonough, 1989). All are characterized by either moderate or strong positive Nb anomalies relative to Th and La, a variable positive Zr and positive Ti anomalies (with the exception of the more fractionated trachy-andesite). Unit 3 rocks have higher HFSE contents typical of non-arc basalts and Nb values (24-75, Table 1) that reflect a relatively large degree of within plate enrichment.

Unit 3 basalt and trachy-andesite samples have non-arc basalt abundances of Th, Hf and Nb and show characteristics of within plate ocean island basalt (rift-related) and enriched mid ocean ridge basalt affinities (Fig. 5a) on the arc *vs.* non-arc tectonic discrimination diagram of Wood (1980). Figure 5b (after Meschende, 1986) uses Nb /Y ratios to separate the within plate basalts into alkalic and tholeiite subgroups and clearly indicates within plate alkalic affinities of Unit 3 rocks.

Paleozoic Intrusions

FKPS

The Late Devonian to Early Mississippian Forrest Kerr Plutonic Suite comprises two individual plutons in the More Creek area, the Forrest Kerr Pluton and More Creek Pluton. Textural, mineralogical, and chemical characteristics of each are surprisingly similar (Logan et al., 2000), and have been interpreted to represent the roots of a Devono-Mississippian volcano-plutonic arc (Logan et al., 1993). Each comprises a peraluminous felsic phase, which ranges from biotite granodiorite to biotite tonalite and trondhjemite, and an older metaluminous mafic phase of mainly hornblende monzodiorite and gabbro composition. They are synvolcanic and probably comagmatic to the Late Devonian and Early Mississippian extrusive rocks recognized regionally in this part of northern Stikinia (McClelland, et al., 1993; Mortensen in Sherlock et al., 1994; Grieg and Gehrels, 1995; Friedman in Gunning, 1996; Childe, 1997).

The major trace element abundances of the FKP suite show a strong Na_2O enrichment and K_2O depletion from mafic (~50 wt% SiO_2) to felsic (>70 wt% SiO_2) compositions and follow the differentiation trend of gabbro-trondhjemite series rocks located in southwest Finland (Arth et al., 1978). The plutons show a wide spectrum of compositions on normative Qz-Pl-Or plots, with most samples lying in the tonalite-trondhjemite field and the diorite and quartz diorite fields (Gunning, 1996; Logan et al., 2000). The FKP suite belong to the low-Al (< 15 wt % Al_2O_3), calcalkaline trondhjemite-tonalite types which are characteristic of subvolcanic arc environments and usually have low abundances of Rb, Sr, slight enrichments in LREE, negative Eu anomalies and flat HREE patterns (Barker and Arth, 1976).

Chondrite normalized REE patterns for trondhjemites from oceanic settings typically have flat or light REE depleted patterns showing whole-rock heavy REE values greater than 10 and negative Eu anomalies (Arth, 1979). Continental rocks (continental-margin and -interior examples) on the other hand have highly fractionated patterns showing HREE values less than 5 and small positive Eu anomalies (Arth, 1979). Trondhjemite (FKP) and tonalite (MKP) have steep chondrite normalized REE patterns (La/Yb_{CN} = 4.56-9.0), with a small negative or positive Eu anomaly and essentially flat or dish-shaped HREE profile (Fig. 4g), with HREE values between 5 and 10 times chondrite (Sun and McDonough, 1989). Early Mississippian diorite (MCP) has flat (La/Yb_{CN} = 1.51-2.13), chondrite normalized REE values 10 to 20 times chondrite. The chondrite normalized REE patterns for the FKPS show a steep highly fractionated LREE profile which corresponds to 'continental' trondhjemites and a flat, slightly depleted HREE profile similar to oceanic arc trondhjemites (Arth, 1979). Primitive mantle-normalized plots for the FKPS are characterized by weak to strong negative Nb anomalies relative to Th and La, a moderate sloping profile from LREE to the HREE, and a negative Ti relative to Eu and Gd (Fig. 4h). On Yb-Al_2O_3 tectonic discrimination diagram, the FKP suite extends from the oceanic (low Yb/Al_2O_3 ratios) into the continental arc (lower Yb and higher Al_2O_3) fields (Arth, 1979).

Tonalite and diorite of the More Creek and Forrest Kerr plutons have Nb-Y compositions (Fig. 5c) that plot within the volcanic arc-field, typical of I- and S-type igneous rocks (VAG; Pearce et al., 1984). The felsic volcanic units (rhyolite A and rhyolite B) have compositions that straddle the boundaries between volcanic-arc (I-type) and within-plate (A-type/OR-type) igneous rocks. The low Rb contents of both intrusive and extrusive rocks (<100 ppm) indicate that they do not have a syn-collisional affinity (Fig. 5d).

Small, <0.5 km^2 equant plugs, dikes and sills of tonalite intrude the metavolcanic rocks in the vicinity of the North zone, above the BRT zone and along the north-facing cliffs of More Creek. The intrusions show pervasive alteration and penetrative deformation that is related to the dominant phase of regional deformation. These are interpreted to be subvolcanic Devono-Mississippian intrusions that are related to the FKPS. Although undated, these intrusions have age and mineralizing implications for the host rocks. Subvolcanic intrusions have been linked to the majority of Archean VHMS deposits (Galley, 1995, 2003), so the spatial association of these intrusions in metavolcanic and siliciclastic rocks that host the North and BRT VHMS mineralized zones may not be fortuitous and should be tested further as a potential exploration vector.

An undated equigranular, medium grained hornblende-biotite to tonalite sill complex intrudes the well-bedded volcanic siltstones, tuffs and flows which overlie the Early to middle Devonian rocks of Unit 1 at the SG zone. Pervasive propylitic alteration has replaced feldspars and mafic minerals in the intrusion with epidote-quartz-pyrite assemblages. The alteration is focused and limited primarily to the intrusion and probably represents magmatic-hydrothermal alteration associated with late stage fluids.

Mesozoic Intrusions

A 1km^2 leucocratic granodiorite plug intrudes and metamorphoses mafic metavolcaniclastic breccias, maroon phyllite, felsic tuff and argillaceous phyllite west of the terminus of More Glacier. The intrusion is well jointed but not foliated and consists of biotite-hornblende-plagioclase-potassium feldspar and quartz. Metavolcanic rocks adjacent to the contact are converted to amphibolites and contact-metamorphic minerals overprint the dominant foliation in argillaceous phyllite. The intrusion is cut by a series of east-trending auriferous quartz veins (Harris, 2002) that, have Jurassic galena lead model ages (Logan et al., 2000), suggesting that the plug is related to the regionally extensive Early Jurassic intrusive event.

DISSCUSSION

Primitive mantle normalized trace element profiles of the lower (Early to Middle Devonian) and medial (Early to Late Carboniferous) subalkaline volcanic sequences in the Foremore area have trace element patterns that are similar to calcalkaline volcanic arc basalts. They compare well with calc-alkalic rocks from the Sunda arc (Jenner in, Piercey, 1999), which have trace element patterns characterized by a very strongly pronounced negative Nb anomaly, a slight negative Ti anomaly, LREE enrichment and steeply downward trending profiles. Calc-alkaline basalts reflect more mature arc evolution and/or the influence of continental crust on arc-basalt petrogenesis (Pearce and Peate, 1995). Primitive mantle normalized trace element profiles of the upper (Late Carboniferous) alkaline volcanic sequence have trace element patterns that are similar to non-arc ocean island basalts (OIB) of rift affinities. The calcalkaline and alkaline magmatic events in the Foremore area are two distinct magmatic events of different ages and stratigraphic position. The switch from subduction arc magmatism to within-plate rifting has regional tectonic implications with respect to arc configuration and polarity, but because rifting is characterized by high heat flow, rapid and shallow emplacement of intrusions and development of second or third order basins it can be an important period of VHMS generation.

The variable Th/Yb ratio of rhyolite A (1.2-1.9), and rhyolite B (0.6-0.9) is good evidence that the two are the result of different magma sources and/or volcanic centre. The two rhyolites type A and B also display subtle variations in their chondrite normalized REE patterns and primitive mantle normalized trace element plots. Felsic suites have variably negative Nb, Eu and Ti anomalies (Fig. 4f). The negative Eu and Ti anomalies are consistent with fractional crystallization of feldspar and oxides, respectively, or retention of such phases as a restite in the source region. The overall REE patterns of rhyolite A and B fall within the range of rifted mature arcs and continental back arc rift settings that compare with calcalkaline arc basalt profile from the Sunda arc.

Felsic phases of the FK and MK plutons are coeval with extrusive felsic tuff and flow units (Logan et al., 2000). The limited trace element and REE data available shows abundances for hornblende diorites from the Early Mississippian More Creek pluton that are identical to Early Carboniferous Unit 2 basalt samples (Table 3). Primitive mantle normalized trace element patterns of tonalite and trondhjemite of the FKPS are characterized by elevated LREE and with the exception of a positive Y anomaly relative to Dy and Er; flat HREE profile that are depleted relative to patterns for Unit 1 (rhyolite A) and Unit 2 (dacite and rhyolite B). The characteristic pattern of depleted HREE is related to the partition coefficient for hornblende. The FKPS also show a decoupling between niobium and zirconium typical of relatively reduced melts (Galley, 2003). Large synvolcanic intrusions of quartz diorite-tonalite-trondhjemite composition are spatially associated with many of the Precambrian VMS camps (Noranda, Sturgeon Lake and Snow Lake VMS camps, Galley, 2003). Limited geochemistry (Logan et al., 2000; and unpublished data) indicates that the tonalite-trondhjemite phases of the FK and MC plutons have low Al_2O_3 (<14.7 wt. %), high SiO_2 (>70 wt. %) and low-K_2O (<1.5 wt. %) which are characteristic of the synvolcanic trondhjemite-tonalite intrusive complexes that are known to be associated with Archean VHMS mineralization (Noranda, Manitouwadge and Snow Lake VMS districts; see Galley, 1995; Galley, 2003).

Drobe and Logan (1992) and Logan et al., (1993) proposed that this part of northern Stikinia evolved in a mainly intraoceanic setting. This conclusion is based on: low initial Sr-ratios, + ϵ_{Nd} values and lack of inheritance patterns in zircons from the FKPS intrusions. The Proterozoic inheritance in zircons at Tulsequah (Childe, 1997) indicate a north and westward transition from an intraoceanic-setting to one either underlain by transitional or pericratonic crust or continent-derived sediments, similar to the modern Aleutian Arc. Gunning (1996) on the other hand postulated a long-lived (~150 Ma) continental margin arc setting for the Paleozoic Stikine assemblage rocks based on: the predominantly differentiated calcalkaline character of the volcanic rocks, the presence of a large, I-type polyphase pluton (FKPS) and trace element abundances of volcanic domains in the Iskut River area, and made analogy with the Java portion of the Sunda arc. The Sunda arc is characterized by calcalkaline basalt, dacite and rhyolite volcanic succession developed on 25-30 km of continental crust (Nicholls and Whitford, 1976; and Gill, 1981). The volcanics of Unit 2 have low Zr/Y ratios (Table 1 and 2) corresponding to oceanic arc and high Ta/Yb ratios of calcalkaline oceanic arc fields (Pearce, 1983; Pearce et al., 1981).

VHMS deposits form in a number of different geotectonic environments and most are associated with felsic volcanic-bearing sequences. Major- and trace element geochemical abundances of mafic (Pearce and Cann, 1973; Pearce et al., 1977; Wood, 1980; Shervais, 1982; Meschede, 1986) and felsic (Pearce et al., 1984; Whalen et al., 1987; Christiansen and Keith, 1996) volcanic rocks have been shown to reflect their source and geotectonic environments of formation. Various workers have used felsic volcanic geochemistry to define prospective versus nonprospective volcanic environments for VHMS deposits (Lesher et al., 1986; Lentz, 1998). These studies are based on HFSE-REE systematics of the felsic rocks (see Piercey et al., 2001). Preliminary geochemistry from the felsic volcanic rocks in the More Creek area (Logan et al., 2000; unpublished data and this study) have low Zr/Y ratios and Low La_{CN}/Yb_{CN} that are also similar to Archean and Phanerozoic VHMS associated felsic rocks (Barrie et al., 1993; Lentz, 1998), but rather than tholeiitic have calcalkaline affinities that have more analogies with Phanerozoic VHMS associated felsic rocks (Lentz, 1998; Piercey, et al., 2001). Calcalkaline fractionated sequences, which probably formed in arc-building (neutral to compressional) environments, are not as favorable as extensional tectonic settings (Fig. 10 in, Lentz, 1998) to host VHMS deposits.

The $(La/Yb)_{CN}$ ratios reflect the slope of the chondrite-normalized REE patterns (Fig. 4e, Table 1) and when plotted against Yb_{CN} can be used to evaluate the relative degree of compatibility between LREE versus HREE. In addition, they have been used to distinguish VHMS favorability (Lesher et al., 1986; Barrie et al., 1993; Lentz, 1998). Low $(La/Yb)_{CN}$ ratios are characteristic of tholeiitic or alkaline affinity and high ratios reflect calcalkaline affinity (Cullers and Graf, 1984, in Lentz, 1998). Figure 5e compares the Foremore/More Creek samples to the fields of Phanerozoic felsic-VHMS deposits (Lentz, 1998) formed in four different geotectonic settings. Rhyolite B and the FKPS granites have variable LREE/HREE ratios (1.5-9.5), which are dispersed along the estimated calcalkaline fractionation trend and plot in the Mt. Windsor (intra-continental back-arc) field of Lentz (1998). Rhyolite A samples, cluster together in the field for Kuroko (rifted mature intra-oceanic island-arc) rocks, which overlap with the data from the Mt. Windsor district. Both rhyolites overlap productive fields for Phanerozoic VHMS deposits. The commonality between these settings is that they are underlain by evolved continental crust (Ohmoto and Skinner, 1983; Stoltz, 1995; Lentz, 1999). Gunning (1996) suggests development of the Late Devonian Stikine arc on transitional continental crust, and old (up to 2040 Ma) ages from zircons at Tulsequah indicate inheritance of older Proterozoic zircons. Initial $^{87}Sr/^{86}Sr$ values from the diorite and tonalite phases of FKPS range between 0.7039 to 0.7043 and suggest a relatively primitive magma source region; consistent with the juvenile Nd-isotopic signatures from the felsic phases (unpublished data). The source for the enriched, calcalkaline rhyolites (A and B) is not compatible by simple fractionation but rather requires crustal contamination or addition.

STRUCTURE

The structural characteristics in the More Creek and Mess Creek areas are summarized by Holbek (1988), Gunning (1996) and Logan et al. (2000) and for the Foremore property in particular by Oliver (2003). Planar fabrics preserved in rocks of the area clearly indicate three and probably four phases of deformation.

Briefly, the earliest phase (D1) is characterized by large scale(?) recumbent to tight isoclinal folds and thrust faults. The flat-lying dominant foliation (Sn) is interpreted to be axial planar to these early structures. Bedding-cleavage intersections and minor folds suggest the earliest structures trended north and verged west-southwesterly(?). Younger, second generation folds deform bedding and the dominant foliation (Sn) about open, generally northwest-trending, southeast plunging D2 folds. The second phase cleavage (S_{n+1}) is not always well developed and is often represented by a spaced fracture cleavage rather than a good penetrative cleavage. Third phase (D3) structures are characterized by millimeter up to several meter amplitude east-trending folds, that crenulate earlier foliations (Sn and S_{n+1}) and produced an east-trending steep crenulation cleavage indicative of a north-south compressional event. A younger phase of regional folding, characterized by north-trending, upright, broadly open folds with wavelengths in the order of 1 to 2 kilometers may be the youngest phase of deformation in this part of Stikinia. It has been correlated with Cretaceous deformation that produced the Skeena fold and thrust belt located east of the Foremore property (Evenchick, 2001).

Faults

The North Zone Fault (NZF) is a north-northwest verging reverse fault that has localized quartz-pyrite-base metal ± precious metal mineralization, alteration and ductile deformation (Oliver, 2003). It does not appear to be folded by D1 or D2 and is interpreted to have evolved relatively late in the tectonic history of the area (Oliver, 2003). Kinematic data support north-northwest verging, reverse motion as the youngest movement on the NZF, but its overall parallelism with the dominant early foliation (Sn) suggest it may be an older structure related to inter-limb thrust failure during D1 deformation, that has since been reactivated.

MINERALIZATION

Cominco staked and began exploration on the Foremore property following the discovery of auriferous quartz vein float and several hundred mineralized boulders containing very fine-grained pyrite, barite, sphalerite, with minor galena and tetrahedrite (Mawer, 1988). The auriferous quartz vein material was traced to outcrop mineralization (Westmore gold zone), but the distribution of the massive sulphide boulders, located in outwash plains at the north and eastern lobes of the More glacier (i.e. north boulder field (NBF) and south boulder field (SBF) respectively) was interpreted to suggest the source lay to the west and beneath the main ice sheet of More glacier. Cominco drilled several holes through the glacier without success.

Current work by Roca Mines Inc. has resulted in the discovery of new mineralization located proximal to but, topographic above the mineralized boulder fields. The North and newly discovered BRT zones are situated above and northeast of the NBF; and the SG zone, located in the Hanging valley occurs above and up ice-flow direction of the SBF. These exploration successes permit reinterpretation of the probable source and the prospectivity of the intervening areas located above the two main boulder fields.

Felsic volcanic and sediment-hosted zinc-lead-copper±gold mineralization at the North/BRT and SG zones on the Foremore property share many of the characteristics of the Kuroko/Noranda VHMS deposits and this subclass of VHMS deposits is a prime exploration target in Paleozoic volcanic rocks of northern British Columbia. The polymetallic massive sulphide deposits, or Kuroko/Noranda subclass typically form within calcalkaline, bimodal, arc volcanic sequences characterized by basalt, andesite, dacite and rhyolite. The polymetallic massive sulphide lenses are general hosted within or adjacent to fragmental dacite or rhyolite rocks but which almost always comprise a subordinate component of the bimodal volcanic pile. The evolved tenor of the Foremore VMS mineralization (Zn-Pb-Cu-Ag-rich) is typical of evolved arc and back-arc felsic, volcaniclastic rock dominated successions.

Felsic Volcanic-Hosted Sulphide Mineralization

SG

SG mineralization consists of a 5-8 m thick stratabound zone comprised of 2-3 cm wide foliation parallel and discordant, quartz-carbonate veins mineralized with sphalerite-galena. The mineralization occupies the lower contact of a felsic dome complex and limestone-sedimentary package that projects northeastward beneath ice and snow cover. Trenching and sampling can follow the horizon for approximately 200 m southwest. A number of large boulders of heterolithic carbonate-rich debris flow containing felsic fragments and oxidized sulphide fragments occur immediately down ice (SW) from the SG zone. This unit has been interpreted by Oliver (2003) to stratigraphically overlie the felsic complex in a position upslope and covered beneath glacial ice. Sulphide clast-bearing breccias located at the top or flanks of the felsic complex are additional VMS exploration targets, which because of ice cover and the potential unconformable contact with the younger volcaniclastic units are difficult to assess.

Mapping has traced the footwall stratigraphy northeastward 1000 m at which point the felsic tuff /limestone-sill contact (mineralized horizon) re-emerges from the ice field, trending southeastward. Cominco defined a northwest trending 4-line, UTEM conductor (conductor "B") with coincident anomalous HLEM response in this area and based on the presence of SG-style float boulders recommended the conductor for drill testing (Holroyd, 1989). At the southeast end of the conductor, the felsic units are mineralized primarily with pyrite and overprinted with low temperature iron-carbonate alteration (although only limited geochemical sampling has been completed). The low conductance-conductor is interpreted to deepen westward under thickening ice (Holroyd, 1989). The area has not been drilled but the results of a Max-Min electromagnetic survey over the prospective area have delineated a 200m long anomaly, coincident with both the HLEM and UTEM anomalies obtained by Cominco (Roca Mines News release, Oct 10, 2003).

At the SG, a 4-hole, 225m diamond drill program tested base metal mineralization exposed in trenches at the base of the glacier. The holes were shallow ($3 < 50$ m) and encountered narrow widths of galena and sphalerite mineralization concentrated near the base of the felsic complex, before entering the non-mineralized-footwall limestone-sill sequence. The lower part of the felsic complex is a sericite-altered intermediate to felsic tuff/tuff breccia variably replaced by calcite and quartz veinlets and stockwork stringers which carry mineralization. Vein mineralogy includes sphalerite, galena, pyrite, tetrahedrite, and arsenopyrite, locally with gold values. The stratabound Pb-Zn-Ag mineralization at the SG was focused by permeability along stratigraphic contacts near the base of the felsic dome complex. The alteration and sulphide mineralogy suggests low temperature fluids, possibly derived from leakage and/or lateral flow away from a higher temperature (>300°C) Cu-Zn rich system associated with the felsic dome complex.

North Zone

Mineralization at the North zone consists of thin foliation parallel disseminations and lenses of pyrite, sphalerite and galena.

BRT Zone

Mineralization at the BRT zone consists of layered semi-massive to massive sphalerite, galena, pyrite and trace chalcopyrite. At the discovery outcrop the BRT sulphide horizon is 0.4 to 0.5 m thick (Photo 2). Deformation has significantly thickened the sulphide layer (1.78 m in hinge zones) and folded it into a shallow, southeast-plunging anticline. Assay results from 6 chip samples across 2.95 m at the BRT discovery zone returned a weighted average of 10.24% Zn, 8.58% Pb, 0.27% Cu, 186.6 g/t Ag and 2.04 g/t Au (Roca Mines News release, July 18, 2003). Trenching to the southwest has extended the strike length of the horizon 30 m before the 0.8 m wide zone plunges into the hillside. A chip sample across the zone at this location returned 7.5% Zn, 13.9% Pb, 444.8 g/t Ag and 1.4 g/t Au over 0.8 m.

Detailed mapping (Oliver, 2003) and regional mapping (this study), recognize a structurally complex

Photo 2. Discovery outcrop, BRT zone. Massive and semi-massive galena, sphalerite, pyrite and trace chalcopyrite layers.

package of interleaved mafic breccias and tuffs, felsic tuffs and epiclastic and sedimentary rocks which in drill core comprise three main lithologies; a structural upper, maroon and green mafic volcaniclastic unit, a medial intermediate to felsic chlorite-sericite+/-pyrite altered volcaniclastic and epiclastic unit (host to the gold-enriched base metal sulphide horizon at BRT zone), and a lower black graphitic and siliclastic sedimentary unit.

The drilling on the BRT zone totaled 896m in 7 holes, from three drill sites. The three drill setups tested the sulphide-bearing horizon along 100 m of strike length, southwest from the discovery outcrop. Results from this first phase drill program at the BRT zone intersected a thick section of variably altered and tectonized intermediate to felsic volcaniclastic rock package that is mineralized by semi-massive cm-thick layers of foliation parallel pyrite and wide m-thick intervals of disseminated blebs and streaks of pyrite. Deformation has transposed the primary features of the host lithology and recrystallized and remobilized the sulphides into interstial-matrix positions and foliation parallel concentrations. Pyrite comprises the majority of the sulphides. Preliminary gold assays from drill core have recognized a 2.3 m interval within Drill hole FM03-11 that contains 7.92 g/t Au. This zone is contained within a thicker 15.9 m sulphide-enriched interval from 85.1 m to 101.0 m. Analyses from the drilling returned low base metal values.

Broken Antler

The Broken Antler consists of a gossanous outcrop (110 x 70 m) of brecciated felsite, located one kilometer northeast of the terminus of Alexander Glacier. The mineralization was first described by Gunning (1994) and attributed to a rhyolite dome complex (~2km in diameter). Subsequent work (Harris, 2002; this study) concluded that the felsite was probably a high level differentiated phase related to the More Creek Pluton that outcrops one kilometer to the east. The felsite is a fine-grained, grey to pale pink-weathering siliceous, brittle rock commonly veined by white quartz stockwork veinlets. Microgranitic-textured tonalite or granite occupies the core of the complex. Locally, a well-developed magmatic/tectonic(?) foliation is defined by segregations of chloritized biotite, plagioclase and quartz ± potassium feldspar in the coarser-grained interior phases of the intrusive complex. At the showing (1 km north), the felsite clearly intrudes and incorporates foliated metavolcanic rocks along its margins. Mineralization is focused along the structural footwall of the felsite and comprises coarse seams, fracture-fillings and disseminated pyrite that is deeply oxidized and leached. Analyses of seven samples (Gunning, 1994) returned a maximum of 200 ppb gold and low base metal values. Additional felsite bodies, numerous 1-2 meter thick feldspar-phyric and rare quartz-phyric rhyolite dikes intrude the metavolcanic rocks north and south of Alexander Glacier. Some are gossanous and many remain virtually untested.

ISOTOPES

Galena Pb-isotopes from the newly discovered SG zone mineralization overlap with feldspar Pb-isotope values calculated from feldspar separates of the Late Devonian (369±5 Ma) Forrest Kerr Pluton (Westcott, 1991; Godwin, 1993; Childe, 1997; Logan, 2000). They lie midway between values from epigenetic Zn-Pb-Ag (Type C boulders) samples and the more radiogenic conformable VHMS Zn-Pb-Cu±Au (Type D boulders) mineralized samples on conventional Pb evolution curves. Mineralization at the SG is hosted in rhyolite interpreted to be Devonian age, while the mineralization at the BRT and north zones is thought to be younger, possibly hosted in the Early Carboniferous volcanic cycle. In addition, the Foremore data cluster together with galena Pb-isotope values from the Late Devonian (377 +9/-7 Ma) Ecstall VMHS prospect located 380 km south in the Coast belt. However, comparison with the Early Mississippian (327±1 Ma), polymetallic (Pb-Zn-Cu-Au-Ag) Tulsequah Chief deposit located 350 km northwest shows that the Pb-isotopic signatures from the Foremore, Ecstall and FKP are significantly less radiogenic. The anomalous highly radiogenic Pb-isotopes and Proterozoic inheritance in zircons at Tulsequah indicate the area is underlain by evolved pericratonic crust or continental-derived sediments which interacted with and modified the Early Mississippian magmas and by inference suggest that the Devonian and Mississippian mineralization at Foremore formed in a more primitive, mainly intraoceanic setting (low initial Sr-ratios, + ϵNd values and lack of inheritance patterns in zircons). Neodymium and strontium isotope studies of volcaniclastic rocks (Samson et al., 1989) and the Forrest Kerr Pluton (Logan et al., 1993) indicate that in the Iskut River, Stikine assemblage strata are indicative of a juvenile, mantle-derived magma source compatible with an orogenic volcano-plutonic complex that evolved in an intra-oceanic environment with no continental detrital influences.

CONCLUSIONS

Mapping and preliminary lithogeochemistry has identified three distinct and regionally extensive submarine volcanic cycles of Late Paleozoic age in Stikine assemblage rocks of the More Creek area. These include: Early to middle Devonian, Early Carboniferous and Late Carboniferous intervals. Polymetallic (gold-enriched) volcanic hosted massive sulphide mineralization is associated with felsic intervals in the Early to middle Devonian and Early Carboniferous cycles. These magmatic cycles have calcalkaline affinities. The FKPS show LREE profiles, which correspond to 'continental' trondhjemites, and a flat, slightly depleted HREE profile similar to oceanic arc trondhjemites. Small tonalite sills present near the North and BRT zones may represent the well-described association of tonalite-trondhjemite subvolcanic sills and Archean VHMS deposits (Galley, 2003).

The stratigraphy at the North and BRT zones and conformable mineralization are thought to be Early Mississippian in age, based in part on the Pb-isotope analyses of the mineralization. There is no clear age constraint and it is possible these rocks and mineralization are also Devonian. The major and trace element abundances define a Devonian group of rhyolites (A) and an Early Carboniferous group of rhyolites (B).

The Late Carboniferous volcanic cycle is characterized by non-arc basalt volcanism with alkalic affinities. Age constraints on this volcanic cycle are not tightly constrained in the study area, but correlated regionally. Rifting associated with this event may have potential to deliver heat, magma and fluids to upper levels of the crust quickly and drive hydrothermal circulation cells that could deposit massive sulphide mineralization.

Further lithogeochemical work is necessary to establish the felsic volcanic and sedimentary facies that are most prospective. Additional age dating could focus exploration onto the more prospective volcanic cycles in the Foremore area.

REFERENCES

Armstrong, R.L. (1988): Mesozoic and Early Cenozoic magmatic evolution of the Canadian Cordillera; in Rodgers symposium volume, *Geological Society of America*, Special Paper 218, pages 55-91.

Arth, J.G., Barker, F., Peterman, Z.E. and Friedman, I. (1978): Geochemistry of the gabbro-diorite-tonalite-trondhjemite suite of southwest Finland and its implications for the origin of tonalitic and trondhjemitic magmas; *Journal of Petrology*, Volume 19, Part 2, pages 289-316.

Barker, F. and Arth, J.G. (1976): Generation of trondhjemitic-tonalitic liquids and Archean bimodal trondhjemite-basalt suites; *Geology*, Volume 4, pages 596-600.

Barnes, D.R. (1989): Geological-Geochemical Report, Foremore Group, Liard Mining District; B.C. Ministry of Energy, Mines and Petroleum Resources, Assessment Report 19,379.

Barrett, T.J., and MacLean, W.H. (1994): Chemostratigraphy and hydrothermal alteration in exploration for VHMS deposits in greenstones and younger volcanic rocks, in Alteration and Alteration Processes, Lentz, D.R. ed.; *Geological Association of Canada*, Short Course Notes, Volume 11, pages 433-467.

Barrett, T.J., and MacLean, W.H. (1999): Volcanic sequences, Lithogeochemistry, and hydrothermal alteration in some bimodal volcanic-associated massive sulfide systems, in Volcanic-associated massive sulfide deposits: processes and examples in modern and ancient settings, C.T. Barrie and M.D. Hannington eds; *Society of Economic Geologists*, Reviews in Economic Geology, Volume 8, pages 101-131.

Barrie, C.T., Ludden, J.N., and Green, T.H. (1993): Geochemistry of volcanic rocks associated with Cu-Zn and Ni-Cu deposits in the Abitibi subprovince; Economic Geology, Volume 88, pages 1341-1358.

Childe, F. (1997): Chronology and radiogenic isotopic studies of the Kutcho, Granduc, Anyox and Tulsequah Chief volcanogenic massive sulphide deposits; in Volcanogenic massive sulphide deposits of the Cordillera project, Unpublished M.Sc. thesis, *The University of British Columbia*, 298 pages.

Christiansen E.H., and Keith J.D. (1996): Trace element systematics in felsic magmas: a metallogenic perspective, *in* Trace element geochemistry of volcanic rocks: applications for massive sulfide exploration, D.A.

Wyman ed.; *Geological Association of Canada*, Short Course Notes, Volume 12, pages 115-154.

Evenchick, C.A. (2001): Northeast-trending folds in the western Skeena Fold Belt, northern Canadian Cordillera: a record of Early Cretaceous sinistral plate convergence; Journal of Structural Geology, Volume 23, pages 1123-1140.

Gabrielse, H. and Yorath, C.J. (1991): Tectonic Synthesis, Chapter 18; in Geology of the Cordilleran Orogen in Canada, Gabrielse, H. and Yorath, C.J., eds, *Geological Survey of Canada*, Geology of Canada, no 4, pages 677-705.

Galley, A.G. (1996): Geochemical characteristics of subvolcanic intrusions associated with Precambrian massive sulfide districts, *in* Trace element geochemistry of volcanic rocks: applications for massive sulfide exploration, D.A. Wyman ed.; *Geological Association of Canada*, Short Course Notes, Volume 12, pages 239-278.

Galley, A.G. (2003): Composite synvolcanic intrusions associated with Precambrian VMS-related hydrothermal systems; *Mineralium Deposita*, Volume 38, number 4, pages 443-473.

Gill, J.B. (1981): Orogenic andesites and plate tectonics; Springer-Verlag, 390 pages.

Godwin, C.I. (1993): Arc and back-arc related galena lead: Stikine terrane; in Metallogenesis of the Iskut River area, northwestern B.C., second annual report, Mineral Deposit Research Unit, The University of British Columbia.

Gunning, D. R. (1995): Report on the Antler Property; B.C. Ministry of Energy, Mines and Petroleum Resources, Assessment Report 24076.

Gunning, M.H. (1996): Definition and interpretation of Paleozoic volcanic domains, northwestern Stikinia, Iskut River area, British Columbia; Unpublished Ph.D. thesis, *University of Western Ontario*, 389 pages.

Gunning, M.H., Patterson, K. and Green D. (1994): New Sulphide occurrences in the Northeastern part of Iskut River map area and southeastern part of Telegraph Creek map area, Northwestern British Columbia; in Current Research 1994 Part A, *Geological Survey of Canada*, Paper 94-1, pages 25-36.

Harris, A.S. (2002): Summary report on the Foremore project; unpublished company report, Equity Engineering Ltd., 34 pages.

Höy, T. (1991): Volcanogenic massive sulphide deposits in British Columbia; in Ore deposits, tectonics and metallogeny in the Canadian Cordillera, *B.C. Ministry of Energy, Mines and Petroleum Resources*, Paper 1991-4, pages 89-123.

Holroyd, R.W. (1989): Foremore property assessment report on geophysical surveys 1989; *B.C. Ministry of Energy, Mines and Petroleum Resources*, Assessment Report 19380.

Lentz, D.R. (1996): Trace element systematics of felsic volcanic rocks associated with massive-sulfide deposits in the Bathurst Mining Camp: Petrogenetic, tectonic and chemostratigraphic implications for VMS exploration, *in* Trace element geochemistry of volcanic rocks: applications for massive sulfide exploration, D.A. Wyman ed.; *Geological Association of Canada*, Short Course Notes, Volume 12, pages 359-402.

Lentz, D.R. (1998): Petrogenetic evolution of felsic volcanic sequence associated with Phanerozoic volcanic-hosted massive sulphide systems: the role of extensional geodynamics, in Ore Geology Reviews 12, Elsevier, New York, pages 289-327.

Lesher, C.M, Goodwin, A.M., Campbell, I.H., and Gorton, M.P. (1986): Trace element geochemistry of ore-associated and barren felsic metavolcanic rocks in the Superior Province, Canada; Canadian Journal of Earth Sciences, Volume 23, pages 222-237.

Logan, J.M., and Koyanagi, V.M. (1994): Geology and mineral deposits of Galore Creek area (NTS 104G/3 & 4); *B.C. Ministry of Energy and Mines*, Bulletin 92, 96 pages.

Logan, J.M., Drobe, J.R., McClelland W.C., and Anderson, R.G. (1993): Devonian intraoceanic arc magmatism in northwestern Stikinia; *Geological Association of Canada/Mineralogical Association of Canada*, Edmonton '93, Program with Abstracts, page A60.

Logan, J.M., Drobe, J.R, and McClelland, W.C. (2000): Geology of the Forrest Kerr - Mess Creek area, northwestern British Columbia (NTS 104B/10, 15 & 104G/2 &7W); *B.C. Ministry of Energy and Mines*, Bulletin 104, 164 pages.

McClelland, W.C. (1992): Permian and older rocks of the southwest Iskut River map area, northwestern British Columbia; *in* Current Research, Part A, *Geological Survey of Canada*, Paper 92-1A, pages 303-307.

McClelland, W. C., Mattinson, J.M., Anderson, R. G., Logan, J.M. and Drobe, J.R. (1993): Late Devonian plutonism in the Stikine terrane, British Columbia (abstract); *Geological Society of America*, Abstracts with Programs, Volume 25, page 117.

Mawer, A.B. (1988): Geological-Geochemical Report, Foremore Group; *B.C. Ministry of Energy, Mines and Petroleum Resources*, Assessment Report 18105.

Meschede, M. (1986): A method of discriminating between different types of mid-ocean ridge basalts and continental tholeiites with the Nb-Zr-Y diagram; *Chemical Geology*, Volume 56, pages 207-218.

Mihalynuk, M.G. Smith, M.T., Hancock, K.D. and Dudka, S. (1994): Regional and economic geology of the Tulsequah River and Glacier Areas (104K/12 & 13); in Geological Fieldwork 1993, B. Grant and J.M. Newell, eds; *B.C. Ministry of Energy, Mines and Petroleum Resources*, Paper 1994-1, pages 171-197.

Monger, J.W.H. (1977): Upper Paleozoic rocks of the western Cordillera and their bearing on Cordilleran evolution; *Canadian Journal of Earth Sciences*, Volume 14, pages 1832-1859.

Murphy D.C., and Piercey, S.J. (1999): Finlayson project: geological evolution of Yukon-Tanana terrane and its relationship to Campbell Range belt, northern Wolverine Lake map area, southeast Yukon; *in* Yukon Exploration and Geology 1998, Exploration and Geological Services Division, Yukon, *Indian and Northern Affairs Canada*, pages 47-62.

Murphy, D.C., van der Heyden, P., Parrish, R.R., Klepacki, D.W., McMillan, W., Struik, L.C. and Gabites, J. (1995): New Geochronological Constraints on Jurassic deformation of the western edge of North America, southeastern Canadian Cordillera; in Miller, D.M., and Busy, C., Jurassic Magmatism and Tectonics of the North

American Cordillera: Boulder Colorado, *Geological Society of America*, Special Paper 299, pages 159-171.

Nelson, J. and Payne J.G. (1984): Paleozoic volcanic assemblages and volcanogenic massive sulphide deposits near Tulsequah, British Columbia; *Canadian Journal of Earth Sciences*, Volume 21, pages 379-381.

Nelson, J. and Mihalynuk, M.G. (1993): Cache Creek Ocean: Closure or Enclosure?; *Geology*, Volume 21, pages 173-176.

Nicholls, I.A., and Whitford, D.J. (1976): Primary magmas associated with Quaternary volcanism in the western Sunda Arc, Indonesia; in Volcanism in Australasia, R.W. Johnson ed., Elsevier, pages 77-90.

Ohmoto, H. and Skinner, B.J. (1983): The Kuroko and related volcanogenic massive sulfide deposits: introduction and summary of new findings; in The Kuroko and related volcanogenic massive sulfide deposits, H. Ohmoto and B.J. Skinner eds., *Economic Geology*, Monograph 5, pages 1-8.

Oliver, J.L. (2003): Summary of geological observations: Roca Mines's Foremore property, northwestern B.C.; unpublished report for Roca Mines Inc., 30 pages.

Okulitch, (2002): Time scale, Geological Survey of Canada.

Pearce, J.A. (1996): A user's guide to basalt discrimination diagrams, *in* Trace element geochemistry of volcanic rocks: applications for massive sulfide exploration, D.A. Wyman ed.; *Geological Association of Canada*, Short Course Notes, Volume 12, pages 79-113.

Pearce, J.A., and Cann, J.R. (1973): Tectonic setting of basic volcanic rocks determined using trace element analyses; *Earth and Planetary Science Letters*, 19, pages 290-300.

Pearce, J.A. and Norry, M.J. (1979): Petrogenetic implications of Ti, Zr, Y and Nb variations in volcanic rocks; *Contributions to Mineralogy and Petrology*, Volume 69, pages 33-47.

Pearce, J.A., Harris, N.B.W., and Tindle, A.G. (1984): Trace element discrimination diagrams for the tectonic interpretation of granitic rocks; *Journal of Petrology*, 25, pages 956-983.

Piercey, S.J., Paradis, S., Murphy, D.C., and Mortensen, J.K. (2001): Geochemistry and paleotectonic setting of felsic volcanic rocks in the Finlayson Lake volcanic-hosted massive sulphide district, Yukon, Canada; Economic Geology, Volume 96, pages1877-1905.

Rautenschlein, M., Jenner, G.A., Hertogen, J., Hofmann, A.Q.W., Kerrich, R., Schminke, H.U., and White, W.M. (1985): Isotopic and trace element composition of volcanic glasses from the Akaki Canyon, Cyprus: implications for the origin of the Troodos ophiolite; *Earth and Planetary Science Letters*, 75, pages 369-383.

Samson, S.D., McClelland, W.C., Patchett, P.J., Gehrels, G.E. and Anderson, R.G. (1989): Nd isotopes and Phanerozoic crustal genesis in the Canadian Cordillera; *Nature*, Volume 337, pages 705-709.

Sawkins, F.J. (1990): Metal deposits in relation to plate tectonics; Second Edition, *Springer-Verlag*, 461 pages.

Sebert, C. (1998): Stratigraphy, lithogeochemistry, alteration and mineralization at the Tulsequah Chief massive sulphide deposit, northwestern British Columbia; Unpublished M.Sc. thesis, *The University of British Columbia*, 331 pages.

Sherlock R.L., Childe, F., Barrett, T.J., Mortensen, J.K. Lewis, P.D., Chandler, T., McGuigan, P., Dawson, G.L. and Allen, R. (1994): Geological investigations of the Tulsequah Chief massive sulphide deposit, northwestern British Columbia; *in* Geological Fieldwork 1993, B. Grant and J.M. Newell, eds; *B.C. Ministry of Energy, Mines and Petroleum Resources*, Paper 1994-1, pages 279-285.

Shervais, J.W. (1982): Ti-V plots and the petrogenesis of modern and ophiolitic lavas; *Earth and Planetary Science Letters*, 59, pages 101-118.

Stolz, A.J. (1995): Geochemistry of the Mount Windsor volcanics: implications for the tectonic setting of Cambro-Ordovician volcanic-hosted massive sulphide mineralization in northeastern Australia; *Economic Geology*, Volume 90, 1080-1097.

Sun, S.S., and McDonough, W.F. (1989): Chemical and isotopic systematics of oceanic basalts: Implications for mantle composition and processes, in Saunders, A.D., and Norry, M.J., eds., Magmatism in the Ocean Basins; *Geological Society of London*, Special Publication 42; pages 313-345.

Webster, I.C.L. and Ray, G.E. (1991): Skarns in the Iskut River-Scud River region, Northwest British Columbia; *in* Geological Fieldwork 1990, *B.C. Ministry of Energy, Mines and Petroleum Resources*, Paper 1991-1, pages 245-253.

Westcott, M.G. (1991): An investigation of possible genetic and/or spatial links between four distinct mineralized boulder populations located on the Foremore claim group, northwest British Columbia, Unpublished M.Sc. Thesis, *Queen's University*, 45 pages.

Westcott, M.G. (1991): Geological work on Fore 29 and Fore 30 mineral claims, Liard Mining Division; *B.C. Ministry of Energy, Mines and Petroleum Resources*, Assessment Report 21936.

Whalen, J.B., Currie, K.L., and Chappell, B.W. (1987): A-type granites: geochemical characteristics, discrimination and petrogenesis; Contributions to Mineralogy and Petrology, Volume 95, pages 420-436.

Wheeler, J.O. and McFeely P. (1991): Tectonic assemblage map of the Canadian Cordillera and adjacent parts of the United States of America; *Geological Survey of Canada*, map 1721A.

Winchester, J. A., and Floyd, P. A. (1977): Geochemical discrimination of different magma series and their differentiation products using immobile elements; *Chemical Geology* (Isotope Geoscience Section), Volume 20, pages 325-343.

Wood, D.A. (1980): The application of the Th-Hf-Ta diagram to problems of tectonomagmatic classification and to establishing the nature of crustal contamination of basaltic lavas of the British Tertiary volcanic province; *Earth and Planetary Science Letters*, 50, pages 11-30.

Zartman, R.E. and Doe, B.R. (1981): Plumbotectonics - The model, in Evolution of the Upper Mantle, Zartman, R.E. and Taylor, S.R., eds; Tectonophysics, Volume 75, pages 135-162.

THE B.C. MINERAL POTENTIAL PROJECT - NEW LEVEL 2 MINERAL RESOURCE ASSESSMENT METHODOLOGY AND RESULTS

By D.G. MacIntyre, N.W.D. Massey and W.E. Kilby

KEYWORDS: Mineral potential, resource assessment, Level 1, Level 2, Mark 3B simulator, Gross-in-place-value, ordinal ranking, expert workshops, sub-tracts, redistribution

INTRODUCTION

In August 2002, the Geological Survey Branch (GSB) of the Ministry of Energy and Mines was asked by the Ministry of Sustainable Resource Management to undertake a Level 2 Mineral Resource Assessment (MRA) of the Coast Information Team's (CIT) project area which encompasses approximately 11 million hectares. This was followed by a similar request in February 2003 to do the Lillooet Land Resource Management Plan (LRMP) area. The primary purpose of these assessments was to provide more detailed information on metallic and industrial mineral resource potential in support of concluding detailed land use plans. The Coastal resource assessment was carried out in early October, 2002 and final results delivered to the Ministry of Sustainable Resource Management and the CIT at the end of December 2002. The Lillooet assessment was completed in April 2003. This report summarizes the methodology used in these projects and briefly reviews the results which are now posted on the MapPlace website (http://www.mapplace.ca). A review of the original Level 1 MRA methodology is also included here because the Level 2 MRA used the results from the original assessment.

All users of mineral resource assessments should be aware that they are based on historic information and current knowledge. They are, therefore, a snapshot in time which can change with more information and knowledge. One only has to think of the discovery of diamond mines in Canada in the 1990s to recognize the difficulty of assessing hidden resources. For this reason areas of low mineral potential may reflect our lack of understanding of the geology of the region, not an absence of future mines. As well, mineral potential assessments can only be used effectively at the scale at which they were completed. Just as one wouldn't use a map of the province to locate a house in your community, provincial scale mineral potential maps cannot be used for detailed resource assessments in small areas.

HISTORY OF THE MINERAL POTENTIAL PROJECT

Early in 1992, the British Columbia Geological Survey Branch of the Ministry of Energy, Mines and Petroleum Resources (later Employment and Investment and now Energy and Mines) launched the Mineral Potential Project to develop the information required by the Commission on Resources and the Environment (CORE) over a 5-year period. The Geological Survey Branch dedicated in excess of 30 geologist-years to meet this information requirement. Completion of the assessments in step with the land use planning processes was critical. This earlier assessment is referred to here as a Level 1 MRA. Results of this MRA are presented in Figure 1.

The first major task of the Mineral Potential Project group was to determine the type of information that would be useful in land use negotiations and develop a methodology which would best produce this information. A two-day workshop involving participants with recent experience in producing and using Mineral Resource Assessments in Canada and around the world determined that the MRA products must be quantitative rather than qualitative, provide a ranking of the land base, have major input from experts from the mining and exploration industries, produce digital GIS-compatible products and be readily available.

Quantitative, easily understood results were desired because the LRMP process involved people with a wide range of technical and non-technical backgrounds who had to consider the MRA results in the decision-making process. In addition, quantitative information can be used in subsequent socio-economic analysis. Ranking of the land base was necessary because the Protected Areas Strategy dictated that a target of 12% of the land area in each region would be protected, double the amount protected at that time. A major objective of the Mineral Potential Project was therefore to rank the relative mineral potential of the land base so that planners could easily identify areas with the lowest relative mineral potential during their land use planning.

The mining and exploration industries of BC have built an enormous knowledge base that is not in the public domain. Their involvement and cooperation gave us access to some of this knowledge and also enabled us to familiarize public sector stakeholders with the strengths and limitations of the MRAs. Government dictated production of all information for the land use planning processes in Geographic Information System compatible digital format. Adherence to this policy assured the information was easily incorporated into the analysis systems used by the planners. In addition, storage of the information in digital format provides an opportunity to more easily upgrade the information in the future. Virtually all the data and map products discussed in the article are now available over the Internet at **www.em.gov.bc.ca/Mining/Geolsurv**.

LEVEL 1 MINERAL RESOURCE ASSESSMENTS

Based on the results of the workshop, a plan for the production of MRAs in BC was developed that was based on the United States Geological Survey's "Three Part Mineral Assessment Methodology" (Singer, 1993). Modifications were made to their procedure to meet the specific requirements of this project. Early in the life of the project, a number of minor adjustments were made to the initial methodology. This methodology has been applied consistently to all assessment regions, so the results from one region may be compared to the results from a neighboring region. Two different techniques are used to assess metallic and industrial mineral commodities due to their very different dependence on infrastructure and markets. A six-step process is used for the **metallic resource assessments**:

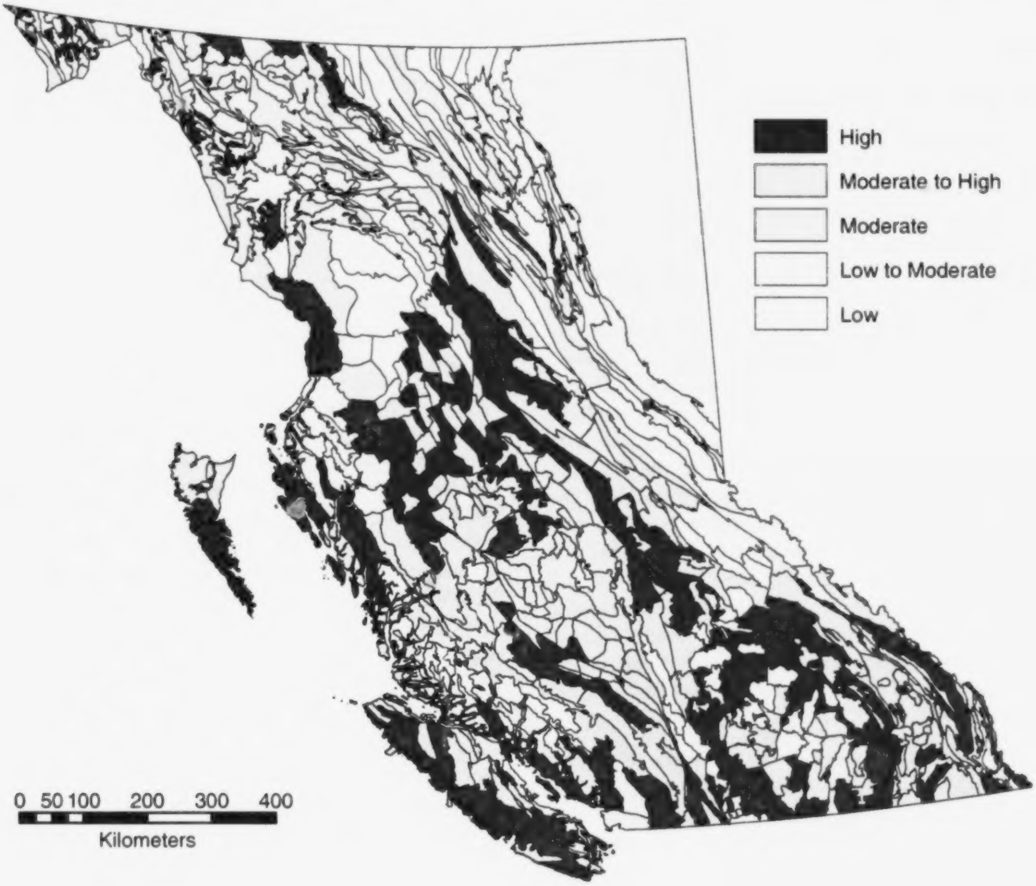

Figure 1. Metallic mineral potential map for B.C. based on the Level 1 MRA completed in 1997. Total number of tracts is 794.

1. compile geology
2. select mineral assessment tracts

3. tabulate discovered resources and construct deposit models
4. employ a team of industry and government experts to estimate the number of undiscovered deposits by deposit type and tract
5. determine quantities of metallic commodities remaining to be discovered using the Mark3B Mineral Resource Assessment Monte Carlo simulator
6. calculate the gross in place value (GIPV) of each tract based on the undiscovered and known commodities it contains.

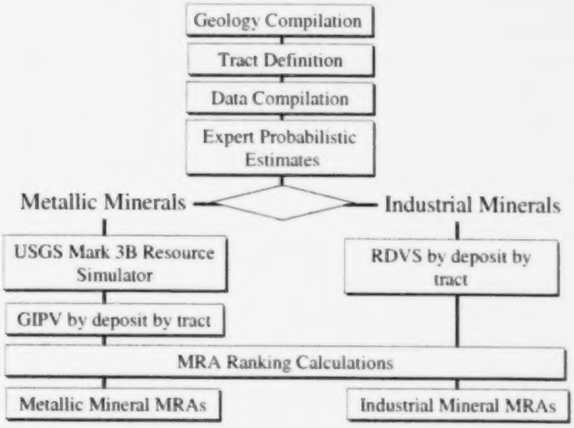

Figure 2. Flow chart for the Level 1 MRA process.

For **industrial mineral assessments** the first 4 steps are the same. However, instead of using the Mark3B simulator and associated GIPV, a relative ranking of industrial mineral deposit types was employed (Kilby *et al.*, 1999). All industrial mineral deposit types were given a relative ranking score from 1 to 100 based on their perceived value and viability. This relative deposit value score (RDVS) was used to determine the importance of each tract with respect to undiscovered deposits. The estimates are then blended with the value of discovered industrial mineral deposits to produce the overall industrial mineral tract assessment ranking.

Industrial Minerals Relative Deposit Value Scores (RDVS)

Metallic and industrial mineral deposit evaluations require different valuing methods. A methodology was developed for the Level 1 MRA project to provide a meaningful comparison between resource assessment tracts based on their industrial mineral potential. This methodology is described in Kilby *et al.* (1999).

Generally, metals are sold on the world market, they are relatively highly priced, and transportation costs are relatively minor compared to mining and refining costs. Providing that a company can produce the metal at or below market price it can generally sell the product relatively easily. Therefore, metal mines can be developed at considerable distances from population centres or processing plants. With industrial minerals the situation is more complex. Many industrial mineral commodities have low unit values. Thus transportation costs are a major consideration and deposits have to be close to market, or have access to inexpensive transportation, to become producers. This situation exists because the geological resources far exceed the anticipated demand for the commodity in the foreseeable future. For example, in some parts of British Columbia there is excellent potential to locate large limestone deposits in areas where it is impossible to transport the rock or possible products (e.g. cement, lime) economically to the market. In other words, there are significant potential geological resources, but the demand for the commodity limits the value of the resource for the foreseeable future (a relatively uncommon situation for metallic deposits). If the value of in-place resources for deposits like this were used in mineral potential assessments, it would overshadow the value of smaller deposits with readily available markets or high unit values. Since there is a limited market for most of the industrial minerals, estimates of the relative value of industrial mineral resources must often be "capped" to provide a meaningful value for planning processes.

Given the difficulties associated with determining a realistic "gross in place value" (GIPV) for industrial mineral assessments, the GSB developed a new approach. In this process two different assessments are made, one for metallic commodities, and one for industrial mineral commodities. The results are presented separately and no attempt is made to equate or combine the results of the two assessments.

The Level 1 ranking of the land base for metallic deposits is based on the GIPV of commodities in each tract contained in both known and a predicted number of undiscovered deposits. The GIPV of the commodities in each deposit are used to generate a total dollar score per hectare for each tract (Kilby, 1995, 1996). These total dollar scores per hectare are then used to rank all of the tracts under consideration. The GIPV of many industrial mineral deposits is not an acceptable way to compare their relative values because of market constraints. The industrial mineral assessment used a deposit score system where each deposit type was given a "relative deposit value score" (RDVS) from 1 to 100. The RDVS provides a relative ranking for the industrial mineral deposit types and may vary from one geographic area of the province to another. So while the relative deposit rank of metallic deposits is based solely on the value of contained metals or the "gross in place value" (GIPV) industrial mineral deposit relative rankings consider the following six characteristics:

1. commodity unit-value,
2. size and location of potential market,

3. deposit grade and size,
4. transportation costs,
5. existing infrastructure, and
6. extraction costs.

In the industrial mineral resource assessment process, the RDVS is used in the same manner as the total GIPV of all the commodities in a metallic mineral deposit to describe the relative value of each undiscovered deposit type.

Deposit Models

Descriptive deposit models were developed as part of the Level 1 MRA for mineral deposits that were known and believed to exist in British Columbia. This work built on the work by the USGS and others (Cox and Singer, 1986) but updated these global models and more closely described characteristics expected in BC. Along with the descriptive models, a classification framework was established in which deposit types were ordered according to their genetic characteristics (Lefebure and Ray, 1995, Lefebure *et al.*, 1995 and Lefebure and H y, 1996; Simandl *et al.*, 1999).

Descriptive deposit models are essential to the BC mineral resource assessment process. They provide the standardization required to assure that all participants and users understand exactly what is meant when discussing a given deposit type. The deposit examples given in each model help the estimators visualize the deposit type being estimated. The deposit description assists the estimators during the estimation process by identifying characteristic geological, geochemical, geophysical, alteration and weathering features.

MINFILE deposit classification

The MINFILE database of mineral occurrences in the province contains about 12,000 entries. At the start of the Level 1 MRA, this database was in good shape but did not contain uniform deposit classification information. Consequently, a series of contracts were let to industry consultants to classify the deposits that were listed in MINFILE. The contractors assigned a given deposit up to four possible classifications in order of importance. This classification information is now incorporated into MINFILE. Classification of all known occurrences provided a database that was used for several purposes during the mineral resource assessment. First, the classifications allowed associated resource tonnages to be included in the calculations if they met the qualifying criteria for inclusion in the digital models. Second, knowing the locations of all deposits of a given deposit type in MINFILE was very helpful to the experts during the estimation process.

Geology Compilation

Mineral Resource Assessments rely on accurate, up-to-date geologic information since geology is the primary control for the distribution of mineral resources in the Earth's crust. A major task during the original Level 1 MRA was to compile the geology of the province at a scale of 1:250 000. All available information was examined and reinterpreted using the latest information on the geology of the region. Typically, all available provincial, federal, academic and industry work was compiled and digitized to form the final map product. More than 30 geologist-years were dedicated to this effort. All compilations were produced in GIS compatible digital format and were made available for download and viewing over the Internet (http://www.mapplace.ca). This geological compilation formed the basic framework on which all subsequent MRA analysis was performed.

MRA Tracts

Upon completion of the geological compilation, the province was divided into mineral assessment tracts. These tracts are based on common geologic features and their boundaries correspond to existing geologic boundaries such as faults or significant changes in the age and types of rocks present. Once defined, these tracts become the base unit areas in which the assessments are performed. The original Level 1 MRA resulted in the definition of 794 tracts in the province. The size of tracts can vary significantly but in general were intended for use on a broad regional scale (e.g. 1:250 000). The average size of tracts in the Level 1 assessment is about 100 000 hectares. For each tract, permissive deposit types were determined and an estimate for their existence within the tract in question was made by a panel of experts.

Deposit Model Data Preparation

The two types of input required for the Monte Carlo Mineral Resource Simulator are the experts' estimates of the potential for new discoveries and the digital deposit models describing the grade and tonnage distribution of each deposit type for which the simulator will be used. The digital deposit model contains a list of realistic deposit grades and tonnages for the model types that might be found in the area being assessed. The USGS has constructed many of these models using deposits from around the world. In some cases the parameters of these models were modified to better describe probable grade and tonnage distributions for deposits likely to be found in British Columbia. New models were required where an adequate model did not exist. In some cases existing USGS models were combined or subdivided to better accommodate the British Columbia situation (Grunsky, 1995).

Known Resources

The final resource assessment value for each tract incorporates both the known and yet to be discovered resources. The known resource values were compiled as part of the Level 1 MRA project. Each mineral occurrence in the provincial database was researched to see if any resource values had ever been published. All deposits with resource values were tabulated and their deposit types evaluated. These values were incorporated into the digital deposit models that are used as part of the input to the Mark3B simulator. The results of this resource compilation work were subsequently incorporated into the MINFILE database and have been published as Open File 1995-19 (MINFILE Team, 1995). This publication is the source of resource values used in the final calculation of the Level 1 tract assessment score. The resource values were converted to a dollar value based on a commodity price list developed for the Level 1 assessment.

Commodity Values

A dollar value was established for each commodity to allow the calculation of gross in-place values (GIPV) for each tract. In the Level 1 MRA, the dollar value used for each commodity was the average market value of that commodity for the ten-year period from 1981 to 1990. The dollar values used for the Level 2 MRA described in this report are based on either December, 2002 commodity prices or averages for the last ten years as of the end of 2002.

Resource Estimation

Mineral resource assessments have a long history and an associated large number of assessment methodologies. At the beginning of the Level 1 MRA project a workshop was organized to obtain input from government, university and industry sources on the type of methodology that would be best suited to our required products, our existing databases, our resources and our time constraints. The workshop was held in Victoria, BC on April 22 and 23, 1992. The content and results of the workshop are described in detail in Kilby, 1992.

The estimation procedure that was developed for the Level 1 MRA project incorporated several significant modifications to the USGS three part methodology. In the USGS methodology a single set of estimation values is sent to the simulator. If a group of estimators were involved, this single estimation would have been obtained by consensus. A great deal of work in the field of psychometrics has shown that a true consensus may be unachievable, and certainly would not be achievable within the time constraints most resource assessment projects are faced with. The interaction of people's personalities and agendas would override the information being solicited in a group setting (Acquired Intelligence Inc., 1993). In order to reduce stress and undo influence, each estimator was allowed to make estimates in confidence. The weighted scores provided by the estimators were then used to produce a weighted average of the estimates and obtain a single group estimate for input to the simulator.

The Mark3B simulator requires estimation input at discrete confidence intervals. However, making estimates at specific confidence intervals is believed to restrict the accurate expression of the estimators' true feelings. This is believed to be due to the fact that a great deal of concentration is diverted to thinking about the confidence intervals rather than the estimate being made. An alternative way to record the estimates, and the one used in both the Level 1 and Level 2 MRA projects, is based on fuzzy logic theory. In this method the estimator records the value as a position between two end points. The two end points being, "no chance of a deposit" (0% confidence) and "certainty of a deposit" (100% confidence) (Acquired Intelligence Inc., 1993). The simple linear scale is believed to capture a more realistic sample of the estimator's feelings than the discrete probability level entry style of the USGS three-part methodology. Once the estimates are recorded in this manner discrete probability level values are derived numerically.

Estimation Workshops

The Level 1 MRA involved convening estimation workshops for different regions in the province in order to solicit the required expert estimations for the assessment. Industry and government personnel familiar with a given region and mineral deposit types being assessed were invited to the workshops. These experts were divided into groups of 3 to 4 individuals and each group was assigned a series of deposit types to assess. A large amount of background information, such as the geological compilation, MINFILE occurrence maps and geochemical maps were prepared prior to the workshop to assist the estimators. Today most of this information is provided on-line through the MapPlace web site (www.MapPlace.ca).

Estimators

Estimators were invited to the workshops based on their expertise in the area being assessed and their familiarity with specific deposit types. Naturally, for any given area, one or more individuals might have a better level of knowledge to bring to the table. In order to capture this variability and allow for some weighting of the estimates, each estimator was asked to give a numerical score for their fellow estimators that reflected how they perceived each persons knowledge level.

Estimators were not asked to rate their own knowledge level and were automatically given a score of 50.

Workshop Data

Geological information forms the basis of all discussions during both the Level 1 and Level 2 MRA workshops. At the workshops, this basic information was provided as both paper maps at 1:250 000 scale and as online access to the MapPlace web site. Other spatial data sets such as geochemistry, mineral occurrences and tract outlines were usually superimposed on the geology in the form of overlays or plotted directly on the printed maps. In general, as much as possible of the spatial information was made available in the same projection and at the same scale to facilitate efficient use of time by the estimators.

For some data sets it proved to be more important to have the supporting information available in its original format rather than in a totally integrated format because that was how the estimators were familiar with it. Geophysical information, for example, was always made available but was usually in its published format. Though the format was not digital, it was used for some deposit types and proved to be easily integrated by the estimators.

In addition to the information presented in map format, a large amount of material was made available in text format. A compendium of the following information was provided to each estimation table:

- descriptive deposit models
- graphs of the digital deposit models
- a list of all deposit types with their median tonnages and grades
- a small map displaying all tracts in the study area
- a list of all tracts and their areas
- a list of all resource bearing deposits by tract
- a list of all MINFILE occurrences by tract with deposit type information
- a tracking sheet for the table facilitator to log estimates made.

The PC based MINFILE/pc database system was also made available at all workshops.

In addition to information that the project made available at the workshops, estimators brought company information, usually in the form of private reports or works in progress that proved extremely useful. This private information was freely shared at the estimation tables and was essential to the success of the process. More important still was the personal experience and knowledge of the estimators; it was key to the success of the assessments.

Estimation Process

Each Level 1 estimation workshop began with a presentation that described the estimation process, its rules, the information available, the estimator's responsibilities and how the estimation results would be processed. A second presentation by a geologist involved in the area's geological compilation and tract selection described the geology and metallogeny.

The invited estimators were divided into groups of 3 to 4 people. Each group was assigned a series of mineral deposit types and their task was to provide estimates for each tract in the entire study area. For example, they might be asked to estimate the number of copper and iron skarns and multi-element veins deposits for the whole of Vancouver Island. Each group or table consisted of these estimators and one facilitator. The facilitator's purpose was to keep the process on track, manage the coding sheets and make sure the rules of estimation were followed. The facilitator did not make any estimates but was free to participate in any discussions or assist in any way possible. Each group was assigned a table to work at and all tables were relatively close to each other to promote consultation with other tables should the need arise.

Four basic guidelines were followed by the estimators:

1. The estimators made their own estimate in confidence. No table consensus was sought.
2. Each person made a confidential evaluation of the other estimators with respect to each tract/deposit model combination.
3. If all estimators agreed that a particular deposit type would not be found in a tract, then no estimate was made, but if at least one estimator felt there was a chance for the deposit type to occur in the tract then everyone made an estimate.
4. The deposit size, for this process, was the median tonnage of the digital deposit model for the deposit type.

A typical sequence of actions for the estimate of a single tract/deposit type combination would be:

1. A general table discussion of the tract geology and the characteristics of the deposit type would often result in the group identifying characteristics of the tract that were favourable for the deposit type. All available information sources would be used during this step, such as MINFILE, geochemistry, geology, geophysics and personal knowledge.
2. The group would identify any known occurrences of the deposit type being estimated from MINFILE. Care was taken to properly include these known occurrences. So long as an occurrence did not have defined resources, it

influenced the estimates of undiscovered deposits. If it had significant known resources but was not expected to be enlarged through additional exploration by at least the amount of the digital deposit model median tonnage, it was excluded because the resources would be counted as inventory. If there was an opportunity for a deposit to be increased in size by at least the amount of the median tonnage for the deposit model type, an estimate for this additional amount could be considered in estimators' evaluation. In this case, the already known resources would be considered as inventory and the potential new resources possible through additional exploration would be considered as potential resources.

3. When each estimator recorded estimates for a single deposit type they would do the following:
   - Ask themselves "How confident am I that at least one more deposit of the median tonnage size can be found in this tract?" They would then place a tick mark on the estimation scale and the number one above it to record the number of deposits associated with the estimation tick mark (Figure 3).
   - Then they would proceed by asking themselves how confident they were that at least two deposits of the median tonnage could be found. In this instance the probability estimate tick mark is labeled 2. Estimators were not restricted to increments of one deposit but could choose any number that was appropriate. They were, however, limited to a total of six tick marks on the scale.
   - Then if they wished, they could add a single tick mark to the scale, which recorded the confidence level, at which they were confident no deposits could be found. This option was often confusing and required care in use. If this option was not provided, then the simulator assumed a default value for zero deposits because the program always assumes that there is some chance of the deposit type existing. Although this feature is used to help constrain the simulator, it was seldom used by the estimators.
   - Following completion of their estimates, they were required to evaluate each of the other estimators for that tract/deposit type combination. To do this they recorded the estimators' initials and record a ranking score. They were required to distribute 50 ranking points between the other estimators at the table. In this way they could adjust the weight placed on the others' estimates in accordance to their feeling of each person's knowledge of the tract and deposit type.
   - Finally the estimators would place one tick on the estimation confidence scale recording their overall feeling of the quality of that estimate. This was not a measure of their confidence in their own estimation but was a measure of their confidence in the quality of the estimation made by the group as a whole that included the general group knowledge of the tract and deposit type, the quality of the information available and the quality of the estimators. This value is not used in calculating the potential of the tracts but has value for gauging the quality of the estimate should the issue arise in the future.
4. Once all the estimates for the tract/deposit type combination were completed, the facilitator would check to make sure all required information had been recorded and then staple all the work sheets together.
5. The table would then move on to the next tract/deposit type combination.

Pre-Simulation Estimate Preparation

Upon completion of the estimation of the potential for undiscovered mineral deposits in a tract, the information captured on the coding sheets was converted into digital files. These files were then processed to provide input into either the Mark3B simulator or the industrial mineral evaluation process.

The estimation coding sheets were processed once a workshop was completed. The initial step was to digitize the linear Estimate Scale on each sheet. This digitization involves measurement of the distance along the estimation bar, from 0 to 100 for each tick mark made by the estimator.

Once all the estimation-coding forms were digitized the information was recorded into computer files. Upon completion of the data entry phase, the multiple estimates for each group/tract/deposit combination must be reduced to a single weighted estimate based on the weights assigned by each estimator at the table. The QuickBasic program RAW2MARK.exe written by Ward Kilby produces a single weighted estimate for each tract/deposit type. Two output files are created by the program, one containing a script of input values for the Mark3B simulator and the other containing the weighted estimates of the number of deposits that the group thought could be found in the tract at the 90, 50, 10, 5 and 1 percent confidence levels. The program uses linear interpolation between the values noted on the coding sheet to calculate the number of deposits expected at the five discrete confidence points needed for input to the Mark3B simulator. Simple weighted averaging is used to combine all the estimates for a single tract/deposit type combination.

As described earlier, each estimator was required to rate each of the other estimators at the table by distributing 50 ranking points between the other estimators based on the estimator's feeling of their relative knowledge of the deposit type and tract being estimated. Each estimator was also assigned 50 ranking points to assure that each estimator's estimations provided at least some input to the group estimate as the estimators could not apply any ranking points to their own estimations. Thus the total number of points for any estimate would be 100 times the number of estimators. The weighting of each estimator's values in the combined result would then be their total number of points divided by the total number of points for the whole table.

Industrial Mineral Resource Calculation

As described earlier, the industrial mineral (IM) resource assessment calculations differ from those performed for metallic minerals. The processing of the estimate information for the two types of commodities diverges after the weighting stage. Once the weighted mean estimates for each IM deposit type in each tract have been calculated, the deposits are valued by multiplying the number of deposits by the RDVS.

At this point, the estimate portion of the industrial mineral assessment is ready to be integrated with tract area and inventory information to allow final tract ranking calculations to be performed. This integration and calculation step is performed in MS Access. Two MS Access queries are used to perform some simple calculations on this data, add some additional fields and perform the ranking of the tracts.

The calculations performed in MS Access are identical for industrial minerals and metallic minerals. The only difference is that the values in the estimation fields for metallic commodities are in dollars and the corresponding values for industrial minerals are RDVS.

MARK3B MINERAL RESOURCE ASSESSMENT MONTE CARLO SIMULATOR

The original Mark3 simulator was developed by the USGS and has been used in many mineral resource assessment projects (Brew, 1992, Brew *et al.*, 1991, Cox and Singer, 1986, Cox, 1993, Root *et al.*, 1992 and Spanski, 1992). An excellent example of one of these projects, and a description of the operation of the simulator, can be found in Root *et al.*, 1992. The simulator itself was released in 1998 (Root *et al.*, 1998). Originally the simulator was available in the Fortran computer language and required significant computer resources to operate. During the Level 1 MRA project the Mark3 simulator was rewritten in QuickBasic by the USGS so that it could be operated on the more common PC platforms. This new simulator was called Mark3B to designate its QuickBASIC source code. This QuickBASIC version was provided to the GSB along with considerable advice and recommendations (Root, Pers. Commun. 1993). The Mark3B was modified slightly to provide a custom output file that simplified the data processing involved in producing tract rankings. The functions of the simulator have been described elsewhere (Brew, 1991 and Root *et al.*, 1992) but the eleven basic steps that the simulator goes through during a calculation are summarized here (from Root, unpublished).

1. Choose, at random, the number of deposits for this iteration. If it is zero, go to step 10 otherwise go to step 2.
2. Choose, at random, a suite of metals. Go to step 3.
3. Evaluate, at random, m+1 independent standard normal random variables (m= the number of metals in the model). Go to step 4.
4. Calculate the linear combinations of the values of the standard normal random variables from the matrix of coefficients in the "bem" file to obtain the values of m+1 dependent standard normal random variables. Go to step 5.
5. Find dependent uniform values from the dependent standard normal random variables (by the inverse of the cumulative standard normal distribution function evaluated at the values determined in step 4). Go to step 6.
6. Find tonnage and grade values from the dependent uniform values and the inverse of their cumulative distributions. Go to step 7.
7. Add the amount of each metal to its total for the deposits in this iteration. Go to step 8.
8. Check to see whether there is another deposit to do in this iteration. If there is, go to step 2, otherwise go to step 9.
9. Check to see whether 4,999 iterations have been completed. If not, go to step 1, otherwise go to step 10.
10. For each metal, sort the 4,999 totals from each iteration (least being rank1 and greatest being 4,999).
11. Graph 1 minus the rank divided by 4,999 on the y-axis versus the quantity of metal on the x-axis to obtain the assessed distribution of the metal in the area.

In addition to the above steps, a modification to the program extracted the total amount of each commodity calculated for each tract at five probability ranks (0.9, 0.5, 0.1, 0.05, 0.01) and output this information into a file called S!MTOT.all.

Operation of the simulator can be performed either in interactive or batch mode. With the output from the RAW2MARK.exe program the batch mode of operation is very straightforward.

The results in the simulator output, SIMTOT.all, are the tract number, the deposit type number, the commodity, a mean tonnage value, and the volume of the commodity in tonnes expected to be discovered at the five confidence levels (.9, .5, .1, .05, .01). The next step in the processing of the metallic mineral estimates is to convert the commodity amounts to dollar values to allow integration of all the commodities into one value for the deposit and subsequently the tract. This can be done easily in either MS Access or MS Excel or by using the SIM-VALU program created by Ward Kilby.

Once total tract dollar values have been calculated, this number is normalized for tract area to give a GIPV per hectare value. In the Level 1 MRA this value is integrated with inventory information to allow final tract ranking calculations to be performed. This integration and calculation step is performed in MSAccess.

Post-Simulation Calculations

Final ranking of tracts for both the metallic and industrial minerals assessment are performed in exactly the same way once the valued estimation information has been merged with the resource inventory and tract area information. MS Access is used to perform the manipulations required to produce the final rankings. The calculations are all based on a per hectare basis. In the calculations, each tract is ranked using each of the six confidence interval values individually, and then the six rankings are weighted by their probability and combined to produce the final rank value. This is done to isolate the estimates at the various confidence levels so they do not bias the final ranking score. This approach prevents an extremely high ranking at a low confidence level from overshadowing a lower ranking at a high confidence level.

For each of the variables (confidence interval levels), the tract is assigned a rank based on that variable normalized for the size of the tract (area). The rank numbers run from one, for the lowest ranking, to the total number of tracts for the highest ranked tract for that variable. The rank numbers for each variable are then weighted by their confidence value and summed to give a total score for each tract. For the final ranking, the scores for each of the tract are sorted from lowest to highest and assigned ordinal numbers from 1 to the total number of tracts (794) to give the final ranking.

The weightings assigned to the variables are, 1.0 for the inventory values, .9 for the 90% confidence values, .5 for the 50% confidence values, .1 for the 10% confidence values and .01 for the 1% confidence values.

Tract Ranking Maps

Two provincial scale maps were generated to display the relative ranking of the mineral potential across the province for the Level 1 MRA. One map illustrated the mineral potential ranking based on the metallic mineral commodities and the second map illustrated the mineral potential based on the industrial mineral commodities. These maps are useful to illustrate very broad trends in the potential but are not valid for detailed analysis of tract rankings. The maps do not include any measure of important variables that have affected resource development in the province such as regional exploration histories and infrastructure development. The mineral assessment evaluation was carried out on a regional basis.

Limitations of Mineral Resource Assessments

Mineral Resource Assessment maps and products are a very valuable component in any land use planning process. In jurisdictions containing substantial mineral resources such as British Columbia they are essential. Although considered essential to the process they are only a component of the information needed to make an informed decision on land use. There are a number of limitations to any Mineral Resource Assessment product.

COMPARISON OF TRACTS

Comparison of tract rankings from widely separated regions may result in flawed analysis due to their very different histories. Two tracts may have exactly the same mineral potential but due to the remote location of one relative to the other it will not have received the exploration attention over time and will likely have a lower mineral potential ranking than the tract that received the most exploration. Detailed comparison of tract rankings within a region or closely separated tracts in two adjacent regions is valid, as they will in most cases have shared a common exploration and developmental history.

TIME RELATED ISSUES

The principle limitation is the timeliness of the assessment. All assessments are made based on historic information and current knowledge. They are therefore, a snapshot in time. They cannot be expected to accurately portray the mineral potential of a portion of land far into the future. Our knowledge of mineral deposits will advance with time changing our ability to discover and

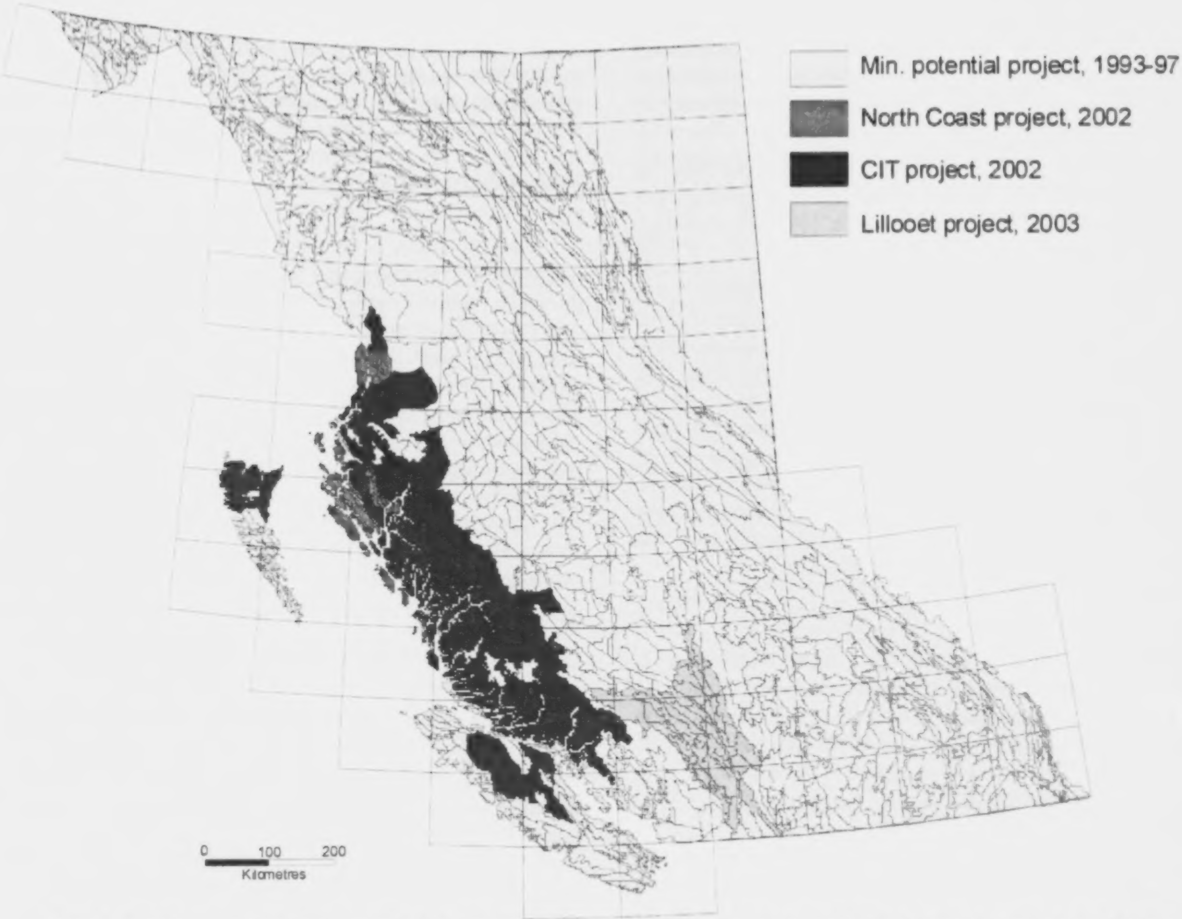

Figure 3. Mineral potential tract map for B.C. Tracts that were subdivided during the North Coast, CIT and Lillooet Level 2 Mineral Resource Assessment projects are shown in cyan, blue and pink respectively.

develop deposits in unimagined environments, at greater depths and with lower grades. New technologies will allow certain deposit types to be discovered with greater ease and will allow the profitable exploitation of deposits that are currently uneconomic. In addition deposit types that were not believed to exist in the study area during the analysis may subsequently be found within the area. Societal demands for certain commodities will change causing the relative values of deposits to change and thus the relative ranking of mineral assessment tracts.

SCALE RELATED ISSUES

The Level 1 MRA was conducted at a scale of 1:250 000. This scale was dictated by the client of the information and was used to present all resource evaluation information from all sectors to the various planning processes. The scale of analysis dictates the required resolution of the analysis units (tracts). Tract size limits the size of planning areas in which the tract can provide any information of value in differentiating the planning area. For example, if a planning area contains a single mineral assessment tract the mineral assessment information adds nothing to the planners' abilities to subdivide the planning area on the basis of mineral potential. In British Columbia as the planning process progressed, smaller and smaller study areas were proposed and land use planning initiated. In some LRMP areas only a few 1:250 000 scale mineral assessment tracts covered the whole LRMP. In these small areas an analysis of greater detail than the initial 1:250 000 study was required to be able to make any reasonable contribution with respect to mineral potential.

In some cases, the information in the provincial scale MRA can be used to generate a more detailed product without conducting a new estimation of undiscovered resources. Usually, the mineral resource assessment tracts contain a variety of geological units. The units, though grouped at a scale of 1:250 000, may in fact be permissive for different types of mineral deposits. If deposit types contributing significantly to the total value of a tract prove to be controlled by geological or topographical features that can be delineated within the tract then the associated values of known and estimated resources can be placed in these sub-tracts. By this means it may be

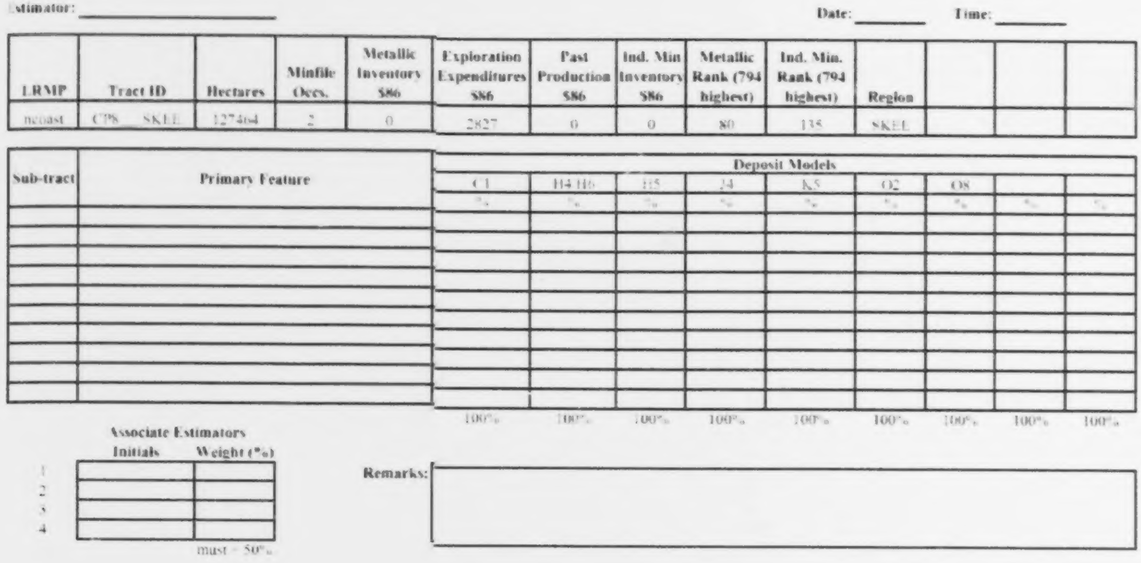

Estimator: ____________ Date: ______ Time: ______

LRMP	Tract ID	Hectares	Minfile Occs.	Metallic Inventory $86	Exploration Expenditures $86	Past Production $86	Ind. Min Inventory $86	Metallic Rank (794 highest)	Ind. Min. Rank (794 highest)	Region			
ncoast	CP8__SKEE	127464	2	0	2827	0	0	80	135	SKEE			

Sub-tract	Primary Feature	Deposit Models								
		C1	H4 H6	H5	J4	K5	O2	O8		
		%	%	%	%	%	%	%	%	%
		100%	100%	100%	100%	100%	100%	100%	100%	100%

Associate Estimators

	Initials	Weight (%)
1		
2		
3		
4		
		must = 50%

Remarks:

Figure 4. Typical Level 2 MRA coding form used to redistribute exisiting estimates to sub-tracts.

possible to extract greater spatial resolution from the original study without performing a new assessment but simply redistributing the previously calculated values. These more detailed assessments are referred to as Level 2 MRAs.

LEVEL 2 MINERAL RESOURCE ASSESSMENTS

In order to provide a more detailed MRA for the CIT and Lillooet project areas, Level 2 assessments were conducted in October, 2002 and February 2003 respectively. The areas covered by these assessments are shown in Figure 3. These assessments incorporate elements from the Level 1 assessment (Bellefontaine and Alldrick, 1994, 1995; MacIntyre *et al.*, 1994, 1995; Massey, 1994, 1995) for undivided tracts and a preliminary Level 2 MRA applied to selected tracts within the North Coast LRMP that was done in February 2002

A major philosophical change was incorporated into presentation of Level 2 MRA results. The tracts were ranked only on the estimate of the undiscovered resources to emphasisze the potential for new discoveries. The known resources are shown by plotting the mineral occurrences and deposits as point data showing their gross-in-place-value (GIPV). In Level 2 maps this data is often superimposed on the MRA tract plots. This change means that Level 1 and Level 2 tract values cannot be directly compared.

The following tasks were completed in chronological order to produce the final Level 2 MRAs for the CIT and Lillooet LRMP areas.

Selection of MRA tracts for subdivision

Existing Level 1 MRA tracts that intersected or were within the CIT and Lillooet LRMP areas were examined and candidate tracts for subdivision were selected. All tracts with significant area within the LRMP boundaries and in excess of 100,000 hectares were targeted for subdivision. A final list of tracts was compiled together with pertinent information from the Level 1 MRA. A preliminary map in ESRI shape file format showing the tracts targeted for subdivision was prepared and posted to a MapGuide website prepared especially for each project.

Invitation to Quote for Metallic and Industrial Mineral Experts

Upon approval to proceed with the Level 2 assessments, an Invitation to Quote (ITQ) was prepared and posted to the BC-Bids website inviting metallic and industrial mineral experts with knowledge of the project areas to participate in an "experts workshop". Selection of participants was based on a review of pertinent credentials and their daily contract rate.

Expert Workshops

The first task assigned to the metallic mineral tables was to examine the geology of the existing Level 1 tracts targeted for subdivision and decide how they should be subdivided. Depending on the complexity of the geology

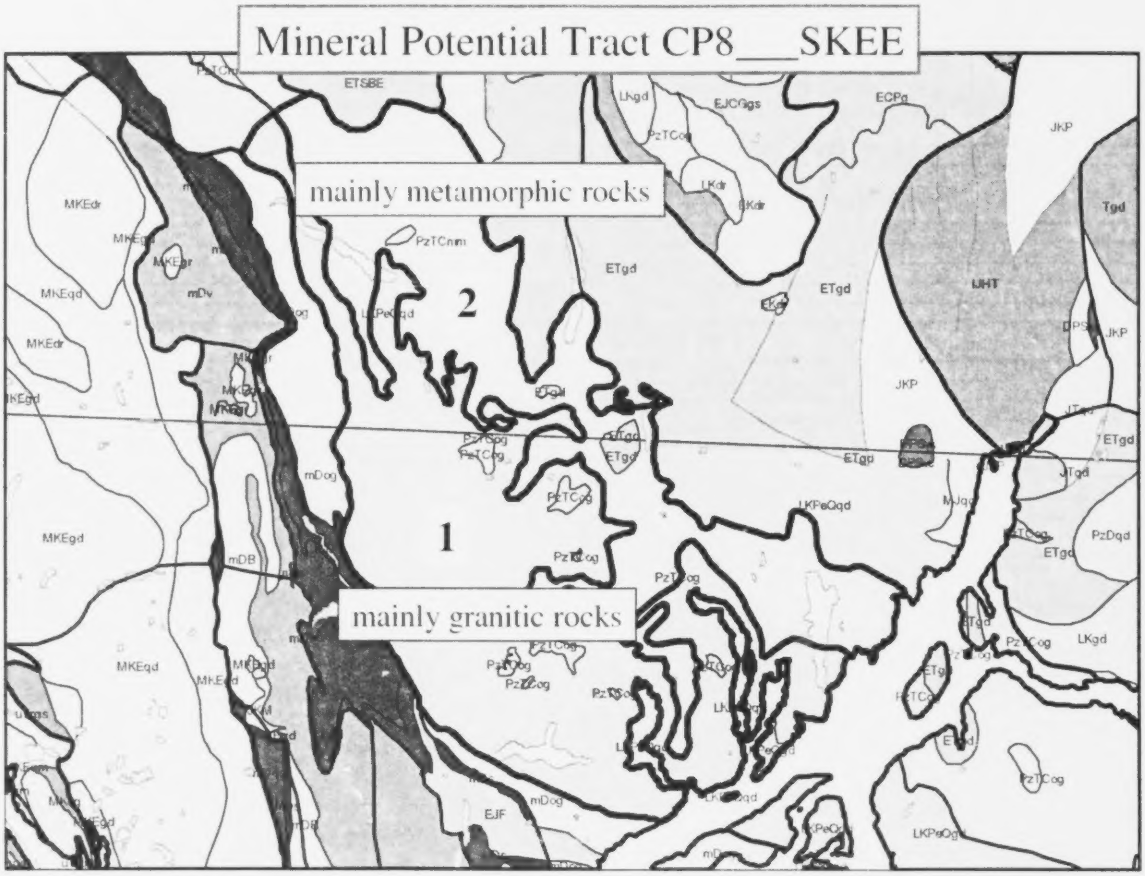

Figure 5. Map of tract CP8_SKEE showing a simple subdivision into two sub-tracts, one dominated by granitic rocks, the other by metamorphic rocks.

within the tract, anywhere from 1 to 5 sub-tracts were defined. Sub-tract boundaries were drawn directly onto coloured geology maps that were plotted specifically for each project. Sub-tracts were given a numeric label i.e. 1, 2 etc. The industrial minerals table that was convened the following week used the same sub-tract boundaries established by the metallic mineral experts.

Once the sub-tract boundaries were established, coding sheets were handed out for each tract being subdivided. As shown in Figure 4, these sheets contained information from the Level 1 MRA such as dollar values for inventory, exploration expenditures, number of MINFILE occurrence, tract hectares, etc., plus columns for each of the deposit models considered in the Level 1 MRA. Blank columns were also provided for any new deposit model estimates. These columns were labeled with the deposit code used in the original MRA. A lookup sheet was provided so that these codes could be cross-referenced to existing deposit profiles. For each sub-tract, a row was added to the table grid and a brief description of the primary geologic features of the sub-tract entered in the cell next to the sub-tract number.

For each deposit model, the experts were given time to discuss the likelihood of that type of deposit occurring in each of the sub-tracts. To assist this discussion, the facilitator used a notebook computer connected to the Internet and a digital projector to display information on the geology, mineral occurrences, geochemistry and geophysics in the vicinity of the tract under consideration. Most of this information was derived on-line from the MEM MapPlace website (www.mapplace.ca). Also included in the discussion was an evaluation of the models considered in the Level 1 MRA and whether new models should be estimated for. If the table decided that new models should be considered, estimation forms for that model were distributed and the experts were asked to fill these out using the same methodology used in the Level 1 MRA. Once this task was completed the experts were then asked to indicate the percentage of each deposit model estimate that should be assigned to each sub-tract. These redistribution percentages were based on the geologic characteristics of the sub-tracts and the relatively likelihood that a particular deposit model would occur in that sub-tract. In some cases, because the deposit model

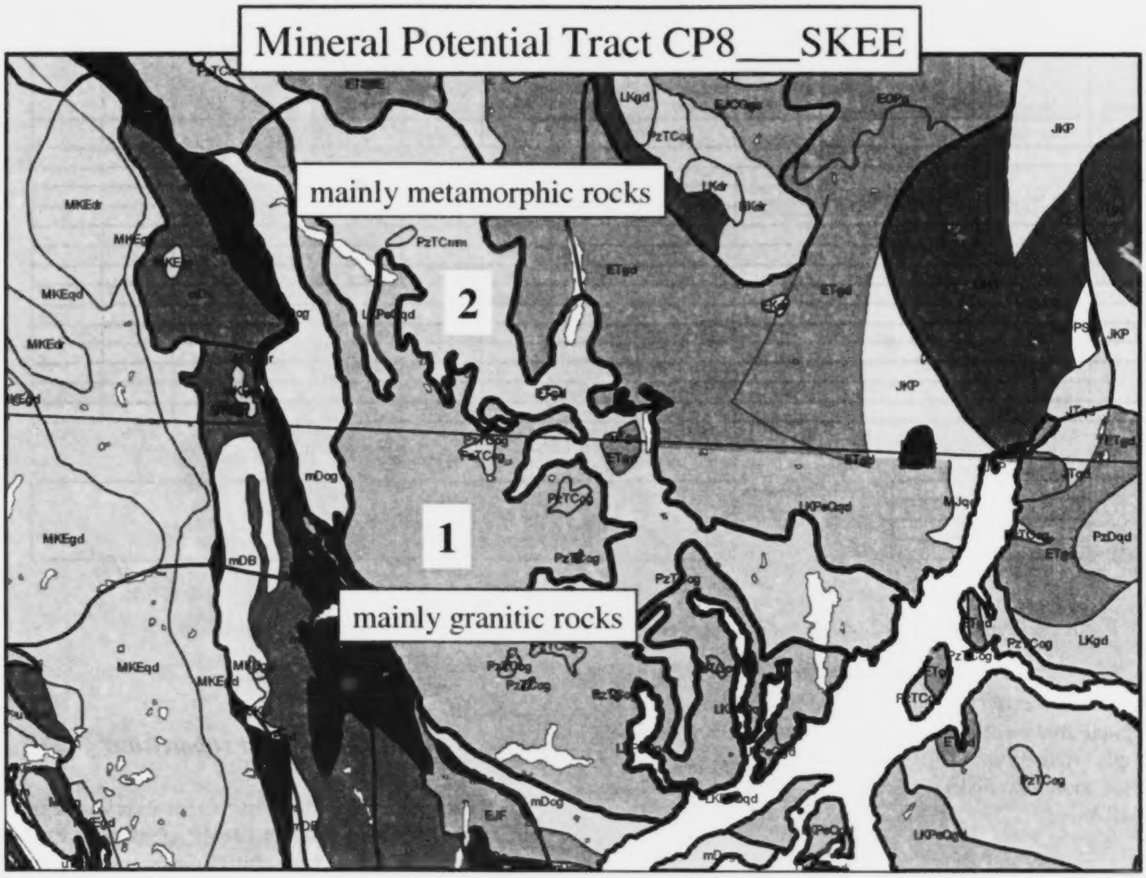

Figure 5. Map of tract CP8_SKEE showing a simple subdivision into two sub-tracts, one dominated by granitic rocks, the other by metamorphic rocks.

within the tract, anywhere from 1 to 5 sub-tracts were defined. Sub-tract boundaries were drawn directly onto coloured geology maps that were plotted specifically for each project. Sub-tracts were given a numeric label i.e. 1, 2 etc. The industrial minerals table that was convened the following week used the same sub-tract boundaries established by the metallic mineral experts.

Once the sub-tract boundaries were established, coding sheets were handed out for each tract being subdivided. As shown in Figure 4, these sheets contained information from the Level 1 MRA such as dollar values for inventory, exploration expenditures, number of MINFILE occurrence, tract hectares, etc., plus columns for each of the deposit models considered in the Level 1 MRA. Blank columns were also provided for any new deposit model estimates. These columns were labeled with the deposit code used in the original MRA. A lookup sheet was provided so that these codes could be cross-referenced to existing deposit profiles. For each sub-tract, a row was added to the table grid and a brief description of the primary geologic features of the sub-tract entered in the cell next to the sub-tract number.

For each deposit model, the experts were given time to discuss the likelihood of that type of deposit occurring in each of the sub-tracts. To assist this discussion, the facilitator used a notebook computer connected to the Internet and a digital projector to display information on the geology, mineral occurrences, geochemistry and geophysics in the vicinity of the tract under consideration. Most of this information was derived on-line from the MEM MapPlace website (www.mapplace.ca). Also included in the discussion was an evaluation of the models considered in the Level 1 MRA and whether new models should be estimated for. If the table decided that new models should be considered, estimation forms for that model were distributed and the experts were asked to fill these out using the same methodology used in the Level 1 MRA. Once this task was completed the experts were then asked to indicate the percentage of each deposit model estimate that should be assigned to each sub-tract. These redistribution percentages were based on the geologic characteristics of the sub-tracts and the relatively likelihood that a particular deposit model would occur in that sub-tract. In some cases, because the deposit model

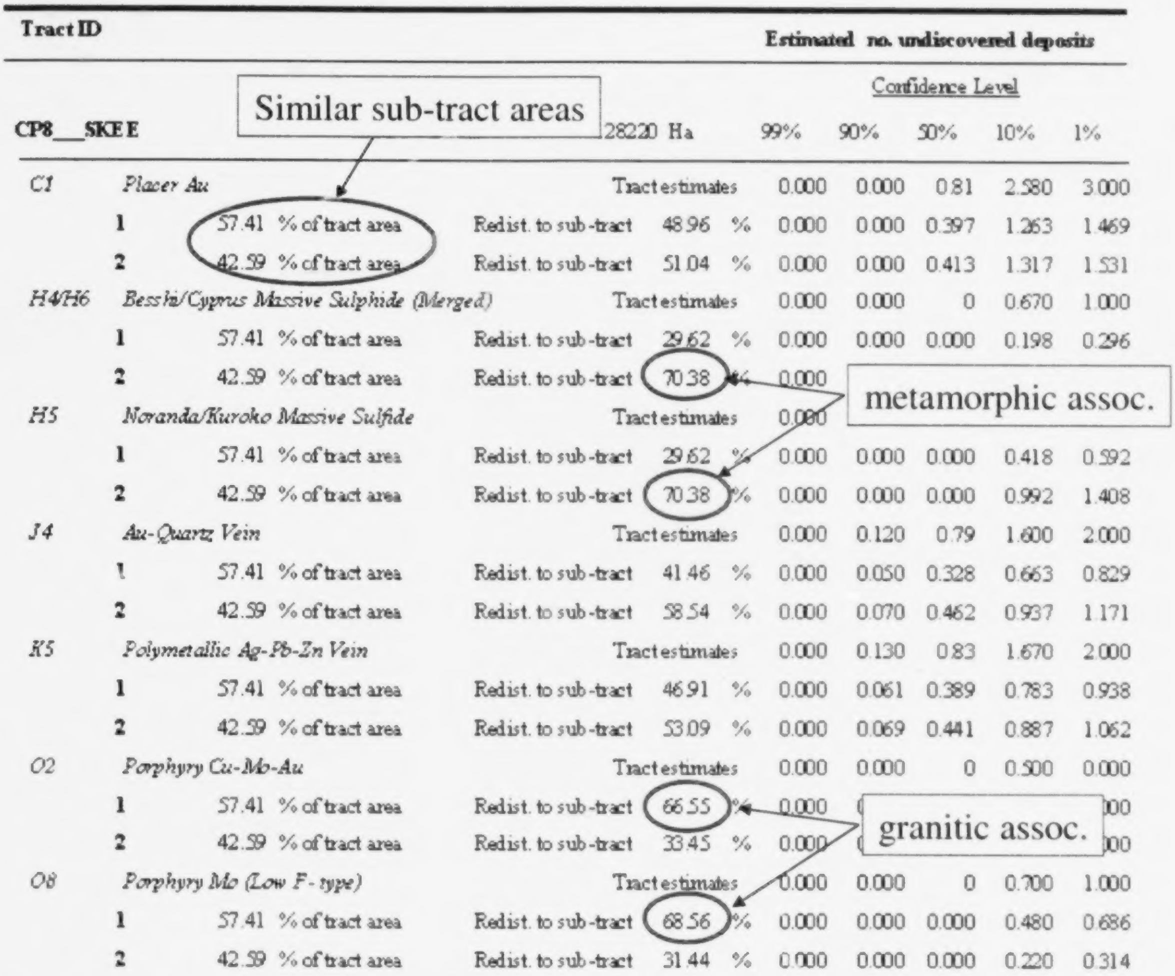
Similar sub-tract areas
metamorphic assoc.
granitic assoc.

Tract ID				Estimated no. undiscovered deposits				
				Confidence Level				
CP8__SKEE			28220 Ha	99%	90%	50%	10%	1%
C1	*Placer Au*		Tract estimates	0.000	0.000	0.81	2.580	3.000
	1	57.41 % of tract area	Redist. to sub-tract 48.96 %	0.000	0.000	0.397	1.263	1.469
	2	42.59 % of tract area	Redist. to sub-tract 51.04 %	0.000	0.000	0.413	1.317	1.531
H4/H6	*Besshi/Cyprus Massive Sulphide (Merged)*		Tract estimates	0.000	0.000	0	0.670	1.000
	1	57.41 % of tract area	Redist. to sub-tract 29.62 %	0.000	0.000	0.000	0.198	0.296
	2	42.59 % of tract area	Redist. to sub-tract 70.38 %	0.000	[illegible]	[illegible]	[illegible]	[illegible]
H5	*Noranda/Kuroko Massive Sulfide*		Tract estimates	0.000	[illegible]	[illegible]	[illegible]	[illegible]
	1	57.41 % of tract area	Redist. to sub-tract 29.62 %	0.000	0.000	0.000	0.418	0.592
	2	42.59 % of tract area	Redist. to sub-tract 70.38 %	0.000	0.000	0.000	0.992	1.408
J4	*Au-Quartz Vein*		Tract estimates	0.000	0.120	0.79	1.600	2.000
	1	57.41 % of tract area	Redist. to sub-tract 41.46 %	0.000	0.050	0.328	0.663	0.829
	2	42.59 % of tract area	Redist. to sub-tract 58.54 %	0.000	0.070	0.462	0.937	1.171
K5	*Polymetallic Ag-Pb-Zn Vein*		Tract estimates	0.000	0.130	0.83	1.670	2.000
	1	57.41 % of tract area	Redist. to sub-tract 46.91 %	0.000	0.061	0.389	0.783	0.938
	2	42.59 % of tract area	Redist. to sub-tract 53.09 %	0.000	0.069	0.441	0.887	1.062
O2	*Porphyry Cu-Mo-Au*		Tract estimates	0.000	0.000	0	0.500	0.000
	1	57.41 % of tract area	Redist. to sub-tract 66.55 %	0.000	[illegible]	[illegible]	[illegible]	[illegible]
	2	42.59 % of tract area	Redist. to sub-tract 33.45 %	0.000	[illegible]	[illegible]	[illegible]	[illegible]
O8	*Porphyry Mo (Low F-type)*		Tract estimates	0.000	0.000	0	0.700	1.000
	1	57.41 % of tract area	Redist. to sub-tract 68.56 %	0.000	0.000	0.000	0.480	0.686
	2	42.59 % of tract area	Redist. to sub-tract 31.44 %	0.000	0.000	0.000	0.220	0.314

Figure 6. Summary of redistribution results for tract CP8__SKEE.

was not strongly controlled by a specific geologic characteristic there would be roughly equal likelihood that a deposit might be found in each of the sub-tracts. For other deposit models, such as those associated with specific rock types such as intrusions, the occurrence or absence of these features in a sub-tract would significantly influence the percentage of the original estimate to be assigned to that sub-tract. Naturally, column totals for each deposit model must total 100%. The experts were also asked to indicate on the redistribution form a personal confidence level (PCL) as a score out of 100, which would reflect how they felt about their personal knowledge of the tract and mineral deposit models being discussed. In addition, they were also asked to rank the other experts at the table by assigning points, the total of which must add up to 50. Figure 5 shows a typical tract which has been subdivided into two subtracts. Figure 6 shows the final redistribution results based on input from each member of the expert panel.

Data Processing

Data processing was done by GSB staff and began immediately after the expert workshops were completed. The first task involved processing metallic and industrial mineral deposit estimation forms. For each estimator and each deposit model this involved measuring the location of tics on a probability bar, converting these values to a probability percentage, recording the number of deposits estimated at each probability level and recording the weights given to the other estimators at the table. This raw data was entered into separate excel spreadsheets for metallic and industrial mineral deposits. This data was then reformatted and exported as a comma delimited ASCII file for input into the RAW2MARK QuickBasic program written by Ward Kilby. This program calculates the weighted average number of deposits for each deposit

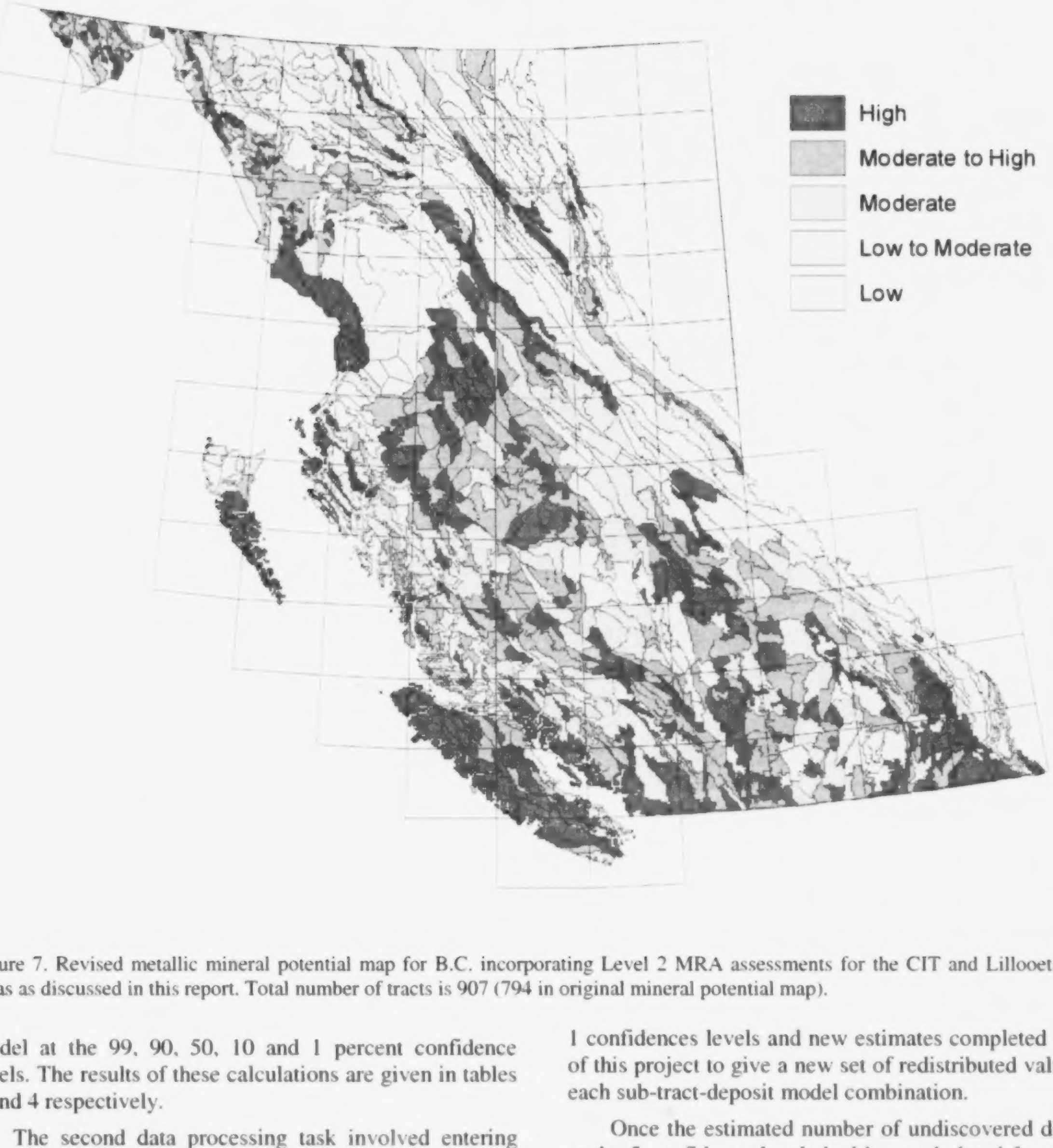

Figure 7. Revised metallic mineral potential map for B.C. incorporating Level 2 MRA assessments for the CIT and Lillooet LRMP areas as discussed in this report. Total number of tracts is 907 (794 in original mineral potential map).

model at the 99, 90, 50, 10 and 1 percent confidence levels. The results of these calculations are given in tables 3 and 4 respectively.

The second data processing task involved entering the redistribution percentages, personal confidence levels and weights assigned to the other estimators at the table from the redistribution worksheets. Redistribution percentages were recorded in an MS Excel spreadsheet with one record created for each value recorded on the worksheets. Personal confidence levels and weights given to associated estimators were entered in separate spreadsheets. All this data was imported into an MS Access Database where a series of queries were used to calculate a weighted average redistribution percentage for each deposit model in each sub-tract. These percentages were then applied to existing Level 1 estimates of the number of undiscovered deposits at the 99, 90, 50 , 10 and 1 confidences levels and new estimates completed as part of this project to give a new set of redistributed values for each sub-tract-deposit model combination.

Once the estimated number of undiscovered deposits at the 5 confidence levels had been tabulated for each of the tracts and sub-tracts in the project area, this data was reformatted for input into the Mark3B resource simulator. The input required to run the simulator includes the tract number, deposit model number, number of iterations to perform, number of confidence levels to use and the estimated number of undiscovered deposits at each of the confidence levels. Since the tract names are too long for input into the simulator a key number was created for each tract and subtract deposit numbers used by the simulator correspond to the names of a series of files containing commodity, grade and tonnage information used in the Monte Carlo simulation process.

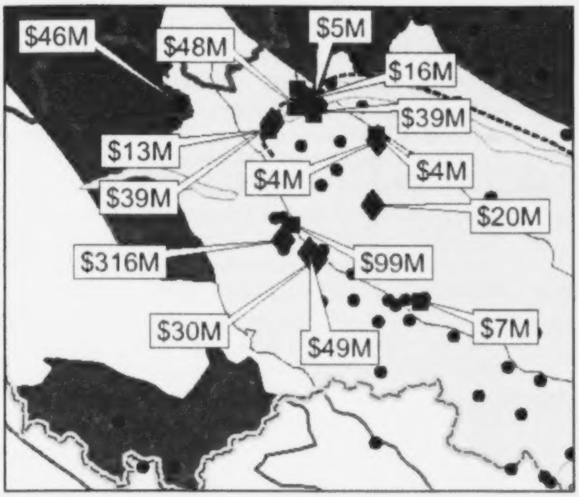

Figure 8. Level 2 MRA tract map of the area around the Bralorne Mine. Tract rankings are the same as shown in Figure 7. Superimposed on the Level 2 map are the GIPV for known resources in the Bralorne area.

For this.project the number of iterations for each tract-deposit model combination was set at 2000 and estimation data was entered for the 90, 50 and 10 percent confidence levels. The output from the simulator is written to a comma-delimited, ASCII text file (SIMTOT.ALL). Each record has the tract number, deposit, number, commodity name and predicted tonnes for the mean and 90, 50, 10, 5 and 1 percent confidence levels. In order to have a base to compare rankings across the entire province, all tracts were re-run through the simulator. This resulted in an increase in the overall number of tracts from 794 to 907, this increase being a result of the subdividing of tracts that occurred as part of the Level 2 assessments described in this report.

The final data processing task for the metallic mineral deposit models was to determine the relative tract rankings using Gross-In-Place-Values (GIPV). This procedure for ranking metallic mineral tracts is the same as that used in the Level 1 MRA with the exception that the value of known resources was not included in the calculation. The Level 2 MRA rankings are based strictly on the predicted value of undiscovered resources determined by the Mark3B resource simulator as described above. To determine the Level 2 rankings the predicted tonnes of commodity for each deposit model in a tract at the various confidence levels was multiplied by the per tonne value in current Canadian dollars. The values used for this calculation are listed in Table 7. The dollar values were then totaled for the tract and divided by the tract area to give a GIPV per hectare. These values were then discounted by factors of 0.9, 0.5, 0.1, 0.05 and 0.01 for the 90, 50, 10, 5 and 1 percent confidence levels respectively. Finally, these discounted values were given an ordinal ranking for each of the confidence levels. These ordinal ranks were then summed for each of the tracts or sub-tracts and this value was used to produce the final ordinal ranking for the tract. All of these calculations were done within an MS Access database. The rankings were then categorized into 5 divisions, each division representing 20% of the total land area of the province. A new Level 2 MRA map for B.C. was generated and is shown in Figure 7. This is map is now posted on the MapPlace website (www.mapplace.ca).

The ranking of tracts for industrial mineral potential does not use data from the Mark3 resource simulator. Instead a Relative Deposit Score Value is used as described for the Level 1 MRA. The number of predicted deposits is multiplied by the RDVS and then normalized to the tract area. These normalized values are discounted and ranked in the same way as the GIPV/HA values for metallic mineral deposits described above.

Known In-ground Resources

Unlike the Level 1 MRA, known in-ground resources (reserves) have not been included in the tract rankings. These values have been recalculated using current commodity prices and are presented as a point map for use with the Level 2 MRA ranking maps. An example of how the data is presented on such a map is shown in Figure 8. The map shows the GIPV of resources defined in the Bralorne Mine area of the Lillooet LRMP. Note that even though there are significant resources in the area, the tracts that contain most of the deposits are only given a Moderate to High ranking (pink colour) for potential for new discoveries. Adjacent tracts, on the other hand, are given a High ranking (red colour) for new discoveries. This approach clearly separates the known from the unknown and should assist land-use planners in assessing the potential for new mineral discoveries in a given MRA tract.

CONCLUSIONS

The Level 2 MRAs completed to date represent a significant improvement over the original Level 1 MRA because;

1. In general tract (sub-tract) areas are smaller and more appropriate for regional land-use planning
2. The subdivision of tracts into sub-tracts based on geology has resulted in a better definition of the potential within tracts to host specific types of deposits. This has resulted in a better definition of the areas within the CIT project area that have the highest mineral potential.
3. Values used for ranking are based on current commodity prices
4. Estimates for deposit models not included in the Level 1 MRA were added to the assessment and included in the final tract ranking.
5. The final tract rankings for the Level 2 MRA are based on the potential for new discoveries only

and are not influenced by known resources (in-ground reserves).

6. Known resources have been re-valued using current commodity prices and will be presented as a separate map layer in the future. Therefore, Level 1 and Level 2 tracts cannot be compared directly as they incorporate different datasets.

REFERENCES

Acquired Intelligence Inc., (1993): The Estimation Process for Undiscovered Deposits on Vancouver Island; internal report prepared under contract # 93-712.

Bellefontaine, K.A and Alldrick, D.J. (1994): Mineral Potential - Mid-Coast Area, B.C.; *B.C. Ministry of Energy, Mines and Petroleum Resources*, Open File 1994-17.

Bellefontaine, K.A and Alldrick, D.J. (1995): Highlights of the Mid-Coast Mineral Potential Project; in Geological Fieldwork 1994, Grant, B. and Newell, J.M., Editors, *B.C. Ministry of Energy, Mines and Petroleum Resources*, Paper 1995-1, pages 449-458.

Brew, D.A., (1992): Decision Points and Strategies in Quantitative Probabilistic Assessment of Undiscovered Mineral Resources; *U.S. Geological Survey*, Open File 92-308, 23 pages.

Brew, D.A., Drew, L.J., Schmidt, J.M., Root, D.H. and Huber, D.F. (1991): Undiscovered Locatable Mineral Resources of the Tongass National Forest and Adjacent Lands, Southern Alaska; *U.S. Geological Survey*, Open File 91-10, 370 pages.

Cox, D.P. and Singer, D.A., Editors, (1986): Mineral deposit Models, *U.S. Geological Survey*, Bulletin 1693, 379 p.

Cox, D.P., (1993): Estimation of Undiscovered Deposits in Quantitative Mineral Resource Assessments- Examples from Venezuela and Puerto Rico; *Nonrenewable Resources*, Volume 2, No. 2, pages 82-91.

Grunsky, E.C., (1995): Grade and Tonnage Data for British Columbia Mineral Deposit Models: in Geological Fieldwork 1994, Grant, B. and Newell, J.M., Editors, *B.C. Ministry of Energy, Mines and Petroleum Resources*, Paper 1995-1, pages 417-423.

Kilby, W.E. (1992): Mineral Potential Workshop, Report of Proceedings April 22-23, 1992, Victoria, British Columbia. *B.C. Ministry of Energy, Mines and Petroleum Resources*, Information Circular 1992-22, 50 pages.

Kilby, W.E. (1995): Mineral Potential Project - Overview; in Geological Fieldwork 1994, Grant, B. and Newell, J.M., Editors, *B.C. Ministry of Energy, Mines and Petroleum Resources*, Paper 1995-1, pages 411-416.

Kilby, W.E. (1996): Mineral Potential Project - An Update: in Geological Fieldwork 1995, Grant, B. and Newell, J.M., Editors, *B.C. Ministry of Energy, Mines and Petroleum Resources*, Paper 1996-1.

Kilby, W.E., Simandl, G.J., Lefebure, D.V., Hora, Z.D., Grunsky, E.C. and Desjardins, P. (1999): Systematic Evaluation of Industrial Mineral Potential, British Columbia, Canada - Possible World-Wide Applications; CIM, Special Volume 50 - 33rd Forum on the Geology of Industrial Minerals, Proceedings, Pages 249-256.

Lefebure, D.V. and Hoy, T. (1996): Selected British Columbia Mineral Deposit Profiles, Volume II - More Metallic Deposits; *B.C. Ministry of Employment and Investment*, Open File 1996-13, 172 pages.

Lefebure, D.V. and Ray, G.E. (1995): Selected British Columbia Mineral Deposit Profiles, Volume I - Metallics and Coal; *B.C. Ministry of Energy, Mines and Petroleum Resources*, Open File 1995-20, 136 pages.

Lefebure, D.V., Alldrick, G. J., Simandl, G.J. and Ray, G. (1995): British Columbia Mineral Deposit Profiles; in Geological Fieldwork 1994, Grant, B. and Newell, J.M., Editors, *B.C. Ministry of Energy, Mines and Petroleum Resources*, Paper 1995-1, pages 469-490.

MacIntyre, D.G., Ash, C. and Britton, J. (1994): Mineral Potential - Nass-Skeena Area; *B.C. Ministry of Energy, Mines and Petroleum Resources*, Open File 1994-14.

MacIntyre, D.G., Ash, C., Britton, J., Kilby, W.E. and Grunsky, E.C. (1995): Mineral Potential Evaluation of the Nass-Skeena Area; in Geological Fieldwork 1994, Grant, B. and Newell, J.M., Editors, *B.C. Ministry of Energy, Mines and Petroleum Resources*, Paper 1995-1, pages 459-468.

Massey, N.W.D. (1994): Mineral Potential - Vancouver Island; *B.C. Ministry of Energy, Mines and Petroleum Resources*, Open File 1994-6.

Massey, N.W.D. (1995): The Vancouver Island Mineral Potential Project (92B, C, E, F, G, K, L and 102I); in Geological Fieldwork 1994, Grant, B. and Newell, J.M., Editors, *B.C. Ministry of Energy, Mines and Petroleum Resources*, Paper 1995-1, pages 435-448.

MINFILE Team (1995): Reserves and Resources Inventory (paper printout), *B.C. Ministry of Energy, Mines and Petroleum Resources*, Open File 1995-19.

Root, D.H., Menzie, W.D. and Scott, W.A. (1992): Computer Monte Carlo Simulation in Quantitative Resource Assessment; *Nonrenewable Resources*, Volume 1, No. 2, pages 125-138.

Root, D.H., Scott, W.A. Jr. and Schruben, P (1998): Mark3B Resource Assessment Program for Macintosh; *United States Geological Survey*, USGS Open File Report 98-356.

Simandl, G.J., Hora, Z.D. and Lefebure, D.V. (1999): Selected British Columbia Mineral Deposit Profiles, Volume 3 – Industrial Minerals and Gemstones, *B.C. Ministry of Energy and Mines*, Open File 1999-10, 136 pages.

Singer, D.A. (1993): Basic Concepts in Three-part Quantitative Assessments of Undiscovered Mineral Resources; *Nonrenewable Resources*, Volume 2, No. 2, pages 69 - 81.

Spanski, G.T., (1992): Quantitative Assessment of Future Development of Copper / Silver Resources in the Kootenay National Forest, Idaho / Montana: Part 1 - Estimation of the Copper and Silver Endowments; *Nonrenewable Resources*, Volume 1, pages 163-183.Old Mineral Deposit and Land Use Maps

Composition of Logtung Beryl (aquamarine) by ICPES/MS: A Comparison with Beryl Worldwide

by Mitchell G. Mihalynuk and Ray Lett

Keywords: Beryl, aquamarine, Logtung deposit, ICPMS, chemical analysis

INTRODUCTION

Beryl is a beryllium-aluminum-silicate mineral. When it grows unimpeded, it forms hexagonal prisms. In its simplest form, its chemical formula is $Be_3Al_2[Si_6O_{18}]$, and it is clear or white in colour. Addition of Cr, V, Mn, or Fe into the formula can result in some of the world's most sought after gemstones: green emerald (Cr, ±V), pink morganite (Mn), yellow heliodor (Fe), and blue aquamarine (Fe). Yet, no simple addition of these key elements will do; the amount and valence of the element and site of its occupancy within the crystal lattice are key to colour. Beryl's molecular structure is dominated by hexagonal rings comprised of six Si-O tetrahedra (Figure 1). Linking the rings are tetrahedrally coordinated Be (±Fe, Mn, Mg) and octahedrally coordinated Al (±Fe, Cr, V). The rings are stacked parallel to the crystal prism (z axis) producing hollow channels. This "zeolite" structure, named after a family of minerals known as molecular sieves, permits occupancy of water and cations (particularly alkalis, Na, Li, K, Cs, Rb) within the crystal lattice, but outside of the crystal formula unit. Thus, up to 8% alkalis (Deer *et al.*, 1966) in igneous beryl, and an amazing 14% in hydrothermal beryl (Vianna *et al.*, 2002b) can be accommodated along with a charge balance not accounted for in the formula unit. Schaller *et al.* (1962) described beryl chemistry as an isomorphic series between the end members $Be_3Al_2Si_6O_{18}$, $(Na, Cs)Be_2Al(Al, Li)Si_6O_{18}$, and $(Na,K,Cs)Be_3R^{3+}R^{2+}Si_6O_{18}$ where R^{3+} = Al, Fe, Cr and Sc, and R^{2+} = Be, Fe, Mn and Mg. In consideration of the channel components, the formula may be generally presented as: $R^{2+}Be_2R^{3+}Al[Si_6O_{18}].(H_2O)(Na, \square)$.

Refractive index of beryl increases with increasing content of alkalis in the channels as the channels would otherwise be empty space within the crystal structure. When iron occupies the channels it appears to be a quintessential agent in the colouration (*i.e.* the chromophore) of aquamarine gemstones (Price *et al.*, 1976; Vianna *et al.*, 2002a). A correlation between Fe content and colour of aquamarine has long been known, although some authors have attributed colouration to other agents such as Cs (Sosedko, 1957). Mössbauer spectroscopy in particular has helped to isolate the chromophore's position within the crystal lattice. Combining this technique with other spectroscopic methods it can be reasonably inferred that ferric iron with octahedral coordination produces a yellow colour, while ferrous iron in the octahedral site has no effect on colour, and ferrous iron within channels produces a deep blue colour (Vianna *et al.*, 2002b). These same authors showed that in one small population of samples deep blue aquamarines have little Fe^{3+} and greener samples contain more Fe^{3+} or less Fe^{2+} in channels. The common process of heat-treating aquamarine to produce darker blue colour may work through charge transfer of Fe^{3+} to Fe^{2+}, thereby eliminating the greenish cast (Blak *et al.*, 1982).

In this paper we report on the chemical composition of blue beryl that is abundant at the Logtung tungsten-molybdenum deposit of northwestern BC (Figure 2). Mineralization is associated with a porphyritic quartz monzonite intrusion dated at ~58 Ma (U-Pb zircon; Mihalynuk and Heaman, 2002) although previous isotopic age determinations suggest an age of around 109 ±2 Ma (K-Ar muscovite; Hunt and Roddick, 1987) to 118 ±2 Ma (Rb-Sr; Stewart and Evensen, 1983).Observations reported on here are limited to a few person-days devoted mainly by Ministry of Energy and Mines personnel to mapping the area around the Logtung deposit as part of the National Mapping Program (Ancient Pacific Margin NATMAP, 1999-2000; Mihalynuk *et al.*, 2000). Geological work un-

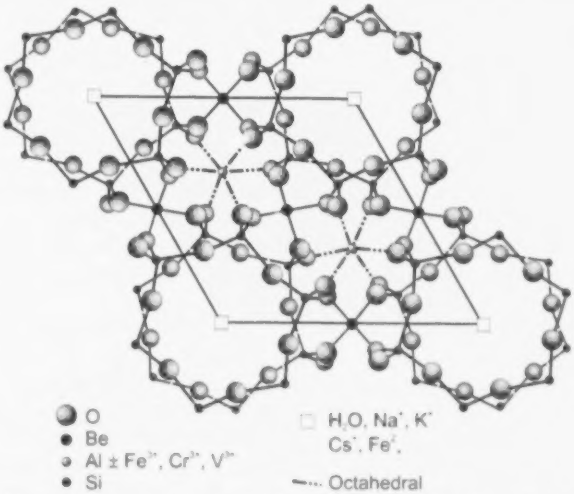

Figure 1. Atomic structure of Beryl, modified after (Deer *et al.*, 1966). Atom loci are projected onto basal 0001 plane and the lower Si-O ring is shown by dashed bonds. Grey trapezoid outlines the unit cell. Ring channels may be occupied by water alkalis and ferrous iron.

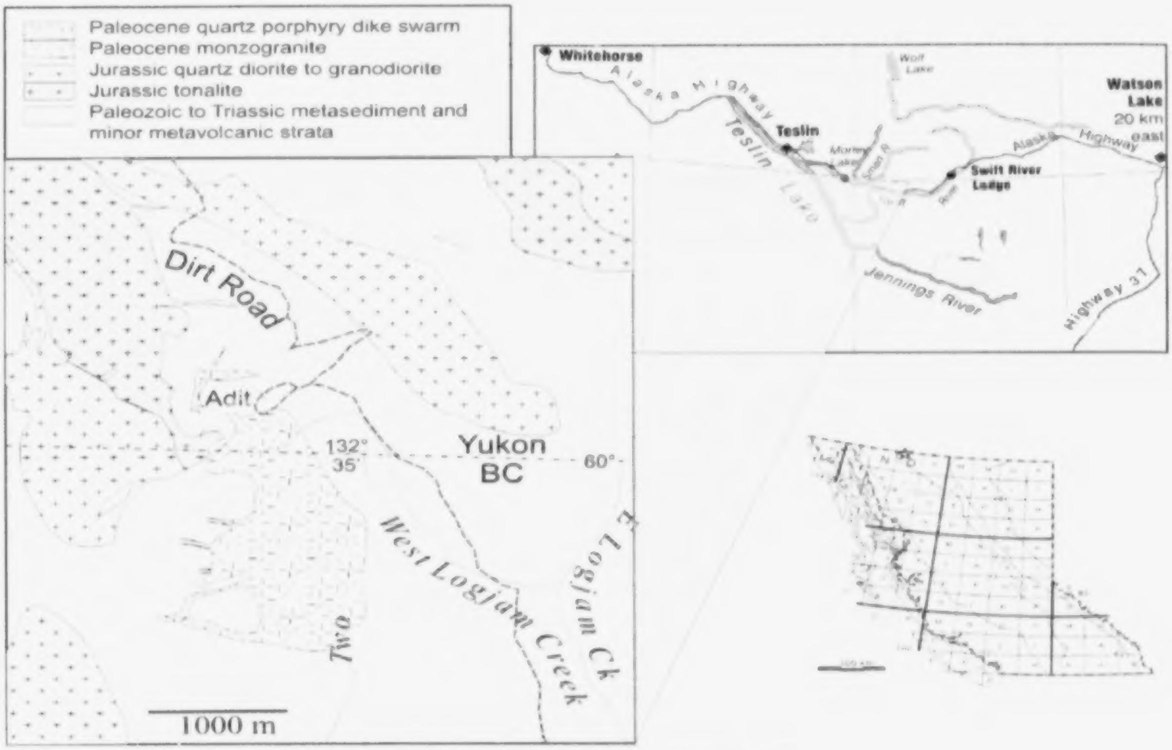
Paleocene quartz porphyry dike swarm
Paleocene monzogranite
Jurassic quartz diorite to granodiorite
Jurassic tonalite
Paleozoic to Triassic metasediment and minor metavolcanic strata
Whitehorse
Alaska Highway
Wolf Lake
Watson Lake
20 km east
Teslin
Teslin Lake
Morley Lake
Swan R.
Swift River Lodge
Alaska Highway
Jennings River
Highway 37
Dirt Road
Adit
132° 35'
Yukon
BC
60°
West Logjam Creek
E Logjam Ck
Two
1000 m

Figure 2. Location of the Logtung porphyry, adapted from (Mihalynuk and Heaman, 2002).

der the NATMAP program was not specifically aimed at beryl, however, blue beryl was reported previously at the Logtung deposit (MINFILE number 104O 016) and we found to it be common, with crystals up to 1.5 cm in diameter and 3 cm long. Unfortunately, all large specimens observed were cloudy or heavily included. Clear crystals tended to be less than 3 mm in diameter.

If large, gem quality stones are to be found at Logtung, a more methodical and intense exploration program than our ancillary approach will be required. To help determine if such exploration is worthwhile, we analyzed a sample of Logtung beryl to compare its chemical affinity with known gem occurrences from around the globe. The chemistry and structure of beryl from some of these occurrences is very well characterized, providing a good benchmark for comparison.

Methods

About 2 grams of beryl were extracted from a single fist-sized sample, crushed with an agate mortar and pestle to a particle size of less than ~1 mm and then carefully sorted. Clear, inclusion-free grains were separated and powdered in the mortar and pestle, resulting in a final sample yield of 0.8 g. The powder was submitted to ACME Analytical Laboratories, Vancouver, for analysis by lithium metaborate ($LiBO_2$)fusion followed by Inductively Coupled Plasma Emission and Mass Spectrometry (ICPES/MS).

A sample aliquot of 0.2g was fused at 900°C with $LiBO_2$which enables complete dissolution of the residue in HNO_3 for analysis by ICPES/MS. This technique provides an analytical sensitivity with a small sample size that is comparable to wet chemical or microprobe analyses of beryl published previously (Table 1). Benefits of ICPES/MS include ease of sample preparation, and the large number of major and trace elements can be determined simultaneously. Drawbacks include the inability to analyze Li_2O content because of the addition $LiBO_2$ and possible loss of Li during fusion, inability to distinguish Fe valance state, and lack of volatiles determination (e.g. H_2O). As discussed above, H_2O+ and H_2O- are principally restricted to crystal channels and do not enter into the crystal structure. Fe^{3+}/Fe^{2+} can be estimated from cationic site occupancy balance. However, lack of Li_2O is a serious drawback because the beryl crystal structure can incorporate a large proportion of Li. In the case of the Logtung beryl, Li may be an important constituent based upon the low oxide totals and the results of cationic ratio calculations (Tables 1 and 2).

Results

ICPES/MS analytical results are reported at the bottom of Table 1. ICPES/MS detection limits reported are comparable or better than those reported for the results by other methods listed in Table 1. Figure 3a shows that the most abundant oxides of Si and Al are low in the Logtung beryl

TABLE 1. COMPOSITION OF BERYL FROM OCCURRENCES WORLDWIDE.

Sample No.	Ref.	Method**	SiO2	TiO2	Al2O3	Cr2O3	Fe2O3	V2O3	FeO	BeO	MnO	MgO	CaO	Na2O	K2O	Rb2O	Cs2O	Li2O	H2O+	H2O-	Total
1. Ingersoll	1		64.76		18.91					12.83				1.23	0.23			0.14	1.96	0.01	100.07
2. Aquamarine	1		64.99		17.17		0.97			12.89		0.31		1.08	0.29				1.62	0	100.08
3. Biotite schist	1		63.1	0.04	14.08				0.7	11.07	0.03	3.37	2.31	3.32	0.29				2.76	0	100.07
Be 609	2		66	0.03	19.34		2.04			10.75	0.02			0.04	0.03				0.59	0.38	99.22
Be 522	2		63.66		20.89		0.83			12.49	0.01	0.01		0.24	0.05				0.74	0.38	99.30
Be551	2		63.94	0.01	20.98		2.04			10.08	0.02			0.32	0.09				1.15	0.47	99.11
DHZ4	3		59.52	0.05	10.63	0.09	2.08		2.24	12.49	0.29	2.16	0.11	1.16	0.16		6.68	0.23	1.62		99.88
1	4	microprobe#	65.12		18.84	0.01		0.03	0.46	13.6		0.03		0.1				0.02	0.95		99.21
2	4	microprobe#	65.45		18.24				0.89	13.65		0.04		0.17				0.02	1.04		99.50
3	4	microprobe#	65.83		18.7	0.02		0.01	1.13	13.65		0.02		0.14				0.02	1.04		100.56
4	4	microprobe#	65.53		18.39	0.08		0.06	0.31	13.7		0.2		0.15				0.01	1.13		99.56
DHZ1	5*		65.14	0.06	18.2		0.65		0.28	12.82		0.5		0.4	0.05				1.98	0.23	100.31
DHZ2	6*		64.16		18.73		0.28			12.98				1.27	0.39		0.42	0.08	1.44	0.02	99.77
DHZ3	7		61.88	0.01	17.1		0.08			10.54		0.22	0.44	2.5			4.13	0.6	2.26	0.16	99.92
Rbba1	8	XRF/EDS/ICP	67.0		18.3		0.25		0.66	13.5	0.01	0.09	0.04	0.13		0.01	0.006	0.1	1.05		101.20
Rbba2	8	XRF/EDS/ICP	67.9		18.0		0.22		0.65	13.6	0.03	0.1	0.03	0.12		0.01	0.006	0.09	0.99		101.80
Rbip1	8	XRF/EDS/ICP	67.3		18.2				0.53	12.9	0.05	0.2	0.05	0.53		0.02	0.04	0.13	1.36	0.61	101.90
Rbip2	8	XRF/EDS/ICP	67.1		17.9				0.62	12.9	0.01	0.26	0.02	0.57		0.02	0.04	0.11	1.22	0.81	101.60
Rblf1	8	XRF/EDS/ICP	65.4		15.8		0.12		1.66	12.1	0.01	0.7	0.03	1.35	0.14	0.06	0.35	0.52	0.24	1.85	100.30
Rblf2	8	XRF/EDS/ICP	65.5		15.3		0.19		2.35	12.3	0.01	0.88	0.05	1.38	0.15	0.06	0.35	0.5	0.2	2.12	101.30
Rbsc1	8	XRF/EDS/ICP	66.5		17.7		0.05		0.76	12.4	0.02	0.1	0.09	0.36		0.01	0.04	0.12	1.25	0.32	99.70
Rbsc2	9	XRF/EDS/ICP	66.8		17.9		0.06		0.87	12.9	0.03	0.1	0.03	0.54		0.01	0.04	0.14	0.87	0.66	101.00
MMI03-Be	**9**	**ICPES/MS**	**64.36**	**0.02**	**16.83**		**1.52**	**0.008**		**10.838**	**0.02**	**0.2**	**0.01**	**0.49**	**0.1**	**0.014**	**0.209**				**94.62**
ICPES/MS detection limit			0.01	0.01	0.01	0.001	0.01	0.0007	0.01	0.001	0.01	0.01	0.01	0.01	0.04	0.006	0.001				

References (Ref.): 1 = Jacob, J., 1938; 2= Radcliffe and Campbell, 1966; 3= Schaller, W.T., et al., 1962; 4 = Lind, T., et al., 1986; 5* = Huton, C.O. and Seelye, F.T., 1945; 6 = Quesnel, P., 1937; 7 = Sosedko, T.A., 1957; 8 = Schaller, W.T. et al., 1962

* = in Deer, et al. (1966)

** = blank if not reported, incompletely reported, or if a wide variety of wet chemical and spectrographic methods employed on an element by element basis.

Mean SiO_2 and Al_2O_3 excluding Logtung analysis are: 65.12 and 17.7 Wt % respectively.

#-Li_2O, BeO and H_2O by standard wet chemical techniques; identical values for some oxides of samples 3 and 4 indicate not analyzed but averaged 1 and 4

TABLE 2. NUMBER OF CATIONS IN BERYL ON THE BASIS OF 18 (O)

Sample	Location	Colour	Si	Al	Ti	Fe^{3+}	Cr	Be	Mg	Li	Fe^{2+}	Mn	Na	Ca	K	Cs	Rb	Cations	Th	Oh	R+
1Ingersoll	S. Dakota	clear	5.974	2.054				2.843					0.22		0.027			11.118	2.817	2.054	0.247
2Aqua	Switzerland	blue	6.027	1.875		0.068		2.872	0.043				0.194		0.034			11.113	2.899	1.986	0.228
3Bt schist	Austria	green	6.001	1.577	0.003			2.529	0.478		0.056	0.002	0.612	0.235	0.035			11.528	2.586	2.055	0.647
Be 609	Saskachewan	green	6.11	2.108	0.002	0.142		2.391				0.002	0.007		0.004			10.766	2.501	2.25	0.011
Be 522	Saskachewan	yellow	5.862	2.265		0.057		2.763	0.001			0.001	0.043		0.006			10.998	2.625	2.323	0.049
Be551	Colorado	aqua	5.998	2.318	0.001	0.144		2.271				0.002	0.058		0.011			10.803	2.269	2.462	0.069
DHZ4	Arizona	bluish	6.003	1.263	0.004	0.158	0.007	3.026	0.325		0.189	0.025	0.227	0.012	0.021	0.287		11.547	3.029	1.942	0.535
1	Nigeria	med. blue	5.957	2.03			0.001	2.989	0.004		0.035		0.018					11.034	2.981	2.035	0.018
2	Nigeria	light blue	5.983	1.964				2.997	0.005		0.068		0.03					11.047	3.048	1.969	0.03
3	Nigeria	light green	5.965	1.995			0.001	2.971	0.003		0.086		0.025					11.046	3.022	1.999	0.025
4	Nigeria	med. green	5.977	1.975			0.006	3.002	0.027		0.024		0.027					11.038	3.003	2.008	0.027
DHZ1	New Zealand	pale green	5.998	1.974	0.004	0.045		2.836	0.069		0.022		0.071		0.006			11.025	2.856	2.088	0.077
DHZ2	Sweden	clear	5.937	2.041		0.019		2.886					0.228		0.046	0.017		11.174	2.823	2.06	0.291
DHZ3		pink	6.003	1.954	0.001	0.006		2.456	0.032	0.39			0.47	0.046		0.171		11.529	2.849	1.992	0.641
Rbba1	Brazil	green-blue	6.032	1.94		0.017		2.92	0.012		0.05	0.001	0.023	0.004			0.001	11	3.002	1.969	0.024
Rbba2	Brazil	green-blue	6.068	1.894		0.015		2.92	0.013		0.049	0.002	0.021	0.003			0.001	10.986	3.037	1.922	0.022
Rbip1	Brazil	light blue	6.083	1.937				2.801	0.027		0.04	0.004	0.093	0.005		0.002	0.001	10.993	2.924	1.964	0.096
Rbip2	Brazil	light blue	6.089	1.913				2.812	0.035		0.047	0.001	0.1	0.002		0.002	0.001	11.002	2.948	1.948	0.103
Rblf1	Brazil	dark blue	6.071	1.727		0.008		2.698	0.097	0.373	0.129	0.001	0.243	0.003	0.017	0.014	0.004	11.385	3.271	1.832	0.278
Rblf2	Brazil	dark blue	6.119	1.683		0.013		2.76	0.123		0.184	0.001	0.25	0.005	0.018	0.014	0.004	11.174	3.063	1.819	0.286
Rbsc1	Brazil	light blue	6.126	1.92		0.003		2.744	0.014		0.059	0.002	0.064	0.009		0.002	0.001	10.944	2.929	1.937	0.067
MM103-Be	**Logtung, BC**	**light blue**	**6.19**	**1.906**	**0.001**	**0.11**		**2.502**	**0.029**			**0.002**	**0.091**	**0.001**	**0.012**	**0.009**	**0.001**	**10.854**	**2.692**	**2.045**	**0.113**

Notes: "Th" is total cations estimated in the tetrahedral site calculated as: Be + (Si-6) + Mg + Mn + FeO. "Oh" is total number of cations in the octahedral site calculated as: Al2O3 + Cr2O3 + Fe2O3 + V2O3. "R+" is estimated total cations in channels calculated as: Na + K + excess FeO.

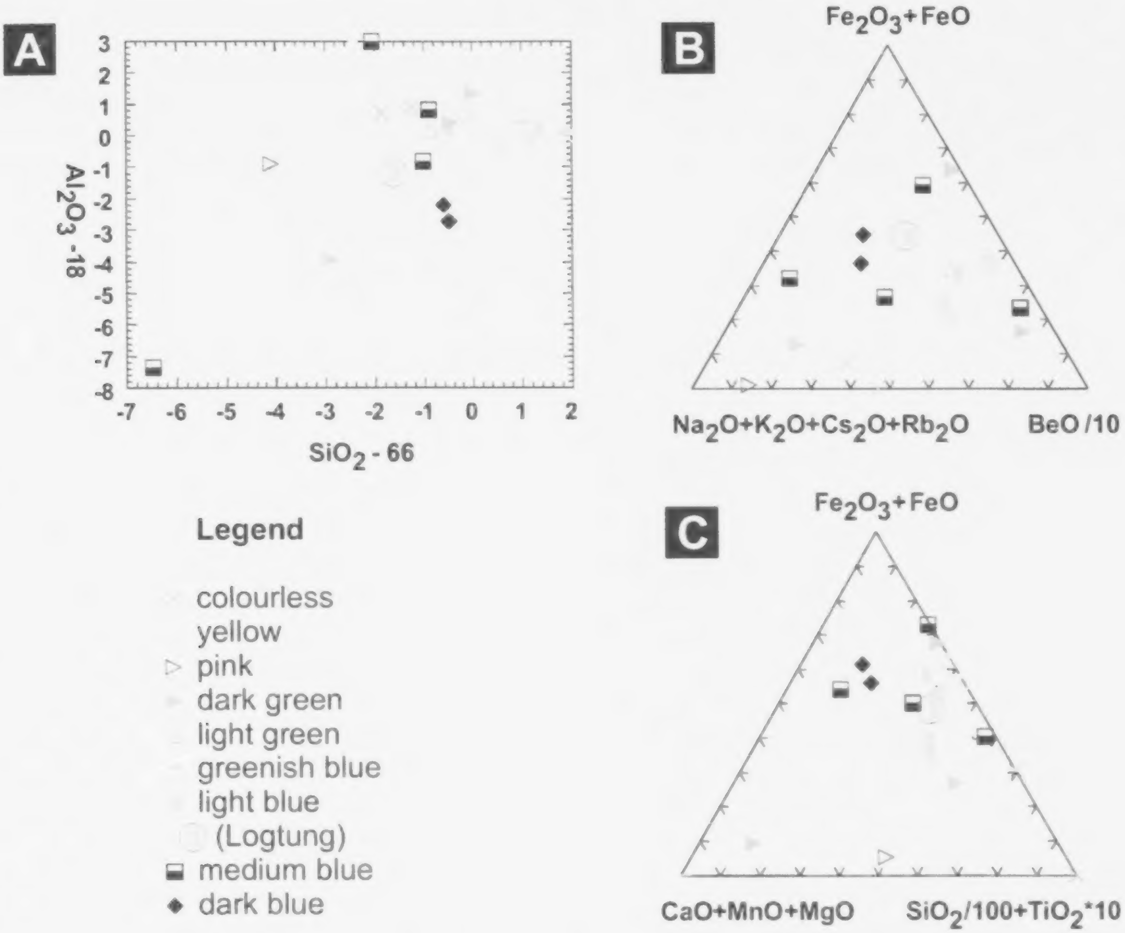

Figure 3. A. variance of SiO_2 and Al_2O_3 content of beryl about a visually estimated mode from analyses in Table 1 of 66 wt. % SiO_2 and 18 wt. % Al_2O_3. Logtung analysis is highlighted by a shaded circle.

when compared to the visually estimated mean of 65 wt. % SiO_2 and 18 wt. % Al_2O_3 from the data set, possibly contributing to the low total and the 0.3 atomic formula unit deficit in the tetrahedral site (Th, Table 2).

Iron on the other hand, compares favourably with Fe contents in blue (and green) gem beryl worldwide (Figure 3b, c). Only beryl which lack blue or green colouration have lower Fe contents as listed in Table 1 and shown on Figures 3b and 3c.

Conclusions

Inductively Coupled Plasma Emission and Mass Spectrometry (ICPES/MS) permits analysis of small samples (0.2g) with low detection limits. As a result, the method is ideally suited to elemental determination of coarse, single crystals. Drawbacks of the method are acute for minerals that contain significant Li_2O because fusion of the sample for ICPES/MS analysis requires addition of $LiBO_2$. Where OH- is a key components of the crystal chemistry, it must be also be determined by a separate method. Nevertheless, ICPES/MS provides a quick and cost effective method for determining the elemental abundance of key chromophores. In the case of the Logtung beryl, Fe content compares with gem aquamarine (and emerald) elsewhere in the world. On the basis of Fe content, the Logtung beryl can be classified as aquamarine, although the presence of gem-quality aquamarine at this locality has yet to be established.

Acknowledgments

Dave Lefebure collected the sample of aquamarine and generously allowed us to destroy one of the large crystals for analysis. Sample collection was made possible by joint Federal and Provincial funding of the Ancient Pacific Margin NATMAP program.

References Cited

Blak, A., Isotani, S. and Watanabe, S. (1982): Optical absorption and electron spin resonance in blue and green natural emerald: *Physics and Chemistry of Minerals*, Volume 8, pages 161-166.

Deer, W., Howie, R. and Zussman, J. (1966): An Introduction to the Rock Forming Minerals; London, Longman Group Limited, 528 pages.

Hunt, P.A. and Roddick, J.C. (1987): A compilation of K-Ar ages; *in* Radiogenic and isotopic studies: Report 1, *Geological Survey of Canada*, Paper 87-2, pages 143-210.

Mihalynuk, M.G., Nelson, J.L., Roots, C.F., Friedman, R.M. and de Keijzer, M. (2000): Ancient Pacific Margin Part III: Regional Geology and Mineralization of the Big Salmon Complex (NTS 104N/9E, 16 & 104O/12, 13, 14W: *in* Geological Fieldwork 1999, Paper 2000-1, pages 27-46.

Mihalynuk, M.G and Heaman, L.M. (2002): Age of mineralizated porphyry at the Logtung deposit W-Mo-Bi-Be (beryl, aquamarine), northwest BC: *in* Geological Fieldwork, *BC Ministry of Energy and Mines*, Paper 2002-1, pages 35-39.

Price, D., Vance, E., Smith, G., Edgar, A. and Dickson, B. (1976): Mossbauer effect studies of beryl; *Journal of Physics Colloquium*, Volume C6, Supplement 12, 37, pages 811-817.

Schaller, W.T., Stevens, R.E. and Jahns, R.H. (1962): An unusual beryl from Arizona; *American Mineralogist*, Volume 47, pages 672-699.

Sosedko, T. (1957): The change of structure and properties of beryls with increasing amounts of alkalis; *Memoir all Union Mineralogical Society*, Volume 86, pages 495-499.

Stewart, J.P. and Evensen, N.M. (1983): The Logtung W (scheelite) - Mo deposit, S. Yukon: petrology and geochemistry of spatially associated felsic igneous rocks, Geological Association of Canada, A65.

Vianna, P., da Costa, G., Grave, E., Evangelista, H. and Stern, W. (2002a): Characterization of beryl (aquamarine variety) by Mossbauer spectroscopy; *Physics and Chemistry of Minerals*, Volume 29, pages 78-86.

Vianna, R., Jordt-Evangelista, H., da Costa, G and Stern, W. (2002b): Characterization of beryl (aquamarine variety) from pegmatites of Minas Gerais, Brazil; *Physics and Chemistry of Minerals*, Volume 29, pages 668-679.

Proximal gold-cassiterite nuggets and composition of the Feather Creek placer gravels: clues to a lode source near Atlin, B.C.

By Patrick J. Sack and Mitchell G. Mihalynuk

KEYWORDS: Geochemistry, Cache Creek Terrane, Placer gold, Pluton related gold, Staniferous placers, Atlin placer camp

INTRODUCTION

Placer gold was discovered on Pine Creek east of Atlin in 1898 (Robertson, 1899). Since that time, exploring for a lode source for the rich Atlin placers has been a local preoccupation. Traditionally, lode exploration has focused within and adjacent to the eye-catching, bright orange, extensively quartz-veined listwanitic alteration zones in the Atlin placer camp. These zones of quartz, iron carbonate and mariposite (Cr-mica), which comprise the listwanite alteration assemblage, contain sporadic visible gold. So far, however, there has been no significant lode-gold production from such settings, in contrast to similar alteration zones in the famous Alleghany district of California (Böhlke, 1999).

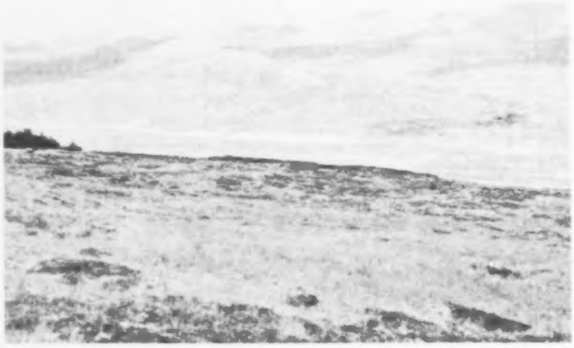

Figure 1. View to the northeast, over the broad Feather Creek valley. The placer workings are located near the centre of the photo.

Numerous lode-gold showings are known in the Atlin area, although the character of such mineralization is not in accordance with the richness of the Atlin placers and certainly not with the coarseness of some of the nuggets recovered. Also there are no producers of lode gold known within the Atlin camp*. The question remains: "What was the source of the Atlin placers?" In 1959, the Geological Survey of Canada published the Atlin Map-Area memoir by J. Aitken that included a comprehensive synopsis of placer mining activity in the Atlin camp. About the source of the gold, Aitken (1959) concluded: "*…it is significant that many acres of bedrock in the most favourable area have been stripped in the course of placer mining without a single promising vein being uncovered…. It appears likely, therefore, that the known lodes of the area and perhaps some of the multitude of barren quartz veins are the roots of lodes, now completely eroded, that may have been the source of the placer gold.*" (page 78). A contemporary view by Ash (2001) is more specific about the host lithologies, suggesting an ophiolitic association, but he comes to essentially the same conclusion: "*The placers are considered to be derived from quartz lodes previously contained within the ophiolitic crustal rocks.*"(page 25). Implicit in these assertions is that coarse gold has undergone transport in a dominantly vertical direction (eluvial); from its eroded source somewhere directly above or slightly upstream of the point in the creek bed from which the gold was recovered. Such an assertion requires that the process(es) which transported boulders up to 4 metres across into lithologically alien streambeds, did not result in long distance transport of gold nuggets.

The total erosion hypothesis advocated by Aitken (1959) and total erosion of a listwanite-altered ophiolitic source by Ash (2001), have not been systematically tested, principally because the most obvious subject of investigation no longer exists. The fact that a viable lode-gold source has not been found after more than a century of searching, appears to support these hypotheses. Even if totally eroded, however, the source should leave some telltale traces in addition to placer gold. For example, altered ultramafic clasts would occur within pay gravels. The problem lies in avoiding background sources of the proposed host rocks; sources that may have nothing to do with the lode gold, but which

---

[1] *University of Victoria, Victoria, BC*

[2] *Geoscience, Research and Development Branch, Ministry of Energy and Mines, Victoria, BC*

* *The Imperial Mine is classified as a "past producer" in MINFILE (104N008), but only 3 kg of gold production was recorded, more than 90% from mining operations in 1899. Mining ceased in 1900. Gold was not in gold "ore", considering that "ore" is raw mineral matter from which elements can be extracted at a profit.*

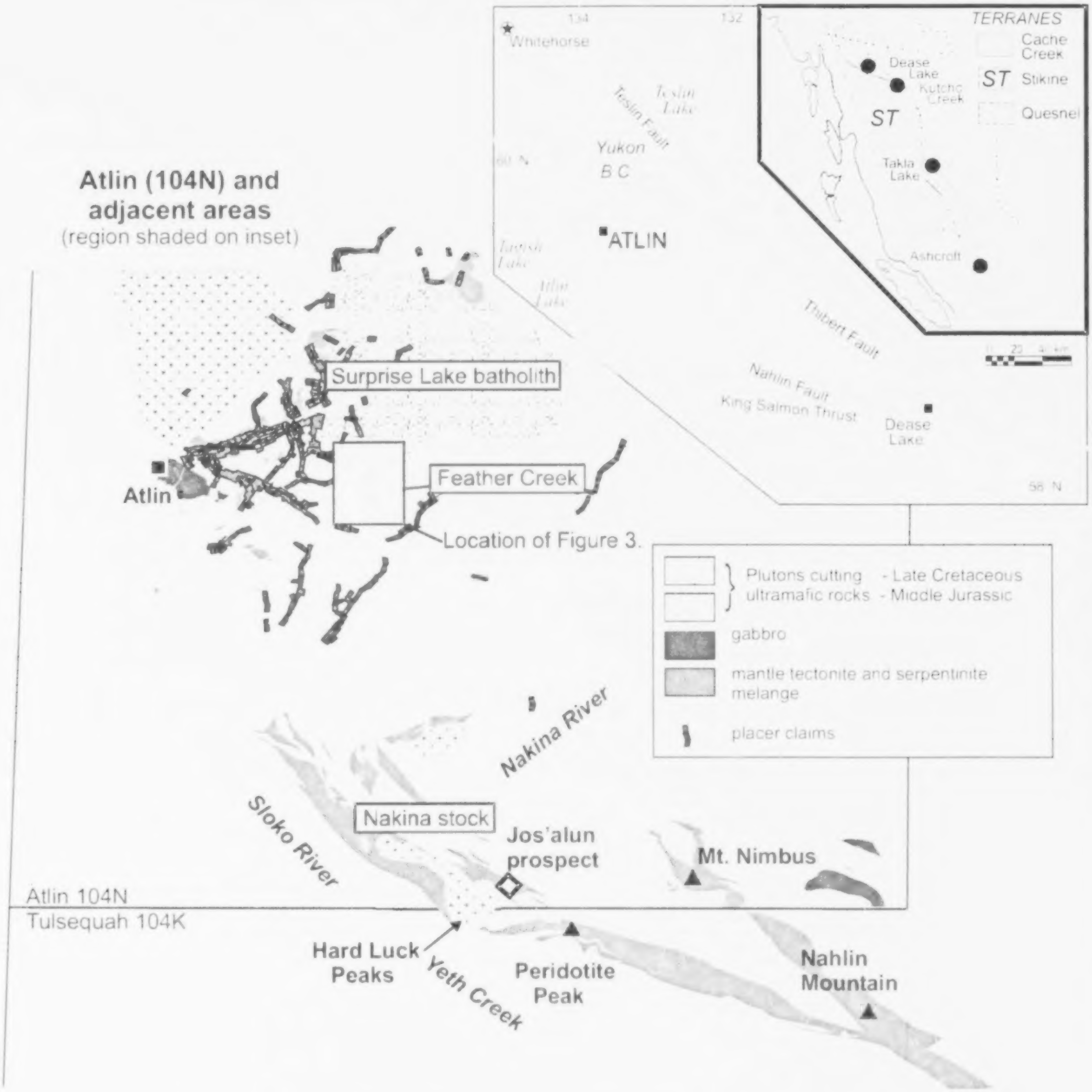
Atlin (104N) and adjacent areas
(region shaded on inset)
134
132
Whitehorse
Teslin Lake
Teslin Fault
60 N
Yukon
B C
ATLIN
Tagish Lake
Atlin Lake
TERRANES
Cache Creek
ST Stikine
Quesnel
Dease Lake
Kutcho Creek
ST
Takla Lake
Ashcroft
Thibert Fault
Nahlin Fault
King Salmon Thrust
Dease Lake
0 20 40 km
58 N
Surprise Lake batholith
Atlin
Feather Creek
Location of Figure 3.
Plutons cutting ultramafic rocks - Late Cretaceous - Middle Jurassic
gabbro
mantle tectonite and serpentinite melange
placer claims
Nakina River
Nakina stock
Sloko River
Jos'alun prospect
Mt. Nimbus
Atlin 104N
Tulsequah 104K
Hard Luck Peaks
Yeth Creek
Peridotite Peak
Nahlin Mountain

Figure 1. Location of Feather Creek, in relation to major intrusive bodies and mantle rocks.

find their way into the pay gravels. Lower portions of mature drainages are particularly afflicted by this problem. An additional level of uncertainty arises from the regional transportation of placer gold by glacial ice or ancient watercourses. Perhaps the placer gold itself carries a fingerprint of its source. Thus far, however, compositional analysis of gold nuggets within the Atlin camp has not yet revealed a fingerprint of the lode gold source (Ballantyne and MacKinnon, 1986). Mineral matter attached to the gold nuggets may however, provide insight into the gold source. We know of no prior attempt to characterize mineral matter included or intergrown with the Atlin placer gold to fingerprint its source, and consider this method a potentially fruitful avenue of investigation.

In our reconnaissance study we attempted, as much as possible, to remove the uncertainty of extraneous clast sources. We utilized a valley with dominantly local sediment (Levson, 1992), Feather Creek, to examine the composition of clasts comprising the gravels; within these gravels, coarse crystalline gold (not rounded by alluvial transport) is commonly recovered (Figure 7). Because crystalline gold is most probably not far traveled, we assume that it is from a single source. Nuggets from Feather Creek were examined visually to identify those with at-

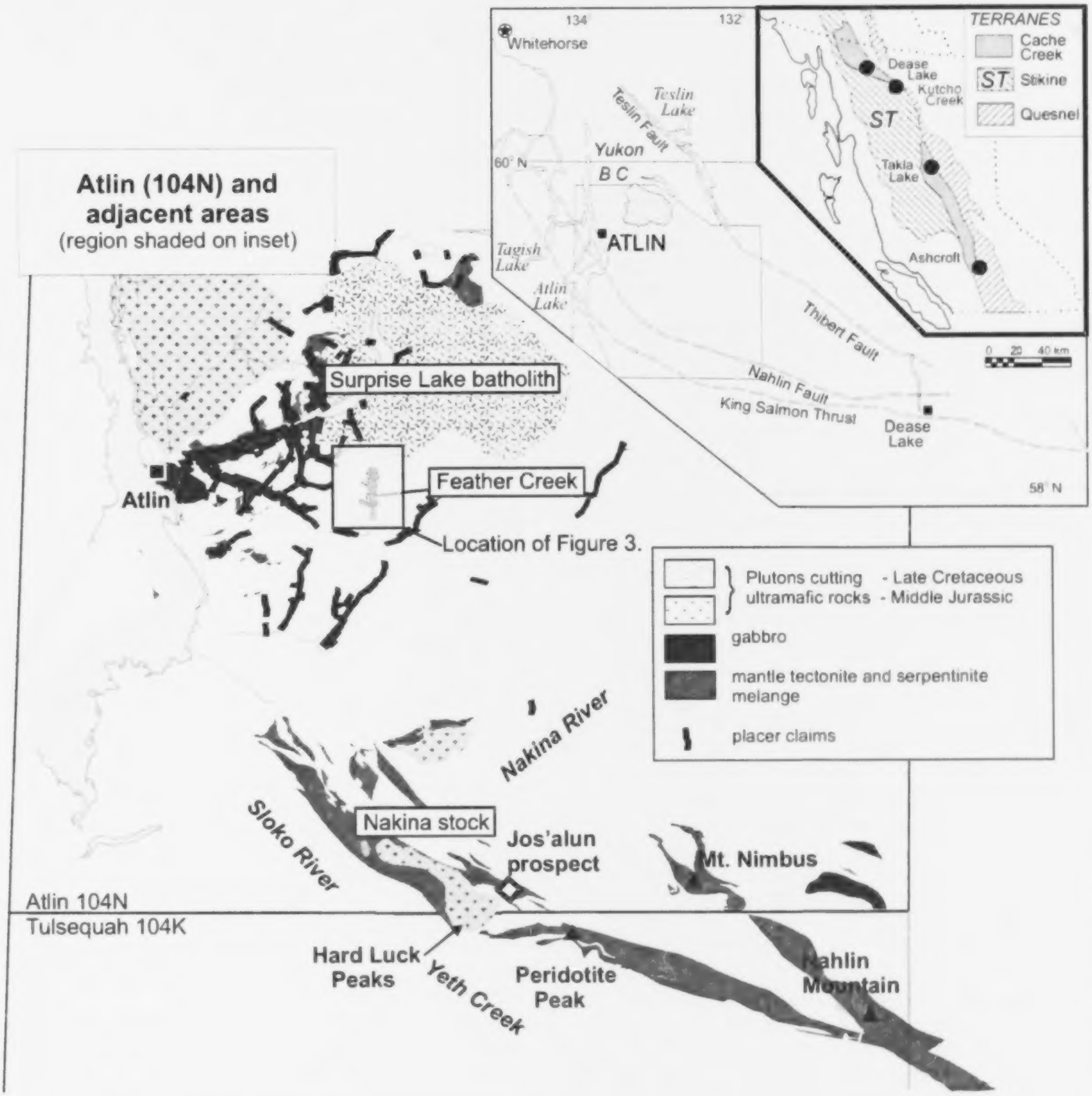
Atlin (104N) and adjacent areas
(region shaded on inset)
134
132
Whitehorse
Teslin Lake
Teslin Fault
Yukon
BC
60° N
Tagish Lake
Atlin Lake
ATLIN
Thibert Fault
Nahlin Fault
King Salmon Thrust
Dease Lake
58° N
TERRANES
Cache Creek
ST Stikine
Quesnel
Dease Lake
Kutcho Creek
ST
Takla Lake
Ashcroft
0 20 40 km
Surprise Lake batholith
Atlin
Feather Creek
Location of Figure 3.
Plutons cutting - Late Cretaceous
ultramafic rocks - Middle Jurassic
gabbro
mantle tectonite and serpentinite melange
placer claims
Nakina River
Sloko River
Nakina stock
Jos'alun prospect
Mt. Nimbus
Atlin 104N
Tulsequah 104K
Hard Luck Peaks
Yeth Creek
Peridotite Peak
Nahlin Mountain

Figure 1. Location of Feather Creek, in relation to major intrusive bodies and mantle rocks.

find their way into the pay gravels. Lower portions of mature drainages are particularly afflicted by this problem. An additional level of uncertainty arises from the regional transportation of placer gold by glacial ice or ancient watercourses. Perhaps the placer gold itself carries a fingerprint of its source. Thus far, however, compositional analysis of gold nuggets within the Atlin camp has not yet revealed a fingerprint of the lode gold source (Ballantyne and MacKinnon, 1986). Mineral matter attached to the gold nuggets may however, provide insight into the gold source. We know of no prior attempt to characterize mineral matter included or intergrown with the Atlin placer gold to fingerprint its source, and consider this method a potentially fruitful avenue of investigation.

In our reconnaissance study we attempted, as much as possible, to remove the uncertainty of extraneous clast sources. We utilized a valley with dominantly local sediment (Levson, 1992), Feather Creek, to examine the composition of clasts comprising the gravels; within these gravels, coarse crystalline gold (not rounded by alluvial transport) is commonly recovered (Figure 7). Because crystalline gold is most probably not far traveled, we assume that it is from a single source. Nuggets from Feather Creek were examined visually to identify those with at-

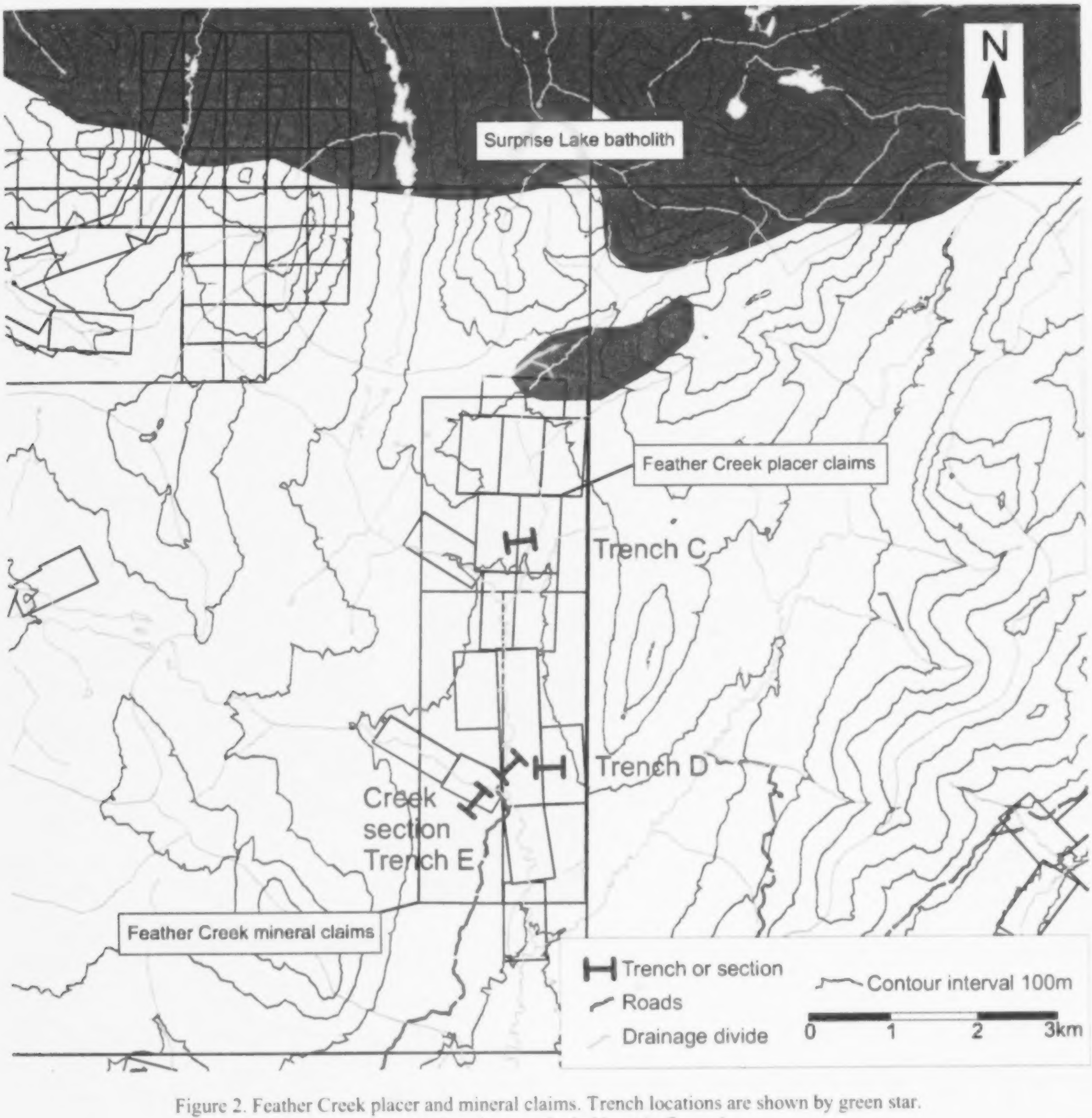
N
Surprise Lake batholith
Feather Creek placer claims
Trench C
Trench D
Creek section Trench E
Feather Creek mineral claims
Trench or section
Roads
Drainage divide
Contour interval 100m
0
1
2
3km

Figure 2. Feather Creek placer and mineral claims. Trench locations are shown by green star. For map location see shaded inset in figure 1.

tached, non-quartz mineral matter. Scanning Electron Microscope (SEM) and Energy Dispersive Spectroscopy (EDS) techniques were then used to analyze the mineral matter with the aim of acquiring a geochemical fingerprint for the geological host unit.

Our preliminary findings show that neither ultramafic nor listwanite are a significant source for river gravels in the Feather Creek placers as no ultramafite nor listwanite clasts (> 2 mm in diameter) could be found (Table 1). Furthermore, in all cases where Feather Creek gold is attached to non-quartz mineral matter, the mineral matter is primarily composed of tin oxide (cassiterite) as determined by SEM – EDS analysis. When considered in conjunction with the local and regional geology, these findings have important implications for lode gold exploration in the Atlin camp.

GEOLOGY

The Atlin placer camp is located in the northwest corner of the northern Cache Creek Terrane (Figure 1). In northwestern BC, the Cache Creek Terrane consists largely of an accreted complex of oceanic sedimentary strata of Mississippian to Jurassic age (Monger, 1975; Mihalynuk,

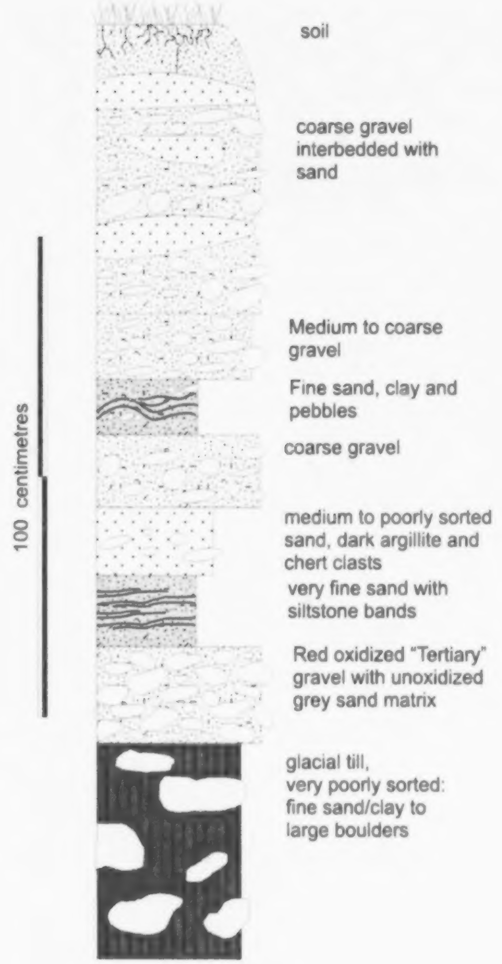
soil
coarse gravel interbedded with sand
Medium to coarse gravel
Fine sand, clay and pebbles
coarse gravel
medium to poorly sorted sand, dark argillite and chert clasts
very fine sand with siltstone bands
Red oxidized "Tertiary" gravel with unoxidized grey sand matrix
glacial till, very poorly sorted: fine sand/clay to large boulders
100 centimetres

Figure 4a. Trench C, which had the highest gold value on the property (sample series MMI03-24-3). Total thickness represented is 1.85 m.

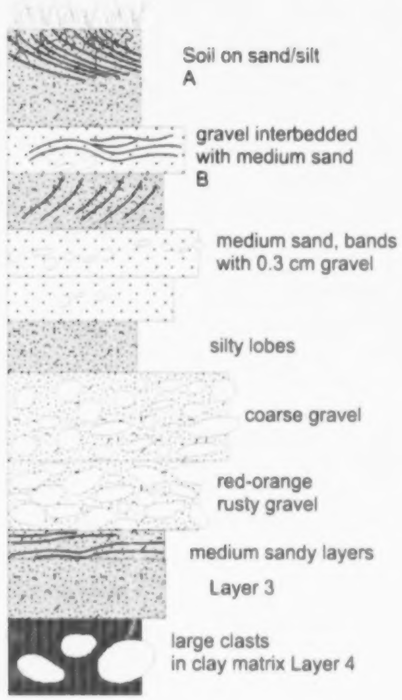
Soil on sand/silt
A
gravel interbedded with medium sand
B
medium sand, bands with 0.3 cm gravel
silty lobes
coarse gravel
red-orange rusty gravel
medium sandy layers
Layer 3
large clasts in clay matrix Layer 4

Figure 4b. Coomposite stream bank section D (KWI03-15-4) based upon the field notes of K. Wight (2003). Analyses of samples from this section included the second highest gold value that we obtained from the property.

1999) and ophiolitic rocks of Late Permian to Triassic age. Cache Creek strata were deformed and amalgamated to the ancestral continental margin between 174 and 172 Ma (Middle Jurassic) and were intruded by post collisional Middle Jurassic plutons (Mihalynuk et al., in press) and younger Cretaceous and Tertiary felsic intrusives (Mihalynuk, et al., 1992).

Near the townsite of Atlin, remnant ocean crust and upper mantle is referred to as the "Atlin Ophiolitic Assemblage" and is interpreted by Ash (2001) to have been thrust over pelagic meta-sedimentary rocks referred to as the "Atlin Accretionary Complex" (ibid.) which is the dominant lithology to the east. North of Atlin, both mantle and dismembered ophiolite are intruded by the Fourth of July Batholith (172 Ma) and, farther to the northeast, by the Surprise Lake Batholith (84 – 80 Ma; Mihalynuk et al., 1992; 2003a).

Units that underlie the lower stretches of Feather Creek drainage are ribboned and massive chert, quartz-bearing wacke, pyritic carbonaceous phyllite, volcanic conglomerate, and minor carbonate. The creek's headwaters are underlain by the Surprise Lake batholith (Aitken, 1959; Figure 2) and its thermal metamorphic aureole, as shown by the aeromagnetic response (Dumont et al., 2001).

Quaternary glaciation affected the region, and the dominant ice flow direction is north-northwest (Levson, 2003). Younger alpine glaciers north and south of placer workings at Feather Creek carved cirques and steep valleys in mountainous granitic terranes. Feather Creek occupies a broad, fluvially modified glacial valley with a relatively high gradient (Figure 3).

TABLE 1. FEATHER CREEK PLACER GRAVEL COMPOSITIONS

Sample #	Sedimentary										
	b Chert	l. g Chert	t Chert	r Chert	v Chert	c Wacke	Wacke	r Wacke	Argillite	Limestone	Feldspar
KWI03-15-5B pebbles	56	3		1	4		3			6	4
KWI03-15-5B granules	833	32	52	10		50	31				
KWI03-15-4E pebbles	287	16		3	4		8			8	
KWI03-15-4E ganules	776	17	7	13			48			39	
KWI03-15-4D pebbles		9					2				
KWI03-15-4D granules		9					10		1		
MMI03-24-4B pebbles		2									
MMI03-24-4B granules		4				1		1			
MMI03-24-3 pebbles	194	7	5			5					
MMI03-24-3 granules	1058	40	35	5							
MMI03-24-2A pebbles		3	2			3	22				
MMI03-24-2A granules	405	208	24	10			6				

						Metamorphic			Total Sample		Total	Total
	f Volcanic	FspPorph	Dioritic	Granitic	gr Volanic	Quartzite	Qtz-Vein	Meta - Wacke	Magnetic	**Weight**	Pebbles	Granules
KWI03-15-5B pebbles		3	2								5	
KWI03-15-5B granules	4	3	14	61		10	14	2	20	207. 0 g		128
KWI03-15-4E pebbles	4		4	3		5	4				20	
KWI03-15-4E ganules	8		5	25		100	13		5	345.0 g		156
KWI03-15-4D pebbles	4										4	
KWI03-15-4D granules							1	3		38.0 g		4
MMI03-24-4B pebbles									2		2	
MMI03-24-4B granules							1		10	2.9 g		11
MMI03-24-3 pebbles	2			2	2	2	6				14	
MMI03-24-3 granules	1			203		3	2			1144.9 g		209
MMI03-24-2A pebbles						2					2	
MMI03-24-2A granules				14		5	3			248.7 g		22

f = felsic, r = rusty, c = cherty, l.g = light grey, gr = green, b = black, t = tan, r = red, v = veined

METHODOLOGY

GEOCHEMICAL ANALYSIS OF FEATHER CREEK PLACER GRAVELS

Three trenches up to 2.5 m deep provide sections through unconsolidated material over fractured bedrock. These sections are similar (Figure 4) and at their base have rusty red, weakly cemented "Tertiary" gravels typically 25 cm thick, overlain by "Quaternary" lacustrine, alluvial and colluvial units, typically over a metre thick. Throughout the Atlin camp, red, oxidized gravels of assumed Tertiary age contain much of the placer gold. With the notable exception of some pay streaks along Spruce Creek, Quaternary gravel does not contain large concentrations of placer gold. Oxidized, red, angular and incipiently lithified gravels along Feather Creek resemble Tertiary gravel elsewhere in the Atlin camp, but it is underlain by poorly-sorted material

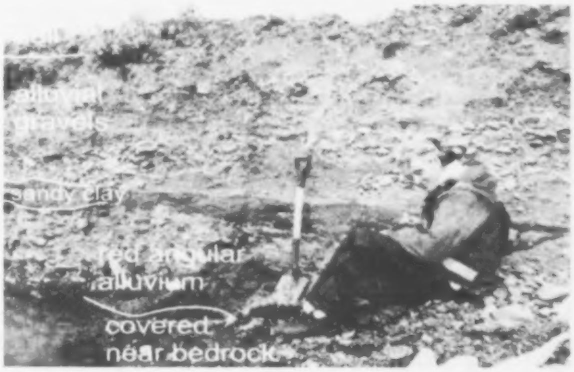

Figure 4c. Representative trench on Feather Creek showing a section of red angular alluvium, sandy clay and alluvial gravels.

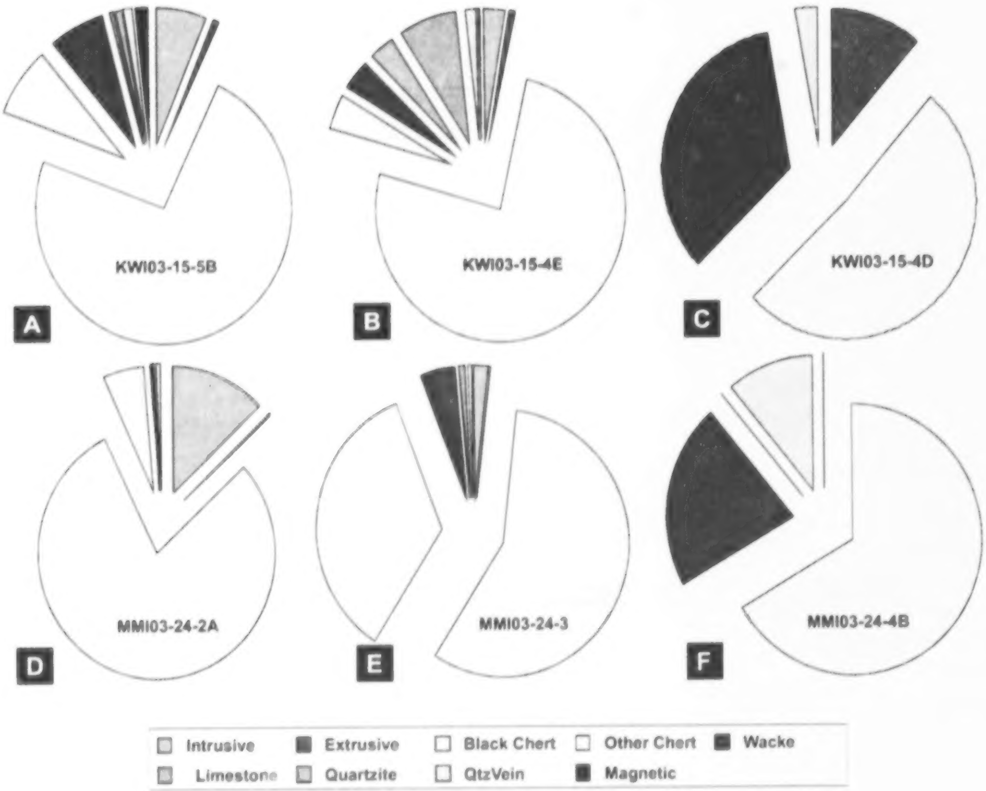

Figure 5. Clast counts for six samples; pebble and granule fractions are combined. Intrusive = diorite and granitoid; Extrusive = felsic volcanic, green volcanic, feldspar porphyry; Other chert = light grey, tan, red, and veined chert; Wacke = cherty-wacke, rusty wacke and grey wacke.

with clasts up to boulder size in a clay-rich matrix. We interpret this underlying material as glacial till. Hence, most of the sections that we sampled are probably Quaternary and younger in age. Representative samples, 1 – 2 kg, were collected from the three main units exposed in each trench. One composite sample was collected from a well exposed cut bank of Feather Creek as well as a sample from the sluice box clean up reject pile. In all, 15 samples were collected from Feather Creek. Analytical results from the 60 samples are reported in Tables 2 and 3.

Each of the fifteen samples was split into four size fractions: +10 mesh (>2 mm), -10 to +18 mesh (2 - ~1 mm), -18 to +80 mesh (1 – 0.2 mm) and -80 mesh (<0.2 mm). Resultant fractions were weighed with approximately half of the +10 mesh fraction reserved for clast identification. Grain mounts were made from a small proportion (~5%) of grains between -10 and +18 mesh to provide independent petrographic verification of clast compositions. Remaining material was reweighed. Approximately 50 g of material was split from each fraction using a Jones splitter and ground in a steel disk mill. Geochemical analyses of the "Tertiary" and "Quaternary" material was performed by inductively coupled plasma emission spectroscopy (ICPES) at ACME Analytical Laboratories Ltd., Vancouver; and by instrumental neutron activation analysis (INAA) at Activation Laboratories, Ancaster, Ontario.

The size of sample needed to accurately represent the gold content of an alluvial placer material is on the order of 2 m^3 per sample (Royle, 1987). The size of samples taken for this project were 0.02 m^3, therefore the concentrations of gold reported are not taken as representative of the grade on the property.

COMPOSITION OF ATTACHED MINERAL MATTER IN GOLD NUGGETS

Six gold nuggets with attached mineral matter (other than quartz) were obtained from the placer operation on Feather Creek. Each nugget was analyzed using a Hitachi S-3500N Scanning Electron Microscope (SEM) with an Oxford Instruments Link ISIS Energy Dispersive X-Ray Spectroscope (EDS) attached. All nuggets were attached to aluminum stubs with double-sided carbon tape. It was not necessary to apply carbon or gold coating to the electrically conductive samples. EDS analysis provided relative abundances of elements present. Elements identified during spectroscopic analysis of four of these nuggets are presented in Table 4.

TABLE 2. ENERGY DISPERSIVE SPECTROSCOPY (EDS) RESULTS FOR FOUR GOLD NUGGETS WITH ATTACHED, NON-QUARTZ MINERAL MATTER.

Sample Number	PSA03-1-1	PSA03-1-2	PSA03-1-4	PSA03-3-1
Elements present	**Au**, Sn, O (SnO_2 cassiterite), Si (quartz), Cl, Fe (oxide/ chloride coating?)	**Au**. Sn, O, (SnO_2 cassiterite) Si (quartz), Fe, Cu (in Au)	**Au**. Sn, O (SnO_2 cassiterite), Si (quartz), Th ($ThSiO_4$ thorite), Fe (surface coating?)	**Au**. Sn, O (SnO_2 cassiterite), Cl, Pb, C, Fe (surface coating?)

RESULTS

CLAST COUNTS

Fifteen samples were collected for analysis from three trenches, one exposed creek section and one from a pile of sluice box clean-up rejects. The +10 fraction was sieved to +5 mesh (> ~4 mm) and -5 to +10 mesh (~4 – ~2 mm). The +5 size range is referred to as the pebble fraction and the -5 to +10 size range is the granule fraction, conforming to the Wentworth scale size class divisions. Cobbles (>64 mm) are not present in the samples. Six clast counts were completed on samples which displayed gold INAA values in excess of 20 ppb, or had the highest gold values at their location. A complete clast count by lithology and size class is presented in Table 1.

Trench and Creek Sections

Proportions of major clast types are shown in Figure 5. In sample KWI03-15-5B, about 75% of pebbles and granules are black chert, with minor (<5%) light grey chert, tan chert, cherty wacke, and wacke pebbles. Granitoid granules comprise 6% of the sample (Figure 5a).

Sample KWI03-15-4E pebbles and granules are about 0% black chert, 10% quartzite with minor limestone, wacke and granitoid granules (Figure 5b).

Sample KWI03-15-4D pebbles are about 60% light grey chert; 30% felsic volcanic, and 10% wacke. Granules are 45% wacke, 40% light grey chert, and 15% metawacke. The sample contains no granitoid pebbles or granules (Figure 5c).

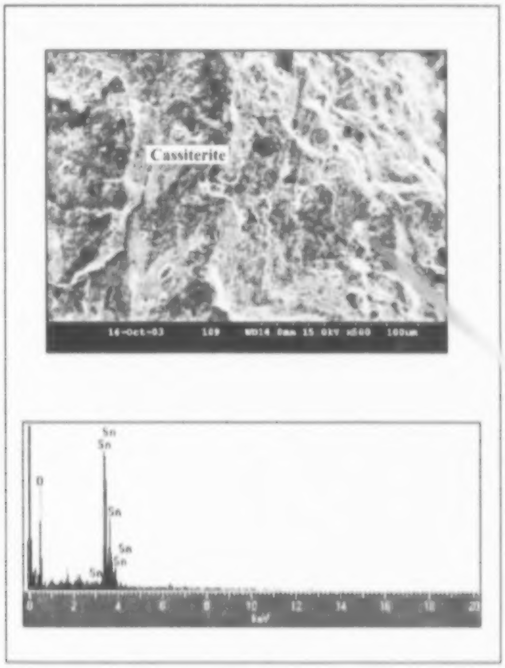

Figure 6a. SEM photomicrograph of tin-oxide (cassiterite) and EDS spectrum. The cassiterite is attached to a Feather Creek coarse crystalline crystalline gold nugget (Sample PSA03-1-1).

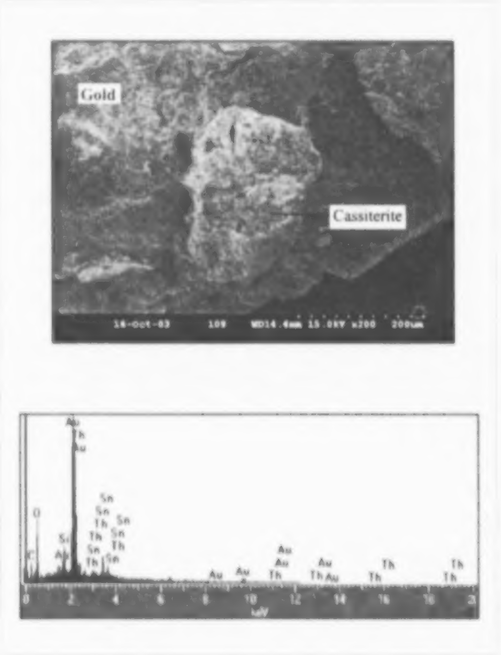

Figure 6b. SEM photomicrograph and EDS spectrum of tin-oxide (cassiterite), with thorium (thorite) on a Feather Creek gold nugget (Sample PSA03-1-4).

TABLE 3. INSTUMENTAL NEUTRON ACTIVATION ANALYSIS (INAA) FOR FEATHER CREEK PLACER GRAVELS

	Element	Au	As	Ba	Br	Ca	Co	Cr	Cs	Fe	Hf	Na	Rb	Sb	Sc	Ta	Th	U	W	La	Ce	Nd	Sm	Eu	Tb	Yb	Lu	Mass
	Units	ppb	ppm	ppm	ppm	%	ppm	ppm	ppm	%	ppm	%	ppm	ppm	ppm	ppm	ppm	ppm	ppm	ppm	ppm	ppm	ppm	ppm	ppm	ppm	ppm	g
	Detect Limit	2	0.5	50	0.5	1	1	5	1	0.02	1	0.01	15	0.1	0.1	0.5	0.5	0.5	1	0.1	3	5	0.1	0.2	0.5	0.2	0.05	0.1
Sample Number/ Location	Grain Size																											
MMI03 - 24 - 2A	>2mm	5	9	1700	-0.5	-1	14	105	2	4.03	2	1.55	23	1.2	17	-0.5	1.8	-0.5	-1	7.7	18	8	2.1	0.5	-0.5	1.5	0.25	30.24
600847 mE +/- 4m	1 - 2mm	-2	10.7	2300	-0.5	-1	12	144	4	3.46	3	1.27	53	1.2	14.8	-0.5	3.6	1.8	-1	13.5	30	17	2.8	0.6	-0.5	2.1	0.33	20.08
6600989 mN	.18 - 1mm	11	14.2	2100	-0.5	-1	11	184	3	3.22	3	1.35	50	1.5	13.7	1	3.8	1.5	-1	14.7	31	15	2.9	0.8	-0.5	2.2	0.33	21.42
	<.18mm	-2	12.7	1800	-0.5	-1	12	180	2	2.84	4	1.61	39	1.3	11.5	1.3	5.5	2.8	-1	19.2	39	14	3.5	1.1	-0.5	2.5	0.38	23.45
MMI03 - 24 - 2B	>2mm	7	8.2	1900	-0.5	-1	11	140	2	3.94	3	1.29	45	1.6	17.5	1.4	3	-0.5	-1	11.5	24	12	2.6	0.7	-0.5	2.1	0.31	22.75
	1 - 2mm	2	7.6	1800	-0.5	-1	11	122	2	3.76	2	1.43	40	1.6	17.1	-0.5	3	-0.5	-1	11.1	24	15	2.6	0.7	-0.5	2	0.3	28.46
	.18 - 1mm	-2	11	1700	-0.5	-1	10	154	2	3.19	2	1.36	32	1.6	14.2	-0.5	3.3	-0.5	-1	11.9	25	10	2.7	0.7	-0.5	1.8	0.28	26.56
	<.18mm	5	10.5	1800	-0.5	-1	9	170	2	2.57	4	1.55	40	1.1	10.7	-0.5	4.9	1.4	-1	17.4	35	16	3.3	1.1	0.5	2.5	0.38	28.39
MMI03 - 24 - 3	>2mm	-2	5.9	2400	-0.5	-1	4	141	3	2.09	3	0.78	52	1.2	12.2	-0.5	6.5	3	-1	19.1	38	15	3	0.6	-0.5	2.7	0.41	28.52
600925 mE +/- 12m	1 - 2mm	11	8.6	2200	-0.5	-1	9	144	2	2.89	2	1	61	1.4	11.7	-0.5	4.8	3.4	-1	15.1	29	16	2.7	0.7	-0.5	2.1	0.3	33.57
6603714 mN	.18 - 1mm	14	14.7	2300	-0.5	-1	13	380	3	4.09	3	1.01	80	2.3	13.9	-0.5	6.1	3.7	-1	20.1	40	21	3.7	1	-0.5	2.8	0.55	23.33
	<.18mm	112	18.3	2300	2.8	-1	17	175	4	5.73	5	0.97	82	4.2	16.5	-0.5	9	6.4	-1	28.1	54	26	5.5	1.7	0.8	3.8	0.56	22.46
MMI03 - 24 - 3A	>2mm	11	8.2	2800	-0.5	-1	8	147	3	2.97	3	0.98	67	1	11.7	-0.5	5	3	-1	16.3	38	13	2.9	0.7	-0.5	2.1	0.32	26.16
	1 - 2mm	7	10	2800	-0.5	-1	7	136	3	2.61	3	0.93	49	1.3	11.3	-0.5	5.4	2.4	-1	16.8	38	18	3	0.7	-0.5	2.1	0.32	20.54
	.18 - 1mm	-2	9.2	2400	-0.5	-1	7	156	2	2.4	2	0.94	61	1.3	10	-0.5	5	2.8	-1	16.6	37	14	2.8	0.7	-0.5	1.8	0.26	31.02
	<.18mm	11	14.6	2500	-0.5	-1	13	273	3	3.54	5	1.21	63	2	12.8	-0.5	6.8	3.7	-1	27.1	61	22	4.9	1.5	-0.5	3.7	0.55	20.28
	1-2mm duplicate	8	10.7	2400	-0.5	-1	8	186	2	2.55	2	0.91	51	1.3	10.6	-0.5	5.3	2.7	-1	15.7	32	18	2.8	0.5	-0.5	1.8	0.26	23.8
MMI03 - 24 - 3B	>2mm	-2	6.4	2300	-0.5	-1	5	108	2	2.06	2	1.16	44	0.8	10.8	-0.5	3.9	1.4	-1	11	28	7	2.1	0.5	-0.5	1.6	0.24	31.68
	1 - 2mm	-2	7.1	2400	-0.5	-1	6	83	2	1.99	2	0.79	54	0.9	9	0.7	4.1	-0.5	-1	12.2	26	11	2	0.4	-0.5	1.4	0.21	36.11
	.18 - 1mm	6	7.9	2600	-0.5	-1	8	186	2	2.35	2	1.04	63	1	10.4	-0.5	5.6	2.8	2	17.3	36	13	2.8	0.5	-0.5	2	0.31	27.01
	<.18mm	12	6.3	2300	-0.5	1	9	300	2	2.43	5	1.37	60	1	10.5	2.1	5.4	3.9	-1	23.2	46	23	3.8	0.9	0.5	2.8	0.42	24.62
	>2mm duplicate	-2	4.9	2200	-0.5	-1	6	158	2	1.86	2	0.65	62	0.5	9.4	-0.5	3.9	1.5	-1	12.6	25	10	2	0.4	-0.5	1.4	0.21	27.49
MMI03 - 24 - 4B	>2mm	17000	80.8	1800	-0.5	-1	47	7050	1	33	3	0.57	41	8.4	10	-0.5	2.9	-0.5	6	12.1	25	5	2.4	0.6	-0.5	1.8	0.26	20.16
600814 mE +/- 6m	1 - 2mm	5660	89.7	1400	-0.5	-1	60	8540	-1	40.8	3	0.5	-15	9.1	9.4	-0.5	2.1	-0.5	20	12.4	30	8	2.4	0.6	-0.5	1.9	0.31	20.67
6600242 mN	.18 - 1mm	90	12.6	1700	-0.5	-1	41	7420	2	30	5	0.71	-15	2	9.2	-0.5	5.5	2.1	-1	15.7	34	12	2.8	1	0.8	2.1	0.32	19.85
	<.18mm	12700	9.3	2300	-0.5	-1	24	2930	2	17.3	8	1.19	44	1.6	11.5	2.1	5.9	-0.5	7	25.7	52	24	4.4	1.2	-0.5	3.2	0.5	12.5
	GSB 99 standard	28	60	1100	2.7	-1	42	399	-1	8.26	4	2	52	15.1	29.9	-0.5	6.4	-0.5	-1	30.3	54	30	6.4	2.5	-0.5	3.1	0.47	17.85
	STD-4 standard	4	15.8	2800	12.5	2	14	91	3	4.35	6	2.16	41	7.1	13.5	-0.5	4.3	4.2	-1	22.8	46	22	4.6	1.3	-0.5	3.5	0.54	18.42
KWI03 - 15 - 4	>2mm	-2	6.3	2100	-0.5	1	10	139	2	2.47	2	0.68	34	0.7	10.4	-0.5	2.4	-0.5	-1	9.1	19	9	2	0.4	-0.5	1.3	0.19	43.21
660858 mE +/- 14m	1 - 2mm	-2	8.7	2700	-0.5	-1	7	152	2	2.14	2	0.85	53	0.9	9	-0.5	4.2	-0.5	3	14.2	30	11	2.4	0.5	-0.5	1.6	0.26	21.68
6600903	.18 - 1mm	11	14	3300	-0.5	-1	10	322	3	3.13	3	1.05	53	1.4	11.3	-0.5	5	1.8	-1	18.5	34	14	3	0.8	-0.5	2.1	0.31	9.72
KWI03 - 15 - 4A	>2mm	-2	7	2300	-0.5	-1	7	120	2	2.41	2	0.99	47	0.8	9.7	-0.5	3.5	1.2	-1	11.5	27	11	3.2	0.6	-0.5	1.6	0.25	29.26
	1 - 2mm	-2	6.7	2400	-0.5	-1	6	102	2	2.09	2	0.82	47	0.9	8.8	-0.5	3.4	1.2	-1	12	25	8	2.2	0.6	-0.5	1.7	0.26	34.17
	.18 - 1mm	-2	7.7	2600	-0.5	-1	7	159	2	2.32	2	0.96	46	1.1	9.4	-0.5	4	1.9	-1	13.7	31	10	2.8	0.4	-0.5	1.7	0.26	27.87
	<.18mm	10	8.4	2800	2.3	-1	9	331	3	3.01	4	1.21	42	1.2	11.6	-0.5	5.9	2.2	-1	21.6	51	20	3.9	1	-0.5	2.8	0.42	20.12
KWI03 - 15 - 4B	>2mm	5	8.9	2400	-0.5	-1	8	171	1	2.19	2	0.73	44	1.2	9.4	-0.5	3.9	1.2	-1	11.2	28	11	2.4	-0.2	-0.5	1.7	0.28	20.45
	1 - 2mm	5	8.5	2400	-0.5	-1	10	131	2	2.54	3	0.99	42	1.1	10.3	1.3	4.3	1.1	-1	15.8	36	16	3.3	0.5	-0.5	2	0.3	25.17
	.18 - 1mm	2	8.8	2700	1.3	-1	9	149	2	2.61	3	1.13	55	1.1	10.6	-0.5	5.2	1.9	-1	16.6	38	14	3.3	0.6	-0.5	2.2	0.36	20.9
	<.18mm	5	8.6	2200	1.2	-1	9	235	2	2.72	4	1.17	54	1.1	11	-0.5	5	2	2	20.4	43	18	4	0.9	-0.5	2.8	0.41	27.96
	.18-1mm duplicate	10	8.4	2500	-0.5	-1	8	141	2	2.54	3	1.11	49	1	10.1	-0.5	4.6	2.1	-1	16.2	39	15	3.3	0.7	-0.5	2.3	0.36	20.34
KWI03 - 15 - 4C	>2mm	-2	6.2	1500	0.8	-1	7	255	1	2.47	2	0.49	24	0.5	9.5	-0.5	3.1	0.8	-1	7.7	16	7	1.9	0.4	-0.5	1.3	0.2	24.71
	1 - 2mm	4	13	2100	1.3	1	7	87	2	2.99	2	0.82	58	1	8.6	-0.5	3.8	1.6	-1	11.8	28	10	2.4	0.4	-0.5	1.7	0.25	32.76
	.18 - 1mm	6	17.7	2300	1.3	-1	8	143	2	3.44	3	0.96	33	1.2	9.1	-0.5	4.5	1.5	-1	14.3	32	10	2.8	0.5	-0.5	1.9	0.28	26.83
	<.18mm	7	44	2400	4.2	-1	21	185	2	7.02	4	1.02	49	1.6	11.2	1.1	7.7	2.8	-1	21.9	48	17	4.5	1.1	-0.5	2.9	0.41	24.35
	>2mm duplicate	-2	10.7	2000	0.8	-1	8	288	1	2.62	2	0.91	40	0.5	8.5	-0.5	3.3	1	-1	10.5	21	10	2.5	0.4	-0.5	1.4	0.21	16.32
KWI03 - 15 - 4D	>2mm	4	7.8	2000	-0.5	-1	8	192	2	2.1	2	0.66	42	0.9	8.8	-0.5	3.4	1.6	-1	10.3	22	11	2.4	0.7	-0.5	1.5	0.23	20.49
	1 - 2mm	10	6.1	2600	1.6	-1	8	220	2	2.15	3	1.01	50	0.9	11.5	-0.5	5.6	1.4	-1	18.7	38	15	3.3	0.6	-0.5	2.2	0.34	22.82
	.18 - 1mm	17	5	2400	1.4	-1	7	219	3	1.85	3	1.06	53	1	10	-0.5	5.1	2	-1	17.9	35	14	3	0.6	-0.5	2.1	0.32	32.2
	<.18mm	85	4.3	2300	-0.5	-1	9	216	3	2.23	4	1.2	44	0.8	11.7	-0.5	5.9	1.5	-1	23.1	46	19	4	1.1	-0.5	2.9	0.42	26.32
KWI03 - 15 - 4E	>2mm	4	7.5	1600	-0.5	4	6	135	-1	1.96	2	0.69	38	0.8	8.4	-0.5	2.9	1.3	-1	9	21	10	1.9	0.4	-0.5	1.4	0.22	27.56
	1 - 2mm	5	8.3	1700	-0.5	4	8	125	2	2.21	2	0.76	43	1	9.1	1.1	4	1.1	-1	12	24	11	2.4	0.5	-0.5	1.7	0.26	25.2
	.18 - 1mm	10	11.5	2000	-0.5	4	11	103	2	2.78	3	0.97	38	1.6	11.2	-0.5	4.8	2.4	-1	16.2	32	13	3	0.8	-0.5	2.4	0.35	24.83
	<.18mm	24	10.7	2000	-0.5	3	13	122	3	3.03	3	1.06	54	1.6	12.2	-0.5	5.2	1.9	-1	17.2	37	15	3.4	0.9	-0.5	2.4	0.36	28.21

	Element	Au	As	Ba	Br	Ca	Co	Cr	Cs	Fe	Hf	Na	Rb	Sb	Sc	Ta	Th	U	W	La	Ce	Nd	Sm	Eu	Tb	Yb	Lu	Mass
	Units	ppb	ppm	ppm	ppm	%	ppm	ppm	ppm	%	ppm	%	ppm	ppm	ppm	ppm	ppm	ppm	ppm	ppm	ppm	ppm	ppm	ppm	ppm	ppm	ppm	g
	Detect Limit	2	0.5	50	0.5	1	1	5	1	0.02	1	0.01	15	0.1	0.1	0.5	0.5	0.5	1	0.1	3	5	0.1	0.2	0.5	0.2	0.05	0.1
KWI03 - 15 - 5A	>2mm	7	6.2	2300	-0.5	-1	8	104	2	2.33	2	0.95	32	0.8	9.7	-0.5	3.5	1.5	-1	12.3	25	11	2.3	0.5	-0.5	1.6	0.24	32.19
600415 mE +/- 6m	1 - 2mm	8	8.8	2300	0.8	-1	7	100	3	2.44	2	0.79	57	1.5	9.9	0.9	4.4	1.5	-1	15.5	33	12	2.6	0.5	-0.5	1.9	0.29	32.25
6600471 mN	.18 - 1mm	10	10.1	2500	-0.5	2	8	165	2	2.75	3	1.01	52	1.5	10.1	-0.5	5.3	1.8	2	17.8	33	14	2.9	0.6	-0.5	1.8	0.26	28.8
	<.18mm	6	7.4	2100	-0.5	-1	8	145	2	2.27	4	1.24	34	1.2	9.9	2.1	6.2	1.5	-1	22.6	48	18	3.7	1	-0.5	2.3	0.35	27.91
KWI03 - 15 - 5B	>2mm	-2	5.9	1800	-0.5	3	8	213	1	2.31	2	0.67	37	0.7	10.2	-0.5	3.1	1.3	-1	9.8	21	10	1.5	0.4	-0.5	1.4	0.21	29.38
	1 - 2mm	7	7.3	1800	-0.5	4	11	162	2	2.7	2	0.96	45	1	11	-0.5	4	1.9	-1	14.5	29	13	2.6	0.8	-0.5	1.8	0.26	30.06
	.18 - 1mm	4	8.4	1900	-0.5	3	14	152	3	3.13	3	1.1	50	1.1	12.6	-0.5	4.9	1.6	-1	17.3	34	16	3.3	0.6	0.6	2.1	0.31	28.19
	<.18mm	7	12.1	2100	-0.5	3	18	185	2	3.89	4	1.3	85	1.5	15.2	-0.5	6.8	2.1	-1	22.1	44	15	4	1.1	-0.5	2.8	0.42	16.3
KWI03 - 15 - 5C	>2mm	-2	7.7	1600	-0.5	4	5	128	1	1.78	1	0.44	33	0.6	6.5	-0.5	2.3	1.2	-1	7.7	17	-5	2.3	0.4	-0.5	1.1	0.17	24.82
	1 - 2mm	-2	12.2	1800	-0.5	-1	11	143	2	3.1	3	1.03	36	1.1	12.7	-0.5	4.6	1.2	-1	15.9	36	16	3.3	0.8	-0.5	2.4	0.36	27.92
	.18 - 1mm	-2	15.5	2400	-0.5	1	15	171	3	3.84	4	1.19	63	1.5	15.5	-0.5	6.3	1.3	-1	19.9	43	19	3.8	0.9	-0.5	2.6	0.39	20.94
	<.18mm	9	14.5	2000	1.5	-1	16	172	3	3.62	4	1.18	56	1.7	14.3	-0.5	6.1	1.6	-1	20.9	43	14	3	1.1	0.6	2.6	0.4	24.3
	GSB 99 standard	32	62.6	1100	-0.5	-1	43	378	2	8	4	1.96	45	14.7	30.1	2.3	6.2	-0.5	-1	30.2	68	21	6.2	2.2	-0.5	2.8	0.42	20.52
Q/C																												
KWI03 - 15 - 4	1 - 2mm	7	10	2600	-0.5	-1	7	135	3	2.61	3	0.93	49	1.3	11.3	-0.5	5.4	2.4	-1	16.8	38	18	3	0.7	-0.5	2.1	0.32	20.54
	1 - 2mm duplicate	8	10.7	2400	-0.5	-1	8	166	2	2.55	2	0.91	51	1.3	10.6	-0.5	5.3	2.7	-1	15.7	32	15	2.8	0.5	-0.5	1.8	0.26	23.8
	% difference	13.3	6.8	8.0	0.0	0.0	13.3	20.6	40.0	2.3	40.0	2.2	4.0	0.0	6.4	0.0	1.9	11.8	0.0	6.8	17.1	18.2	6.9	33.3	0.0	15.4	20.7	14.7
MMI03 - 24 - 3B	>2mm	-2	6.4	2300	-0.5	-1	5	108	2	2.06	2	1.16	44	0.8	10.8	-0.5	3.9	1.4	-1	11	26	7	2.1	0.5	-0.5	1.6	0.24	31.68
	>2mm duplicate	-2	4.9	2200	-0.5	-1	6	158	2	1.86	2	0.65	62	0.5	9.4	-0.5	3.9	1.5	-1	12.6	25	10	2	0.4	-0.5	1.4	0.21	27.49
	% difference	0.0	26.5	4.4	0.0	0.0	18.2	37.6	0.0	10.2	0.0	56.4	34.0	46.2	13.9	0.0	0.0	6.9	0.0	13.6	3.9	35.3	4.9	22.2	0.0	13.3	13.3	14.2
KWI03 - 15 - 4B	.18 - 1mm	2	8.8	2700	1.3	-1	9	148	2	2.61	3	1.13	55	1.1	10.6	-0.5	5.2	1.9	-1	16.6	38	14	3.3	0.6	-0.5	2.2	0.36	20.9
	.18 - 1mm duplicate	10	8.4	2500	-0.5	-1	8	141	2	2.54	3	1.11	49	1	10.1	-0.5	4.6	2.1	-1	16.2	39	15	3.3	0.7	-0.5	2.3	0.36	20.34
	% difference	133.3	4.7	7.7	450.0	0.0	11.8	4.8	0.0	2.7	0.0	1.8	11.5	9.5	4.8	0.0	12.2	10.0	0.0	2.4	2.6	6.9	0.0	15.4	0.0	4.4	0.0	2.7
Standards	STD-4 standard	4	15.8	2800	12.5	2	14	91	3	4.35	6	2.16	41	7.1	13.5	-0.5	4.3	4.2	-1	22.8	46	22	4.6	1.3	-0.5	3.5	0.54	18.42
	CANMET Ref. values*	4	15	2000	13		13	93	1.9	4.1	5.5		39	7.3	14	0.6	4.3	3	-4	24	44	21	5	1.2	0.8	2.6	0.5	
	% difference	0.0	5.2	33.3	3.9		7.4	2.2	44.9	5.9	8.7		5.0	2.8	3.6	2200	0.0	33.3	-120	5.1	4.4	4.7	8.3	8.0	867	29.5	7.7	200.0

Notes:
Prep. Sediment samples prepared @ GSB, Victoria.
INA - Instrumental neutron activation analysis
ACT - ActLabs, Ancaster, Ontario.
% Difference = ABS ((x1-x2)/(x1+x2)/2)x100
BAL = Balance
* CANMET Reference value (Bowman, 1994)

Elements Ag, Hg,Ir, Mo, Ni, Se, Sn, Sr, Zn were included in analysis, but results were either below detection or unreliable.

TABLE 4. INDUCTIVELY COUPLED PLASMA EMISSION SPECTRSOSCOPY (ICPES) FOR FEATHER CREEK PLACER GRAVELS.

	Element	Mo	Cu	Pb	Zn	Ag	Ni	Co	Mn	Fe	As	U	Au	Th	Sr	Cd	Sb	Bi	V	Ca	P	La	Cr	Mg	Ba	Al	Na	K	W	Sc	S	Hg	Se	Te	Ga
	Units	ppm	ppm	ppm	ppm	ppb	ppm	ppm	ppm	%	ppm	ppm	ppb	ppm	ppm	ppm	ppm	ppm	ppm	%	%	ppm	ppm	%	ppm	%	%	%	ppm	ppm	%	ppb	ppm	ppm	ppm
	Detect Limit	0.01	0.01	0.01	0.1	2	0.1	0.1	1	0.01	0.1	0.1	1	0.1	0.5	0.01	0.02	0.02	2	0.01	0	0.5	0.5	0.01	0.5	0.01	0.001	0.01	0.2		0.02	5	0.1	0.02	0.02
Sample Number	Grain Size	ppm	ppm	ppm	ppm	ppb	ppm	ppm	ppm	%	ppm	ppm	ppb	ppm	ppm	ppm	ppm	ppm	ppm	%	%	ppm	ppm	%	ppm	%	%	%	ppm	ppm	%	ppb	ppm	ppm	ppm
MMI03 - 24 - 2A	>2mm	0.78	64.3	2.84	70.1	57	29.8	14.4	631	3.67	8.6	0.2	1.7	1.1	14.6	0.2	0.53	0.05	47	0.23	0.05	4.7	59.6	1.41	196	2	0.015	0.07	<.1	4	<.01	21	0.1	0.02	5.3
	1 - 2mm	1.56	48.8	4.31	58.6	109	27.7	9.4	762	2.47	8	0.4	1.6	2	17.8	0.23	0.57	0.1	32	0.25	0.05	7.9	50	0.81	164	1.2	0.011	0.07	<.1	2.8	0.02	30	0.2	0.03	3.6
	.18 - 1mm	1.84	55	5.47	63.9	113	30.7	11.2	830	2.59	9.9	0.5	1.9	2.4	20.9	0.29	0.7	0.13	37	0.28	0.05	9.4	76.8	0.76	230	1.28	0.02	0.12	<.1	3.5	0.01	33	0.3	0.05	3.8
	<.18mm	1.95	57.5	6.82	62.1	111	31.5	11.8	835	2.26	10	0.5	3.5	2.9	23.2	0.27	0.73	0.15	34	0.33	0.06	11.4	57.8	0.53	191	1.03	0.018	0.08	<.1	3.4	0.02	49	0.2	0.06	3.1
MMI03 - 24 - 2B	>2mm	2.19	71.8	4.88	73.2	53	31	11.8	624	3.27	6.3	0.4	0.8	2.1	15.7	0.18	0.61	0.17	43	0.25	0.04	7.8	73.8	1.31	202	1.94	0.018	0.13	<.1	3.8	0.01	15	0.2	0.08	5.2
	1 - 2mm	0.91	54.9	3.57	66.9	64	28.6	11.8	688	3.06	6.7	0.3	1.9	1.7	14.5	0.19	0.61	0.1	43	0.27	0.05	6.7	51.7	1.19	134	1.69	0.01	0.06	<.1	3.7	0.01	19	0.2	0.06	4.7
	.18 - 1mm	1.17	55.8	4.45	63	95	29.2	11	748	2.83	7.4	0.4	2.1	2.1	18.7	0.2	0.73	0.11	44	0.28	0.05	8.1	75.3	1.01	207	1.55	0.021	0.1	<.1	4	0.02	27	0.2	0.04	4.3
	<.18mm	1.65	49.7	4.93	51.9	117	27	9.2	540	2.04	8.4	0.5	3	2.7	19.9	0.22	0.69	0.12	33	0.28	0.05	10.2	47	0.48	164	0.91	0.012	0.06	<.1	3	0.04	37	0.3	0.05	2.9
MMI03 - 24 - 3	>2mm	3.36	31.5	3.5	47.4	90	14.8	4.4	264	1.6	3	0.9	< 2	5.3	11.9	0.17	0.44	0.09	24	0.12	0.02	15.9	60.5	0.58	221	0.87	0.011	0.16	<.1	1.8	0.03	33	0.3	<.02	2.9
	1 - 2mm	4.83	48.5	5.71	69	99	26.2	8.3	402	2.4	6.4	1.2	1.4	3.5	20.1	0.32	0.77	0.19	30	0.31	0.04	11.9	71.1	0.53	218	0.96	0.02	0.14	<.1	2.3	0.02	34	0.8	0.08	3.2
	.18 - 1mm	7.53	69.3	8.09	93.4	148	31.8	10.7	482	3.08	9.5	1.6	6.2	4.3	22.2	0.37	1.24	0.3	40	0.29	0.05	14.3	87.9	0.61	224	1.09	0.017	0.16	<.1	2.6	0.03	58	1.2	0.08	3.6
	<.18mm	21.3	128	18.5	139	480	44.9	16.5	726	4.68	13.6	3.8	51.7	6.5	26.4	0.66	2.64	0.62	44	0.28	0.07	21.5	54.1	0.63	225	1.31	0.009	0.14	<.1	3.8	0.04	213	4.5	0.36	4
	ACME Q/C	21.7	131	19	143	491	48.7	16.5	743	4.8	14.1	3.8	48.6	6.5	27	0.69	2.67	0.65	44	0.29	0.08	22.1	55.1	0.65	231	1.33	0.01	0.15	0.1	3.7	0.04	232	4.7	0.4	4
MMI03 - 24 - 3A	>2mm	3.81	47.1	5.43	68.8	104	36.5	7.9	378	2.51	5.7	0.9	0.6	3.3	16.9	0.38	0.53	0.13	41	0.23	0.05	12.4	76.3	0.55	372	1.03	0.024	0.19	0.1	3.1	0.07	33	0.4	0.03	3.8
	1 - 2mm	5.57	53.9	6.05	76.3	122	36.3	7.1	690	2.15	6.6	1.1	0.9	3.7	18.1	0.64	0.68	0.3	27	0.23	0.04	12.5	60.4	0.45	221	0.87	0.013	0.12	<.1	2.2	0.03	42	0.4	0.07	2.8
	.18 - 1mm	5.16	55.4	6.43	83.1	135	38.3	7.4	682	2.08	7.3	1.1	2.5	3.5	15.4	0.68	0.73	0.19	26	0.2	0.05	12	40.5	0.43	161	0.78	0.008	0.08	<.1	2.1	0.01	55	0.4	0.07	2.7
	<.18mm	10.9	101	11.2	129	256	87.1	12.2	2087	2.77	10	2	5.7	4.4	22	2.45	1.03	0.3	40	0.29	0.08	17.5	65.5	0.51	295	1.1	0.012	0.12	0.4	3.6	0.01	147	0.5	0.1	3.6
	1-2mm duplicate	4.85	53.6	5.79	79.3	109	37.3	7.7	739	2.29	8.2	1.1	0.5	3.6	22.8	0.68	0.7	0.17	32	0.27	0.06	12.6	94.9	0.47	307	1	0.02	0.18	<.1	2.5	0.02	53	0.4	0.08	3.3
MMI03 - 24 - 3B	>2mm	1.2	28.3	4.8	58.1	28	22.4	5.6	319	1.79	4.9	0.4	0.2	2.8	61	0.26	0.3	0.12	31	0.22	0.04	8.8	53.3	0.55	292	0.97	0.014	0.09	<.1	2.4	0.02	12	0.2	0.03	3.2
	1 - 2mm	3.13	38.8	5.28	73.1	34	25.1	6.2	348	1.79	6	0.7	1.7	2.9	11	0.35	0.51	0.16	22	0.14	0.04	10.2	41.8	0.39	148	0.81	0.008	0.09	<.1	1.7	0.02	23	0.3	0.05	2.5
	.18 - 1mm	3.18	45.3	5.92	84.5	49	29.9	7.2	321	1.96	6.4	1	2.8	3.2	13.5	0.34	0.59	0.2	26	0.15	0.04	12.7	72.3	0.42	210	0.95	0.012	0.12	<.1	2.1	0.02	21	0.4	0.06	3.1
	<.18mm	2.58	45.8	6.04	86.7	79	32.5	8.1	317	1.8	5.1	1.5	3.4	3.2	18.7	0.42	0.53	0.24	34	0.24	0.06	14.7	97.5	0.43	234	1.02	0.022	0.13	0.2	2.7	0.03	47	0.2	0.05	3.3
	>2mm duplicate	1.62	29.7	4.33	60.7	30	27.7	6.1	405	1.58	3.8	0.5	0.3	2.6	8.1	0.17	0.26	0.24	28	0.08	0.03	9	91.6	0.42	234	0.79	0.018	0.16	<.1	2.5	0.02	6	0.1	0.05	2.6
MMI03 - 24 - 4B	>2mm	17.6	197	16.5	92.5	1636	159	34.3	3638	24.7	70.7	1.5	22780	2.6	21.3	1.16	7.15	1.47	399	0.34	0.05	11.8	559	0.51	765	0.77	0.014	0.08	0.9	2.6	<.01	180	5.1	1.53	8
	1 - 2mm	27.3	326	15.6	84.5	411	236	40.8	3645	32.1	58.4	1.4	91.3	2.5	17.4	0.63	8.82	0.79	464	0.3	0.05	12	649	0.49	803	0.74	0.011	0.07	2.8	2.4	<.01	96	2.3	0.75	9.7
	.18 - 1mm	5.19	46.3	6.72	70.5	76	95.1	21.3	951	18.7	8.2	0.8	14.8	2.8	13.7	0.34	1.22	0.22	460	0.31	0.05	11.7	410	0.36	216	0.61	0.01	0.06	0.2	1.8	<.01	35	0.2	0.04	7.1
	<.18mm	4.86	38.8	7.52	78.9	1493	65.3	16	1047	13	6.7	1.1	14140	4	23.3	0.41	0.92	0.26	352	0.43	0.05	17.6	331	0.43	366	0.93	0.035	0.13	1.5	2.7	<.01	1022	0.2	0.03	7.5
	GSB 99 standard	0.94	159	221	330	1351	195	42	1331	6.6	55.1	0.5	21	3.8	16.7	0.66	9.16	0.25	97	0.34	0.1	16.7	251	2.55	337	2.82	0.005	0.04	<.1	14.9	<.01	327	0.5	0.22	9.1
	STDS-4 standard	1.36	64.4	14.6	84.4	306	23.7	10	1185	2.59	11.7	2	2.7	1.5	58.4	0.37	5.02	0.21	49	1.07	0.08	13.4	31	0.65	1009	1.06	0.033	0.09	0.2	3.1	0.12	817	0.8	0.02	3.7
KWI03 - 15 - 4	>2mm	1.37	37.1	3.03	48.4	91	31.4	9.6	390	1.99	6.5	0.3	0.9	1.5	18.6	0.71	0.3	0.12	30	0.49	0.04	5.8	65.7	0.55	260	0.84	0.013	0.07	<.1	2.7	0.07	19	0.3	0.04	3
	1 - 2mm	2.53	33.3	4.32	53.8	59	27.1	6.7	581	1.76	6.8	0.5	1	3	25.6	0.39	0.5	0.17	25	0.97	0.04	11.9	80.9	0.45	264	0.78	0.016	0.13	<.1	2.2	0.05	30	0.3	0.04	2.9
	.18 - 1mm	2.35	37.9	5.22	57.9	75	33.9	8	873	2.09	7.7	0.6	1.2	2.8	33.3	0.48	0.52	0.14	34	1.33	0.04	10.8	162	0.54	489	1.13	0.042	0.25	<.1	3.2	0.03	39	0.3	0.05	4
	<.18mm	3.54	52	8.78	71.2	115	52.9	10.9	1860	2.54	10.5	0.7	4.7	3.1	48.6	0.97	0.77	0.16	42	2.48	0.05	12.6	180	0.66	566	1.25	0.046	0.24	0.1	4	0.03	64	0.4	0.05	4.4
KWI03 - 15 - 4A	>2mm	1.61	31.3	4.22	61.4	51	24.5	7.1	426	2.07	5.7	0.4	0.8	2.1	13.6	0.23	0.36	0.12	26	0.23	0.04	8.7	60.9	0.54	170	0.86	0.014	0.12	<.1	2.5	0.02	11	0.2	0.09	3.4
	ACME Q/C	12.4	135	25	132	260	22.8	11.6	737	2.88	17.5	6.2	40.8	2.8	46.6	5.17	3.52	5.68	57	0.71	0.09	11	179	0.64	135	2.01	0.032	0.13	4.2	3.4	0.05	170	4.8	0.82	6.5
	1 - 2mm	1.95	33.9	4.42	56.4	62	26.8	7	456	1.74	6.6	0.4	1.4	2.4	14.8	0.32	0.48	0.11	21	0.22	0.04	9.3	49.8	0.41	152	0.71	0.011	0.1	<.1	1.9	<.01	24	0.2	0.04	2.4
	.18 - 1mm	2.06	36.1	4.76	63	76	27.5	7.2	419	1.86	6.8	0.4	2	2.6	15.1	0.28	0.5	0.14	26	0.25	0.04	10.3	76.6	0.43	185	0.83	0.016	0.14	<.1	2.3	<.01	30	0.2	0.04	2.8
	<.18mm	2.26	44.3	5.96	81	163	34.1	8.8	549	2.22	7.7	0.5	2.3	3.2	21.5	0.36	0.59	0.18	38	0.39	0.06	14	106	0.55	243	1.17	0.028	0.21	<.1	3.6	<.01	52	0.3	0.06	3.7
KWI03 - 15 - 4B	>2mm	1.53	31.1	4.46	49.1	41	26.1	6.4	583	1.61	7.4	0.4	1.2	2.2	14.1	0.32	0.51	0.11	22	0.2	0.04	8.1	84.9	0.36	204	0.65	0.013	0.12	<.1	2	<.01	22	0.2	0.03	2.2
	1 - 2mm	2.78	48.2	5.9	79.5	91	36.6	10.3	883	2.05	8.2	0.5	1.9	3	15	0.49	0.6	0.18	29	0.28	0.04	11.8	57.1	0.49	200	0.9	0.011	0.12	<.1	2.7	<.01	31	0.3	0.04	3
	.18 - 1mm	2.36	37.9	5.04	67.9	71	29.3	8.2	515	1.82	6.8	0.5	1.5	2.7	13.4	0.31	0.53	0.17	25	0.24	0.04	10.7	50.6	0.43	157	0.76	0.011	0.1	<.1	2.2	<.01	40	0.2	0.04	2.6
	<.18mm	2.14	41.9	5.5	76.3	107	31.8	8.5	527	1.99	7.2	0.5	3.3	2.6	16.7	0.31	0.56	0.2	31	0.32	0.05	12.3	61.5	0.47	181	0.87	0.014	0.12	<.1	2.8	<.01	42	0.3	0.03	2.9
KWI03 - 15 - 4C	>2mm	1.21	26.5	2.58	33.9	36	21.3	6.5	557	1.73	5.8	0.3	0.3	1.8	11.8	0.18	0.28	0.06	29	0.32	0.02	5.7	158	0.42	292	0.71	0.036	0.14	<.1	2.6	<.01	11	0.2	<.02	2.4
	1 - 2mm	3.14	34	3.95	53.4	48	25.9	7.1	658	2.47	13.1	0.5	1.4	2.5	13.1	0.4	0.55	0.11	22	0.21	0.04	8.8	44.2	0.37	151	0.65	0.01	0.09	<.1	1.8	<.01	21	0.2	0.04	2.2
	.18 - 1mm	4.01	38.6	4.47	61.1	64	31.5	8.6	709	2.94	17.1	0.5	2.1	3	14.3	0.5	0.66	0.13	26	0.25	0.04	10.8	63.6	0.4	199	0.73	0.013	0.11	<.1	2.2	<.01	40	0.3	0.03	2.6
	<.18mm	11.9	82	8.98	109	165	92.6	22.8	4896	6.48	44.2	1.2	4.8	4.7	20.1	3.3	1.33	0.22	51	0.47	0.07	16.7	65.6	0.61	535	1.2	0.016	0.17	0.1	4.1	<.01	82	0.5	0.08	4.4
KWI03 - 15 - 4D	>2mm	0.95	33.5	3.82	42.8	58	19.4	6.1	298	1.63	6.3	0.4	0.4	2	13.5	0.22	0.35	0.11	28	0.24	0.03	7.7	99.7	0.41	209	0.75	0.017	0.13	<.1	2.2	0.02	11	0.2	0.04	2.8
	1 - 2mm	1	39.3	5.98	87.2	108	29.4	8.2	201	1.7	4.1	0.4	3	3.1	19	0.14	0.39	0.2	31	0.33	0.04	13.1	110	0.53	274	1.21	0.025	0.18	<.1	3.3	<.01	39	0.2	0.03	3.7
	.18 - 1mm	1.02	35.5	5.77	87.6	112	29	7.4	170	1.55	2.9	0.4	18.4	3.2	18	0.14	0.35	0.21	29	0.3	0.04	13.7	104	0.52	243	1.1	0.023	0.16	<.1	2.9	0.01	29	0.1	0.03	3.5
	<.18mm	0.93	41.8	8.8	107	119	34	8.4	175	1.62	3.2	0.5	2	3.4	18.9	0.17	0.39	0.25	31	0.36	0.05	14.4	72.8	0.55	207	1.15	0.017	0.12	<.1	3.3	<.01	42	0.1	0.05	3.6
	ACME Q/C	0.95	40.1	6.21	102	112	32.3	7.7	173	1.59	2.8	0.4	5.6	3.2	18.3	0.15	0.38	0.24	29	0.35	0.05	13.5	69.7	0.54	195	1.11	0.016	0.11	0.1	3.2	0.01	42	0.1	0.04	3.4
	<.18mm duplicate	0.92	40.2	6.15	103	116	32.5	7.9	169	1.58	2.9	0.4	7.8	3.2	18	0.15	0.36	0.24	29	0.35	0.04	13.2	68.8	0.54	194	1.1	0.015	0.11	0.1	3.1	<.01	43	0.1	0.03	3.4

KWI03 - 15 - 4E	>2mm	1.63	29	3.66	38.9	60	14	5.3	280	1.43	5.6	0.6	<.2	1.7	81.9	0.18	0.37	0.07	28	3.61	0.04	6.6	62.6	0.58	166	0.75	0.037	0.1	<.1	2.2	0.02	22	0.3	0.02	2.5
	1 - 2mm	1.76	35.7	5.71	52.5	92	30.5	7.7	402	1.78	6.2	0.7	0.3	2.5	61.8	0.32	0.6	0.11	31	3.84	0.05	9.1	63.1	0.7	188	0.85	0.015	0.14	<.1	3	0.03	59	0.5	0.04	3.1
	.18 - 1mm	2.23	52.6	7.32	72.6	124	45.8	11.1	601	2.31	8.5	0.9	0.7	3.6	62.9	0.48	0.79	0.16	45	3.9	0.06	13.3	82.3	0.81	297	1.37	0.024	0.23	<.1	4.5	0.01	87	0.6	0.06	4.5
	<.18mm	2.39	57.8	8.04	75.8	148	50.2	12.3	729	2.39	8.9	0.8	0.5	3.6	62	0.56	0.79	0.17	43	3.97	0.07	13.5	52.8	0.83	269	1.29	0.016	0.18	<.1	4.6	0.01	102	0.7	0.05	4.2
KWI03 - 15 - 5A	>2mm	2.45	39.5	5.02	54.2	49	21.2	6.8	383	1.95	4.5	0.6	1	2.3	23.6	0.17	0.44	0.12	34	0.31	0.04	9	52.9	0.43	237	0.89	0.019	0.1	<.1	2.6	0.02	32	0.3	<.02	3.3
	1 - 2mm	2.95	48.4	6.88	57.1	50	26.2	7.7	620	2.13	8.5	0.7	4.5	3.3	14.3	0.19	0.73	0.18	27	0.16	0.04	13.2	48.3	0.37	220	0.86	0.008	0.08	<.1	2.3	<.01	27	0.5	0.05	3
	.18 - 1mm	3.58	50.1	6.95	57.2	60	27.7	8.1	676	2.24	7.6	0.8	3.4	3.3	15.7	0.2	0.84	0.25	30	0.17	0.04	13.8	85.5	0.39	288	1.05	0.018	0.13	<.1	2.7	<.01	31	0.5	0.06	3.3
	<.18mm	1.83	36.8	5.49	45.4	41	26	7.3	457	1.7	5.5	0.7	5.1	3	15.5	0.14	0.49	0.17	32	0.21	0.04	15.5	58.6	0.41	207	0.93	0.014	0.07	<.1	2.9	<.01	31	0.3	0.03	3
KWI03 - 15 - 5B	>2mm	0.56	28.7	2.84	37.7	59	29.3	5.8	272	1.55	4.2	0.3	<.2	1.5	41.3	0.11	0.29	0.08	21	2.17	0.03	6.1	63.5	0.7	126	0.77	0.007	0.09	<.1	1.8	0.01	37	0.2	0.03	2.8
	1 - 2mm	1.43	44.4	5.53	59.6	100	54.5	11.1	516	2.16	6.3	0.6	0.7	3	50.6	0.33	0.52	0.12	42	2.9	0.06	11.6	77.7	0.92	209	1.24	0.016	0.18	<.1	4.1	<.01	79	0.3	0.04	4.1
	.18 - 1mm	1.56	54.7	6.73	71.7	124	69	13.7	623	2.46	7.1	0.7	1.1	3.6	49.2	0.35	0.63	0.15	47	2.93	0.06	13.7	68	1.03	210	1.39	0.012	0.18	<.1	5	<.01	79	0.2	0.06	4.5
	<.18mm	1.69	62.1	7.72	81	134	79.8	15.6	723	2.68	8.4	0.7	1.4	3.9	50.5	0.43	0.67	0.16	53	3.1	0.07	15.2	74.3	1.1	248	1.53	0.015	0.21	<.1	5.5	<.01	110	0.2	0.04	5.1
	<.18mm duplicate	1.7	61.3	7.69	75.1	141	77.1	15	727	2.73	7.8	0.8	1.7	4	52.7	0.44	0.64	0.15	56	3.1	0.07	15.3	99.5	1.12	299	1.67	0.026	0.26	<.1	5.7	<.01	97	0.3	0.06	5.5
KWI03 - 15 - 5C	>2mm	0.89	29.7	4.2	30.9	72	15.6	4.7	398	1.44	3.6	0.6	<.2	1.3	145	0.75	0.29	0.07	20	3.48	0.07	6.1	62.3	0.38	198	0.64	0.008	0.08	<.1	1.9	<.01	32	0.3	0.02	2.3
	1 - 2mm	1.77	52.8	6.66	65.2	103	56	11.8	572	2.46	7.5	0.5	7.8	3.3	24.4	0.28	0.64	0.17	45	0.53	0.06	12.8	70.6	0.78	199	1.37	0.014	0.13	<.1	4.1	<.01	76	0.4	0.04	4.4
	.18 - 1mm	1.97	60.5	7.29	75.7	116	66.9	14	680	2.7	8.6	0.6	2.1	3.9	24.5	0.34	0.68	0.16	50	0.57	0.06	14.2	70.8	0.88	215	1.56	0.014	0.15	<.1	4.7	<.01	91	0.3	0.06	5
	<.18mm	2	68.9	8.03	80.8	138	75.3	15.3	752	2.91	9.3	0.6	2.3	4.2	26.1	0.4	0.76	0.18	56	0.64	0.07	16	74.2	0.95	243	1.71	0.014	0.17	<.1	5.5	<.01	112	0.3	0.04	5.5
Std. DS5	ACME Q/C	13.2	141	25.2	139	294	24.8	11.8	791	2.98	19.1	6.4	40.1	3	48.5	5.69	3.8	5.85	59	0.75	0.1	11.8	190	0.68	135	2.09	0.035	0.14	4.2	3.6	0.03	172	5.1	0.89	6.7
	.18-1mm duplicate	1.79	59.7	7.22	73.8	101	64.8	13.8	634	2.62	7.5	0.6	5	3.3	24	0.33	0.67	0.16	49	0.54	0.06	14.1	72.4	0.86	206	1.52	0.013	0.15	<.1	4.9	<.01	81	0.2	0.06	4.7
	GSB 99 standard	0.84	166	206	346	1297	200	43.8	1277	6.64	51	0.5	22	3.3	17.6	0.68	8.76	0.24	100	0.35	0.1	16.3	245	2.67	277	2.91	0.006	0.04	<.1	15	<.01	326	0.4	0.3	8.4
Std. DS5	ACME Q/C	13.1	145	25.6	139	282	24.9	12.6	744	2.99	17.2	6.4	42.5	2.8	48.4	5.57	3.83	5.7	61	0.74	0.1	12.1	183	0.69	133	2.09	0.034	0.14	4.4	3.6	0.01	169	5.1	0.86	6.6

Q/C

	Element	Mo	Cu	Pb	Zn	Ag	Ni	Co	Mn	Fe	As	U	Au	Th	Sr	Cd	Sb	Bi	V	Ca	P	La	Cr	Mg	Ba	Al	Na	K	W	Sc	S	Hg	Se	Te	Ga
MMI03 - 24 - 3A	1 - 2mm	5.57	53.9	6.05	76.3	122	36.3	7.1	690	2.15	6.6	1.1	0.9	3.7	18.1	0.64	0.68	0.3	27	0.23	0.04	12.5	60.4	0.45	221	0.87	0.013	0.12	-0.1	2.2	0.03	42	0.4	0.07	2.8
	1-2mm duplicate	4.85	53.6	5.79	79.3	109	37.3	7.7	739	2.29	8.2	1.1	0.5	3.6	22.8	0.68	0.7	0.17	32	0.27	0.06	12.6	94.9	0.47	307	1	0.02	0.18	-0.1	2.5	0.02	53	0.4	0.08	3.3
	% difference	13.8	0.6	4.39	3.86	11.3	2.72	8.11	6.86	6.31	21.6	0	57.14	2.74	23	6.06	2.9	55.3	16.9	16	26.3	0.8	44.4	4.35	32.6	13.9	42.42	40	0	12.8	40	23.2	0	13.3	16.4
MMI03 - 24 - 3B	>2mm	1.2	28.3	4.8	58.1	28	22.4	5.6	319	1.79	4.9	0.4	0.2	2.8	61	0.26	0.3	0.12	31	0.22	0.04	8.8	53.3	0.55	292	0.97	0.014	0.09	-0.1	2.4	0.02	12	0.2	0.03	3.2
	>2mm duplicate	1.62	29.7	4.33	60.7	30	27.7	6.1	405	1.58	3.8	0.5	0.3	2.6	8.1	0.17	0.26	0.24	28	0.08	0.03	9	91.6	0.42	234	0.79	0.018	0.16	-0.1	2.5	0.02	6	0.1	0.05	2.6
	% difference	29.8	4.8	10.3	4.38	6.9	21.2	8.55	23.8	12.5	25.3	22.2	40	7.41	153	41.9	14.3	66.7	10.2	93.3	14.5	2.25	52.9	26.8	22.1	20.5	25	56	0	4.08	0	66.7	66.7	50	20.7
KWI03 - 15 - 4D	<.18mm	0.93	41.8	6.6	107	119	34	8.4	175	1.62	3.2	0.5	2	3.4	18.9	0.17	0.39	0.25	31	0.36	0.05	14.4	72.8	0.55	207	1.15	0.017	0.12	-0.1	3.3	-0.01	42	0.1	0.05	3.6
	<.18mm duplicate	0.92	40.2	6.15	103	116	32.5	7.9	169	1.58	2.9	0.4	7.8	3.2	18	0.15	0.36	0.24	29	0.35	0.04	13.2	68.8	0.54	194	1.1	0.015	0.11	0.1	3.1	-0.01	43	0.1	0.03	3.4
	% difference	1.08	3.93	7.06	4.48	2.55	4.51	6.13	3.49	2.5	9.84	22.2	118.4	6.06	4.88	12.5	8	4.08	6.67	2.82	2.25	8.7	5.65	1.83	6.43	4.44	12.5	8.7		6.25	0	2.35	0	50	5.71
KWI03 - 15 - 5B	<.18mm	1.69	62.1	7.72	81	134	79.8	15.6	723	2.68	8.4	0.7	1.4	3.9	50.5	0.43	0.67	0.16	53	3.1	0.07	15.2	74.3	1.1	248	1.53	0.015	0.21	-0.1	5.5	-0.01	110	0.2	0.04	5.1
	<.18mm duplicate	1.7	61.3	7.69	75.1	141	77.1	15	727	2.73	7.8	0.8	1.7	4	52.7	0.44	0.64	0.15	56	3.1	0.07	15.3	99.5	1.12	299	1.67	0.026	0.26	-0.1	5.7	-0.01	97	0.3	0.06	5.5
	% difference	0.59	1.33	0.39	7.56	5.09	3.44	3.92	0.55	1.85	7.41	13.3	19.35	2.53	4.26	2.3	4.58	6.45	5.5	0	2.94	0.66	29	1.8	18.4	8.75	53.66	21.3	0	3.57	0	12.6	40	40	7.55
KWI03 - 15 - 5C	.18 - 1mm	1.97	60.5	7.29	75.7	116	66.9	14	680	2.7	8.6	0.6	2.1	3.9	24.5	0.34	0.68	0.16	50	0.57	0.06	14.2	70.8	0.88	215	1.56	0.014	0.15	-0.1	4.7	-0.01	91	0.3	0.06	5
	.18-1mm duplicate	1.79	59.7	7.22	73.8	101	64.8	13.8	634	2.62	7.5	0.6	5	3.3	24	0.33	0.67	0.16	49	0.54	0.06	14.1	72.4	0.86	206	1.52	0.013	0.15	-0.1	4.9	-0.01	81	0.2	0.06	4.7
	% difference	9.57	1.46	0.96	2.54	13.8	3.19	1.44	7	3.01	13.7	0	81.69	16.7	2.06	2.99	1.48	0	2.02	5.41	4.96	0.71	2.23	2.3	4.37	2.6	7.407	0	0	4.17	0	11.6	40	0	6.19
	STDS-4 standard	1.36	64.4	14.6	84.4	306	23.7	10	1185	2.59	11.7	2	2.7	1.5	58.4	0.37	5.02	0.21	49	1.07	0.08	13.4	31	0.65	1009	1.06	0.033	0.09	0.2	3.1	0.12	817	0.8	0.02	3.7
	CANMET Ref. values*	2	66	13	82	300	23	11	1200	2.8	11	3	4	4.3	350	0.8	3.6		51			24	30		2000				-4	14	0.09	930			
	% difference	-9.52	-0.61	2.92	0.72	0.5	0.75	-2.4	-0.31	-0.1	1.54	-10	-9.701	-24.1	-35.7	-11.9	8.24	50	-1			-14.2	0.82		-16.5				-55.3	-31.9	7.14	-3.23			50

Notes:

Prep. Sediment samples prepared @ GSB, Victoria.
ARMS = 2-2-2-HCl:HNO$_3$:H$_2$O digestion - Inductively coupled plasma mass spectrometry (1 gram sample)

ACM = ACME Analytical, Vancouver

% Difference = ABS ((x1-x2)/(x1+x2)/2)x100
CANMET Reference values based on cocentrated HNO$_3$-HCl digestion

* CANMET Reference value (Bowman, 1994)

Elements B, Ti, Tl were included in analysis, but results were either below detection or unreliable.
For location of samples see Table 1. Instrumental Neutron Activation (INAA) results for Feather Creek.

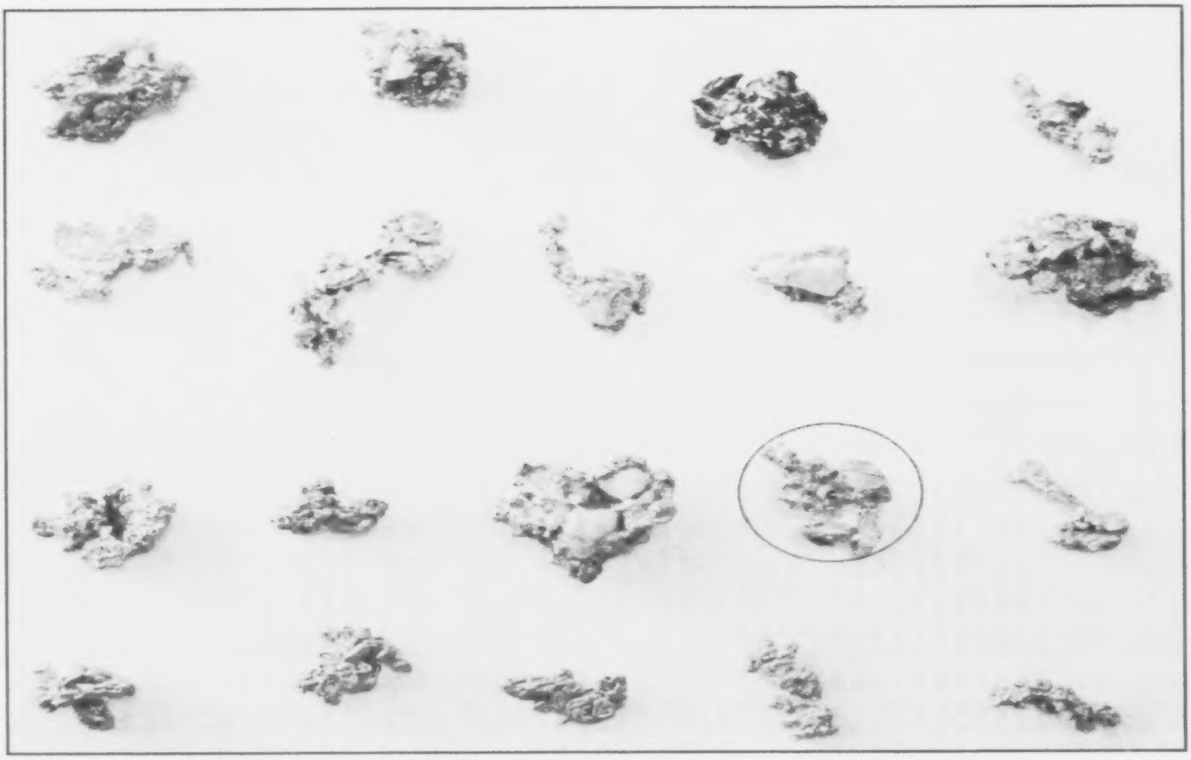

Figure 7. Representative crystalline and hackly gold from Feather Creek which indicates either a proximal source, or transport in clasts that released the gold near its point of recovery

Sample MMI03-24-3 pebbles and granules are about 80% black chert, with minor light grey chert and tan chert. Granitiod granules comprise 15% of the clasts (Figure 5d).

Sample MMI03-24-2A pebbles are 70% wacke, with minor light grey chert, tan chert, cherty wacke, and quartzite. Granules are 60% black chert, 30% light grey chert with minor tan chert, red chert and wacke (Figure 5e).

Sluice box clean-up rejects

Most of the sluice box clean-up reject sample consists of magnetite grains partly cemented with iron oxide and hydroxides. Only about 10% of the sample consisted of the grain size fraction used for the clast identification (> 2 mm). The pebble fraction of sample MMI03-24-4B consists of light grey to tan chert, plus an equal abundance of clumps of magnetite grains cemented by iron-oxide and hydroxides, which results from weathering of the reject pile. The granule fraction is comprised of 75% grey to tan chert, 15% cherty wacke, and 10% vein quartz (Figure 5f).

GEOCHEMICAL RESULTS

ICPES analyses may result in lower gold values than INAA analyses due to the acid digestion in the ICPES not releasing all of the gold. For this reason, the INAA values are considered here (Table 2). ICPES results are shown in Table 3 for comparison and quality control. Sample MMI03-24-4B contained the highest reported gold values, which is expected as the sample was collected from sluice box clean-up rejects. The sample contains mainly heavy minerals that are the product of gravimetric concentration; first in the trommel, and then in the sluice during primary placer gold recovery, and then reconcentrated on an oscillating table during final gold recovery. The +10 and the −80 fractions returned the highest gold values with 17000 ppb and 12700 ppb respectively.

Trench and Creek Sections

Two samples were collected across the unoxidized and oxidized strata of Trench B. The highest gold value is 11 ppb in sample MMI03-24-2A, in the -18 to +80 fraction. This is the only value over 10 ppb from samples collected in this trench.

Two Quaternary and Tertiary stratigraphic samples and one composite sample were collected from Trench C. Composite sample MMI03-24-3 contained 112 ppb Au in the -80 fraction; the highest gold value from a trench. Five other samples from this trench contain gold values above 10 ppb.

Five stratigraphic samples and one composite sample were collected from Trench D. This trench contained the second highest gold value with 85 ppb in sample KWI03-15-4D in the -80 fraction, as well as the third highest gold value in sample KWI03-15-4E with 24 ppb in the -80 fraction. Five other samples from this trench had over 10 ppb gold.

Three stratigraphic samples were collected from Trench E. Sample KWI03-15-5A, is the only sample containing 10 ppb Au, or greater, in the -18 to +80 size fraction.

ATTACHED MINERAL MATTER COMPOSITION

Six nuggets were scanned by SEM and relative elemental abundances in attached mineral matter were obtained with the EDS. Figure 6 contains SEM images of the attached mineral matter. All nuggets are less than 2mm diameter and are hackly, possibly indicating proximity to source, although nuggets in this size fraction are not readily rounded. Nuggets up to 15 mm in size are also crystalline or hackly in nature (Figure 7).

Mineral matter attached to the gold is mainly tin oxide with one grain containing significant thorium (Figure 6b, Table 4: PSA03-1-4). SEM photographs and their accompanying spectra responses are shown in Figure 6.

SUMMARY

Dominant clast types within the Feather Creek placer gravels are: black chert which constitutes at least half of the clasts; grey, tan or red chert; and wacke. Some samples contain significant proportions of quartz or granitoid clasts. Ultramafite or listwanite clasts were not identified in any sample.

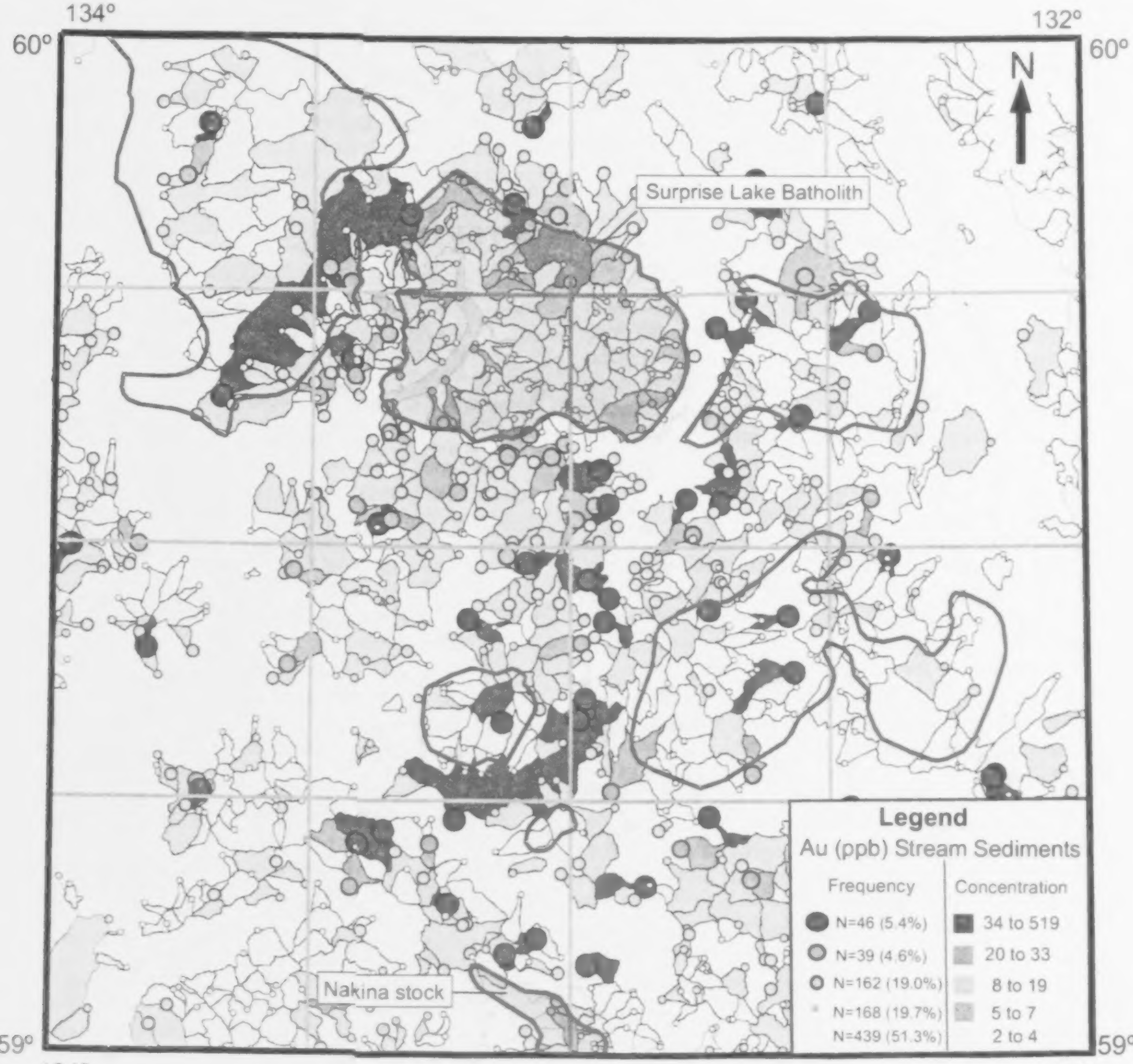
134°
132°
60°
60°
N
Surprise Lake Batholith
Nakina stock
59°
59°
134°
132°
Legend
Au (ppb) Stream Sediments
Frequency
Concentration
N=46 (5.4%)
N=39 (4.6%)
N=162 (19.0%)
N=168 (19.7%)
N=439 (51.3%)
34 to 519
20 to 33
8 to 19
5 to 7
2 to 4

Figure 8. Regional stream geochemistry showing streams draining the margins of plutonic bodies (outlined by heavy red line) including the Surprise Lake batholith and Nakina stocks (shaded), are elevated in gold. Geology after Mihalynuk et al. (1996).

Analyses of gravels from trenches revealed three samples with gold content greater than 20 ppb. The highest value obtained from a trench sample was 112 ppb Au in the -80 fraction of sample MMI03-24-3; followed by 85 ppb in the -80 fraction of sample KWI03-15-4D. Sample KWI03-15-4E has 24 ppb Au in the -80 fraction. For samples containing more than 20 ppb Au, the amount of gold increased as the size fraction decreased.

Two of three samples with the highest gold values contained a significant population of granitoid clasts. The sample with the highest gold value contained 15% granitoid granules, while the sample with 24 ppb Au contained 6% granitoid granules (note that higher gold values were obtained from the sample of sluice clean-up rejects). One sample with 85 ppb gold does not contain granitoid clasts, however, the clast count sample was relatively small (39 clasts) and may not be representative. Overall, the samples analyzed are too small to provide a reliable indication of gold content, and the results of this geochemical orientation study are preliminary and should be verified with geochemical and clast population analysis of much larger samples. Nevertheless, the clues provided by our orientation study corroborate those based on government, regional geochemical stream survey results, and the spatial distribution of placer workings and coarse gold nuggets in proximity to the Surprise Lake batholith.

If gold in the Atlin placer camp bears an association with altered ultramafic rocks, it is not borne out in the juvenile gold placers of Feather Creek. On the contrary, ultramafic or listwanite clast were not identified from these placer gravels. Ascribing the lack of clasts of the ultramafic host rocks to comminution during alluvial transport seems inappropriate given the hackly nature of much of the gold. Gravels with elevated gold do contain a significant proportion of granitoid clasts, as well as ubiquitous sedimentary clasts with lithologies matching geological units within the immediate drainage basin. Does this observation warrant the suggestion of a plutonic-related gold source? On its own, probably not, but combined with the identification of cassiterite in six of six gold nuggets analyzed, a stronger argument can be made for linkage with the evolved, tin-rich Surprise Lake batholith. Further evidence includes, the distribution of 95th percentile gold values in stream sediments collected from streams that drain the flanks of intrusions east of Atlin (Figure 8), as well as the distribution of placer streams, with past and present placer operations on all sides of the Surprise Lake batholith (Figure 1). Finally, consider that the coarsest placer gold is recovered primarily from streams located along the margin of the Surprise Lake batholith. The coarsest gold is recovered from Wright, Otter, Boulder, Ruby, McKee and Spruce creeks (J. Harvey, Personal Communication, 2003). Of these, only the McKee Creek workings are not situated on the margin of the Surprise Lake batholith.

Gold is associated with ultramafic rocks in the Atlin camp as can be shown by the number of lode occurrences in which native gold is seen within listwanite. Perhaps the key to the listwanite-related gold deposition is the late-synorogenic to early post-orogenic granitic batholiths. This is consistent with Middle Jurassic U-Pb ages of chrome micas within the listwanite, which are interpreted as cooling ages related to batholiths such as the Fourth of July body (Ash, 2001). If ophiolites are the source of gold, then other areas in the northern Cache Creek terrane displaying the same listwanite altered zones should also be associated with gold occurrences. One such area would be along the Nahlin ultramafic body where it is cut by large plutons coeval with the Fourth of July batholith (*e.g.* Mihalynuk *et al.*, 2003b). In this region, indications of placer gold are sporadic: an inactive placer in Goldbottom Creek, and gold discovered as part of a heavy mineral sampling program in bulk stream sediment samples from north of Peridotite Peak, as well as near "Scarface Mountain" (Canil *et al.*, this volume; Figure 1). However, no significant placer or lode occurrence has yet been found in this area. It is prudent to ask if these tantalizing specks of gold and bright orange listwanitic alteration zones have not been a mineral exploration red herring but insufficient data exists on which to base resonable conclusions. However, our preliminary results from Feather Creek strongly suggest a link between placer gold and the evolved Surprise Lake batholith, with significant implications for lode gold exploration in the region.

REFERENCES

Aitken, J.D. (1959): Atlin map-area, British Columbia; *Geological Survey of Canada*, Memoir 307, 89 pages.

Ash, C.H. (2001): Relationship between ophiolites and gold-quartz veins in the North American Cordillera; *BC Ministry of Energy and Mines*, Bulletin 108, 140 pages.

Ballantyne, S.B. and MacKinnon, H.F. (1986): Gold in the Atlin Terrane, British Columbia; *in* Gold '86, an international symposium on the geology of gold deposits: poster paper abstracts., Chater (Editor), *Geol. Assoc. Can.*, pages 16-17.

Böhlke, J.K. (1999): Mothe Lode gold; *Geological Society of America*, Special Paper 338, pages 55-67.

Bowman, W.S. (1994): Catalogue of Certified Reference Material; *Canadian Certified Reference Material Project (CCRMP)*, CCRMP 94-1E, pages 55-57.

Canil, D., M. Mihalynuk, J.M. MacKenzie, S.T. Johnston, L. Ferreira and B. Grant (2004): Diamond and other indicator minerals in the Atlin-Nakina area (NTS 104N and 104K); *in* Geological Fieldwork, *BC Ministry of Energy and Mines*, Paper 2004-1, this volume.

Clifton, H.E., Hunter, R.E., Swanson, F.J. and Phillips, R.L. (1969): Sample size and meaningful gold analysis; *US Geological Survey*, Professional Paper 625-C, 17 pages.

Dumont, R., Coyle, M. and Potvin, J. (2001): Aeromagnetic total field map British Columbia: Lina Range, NTS 104N/13; *Geological Survey of Canada*, Open File, 4093.

Gebre-Mariam, M., Hagemann, S.G. and Groves D.G. (1995): A classification scheme for epigenetic Archean lode-gold deposits; *Mineralium Deposita*, Volume 30, pages 408- 410.

Hallbauer, D.K. and Utter, T. (1977): Geochemical and morphological characteristics of gold particles from recent river deposits and the fossil placers of the Wittwatersrand; *Mineralium Deposita*, Volume 12, pages 293-306.

Hilchey, G.R. (1990): Techniques of placer exploration and mining in Canada; *Energy of Mines and Resources Canada*, Canadian Exploration Incentive Program, 96 pages.

Jackaman, W. (2000): British Columbia Regional Geochemical Survey, NTS 104N/1 - Atlin; *BC Ministry of Energy and Mines*, BC RGS, 51.

Landefeld, L.A. (1988): The Geology of the Mother Lode Gold Belt, Sierra Nevada Foothills Metamorphic Belt, California; in Proceedings Volume, North American Conference on Tectonic Control of Ore Deposits and the Vertical and Horizontal Extent of Ore Systems, *University of Missouri - Rolla*, pages 47-56.

Lehmann, B. and Grabezhev, A.I. (2000): The Bereznjakovskoje gold trend, southern Urals, Russia - a reply; *Mineralium Deposita*, Volume 35, pages 388-389.

Levson, V.M. (1992): Quaternary geology of the Atlin area (104N/11W, 12E); *in* Geological Fieldwork, *BC Ministry of Energy and Mines*, Paper 1992-1, pages 375-390

Levson, V.M., Kerr, D.E., Lowe, C. and Blythe, H. (2003): Quaternary geology of the Atlin area, British Columbia; *British Columbia Geological Survey Branch*, Geoscience Map 2003-1 and Geological Survey of Canada, Open File 1562, scale 1: 50,000.

Mihalynuk, M.G., Anderson, R.G., Lowe, C., Villeneuve, M., Johnston, S.T., English, J.M. and Cordey, F. (2003a): Atlin TGI update and new massive sulphide discovery in Cache Creek rocks; Cordilleran Exploration Roundup 2003, *British Columbia and Yukon Chamber of Mines*, 6-7.

Mihalynuk, M.G., Johnston, S.T., English, J.M., Cordey, F., Villeneuve, M.J., Rui, L. and Orchard, M.J. (2003b): Atlin TGI Part II: Regional geology and mineralization of the Nakina area (NTS 104N/2W and 3); *in* Geological Fieldwork, *BC Ministry of Energy and Mines*, Paper 2003-1, pages 9-37.

Mihalynuk, M.G., Smith, M., Gabites, J.E., Runkle, D. and Lefebure, D. (1992): Age of emplacement and basement character of the Cache Creek terrane as constrained by new isotopic and geochemical data; *Canadian Journal of Earth Sciences*, Volume 29, pages 2463-2477.

Mihalynuk, M.G. (1999): Geology and mineral resources of the Tagish Lake area, northwestern British Columbia; *BC Ministry of Energy and Mines*, Bulletin 105, 217 pages.

Monger, J.W.H. (1975): Upper Paleozoic rocks of the Atlin terrane; *Geological Survey of Canada*, Paper 74-47, 63 pages.

Robertson, W.F. (1899): Cassiar District; In Annual report of the Minister of Mines, 1898, *BC Department of Mines*, pages 985-991.

Royle, A.G. (1987):Alluvial sampling formula and recent advances in alluvial deposit evaluation; *Extractive industry geology '87*, 4 pages.Heavy Mineral Sampling of Stream Sediments for

COMPILATION AND ANALYSIS OF REGIONAL GEOCHEMICAL SURVEYS AROUND THE BOWSER BASIN

By Dani Alldrick[1], Wayne Jackaman[2] and Ray Lett[1]

KEYWORDS: Regional stream sediment surveys, regional geochemical survey, Rocks To Riches, Bowser Basin, mineral deposits.

INTRODUCTION

More than two-thirds of British Columbia has now been sampled as part of the jointly funded federal-provincial stream sediment survey program (Figure 1).

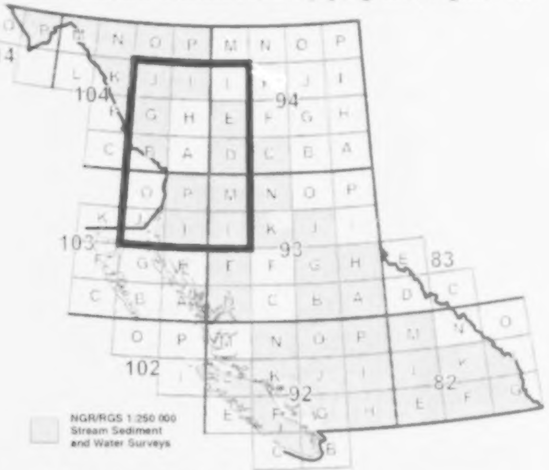

Figure 1. Location of project area.

The database is sufficiently large to begin the assembly of individual mapsheets into seamless provincial-scale maps of survey results for publication in an "atlas" volume. This amalgamation of survey data acquired in different years presents significant challenges due to different sampling intervals, different analytical equipment and techniques, and different detection limits applied since the first regional geochemical survey was completed in 1976.

The Rocks To Riches program (http://www.bc-mining-house.com) has funded a project designed to identify and solve these problems. A large 'test area' with exceptionally high mineral potential was selected for this development work. Ten 1:250,000 mapsheets surrounding the Bowser sedimentary basin in northwestern British Columbia cover a series of island arc complexes hosting an array of important mineral deposit types including epithermal veins, porphyry copper-gold deposits and volcanogenic massive sulphide deposits.

The British Columbia RGS database contains field information and analytical data for up to 50 elements from 48,000 sample sites covering 47 out of the 69 1:250,000 mapsheets that cover the entire province. Planning is now underway for preparation of a full geochemical atlas for British Columbia similar to existing volumes (Webb *et al.*, 1978). These assembled maps will display regional element concentrations reflecting major geological units (strata and plutons) as well as comparing and contrasting the geochemical signatures of different tectonic terranes. Large mineral deposits as well as small mineral prospects with large geochemical footprints, such as showings located near ridge crests, can still be delineated at these smaller map scales. Geochemical anomalies generated by large alteration haloes can also be discerned. Entire mining camps, mineral districts and metallogenic belts can be recognized and delineated due to geochemical anomalies generated by their favourable lithologies.

Development work includes:

- Software preparation, base map acquisition and data compilation for the RGS data from 10 NTS mapsheets.
- "Leveling" of analytical suites of elements between mapsheets to correct for differences in analytical procedures.
- Develop and test discriminant functions for detection of geochemical signatures of particular mineral deposit types.
- Produce final map files incorporating contoured analytical data, various base map layers and reference grids.

RESULTS AND DISCUSSION

There are a total of 11,478 individual stream sediment sample sites located in the 10 survey areas. The area covered is 136,500 km^2 and the average sample density is 1 sample site every 12 km^2. Sampling density is not consistent throughout the study area; increased funding provided a higher sample density for sheets 103I/J and O/P (1 site per 10 km^2).

---

[1] *British Columbia Ministry of Energy and Mines, Geoscience Research and Development Branch*

[2] *3011 Felderhof Road, Sooke, BC, V0S 1N0*

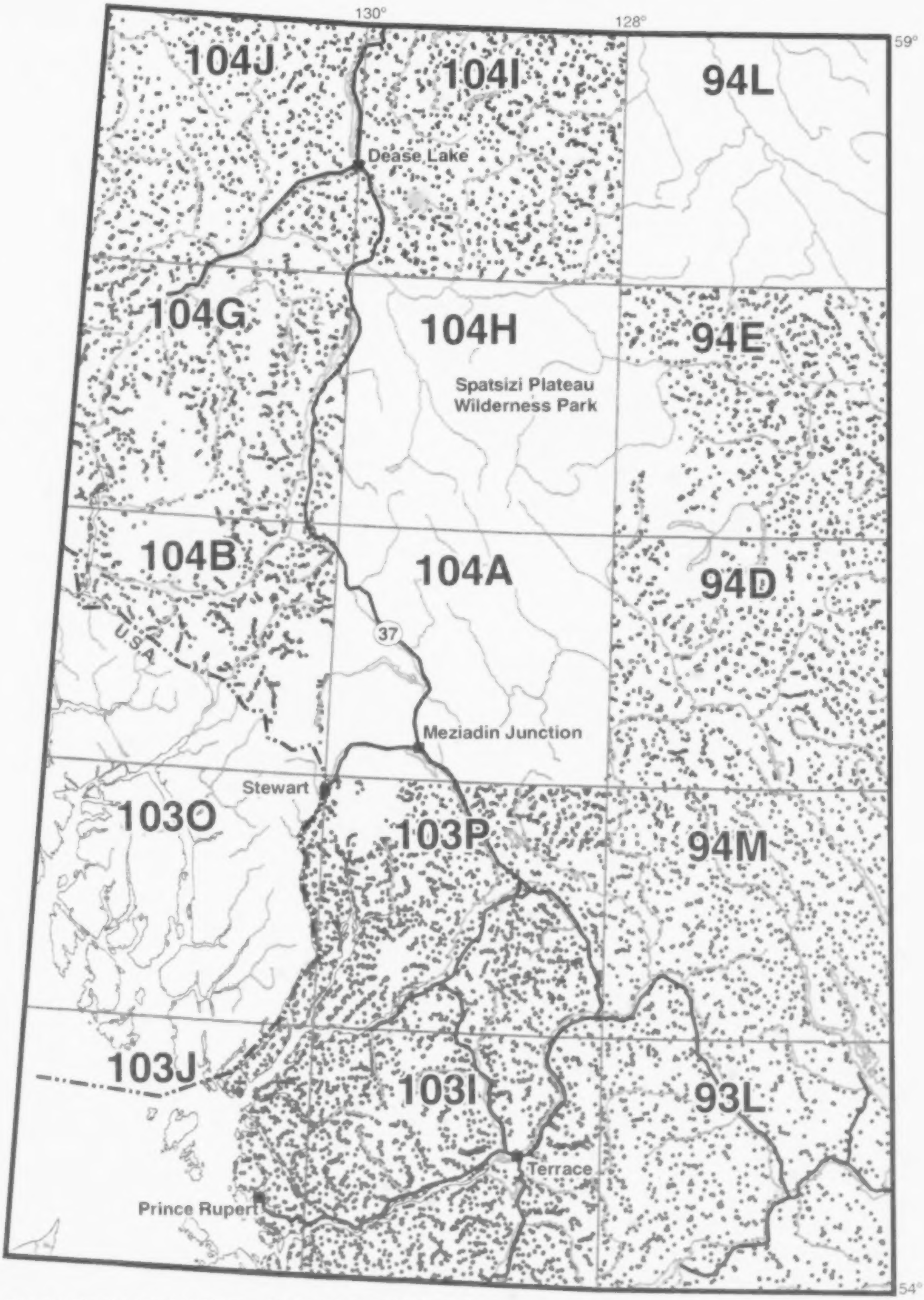
130°
128°
59°
54°
104J
104I
94L
Dease Lake
104G
104H
94E
Spatsizi Plateau
Wilderness Park
104B
104A
94D
U.S.A.
37
Meziadin Junction
Stewart
103O
103P
94M
103J
103I
93L
Terrace
Prince Rupert

Figure 2. Distribution of 11,478 sample sites contoured in this study.

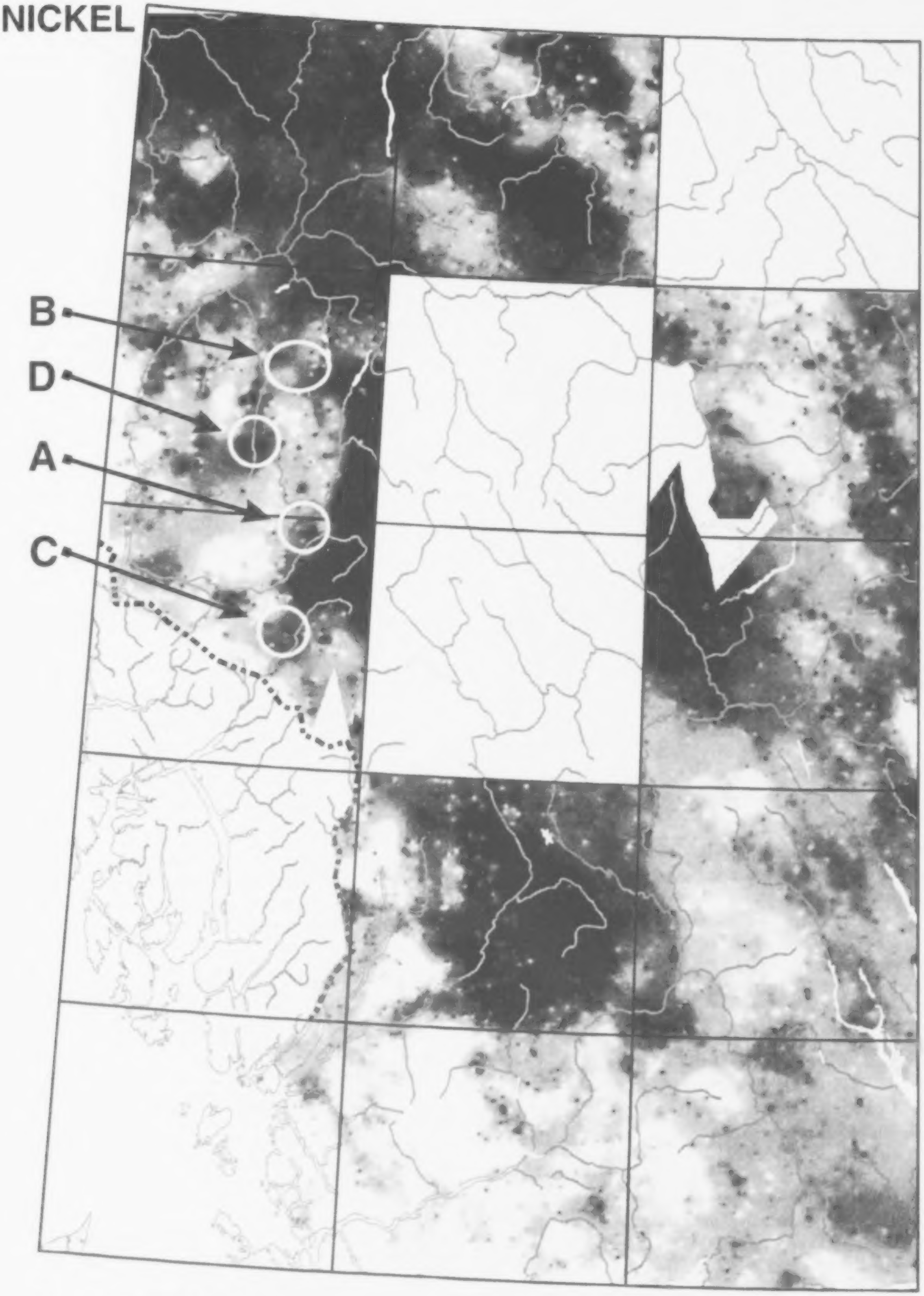
NICKEL
B
D
A
C

Figure 3. Nickel in RGS samples.

In contrast, mapsheets 104B, 104G and 104J tend to have a lower sample density (1 site per 14 km^2) due to factors that limited sample availability (i.e. ice, or low-lying heavily overgrown terrain).

A single composite mapsheet has been contoured in grayscale (Figure 3) to illustrate some of the capabilities and applications of contouring the 'leveled' RGS dataset at these small scales. The RGS dataset for nickel in northwestern BC shows large-scale and small-scale features, all of which have implications for mineral potential and mineral exploration.

A strong, regional-scale nickel anomaly is associated with the fine clastic carbonaceous sedimentary rocks of the Bowser Basin of north-central British Columbia. The elevated nickel concentrations in these rocks is similar to other regions of the world where nickel accumulates in fine-grained, reduced clastic rocks (Lefebure and Coveney, 1995).

The distribution of strongly anomalous nickel signatures sheds new light on existing regional-scale geology maps. In the northeast corner of NTS 104B an area of anomalous nickel values (Area A on Figure 3) indicates terrain likely underlain in part by an outlier of strata of the Bowser Lake Group. The most recent geology map (Logan *et al.*, 1997) published for this area identifies sedimentary units as part of the underlying Hazelton and Stuhini Groups. In contrast, sedimentary strata exposed along the deeply eroded Raspberry Pass (Area B of Figure 3) that cuts through the Mount Edziza Volcanic Complex has historically been correlated with Bowser Lake Group rocks (Souther, 1972). The lack of a similar anomalous nickel signature in this area suggests that these sedimentary units may be exposures of older Triassic strata that have been identified elsewhere underlying the Late Miocene to Recent Edziza volcanics.

On the eastern side of the composite map area, strata of the Bowser Lake Groups and Sustut groups both display high nickel concentrations and the two stratigraphic packages are indistinguishable using nickel RGS data. The eastern perimeter of the Sustut Basin is as sharply defined against older arc rocks as the perimeter of the Bowser Basin on the west side of the map area.

E & L Nickel (MINFILE 104B 006) is the largest nickel deposit in northern British Columbia. A series of moderate RGS nickel anomalies are scattered over the area (Area C on Figure 3) surrounding the string of small gabbroic stocks which host E & L Nickel (Alldrick and Britton, 1992; Britton et al., 1989). In contrast, in the centre of the next NTS mapsheet to the north (104G), the Hickman Ultramafic Complex generates a much broader and stronger RGS nickel anomaly (Area D on Figure 3) even though there is no documented nickel mineralization (Nixon *et al.*, 1989).

Readers can also compare and contrast the effectiveness of the processing and presentation of RGS data using computer contouring or drainage basin plots by comparing Figure 3 with illustrations in Lett and Jackaman (this volume).

CONCLUSIONS

Compilation and contouring of regional stream sediment survey data provides new perspectives on the extent of regionally distributed lithologic units and reveals areas of interest for mineral exploration.

ACKNOWLEDGEMENTS

We thank the 2003 Rocks To Riches Geoscience Program of the British Columbia and Yukon Chamber of Mines for the financial support provided.

REFERENCES

Alldrick, D.J. and Britton, J.M. (1992): Unuk River Area Geology, BC Ministry of Energy, Mines and Petroleum Resources, Open File Map 1992-22, Scale 1:20 000, 5 sheets.

Britton, J.M., Webster, I.C.L. and Alldrick, D.J. (1989): Unuk Map Area; B.C. Ministry of Energy, Mines and Petroleum Resources, Geological Fieldwork 1988, Paper 1989-1 p.241-250.

Lefebure, D.V. and Coveney, R.M. Jr. (1995): Shale-hosted Ni-Zn-Mo-PGE; British Columbia Ministry of Employment and Investment, Selected British Columbia Mineral Deposit Profiles, V.1, Open File Report 1995-20, p.45-48.

Lett, R. and Jackaman, W. (2004): New exploration opportunities in the B.C. regional geochemical survey database; (this volume).

Logan, J.M., Drobe, J.R., Koyanagi, V.M. and Elsby, D.C. (1997): Geology of the Forest Kerr - Mess Creek Area, Northwestern British Columbia (104B/10,15 & 104G/2 & 7W), Ministry of Employment and Investment, Geoscience Map 1997-3, 1:100 000 scale.

Nixon, G.T., Ash, C.H., Connelly, J.N. and Case, G. (1989): Alaskan-type mafic-ultramafic rocks in British Columbia - the Gnat Lakes, Hickman and Menard Creek complexes; Ministry of Energy, Mines and Petroleum Resources, Geological Fieldwork 1988, Paper 1989-1, p.429-442.

Souther, J.G. (1972): Telegraph Creek map-area, British Columbia; Geological Survey of Canada, Paper 71-44, 39p.

Webb, J.S., Thornton, I., Thompson, M., Howarth, R.J. and Lowenstein, P. (1978): The Wolfson Geochemical Atlas of England and Wales; Oxford University Press, 66p.

MINERALOGY AND GEOCHEMISTRY OF BERYL AND RARE-METAL-BEARING GRANITIC PEGMATITES IN THE KOOTENAY REGION OF SOUTHEASTERN BRITISH COLUMBIA

By Jarrod A. Brown, M.Sc. (Geological Consultant, Nelson BC)

KEYWORDS: PEGMATITE, MINERALOGY, GEOCHEMISTRY, GEMSTONES, RARE METALS, BERYL, AQUAMARINE, EMERALD, KOOTENAY REGION, BAYONNE BATHOLITH, WHITE CREEK BATHOLITH, SHAW CREEK STOCK, HELLROARING CREEK STOCK, GREENLAND CREEK STOCK, SLOCAN VALLEY.

INTRODUCTION

LCT-granitic pegmatites as defined by (Cerny, 1991) are anomalously enriched in Li, Rb, Cs, Be, Sn, Ga, Ta>Nb, (B,P,F) and are host to many of the worlds most precious gemstones including emerald, chrysoberyl and topaz (Minas Gerais, Brazil), sapphire and ruby (Afghanistan and Pakistan), and gem tourmaline (Pala District, California). Twelve Minfile (MF) occurrences of LCT-pegmatites are recorded in BC, with all but one located within the Omineca Belt.

A review of BC-Minfile occurrences of beryl-bearing LCT-granitic pegmatites in southern BC reveals the majority are proximal to metaluminous to peraluminous granitoids either within the Cretaceous Bayonne magmatic belt (Geoscience Map 2002-1), or within, or near the eastern margins of the Valhalla and Monashee Complexes (Table I). Beryl, as well as gem quality corundum, cordierite, garnet, quartz and feldspar have been found in pegmatites, or in the alteration haloes of pegmatites. Some of these pegmatites also contain significant rare-metal mineralization, particularly Be, Ta, and Nb.

Two to three different ages of pegmatites are known in the Kootenay Region: 1) Beryl- and tourmaline-bearing dykes and stocks comprise major proportions of the Proterozoic Greenland Creek Stock, and the Hellroaring Creek Stock (Figures 1,2,5); 2) Significant gem-beryl-bearing pegmatites occur within and proximal to middle to late Cretaceous batholiths and stocks east and west of Kootenay Lake (Figures 1,5,11); and 3) Various gemstone varieties are associated with pegmatites of the Slocan Valley (Figure 13), related to either Eocene? or Cretaceous? plutonism.

The recent discovery of emerald and aquamarine in the Finlayson District of southeastern Yukon has piqued interest in the potential for gemstones in the Canadian Cordillera. Emeralds at Regal Ridge are hosted in and around quartz-tourmaline-scheelite veins proximal to a geochemically evolved middle Cretaceous granitoid, with associated pegmatites and aplites (Groat et al., 2002). Gemstone deposits of the Finlayson district and the Kootenay Region share two similar characteristics: I) Regional tectonic setting (Omineca belt, close to large-scale regional fault structures) and II) proximity to peraluminous Cretaceous intrusions.

The purpose of this paper is to provide a baseline description of the mineralogy and geochemistry of some of the historical and new pegmatite showings in the Kootenay Region. This study was funded through the Rocks to Riches Program, administered by the BC and Yukon Chamber of Mines. This paper complements other recently initiated studies of British Columbia pegmatites by Andrew Legun of the BC Geological Survey, and Lee Groat at the geology department of the University of British Columbia. A coordinated study, in light of the recent excitement from gem discoveries in the Yukon and North West Territories may yield significant investment potential for British Columbia.

Table I: Three groups of pegmatite associated deposits in southern BC, based on age and spatial or tectonic setting. Alphanumeric entries refer to Minfile reports. Data and discussions are presented for underlined entries only.

WEST	CENTRAL	CENTRAL TO EAST
Valhalla and Monashee Complexes	Bayonne Magmatic Belt	Bayonne Magmatic Belt
Eocene or Cretaceous?	Mid-late Cretaceous	Proterozoic
Airey Creek (BQ claims) 082FNW250	White Creek 082FNE159	Hellroaring Creek 082FNE110
Blu Starr 082FNW259	Midge Creek 082FSE091	Greenland Creek 082FNE112
Mount Begbie 082LNE015	Doctor Creek (Blue Hammer)	Lightening Creek
	Kootenay Gemstone (Laib and Topaz creeks)	Mathew Creek

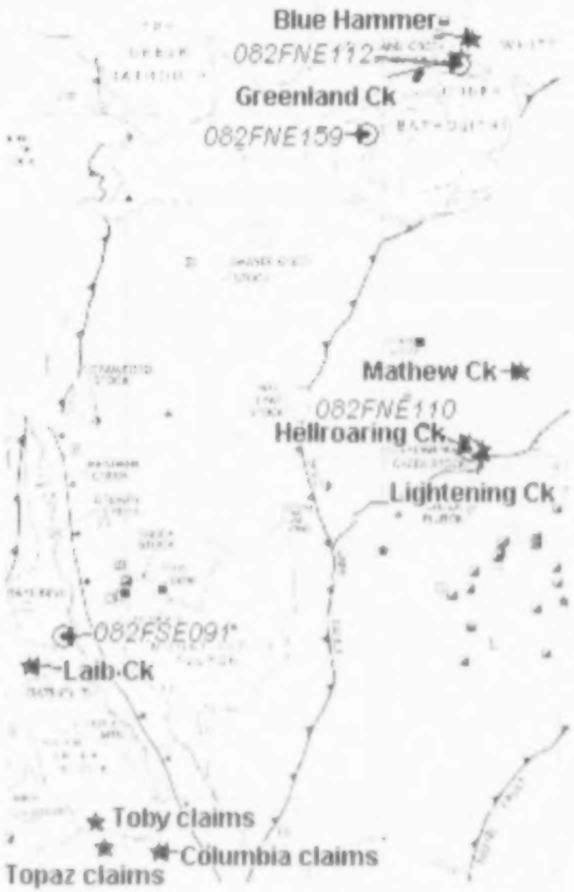

Figure 1 Field locations (stars) and known pegmatite Minfiles (circles with Minfile reference) within the Bayonne magmatic belt in the southern Kootenay Region (after Geoscience Map 2002-1). Grid squares are 10 by 10 km.

GEOLOGIC SETTING

Except for field locations in the Slocan Valley, all other field sites discussed in this report are located within the Cretaceous Bayonne Magmatic/Plutonic Belt (Figure 1). This belt comprises an 80 to 100 kilometre wide arcuate train of middle to late Cretaceous batholiths and stocks of granodioritic, monzonitic and quartz monzonitic compositions. Most of the plutonic bodies are post-metamorphic and are discordant to the country rock. Typically they form multiphase intrusions comprising significant volumes of metaluminous to weakly peraluminous, medium- to coarse-grained granitoids, with lesser strongly peraluminous two-mica granite and subordinate aplite and pegmatite (Logan et al., 2000). The belt is also host to two known Proterozoic pegmatitic stocks, namely the Hellroaring and Greenland Creek pegmatites (Smith and Brown, 1998) (Figure 1).

The Cretaceous White Creek Batholith and Proterozoic Hellroaring and Greenland Creek stocks straddle the central axis of the Purcell anticlinorium. The anticlinorium is a broad, gently north-plunging structural culmination cored by the Proterozoic Purcell Supergroup, and flanked by Late Proterozoic Windermere rocks and Lower Paleozoic cratonic rocks (Brown and Termuende, 1998). The Shaw Creek stock, west of Kootenay Lake is proximal to the westernmost limit of the Purcell anticlinorium where it is coincident with the Kootenay Arc (Carr, 1995).

Most of the field areas are underlain by argillites, siltstones and fine-grained quartzites of the Lower to Middle Aldridge Formation. The Lower Aldridge is typically rusty-brown and thinly bedded to laminated siltstone, argillite with lesser sandstone, in contrast to the middle Aldridge, which is a grey-weathered medium to thick bedded turbidite (Brown and Termuende, 1998). Locally, and especially adjacent to granitoid intrusions, much of the Aldridge is muscovite-biotite schist with localized influxes of tourmaline. Further to the west, the Shaw Creek stock intrudes grey siltites and black argillites of the La France Creek Group, dolomite and argillite of the Mt. Nelson Formation, and polymict conglomerate of the Windermere Group Toby Formation. Middle Aldridge lithologies south and east of the Shaw Creek stock predominately comprise biotite-muscovite or amphibolite schists with reports of upper amphibolite metamorphic assemblages (Archiblad et al, 1983).

The Middle Proterozoic Moyie Sills and lesser dykes are the oldest known intrusives in the area. They comprise extensive bodies of gabbro and diorite that intrude the lower and middle Aldridge Formation. Amphibolitic gabbro is the dominant lithology forming dark green to brown weathering sills, and rare crosscutting dykes. Sills in the field area east of Kootenay lake are 10 to 100 m thick and comprise up to 25% of the lower Aldridge section. The size and abundance of Moyie intrusions is significantly less within Middle Aldridge lithologies south of the Shaw Creek stock.

Major structures in the study area include the St. Mary fault, an east- to southeast trending reverse thrust truncated by the post tectonic Cretaceous Reade Lake stock (Hoy and van der Heyden, 1988), and the Hall Lake fault, a right lateral reverse fault that cuts obliquely across the Purcell anticlinorium. It is truncated by the White Creek Batholith in the Buhl Creek area (Reesor, 1996).

HELLROARING CREEK STOCK

The Hellroaring Creek stock is located approximately 20 kilometres southwest of Kimberly, BC, centered near 116° 10' W longitude and 40° 34' N latitude (UTM11 559 677 E / 5 490 561 N). The main body is exposed over approximately 10 square kilometres with the long axis of the pegmatite trending north-northwest for 4 kilometres within a package of lower Aldridge sediments and Moyie sills (Figure 2). The southernmost end of the pegmatite stock is truncated by the St Mary thrust fault, where the stock is in contact with siltite, quartzite and argillite of the Creston Formation.

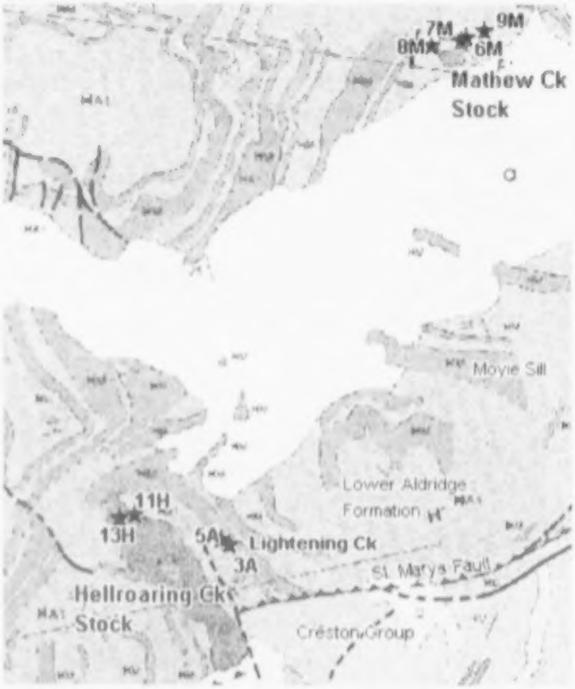

Figure 2 Field locations in the St. Mary river valley 20 kilometres west of Kimberley BC (after Reesor, 1996). Pegmatite comprises major volumes of the Proterozoic Hellroaring Creek stock and Mathew Creek stock. St. Mary's lake (upper left) is approximately 3 kilometres long.

The pegmatite stock is up to 1.5 kilometres wide. Historical drilling, over the last 50 years for rare-metals and industrial grade feldspar, has encountered pegmatite thicknesses up to 150 metres (MF 082FNE110). Previous workers have noted several intrusive phases in outcrop and in drill core, including granodiorites, muscovite-tourmaline and tourmaline-muscovite granites, leucogranites, and aplite (EMPR ass rpt 26701). Essential features of the stock, as a whole, are the widespread occurrences of micropegmatite and pegmatite textures, with localized segregations of very large K-feldspar, tourmaline and micas. Significant mineralization includes the near ubiquitous presence of black tourmaline (locally in excess of 10%), minor garnet to several percent, and accessory beryl and fluroapatite.

Significant alteration related to the Hellroaring creek stock was reported in Chapleau Resources Ltd. news release dated November 24, 2000:

> "The Hellroaring Stock is a multiphase granitic intrusive strongly altered by albitization and griesenization processes… Both intrusive and country rocks were subjected to intensive griesenization and bear elevated to high grades of beryllium, cesium, and rubidium."

Several satellitic intrusions and dyke swarms are reported to occur within hundreds of metres to a few kilometres of the main Hellroaring Creek body. The pegmatite at *Lightening Creek* is traced in outcrop for 100 metres, and consists of coarsely crystalline pegmatite with an estimated 30 metres of thickness. It is located immediately east of the confluence of Lightening Creek with Angus creek. The *Lower Jack Showing*, located 6 kilometres southwest of the main body, comprises a 20 to 50 metre thick dyke which sporadically outcrops over 500 metres. Several occurrences of pegmatite dykes are also reported on the hill side facing the main body, on the west side of Hellroaring Creek.

The *Mathew Creek Stock*, located approximately 10 kilometres to the northeast, is tentatively considered a satellitic intrusion of the Hellroaring Creek Stock. It is exposed over an area about 1000 by 300 metres, and comprises simple micropegmatite textures and lithologies to the west, with an eastwards progression to medium- and coarse -grained beryl-bearing pegmatite. The general textures and mineralogy of the pegmatite is comparable to those identified at the Hellroaring Creek stock.

Field Observations

The author spent two days on the main pegmatite body, and one day at each of the satellitic pegmatites at Lightening Creek and Mathew Creek. Notes and impressions gathered at each site are as follows:

Stop 11H: Hellroaring Creek pegmatite (main zone)

UTM 11 559555E / 5491462N in the vicinity of Bearcat drilling and trenches at 1433 metre (EMPR ass rpt 15760): The area is underlain by broad exposures of equigranular pegmatite with average 1 to 3 centimetre crystal sizes comprising 50% feldspar, 30% quartz, 15% muscovite, and minor but variable black tourmaline and garnet.

Subordinate volumes of the main body are represented by a coarse to very coarse pegmatite comprising a core assemblage of megacrystic euhedral K-feldspar crystals (up to 50 by 30 centimetres), coarse euhedral silvery muscovite to 20 centimetres commonly intergrown with anhedral light grey and occasionally smoky quartz. Where visible, beryl crystals are commonly found within quartz-muscovite assemblages at the margin between the coarse core assemblage and the fine to medium -grained pegmatite assemblage. The beryl occurs as white to yellowish-white, opaque, euhedral to subhedral hexagonal crystals, with 0.3 to 1 centimetre diameter crystals the most common, but occasional within a package of lower Aldridge sediments and Moyie sills (Figure 2). The southernmost end of the pegmatite stock is truncated by the St Mary thrust fault, where the stock is in contact with siltite, quartzite and argillite of the Creston Formation.

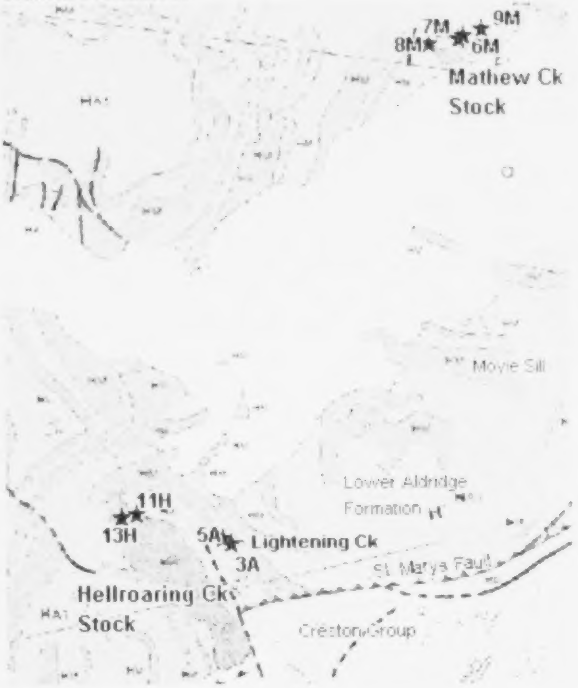

Figure 2 Field locations in the St. Mary river valley 20 kilometres west of Kimberley BC (after Reesor, 1996). Pegmatite comprises major volumes of the Proterozoic Hellroaring Creek stock and Mathew Creek stock. St. Mary's lake (upper left) is approximately 3 kilometres long.

The pegmatite stock is up to 1.5 kilometres wide. Historical drilling, over the last 50 years for rare-metals and industrial grade feldspar, has encountered pegmatite thicknesses up to 150 metres (MF 082FNE110). Previous workers have noted several intrusive phases in outcrop and in drill core, including granodiorites, muscovite-tourmaline and tourmaline-muscovite granites, leucogranites, and aplite (EMPR ass rpt 26701). Essential features of the stock, as a whole, are the widespread occurrences of micropegmatite and pegmatite textures, with localized segregations of very large K-feldspar, tourmaline and micas. Significant mineralization includes the near ubiquitous presence of black tourmaline (locally in excess of 10%), minor garnet to several percent, and accessory beryl and fluroapatite.

Significant alteration related to the Hellroaring creek stock was reported in Chapleau Resources Ltd. news release dated November 24, 2000:

> "The Hellroaring Stock is a multiphase granitic intrusive strongly altered by albitization and griesenization processes… Both intrusive and country rocks were subjected to intensive griesenization and bear elevated to high grades of beryllium, cesium, and rubidium."

Several satellitic intrusions and dyke swarms are reported to occur within hundreds of metres to a few kilometres of the main Hellroaring Creek body. The pegmatite at *Lightening Creek* is traced in outcrop for 100 metres, and consists of coarsely crystalline pegmatite with an estimated 30 metres of thickness. It is located immediately east of the confluence of Lightening Creek with Angus creek. The *Lower Jack Showing*, located 6 kilometres southwest of the main body, comprises a 20 to 50 metre thick dyke which sporadically outcrops over 500 metres. Several occurrences of pegmatite dykes are also reported on the hill side facing the main body, on the west side of Hellroaring Creek.

The *Mathew Creek Stock*, located approximately 10 kilometres to the northeast, is tentatively considered a satellitic intrusion of the Hellroaring Creek Stock. It is exposed over an area about 1000 by 300 metres, and comprises simple micropegmatite textures and lithologies to the west, with an eastwards progression to medium- and coarse -grained beryl-bearing pegmatite. The general textures and mineralogy of the pegmatite is comparable to those identified at the Hellroaring Creek stock.

Field Observations

The author spent two days on the main pegmatite body, and one day at each of the satellitic pegmatites at Lightening Creek and Mathew Creek. Notes and impressions gathered at each site are as follows:

Stop 11H: Hellroaring Creek pegmatite (main zone)

UTM 11 559555E / 5491462N in the vicinity of Bearcat drilling and trenches at 1433 metre (EMPR ass rpt 15760): The area is underlain by broad exposures of equigranular pegmatite with average 1 to 3 centimetre crystal sizes comprising 50% feldspar, 30% quartz, 15% muscovite, and minor but variable black tourmaline and garnet.

Subordinate volumes of the main body are represented by a coarse to very coarse pegmatite comprising a core assemblage of megacrystic euhedral K-feldspar crystals (up to 50 by 30 centimetres), coarse euhedral silvery muscovite to 20 centimetres commonly intergrown with anhedral light grey and occasionally smoky quartz. Where visible, beryl crystals are commonly found within quartz-muscovite assemblages at the margin between the coarse core assemblage and the fine to medium -grained pegmatite assemblage. The beryl occurs as white to yellowish-white, opaque, euhedral to subhedral hexagonal crystals, with 0.3 to 1 centimetre diameter crystals the most common, but occasional crystals 2 to 5 centimetres in diameter and up to 15 centimetres long, were noted.

Occasional pods of banded garnetiferous aplite were also noted within the main area. One notable occurrence in particular (Figure 3) occurs as a 10 to 50 centimetre thick pod along the contact between medium- and coarse-grained pegmatite assemblages. Arcuate accumulations of garnet and black resinous oxide crystals delineate crystallization fronts within the aplite pod. The outer interface, with the medium-grained pegmatite, is rich in muscovite and fine-grained tourmaline. Aplite pods similar to these found at the Tanco pegmatite in southeastern Manitoba, are known to contain economic grades of Ta +/- Nb mineralization.

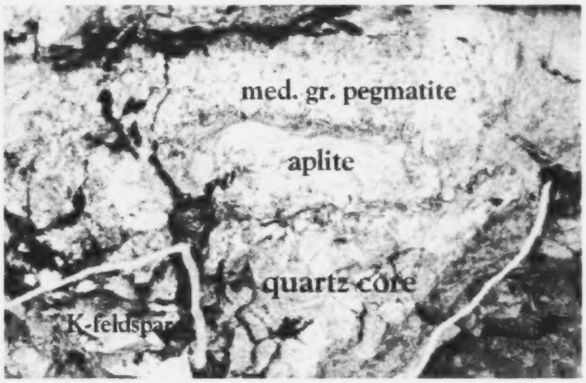

Figure 3 Garnet- and oxide-bearing aplitic albite pod sandwiched between a quartz core and medium-grained pegmatite (above) and very coarse-grained K-feldspar pegmatite (left). Aplite pod is approximately 80 centimetres wide.

A sample of dark grey altered (tourmalinized) host rock (possible xenolith) was collected in this area, and tested for geochemical signatures, particularly Be and Cr.

Stop 13H: Hellroaring Creek pegmatite (south_central)

UTM 11 559269E / 5491422N: Medium-grained pegmatite at this location is crosscut by a late 3 to 10 centimetre wide vuggy quartz-muscovite vein containing subordinate euhedral feldspar crystals and a tourmaline laden alteration selvage. A single, one centimetre diameter, translucent, light yellowish-green, euhedral beryl crystal was found within one of the vugs. Several other poor quality Fe-stained, opaque beryls were also noted in vugs, and within the alteration halo around the vein. The mineralogy and texture of this vein is consistent with a greisen style origin. This is the first and only reference I know of, pertaining to beryl crystals with gem potential at the Hellroaring Creek stock.

Stops 2-5A: Lightening Creek pegmatite

UTM 11 561250 / 5490851: Overall mineralogy and distribution of medium- and coarse-grained pegmatites is similar to the main Hellroaring Creek body except for slight variations in mineral modes, and a notable elevated tourmaline content. Overall pegmatite grain size and modal abundance of tourmaline increases from east to west over the 100 metres of exposure. Mineral mode is noted below:

Feldspar (60%): bluish-grey, euhedral to subhedral, 0.5 to 2 centimetre long in medium-grained pegmatite, with albite twinning (plagioclase). Crystal sizes exceed 30 centimetres in length in coarse pegmatite.

Quartz (25%): light-grey, sub- to anhedral, dispersed as matrix throughout. Occasional intergrowth with muscovite.

Muscovite (10%): silver to silvery-green, euhedral books to 2 centimetres in medium-grained pegmatite, and 15 by 10 by 5 centimetres in coarse pegmatite.

Tourmaline (0.5 to 5 %): black, euhedral columns averaging 0.5 by 3 centimetres. Exceptional crystals in coarse pegmatite reach 20 by 10 centimetres. Occasional 'boron blasts' are noted in very coarse assemblages. Size and abundance of crystals are highly variable.

Fluroapatite? (trace): possibly identified as grey, subhedral, pseudohexagonal crystal with dimensions 20 by 10 centimetres.

Beryl (trace): rare, white, opaque, euhedral, hexagonal crystals up to 3 by 12 centimetres, hosted in medium- to coarse-grained feldspar-quartz-muscovite-tourmaline pegmatite.

Stops 6-9M: Mathew Creek Stock

UTM 11 564916E / 5499824N: This coordinate (stop 8M) represents the westernmost outcrop examined. Approximately 900 metres to the east (stop 9M), the pegmatite was drilled in 2001, where beryl abundances are greatest (EMPR ass rpt 26701). The pegmatite is medium- to coarse-grained with the following mineral mode:

Feldspar (65%): Porphyritic K-feldspar is generally discernable from finer grained matrix-filling plagioclase. K-feldspar is blocky, pinkish-white and visibly perthitic. 5 by 3 centimetre blocks are common in the coarser grained assemblage. The ratio of K-feldspar to plagioclase is close to 3:2, but appears to increase in favour of K-feldspar from west to east.

Muscovite (15%): Is silver to reddish silver with euhedral books up to 3 by 3 by 1.5 centimetres.

Quartz (17%): Occurs typically as light-grey, anhedral matrix, and occasionally as quartz-rich segregations or cores, especially at the main area of drilling towards the east.

Beryl (trace to X%): Occurs as white to light-bluish-grey, opaque, subhedral to euhedral crystals (Figure 4). Towards the west, rare beryl crystals are found in several outcrops, up to 4 by 1 centimetres in size. At the main area of drilling in the east, there is spectacular abundances of beryl, locally approaching several percent. Crystals up to 15 by 5 centimetres were noted, with average size of 4 by 1 centimetres.

Tourmaline is generally absent from the pegmatite assemblages, but occurs, up to 10%, in metasomatically altered tourmalinized schist host rock at the eastern extent of the pegmatite.

Several evolving textural and mineralogical features, i.e. increase in grain size, beryl abundance and K-feldspar: plagioclase ratio, strongly suggest a west to east increase in fractionation and mineralization potential.

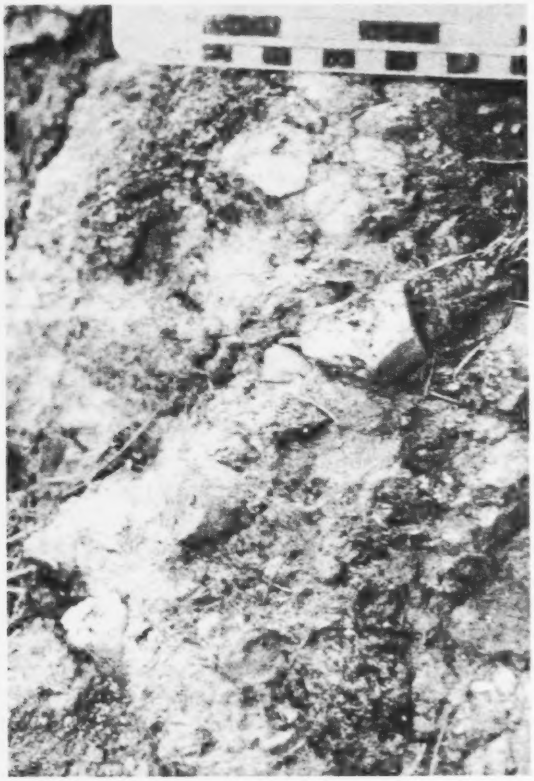

Figure 4 Beryl crystals in medium -grained pegmatite of the Mathew Creek stock, near the main drilling site.

Drilling on the property occurred at the eastern limit of the exposed part of the Mathew Creek stock. Results showed BeO greater than 1000 g/t over 6 metres (including. 2908 g over 1 metre), and Ta_2O_5 approaching 100 g/t over several metres (EMPR ass rpt 26701). These values, although not exceptional, are significant and could be considered encouraging. Does the pegmatite continue in the subsurface towards the east and northeast?

Significance and Interpretations of the Hellroaring Creek Stock

Based on the known mineralogy and geochemistry of the pegmatites at Hellroaring Creek and Mathew Creek, the pegmatites can be classed as beryl - (columbite) pegmatites as defined by Cerny (1991).

The volume of pegmatite at the Hellroaring Creek stock is impressive, rivaling the size of world class economic LCT-pegmatites such as the Greenbushes pegmatite in Australia (with dimensions 3300 by 400 by >500 metres) and the Tanco pegmatite in Manitoba (1650 by 800 by 125 metres) (Cerny, 1991). In contrast to the above pegmatites however, the Hellroaring Creek stock comprises a simple mineralogy: feldspar, quartz, muscovite, biotite, tourmaline, beryl, garnet, apatite, and occasional oxides, including columbite and ilmenite. The internal zonation of the pegmatite is also relatively simple with only localized, discontinuous pods of more texturally and chemically evolved lithologies, in contrast to th Greenbushes and Tanco pegmatites which exhibit bro concentric and/or layered internal zonation patterns. The Hellroaring Creek pegmatite is structurally complex in that it is interpreted as a multiphase system of dyke swarms (EMPR ass rpt 26701), however, internal zonation within individual intrusions appears limited.

The Mathew Creek stock, although significantly smaller than the Hellroaring Creek stock, exhibits encouraging Be and Ta content, and unexplored potential along both strike and dip directions.

Classic models of fractionation and evolution of mineralization in pegmatites suggest the farther a pegmatite forming melt traveled from its parental source, the more fractionated and enriched in incompatible elements such as Be, Li, Rb, Cs, Ta the resulting pegmatite will be (Cerny, 1992). In the case of the Hellroaring Creek stock and surrounding 'satellitic' pegmatites, it is tempting to ask whether the main stock is proximal to a parental source, and if the satellites represent more distal expressions of this system.

GREENLAND CREEK STOCK

The Greenland Creek stock is a north to northwest trending swarm of pegmatite dykes and sills that intrude lower Aldridge sediments and Moyie Sill gabbros and diorites (Figure 5). The elongate and arcuate lobe shaped intrusions have a total average strike length of approximately 2 kilometres, with individual lobes 100 to 500 metres wide. The stock is located approximately 45 kilometres northwest of Kimberley BC, and straddles the west trending ridge between Greenland and Skookumchuck creeks.

Preliminary work on the geological setting, mineralogy and age relationship of the Hellroaring Creek stock to the White Creek batholith and the Greenland

Creek stock, was undertaken by Smith and Brown (1998). Several historical and ongoing exploration projects occur within a 10 kilometre radius of the pegmatite (Brown and Termuende, 1998), but no exploration work has been directed specifically to the Greenland Creek pegmatites. In 2000, Kennecott Canada Exploration drilled one hole on the Greenland Creek Ag-Pb-Zn showing (MF 082FNE107), located approximately 2 kilometres west of the pegmatitic stock. Hole DH-G00-01 intersected feldspar-muscovite-quartz-tourmaline pegmatite at 228 metres depth and remained in pegmatite to the bottom of the hole at 295 metres (Coombs, 2000).

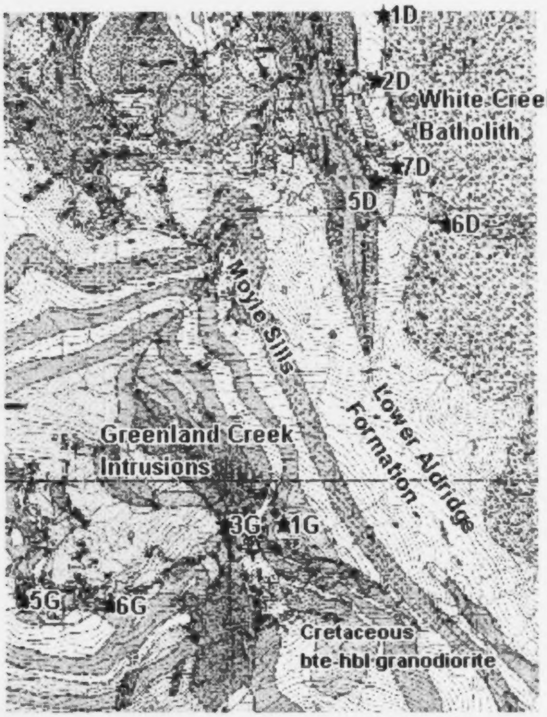

Figure 5 Geology and field sites (stars) visited near the headwaters of Greenland Creek and Doctor Creek (after Greig, 2001). The main body of the Greenland Creek stock is approximately 500 m wide.

Field Observations

The author and assistant set up camp near the eastern limit of the pegmatite swarm, 100 metres north of the ridge line at stop 1G: UTM 11 – 558601E / 5536682 N. Two and a half days were spent examining the pegmatites along the ridge, for two kilometres to the westernmost exposure at stop 5G: UTM11 556709 / 5536133.

Stops 1G-4G: Pegmatites in the eastern one-third of the observed area are composed primarily of fine-grained tourmaline-bearing pegmatitic quartz monzonite to granite, with subordinate but significant volumes of medium- to coarse-grained K-feldspar-quartz-muscovite +/-tourmaline, garnet- and/or beryl-bearing pegmatite. The coarse-grained pegmatite assemblages commonly exhibit significant internal zonation (Figure 6). The best exposures of more evolved pegmatite assemblages were found near camp, at the base of a 300 metre high talus slope. As boulders are typically not large enough to preserve the entire thickness of a zoned pegmatite, it is not possible to ascertain if the pegmatites are zoned symmetrically or layered asymmetrically with respect to central quartz core zones observed up to 1 metre in width. Mineral mode appears to vary systematically from outer zones to inner zones: quartz content increases markedly from 10% to more than 90%, with concurrent increase in muscovite, and decrease in tourmaline content (Figure 6).

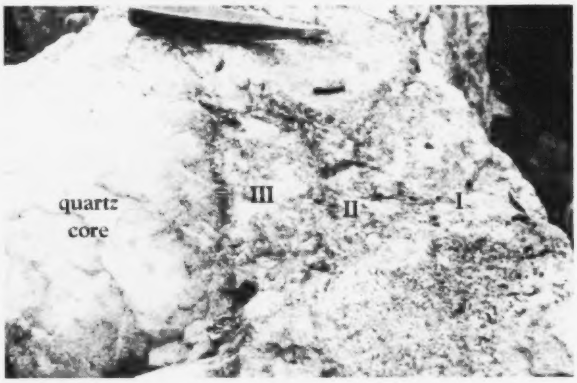

Figure 6 Zoned pegmatite of the Greenland Creek intrusion (stop 2G). I: Fine- to med-grained tourmaline-garnet bearing feldspar +/-muscovite pegmatite. II: Fine- to med-grained feldspar-muscovite pegmatite. III: Medium- to coarse-grained blocky K-feldspar-muscovite pegmatite with quartz matrix. Note: From outer to inner zones (I to quartz core) modal quartz and muscovite increase, tourmaline decreases.

At least four beryl occurrences were noted in the medium- to coarse-grained pegmatite assemblages: three north of the ridge, and one south of the ridge. They occur as white to light-grayish-green, opaque to rarely semi-translucent, euhedral hexagonal crystals. Three to seven millimetre diameter crystals are typical, with visible lengths approaching three centimetres.

Localized vuggy quartz-tourmaline-muscovite-fluorite veining, was observed crosscutting both coarse - grained pegmatites in the talus area, and Aldridge sediments at the 2440 metre peak overlooking the talus area.

Stop 5G: At the western edge of the field area is a 100 by 300 metre exposure of medium-grained pegmatite averaging 45% feldspar, 40% quartz, and 15% muscovite. Minor tourmaline and garnet were noted in zones poor in muscovite. Several discontinuous quartz cores were noted, as well as a zoned contact along the southeast margin. The zoned marginal assemblage comprises a 10 centimetre tourmalinite contact zone, followed by a 3 to 5 centimetre light-bluish microcrystalline quartz zone, containing an unknown jarositic-stained, soft, equant mineral. This zone was, in turn, in contact with a tourmaline bearing aplite, followed by standard medium-grained pegmatite (sample 5G-1).

Greisen-like alteration is also noted locally (sample 5G-3).

Stop 6G UTM 11 557339E / 5536097N: Located on the ridge, at the saddle, midway between the eastern and western stops. Mineralogy of this 30 by 100 metre exposed pegmatite is unique. The rock mode is:

75% medium-grained quartz-plagioclase-tourmaline pegmatite. Mineral mode: 60% quartz, 25% plagioclase, 8% black tourmaline, and subordinate K-feldspar (5%), and muscovite (2%). Tourmaline crystals are up to 6 by 2 centimetres.

15% monomineralic light-grey to white quartz, host to occasional large tourmaline crystals.

10% fine -grained aplite (sample 6G-2)

One occurrence of light-bluish white, opaque beryl was noted in the medium -grained tourmaline-bearing pegmatite. At this same locality, a broad exposure of medium-grained pegmatite is transitional to quartz-tourmaline dykes and sills extending out into the surrounding host sediments.

WHITE CREEK BATHOLITH

The middle Cretaceous White Creek batholith is well exposed over a 435 square kilometre area, in the southern Purcell mountains, approximately 45 kilometres northwest of Cranbrook, BC (Figures 1 & 5). The long axis of the exposed bilobate intrusion trends northeasterly, and comprises a complex multiphase southern lobe, and a single-dominant-phase northern lobe. The details of the mineralogy and phase relations of the batholith are described and mapped by Ressor (1958, 1996). Age relationships of the phases are summarized by Smith and Brown (1998).

The southern lobe is composed of a broad succession of generally younging-outward, concentric phases of leucoquartz monzonite, porphyritic quartz monzonite, hornblende-biotite granodiorite, biotite granodiorite, and quartz monzonite. The northern lobe is mapped exclusively as porphyritic quartz monzonite.

Aplite and pegmatite phases are reportedly widespread, but are particularly associated with the porphyritic quartz monzonites. Reesor (1958) reported the aplites and pegmatites are particularly plentiful east of the headwaters of White Creek along the contact to the northeast and down Skookumchuck Creek. Conversely, aplites and pegmatites are absent in the leucoquartz monzonites, and rare in the medium-grained quartz monzonites and mafic-rich granodiorites of the south and west parts of the batholith (southern lobe?).

Rice (1941) noted, "Pegmatite and aplite dykes are common on the borders and in places carry small amounts of black tourmaline and blue-green beryl." One such locality mentioned, west of Mt. Alton (Mulligan 1968), likely corresponds to Minfile 082FNE159.

Field Observations

The purpose of the traverse in this area was to explore the western contact of the White Creek Batholith between Doctor Creek and Greenland Creek (Figure 5). At the time of writing, the area is blanket staked by Eagle Plains Resources as a prospective area for Ag-Pb-Zn Sullivan-style mineralization, and also includes several W+/-Mo mineralized quartz greisen and skarn showings.

Stop 1D to 5D: The traverse started at the Silver Key Ag-Zn-Pb-Cu mine (MF 082KSE053) and continued south past Shrimp Lake (Figure 7), a local name for the tarn at the headwaters of the southern most tributary of Doctor Creek.

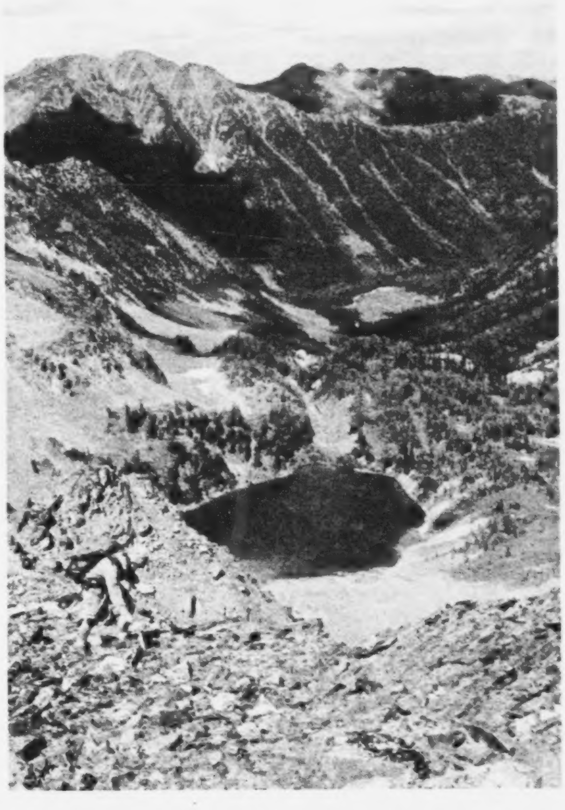

Figure 7 Looking north from stop 5D towards Shrimp Lake.

From here the traverse headed southwards up talus and outcrop, to the peak at stop 5D. Well exposed Lower Aldridge and Moyie Sills were examined for signs of pegmatite and aplite intrusions (Figure 8). No aplite or pegmatite were observed, but a 3 to 5 metre wide quartz sill with notable workings was noted at stop 5D, 50 metres south of the peak. On the ridge, approximately 50 metres east of this same peak, is an occurrence of tourmalinized and albite altered diorite (sample 5D-2), proximal to several veins of tourmaline bearing granite (sample 5D-3).

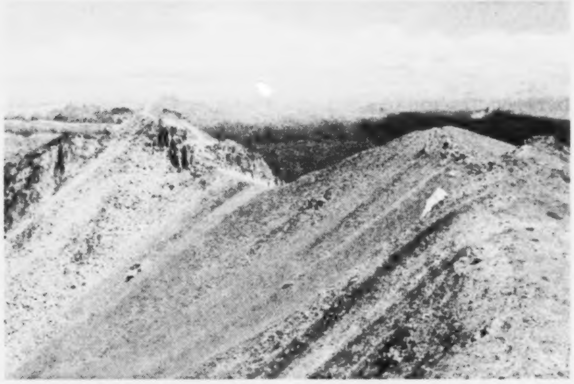

Figure 8 Looking east from stop 5D at rusty lower Aldridge sediments with interbedded grey Moyie diorite sills, and lesser white granitic dykes and veins. Note contact between lower Aldridge sediments and White Creek batholith farther along ridge.

Stop 6D: Blue Hammer showing (UTM 11 559824 E / 5538897 N): Excellent exposure of the contact between the White Creek batholith and Aldridge sediments in this area allowed for careful examination of aplite and pegmatitic dykes and veins hosted within K-feldspar megacrystic quartz monzonite, over a 1500 by 500 metre area (Figure 9). Intrusive phases of the White Creek batholith at this locale are described below:

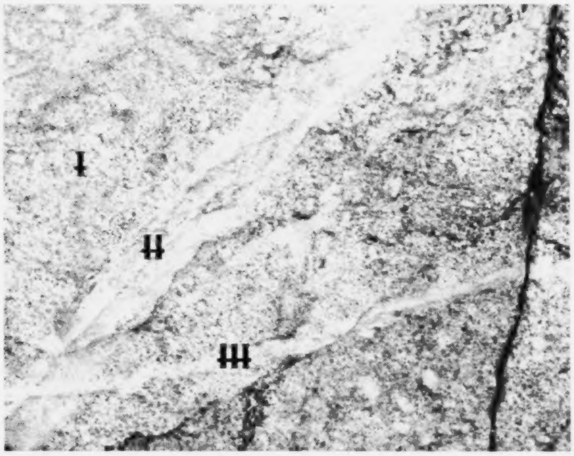

Figure 9 Crosscutting relationships of the three phases in the White Creek Batholith within 5 metres of the Aldridge sediment contact. Three-millimetre long, blue gemmy beryl crystals were found in the 2-3 centimetre wide phase III vein in this photo.

Phase I: K-feldspar megacrystic quartz monzonite, is the dominant phase of the batholith in the area. Euhedral K-feldspar megacrysts greater than 10 centimetres long are pervasive and account for up to 50% of the rock.

Phase II: Medium-grained tourmaline bearing aplite or microgranite crosscuts phase I as veins and dykes up to 10's of metres thick. Contacts between phases I and II are sharp.

Phase III: Fine- to medium-grained beryl-bearing K-feldspar-quartz pegmatite crosscuts phases I and II. Micas are conspicuously rare, but where present, biotite is more common than muscovite. Occasional skeletal intergrowths of tourmaline and quartz were noted. Other minor constituents include fine-grained red garnet, and locally, up to 1% pyrite cubes to 1 centimetre. Contacts with phase II are sharp to diffuse over 1 to 3 centimetres. Contacts with phase I are sharp.

Two gem quality beryls in excess of 8 millimetres in diameter have been found in phase III, in addition to dozens of transparent to translucent crystals less than 3 millimetres (Figure 10). A later beryl-bearing phase has also been noted. Walnut-sized vugs containing inwardly growing euhedral beryl crystals have been noted in quartz-mica +/-tourmaline greisen veins up to 5 centimetres wide. At one location, this vein type was observed crosscutting phase III pegmatite.

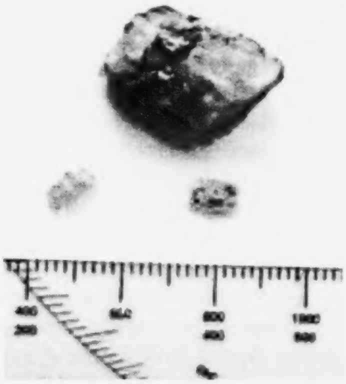

Figure 10 Blue and blue-green aquamarine crystals from the Blue Hammer showing.

In the field area, the volume and number of occurrences of both aplite and pegmatite are greatest at the batholith-sediment contact. Overall rock mode, within 100 metres of the contact, is approximately 75% K-feldspar megacrystic granite (phase I), 20% aplite (phase II) and <5% pegmatite with or without visible beryl (phase III). Cursory traverses in the area revealed an almost complete lack of aplite and pegmatite at distances greater than 100 to 200 metres from the contact. Distances beyond 200 metres were not explored.

Granitoid intrusions as dykes, sills or veins, into the host rocks, also appear to be limited.

This is the first recorded account of beryl crystals associated with the northern lobe of the White Creek batholith. The pegmatite phase in which the beryl crystals are found, appears to be more abundant in areas that also contain significant volumes of aplite. This pegmatite is most often found crosscutting aplite, but beryl-bearing pegmatite veins are also found crosscutting the main body of K-feldspar megacrystic quartz monzonite.

SHAW CREEK STOCK

The Shaw Creek stock is a late Cretaceous, 130 square kilometre intrusion composing the central to southern one-third of the middle to late Cretaceous multiphase Bayonne batholith (Figures 1, 11). The stock is typically light-grey to pinkish-grey biotite +/- hornblende granite with abundant K-feldspar megacrysts averaging 2 to 3 centimetres. Leucoquartz monzonite is locally abundant.

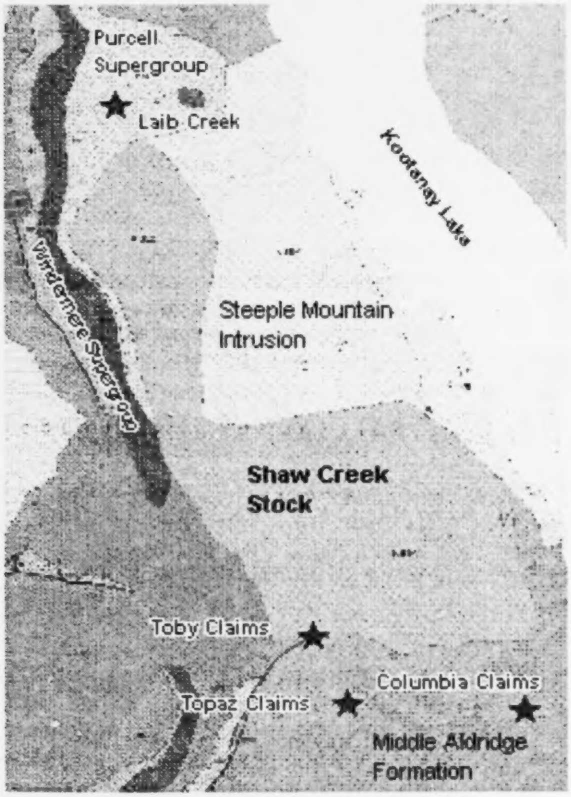

Figure 11 Geology and field sites in the area of the Late Cretaceous Shaw Creek stock (after Reesor, 1996). Kootenay Lake is approximately 5 kilometres wide.

An overview of the area stratigraphy, igneous intrusions, and structural and metamorphic setting is detailed by Brown et al. (1994). The Shaw Creek stock intrudes the Aldridge Formation along the southern and southeastern portion of the map area. Semipelites of the Aldridge Formation in this area have been metamorphosed to amphibolite facies (sillimanite-kyanite-staurolite) (Brown et al., 1994), an expression of the deformation related to the formation of the Kootenay Arc. To the west and southwest, the Shaw Creek stock intrudes grey siltites and black argillites of the La France Creek Group, dolomite and argillite of the Mt. Nelson Formation, and polymict conglomerate of the Windermere Group Toby Formation.

Other intrusions in the area include biotite-hornblende-epidote granodiorite of the Jurassic Mine Stock to the southwest, and biotite-muscovite leucomonzogranite of the mid-Cretaceous Steeple Mountain stock to the east. Eocene Coryell stocks, less than 1 square kilometer, intrude surrounding lithologies approximately 5 kilometres west and northeast of the northernmost extent of the Shaw Creek stock. Lamprophyre dykes are also noted in the region.

Rice (1941) noted that the Bayonne Batholith in general has a highly variable nature and,

> "Masses of pegmatite and dykes of pegmatite and aplite occur everywhere. Some of the pegmatite dykes are over 100 feet wide. A few large crystals of blue-green beryl, pink garnet, magnetite, and a little black tourmaline were seen in these pegmatites."

The details of the above quote refers to the historical Midge Creek showing (MF 082FSE091).

Recent mapping carried out by the author for Cream Minerals Ltd. outlined a further northward extension of the Shaw Creek stock into the Laib Creek area, not previously mapped by Reesor (1996). Beryl showings in the vicinity of the Shaw Creek stock were recently discovered by prospector Lloyd Addie of Nelson BC. In the fall of 2002, Cream Minerals Ltd. of Vancouver, BC, entered into an option agreement with Mr. Addie, to develop the property as an aquamarine and emerald gemstone property. The property includes two large claim groups covering the northern, western and southern contacts of the Shaw Creek stock. More than 25 kilometres separates the northernmost and southernmost showings. In 2003, Cream Minerals Ltd. engaged the author to do geologic mapping and oversee the exploration program in the search for gem-beryl mineralization.

Field Observations

Along the northern and western margins of the Shaw Creek stock, pegmatite and aplite is common as schlieren, dykes, and veins hosted by granite, particularly within one kilometre of the margin. Along the southern contact, pegmatite dykes are observed occasionally within granite dykes, but occur more commonly as pegmatite sills and dykes within Aldridge sediments, typically at a distance greater than one kilometre south of the contact.

Laib Creek (OMG claims)

The OMG claims in the Laib Creek area are underlain by a previously unrecognized lobe of the Shaw Creek stock, which is several square kilometres in area.

Six different rock types were recognized within the property area. In order of abundance they are: biotite +/- muscovite granite (G), K-feldspar-muscovite pegmatitic granite (PG), micaceaos meta-arkose (mma) with subordinate interlayered amphibole-bearing metapelite, garnetiferous sodic aplite (A), medium- to coarse -grained K-feldspar +/- muscovite +/- beryl pegmatite (P), and K-feldspar megacrystic granite (Gk). Textural and cross-cutting relationships suggest the following temporal sequence from oldest to youngest: mma – Gk – G – A – PG – P.

Beryl crystals are most commonly found in the coarser grained P unit, with rare occurrences in the finer grained PG unit. Beryl abundance is generally less than 1%, however volumes greater than 5 % have been noted. Beryl crystals in the pegmatite are pale- to medium- ice-blue to greenish-blue in colour and range up to 10 centimetres in diameter. Some of the best quality aquamarines are found within or along the margin of quartz cores within surrounding coarse-grained pegmatite.

At two known locations, 10 to 30 centimetre wide quartz veins appear to extend out of the quartz cores, through the host coarse-grained pegmatite, and into surrounding aplite and/or sedimentary lithologies. These veins comprise 90% light-grey to smokey quartz with subordinate K-feldspar, trace beryl and molybdenite, and up to 5% vugs, lined with rhimes of very fine -grained micas and/or clays, and occasionally beryl crystals. Several gemmy ice-blue, translucent to transparent, euhedral aquamarine crystals, to 6 millimetres in diameter, have been found in this vein type. Molybdenite occurs as sparse, yet coarse disseminations up to 1.5 centimetres. Smokey quartz is most prevalent in and around vuggy sections of the veins.

In general, quantity and quality of aquamarines in the Laib Creek area, tend to be correlative to increasing grain size of the host pegmatite, presence of zonation in the pegmatite, and presence of smoky quartz. However, some of the bluest crystals were found in narrow pegmatite segregations hosted within thick 3 to 10 meter wide aplite pods (Figure 12).

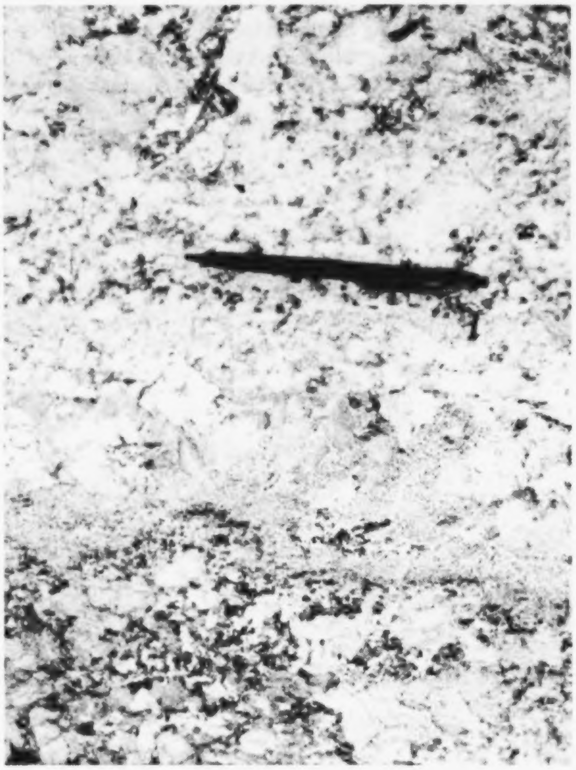

Figure 12 Abundant blue, subhedral to euhedral, translucent and opaque beryl crystals in aplitic albite segregation at centre of medium- to coarse-grained K-feldspar-muscovite pegmatite. Beryl crystals also in pegmatite at bottom of photo within smoky quartz matrix. Location: Laib Creek

Topaz Creek (Toby, Topaz, Columbia claims)

Three claim groups at or near the southern margin of the Shaw Creek stock, were prospected and mapped to outline beryl mineralization. The most significant beryl crystals were found on the Toby claims, which straddle the contact between the Shaw Creek stock and the Mount Nelson Formation.

Preliminary mapping on the Toby claims, discerned five rock types. In order of abundance they are biotite granite (G), schistose semi-pelite (SSP), a mylonitic to cataclastic mafic intrusion or gabbro (M), pegmatitic granite or pegmatite (P), and aplite (A). Textural and cross-cutting relationships suggest the following temporal sequence from oldest to youngest: SSP – M – G – PG – A – P.

The beryl-bearing unit is a fine- to medium-grained K-feldspar-muscovite-biotite pegmatite with a light grey to smokey quartz matrix. The main showing contains bluish-green beryls, some with significant gemmy sections. The largest beryl collected to date is a euhedral, hexagonal, translucent crystal with dimensions of 4 by 0.8 centimetres. The pegmatite is 20 to 30 centimetres wide and is hosted in unit M with distinct, sharp margins. In the area of the best mineralization, pegmatite and granite dykes are hosted in a 50 metre wide zone comprising dominantly dark grey mylonitic and cataclastic gabbro dykes.

The Topaz and Columbia claims are located 1 to 2 kilometres south and southeast, respectively, of the Toby claims. Unlike the claim groups to the north, pegmatites in the Topaz creek area occur as sills and lesser dykes hosted in sediments of the Aldridge Formation. Pegmatite mineralogy consists of feldspar, with significant quartz and muscovite, minor transient red garnet and black tourmaline, and trace white to yellow and rarely pale blue beryl.

On the Columbia claims, 1 to 1.5 metre wide pegmatite sills are most common, hosted in biotite-muscovite schists, containing relict aluminosilicate porphyroblasts. Light bluish-white and yellowish white, opaque beryls are the most common, while translucent beryl crystals up to 5 centimetres long are noted occasionally.

On the Topaz claims, beryl occurs as subhedral to euhedral white, opaque crystals hosted in pegmatite sills and dykes similar to those on the Columbia claims. White opaque beryls, 1 to 3 centimetres wide, were also found on a 50 by 100 metre bluff comprising pegmatitic granite and subordinate fine- to medium-grained pegmatite. Quartz-cassiterite veins occur locally along the margins of the pegmatoid units.

The large outcrop of pegmatite at this location is well foliated in at least two orientations and comprises a mineralogy slightly different than the local pegmatite sills. Textural and mineralogical features of the large pegmatite are somewhat similar to those observed at the Proterozoic Hellroaring Creek stock.

The area has been explored previously for base metal potential (MF 082FSE004). The Minfile report mentions the existence of quartz-cassiterite veins associated with galena and sphalerite, however no reference is made to pegmatites in the area.

SLOCAN VALLEY

Field work in the Slocan Valley included a reconnaissance examination of pegmatites along the Little Slocan River Forest Road, and a detailed viewing of the BQ claim near Yolanda Creek (Figure 13).

Interesting mineralization with gem potential for garnet and moonstone was noted at stop S2.

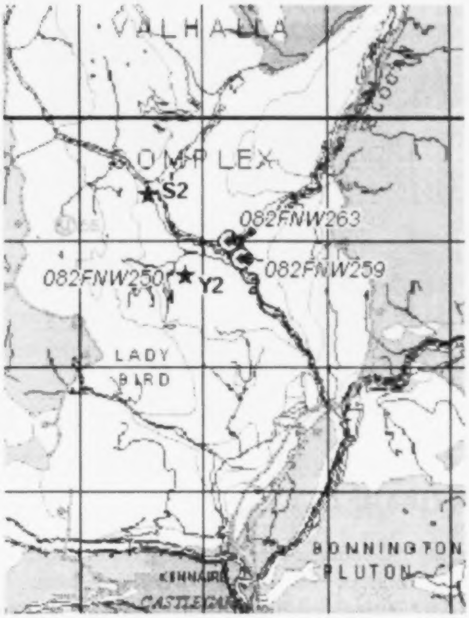

Figure 13 Geology, Minfile and field sites (stars) in the Slocan Valley (after Geoscience Map 2002-1). Grid squares are 10 by 10 km.

Yolanda Creek (BQ claim)

Pegmatites at the BQ claim (stop Y2) occur as quartz monzonite boudined sills hosted in gneissic metasediments and fine to medium-grained quartz monzonite intrusions (Figure 14).

Figure 14 Prospector Ed Varney at his aquamarine-bearing pegmatite showing (BQ claim, Slocan Valley).

Gem quality aquamarine crystals up to 10 centimetres in length have historically been extracted from very coarse -grained vuggy quartz- K-feldspar pegmatite (Figure 15).

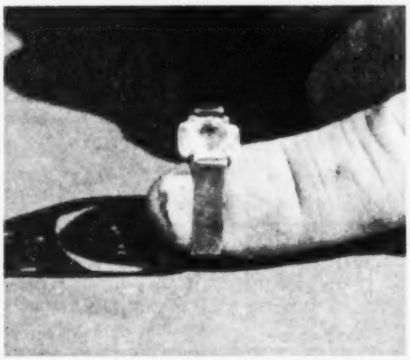

Figure 15 Cut aquamarine gemstone from the BQ claim.

GEOCHEMISTRY

During the course of the 12 field days devoted to this project, a total of 78 samples were collected. This included 42 intrusive and sedimentary samples for whole rock analysis, 27 single crystal K-feldspar and muscovite samples for trace element analysis, 6 beryl crystals for probe analysis, and 3 unknown oxide minerals for XRD identification. Out of the 78 samples collected during field work, 35 of the whole-rock samples were analysed. Samples come from the Hellroaring Creek stock, Lightening Creek, Mathew Creek Stock, Greenland Creek stock, White Creek batholith, and intrusives of the Slocan Valley.

Cream Minerals Ltd. provided a total of 32 analyses from sampling completed by the author in the summer and fall of 2003. Fourteen compositions are from the northern claim groups (OMG, Cultas), the remainder from the southern claim groups (Topaz and Columbia).

All analyses were done by Acme Analytical labs in Vancouver BC, using the analytical packages in Table 2. Analyses provided by Cream Minerals Ltd. did not include Group 4A elements.

Table 2 Analytical packages for whole rock analysis by Acme Labs (http://www.acmelab.com/cfm/index.cfm).

Package	Elements
Group 4A: ICP-ES	Al_2O_3,Fe_2O_3,MgO,CaO,Na_2O,K_2O,TiO_2, P_2O_5,MnO,Cr_2O_3,Ba,Ni,Sc.
Group 4B: ICP-ES&MS	Be,Co,Cs,Ga,Hf,Nb,Rb,Sn,Sr,Ta,Th,U, V,W,Zr,Y,La,Ce,Pr,Nd,Sm,Eu,Gd,Tb,Dy ,Ho,Er, Tm,Yb,Lu
Group 1DX: ICP-MS	Mo,Cu,Pb,Zn,Ni,As,Cd,Sb,Bi,Ag,Au,Hg, Tl,Se

Five different rock types were analyzed:

1) Moyie sill gabbros and diorites
2) Sediments proximal to the Shaw Creek stock
3) Cretaceous granite host to pegmatite
4) Aplite
5) Pegmatite

Average compositions of the different rock types are presented in Table 3. Average compositions of pegmatites from 8 different areas are presented in Table 4.

Significant correlation coefficients for selected pegmatite elements are summarized in Table 5.

Geochemistry of pegmatites

Plots of individual contents (Figures 16 a-i) of pegmatite analyses highlight compositional variations, mineralization trends, and suggest geochemical tools for future geochemical sampling procedures.

There is a discernable inverse correlation between Na2O and K2O (Figure 16b) that corresponds to observed mineral modes at the different properties. K2O vs. Rb (Figure 16d) and Rb vs. Cs (Figure 16e) both exhibit discernable positive correlations. Highest average values of K and Rb occur in pegmatites at White Creek, Mathew Creek and Shaw Creek, respectively. These relationships can be interpreted as a rough, first-pass determinations of relative fractionation of the different pegmatite bodies.

Nb vs. Ta (Figure 16f), Be vs. Ta (Figure 16g), and Be vs. Rb (Figure 16h), all exhibit good to moderate positive correlations. In figures 16g and 16h, there appears to be two parallel but diverging trends at Be > ~50 ppm. Highest average Be contents occur at Mathew Creek, Greenland Creek, and Shaw Creek, while highest Nb and Ta contents occur at Shaw Creek, followed by White Creek, and Mathew Creek. The highest average Ta/Nb value (0.69) occurs at Mathew Creek.

Sn, W, and Bi exhibit moderate to strong positive correlations to each other and moderate to weak positive correlations against Mo, and Cu. This suite of five elements does not correlate well against the suite of LCT-signature elements (K, Rb, Cs, Be, Ta, Nb) mentioned above, and suggests different styles and/or timing of mineralization.

Table 3 Average whole rock compositions by rock type. n (x,y) = number of analyses included in the average (Individual analyses that include Group 4A, Total no. of analyses)

	Moyie gabbro/diorite	Shaw Creek sediments	Cretaceous granite	All aplite	All pegmatite
n	4,8	2,15	4,5	4,5	18,30
SiO2 %	51.67	69.03	71.01	73.12	74.88
Al2O3	13.74	14.78	14.43	15.80	14.32
Fe2O3	14.52	6.23	3.52	0.77	1.17
MgO	4.79	1.77	0.53	0.21	0.17
CaO	9.04	0.65	1.25	1.00	0.68
Na2O	1.92	0.51	3.56	6.06	3.72
K2O	0.56	2.59	3.25	1.91	3.57
TiO2	1.60	0.73	0.25	0.06	0.07
P2O5	0.14	0.45	0.18	0.20	0.22
MnO	0.20	0.12	0.27	0.06	0.05
Cr2O3 *	0.010	0.006	0.001	bd	0.003
Ba (ppm)	110.00	534.23	429.25	101.75	241.44
Ni (ppm)**	79.00	26.00	21.00	bd	27.67
Sc (ppm)	40.25	13.00	3.25	3.00	3.09
LOI	1.55	2.95	1.55	0.75	1.07
SUM	99.76	99.81	99.85	99.93	99.92
Be (ppm)	3.67	5.80	8.25	48.25	99.94
Co	38.68	12.20	2.70	1.20	1.28
Cs	5.98	32.07	11.43	8.65	13.58
Ga	22.83	21.94	21.13	20.10	17.79
Hf	3.23	7.83	3.73	3.13	2.36
Nb	6.90	25.05	59.28	29.75	17.03
Rb	31.40	278.77	236.90	197.68	299.34
Sn	13.00	17.87	4.75	23.75	37.88
Sr	173.18	87.64	215.38	55.83	69.48
Ta	0.48	2.93	5.60	9.85	5.60
Th	4.83	14.05	29.65	6.37	2.59
U	1.30	3.99	19.05	6.10	3.11
V	443.25	101.67	27.25	21.50	17.60
W	26.30	4.43	4.75	9.98	4.48
Zr	101.73	263.12	117.13	74.68	41.89
Y	31.90	39.33	12.03	7.70	10.84
La	14.40	42.27	43.25	5.93	7.78
Ce	34.08	96.57	76.85	12.15	15.89
Pr	3.93	10.76	7.43	1.48	1.85
Nd	17.03	41.34	24.18	5.25	6.95
Sm	4.13	8.31	3.55	1.35	1.72
Eu*	1.30	1.39	1.04	0.26	0.56
Gd	4.64	6.87	2.36	1.21	1.44
Tb	0.80	1.13	0.35	0.22	0.28
Dy	5.11	6.65	1.97	1.19	1.67
Ho*	1.04	1.38	0.35	0.22	0.42
Er	3.11	3.95	1.03	0.65	1.04
Tm*	0.45	0.62	0.18	0.20	0.26
Yb	2.87	3.88	1.27	0.85	1.07
Lu	0.43	0.58	0.22	0.15	0.16
Mo	0.35	0.78	9.40	6.68	1.52
Cu	71.75	23.41	5.88	6.58	8.01
Pb	2.88	4.08	6.45	12.03	6.50
Zn	47.75	55.67	19.25	23.75	19.11
Ni	17.43	12.73	2.28	1.30	2.53
As**	3.85	11.46	2.33	0.95	5.29
Cd**	bd	0.20	bd	0.10	0.23
Sb**	bd	0.10	0.63	0.25	0.10
Bi	0.10	1.00	0.15	1.13	1.88
Ag**	bd	0.17	0.50	0.20	0.73
Au**	1.70	0.85	3.10	1.10	2.18
Hg	bd	0.01	0.02	bd	0.02
Tl	0.20	0.69	0.25	0.10	0.19
Se**	0.80	0.50	bd	bd	bd
Ta/Nb	0.07	0.12	0.09	0.33	0.33
Ga/Al2O3	1.66		1.46	1.27	1.24
Rb/K2O	56		73	104	84

* significant number of contents below detection lead to exaggerated average cont

** majority of contents below detection - average numbers high and suspect

Table 4 Average *pegmatite* whole rock compositions by area. n = number of analyses included in average. ASI (aluminum saturation index) = mol. Al2O3/(CaO+Na2O+K2O)

	Lightening Creek	Slocan BQ claims	Hellroaring Creek	Greenland Creek	Shaw Creek S	Shaw Creek N	Mathew Creek	White Creek
n	3	4	3	4	5	7	3	1
SiO2 %	74.20	74.72	76.83	75.39	nd	nd	73.76	73.02
Al2O3	14.77	14.46	13.31	14.24	nd	nd	14.59	14.87
Fe2O3	0.90	1.12	0.96	0.97	nd	nd	2.13	0.76
MgO	0.06	0.15	0.07	0.21	nd	nd	0.33	0.14
CaO	1.10	0.95	0.31	0.68	nd	nd	0.31	0.49
Na2O	6.12	2.67	5.12	3.17	nd	nd	1.82	3.67
K2O	1.08	4.52	2.32	3.92	nd	nd	4.70	6.14
TiO2	0.02	0.03	0.03	0.04	nd	nd	0.23	0.04
P2O5	0.67	0.11	0.11	0.15	nd	nd	0.17	0.07
MnO	0.06	0.04	0.05	0.03	nd	nd	0.07	0.09
Cr2O3 *	0.002	0.002	bd	0.001	0.001	0.004	0.008	bd
Ba (ppn	26.67	580.50	30.00	239.50	177.90	92.46	191.00	323
Ni (ppm	20.00	26.00	22.50	28.33	nd	nd	47.00	bd
Sc (ppn	1.00	4.50	1.50	2.00	nd	nd	12.00	1
LOI	1.00	0.88	0.83	1.10	nd	nd	1.77	0.5
SUM	99.98	99.90	99.94	99.92	nd	nd	99.89	99.83
Be (ppn	35.67	4.75	29.00	183.50	170.60	96.86	253.33	92
Co	0.50	1.30	0.50	0.73	0.90	2.35	2.57	0.5
Cs	22.43	5.35	8.70	8.70	16.96	14.40	26.00	16.9
Ga	18.43	16.43	13.73	17.70	19.92	30.69	20.00	27.2
Hf	bd	2.37	1.25	1.60	1.40	8.23	4.27	1.9
Nb	14.07	5.38	10.07	16.78	36.82	75.30	24.37	72.4
Rb	197.10	252.33	254.77	313.88	364.96	403.30	425.47	491.3
Sn	48.00	79.00	11.00	40.25	35.60	2.67	34.33	7
Sr	25.97	154.00	11.73	64.60	57.98	44.36	37.17	151.7
Ta	3.90	1.83	2.60	5.98	10.40	51.71	8.53	24.5
Th	0.90	2.30	0.67	1.70	1.52	16.56	6.80	5.5
U	0.70	2.48	1.93	4.28	3.08	11.46	3.77	9.7
V	bd	5.00	bd	7.00	bd	21.50	64.00	5
W	2.60	5.18	2.40	6.68	3.78	2.53	4.17	5.7
Zr	4.53	45.65	12.80	26.70	24.58	91.00	128.10	28.4
Y	2.47	19.30	1.33	14.18	3.80	9.40	13.27	10
La	3.03	7.58	3.85	6.05	3.20	8.24	18.20	6.3
Ce	7.23	14.80	6.37	13.75	5.82	16.71	39.53	12.4
Pr	0.86	1.55	0.74	1.91	0.62	1.74	4.41	1.43
Nd	2.63	5.73	3.70	7.45	2.04	6.01	15.17	4.7
Sm	1.40	1.25	1.10	1.93	0.44	1.31	3.23	1.1
Eu*	0.12	0.69	bd	0.49	0.22	0.36	0.81	0.19
Gd	1.05	1.44	0.58	1.77	0.45	1.23	2.38	0.98
Tb	0.18	0.33	0.09	0.38	0.09	0.21	0.41	0.24
Dy	0.61	2.63	0.32	2.13	0.57	1.39	2.31	1.34
Ho*	0.07	0.59	bd	0.40	0.15	0.47	0.59	0.23
Er	0.13	1.91	0.08	1.27	0.33	0.88	1.19	0.76
Tm*	bd	0.29	bd	0.20	0.19	0.24	0.50	0.15
Yb	0.18	1.82	0.12	1.37	0.39	1.01	1.14	1.22
Lu	0.02	0.27	0.02	0.20	0.06	0.16	0.25	0.17
Mo	0.83	1.03	1.13	3.55	2.04	8.16	0.73	0.9
Cu	1.63	12.23	1.63	17.55	3.28	3.63	3.77	3.9
Pb	4.77	13.68	4.23	3.70	4.88	2.54	5.53	3.9
Zn	11.00	29.25	3.00	21.50	5.60	11.00	28.67	13
Ni	1.53	1.53	1.33	2.53	1.04	1.60	6.60	1
As**	9.73	0.60	7.80	1.50	0.65	bd	3.93	0.8
Cd**	0.50	0.10	0.10	0.10	0.10	0.30	0.10	bd
Sb**	0.10	0.10	bd	0.10	bd	0.10	0.10	0.1
Bi	0.17	7.10	0.20	4.13	0.40	7.10	1.67	0.7
Ag**	bd	0.40	0.10	1.20	0.10	bd	bd	bd
Au**	0.80	0.80	0.60	5.25	0.60	4.73	2.65	bd
Hg	bd	0.04	bd	0.02	0.01	0.01	bd	bd
Tl	0.15	0.20	0.10	0.13	0.13	0.18	0.33	0.1
Se**	bd	bd	bd	bd	bd	bd	bd	bd
Ta/Nb	0.28	0.34	0.26	0.36	0.28	0.69	0.35	0.34
Ga/Al2C	1.25	1.14	1.03	1.24	nd	nd	1.37	1.83
Rb/K2O	183	56	110	80	nd	nd	90	80
ASI	1.11	1.31	1.18	1.47	nd	nd	1.76	1.10

* significant number of contents below detection lead to exaggerated average content

** majority of contents below detection - average numbers high and suspect

Table 5 Significant correlations (pegmatite only)

Element	Strong correlation $r^2 > 0.8$	Moderate correlation $0.8 > r^2 > 0.60$	Significant correlation $0.59 > r^2 > 0.45$
Be		Ta	Nb, Ga
K		Rb	
Rb		K,Nb	Mn,Sn,W,Ta,Cs
Cs		P	Mn,Ga,Nb,Rb
P		Ca,Cs	Mn
Ta	Nb	Be,Ga	Rb,U,Mn
Nb	Ta	Rb,Bi	Mn,U
Ga		Nb,Ta	Be,Cs,Rb
W	Bi	Sn,Cu	Rb,Zn,Mo
Sn		W,Cu,Pb,Bi	P,Cs,Rb,Zn
Mo		Bi,W	Si

Select geochemistry of host sediments and Moyie sills

Known chromophore elements contained in emerald are Cr and V. These elements attain significant contents within mafic and ultramafic lithologies, but are extremely low in uncontaminated felsic granitoids. Special geologic environments are required to mix mafic source Cr and V with felsic Be-bearing granitoids. One important component of an emerald exploration program is the assessment of Cr and V in potential host rocks to Be-bearing granitoids. Tables 6 and 7 report Cr and V statistics of Moyie gabbro/diorite and sediments proximal to beryl occurrences discussed in this report. Additional geochemical data for Moyie intrusions can be found in Hoy and Fournier (2001).

Table 6 Chromium in host rocks

Cr_2O_3 %	n	Average	Max	Min	Stdev
Moyie gabbro/diorite	8	0.008	0.018	<0.001	0.007
Psammite and pelite from Shaw Creek	15	0.006	0.010	<0.001	0.002

Table 7 Vanadium in host rocks

V (ppm)	n	Average	Max	Min	Stdev
Moyie gabbro/diorite	8	362	763	56	209
Psammite and pelite from Shaw Creek	15	102	374	25	110

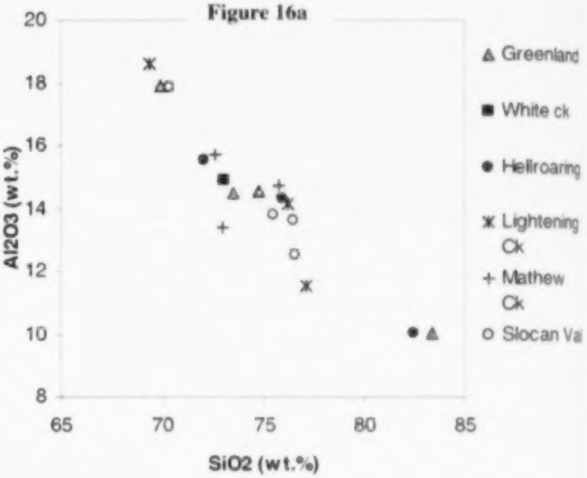

Figure 16a

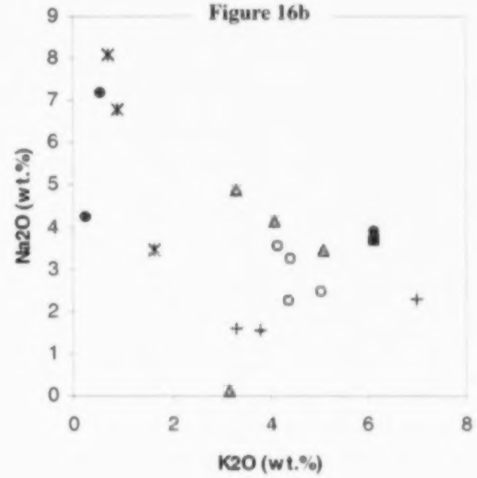

Figure 16b

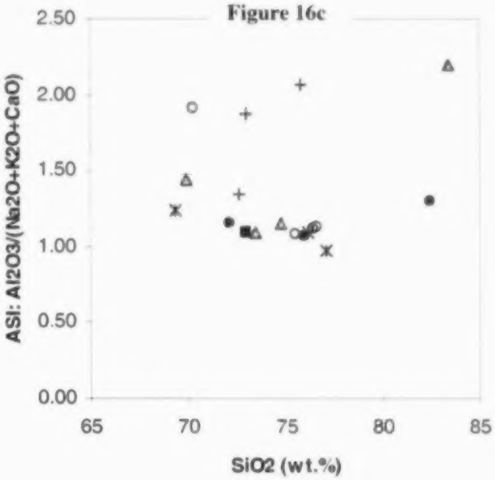

Figure 16c

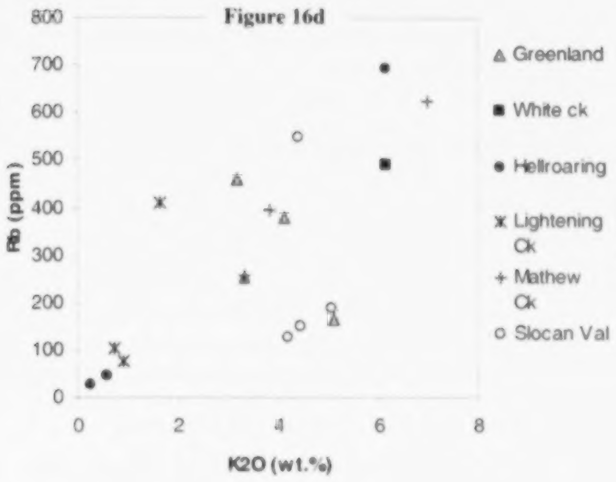
Figure 16d

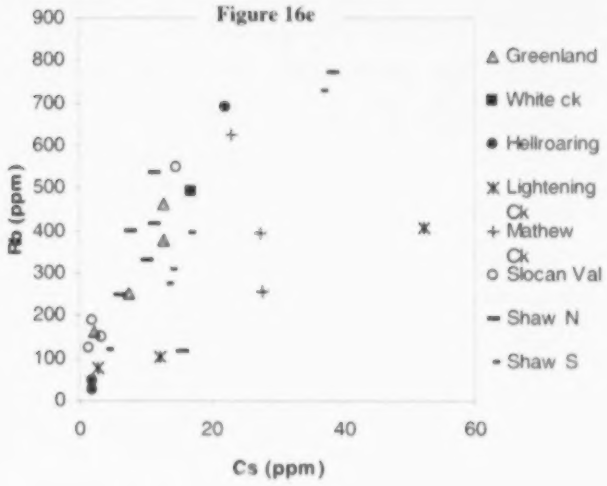
Figure 16e

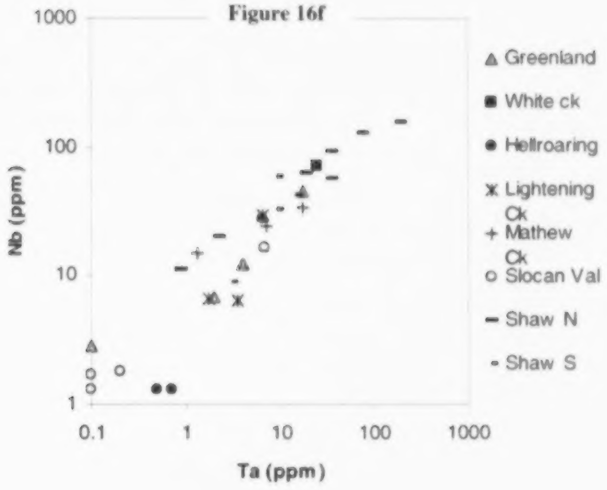
Figure 16f

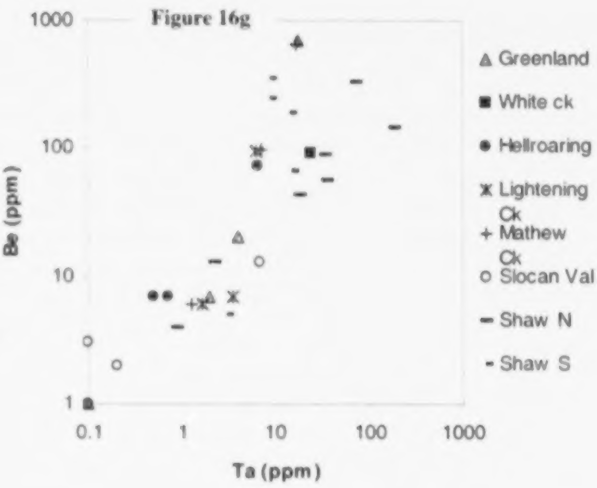
Figure 16g

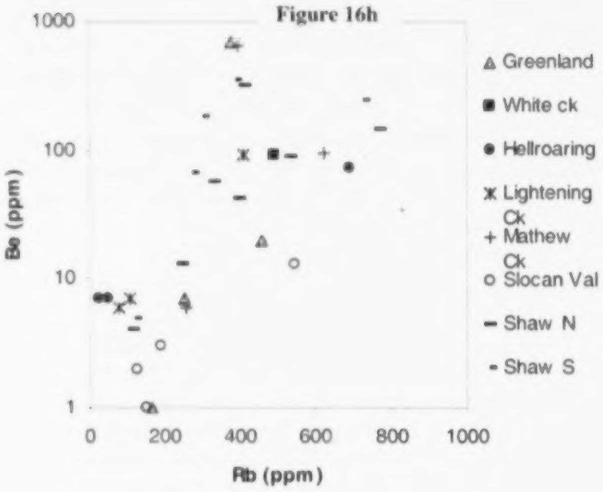
Figure 16h

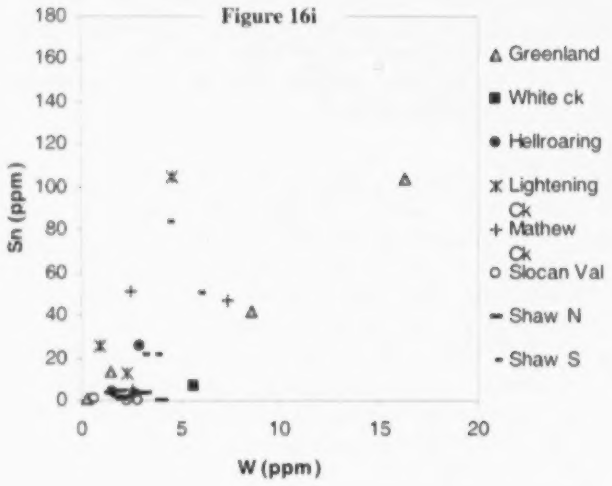
Figure 16i

CONCLUSIONS

Granitic pegmatites are enigmatic deposits host to some of the worlds most rare and precious commodities. In comparison to base and precious metal deposits they are relatively small, with limited alteration and geochemical signatures, making them a difficult deposit type to locate and asses for economic potential.

LCT-granitic pegmatites in the Kootenay Region exhibit a consistent enrichment in Be in early and late magmatic (pegmatite) phases, as well as in pneumatolytic or greisen assemblages. Geochemical data presented here indicate that Be enrichment tends to coincide with enrichments in Ta, Nb, Rb, Cs, and K. Based on the known pegmatite occurrences in the region, it is apparent that there are two target commodity deposit types: I) gemstones in pegmatite or in the alteration halos of pegmatite bodies, and II) rare-element mineralization (e.g. Li, Be, Ta, Nb, Cs) associated with pegmatite.

Pegmatites with the best potential for both commodity types appear to share the following petrologic and mineralogical characteristics:

1. Variable textures with both fine-grained aplite and coarse-grained pegmatite phases present.
2. Extremely coarse-grained pegmatite. These tend to exhibit greater variety and abundance of exotic minerals and ultimately rare-metal contents.
3. Well developed zonation.
4. High ratio of K-feldspar to plagioclase.
5. Significant smoky quartz in the pegmatite especially when accompanied with vugs or miarolitic cavities.
6. Late generations of greisen-style alteration as veins and fracture fill. Common mineralogy includes quartz-muscovite +/-fluorite +/-tourmaline +/-scheelite +/-molybdenite, associated with vugs and rimes of fine-grained white micas and/or clays. Euhedral beryl crystals were noted within vugs of this vein type at the Blue Hammer showing, Laib Creek, and Hellroaring Creek.

The best quality aquamarine and emerald generally comes from pegmatites hosted in middle to late Cretaceous granitoid stocks or batholiths. The pegmatites tend to form as dykes or schlieren with preferred orientations within the granitoid, generally within 100 metres of the contact with neighboring country rocks. Xenoliths and/or roof pendants are generally abundant.

Beryl crystals associated with the Proterozoic pegmatites at Hellroaring, Mathew and Greenland Creek stocks, are invariably white to yellow and opaque. Gem potential appears to be low, however, accumulations of beryl can exceed several percent of the pegmatite volume. The Be mineralization is generally associated with elevated Ta and Nb contents. Considering the substantial size of the Proterozoic pegmatites, there is considerable potential for the discovery of economic reserves of rare-metal commodities.

ACKNOWLEDGMENTS

I would like to thank the prospectors and geologists who contributed to the logistical and technical support of this project. Peter Klewchuck and Craig Kennedy of Kimberley BC, provided access and helpful information for the Hellroaring, and Mathew Creek stocks. Tim Termuende and Chuck Downie of Eagle Plains Ltd. were extremely supportive of traverses to the Greenland Creek and Doctor Creek areas. Ed Varney of Slocan Park, provided access and information on the BQ claim.

Special thanks to the crew and management of Cream Minerals Ltd. for field assistance and access to data from the Shaw Creek stock, and especially to Lloyd Addie for his diligent prospecting which led to the discoveries there.

Also, many thanks to my readers and technical associates: Linda Dandy, Lee Groat and Andrew Legun; to Jess 'eagle-eye' Brown – field assistant extraordinaire, and very special thanks to my wife Amy for her love and support.

REFERENCES

Archibald, D.A., J.K. Glover, R.A. Price, E. Farrar and D.M. Carmichael, 1983. Geochronology and tectonic implications of magmatism and metamorphism, southern Kootenay Arc and neighboring regions, southeastern British Columbia. Part I: Jurassic to mid-Cretaceous. Can. J. Earth Sci. 20: 1891-1913.

Brown, D.A., and T. Termuende, 1998. The Findlay industrial partnership project: Geology and mineral occurrences of the Findlay – Doctor Creek areas, southeastern British Columbia. Geological Fieldwork 1997, Paper 1998-1. 10-1 to 10-9.

Brown, D.A., T.P. Doughty and P. Stinson, 1994. Preliminary Geology of the Creston Map Area, Southeastern British Columbia. Geological Fieldwork 1994, Paper 1995-1. pp. 135-155.

Carr, S.D., 1995. The southern Omineca Belt, British Columbia: new perspectives from the Lithoprobe Geoscience Program. Can. J. Earth Sci. 32: 1720-1739.

Cern , P., 1991. Rare-element granitic pegmatites, Part I: Anatomy and internal evolution of pegmatite deposits. Geosci. Can. (Ore Deposit Models series) 18: 49-67.

Cern , P., 1992. Geochemical and petrogenetic features of mineralization in rare-element granitic pegmatites in the light of current research. Applied Geochemistry 7: 393-416.

Coombs, S., 2000. 2000 diamond drilling report on the Greenland Creek option. Core 3 to 19, core SW, Fin 1-14 mineral claims. Assessment report commissioned by Kennecott Canada Exploration.

Geoscience Map 2002-1: Intrusion Related Mineral Occurrences of the Cretaceous Bayonne Magmatic Belt, Southeast British Columbia, 1: 500 000. Compiled by James Logan (BCGS)

Groat, L.A., D. Marshall, G. Giuliani, D.C. Murphy, S.J. Piercey, J.L. Jambor, J.K. Mortensen, T.S. Ercit, R.A. Gault, D. P. Mattey, D. Schwarz, H. Maluski, M. Wise, W. Wengzynowski, and D. W. Eaton, 2002. Mineralogical and geochemical study of the regal ridge emerald showing, Southeastern Yukon. Can. Min. 40: 1313-1338.

Hoy, T., and M. Fournier, 2001. PGE potential of the Moyie Sills. EMPR GeoFile, 2001-8.

Hoy, T., and P. van der Heyden, 1988. Geochemistry, geochronology, and tectonic implications of two quartz monzonite intrusions, Purcell Mountains, southeastern British Columbia. Can. J. Earth Sci. 25: 106-115.

Logan, J., D. Lefebure, and M. Cathro, 2000. Plutonic-related gold-quartz veins and their potential in British Columbia in The Tintina Gold Belt: Concepts, Exploration, and
Discoveries; Special Volume 2.

Mulligan, R. 1968. Geology of Canadian Beryllium deposits. GSC, Economic geology report, No. 23. pp. 61-62

Reesor, J.E. 1958. Dewar Creek Map-area with special emphasis on the White Creek batholith, British Columbia; Geological survey of Canada, Memoir 292.

Reesor, J.E. 1996. Geology of Kootenay Lake, B.C.; Geological survey of Canada, Map 1864-A.

Rice, H. M. A., 1941. Nelson map area, east half, British Columbia; Geological Survey of Canada, Memoir 228.

Smith, M, and D.A. Brown, 1998. Preliminary report on a Proterozoic (?) stock in the Purcell Supergroup and comparison to the Cretaceous White Creek Batholith, southeastern British Columbia. Geological Fieldwork 1997, Paper 1998-1. 11-1 to 11-7.

AIRBORNE MULTISENSOR GEOPHYSICAL SURVEYS IN THE CENTRAL QUESNEL MINERAL BELT (93A/5, 6, 12)

By M.S. Cathro[1], R.A. Lane[2], R.B.K. Shives[3] and P.M. McCandless[4]

KEYWORDS: Quesnel mineral belt, Quesnel trough, Mount Polley mine, Horsefly, airborne multisensor geophysical survey, radiometric, gamma ray, magnetic, Nicola Group, alkalic porphyry, skarn, placer, propylite, copper, gold.

INTRODUCTION

Two helicopter-borne multisensor (gamma ray spectrometer, magnetometer) geophysical surveys were flown in the Horsefly and Mount Polley mine areas of the central Quesnel mineral belt in September 2003 (Figure 1). Results of both surveys will be released to the public in Spring 2004.

---

[1] *Mining Operations Branch, BC Ministry of Energy and Mines, Kamloops*

[2] *Mining Operations Branch, BC Ministry of Energy and Mines, Prince George*

[3] *Radiation Geophysics Section, Geological Survey of Canada, Ottawa*

[4] *Imperial Metals Corporation, Vancouver*

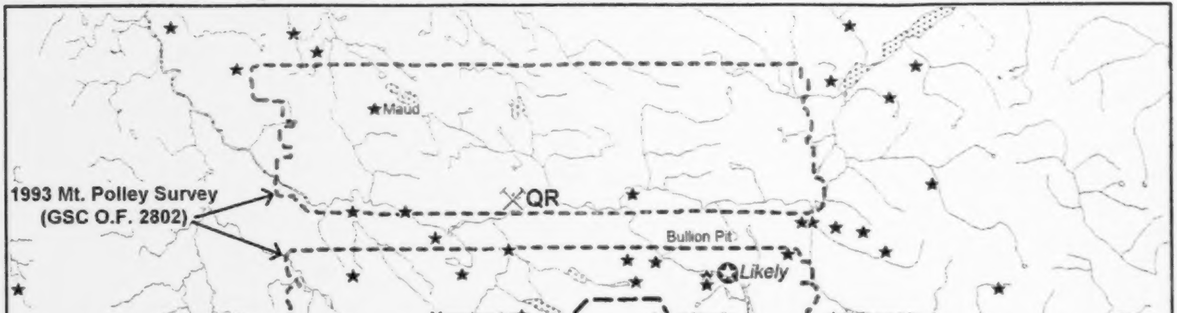
Maud
QR
1993 Mt. Polley Survey
(GSC O.F. 2802)
Bullion Pit
Likely
Moorehead
Lloyd-Nordic
Spanish Mtn
NE (Wishbone)
2003 Mt. Polley Survey
Mt Polley
Bayshore
Quesnel Lake
Gibraltar
Wet
Redgold
2003 Horsefly Survey
McLeese Lake
Kwun L
Beekeeper
Pine
Horsefly
Moffat
Woodjam
Multisensor Geophysical Surveys in the Central Quesnel Belt
Mine
MINFILE Occurrence
Town
N
0
5
10
Kilometers

Figure 1. Location of multisensor geophysical surveys flown in the Mount Polley and Horsefly areas in 1993 and 2003.

Fugro Airborne Surveys carried out the work under contract to the Geological Survey of Canada (GSC) and Imperial Metals Corporation. The BC Ministry of Energy and Mines conceived of the project and provided overall management. Funding was provided by the Rocks to Riches program of the BC and Yukon Chamber of Mines and Imperial Metals Corporation.

The overall purpose of the surveys is to provide modern high-definition radiometric and magnetic data that can be used in the assessment and development of targets for mineral exploration, and to assist in future bedrock and surficial mapping studies. These new helicopter-borne surveys partially overlap and extend southeasterly from a similar survey, flown in 1993 (Shives *et al.*, 1995) using the GSC Skyvan fixed wing aircraft. That survey covered portions of NTS map sheets 93A/12 and 93B/9 including the Mount Polley deposits (prior to start of mining operations).

The 2003 Horsefly survey covered an area of 801 square km and was flown at an average 500-metre line spacing (NE-SW lines) and 135-metre terrain clearance, for a total of 1843 line-km including control lines. The 2003 Mount Polley survey covered 67 square km at an average 100-metre line spacing (E-W lines) and 60-metre clearance, for a total of 738 line-km including control lines (Figure 1).

Rationale

The Horsefly area was chosen because it is highly prospective for alkalic porphyry copper-gold deposits like Mount Polley and Afton, which respond well to radiometric and magnetic survey techniques. The area has excellent access and infrastructure, but only had about 15-20% claim coverage at the time of the survey. The area also has potential for gold and base-metal skarn, calc-alkalic copper-molybdenum porphyry, gold-silver vein, placer gold and a variety of other deposit types (Table 1). Topography is subdued and the extensive cover of glacial till, plateau volcanics and timber has hampered past exploration.

The Geological Survey of Canada has had good results in previous multisensor surveys over similar BC porphyry deposits (e.g. Afton and Mt. Milligan). The radiometric (K and eTh/K ratio) and magnetic (total field and calculated vertical gradient) maps are particularly useful in identifying potassic alteration and magnetite enrichment/depletion zones associated with these copper-gold deposits, and in mapping bedrock lithologies and structures.

Interestingly, the Mount Polley porphyry copper-gold deposit was discovered in 1964 by follow-up prospecting "*at the site of a prominent aeromagnetic anomaly indicated by newly published federal-provincial surveys*" (C.J. Hodgson, R.J. Bailes, & R.S. Verzosa, 1975, CIM Special Volume 15, page 388). It is hoped that by utilizing newer technology, the current surveys could lead to new discoveries in the Quesnel mineral belt.

Project Area Description

The Horsefly area is part of the Cariboo Plateau, an area of relatively gentle topography with low hills and broad valleys. Elevations range from about 800 to 1200 m. Quesnel and Horsefly lakes dominate the landscape to the east and numerous other small lakes and ponds occur throughout the area. Larger drainages are the Cariboo, Quesnel and Horsefly rivers. The small communities of Horsefly and Likely in the area, and the nearest large town is Williams Lake, some 50 km to the southwest. An extensive network of paved highways and gravel logging roads provides excellent access.

Regional Geology, Exploration History and Mineral Potential

Panteleyev *et al.* published an excellent summary of the bedrock geology and mineral deposits of the central Quesnel trough in 1996, and much of the following is taken from that work. The belt is underlain by the Late Triassic-Early Jurassic Nicola volcano-plutonic island arc assemblage, part of the Quesnel Terrane. It is comprised of mafic to intermediate volcanic, volcaniclastic and lesser sedimentary rocks that are intruded by partly coeval Early Jurassic alkalic diorite, monzonite and syenite intrusions. Less common are calc-alkalic intrusions of Early Jurassic and Cretaceous age. Jurassic sedimentary rocks and Permo-Triassic oceanic rocks of the Cache Creek Terrane occur to the west, while Triassic "black clastics" and older metasediments occur to the east. The Nicola volcanic rocks are overlain in places by Eocene volcanics and sediments, Miocene plateau basalts and locally extensive glaciofluvial deposits.

The area has a long history of mining and exploration. Placer mining began on the Horsefly and Quesnel Rivers during the Cariboo gold rush in about 1860. Several large placer operations were active in the early days, including the famous Bullion Pit near Likely. A variety of lode metal deposits are also known (Table 1) and several deposits have been mined in the past. Three dormant, open-pit metal mines are situated close to the survey area: Gibraltar (Cu-Mo), Mount Polley (Cu-Au) and QR (Au). Each of these mine/mill complexes is currently on care and maintenance awaiting higher metal prices and/or discovery of new or higher-grade deposits. Recent exploration activity in this belt has focused on bulk tonnage alkalic porphyry and skarn deposits (e.g. Mount Polley, Lloyd-Nordik, QR, Cariboo, Redgold and Woodjam). Imperial Metals made a significant new discovery of porphyry Cu-Au mineralization on the Mt. Polley property in September 2003. Called the Wishbone or Northeast zone, the deposit occurs close to surface and appears to have much higher copper grades than ore previously mined.

TABLE 1
POTENTIAL DEPOSIT TYPES IN THE MT. POLLEY - HORSEFLY AREA

Deposit Type	Examples
Alkalic porphyry Cu-Au-Ag-Pd	Mount Polley mine, Wishbone (Northeast), Lloyd Nordic, Redgold, Woodjam, Pine, Beekeeper, etc.
Propylite (skarn) Au-Ag-Cu	QR mine
Mesothermal Au veins	Spanish Mountain, Frasergold
Calc-alkalic porphyry Cu-Mo-Au-Ag	Wet, Boss Mountain, Gibraltar
Volcanic disseminated Cu	Red, Moffat, B, Moorehead, Mary
Polymetallic veins	Mandy
Epithermal As-Sb-Ag (Au?)	Minor occurrences
Cu-Au Stockwork in Eocene volcanics	Megabucks
Cu-Au magnetite skarn	Spout Lake, Deer Lake, Craigmont
Placer Au	Bullion pit, Quesnel River, Miocene, Horsefly, Antoine Creek

Methods

The two surveys were completed between September 23, 2003 and September 29, 2003, using an Aerospatiale AS350 helicopter (Photo 1). The flight path was recovered using a post-flight differential Global Positioning System. A vertically mounted video camera was used for verification of the flight path. The traverse lines were flown at an average spacing of 500 m (100 m for Polley) with control lines flown at 4000 m intervals (2000 m). Helicopter flight height was maintained at an average ground clearance of 135 m (60 m).

The gamma ray spectrometry data were recorded at a 1.0 second sample rate using a 256-channel Exploranium GR820 spectrometry system with 33.6 liters of downward-looking and 4.2 liters of upward-looking sodium iodide detectors. The aeromagnetic data were recorded at a 0.1 second sample rate using a 0.01 nT split-beam line cesium vapour magnetometer suspended below the helicopter.

Results

Final results will be presented in GSC and BCGS Open File formats in Spring 2004. The Open Files will consist of digital data (Geosoft compatible line and

Photo 1. Fugro Airborne Surveys helicopter and magnetometer bird in the Likely area, September 2003.

gridded formats) and colour interval maps at 1:20,000 and 1:50,000 scales, for 10 layers (listed below). Map images will be presented as georeferenced .tif files for easy import into GIS programs and as .pdf files with marginal notes, legend and topographic base information. Data will be made available for purchase as digital line or grid data on CD-ROM (from GSC only), in paper format as print-on-demand colour maps from GSC and BCGS and as web-viewable, downloadable images in PDF format, at no cost, from BCGS and GSC-NATGAM websites.

Analogue and digital products will include data for eight radiometric and two magnetic parameters:

Ternary radioelement map (K, eU, eTh)
Natural air absorbed dose rate (ADRN, nGy/h)
Potassium (K, %)
equivalent Uranium (eU, ppm)
equivalent Thorium (eTh, ppm)
equivalent Uranium/equivalent Thorium (eU/eTh)
equivalent Uranium/Potassium (eU/K, ppm/%)
equivalent Thorium/Potassium (eTh/K, ppm/%)
Magnetic total field (nT)
Magnetic vertical gradient (computed, nT/m)

CONCLUSIONS

Multisensor geophysical data will be released in Spring 2004 for two surveys in the central Quesnel mineral belt. This new data should assist in exploration for alkalic porphyry and other deposit types in this highly prospective area.

REFERENCES

Panteleyev, A., Bailey, Bloodgood, M.A. and Hancock, K.D. (1996): Geology and Mineral Deposits of the Quesnel River - Horsefly Map Area, Central Quesnel Trough, British Columbia; *B.C. Ministry of Employment and Investment*, Bulletin 97, 156 pages.

Shives, R.B.K., Holman, P.B., Rebolledo, L., Hetu, R.J. (1995): Airborne geophysical survey, Mount Polley area, B.C.; *Geological Survey of Canada*, Open File 2802, 82 pages.

Sulfur Isotopic Zonation in Alkalic Porphyry Cu-Au Systems: Applications to Mineral Exploration in British Columbia

By Cari L. Deyell Shane Ebert and Richard M. Tosdal

KEYWORDS: Alkalic porphyry Cu-Au, sulfur isotopes

Alkalic Au-Cu porphyry deposits are associated with alkalic or high-K calc-alkalic igneous rocks. The deposits also have distinctive alteration zones, including sodic and calc-potassic assemblages. These deposits occur in only a few mineral provinces worldwide and some of the best-known examples are from British Columbia (e.g., Galore Creek, Mt. Polley, Afton/Ajax, Copper Mountain). The Lachlan Fold Belt of New South Wales, Australia is the second largest alkalic porphyry district (e.g., Cadia, Goonumbla) and other isolated alkalic systems are known from the Philippines (Dinkidi), Greece (Skouries), Colorado (Allard Stock) and Mongolia (Oyu Tolgoi).
Alkalic porphyry deposits are of increasing economic significance and represent some of the world's highest-grade porphyry gold resources (e.g., Cadia, Australia). In B.C., the largest alkalic porphyry systems (Copper Mountain, Mount Milligan, and Galore Creek) have a combined resource of over 900 Mt (Lang et al., 1995), and new discoveries at Afton and Lorraine may significantly add to this figure. These deposits are difficult exploration targets, however, since high-grade deposits are associated with small volume pipe-like intrusions that may have areal extents of only a few hundred square meters (e.g., Wilson et al., 2002). The alkalic systems have no associated advanced argillic alteration assemblages, and phyllic alteration is typically restricted to deep-penetrating fault zones. Supergene enrichment zones will therefore be poorly developed at best due to the low sulfide contents of the alteration assemblages (Cooke et al., 2002). The lack of extensive peripheral hypogene alteration assemblages makes identifying the focus for fluid flow difficult when more than several hundred meters away from the mineralized porphyry centre. Effective exploration therefore requires the means to recognize subtle alteration zones or geochemical halos that highlight proximity to an alkaline intrusive centre.

Preliminary research into the alkalic porphyry deposits of Australia has suggested that systematic vertical and lateral sulfur isotopic zonation may occur around several mineralized porphyry complexes (e.g., Goonumbla and Cadia: Lickfold, 2001; Wilson, 2003). Data collected by the Centre for Ore Deposit Research (CODES) at the University of Tasmania indicates sulfide compositions in these systems are between –2 and –10‰. The most negative values lie towards the top of the mineralized monzonite pipes, with a transition to near zero values with distance upwards or outwards from the pipe (Lickfold, 2001; Wilson, 2003). The initial studies lead to the obvious question of whether sulfur isotopes provide the "magic-

---

Cari L. Deyell < cdeyell@utas.edu.au> University of Tasmania, Hobart, Tasmania, Australia

Shane Ebert sebert@eos.ubc.ca and Richard M. Tosdal < rtosdal@eos.ubc.ca> The University of British Columbia, Vancouver, British Columbia

bullet" for exploration in these system. Before sulfur isotope mapping can be widely applied however, it must be established whether the zonation is a phenomenon common to these deposits on a worldwide basis.

The current study aims to test whether systematic sulfur-isotopic zonation of sulfide and sulfate minerals characterizes alkalic porphyry deposits in British Columbia. If this zonation proves to be a robust and predictable phenomena, then it could be a highly valuable tool in the exploration for new mineral deposits (or extensions to known ore bodies) in the alkalic porphyry provinces of British Columbia.

Research in this study is focused on several sites including Galore Creek, Afton, Lorraine, Mt. Polley, and Red Chris. Over 250 samples from these deposits will be analyzed by conventional sulfur isotope methods at the University of Tasmania, Australia. Preliminary results from two of these sites (Afton and Galore Creek) indicate a wide range of sulfide □^{34}S values from –11.3 to +16.9‰. All results will be reported to the Rocks to Riches program and, if a consistent sulfur isotope zonation is recognized, the origin and significance of this zonation and its applicability to other deposits will be tested by further study.

References

Cooke, D.R., Wilson, A.J., Lickfold, V., and Crawford, A.J. (2002): The alkalic Au-Cu porphyry province of NSW; AusIMM 2002 Annual Conference, Auckland, New Zealand, pages 197-202.

Lang, J. R., Stanley, F.R., Thompson, J. F. H., and Dunne, K. F. (1995): Na-K-Ca magmatic-hydrothermal alteration in alkalic porphyry Cu-Au deposits, British Columbia; Mineralogical Association of Canada, Short Course vol. 23, pages 339-366.

Lickfold, V. (2001): Volatile evolution and intrusive history at Goonumbla, central western NSW; Unpublished Ph.D. thesis, University of Tasmania, Australia.

Wilson, A. (2003): The genesis and exploration context of porphyry copper-gold deposits in the Cadia district, NS;. Unpublished Ph.D. thesis, University of Tasmania, Australia.

Wilson, A., Cooke, D.R., and Thompson, J. F. H. (2002): Alkalic and high-K calc-alkalic porphyry Au-Cu deposits; CODES Special Publication 4, pages 51-55.

ST. MARY MAP-SHEET, PURCELL SUPERGROUP, SOUTHEASTERN BRITISH COLUMBIA

By Trygve Höy[1], Wayne Jackaman[2], David Terry[3] and Brian Grant[3]

KEYWORDS: *Regional Geology, Middle Proterozoic, Purcell Supergroup, Aldridge Formation, Sullivan deposit, sedex deposits, lead-zinc-silver veins.*

INTRODUCTION

The St. Mary sheet (NTS 82F/09) in the Purcell Mountains of southeastern British Columbia (Figure 1) is underlain mainly by the Middle Proterozoic Purcell Supergroup. The Sullivan deposit, a world-class sedex deposit, is located in the eastern part of the map sheet. It closed in 2001 after having mined more than 160 million tonnes of lead-zinc-silver ore. Exploration for sedex deposits continues in the Purcell Supergroup, with at least one company actively drilling targets in the St. Mary map area.

The St. Mary area was mapped initially by Leech (1957). The geology of portions of the sheet have been mapped by Reesor (1958), Höy (1984a) and by a number of exploration companies, including Cominco Ltd., Rio Algom and Kennecott. This project has compiled and reinterpreted this data, as well as data released in numerous assessment reports. Field checks of selected areas and discussions with geologists working in the area have added to the base. The geology of the area will be released as a 1:50 000-scale map in both digital and hardcopy format in early 2004. The map sheet is contiguous with Geoscience Map 1998-3 (Brown, 1998) and overlaps the area of the detailed government airborne geophysical surveys flown over in the late 1990s. Also included in the release is a summary of existing regional geochemical data; these data, including the geophysical surveys, will help in the development of a metallogenic overview that will direct regional exploration

A second component of the project involves updating all mineral occurrences (approximately 30) in St. Mary map sheet as well as adding new occurrence information.

This project is financially supported by the BC and Yukon Chamber of Mines, Rocks to Riches geoscience program 2003.

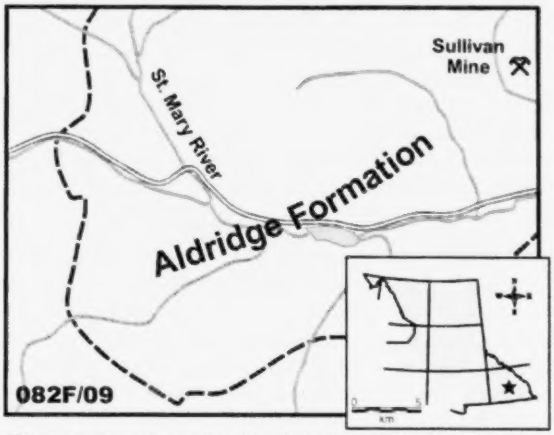

Figure 1: Location and regional geology of the St. Mary map sheet (082F/09).

REGIONAL GEOLOGY

Stratigraphy

The St. Mary map area is underlain mainly by Middle Proterozoic metasedimentary rocks of Purcell Supergroup. The Purcell Supergroup and its correlative in the United States, the Belt Supergroup, is generally considered to represent the infilling of an intracratonic rift (Hoffman, 1991; and summaries in Höy *et al.*, 2001 and Lydon, 2001). The basal part of the succession, the Aldridge Formation records the early synrift fill and overlying Creston, Kitchener and younger strata, the rift cover succession.

The Aldridge Formation has been divided into three members. The lower Aldridge, generally exposed throughout the central part of the St. Mary map sheet, comprises mainly thin to medium-bedded, pyrrhotite-rich, distal argillaceous turbidites. A prominent quartzitic turbidite sequence, several hundred metres thick, is part of the lower Aldridge stratigraphy in the Sullivan mine area and can be traced westward throughout a large part of the St. Mary map sheet. The Middle Aldridge comprises up to 2400 metres of medium-bedded quartzitic turbidites with prominent intervals of laminated marker siltstones. The upper Aldridge comprises approximately 300 metres of thin-bedded to laminated siltstone and argillite deposited on a shallowing basin plain.

---

[1] 2450 Dixon Road, Sooke BC, V0S 1N0

[2] 3011 Felderhof Road, Sooke BC, V0S 1N0

[3] BC Ministry of Energy and Mines

The Creston Formation conformably overlies the Aldridge Formation in the western part of the map area. It comprises green to grey siltstone, argillite and quartzite, with numerous sedimentary structures indicative of shallow water deposition. It is overlain by the Kitchener Formation, metasedimentary rock that is characterized by the presence of carbonate. The Kitchener Formation comprises mainly calcareous and dolomitic siltstone and argillite, some buff-weathering impure dolomite and dark impure limestone. Overlying, mainly metasedimentary rocks, and a thin volcanic succession, are only exposed in the very southeast corner of the St. Mary map sheet.

Numerous mafic sills, the Moyie intrusions, form a large part of the lower and middle Aldridge stratigraphic package. They range from gabbro to diorite in composition and have been shown to be intruded, at least in part, into wet, unconsolidated sediments (Höy, 1984b; Höy *et al.*, 2001). Hence, they record a magmatic event during deposition of the Aldridge Formation and provide supporting evidence for a syn-rift model for the basal part of the Purcell Supergroup. A concordant U-Pb zircon date of 1467+/-3 Ma for a sill located farther south (Anderson and Davis, 1995) provides a minimum age for early subsidence of the Purcell basin and for synsedimentary deposits such as Sullivan.

Intrusive Rocks and Tectonism

Several intrusive bodies occur in the St. Mary sheet area. These include the Middle Proterozoic Hellroaring Creek stock and several smaller related intrusion, and Middle Cretaceous intrusions such as the Hall Lake stock.

The Hellroaring Creek stock is a small pegmatitic body exposed in the St. Mary valley south of St. Mary Lake. It has been assessed for its beryllium content and, more recently, for its potential for semiprecious beryls (Legun, 2004). The stock, dated at *ca.* 1360 Ma (J. Mortenson, unpublished data) is interpreted to cut both foliation and folds in the Aldridge Formation (Leech, 1960), and provided some of the evidence for the existence of a Middle Proterozoic compressional event referred to as the East Kootenay orogeny (McMechan and Price, 1982). More recently, however, this event has been interpreted to result from crustal extension associated with deep seated magmatism (Doughty and Chamberlain, 1996).

The Hall Lake stock is a small Middle Cretaceous granitic intrusion near the western edge of the map-area. It cuts the Hall Lake thrust fault and it, and a similar aged intrusion that cuts the St. Mary fault farther east, provide a minimum age for Mid Cretaceous thrust faulting in the Purcell Mountains.

The southern edge of the White Creek batholith is exposed north of the map-area. It is a zoned intrusion with a granodiorite border phases and quartz monzonite central phases (Reesor, 1958).

Mineral Deposits and Exploration

The Sullivan mine at Kimberley is a classical example of a sedex type of deposit. It was the focus of a collaborative research project involving industry, government agencies and universities that culminated in 2001 with the publication of a comprehensive volume on the deposit and its setting (Lydon *et al.*, 2001). The geology of the Sullivan deposit is dealt with in numerous papers in the "Sullivan volume" and will only be reviewed briefly here.

The Sullivan deposit, largely mined out and closed in 2001, had an initial reserve of approximately 160 million tonnes containing 6.5% Pb, 5.6% Zn, 67 g/tonne silver and 25.9% Fe. The deposit occurred at the transition of the lower and middle Aldridge. It comprised a broadly stratiform, upwardly concave lens, which covered an area of 1.6 x 2.0 km, and consisted mainly of pyrrhotite, sphalerite, galena and lesser pyrite. The western part of the deposit was part of an extensive vent complex, and the eastern part comprised an apron of generally well-laminated sulphides. Several other smaller sedex deposits occurred in the immediate vicinity of the Sullivan deposit, within a south-trending, disrupted geothermal field referred to as the Sullivan-North Star graben.

The lower to middle Aldridge transition, commonly referred to as the Sullivan horizon, has been the focus of considerable exploration in the St. Mary sheet and elsewhere throughout the Purcell basin. At Sullivan, the horizon is marked by an anomalous thickness of sedimentary fragmentals, interpreted as mud volcano deposition, and by cross-cutting discordant fragmentals that appear to record movement along growth faults. Farther west in the St. Mary map sheet, exposures of the Sullivan horizon are also marked by a thick, fairly coarse sedimentary fragmental unit; here the horizon has been tested by several deep drill holes. Exploration continues along this horizon, with Klondike Gold Corp. drilling or extending several holes to the Sullivan horizon in late 2003.

Other deposit types in the St. Mary map sheet include mainly polymetallic vein occurrences. Many of these are considered important as they may target areas that have the potential for discovery of sedex deposits; several occur in the vicinity of the Sullivan deposit.

As noted above, exploration for beryllium and semiprecious gemstones been focused on the Hellroaring Creek stock.

SUMMARY

The geology of the St. Mary map sheet, despite containing the Sullivan sedex deposit, has not been updated since the mid 1950s (Leech, 1957). The updated 1:50 000-scale geological map, scheduled for release at Roundup 2004, summarizes the results of approximately 50 years of exploration and mapping in the area, mainly by exploration companies but also by provincial and federal government surveys. The data is presented in digital and hardcopy format, on a composite 1:50 000-scale trim base. It includes a compilation of all publicly available geologic maps, RGS data, and exploration data such as drill hole locations. The accompanying BC MINFILE data, scheduled for release late in April, 2004, will update the geology of known mineral occurrences in the map area.

ACKNOWLEDGMENTS

The authors gratefully acknowledge the financial support and encouragement received from the BC and Yukon Chamber of Mines, Rocks to Riches geoscience program 2003.

REFERENCES

Anderson, H. E. and Davis, D.W. (1995): U-Pb geochronology of the Moyie sills, Purcell Supergroup, southeastern British Columbia: implications for the Mesoproterozoic geological history of the Purcell (Belt) basin; *Canadian Journal of Earth Sciences*, volume 32, pages 1180-1193.

Brown, R.L. (1998): Geological compilation of the Grassy Mountain (east half) and Moyie Lake (west half) map areas, southeastern British Columbia; *B.C. Ministry of Energy and Mines*, Geoscience Map 1998-3.

Doughty, P.T. and Chamberlain, K.R. (1996): Salmon River arch revisited: new evidence for 1370 Ma rifting near the of the deposition in the Middle Proterozoic Belt basin; *Canadian Journal of Earth Sciences*, volume 33, pages 1037-1052.

Hoffman, P. E. (1991): Did the breakout of Laurentia turn Gondwanaland inside out?; *Science*, volume 252, pages1409-1412.

Höy, T. (1984a): Geology of the Cranbrook sheet and Sullivan mine area; *B.C. Ministry of Energy, Mines and Petroleum Resources*, Preliminary map 54.

Höy, T. (1984b): The age, chemistry and tectonic setting of the Middle Proterozoic Moyie sills, Purcell Supergroup, southeastern British Columbia; *Canadian Journal of Earth Sciences*, volume 29, pages 2305-2317.

Höy, T, Anderson, D., Turner, R.J.W. and Leitch, C.H.B. (2001); Tectonic, magmatic and metallogenic history of the early synrift phase of the Purcell basin, southeastern British Columbia; *in* The Geological Environment of the Sullivan Deposit, British Columbia; J.W. Lydon, T. Hoy, J.F. Slack and M. Knapp, Editors, pages 33-60.

Leech, G.B. (1957): St. Mary Lake, Kootenay District, British Columbia; *Geological Survey of Canada*, Map 15-1957.

Leech, G.B. (1960): Geology, Fernie (west half), Kootenay District, British Columbia; *Geological Survey of Canada*, Map 11-960.

Legun, A. (2004): The potential for emeralds in British Columbia – a preliminary review; *in* Geological Fieldwork 2003, *B.C. Ministry of Energy and Mines*, Open File 2004-1 (In Press).

Lydon, J.W. (2001): A synopsis of the current understanding of the geological environment of the Sullivan deposit; *in* The Geological Environment of the Sullivan Deposit, British Columbia; J.W. Lydon, T. Hoy, J.F. Slack and M. Knapp, Editors, pages 12-31.

Lydon, J.W., Hoy, T., Slack, J.F. and Knapp, M.E. (2001): The geological environment of the Sullivan deposit, British Columbia; Geological Association of Canada, Mineral Deposit Division, Special Publication 1.

McMechan, M.E. and Price, R.A. (1982): Superimposed low grade metamorphism in the Mount Fisher area, southeastern British Columbia – implications for the east Kootenay Orogeny; *Canadian Journal of Earth Sciences*, volume 19, pages 476-489.

Reesor, J.E. (1958): Dewar Creek map area with special emphasis on the White Creek batholith; *Geological Survey of Canada*, Memoir 292, 78 pages.

GOLD EXPLORATION, ROSSLAND-NELSON AREA, SOUTHEASTERN B.C.

By Wayne Jackaman[1] and Trygve Höy[2]

KEYWORDS: Regional geology, metallogeny, Early Jurassic, Rossland Group, Elise Formation, Ymir Group, , mineral occurrences, Rossland Camp, stream geochemistry.

INTRODUCTION

Exploration companies have been successful in locating precious and base metal mineralization in Rossland and Ymir group rocks located in the Nelson-Salmo-Rossland areas of southern British Columbia (Figure 1). Recent discoveries have produced a renewed interest in several known prospects as well as considerable new and ongoing claim staking throughout the region.

To provide assistance to these and future exploration efforts, a geological and metallogenic map of the Rossland and Ymir Group rocks is being prepared as part of the Rocks to Riches program. The work will include a compilation of available geodata, including regional and detailed geological maps, mineral occurrence information and regional geochemical data. This report provides a summary of the project.

REGIONAL GEOLOGY

The study area lies within the Omineca Belt (Figure 2). North American terrane rocks include the Middle Proterozoic Windermere Supergroup and overlying Lower Cambrian Quartzite Range and Reno formations located in the southeast corner of the map area. To the west, these are structurally overlain by the north-trending Kootenay terrane consisting mainly of the Lower Paleozoic Lardeau Group and Active and Laib formations.

The Slide Mountain terrane is represented in the map-area by Upper Paleozoic rocks of the Milford Group. Early Jurassic Rossland and Ymir group rocks of Quesnellia comprise the thickest stratigraphic package, forming a broad northeast-trending belt in the central portion of the map area.

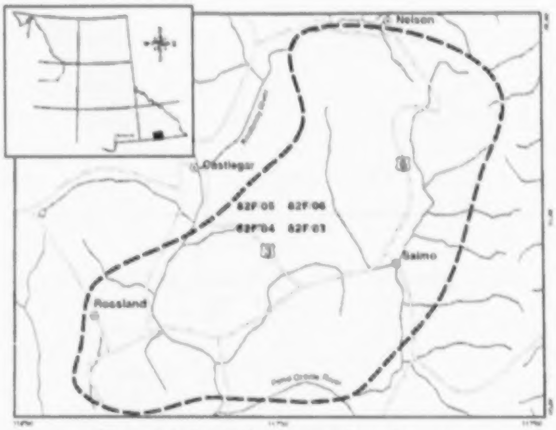

Figure 1: Location map of study area.

Much of the map area is cut by the Middle to Late Jurassic Nelson and related intrusions, including the important Rossland monzonite. Other intrusive suites include Middle Cretaceous granitic rocks and several plutonic suites of Tertiary age. The Valhalla Complex occupies the northwest part of the map sheet. It contains mainly high-grade metamorphic rocks of uncertain age and several orthogneiss bodies of Cretaceous to Tertiary age.

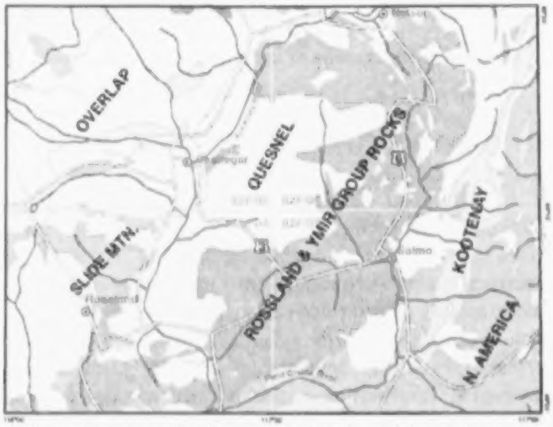

Figure 2: Generalized geological setting of the study area.

MINERAL OCCURRENCES

The area contains more than 380 known mineral occurrences and includes four historically important mining camps or areas (Figure 3). The Sheep Creek camp (Mathews, 1953) ranks sixth in the province in terms of total lode gold produced. The production came from "mesothermal" quartz veins mainly hosted by the Quartzite Range Formation. The Salmo belt in the southern Kootenay Arc (Fyles and Hewlett, 1959) contains carbonate-hosted lead-zinc deposits. The Rossland camp (Fyles, 1964; H y and Dunne, 2001) ranks as the second largest gold producing camp in British Columbia. Gold-copper and polymetallic veins occur in the Elise Formation of the Rossland Group and in the Rossland stock. The deposits of the Ymir-Nelson area have produced more than 16,000 kg of gold and 190,000 kg of silver primarily from vein deposits in the Ymir Group and Elise Formation. Mineral deposit types include Au-Ag-Cu-Pb-Zn veins, porphyry molybdenum-copper deposits, shear-hosted gold occurrences and skarns.

---

[1] 3011 Felderhof Road, Sooke BC, V0S 1N0

[2] 2450 Dixon Road, Sooke BC, V0S 1N0

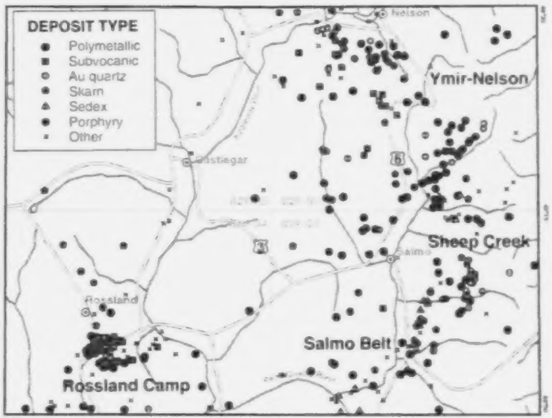

Figure 3: Distribution of known mineral occurrences.

REGIONAL GEOCHEMISTRY

A National Geochemical Reconnaissance (NGR) stream sediment and water survey was conducted in the Nelson (NTS 82F) mapsheet during 1977. Archived sediment pulps were re-analyzed in 1990 by epi-thermal instrumental neutron activation analysis (INAA). This new data along with original survey results were released in 1991 (Matysek *et al*, 1991). Published analytical information includes base metals, precious metals, pathfinders and rare earth elements. A total of 354 NGR sample sites are found within the southwest corner of the Nelson 1:250 000 map sheet (Figure 4).

To help understand the geochemical signature of the various deposit types, a number of stream sediment samples were recently collected and analyzed by inductively coupled plasma mas spectrometry (ICP/MS). This data will give additional information regarding anomaly recognition and will also provide a link between original NGR results and analytical methods currently being used by the exploration sector.

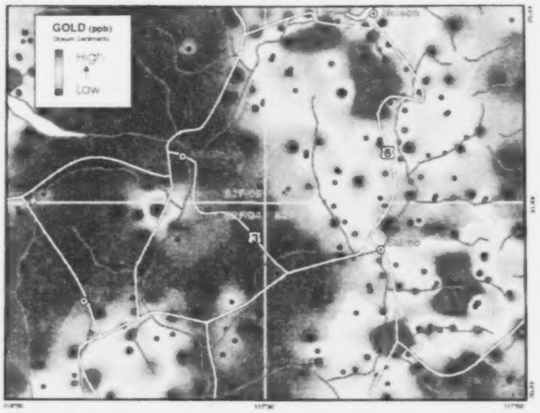

Figure 4: Distribution of NGR sample sites overlaying gridded INAA gold data.

Figure 5 compares original NGR results with new ICPMS data for samples collected downstream from the porphyry molybdenum showing called Fresno (MINFILE 082FSW251). The results are similar for the listed metals with the exception of gold and silver that show an enhanced concentration for the sample material analyzed by ICP/MS. This pattern remains consistent for other data comparisons.

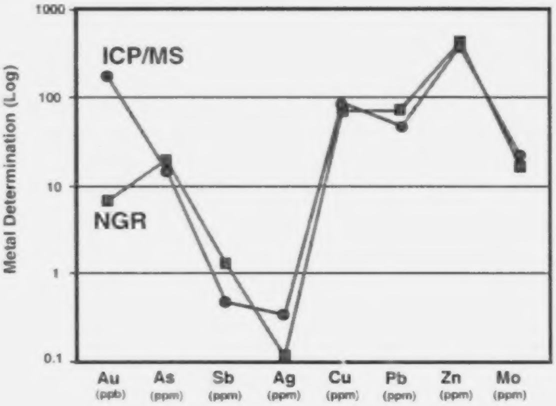

Figure 5: Comparison of original NGR data with new ICP/MS results.

SUMMARY

The project involves a metallogenic evaluation of the Rossland and Ymir Group rocks. Various geodata, including regional and detailed geological mapping, existing regional geochemical survey data, and mineral occurrence information will be integrated to produce geological and metallogenic map(s) (1:50 000 scale) that will be suitable for directing and focusing regional exploration programs.

The full colour digital and hard copy maps (base geology, mineral occurrences and regional geochemical data) plus accompanying metallogenic report are scheduled for release at the 2004 Roundup conference.

SELECTED BIBLIOGRAPHY

Andrew, K.P.E., Hoy, T. and Simony, P. (1991): Geology of the Trail map area, (82F/3,4,5,6); *B.C. Ministry of Energy, Mines and Petroleum Resources*, Open File 1991-16.

Fyles, J.T. (1984): Geological setting of the Rossland Mining Camp (82F/4), *B.C. Ministry of Energy, Mines and Petroleum Resources*, Bulletin 74.

Fyles, J.T. and Hewlett, C.G. (1959): Stratigraphy and structure of the Salmo lead-zinc area; *B.C. Department of Mines*, Bulletin 41, 162 pages.

H y, T. and Dunne, K.P.E. (1998): Geological compilation of the Trail map area, Southeastern British Columbia (82F/3,4,5,6), *B.C. Ministry of Energy, Mines and Petroleum Resources*, Geoscience Map 1998-1.

H y, T. and Dunne, K.P.E. 1997): Early Jurassic Rossland Group, southeastern British Columbia; *B.C. Ministry of Energy and Mines*, Bulletin 102.

H y, T. and Dunne, K.P.E. (2001): Metallogeny and mineral deposits of the Nelson-Rossland map area; *B.C. Ministry of Energy and Mines*, Bulletin 109.

Logan, J.M. (2003): Kena Gold Mountain zone, southern British Columbia; *B.C. Ministry of Energy and Mines*, Geological Fieldwork 2002, pages 133-152.

Mathews, W.H. (1953): Geology of the Sheep Creek Camp (82F/3), *B.C. Ministry of Mines*, Bulletin 31.

Matysek, P.F., Jackaman, W., Gravel, J.L., Sibbick, S.J. and Feulgen, S. (1991): British Columbia Regional Geochemical Survey - Nelson (NTS 82F), *B.C. Ministry of Energy, Mines and Petroleum Resources*, RGS 30.

MINFILE 082FSW (1991): *Researched and compiled by:* Jakobsen, D.E., Payie, G.J., Duffet, L.L., Grant, B., Anderson K.P.E. and H y, T.; Trail Mineral Occurrence Map; *B.C. Ministry of Energy, Mines and Petroleum Resources*, Release date: June 1991.

ISKUT RIVER - TELEGRAPH CREEK: NEW EXPLORATION OPPORTUNITIES IN THE BC REGIONAL GEOCHEMICAL DATABASE

By Ray Lett[1] and Wayne Jackaman[2]

KEYWORDS: Regional stream sediment surveys, archival samples, gold, drainage basins, reanalysis.

INTRODUCTION

This project has been supported by funding from the BC and Yukon Chamber of Mines, Rocks to Riches program.

A primary aim of large-scale (typically 1 sample per 12 to 15 km^2) stream sediment surveys is to identify areas of high mineral potential where mining companies and individuals can focus their search for new deposits. The regional geochemical survey (RGS) in British Columbia has covered almost 70% of the province with stream sediment, moss mat sediment, lake sediment, lake water and stream water samples collected at an average density of 1 sample per 13 square kilomteres from over 40 000 sites. Upgrades to the RGS database are made by the addition of information from new surveys and from the analysis of archival samples for additional elements using new or improved analytical methods. Continual interpretation of existing and new data can reveal new exploration targets. For example, recent follow up of a RGS anomaly resulted in the discovery of new mineralization at the Sickel-Griz Au-Ag occurrence in the Toodoggone River area (Stealth Minerals November 6th News Release).

During the past year rising metal prices and the presence of the operating Eskay Creek mine has stimulated mineral exploration activity in the Iskut River area. This area has been the subject of BC Energy and Mines mapping programs during 2003 (Alldrick *et al.*, 2004). Archived stream sediment samples from 930 RGS sites in the western half of the Iskut River and Telegraph Creek NTS map sheets (NTS 104 B and G) bordering the Bowser sedimentary basin were re-analysed by inductively coupled plasma mass spectrometry. The aim of the re-analysis, funded by a grant from the BC and Yukon Chamber of Mines (Rocks to Riches program), was to generate additional multi-element data to help identify new exploration targets. This paper briefly reviews the new RGS data for the Iskut River region and shows the distribution of selected elements. Areas where the sediment geochemistry suggests a higher potential for different types of mineral deposit are identified.

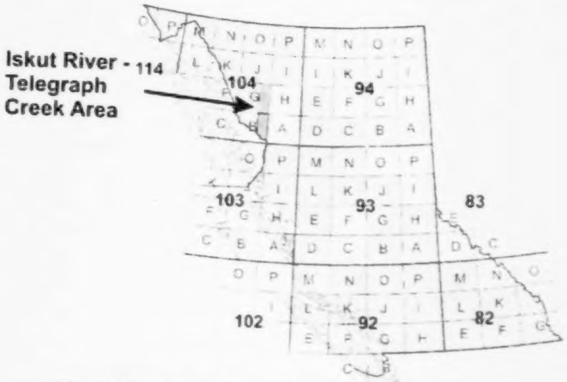

Regional Geochemical Survey Coverage

Figure 1. Archival re-analysis project area

ISKUT RIVER AREA

The Iskut River and Telegraph Creek Map sheets have been covered by regional geochemical surveys in 1987 (Matysek *et al.*, 1988a and b, Day and Matysek, 1989). The archived sediment samples selected for re-analysis are from an area of roughly 8000 square kilometers in these map sheets (Figure 1). Major populations centers in the region are Stewart, Telegraph Creek and Dease Lake (Figure 2).

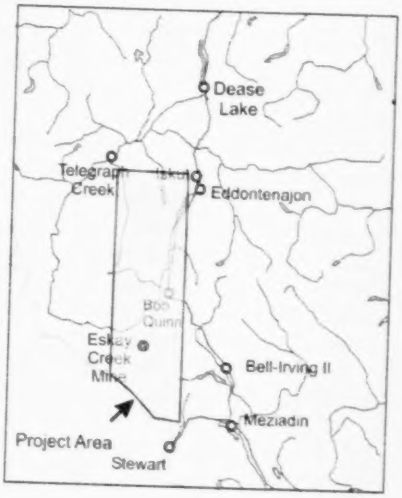

Figure 2. Major centers and roads

---

[1] *British Columbia Ministry of Energy and Mines*

[2] *3011 Felderhof Road, Sooke, BC, V0S 1N0*

The region is crossed by the Tahlan Highlands and Klastiline Plateau and is drained by the Iskut River. Much of the bedrock in this area is concealed beneath ice fields and surficial deposits. Geological units of the Stikine tectonic terrane underlie the eastern part of the Iskut River-Telegraph Creek map sheets. The three most extensive of these units are the Triassic Stuhini Group, the Lower Jurassic Hazelton Group and the Middle Jurassic Bowser Lake Group. The Stuhini Group consists predominantly of volcanoclastic rocks with subordinate mafic to felsic flows. Fosiliferous conglomerate or sandstone at the base of the Hazelton Group rest unconformable on the Stuhini Group. Above the clastic sediments are andesitic to dacitic flows, sills and volcaniclastic rocks. This unit is succeeded by a predominantly felsic volcanic flows, tuffs and breccias with a younger sedimentary strata ranging from sandstone to limestone. The youngest Hazelton Group unit is a bimodal volcanic assemblage with minor sedimentary rocks. Significant precious and base metal mineralization occurs in Stuhini and Hazelton group rocks. Stratigraphically above the Hazelton Group are marine and terrestrial sandstones and conglomerates of the Bowser Lake Group. Neogene volcanic flows of the Mount Edziza Complex partially cover Mesozoic rocks. Intrusive rocks that are related to mineralization range from olivine gabbro (e.g. Nickel Mountain) to granodiorite (e.g. Mitchell Pluton) to feldspar porphyry (Gabrielse and Yorath, 1992).

Within the eastern half of NTS 104 B and G there are a number of past-producing mines and significant advanced prospects in addition to the Eskay Creek gold mine. These are examples of the following BC mineral deposit profiles edited by Lefebure and Höy, (1996):

- **Calc alkaline porphyry (L04).** Mineralization at the Spectrum (MINFILE 104G 036) deposit consists of pyrite, chalcopyrite, pyrrhotite, galena, sphalerite and arsenopyrite in altered Stuhini Group sedimentary and volcanic rocks. The deposit is estimated to contain 504,800 tonnes grading 9.6 g/t Au. East of the Spectrum is the GJ (MINFILE 104G 034) where chalcopyrite and pyrite occur in siliceous sediments of the Stuhini Group and a granodioritic pluton. At the Kerr prospect (MINFILE 104B 191) chalcocite, pyrite, chalcopyrite, copper and gold are disseminated in silicified-sericitized volcanic rocks of the Hazelton Group Unuk River Formation. Reserves are estimated to be 140.8 million tonnes grading 0.36 g/t Au and 0.75% Cu. Pathfinder elements for this deposit type are Cu, Mo, Au and Ag with varying Bi, W, B and Sr levels. There may be a Pb, Zn, Mn, V, Sb, As, Se, Te, Co, Ba, Rb and Hg lithogeochemical halo surrounding the mineralized core zone.
- **Intrusive-related Cu-Ni (M02).** The E and L deposit (MINFILE 104B 006) consists of pyrrhotite, pentlandite and chalcopyrite hosted by the Nickel Mountain olivine gabbro stock. Estimated reserves are 2.9 million tonnes of 0.62 % Cu and 0.8 % Ni with traces of Pd and Pt. Key pathfinders for this deposit type are Cu, Ni, Au, Ag, Pt, Pd and Co.
- **Epithermal and Mesothermal Au-Ag veins (H05, I01).** At the Big Missouri Mine (MINFILE 104B 150) hydrothermally altered Hazelton Group volcanic rocks and granodiorite of the Texas Creek Plutonic suite host high-sulphide base metal-rich Au and low sulphide Au-rich veins. Estimated geological reserves are 1.7 million tonnes grading 2.2 g/t Au. At the Hank prospect (MINFILE 104G 107) pyrite, chalcopyrite, galena and sphalerite occur with carbonate and barite in veins cutting Stuhini Group volcanic rocks. Estimated reserves are 0.5 million tonnes grading 2.2 g/t Au. Pathfinder elements for this deposit type are Au, Ag, Zn, Pb, Cu, As, Sb, Ba, F and Mn with varying Te, Se and Hg.
- **Massive Sulphide – Besshi VMS (G04).** Mineralization at the Granduc Mine (MINFILE 104B 021) consists of massive pyrite, chalcopyrite, pyrrhotite, magnetite, galena, sphalerite, bornite, cobaltite and arsenopyrite in volcanic and sedimentary units of the Hazelton Group Unuk River Formation. Pre-production ore reserves were estimated to be 39.3 million tonnes grading 1.73 % Cu. Pathfinder elements are for this deposit type are Cu, Zn, Ag, Se, Mn and Mg. The Co:Ni ratio is greater the one.
- **Massive Sulphide – Sub aqueous hot-spring (G07, G06).** The most prominent mineralization style at the Eskay Creek mine (MINFILE 104B 008) is massive and disseminated stibnite, pyrite, tetrahedrite, realgar, cinnabar and arsenopyrite in mudstone between rhyolite and basalt units of the Hazelton Group. Reserves are estimated to be over 2.94 million tonnes of ore grading 43.25 g/t Au and 1926 g/t Ag equivalent. Key pathfinder elements are for this deposit type are Au, Ag, Cu, Pb, Zn, Co, As, Sb and Hg.

In addition, there are a number of deposits in the area where there are several styles of mineralization. For example, at the Sulphurets Gold deposit (MINFILE 104B 182) quartz-albite altered Unuk River andesite contains pyrite, chalcopyrite and minor bornite. The highest gold values occur in the most silicified rock. Reserves are estimated to be over 54.8 million tonnes of ore grading 1.02 g/t gold and 0.55 %Cu. This deposit demonstrates both porphyry (L04) and intrusion vein (I02) styles of mineralization. Recent exploration at the Foremore (MINFILE 104G 148) has focused on float boulders of chalcopyrite-sphalerite massive sulphide containing up to 1.5 g/t Au. This occurrence has been tentatively classified as a Kuroko massive sulphide.

TABLE 1.
DETECTION LIMITS FOR ICP/MS AND AAS DETERMINED ELEMENTS

	Units	ICP/MS	AAS
Ag	ppb	2	100
Al	%	0.01	
As	ppm	0.1	1
B	ppm	1	
Ba	ppm	0.5	
Bi	ppm	0.02	
Ca	%	0.01	
Cd	ppm	0.01	0.1
Co	ppm	0.1	2
Cr	ppm	0.5	
Cu	ppm	0.01	2
Fe	%	0.01	0.01
Ga	ppm	0.2	
Hg	ppb	5	5
K	%	0.01	
La	ppm	0.5	
Mg	%	0.01	
Mn	ppm	1	5
Mo	ppm	0.01	1
Na	%	0.001	
Ni	ppm	0.1	2
P	%	0.001	
Pb	ppm	0.01	2
S	%	0.02	
Sb	ppm	0.02	1
Sc	ppm	0.1	
Se	ppm	0.1	
Sr	ppm	0.5	
Te	ppm	0.02	
Th	ppm	0.1	
Ti	%	0.001	
Tl	ppm	0.02	
U	ppm	0.1	
V	ppm	2	5
W	ppm	0.2	
Zn	ppm	0.1	2

Sample Analysis

A total of 945 archive RGS samples (including field duplicates) and 36 samples of 8 different geochemical standards were analysed by leaching a 1 gram of the sample with a HCl-HNO_3-H_2O (2:2:2 v/v) mixture at 95°C for one hour and then measuring the concentration of 37 elements in the diluted solution by inductively coupled plasma mass spectrometry (ICP/MS). ACME laboratories, Vancouver, analysed the archived samples. Detection limits for elements by ICP/MS and also those by the aqua regia digestion-atomic absorption spectrometry (AAS) used in 1987 (Matysek *et al.*, 1988) are shown in Table 1.

The percent relative standard deviation (% RSD) was determined by repeat (typically 4) ICP/MS analyses of the CANMET geochemical standards STSD 1, 2 and 4; LKSD 1,2,3 and 4 and an internal standard. Only Au, B, S, Sb, Te, Th, Ti and W have percent RSD values exceeding 7.5% in 6 of the 8 standards. The lower precision for these elements can be explained by concentrations in a standard close to detection limit. For Au, the large percent RSD values may also reflect the small sample used for analysis and the uneven distribution of Au in the reference material (Clifton *et al.*, 1969).

Results for elements determined by ICP/MS are similar to those obtained by AAS and reported by Matysek *et al.* (1988). For example, the correlation coefficient for As, Ag, Cd, Cu, Co, Mo, Mn, Ni, Pb and Zn by the two techniques is greater than + 0.9; for Fe, Sb and V it is greater that + 0.8 and for Hg the correlation coefficient is +0.76. A scatter plot (Figure 1) for Hg shows that the lower correlation coefficient is due to a small number of samples where there is a large difference in Hg determined by the two methods.

TABLE 2. SUMMARY STATISTICS FOR ELEMENTS BY ICP/MS (*FIRE ASSAY-AAS)

	Units	Mean	95%ile	Max
Ag	ppb	237	798	3931
Al	%	1.61	2.35	5.72
As	ppm	17.0	53.5	446.0
Au*	ppb	28	104	5300
B	ppm	3	7	52
Ba	ppm	177.2	401.3	1528.0
Bi	ppm	0.19	0.62	6.02
Ca	%	0.98	2.59	25.36
Cd	ppm	0.70	2.45	15.28
Co	ppm	18.5	29.9	52.0
Cr	ppm	43.6	98.0	516.4
Cu	ppm	58.42	140.65	909
Fe	%	3.96	5.72	8.89
Ga	ppm	5.4	8.3	16.9
Hg	ppb	111	281	3755
K	%	0.09	0.19	1.17
La	ppm	12.8	33.1	140.9
Mg	%	1.13	1.81	4.41
Mn	ppm	951	1728	10993
Mo	ppm	2.98	10.03	68
Na	%	0.045	0.123	2.169
Ni	ppm	53.4	139.8	349.8
P	%	0.103	0.181	0.305
Pb	ppm	13.38	35.75	300
S	%	0.19	0.67	5.67
Sb	ppm	1.38	4.37	45.61
Sc	ppm	5.5	9.5	13.4
Se	ppm	1.2	3.6	21.0
Sr	ppm	53.5	119.0	503.7
Te	ppm	0.08	0.24	1.93
Th	ppm	1.9	5.0	45.6
Ti	%	0.087	0.281	0.758
Tl	ppm	0.13	0.39	2.33
U	ppm	1.0	3.3	57.4
V	ppm	70	132	219
W	ppm	0.29	0.90	65.70
Zn	ppm	130.6	306.7	1829.9

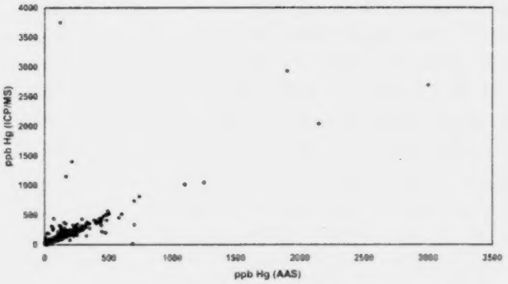

Figure 3. Correlation between Hg by ICP/MS and AAS

The correlation coefficient for Au by ICP/S compared to Au by fire assay-AAS finish reported by Matysek *at al.* (1988) is + 0.14. Again, the poor correlation of Au determinations by the two methods reflects heterogeneous distribution of larger Au grains in the sediment combined with the small sample size used for the ICP/MS analysis. For this reason references to Au in this paper are to values determined by fire assay-AAS finish.

RESULTS SUMMARY

The ICP/MS multi-element element data will be released as Ministry of Energy & Mines Geofile 2003-20 in January 2004. The geochemistry of key ore indicator metals (e.g. Au, Cu, Ag), selected new pathfinder elements (e.g. Se) and the relationship between element associations and different deposit types will be briefly discussed in this paper.

Summary statistics (mean, 95th percentile, maximum value) for the elements determined by ICP/MS and Au by fire assay-AAS are listed in Table 2. The stream sediment geochemistry of selected elements in the eastern half of the Iskut River and Telegraph Creek map sheets is displayed as catchment basin maps in which element variations are shown as colour coded concentrations at the 98th, 95th, 90th, 70th and 50th percentiles. Among the advantages of using catchment basins rather than symbols for displaying RGS sediment geochemistry are that the actual survey coverage and those basins that host actual mineral occurrences are better defined. It is also possible to more realistically estimate the influence of rock type on stream sediment chemistry using the catchment basin as the sediment source area and consequently better define anomaly thresholds based on geology (Matysek and Jackaman, 1996). Figure 4 outlines catchment basins for the RGS archive sample sites and show the location of major mineral deposits and MINFILE mineral occurrences.

Figure 5 shows the distribution of Au by fire assay-AAS finish in the RGS sediments. Most of the RGS sites where Au ranges from 264 ppb to 5300 ppb are south west of Eskay Creek and Sulphurets deposits and to the

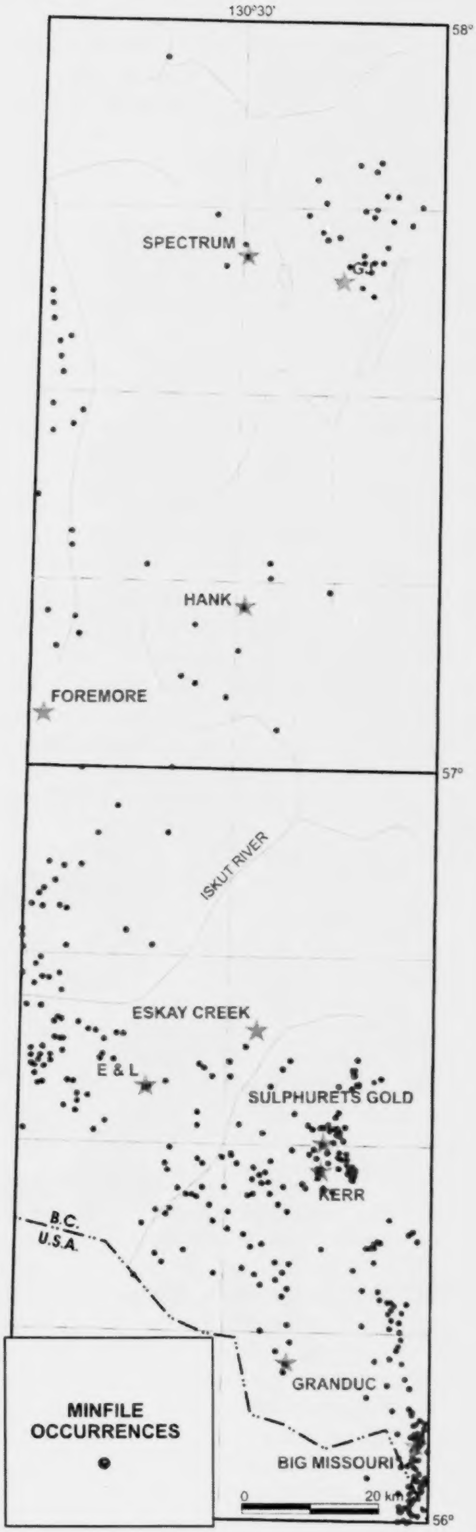

Figure 4. Major deposits and MINFILE occurrences

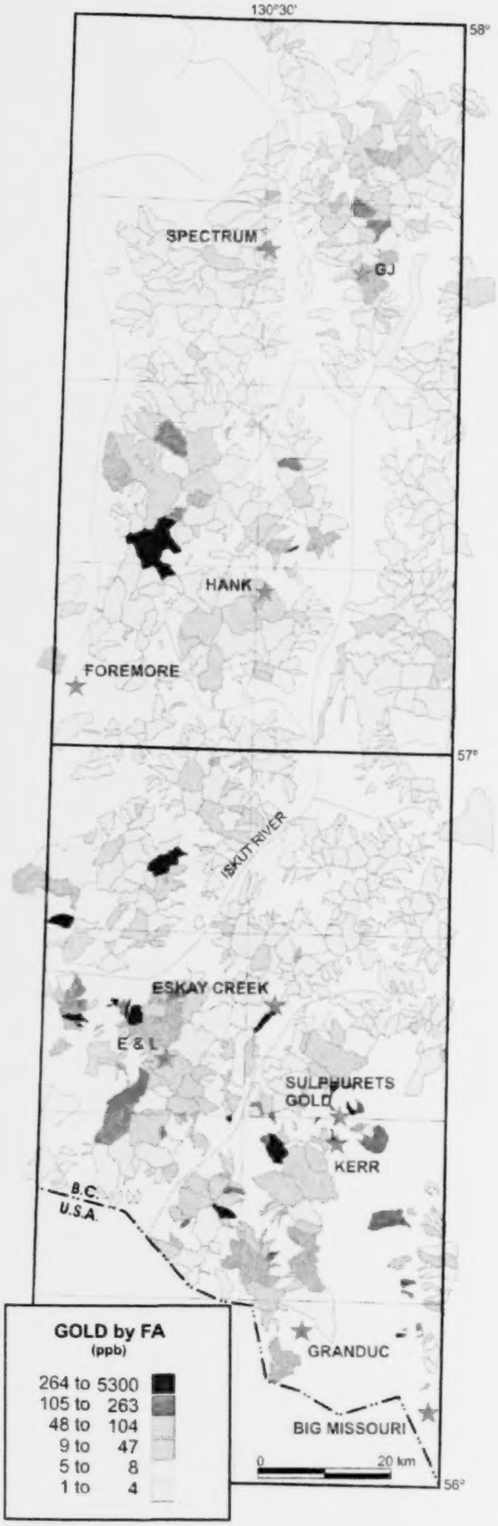
130°30'
58°
SPECTRUM
GJ
HANK
FOREMORE
57°
ISKUT RIVER
ESKAY CREEK
E & L
SULPHURETS
GOLD
KERR
B.C.
U.S.A.
GRANDUC
BIG MISSOURI
0
20 km
56°
GOLD by FA
(ppb)
264 to 5300
105 to 263
48 to 104
9 to 47
5 to 8
1 to 4

Figure 5. Gold in RGS samples.

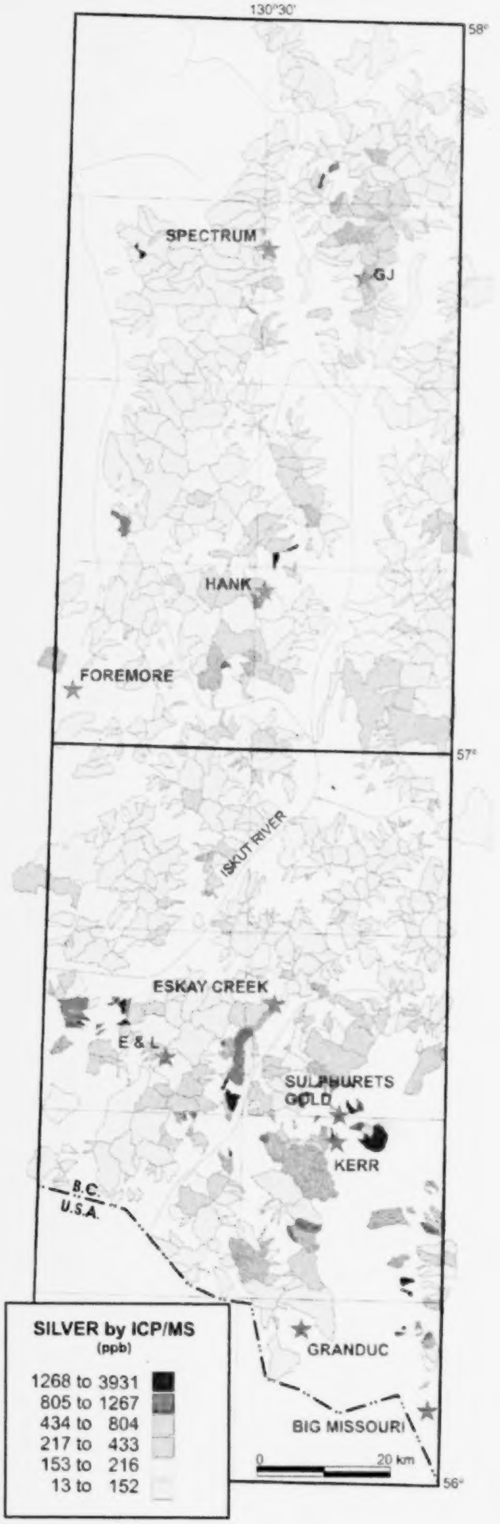
130°30'
58°
SPECTRUM
GJ
HANK
FOREMORE
57°
ISKUT RIVER
ESKAY CREEK
E & L
SULPHURETS
GOLD
KERR
B.C.
U.S.A.
GRANDUC
BIG MISSOURI
0
20 km
56°
SILVER by ICP/MS
(ppb)
1268 to 3931
805 to 1267
434 to 804
217 to 433
153 to 216
13 to 152

Figure 6. Silver in RGS samples

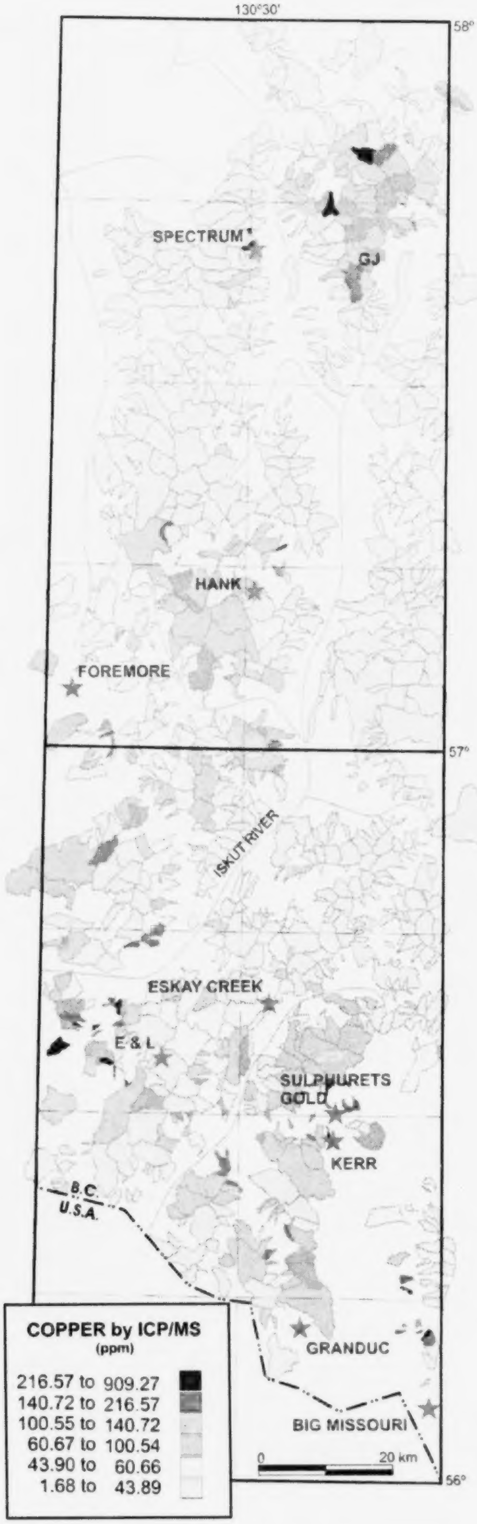
130°30'
58°
57°
56°
SPECTRUM
GJ
HANK
FOREMORE
ISKUT RIVER
ESKAY CREEK
E & L
SULPHURETS
GOLD
KERR
B.C.
U.S.A.
GRANDUC
BIG MISSOURI
0
20 km
COPPER by ICP/MS
(ppm)
216.57 to 909.27
140.72 to 216.57
100.55 to 140.72
60.67 to 100.54
43.90 to 60.66
1.68 to 43.89

Figure 7. Copper in RGS samples

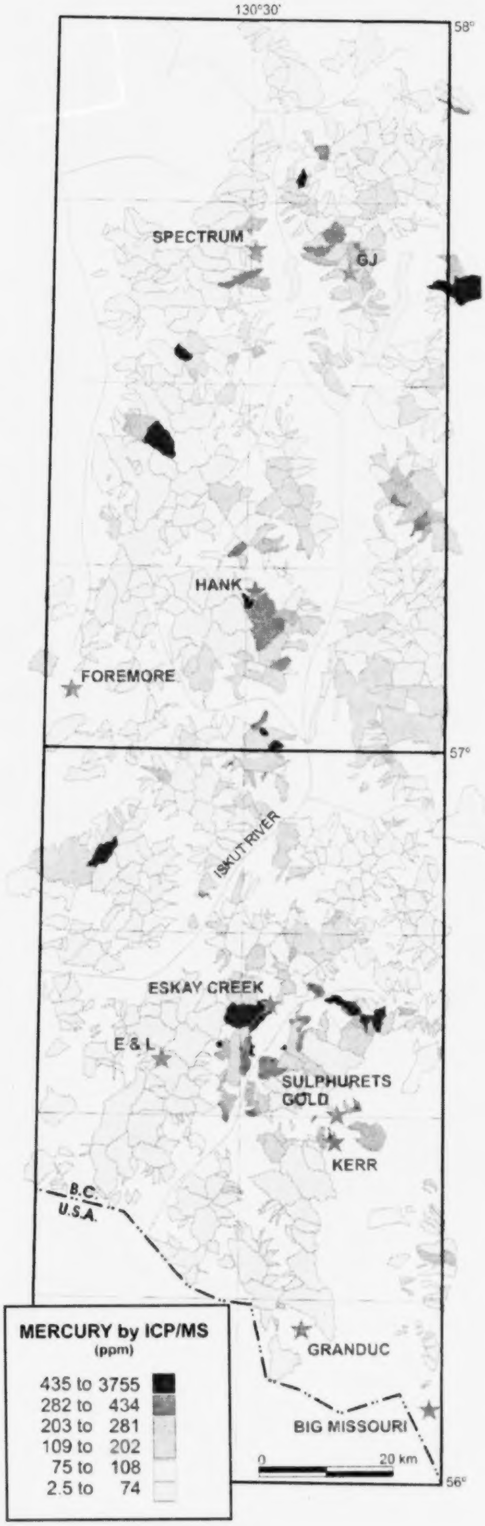
130°30'
58°
57°
56°
SPECTRUM
GJ
HANK
FOREMORE
ISKUT RIVER
ESKAY CREEK
E & L
SULPHURETS
GOLD
KERR
B.C.
U.S.A.
GRANDUC
BIG MISSOURI
0
20 km
MERCURY by ICP/MS
(ppm)
435 to 3755
282 to 434
203 to 281
109 to 202
75 to 108
2.5 to 74

Figure 8. Mercury in RGS samples

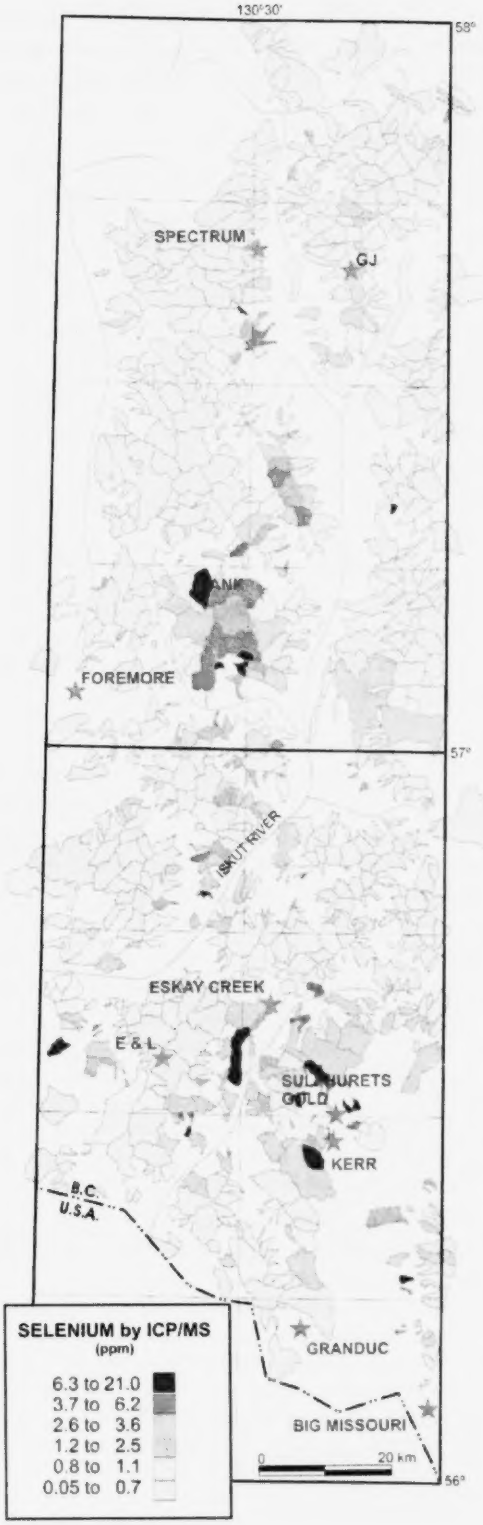
130°30'
58°
57°
56°
SPECTRUM
GJ
HANK
FOREMORE
ISKUT RIVER
ESKAY CREEK
E & L
SULPHURETS
GOLD
KERR
B.C.
U.S.A.
GRANDUC
BIG MISSOURI
0
20 km
SELENIUM by ICP/MS
(ppm)
6.3 to 21.0
3.7 to 6.2
2.6 to 3.6
1.2 to 2.5
0.8 to 1.1
0.05 to 0.7

Figure 9. Selenium in RGS samples

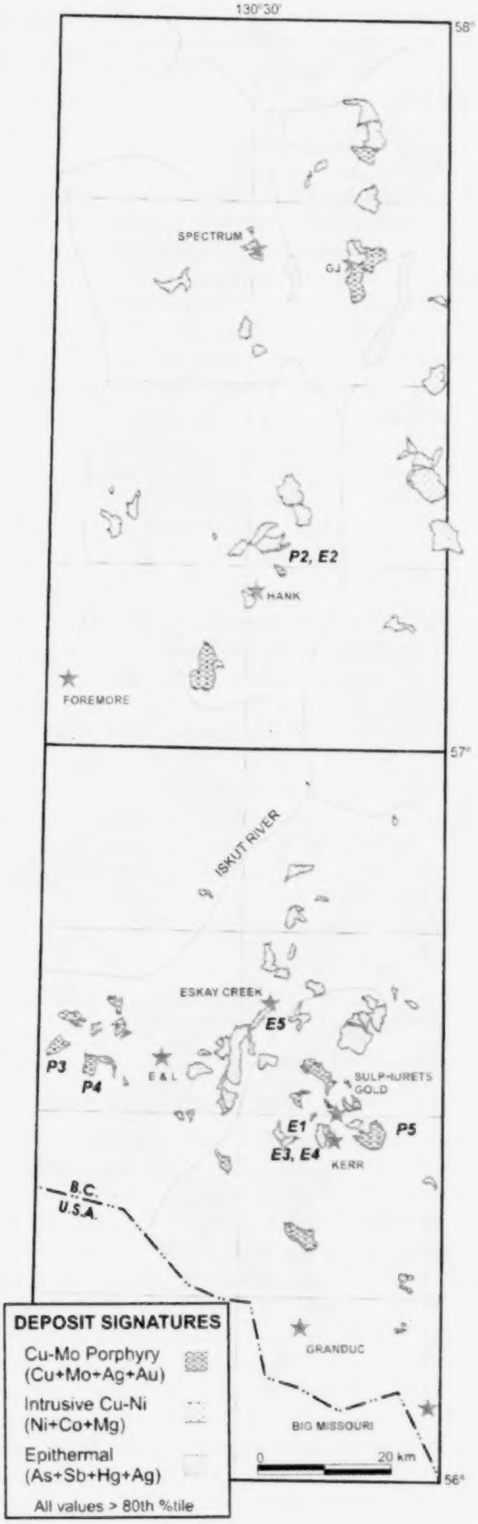
130°30'
58°
57°
56°
SPECTRUM
GJ
P2, E2
HANK
FOREMORE
ISKUT RIVER
ESKAY CREEK
E5
P3
P4
E & L
SULPHURETS
GOLD
E1
P5
E3, E4
KERR
B.C.
U.S.A.
GRANDUC
BIG MISSOURI
0
20 km
DEPOSIT SIGNATURES
Cu-Mo Porphyry
(Cu+Mo+Ag+Au)
Intrusive Cu-Ni
(Ni+Co+Mg)
Epithermal
(As+Sb+Hg+Ag)
All values > 80th %tile

Figure 10. Deposit geochemical signatures

west of the Hank occurrence. The majority of anomalous Ag (> 805 ppb) values occur in samples along a south east trend from the E and L to the Kerr deposits (Figure 6). There are also isolated catchments with anomalous Ag to the north of the Hank and to the west of Spectrum occurrences.

The largest cluster of RGS samples with anomalous Cu (> 216 ppm) values surround the GJ and are west of both the E and L and Hank occurrences (Figure 7). High Hg values (425 to 3755 ppb) occur mainly in samples immediately to the south west and to the east of the Eskay Creek mine (Figure 8). There is also a large area of anomalous Hg (> 282 ppb) east of the Hank and Spectrum occurrences. This Hg anomaly appears to extend east from the Telegraph Creek map sheet into the adjacent Bowser lake sheet. A cluster of sample sites with anomalous (> 3.7 ppm) Se values is present around the Sulphurets Gold and Kerr deposits (Figure 9). However, the largest sediment Se anomalous is west of the Hank occurrence. Samples with anomalous Se in this area typically have high S.

Different mineral deposit types can often be identified from the concomitant association of pathfinder elements in stream sediment. However, the precise discrimination between multi-element associations in RGS data is limited by a common association of many elements (e.g. Cu, Au) in different deposits and the contrasting geochemical mobility of elements (e.g. Zn, Au) in streams. Discrimination between different deposit types in the Iskut River area has been attempted by identifying RGS samples having common enhancement of several elements above their 80th percentile concentration. Element associations selected for three different deposit types are:

- As-Sb-Hg-Ag for epithermal and sub-aqueous hot spring massive sulphide deposits.
- Cu-Mo-Ag-Au for porphyry Cu-Mo deposits.
- Ni-Co-Mg for Cu-Ni intrusive deposits.

Catchment basins with these three signatures are shown in Figure 10. In some instances the multi-element associations effectively distinguish between different deposit types. For example Sulphurets Gold, Spectrum, Kerr and GJ are classified as Cu-Mo porphyry deposits whereas the Eskay Creek mine and Hank are identified as an epithermal deposits. However, the E and L occurrence was not classified as a Cu-Ni intrusive deposit by the sediment geochemistry. Catchment basins with enhanced Co, Ni and Mg are present east of the E and L occurrence and there are also those with a porphyry signature to the west. The apparent failure of the RGS to detect some of the known mineral occurrence reflects the low sample density. For example, there are no RGS sample sites on the west flowing streams from the area around the Foremore occurrence. This is a reminder that all regional geochemical surveys only detect some of the mineralized sites.

While there has been no attempt in this paper to critically evaluate all of the multi-element anomalies identified, the top five ranked porphyry Cu-Mo and epithermal targets are listed in Tables 3 and 4 and identified as numbers (e.g. *P1, E2*) on Figure 10. Decreasing Cu values for the porphyry class and decreasing Au for the epithermal class rank the targets. Several of the targets reflect anomalous drainages close to known mineralization such as deposits in the Sulphurets camp (104B871413) and the Eskay Creek mines (104B871395). Others targets are more remote for mineralized areas and have not been staked at the time this paper was written. One anomaly (sample 104G971347) is classified as both porphyry and epithermal. This shows that the preliminary classification could be refined including additional elements and/or adjusting thresholds.

CONCLUSIONS

Reanalysis of archived RGS stream sediment samples from the Iskut River area by acid digestion - ICP/MS has produced data for 20 additional elements. The new data demonstrate that:

- Many of the RGS Cu, Ag and Au anomalies in the Iskut River area reflect existing mineral deposits.
- There are also catchment basins where there are no mineral occurrences, but where the stream sediment has anomalous levels of deposit pathfinder elements such as Se and Hg.
- It is possible to distinguish between sediment anomalies that have been derived from epithermal Au-Ag, Cu-Mo porphyry and Cu-Ni intrusive deposits using RGS geochemistry. Although discrimination process needs refinement several new and possibly unstaked epithermal and porphyry exploration targets are identified. The location of the five top targets for these deposit types are listed in this paper.
- There are lower detection limits and acceptable precision for ore indicator and pathfinder elements such as Ag and Se. For most elements there is a close comparison between the results produced by acid digestion-ICP/MS and by acid digestion-AAS. However, existing RGS data for Au by fire assay-AAS finish is more reliable than ICP/MS because of the small sample used for the analysis. Data for most of the new elements can be used with confidence to enhance the RGS database.

ACKNOWLEDGEMENTS

The authors would like to thank Dani Alldrick for his helpful remarks on deposits in the Iskut area and for kindly providing an index map. Constructive comments and editing of this paper by Brian Grant and David Lefebure are very much appreciated.

This project has been supported by funding from the BC and Yukon Chamber of Mines, Rocks to Riches program.

TABLE 3.
TOP 5 RGS SAMPLES WITH A CU-MO SIGNATURE. CU IN PPM. UTM ZONE 9. SAMPLES IN BOLD WERE NOT STAKED AS OF DECEMBER 1ST 2003

RGS ID	UTM E	UTM N	Cu	Target
104B871413	424339	6266460	909	P1
104G971347	**415848**	**6349875**	**492**	**P2**
104B871153	381970	6273545	443	P3
104B871133	**390151**	**6268596**	**403**	**P4**
104B871417	420970	6265605	395	P5

TABLE 4.
TOP 5 RGS SAMPLES WITH A AS-SB-HG-AG SIGNATURE. AU IN PPB. UTM ZONE 9. SAMPLES IN BOLD WERE NOT STAKED AS OF DECEMBER 1ST 2003

RGS ID	UTM E	UTM N	Au	Target
104B871431	418220	6261843	493	E1
104G871347	415848	6349875	454	E2
104B871435	421019	6260851	396	E3
104B871416	423596	6265209	383	E4
104B871395	412584	6278020	288	E5

REFERENCES

Alldrick, D. and Stewart, M. (2004): Geology and Mineral Occurrences of the upper Iskut River area, *In* Geological Fieldwork, 2003, *BC Ministry of Energy and Mines*, Open File 2004-1 (In Press).

Clifton, H.E., Hunter, R.E., Swanson, F.J., and Phillips, R.L. (1969): Sample size and meaningful gold analysis, *USGS* Professional Paper 625-C.

Day, S.J. and Matysek, P.F. (1989): Using the Regional Geochemical Survey Database: Examples from the 1988 Release (104B,F,G,K), *BC Ministry of Energy, Mines and Petroleum Resources*, Geological Fieldwork 1988, Paper 1989-1, p.593-602.

Gabrielse, H. and Yorath, C.J., (1992): Geology of the Cordilleran Orogen in Canada, *Geological Survey of Canada*, Geology of Canada, no 4, 843 pages.

Lefebure, D.V. and Hõy, T. (1996): Select British Columbia Mineral Deposit profiles-Volume 2 – Metallic Deposits *Ministry of Employment and Investment*, Open File 1996-13.

Matysek, P.F., Day, S.J., Gravel, J.L. and Jackaman, W. (1988a): 1987 Regional Geochemical Survey 104F-Sumdum and 104G Telegraph Creek, *BC. Ministry of Energy, Mines and Petroleum Resources* RGS 19; *Geological Survey of Canada* Open File 1646.

Matysek, P.F., Day, S.J., Gravel, J.L. and Jackaman, W. (1988b): 1987 Regional Geochemical Survey 104G-Iskut River, *BC. Ministry of Energy, Mines and Petroleum Resources* RGS 18; *Geological Survey of Canada* Open File 1645.

IMAGE ANALYSIS TOOLBOX AND ENHANCED SATELLITE IMAGERY INTEGRATED INTO THE MAPPLACE

By Ward E. Kilby[1], Karl Kliparchuk[2] and Andrew McIntosh[2]

KEYWORDS: MapPlace, Landsat, ASTER, Image Analysis, Structural geology interpretation.

INTRODUCTION

The Image Analysis Toolbox and Enhanced Satellite Imagery, integrated into the MapPlace project of the BC and [illegible]n Chamber of Mines' Rocks to Riches program[illegible] a merging of two initial proposals. The two proje[illegible] though different in purpose shared common data and their results could be distributed through a common method, the MapPlace.

The "Image Analysis Toolbox" project developed and implemented an image analysis capability for the MapPlace and was delivered by Cal Data Ltd. The Toolbox is a framework in which a variety of multi and hyperspectral imagery can be added and processed online by end users. The results of the analysis are georeferenced and can be completely integrated with the information already contained in the MapPlace.

The "Enhanced Satellite Imagery" project produced a series of enhanced Landsat images which facilitate structural interpretations and was delivered by McElhanney Consulting Services Ltd. These images are integrated into the MapPlace so all existing information contained in the system may be referenced to this new set of imagery.

The same Landsat imagery used in the "Enhanced Satellite Imagery" project has been incorporated into the "Image Analysis Toolbox".

IMAGE ANALYSIS TOOLBOX

Purpose

The Image Analysis Toolbox (IAT) was developed to be a system that could hold multispectral and hyperspectral imagery, analyze the imagery and display it through the MapPlace. A suite of initial analysis tools have been provided but the system is designed to be able to incorporate unlimited additional analysis tools. The IAT was added to the Exploration Assistant page of the MapPlace. The appearance and operation of the IAT was designed to maintain the general look and feel of the Exploration Assistant. The purpose of the Toolbox is to provide the ability for MapPlace users to experiment with a variety of imagery and analysis procedures in their search for exploration targets.

Imagery

Twenty Landsat 7 and five ASTER multispectral images and one AVIRIS hyperspectral image have been included in the IAT. All three sets of imagery were available at no cost. The Landsat and ASTER imagery were available orthorectified in UTM NAD83 projections. The AVIRIS image was simply geopositioned in approximately the correct geographic position. The Landsat and AVIRIS images were obtained from the Geogratis website (http://geogratis.ca) and were from their "Landsat 7 Orthorectified Imagery Over Canada" series and a single hyperspectral image example of the Canal Flats area. The ASTER images were obtained from a NASA website (http://asterweb.jpl.nasa.gov) and were obtained from their "DataPool @ LP DAAC" offering of free imagery over the United States. Both these sites provide extensive descriptions of the imagery and its uses. The images used in this project and many more are available as free downloads from these two sites.

The IAT utilizes 6 of the Landsat bands and 14 of the ASTER bands and 223 of the AVIRIS bands. Table 1 lists the bands, their wavelength range and ground sample spacing for Landsat and ASTER. The AVIRIS band centre wavelengths are available from the selection boxes in the Image Analysis Toolbox. All sets of imagery contain radiance measurements. In the future the imagery could be atmospherically corrected to provide reflectance measures that could be compared more successfully to laboratory spectrum for individual ground features. All ground features reflect or absorb solar electromagnetic radiation at different levels across the spectrum. The reflected electromagnetic energy is what is measured by these three sensors. Some of the energy is in the visible light range and provides the colours we see. A large part of the reflected energy is invisible to the human eye but can be measured with these sensors. These three instruments measure energy in the near infrared (NIR), shortwave infrared (SWIR) and thermal infrared (TIR) region of the spectrum. A library of reflectance spectrum for common minerals, rocks, soils and man made materials can be viewed online at the ASTER homepage at the address given above.

---

[1] *Cal Data Ltd.* <wkilby@telus.net>

[2] *McElhanney Consulting Services Ltd.*

BAND	WAVELENGTH	GROUND SAMPLE DISTANCE
L1	.450 - .515	30
L2	.525 - .605	30
L3	.630 - .690	30
L4	.775 - .900	30
L5	1.55 - 1.75	30
L7	2.090 - 2.35	30
L8	.52 - .90	15
A1	.52 - .60	15
A2	.63 - .69	15
A3	.76 - .86	15
A4	1.6 - 1.7	30
A5	2.145 - 2.185	30
A6	2.185 - 2.225	30
A7	2.235 - 2.285	30
A8	2.295 - 2.365	30
A9	2.360 - 2.430	30
A10	8.125 - 8.475	90
A11	8.475 - 8.825	90
A12	8.925 - 9.275	90
A13	10.25 - 10.95	90
A14	10.95 - 11.65	90

TABLE 1. AVAILABLE LANDSAT (L) AND ASTER (A) BANDS, WAVELENGTHS RANGE AND GROUND SAMPLE SIZE.

Knowing the range of the spectrum that each sensor band samples allows one to develop various combinations of the bands that can differentiate between materials on the ground. There is a vast resource of information on remote sensing and image analysis in the literature and on the WWW. A simple search with one of the common search engines will yield a large number of articles describing past experiences using these three sensors to identify features on the ground. Texts such as those by Vincent, (1997) and Lillesand and Kiefer, (2000) provide excellent geology and mineral exploration examples plus a thorough description of the technology.

System

The IAT system was developed using a variety of Commercial Off The Shelf (COTS) software and standard web-based languages such as HTML and JavaScript. The Autodesk MapGuide® Server by Autodesk® is the software that serves many types of spatial data out over the Internet to form map views on the client's computer screen. The MapGuide® Viewer resides on the client's computer and in association with an Internet browser accepts the data sent from various MapGuide® Servers and fabricates the map image as well as providing an Application Program Interface (API) which can be accessed by client-side JavaScript to perform local functions. ColdFusion® by Macromedia was used to generate dynamic web pages, write specialize files for backend processing and access databases. ION™ (IDL ON NET) from Research Systems, Inc. was used to provide the image analysis capability and provide the resultant imagery to the MapGuide® server. IDL® is a specialized image and signal processing language which is used extensively in secondary products related to all types of image processing.

Operation

This section describes the operation of the system from the client's perspective. The image index page is described followed by brief descriptions of the 5 analysis tools. Many of the IAT's functions are common to the individual tool pages and the index page. They will be described as they are first encountered.

INDEX PAGE

Upon selecting the Image Analysis Toolbox by clicking on the appropriate button in the right-side panel of Exploration Assistant a new panel labeled "Image Analysis Toolbox" will appear and several new layers will be added to the map. Depending on the viewing scale of the map either Landsat, ASTER and AVIRIS images or their outlines will be visible. At a scale larger than 1:6 000 000 the images will become visible. The images are presented as a stack of images, often overlapping each other. The ASTER, Landsat and AVIRIS related layers may be toggled on and off with the buttons in the right-side panel. The ASTER group of images will always overlay the Landsat image group and the AVIRIS image overlays all the other image types. To view an image that is partially covered simply, select the image by a single click on the image with the arrow cursor. Then click the "Bring to Top" button and the desired image will be brought to the top of the stack of images. Only one image can be brought to the top at a time. Use the "Clear Selection" button to deselect an image. One can return to the original image stack order by clicking the "Original Order" button. If a particular image cannot be selected with the cursor because it is completely overlain by other images it can be selected by using the MapGuide Pop-Up menu selection option. Simply right mouse click on the map to bring up the Pop-Up menu, then proceed to Select >

Select Map Objects... > then highlight ASTER Analysis Areas or Landsat Analysis Areas and select the desired image number. As there is only one AVIRIS image at this time there is no reason to use this procedure for AVIRIS. The image will then be highlighted on the map and one can proceed as if it were selected with the cursor. The images focus automatically as one zooms in and out but they can be sharpened at anytime by clicking on the "Focus Image" button.

At any time any of the map layers in the left-side legend may be turned off or on or the user may return to one of the other Exploration Assistant tools.

To proceed to the analysis of an image the image must be selected as described above and then the "Analyze Image" button clicked.

IMAGE ANALYSIS TOOLS PAGE

The Image Analysis Tools Page provides a selection of analysis tools in the right-side panel or the opportunity to return to the Exploration Assistant. The map window is centered on the selected image. The map projection is now UTM where the projection of the Image Index map was BC Albers. All analyses are performed using the UTM projected data. Follow the instructions in the lower window, ***WAIT*** until the image has fully loaded. As instructions and data are flowing over the Internet it is possible for some of either to be lost if the user does not wait for each task to complete. When the image has loaded and the system is ready to proceed the lower window will contain some image information such as the system's tracking number for the image, the image's acquisition date and time and a link to the source of the image. The source link for all sets of imagery provides download access to many more images and a thorough description of the imagery and potential uses. The user may zoom into any portion of the image and turn on any of the available map layers contained in the left-side legend. To proceed to an analysis tool simply click on the appropriate button and that tool panel will appear in the right-side panel.

ONE-BAND ANALYSIS

The One-Band Analysis tool provides the ability to examine the readings of a single image band (electromagnetic spectrum range) contained in the image. The "Band" selection box allows the user to select any one of the available bands. The band number and the band's wavelength are displayed in the selection box. Once the desired band has been selected a point of interest may be selected on the main image. To digitize a point of interest first click on the "Digitize Centre of Interest" button and then click on the desired position in the main image. An overlay image will be prepared and sent to the map centered on the digitized point. A histogram equalization stretch is applied to the analysis overlay to provide good contrast of the range of values contained within the analysis area. Initially the overlay image is set to 128 X 128 pixels in size. The user may adjust the size of the analysis overlay from 1 to 1000 pixels by changing the value in the "Analysis Area Pixel Width" input box. The analysis overlay image may be toggled off and on with the "TOGGLE Overlay" button to compare with features between the two images. There are 41 colour schemes that may be applied to the analysis overlay. Simply select the desired colour map from the selection box and re-digitize the area of interest. The various colour maps may be used to highlight features not readily apparent in a grayscale or rainbow coloured image. Different bands have different ground sampling dimensions (pixel widths) therefore a single "Analysis Area Pixel Width" may cover different sized areas with different resolution depending on the band selected. The "Print Image" button opens the print setup dialog box so a hardcopy printout can be configured. Use the "Back to Image Analysis Tools" button to return to the Image Analysis Tools page (Figure 1).

THREE-BAND ANALYSIS

The Three-Band Analysis tool allows the user to create an image by assigning specific bands to the three primary colours: red, green and blue (RGB). The presence of any of the three primary colours in the image represent 100% of that band for that pixel. All pixels containing components of the three bands will appear as secondary colours. This tool provides a visual display of the relative portions of the three selected bands at any pixel location. To assign bands to each colour simply select the desired band in one of the three primary colour selection boxes. Proceed to digitize the area of interest as described earlier. The image values for each of the three selected bands within the analysis area are stretched using the histogram equalization process to enhance the band's image contrast. Some common band combinations for Landsat images are:

$L_{3,2,1}$ will generate a natural colour image

$L_{2,3,5}$ common colour IR composite image highlighting vegetation

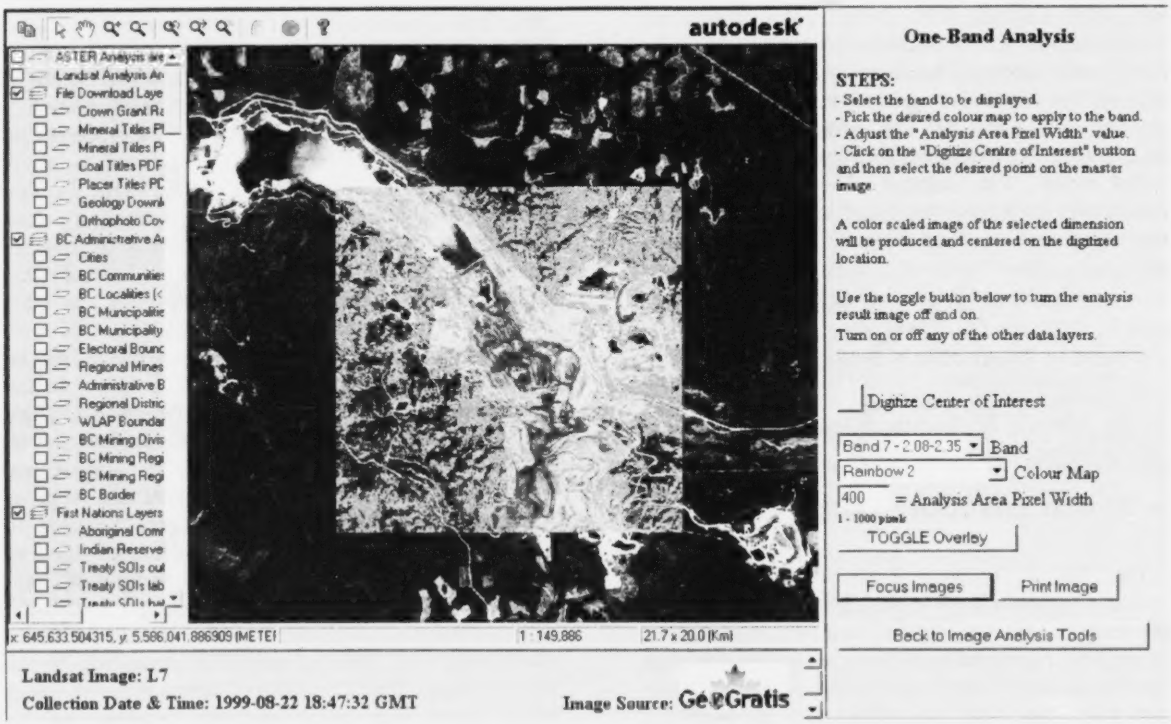
autodesk
☐ ASTER Analysis are
☐ Landsat Analysis An
☑ File Download Laye
☐ Crown Grant Ra
☐ Mineral Titles Pl
☐ Mineral Titles Pl
☐ Coal Titles PDF
☐ Placer Titles PC
☐ Geology Downl
☐ Orthophoto Cov
☑ BC Administrative A
☐ Cities
☐ BC Communities
☐ BC Localities (<
☐ BC Municipalitie
☐ BC Municipality
☐ Electoral Bounc
☐ Regional Mines
☐ Administrative B
☐ Regional Distric
☐ WLAP Boundar
☐ BC Mining Divis
☐ BC Mining Regi
☐ BC Mining Regi
☐ BC Border
☑ First Nations Layers
☐ Aboriginal Comr
☐ Indian Reserve
☐ Treaty SOIs out
☐ Treaty SOIs lab
x: 645,633.504315, y: 5,586,041.886909 (METE
1 : 149,886
21.7 x 20.0 (Km)
Digitize Center of Interest
TOGGLE Overlay
Focus Images
Print Image
Back to Image Analysis Tools
Image Source: GeoGratis

One-Band Analysis

STEPS:

- Select the band to be displayed.
- Pick the desired colour map to apply to the band.
- Adjust the "Analysis Area Pixel Width" value.
- Click on the "Digitize Centre of Interest" button and then select the desired point on the master image.

A color scaled image of the selected dimension will be produced and centered on the digitized location.

Use the toggle button below to turn the analysis result image off and on.

Turn on or off any of the other data layers.

Band 7 - 2.08-2.35 Band

Rainbow 2 Colour Map

400 = Analysis Area Pixel Width

1 - 1000 pixels

Landsat Image: L7

Collection Date & Time: 1999-08-22 18:47:32 GMT

Figure1. Screen view of the One-Band Analysis window illustrating all the major user input components. The overlay analysis image covers a portion of the Highland Valley mining operation. Landsat Band 7 has been selected, the analysis image is 400 pixels square and the Rainbow 2 colour map has been used to colour the image. Most MapPlace data layers are available from the left-side legend.

TWO-BAND RATIO ANALYSIS

The Two-Band Ratio Analysis allows the user to generate band ratio analysis images. The ratio between two bands is used to display the variability between two regions of the electromagnetic spectrum across the analysis area. This type of analysis has been used to discriminate between many features such as minerals, water clarity, water depth and vegetation vigor. The ratio process also reduces the effect of shadows on the analysis. But the result should be used with caution as the ratio for two materials may be the same even though the actual reflectance spectrum values for the materials are completely different. A good example of this is the $L_{3/1}$ ratio. This ratio identifies oxide minerals very well but equally as well identifies ice.

The resultant ratio image is stretched using the histogram equalization process to enhance its contrast. If the same band is selected for both the numerator and the denominator then a ratio image is not generated but a simple one-band image is presented. Assigning various colour maps to the ratio image may enhance features of interest. Some common ratios are:

$L_{3/1}$ oxides

$L_{5/7}$ clays

$L_{5/4}$ ferrous

FALSE COLOUR COMPOSITE ANALYSIS

The False Colour Composite Analysis tool allows the user to assign ratio images to each of the three primary colours and create a RGB image. By selecting band ratios that identify specific characteristics and then combining them into a single image a large amount of information can be conveyed in that image. Each of the three ratio images is stretched using the histogram equalization procedure prior to construction of the final RGB image. A commonly employed combinations is:

$L_{3/1,5/4,5/7}$

NDVI VEGETATION INDEX

The Normative Difference Vegetation Index is a measure of chlorophyll content or plant growth. This measure has long been used with Landsat imagery and uses the Red and near infrared (NIR) bands in ratio (Landsat bands 3 and 4, ASTER bands 2 and 3, AVIRIS 25 and 48). The AVIRIS image (V1) currently loaded is an early image which had poor signal to noise characteristics. The NDVI produced from it is mainly noise. The index is a ratio of NIR+RED / NIR-RED. The resultant NDVI image is again stretched using the histogram equalization procedure to enhance its contrast. This tool can be very useful in assessing vegetation stress differences that could be due to the underlying rock formations or water availability. Age and type of vegetation in logged areas can be inferred with some minor ground verification.

ENHANCED SATELLITE IMAGERY

Purpose

A set of eighteen enhanced satellite images over parts of BC were produced for the purpose of facilitating the interpretation geological structures. This part of the project involved the use of free Landsat 7 ETM data, which is available for download from www.geogratis.ca, and BC TRIM digital elevation models (DEM) provided by the BC government.

The total geographic coverage of the eighteen images comprises approximately 40% of British Columbia (Figure 2). For information about the Landsat 7 ETM satellite, refer to http://landsat7.usgs.gov/index.php.

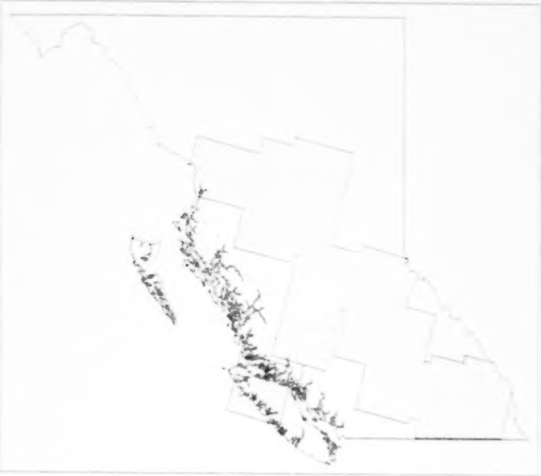

Figure 2. Area covered by enhanced Landsat imagery.

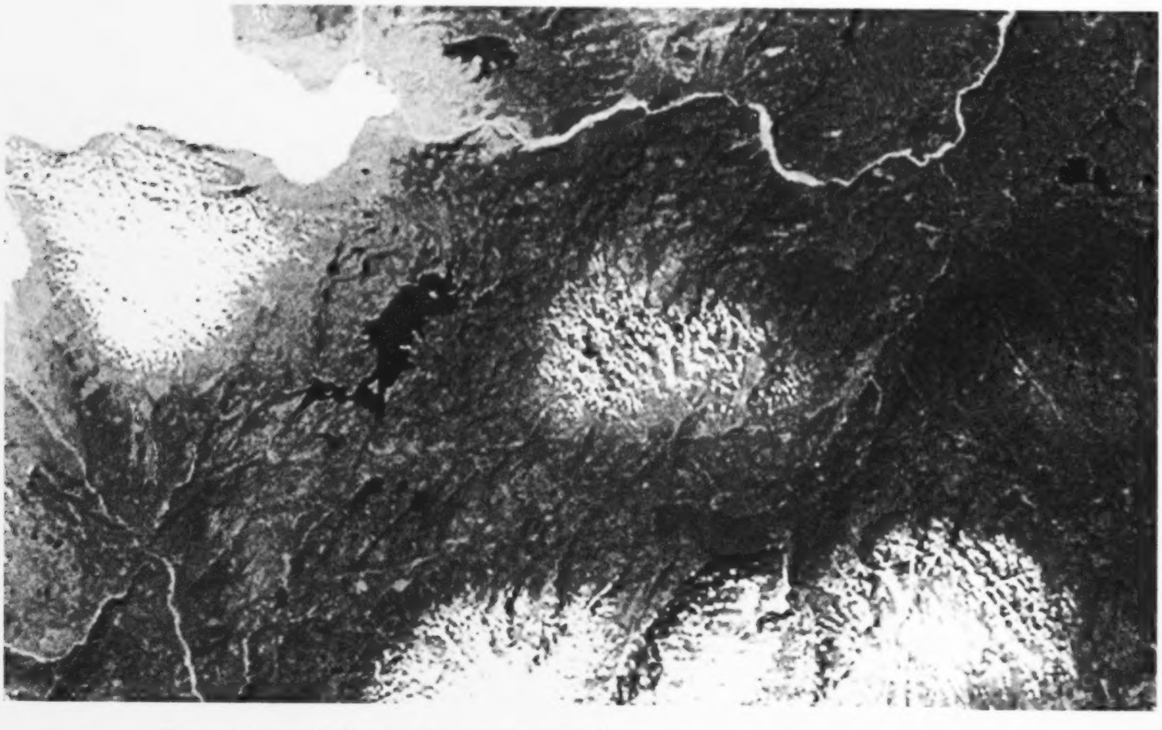

Figure 3. Natural Colour Landsat image based on bands 3, 2, 1 as red, green and blue, respectively.

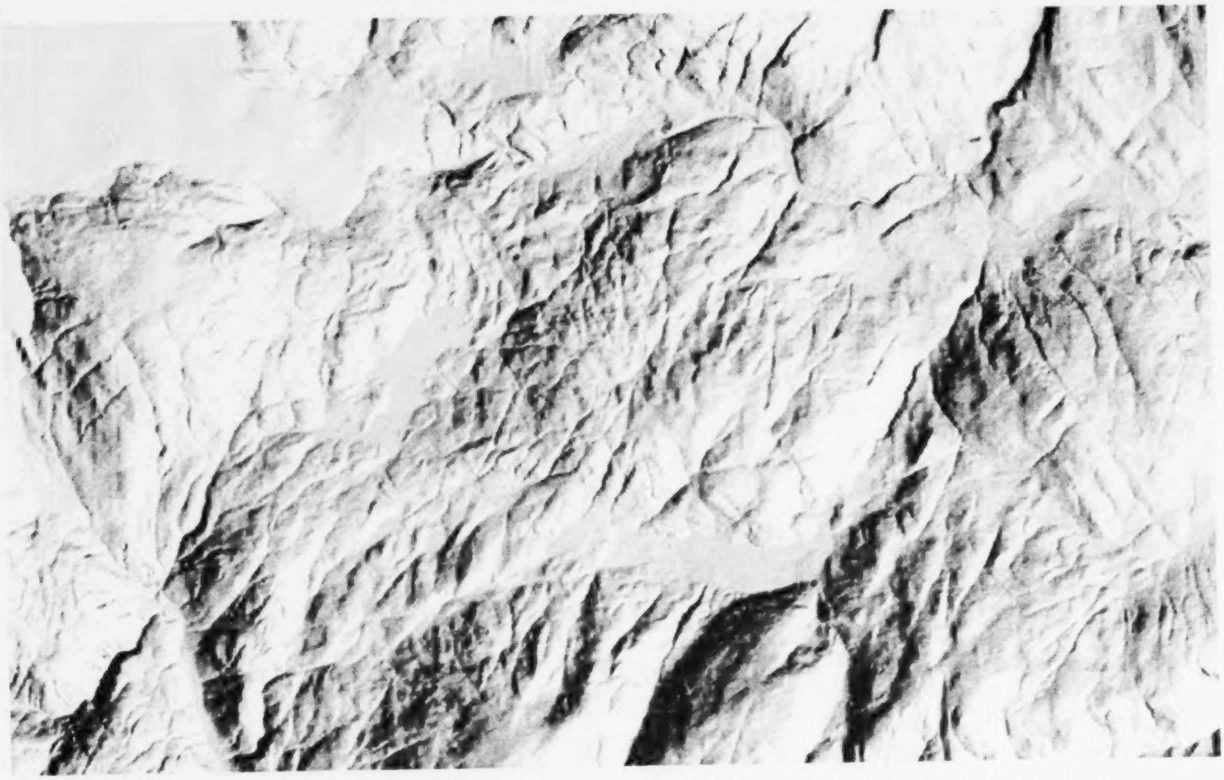

Figure 4. Greyscale "hillshaded" image based on TRIM digital elevation model.

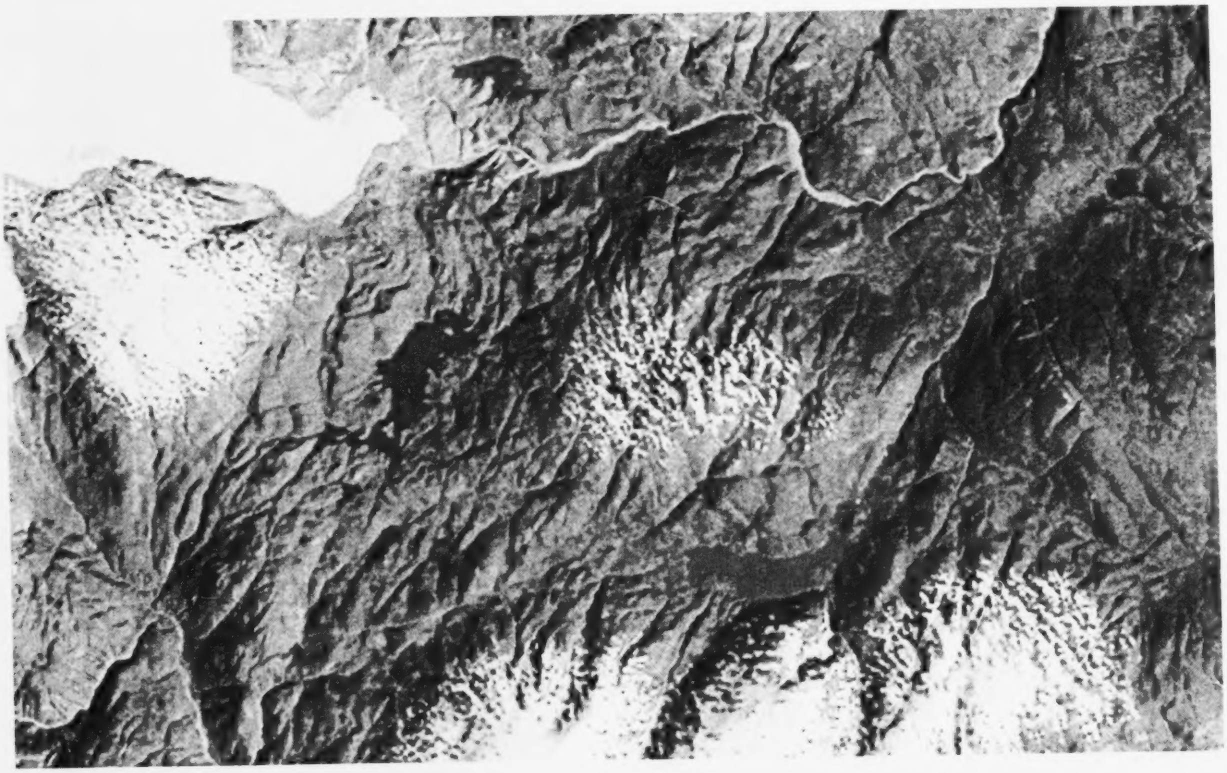

Figure 5. Enhanced Landsat image formed from the fusion of hillshaded image and natural colour image.

Image Enhancement

Image enhancement involved the combination of two types of images:

1. Conventional "natural colour" imagery produced with 30m/pixel Landsat bands 3, 2, 1 as red, green, blue respectively (Figure 3.).
2. Greyscale, "hillshaded" imagery produced by the application of artificial lighting to the 25m/pixel TRIM DEM (Figure 4).

Many geological structures have some topographic expression, often in the form of creeks, ravines, escarpments and on the larger scale, valleys and coastal inlets. By nature, DEMs record topographic features and can therefore be used to aid in the interpretation of geological structures. The fusion of the two image types results in a final product where the visually detectable features of conventional colour imagery (vegetation, water, rocks, ice, snow, etc) are preserved and topographic features (faults, fractures, glacial landforms etc.) are greatly enhanced (Figure 5).

ER Mapper software was used for all aspects of image processing. All images have been provided with 25m/pixel size, in geotiff and ecw formats, in both UTM NAD83 and BC Albers projections.

Uses of Enhanced Imagery

These enhanced images are intended for interpretation at scales between 1:80,000 to 1:100,000. The limitation of scale of use is determined in part by the 30m pixel size of the original Landsat imagery but more importantly by the ground resolution of the BC TRIM DEM.

Geological structures are detectable in all eighteen of the final enhanced images. Furthermore, many glacial features such as drumlins and eskers are also detectable. Each enhanced image was visually compared with the corresponding conventional image. Of particular note here is that many structures detectable in the enhanced images were not detected in the conventional image. It must be noted that there are some problems in the TRIM DEMs where there is a visually noticeable linear smear of data values across the width of a few pixels. These linear artifacts are known by the BC government.

SUMMARY

The project has achieved all of its objectives. Eighteen Landsat 7 ETM images were enhanced to highlight structures with topographic expression. These image products are available for download in several formats and map projections from the MapPlace. An image analysis framework has been added to the Exploration Assistant page of the MapPlace web site to allow basic image analysis processes to be performed on multispectral and hyperspectral images. Twenty Landsat 7 ETM images, five ASTER images and one AVIRIS image have been loaded into the system and are available for analysis. Five general analysis tools are included in this initial version of the site.

This project was designed to test the value and acceptance of providing image products and image analysis tools for use by the exploration community over the Internet. If warranted, additional enhanced Landsat imagery could be produced and added to the system. Addition types of multispectral and hyperspectral imagery can be added to the analysis system as well as additional analysis tools and more complete coverage of existing image types.

ACKNOWLEDGMENTS

This project was made possible by a grant from the Rocks to Riches program of the BC and Yukon Chamber of Mines.

We would like to thank Patrick Desjardins and Larry Jones of the British Columbia Geoscience, Research and Development Branch for invaluable assistance in providing information and access to the MapPlace web-site.

REFERENCES

Vincent, R.K.(1997): Fundamentals of Geological and Environmental Remote Sensing; Prentice Hall, Upper Saddle River, NJ, 366 pages.

Lillesand, T.M. and Kieffer, R.W.(2000): Remote Sensing and Image Interpretation; 4th ed., Wiley, New York, 724 pages.

MapPlace CLIENT-MAPPING TOOLS

By W.E. Kilby[1], L.D. Jones and P.J. Desjardins
[1]Cal Data Ltd.

***KEYWORDS**: geoscience data, geology maps, Internet mapping, geospatial data, mineral deposits, geochemistry, mapping tools, raster projection, MapPlace, Autodesk MapGuide, redline.*

INTRODUCTION

The MapPlace (www.MapPlace.ca) is a website designed to facilitate easy access to the maps and databases of the British Columbia Ministry of Energy and Mines. The site is built using Autodesk MapGuide® technology and has been in operation for about eight years. The site has been highly successful and gained acceptance from its target audience and beyond. Most major datasets that are of value in the promotion and investigation of BC's mineral wealth may be accessed through the site in an interactive format. The site provides a variety of tools to perform sophisticated spatial searches, excellent hardcopy production, and limited GIS functions.

Data themes available on the MapPlace cover a broad range of spatial data in vector and attribute form, including bedrock geology, geochemical surveys, mineral occurrences, exploration assessment reports; and mineral, coal and petroleum tenure locations. These data can be combined with other base data, including administrative boundaries, topographic features and raster images, such as LandSat images and aeromagnetics. User-defined map views can then be printed or pasted into common graphics packages. Many individual map objects are linked to valuable attribute data or to a separate Internet site, allowing further search and retrieval capabilities.

The site has continued to expand both in content and purpose. With each version of MapGuide new functionality has been added to the MapPlace, increasing ease of use, speed of delivery and sophistication of potential products. The quality and quantity of the data content has continually increased. During this time the diversity of users has also greatly increased and this has led to a large array of specialized map products targeted to niche requirements. The site has been used for purposes from simple map viewing to field entry of map data. It has been used in a production environment to manage the Notices of Work information for a district office. Products from the MapPlace have become ubiquitous in the mineral exploration community.

The British Columbia and Yukon Chamber of Mines' 'Rocks to Riches' program funded this project to add 6 new client-mapping tools to the MapPlace including:

1. Redline Mapping Tools
2. Client-defined Grid Overlay
3. Geochemistry Symbol Resizing
4. Copy Maps with Scale Preservation
5. Off-line Map Viewing
6. Re-projection of Raster Images

The objective and expected result of each tool will be described in this article. Subsequent articles will describe the method of delivery and operation of each tool. These enhancements will increase the ways in which clients use and generate products with the MapPlace.

CLIENT-MAPPING TOOLS

REDLINE MAPPING TOOLS

Objective: A set of client-side tools to draw on MapPlace maps. The tools allow the client to draw lines, polygons, symbols and text on any number of 'redline' layers. The client will be able to select the display attributes for these objects and delete objects. The map file (*.MWF) that contains the new 'redline' layers can be saved on the client's computer for later use and distribution.

Expected Result: The feature will provide a simple set of controls in a side panel to MapPlace maps and give the end-user the ability to:

- add new layers to the map
- add linework of any color, width and pattern
- add polygons of any color, fill pattern and edge characteristics
- add text of any size, color and font
- add any symbols included in the original map being able to adjust its rotation and size
- include descriptive text as labels and/or cursor-over displays
- delete any selected 'client added' object
- save the final map file on the client's machine

CLIENT DEFINED GRID OVERLAY

Objective: A capability to generate evenly spaced labeled grid lines in either geographic or map coordinates over the map window.

Expected Result: The user will select separate line spacings for the N-S and E-W lines as well as their colour, thickness and pattern. The lines will be generated on a Redline layer on the client's machine. The grid variables will be retained so that a new grid can be generated by a simple mouse click if the map is panned or zoomed.

GEOCHEMISTRY SYMBOL RESIZING

Objective: A capability to resize the geochemistry symbols to improve the visual clarity of printed output from MapPlace.

Expected Result: The tool will appear in the side panel of the map display. A 'Printer Friendly' dialog will allow the client to define the magnification factor to be applied to a list of layers that the client can select. A new *.MWF file will be generated and sent for printing.

COPY MAPS WITH SCALE PRESERVATION

Objective: A procedure to maintain a selected map scale between the MapPlace map window and a secondary application during a 'Cut&Paste' operation.

Expected Result: A procedure will be recommended that simplifies the process of moving a map view object from the MapPlace into a secondary application while maintaining the same scale, or very close to the same scale, that was present in the map window. The procedure will include the generation of some map window size parameters that are used to structure a frame or window in the secondary application. This product will be a set of instructions for the client along with any required map window parameters.

OFF-LINE MAP VIEWING

Objective: A MapPlace generated product that can be used off-line. An example would be a project map, embedded with a limited number of data themes, such as LandSat, topography, hydrology, roads, MINFILE and geology.

Expected Result: This feature will allow a user-selected window of essential data to be included in the *.MWF file for off-line use. The client will select the themes to be embedded in the map file but there would be protections to ensure that the amount of embedded data remains within acceptable limits.

RE-PROJECTION OF RASTER IMAGES

Objective: Produce additional versions of some selected raster datasets on the MapPlace in different projections to allow their use in more maps.

Expected Result: Selected raster data sets will be reprojected so that they are available in both of the common projections on the MapPlace.

SUMMARY

The MapPlace uses the Internet to provide interactive map access to data relevant for energy and mineral resource evaluation. The addition of new tools will greatly enhance the ability of clients to use the MapPlace and Ministry databases, with their own data, to research and investigate attractive exploration areas. Industry, government, universities and the public benefit from the use of the MapPlace for exploration investment planning, resource management, policy and land-use planning, teaching and research. The MapPlace website can be found at www.MapPlace.ca.

ACKNOWLEDGMENTS

This project was made possible by a grant from the 'Rocks to Riches' of the BC and Yukon Chamber of Mines. The BC Ministry of Energy and Mines will install and host the tools on the MapPlace.

SELECTED BIBLIOGRAPHY

Jones, L. (2003): Web-based Solutions for Geoscience Data - MapPlace.ca, *CAMI 2003 Proceedings* Calgary September 8-10, 2003,

Jones, L., MacIntyre, D., and Desjardins, P. (2002): The MapPlace - An Internet-based Mineral Exploration Tool, *B.C. Ministry of Energy and Mines*, Geological Fieldwork 2001, Paper 2002-1, pages 409-420.

Tupper, D., Jones, L., Kilby, W. and MacIntyre, D. (2001): The MapPlace, Using Web-Based Mineral Exploration Data as an Environmental Tool, *Innovation* June 2001, Volume 5, Number 5.

MacIntyre, D., Jones, L., and Kilby, W. (2001): The MapPlace, An award winning Internet exploration service for B.C. *GEOLOG* Spring 2001, Volume 30, Part 1.

Kilby W E. (1999): The MapPlace — Web-Based GIS Access to British Columbia Mineral Exploration Information. *Proceedings of the Thirteenth International Conference on Applied Geologic Remote Sensing*, Vol. 1 (1999), pp 204-212.

MapPlace Website (December 2003): *http://www.MapPlace.ca*.

Domvile, Julie (2003): The MapPlace A Jewel of a Tool, *Mining Review*, Winter 2003, Vol. 23, No. 4.

THE POTENTIAL FOR EMERALDS IN B.C. - A PRELIMINARY OVERVIEW

By Andrew Legun

KEYWORDS: Beryl, emerald, volatile granite, ultramafics, phlogopite schist, tungsten, Surprise Lake batholith, Cassiar batholith, Hellroaring Creek pegmatite

INTRODUCTION

Discoveries of chromium-rich emerald at Regal Ridge in south-central Yukon, vanadium-rich emerald at Lened near the Yukon/N.W.T. border (Groat *et al.* 2002) has raised interest in the emerald potential of British Columbia and transparent gem exploration in general.

This report reviews associations of beryl, deposit models for chrome-rich beryl (emerald), and the common association of emerald with phlogopite schists. It examines a few areas of interest in B.C. based on a preliminary emerald potential map and literature review. A fieldwork component is focused on several beryl occurrences. Descriptions of three properties are appended and their location shown in figure 1. Examination of the Hellroaring pegmatite stock provided an opportunity to produce an updated map and to determine gem potential within this large target. The Omg claims at Laib Creek illustrate a prospecting success in revisiting old beryl showings. Dortatelle is in a geologic setting which appears conducive to emerald formation but there is no documentation of the showing since its discovery and brief description in the 1940s.

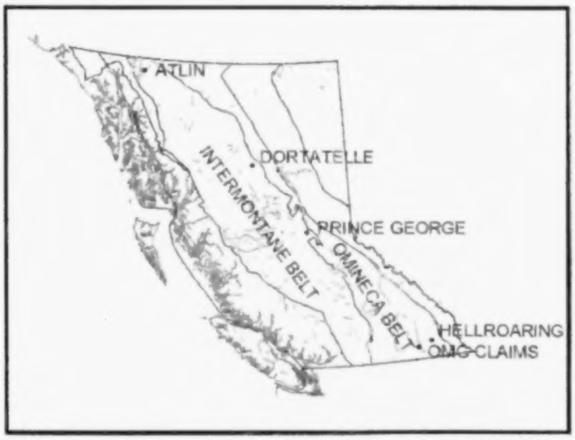

Figure 1: Location of field visits (Omg claims, Hellroaring Creek pegmatite, Dortatelle Creek)

Three weeks were spent in the field in August with the writer returning in October to augment mapping at Hellroaring Creek. A map of the Hellroaring Creek pegmatite body is included in this report. Funding was made available from the BC & Yukon Chamber of Mines, Rocks to Riches Program.

BERYL AND BERYLLIUM

Mulligan (1968) provides an overview of beryllium in Canada while Pell (1990) discusses the geologic setting of beryllium mineralisation in British Columbia. Burt (1982) provides an overview of the minerals of beryllium. Walton (1996) provides an excellent introduction to exploration criteria for emeralds.

Beryl or beryllium aluminum silicate ($Be_3Al_2Si_6O_{18}$) is a hard (7.5 to 8 on Moh scale), resistant mineral, often recognized due to faces of hexagonal prisms that project from the weathered skin of outcrops. It is the most common beryllium mineral in British Columbia. Other Be-bearing minerals in B.C. include the sulphosilicates danalite and helvite, as well as the yttrium bearing gadolinite. Most beryllium minerals are silicates and associated with other lithophile elements and metals such as tungsten, molybdenum, tin, uranium, niobium and tantalum.

Beryl tends to microfracturing and crystal fragments are typically the material found in the light fraction of stream sediments. Beryl, with a specific gravity close to rock forming silicates such as quartz and feldspar has apparently been recognized in placers. Unreferenced locations for beryl include Quesnel River and 111 Mile Creek in the Lillooet District (Mulligan 1966).

Gem-quality beryl is given different names based on color. Thus aquamarine is light-blue, heliodor (yellow-green), morganite (pink), emerald (green), and bixbite is red. Either chrome or vanadium may provide the deep green of emerald.

The variation in color is due to trace element substitutions (for example iron for aluminum). Some ions do not substitute in the framework atoms but occur in the middle of Si-O rings that are stacked parallel to the c-axis of the crystal. These "channel" ions may also affect the color. The oxidation state is also important. Ferric ions give rise to yellow, and ferrous ions in channels give rise to blue hues respectively. Combinations of the two are responsible for the many shades of sea green in aquamarine. Compositional zoning radial or normal to the c-axis can affect the overall hue and result in color banding.

B.C. EXPLORATION WORK

Beryl has received little prospecting attention in the province. It has traditionally been reported as a minor note of interest in geologic reports. A comparison of MINFILE with localities mentioned in a review of transparent gemstone (Wilson, 1997) also shows a proprietary dataset is available to gemologists and mineral collectors.

The regional distribution of beryl is poorly known. There is no regional stream sediment data on beryllium with which to evaluate the distribution of its most common mineral. By way of example, Brinck and Hofmann (1964) provide results of a regional stream sediment assessment for beryllium in Norway.

There are few exploration reports specific to gem beryl. Gauthier and Dixon (1997) working on the Anglo-Swiss claim block in the Slocan area describe beryl pegmatite and gem-corundum exploration targets. Their work followed discovery of aquamarine beryl in vugs in pegmatite (B.Q. claims) during logging operations at Passmore in the early 1990s. Discoveries of gem corundum and cordierite followed. A growing variety of gemstones including iolite, sapphire, garnet and aquamarine have been identified in the Slocan area.

Holland (1956) first described beryl showings from Ingenika Group metasediments cut by pegmatite dikes in the Horseranch area east of Cassiar. The mapping of ultramafics in the area Gabrielse (1963), Plint (1991) eventually led Wilson (1997) and Simandl and Wilson (1998) to prospect for emeralds where these pegmatites cut ultramafic rocks both near the original showing (Cassiar beryl: MINFILE # 104P 024) and at an ultramafic body near Harvey Lake to the north. Six new showings were found in the Harvey Lake area. Aquamarine occurs in simple and zoned pegmatites which carry garnet and tourmaline. Emerald was not found, in spite of pegmatite cutting chrome bearing ultramafic rocks. Simandl and Wilson (1998) concluded hydrothermal activity and structural preparation (shearing) to facilitate fluid interaction was lacking.

Wilson (1997) reported poorly formed vanadian emerald is associated with the Red Mountain porphyry deposit near Stewart but information is minimal.

Beryl has also been evaluated as a potential source of beryllium metal. Recent evaluations include reports on the Hellroaring and Matthew Creek stocks (Anderson 2001, Soloviev 2001) and the wolframite-fluorite-beryl quartz veins peripheral to the Logtung deposit (Wengzynowski 1999). Beryl occurs in the main stockwork of tungsten-molybdenum mineralisation at Logtung. The stockwork has been known for some time but a separate halo of veins was found several kilometers to the south on the B.C. side of the border. The beryl is described as cloudy blue and up to 4 centimetres in length (see Mihalynuk article, this volume). Transparent (uncolored?) crystals up to 2 cm are also found in vugs with quartz.

Recent prospecting efforts in the Bayonne magmatic suite of southern B.C. has led to a number of new beryl localities (Blue Hammer, Omg claims). Jarrod Brown describes them in detail in this volume. The gem quality of beryl at various sites along the margins of the White Creek and Bayonne batholith (Shaw Creek phase) is still under evaluation by Eagle Plains Resources and Cream Minerals Limited.

The number of beryl occurrences in the province is estimated to stand at about 34; 8 new occurrences found in the last few years and 26 listed in MINFILE. Each occurrence may include several showings in proximity to each other.

There are additional reports of beryl or beryllium mineralisation which are not documented in MINFILE or in Wilson (1997). These three are derived from a Ministry industrial minerals file.

NTS 82M/6W Adams Lake

- (51 24 119 24): green crystal of beryl (1 inch diameter) in mica pegmatite near north end of Adams Lake is reported by unknown contact person at B.C. Ministry of Environment.

NTS 103I/16E Massa

- (54 58 128 10): gadolinite identified by x-ray diffraction from sample originating on Massa claims (map 2, ARIS report 8467).

NTS 93G/9 George Creek

- (53 35.4, 122 20): Light-green beryl with garnet and smoky quartz in pegmatite dikes reported in ARIS report 22365.

GEOLOGIC ASSOCIATIONS OF BERYL

Beryl is often associated with granitic intrusives that carry fluxing agents (boron, fluorine, phosphorus). Such magma is less viscous, persists to lower temperatures and later stages of magma differentiation before crystallization. Compositionally these volatile granites are usually peraluminous, mica and alkali feldspar rich, varying in composition from leucocratic granite (alaskite) to quartz syenite and quartz monzonites. They form in continental settings. The suite includes some peralkaline varieties that may carry sodic amphiboles and form in continental but extensional environments. The volatile granites are associated with mineralisation that may include tin, tungsten, molybdenum, uranium, thorium, niobium, tantalum, yttrium and rare earth elements. They are sometimes distinguished as fluorine-rich topaz (specialty) granites or as tourmaline granites. Pell (1990) tended to restrict the volatile-rich granites to the topaz granites of the Surprise Lake and Parallel Creek batholiths. However, tourmaline granites (with minor fluorite) are relatively common in B.C. and if not strictly "specialty" granites by all criteria they are certainly volatile-enhanced.

Griesen is a late stage, mica-rich, mineral assemblage which occurs with fluorine minerals and quartz along fractures in volatile granites and/or country rocks. Lithium micas (lepidolite, zinnwaldite) and tourmaline are also common in griesen. Although griesen has similarities to porphyry style phyllic (sericitic) alteration it is a coarse grained alteration which overlaps pegmatitic and hydrothermal stages of magma crystallization.

Near surface (epizonal) volatile granites, related pegmatites and griesen commonly contain miarolitic cavities. The better examples of gem aquamarines in B.C. are those crystals which line miarolitic cavities. Miarolitic granites are mentioned with fair frequency in B.C. geologic literature.

Apophyses of the larger bodies, smaller intrusions peripheral to larger batholithic bodies and unroofed cupolas may be enriched in beryl.

The volatile granites are more or less equivalent to the "fertile" granites that are parental to rare element pegmatites. Beryl is associated both with the LCT (Li-Cs-Ta) and NYT (Nb-Y-Ta) families of rare-element pegmatites that arise from fractionation of "fertile granites". In these families high field-strength elements (those with small radius but appreciable charge), such as niobium, tantalum, tin, tungsten, beryllium, respond in similar fashion to complex trends of fractionation and may be concentrated together with soluble alkali metals such as lithium, rubidium and cesium. The NYF family tends to be associated with alkaline rocks. Beryl may also be found in simple pegmatites though its gem varieties may be restricted.

DEPOSIT MODELS FOR EMERALD

Two broad types of emerald deposits are recognised worldwide (Schwarz, D. and Guilani, G. (2001). The first relates to the direct and local intrusion of granitic pegmatites within chromium and vanadium-bearing mafic and ultramafic rocks, sediments and metasediments. The second, rather broad in geologic setting (shales, low and high grade metasediments, greenstones, listwanites, suture zones), is linked to thrusts, faults and shear zones. Extended periods of fluid circulation in structurally permeable zones bring Be and Cr/V elements together from source rocks that may be far removed from each other. The common factor to both categories is the exchange of critical elements. In the case of the Columbian deposits the host shales are also the source of both beryllium and chromium (Banks et al., 2000).

Simandl (1999) provides some detailed summaries for emerald deposit types, including schist-hosted emeralds.

EMERALD AND AQUAMARINE

Although exploration for aquamarines may also lead to the discovery of emerald, exploration programs for aquamarine and emerald require slightly differing strategies. Aquamarine has a primary relationship to pegmatites in which the coloring agent (iron) is geochemically abundant.

The relationship of emerald to pegmatite is more indirect. The elemental exchange required for emerald formation tends to occur in the vanadium or chrome bearing wallrock and not the host intrusion (granite or pegmatite). As Cerny (1991) pointed out, hybridization of pegmatites by reaction with wall rocks is very limited. Studies by London (1995) also indicates pegmatites are essentially solidified prior to loss of fluids to wallrocks. This also minimizes opportunity for element exchange in the pegmatite itself. A review of literature does indicate a few examples of emerald in pegmatite. One example is the Australian Emerald Mine near Emmaville in New South Wales. Emeralds occur as 'bunches' in a solid quartz-topaz-mica pegmatite. In another example (Pezzota and Simmons 2001) describe emerald at pegmatite margins forming due to intense wallrock reaction (a kind of endoskarn effect?). On the other hand all Brazilian deposits are schist hosted and associated with K-metasomatism (Guilani et al., 1990).

PHLOGOPITE SCHISTS

The most common host to emerald is phlogopite schist derived from alteration or metamorphism of ultramafics. These are also described as blackwall schists, or glimmerites or phlogopitites.

In a typical example (Franqueira granite pegmatite in Spain) pegmatite cuts a dunite resulting in the formation of emerald-bearing phlogopitite near the pegmatite and tremolite bodies and an anthophyllite rim close to dunite (Fuertes-Fuente et al., 2000). Given that most ultramafics are not potassic, phlogopitite comprising upwards of 75% phlogopite $KMg_3AlSi_3O_{10}$ $(F.OH)_2$ represents potassium metasomatism. It may also represent fluorine metasomatism as fluorine often substitutes for the hydroxyl ion.

The development of phlogopite schists can be considered as part of a griesen assemblage which develops adjacent to volatile granites. According to Siems (1984) griesenisation of ultramafic rocks lead to olivine, pyroxene and amphibole altering to serpentine, phlogopite, talc and chlorite. Alteration minerals are enriched in fluorine, boron and the alkali metals.

Phlogopite schists are not mentioned in descriptions of altered ultramafic rocks in B.C. The usual description (e.g. in Ash, 2000) is listwanites, serpentinites, talc, magnesite, and mica-rich zones of mariposite/fuchsite. Possibly the postulated phlogopite schists are not specifically related to mineral deposits described. They may also be overlooked since the reaction zone at the contact of a small target, such as a beryllium bearing pegmatite, may be less than a metre wide.

Prospective ultramafics in B.C. should show signs of being affected by fluids from mid Cretaceous or later volatile granites. These signs may include high fluorine in water or sediment, presence of minerals such as sericite, fuchsite and tourmaline, phlogopite and other micas that may be sinks for volatile elements. Searching for combinations of serpentinite and fluorite or ultramafic and tourmaline in MINFILE does provide a few hits of interest.

Such prospective associations are supported by the association of emeralds in Pakistan with listwanites, occurring with greenish fuchsite and chrome-rich dravite tourmaline in talc-chlorite schists (Arif, Fallick and Moon 1996).

A YUKON PERSPECTIVE

The Regal Ridge emerald prospect, in the Finlayson district of the Yukon, occurs in mica schists within a metavolcanic unit that is underlain by ultramafics. Both form the roof to an underlying Cretaceous pluton that is part of the mid-Cretaceous Anvil suite. The emerald is found in quartz veins enveloped by tourmaline zones. Groat et al. (2002) note that the prospect is enriched in tungsten (scheelite) and several tungsten skarns are associated with the Anvil suite. The emeralds form in a halo of quartz veining and alteration which extends from the roof of the granite.

The Regal Ridge showing suggests B.C. has potential for emeralds within the veneers of ultramafic rocks and metavolcanics underlain by volatile granites.

Phlogopite schist and skarn host the Lened showing. The phlogopite schist interestingly represents the alteration of adjacent black shales and not ultramafics. Emeralds are found in the quartz veins which cut the skarn (Falck, 2003) and also apparently within the phlogopite schist (Groat et al., 2002). The showing is near tungsten mineralisation within a two-mica pluton, a member of the Selwyn suite. The Lened showing indicates Road River Group shales may be prospective in B.C.

EMERALD POTENTIAL MAP

The emerald potential map is based on the concept that intersects of volatile granites and ultramafics offer the most prospective target for emeralds in B.C. Ultramafics are known to be chrome-bearing and are generally well defined in areal extent. Phlogopite schists, related to ultramafics, are the most common host for emeralds worldwide and thus offer the best opportunity for exploration success. Mineral pathfinders can be drawn from MINFILE and include beryl, other beryllium bearing minerals, fluorite, tourmaline, tungsten, tin, niobium, pegmatite, and chromite. Molybdenum was omitted as it provides a wide scatter and the relationship to tungsten is similar and is geochemically more direct. Very few MINFILE occurrences (3) record lithium minerals such as lepidolite and spodumene. Symbols were chosen that would nest within each other so that sets of association are more easily displayed. Intrusives were subdivided by age. At present only Cretaceous and younger intrusions are plotted, as well as Proterozoic age intrusions related to miogeoclinal rocks at the margin of ancestral North America.

The main area of interest is the Omineca belt which is underlain by continental crust fragments welded by post collisional plutonic suites of a continental magmatic arc that extends along a 1600 kilometre belt into the Yukon. Logan (2002, 2002a) describes intrusive-related metallogenic characteristics of this belt.

In British Columbia dismembered ophiolitic assemblages are present in the Cassiar, Manson, Barkerville and Greenwood-Rossland areas (Ash, 2000). These are the displaced and eroded remnants of the oceanic Slide Mountain terrain.

Discrete ultramafic bodies form a relatively small part of these large klippe-like areas within the Omineca belt. There are nevertheless several juxtapositions of ultramafic bodies and volatile-bearing granites evident on the emerald potential map. Several of these are in areas of little exploration activity. One surprise in the East Kootenays is a little known ultramafic body cut by a border phase of the beryl prospective White Creek batholith.

Though the Atlin area lies in the Intermontane belt it is included as it represents a major intersect of ultramafic rocks of the Cache Creek terrain and mid Cretaceous intrusives.

Areas further to the west also appear to be locally prospective on the basis of associations of beryl, tungsten and tin. Pell (1990) in fact suggested volatile-rich granites might be found anywhere Sr87/86 ratios exceeded 0.704. However they are outside the scope and focus of the present overview.

The areas touched upon in this report include Surprise Lake batholith and the Cassiar batholith near the Yukon border (Figure 2). This area of interest expands on the area described as a potential beryl/emerald camp straddling the B.C./Yukon border (Neufeld et al., 2002, figure 1).

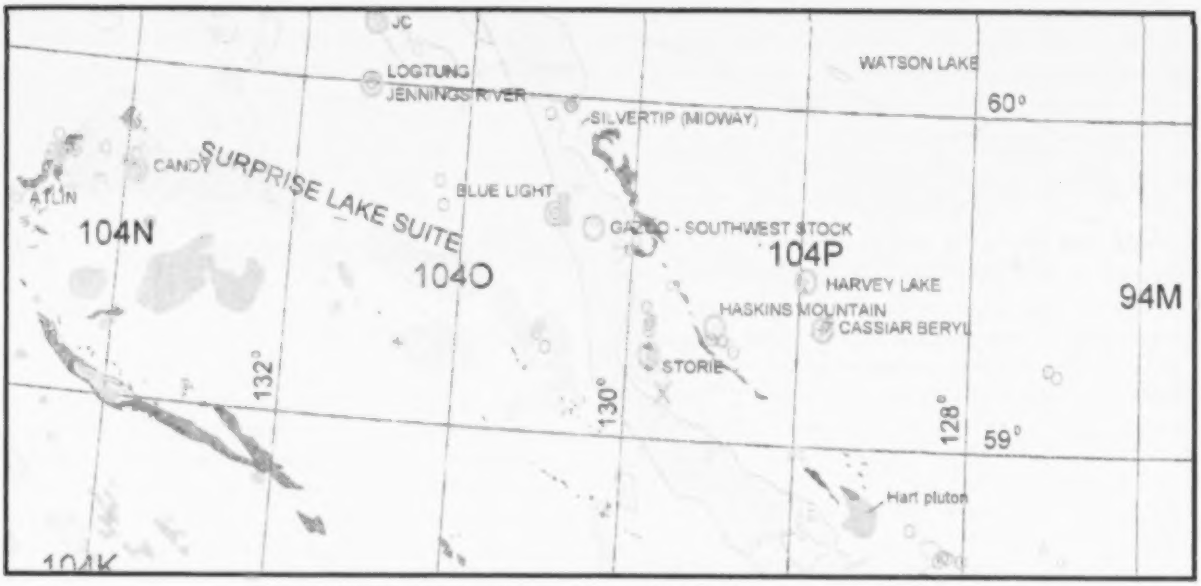

Figure 2: Northern Portion of Emerald Potential Map (NTS 104N, 104O, 104P)

LEGEND

- Pegmatite
- Tourmaline
- Fluorite
- Topaz
- Tungsten
- Tin
- Chromite
- ○ Beryl
- Danalite-Helvite
- ○ Niobium

Plutons
- Mid Cretaceous
- Late Cretaceous
- Early Tertiary

Ultramafic rocks

SURPRISE LAKE BATHOLITH

The Surprise Lake batholith is an equigranular and miarolitic alaskite of Late Cretaceous age. It is host to numerous showings that include tungsten, tin and fluorite. The volatile character of the intrusion is evidenced by the presence of up to 15 % topaz in sheared alaskite at the southern contact of the intrusion (MINFILE 104N 086 Dixie). According to Littlejohn and Ballantyne (1982) an F-rich phase deposited Li-mica, cassiterite, beryl, wolframite, fluorite, arsenopyrite and columbite-tantalite in small pods within roof rocks.

The Surprise Lake batholith intersects ultramafic bodies that are part of Cache Creek ophiolitic complex on its north and west margins. Many large ultramafic roof pendants are also present and are outlined in a map of the batholith (Bloodgood et al., 1989). There are several ultramafic bodies that also border the separate body known as the Mt. Leonard stock. In terms of a griesen model for emeralds there are associations of fluorite with serpentinite and tin/tungsten mineralisation at the south end of the Leonard stock (for example MINFILE 104N 069 Silver Diamond) that merit ground re-examination for beryl.

Beryl is found in the vicinity of Mt. Weir. The area is near the apex of the batholith. Showings include:

- Beryl-quartz veins associated with wolframite or molybdenite-bearing host rocks near Zenazie Creek north of Mt Weir.
- Beryl with fluorite and sphalerite in mafic dikes cutting alaskite near Caribou Creek (Schroeter, 1978).
- Danalite in mafic dikes northeast flank of Mt. Weir (Schroeter ibid).

Gem topaz and beryl in miarolitic cavities in the area reported by Wilson (1997) may be related to the Surprise Lake batholith or a peripheral body.

The Mt. Leonard alaskite hosts a tungsten-molybdenum deposit (Adanac). Any distal wolframite-quartz veins on the periphery of the Adanac porphyry should be scrutinized for beryl. If this halo of veins extends to areas of ultramafic exposure, chrome beryl may be present.

Ballantyne and Littlejohn (1982) mention the lack of a pegmatite phase associated with the Surprise Lake batholith. Some references in Christopher (1980) and MINFILE 104N 066 (Candy) do indicate local pegmatite development and thus rare element pegmatite of the LCT or NYT class may be present together with beryl.

NORTHERN CASSIAR BATHOLITH

This batholith varies from granodiorite to granite in composition and is principally of mid-Cretaceous age.

The intrusive phases of interest for beryl are known as the young Cassiar granites and are of Late Cretaceous age. They are principally peripheral bodies (Kuhn, Lamb Mountain, Contact) or internal phases (Storie, Troutline) that are fluorine-rich, with associated tungsten and molybdenum mineralisation, as well some silver-lead-zinc veins (Bradford and Godwin 1988). Some are known to carry beryl. For example, Pantaleyev (1980) reports rare vuggy quartz veins with green beryl associated with quartz porphyries at the Storie molybdenum deposit. Beryl with quartz veins is also associated with a late quartz monzonite stock intruding the main batholith at Toozaza Creek (Kyba, 1978). There is some pegmatite here as well.

POSSIBLE EXPLORATION TARGETS

A cryptic intrusion, a member of this suite, is invoked as responsible for fluorine-rich, sericitic alteration in Sylvester rocks near the Midway deposit and the presence of topaz-bearing quartz porphyry dikes at the deeper levels of the deposit (Bradford and Godwin, 1987). The interpretation of an intrusive body is supported by aeromagnetic surveys. In the presence of Be-bearing solutions the large alteration halo in Sylvester roof rocks may include a griesen-style emerald deposit. This is an obvious target for ground scrutiny, including baseline stream sediment sampling for beryllium.

The Eocene Mount Haskin and Mount Reed stocks cut Cassiar platformal rocks but are near the Sylvester contact. They are bordered by skarns and reported to carry beryllium minerals (personal communication D. Hora). Tourmaline coats fractures of the leucogranite of Mount Haskin stock and fluorite with phlogopite, molybdenite and scheelite is noted at Mt Reed. Any signs of Eocene intrusive activity in Sylvester rocks immediately to the west should be investigated.

Further to the south in the Cry Lake sheet much of the Sylvester allocthon is in direct contact with batholithic Cassiar rocks. In this area the leucocratic Hart pluton of Eocene age cuts ultramafics of the allochthon and fluorite is noted at the contact (Gabrielse 1998).

Gabrielse (1963, p. 88) mentions granite-pegmatite dikes with quartz, muscovite, potash feldspar, biotite, minor tourmaline and garnet cutting metamorphosed rocks of the Sylvester Group northwest of Blue River. They should be examined to further assess distribution, mineralogy and contact effects.

PART 2: FIELDWORK RESULTS

HELLROARING CREEK BODY

GEOLOGIC SETTING

The Hellroaring Creek pegmatite is an intrusion of middle Proterozoic age (1365 +- 3 Ma, J. Mortensen, unpublished data) that outcrops on a ridge between Hellroaring and Angus Creeks, about 4 kilometers south of St. Mary Lake and 18 km southwest of the town of Kimberley B.C. The intrusive body, up to 1000 metres wide and about 4 kilometres long is oriented along a northwest axis. It intrudes a Lower Aldridge sequence of rusty siltstones with abundant sills of Moyie gabbro (Figure 3). The east-striking St. Mary fault extends across Angus Creek and truncates the south end of the intrusion. A 50-foot- wide exposure of massive quartz is probably a vein that plugs the fault. The St. Mary fault is offset by an acute angled fault such that pegmatite reappears to the south, separated from the northern mass by a fault wedge of Creston Formation. The pegmatite is then truncated again by the continuation of the St. Mary fault.

The intrusion lies at the core of a faulted domal structure and sediments and Moyie sill dip away from the intrusion on its flanks.

The northeast flank of the intrusion is linear and marked in one exposure by a quartz vein at least 4 metres wide in sharp but undulating contact with pegmatite. The vein is believed to plug a fault. A sequence of faults is interpreted to define a down-dropped block on the northeast flank.

In the northwest corner the intrusive contact of the main body dips steeply at about 60 degrees and is bordered by a series of moderately dipping sills within Aldridge sediment. Similar relationships are seen elsewhere on the flanks of the main body.

The trace of the main pegmatite on the southwest flank varies from conformable to crosscutting relationships with the host sequence of Moyie sills and Aldridge sediment. Bedding dips and cleavage development suggest folding in Aldridge sediments. The trace of the contact is subparallel to axial plane cleavage.

The contact on the eastern flank of the body has a large indentation. Moyie Sill outcrops within this "embayment" and there is a v-shaped area of Aldridge sediments dipping at moderate to high angles. Pegmatite

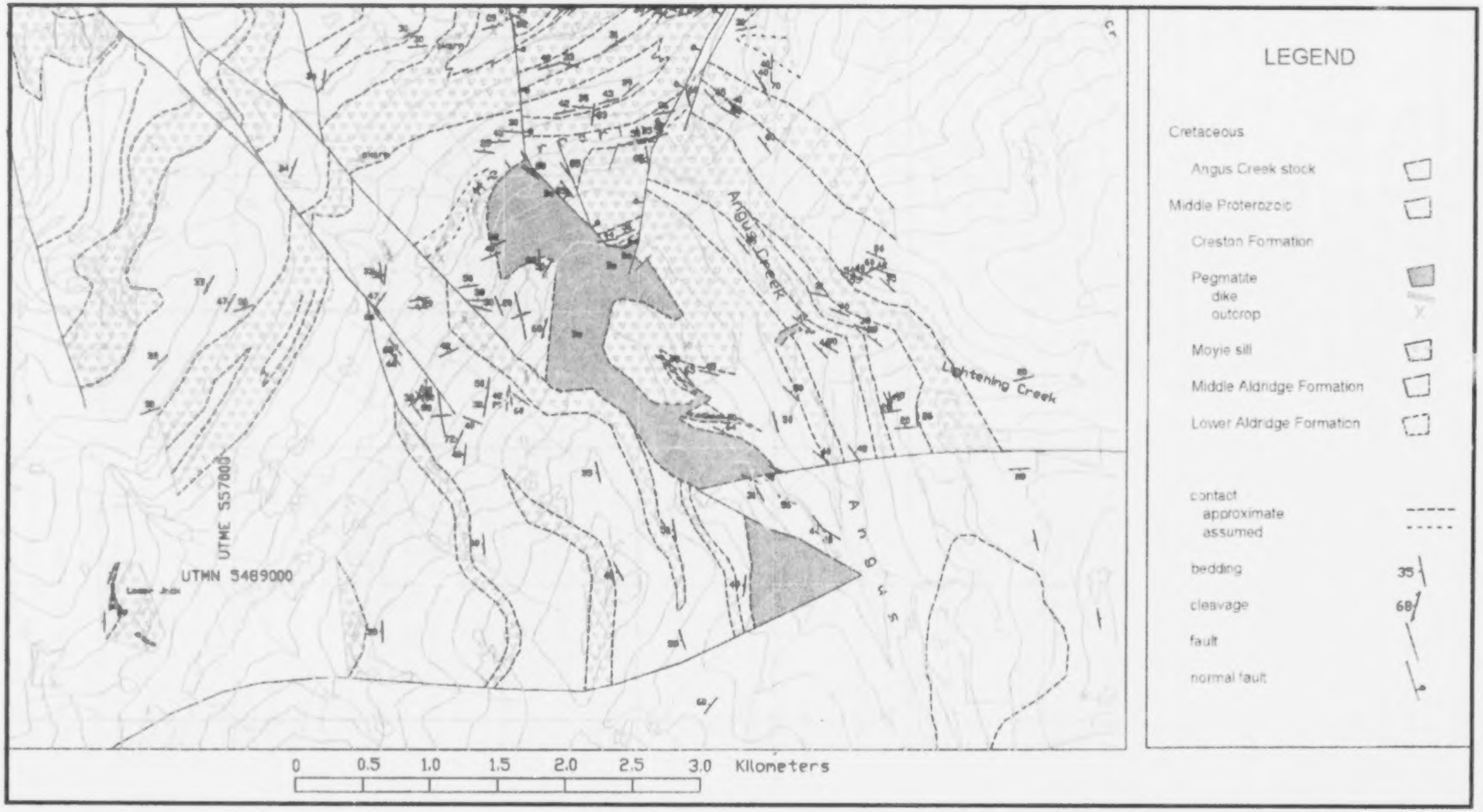
LEGEND
Cretaceous
Angus Creek stock
Middle Proterozoic
Creston Formation
Pegmatite
dike
outcrop
Moyie sill
Middle Aldridge Formation
Lower Aldridge Formation
contact
approximate
assumed
bedding
35
cleavage
68
fault
normal fault
Angus Creek
Lightening Creek
Angus
UTME 557000
UTMN 5489000
0
0.5
1.0
1.5
2.0
2.5
3.0
Kilometers

Figure 3: Geology Map, Hellroaring Creek pegmatite.

sills and wide dikes cut the sequence. The dikes probably connect to the main body of the pegmatite. The embayment suggests a roof zone but the metamorphic effects are less than would be expected in a roof zone. More work is required to define the geometry. One geometric hypothesis is the presence of a steeply plunging fold.

SATELLITIC BODIES

Scattered small dikes and sills occur up to three kilometers from the main body but their extent and orientation is unclear due to poor exposure. A few have been traced for several hundred metres. A small "plug" is only partially exhumed along a tributary to Angus Creek (Lightening Creek). In the valley walls a lower "bench" of pegmatite is mantled by contorted and schistose Aldridge Formation.

Small folds immediately adjacent to dikes appear to be related to intrusion and plastic deformation of wallrock.

Pegmatites are bordered by either Aldridge sediments or Moyie sills. Some pegmatites have clearly intruded along the contact between sills and Lower Aldridge sediments.

There is insufficient data to deduce if there is a geometric pattern to the distribution of dikes and sills.

COMPOSITION

The Hellroaring pegmatite is composed of albite, microcline, quartz, muscovite, tourmaline with very minor garnet and beryl. Most of the main body is alaskite granite with hypidiomorphic granular texture. Concentrations and aggregates of muscovite, tourmaline and quartz occur locally. Tourmaline is commonly developed in wall rocks immediately adjacent to pegmatite. The fabric of the pegmatite may be locally complex with varying intergrowth fabrics, local mineral aggregates, coarser crosscutting pegmatitic phases, irregular quartz veins and masses. Stockscheider fabric (minerals oriented normal to cooling margins) is evident at some dike margins, borders of rafted metasediments, and internal to the pegmatite.

The main body does is not strongly zoned as the same principal mineral phases appear in various parts of the main body but in different proportions. White (1987) suggested a microcline-rich graphic granite phase dominates the north end of the body. Although it dominates a few outcrop areas graphic granite does not form a distinctive body. Whole-rock analytical data ($Na2O$ and $K2O$) does suggest a separation of albitic and potassic phases in the intrusion.

Grain size varies in a striking manner. Muscovite books up to 20 cm across are seen in the Lightening Creek body and quartz and feldspar crystals of the same size occur in a large outcrop area on the northwest side of the main pegmatite body. Tourmaline occurs as large globular masses, also as needle rosettes, and isolated large barrel crystals.

Some pegmatites exhibit microbrecciation together with fine greenish sericite alteration. Others show weak foliation and augen feldspars in a texture of cataclasis.

Quartz veins bordered by thin pegmatite possibly plug minor faults near the contact of Moyie sills and Aldridge sediments.

A small area of skarn adjacent to a pegmatite sill is present on the north side of Hellroaring creek. It is rich in garnet with grey wollastonite. Fluorescence under UV suggests the presence of scheelite. Other skarns, possibly forming a northern arc, are noted in Anderson (1999).

BERYL IN THE HELLROARING CREEK BODY

Beryl occurs as sparse clusters of hexagonal prisms or as single crystals in the northern part of the Hellroaring Creek body. Crystals about a cm wide and 5 or more centimeters long are typical. A 15 cm long dihexagonal crystal is exposed in a pegmatite on the northwest side of the main body. The crystal is white with a very pale patchy bluish hue. Elsewhere very pale whitish-green crystals occur as well as crystals which are more or less translucent. Completely opaque crystals are common.

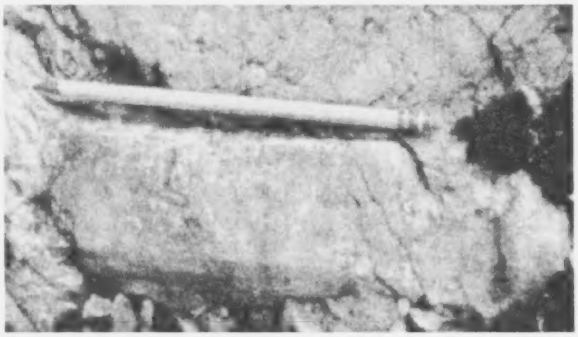

Photo 1: Large crystal of beryl imbedded in Hellroaring Creek pegmatite; pencil for scale.

Two sills peripheral to the Matthew Creek body and a distal sill (Lower Jack) to the main Hellroaring body are enriched in beryl. The Lower Jack pegmatite has a quartz core and is poor in tourmaline. Pale beryl (1 by 5 cm) occurs with quartz and coarse booklets of mica near the enlargement of the sill and its quartz core. Beryl in a sill peripheral to the Matthew Creek pegmatite occurs in an encrusting quartz-poor phase that mantles deformed schistose rafts of Aldridge sediments near the base of the sill. The beryl crystals form a crude arc above the raft. Simple prisms are present with rounded terminations and some crystals appear corroded against matrix.

The beryl of the Hellroaring Creek body is not of gem quality. However, it is not uniformly opaque either and shows variations in crystal development, size, hue and translucence. There is a small potential to discover gem beryl.

LAIB CREEK

The area of the OMG claims on the west side of Kootenay Lake corresponds to an apophysis of the Bayonne batholith that extends up Laib Creek valley and is not shown on the regional map of Reesor (1996). A few days were spent in the area tracing an intrusive-sediment contact on the claims. The main showing consists of the face of a large boulder with beryl crystals in random orientations. The crystal encrusted face may represent one wall of an original fissure vein. The matching wall may be present in other nearby plucked boulders in the lee of an outcrop knob (roche moutonee). The beryl crystals are greenish blue with many hairline fractures. A candy-strip banding normal to the crystal axis is evident with opaque bands and translucent bands alternating.

Elsewhere bluish beryl crystals are widely scattered within a white muscovite granite and crosscutting coarser pegmatite. The pegmatite may contain crystal masses of quartz and mica up to 25 cm diametre. The density of beryl crystals is extremely low, on the order of one per tens of metres in the muscovite granite. Often smoky quartz is associated with this phase and a bit of garnet occurs as small euhedral crystals. In the area of interest muscovite granite contains blocks of biotite granodiorite but also grades into this phase.

Host rocks are metasediments of the Proterozoic La France Group. These vary from phyllitic to schistose shales to more medium bedded quartzose sandstones. A few mafic sills occur in the sediments and they may be the source of a few amphibolitic rafts in the granite.

Traversing from valley floor upwards onto valley slopes the transition is from intrusive rock with abundant raft material into lit par lit alterations of granite and sediments and then into sediment. The Omg claims cover an area where an apophysis of the main batholith is apparently unroofed and exposed along the valley bottom.

The general presence of disseminated beryl in the Bayonne batholith is encouraging. Further work in this area should look for and prospect small satellite intrusions within the sediments outside the main batholith.

DORTATELLE CREEK

The site was visited to examine its emerald potential within juxtaposed volatile granites and chrome bearing ultramafics. The ultramafics are part of a chain of Alaskan ultramafic complexes on the east side of the Intermontane belt near the Ingenika fault. Potential volatile granites include the Davie Creek (Kliyul) molybdenum bearing body found a few miles to the east (MINFILE # 094D 113). It may be Cretaceous in age. The Dortatelle showing is described as hosted in a pegmatite block in moraine (Lord, 1948). Pegmatites are inferred to outcrop nearby and other showings of molybdenite and chromite are noted in the vicinity. Abundant white quartz blocks with molybdenite, and pink granitic debris were located within the moraine. Nearby exposures of serpentinised ultramafics contain chrome mica. The granitic debris is sparse and in strong color contrast to the overwhelming dominance of Takla greenstone and ampibolite in moraine aprons and ridges. No granite or pegmatite outcrops occur in the valley despite abundant outcrop exposures in glacial valley walls and creek ravines. The beryl-bearing block mentioned in the report (Lord, 1948) was not found. This is perhaps not surprising given the extensive boulder fields that comprise moraine aprons and ridges.

The train of granitic debris upslope in the moraine tongue suggests a source from glacial ice that overrode the ridge (or a source that underlies the remnant glacier and obscures bedrock). A traverse was conducted into the adjacent valley into an area of granitic outcrop behind the glacier. Stream sediment samples were taken and submitted for analysis.

Analytical results show very low values of beryllium are present. The conclusion is that the source of beryl mineralisation is not local to the valley.

SUMMARY AND CONCLUSIONS

Beryl is an under-prospected mineral in B.C. Exploration for emerald may complement re-evaluation of alteration halos of granophile tungsten-molybdenum prospects in the vicinity of ultramafic bodies. The Yukon discoveries suggests tungsten showings in the vicinity of ultramafic bodies at Horseranch Range and elsewhere should be revisited.

Exploration for emerald requires a different strategy than aquamarine as it depends on wall rock for an immediate source of chromium or vanadium.

The intersection of ultramafics and volatile granites, together with pathfinder elements, on an emerald exploration map suggests prospecting targets. Discoveries of phlogopite schist zones peripheral to small tourmaline or fluorine-bearing granitic bodies or pegmatite are of prime interest. Griesen alteration of ultramafics, presence of tourmaline, sericite, margarite or fuchsite in altered ultramafics or high fluorine in waters draining areas of ultramafic rocks may be a lead to emeralds, particularly if stream sediment analysis can also demonstrate elevated values of beryllium.

The light coarse fraction of stream sediment in placer areas near altered ultramafics and potassic Cretaceous granites should be examined for beryl.

Field examinations were completed at the Hellroaring Creek, Laib and Dortatelle Creek localities. The Laib occurrence deserves further work. The Hellroaring Creek body is judged to have low potential to discover gem beryl. Further work is necessary to establish if the source of Lord's 1948 pegmatite block can be located.

ACKNOWLEDGMENTS

The support of the Rocks to Riches Program of the BC & Yukon Chamber of Mines is gratefully acknowledged as well as support of manager Brian Grant. Eric Lalande provided cheerful and responsible assistance to the author in the summer. Ray Lett happily responded to numerous investigative queries of RGS data. Dave Pighin provided geologic maps that were incorporated in mapping the Hellroaring Creek body. Nick Massey provided data files for the emerald potential map. Jarrod Brown directed the writer to relevant literature on pegmatites.

REFERENCES

Anderson, D. (1999): Geologic and Prospecting Assessment Report on the Horn Claims, B.C. Ministry of Energy, Mines and Petroleum Resources, Mineral assessment report 25976.

Anderson, D. (2001): Diamond Drilling Assessment Report on the Horn/Beryl Claims; B.C. Ministry of Energy and Mines, Mineral assessment report 26501.

Arif, M., Fallick, A.E. and Moon, C.J. (1996): The genesis of emeralds and their host rocks from Swat, northwestern Pakistan: a stable-isotope investigation, Mineralium Deposita 31, p. 255-268.

Ash, C. (2001): Relationships Between Ophiolites and Gold-Quartz veins in the North Americain Cordillera; B.C. Ministry of Energy and Mines, Bulletin 108, 140 p.

Ballantyne, S.B. and Littlejohn, A.L. (1982): Uranium Mineralization and Lithogeochemistry of the Surprise Lake Batholith, Atlin, British Columbia *in* Uranium in Granites, edited by Y.T. Maurice, G.S.C. Paper 81-23, p. 145-155.

Banks, D.A., Guilani, G., Yardley, B., and Cheilletz, A. (2000): Emerald mineralisation in Columbia: fluid chemistry and the role of brine mixing; Mineralium Deposita, vol. 35, pages 699-713.

Bloodgood, M.A., Rees, C.J. and Lefebure, D.V. (1989): Geology of the Atlin Area (104N/11W, 12E); B.C. Ministry of Energy, Mines and Petroleum Resources, Open File 1989-15.

Bradford, J.A. and Godwin, C.I. (1988): Midway Silver-lead-zinc Manto Deposit, Northern British Columbia (104o/16), B.C. Ministry of Energy, Mines and Petroleum Resources, geological Fieldwork 1987, Paper 1988-1, p 353-360.

Brinck, Johan and Hofmann, Albert (1964): The Distribution of Beryllium in the Oslo Region-Norway-A Geochemical Stream Sediment Study; Economic Geology, vol. 59, pages 79-96.

Brown, G. (1984): Australia's first emeralds, Journal of Gemmology, vol. 19, pages 320-335.

Burt, D.M. (1982): Minerals of Beryllium *in* Short Course in Granitic Pegmatites in Science and Industry; Mineralogical Association of Canada, Short Course Handbook 8, pages 135-148.

Cerny, P. (1991): Rare-element Granitic Pegmatites Part1 Anatomy and Internal Evolution of Pegmatite Deposits; Geoscience Canada, vol. 18, no. 2, pages 49-67.

Christopher, P.A. (1980): Mt. Leonard Boss - Surprise Lake Batholith; B.C. Ministry of Energy, Mines and Petroleum Resources, Geological Fieldwork 1979, Paper 1980-1, p.75-79.

Fuertes-Fuente, Mercedes and Martin-Izard, Agustin et al.. (2000): P-T Path and Fluid Evolution in the Franqueira Granitic Pegmatite, Central Galicia, Northwestern Spain; The Canadian Mineralogist, Vol. 38, pp. 1163-1175.

Gabrielse, H. (1998): Geology of Cry Lake and Dease Lake Map Areas, North-Central British Columbia, Geological Survey Of Canada, Bulletin 504, 147 p.

Gabrielse, H. (1963): McDame Map Area, Cassiar District, British Columbia; Geological Survey Of Canada, Memoir 319, 138 pages.

Gauthier, Guylaine and Dixon, Kathleen, P. (1997): Slocan Valley Gem Project, B.C. Ministry of Energy and Mines, Mineral assessment report 25032.

Groat, Lee et al.. (2002): Mineralogical and Geochemical Study of the Regal Ridge Emerald Showing, Southeastern Yukon, The Canadian Mineralogist, vol. 40, pp.1313-1338.

Guilani, G., Silva, L. and Couto, P. (1990): Origin of emerald deposits of Brazil; Mineralium Deposita, vol. 25, pages 57-64.

Holland, S.S. (1956): Cassiar Beryl; British Columbia; B.C. Ministry of Energy, Mines and Petroleum Resources, Minister of Mines Annual Report - 1955, pages 9-10.

Kyba (1978): Geological and Geochemical Report 6A200 Mineral Claims; B.C. Ministry of Energy and Mines, Mineral assessment report 7148, 72p.

Logan 2002: Intrusion-Related Gold Mineral Occurrences of the Bayonne Magmatic Belt; B.C. Ministry of Energy and Mines, Geological Fieldwork 2001, Paper 2002-1, p. 237-246.

Logan 2002a: Intrusion-Related Gold Mineral Occurrences of the Bayonne Magmatic Belt, Southeast British Columbia; B.C. Ministry of Energy and Mines, Geoscience Map 2002-1.

London, D. (1995): Geochemical Features of Peraluminous Granites, Pegmatites, and Rhyolites as Sources of Lithophile Metal Deposits in Magmas, Fluids, and Ore Deposits, Mineralogical Association of Canada Short Course Series, vol. 23, p. 175-202.

Lord, C.S. (1948): McConnell map-area, Cassiar district, B.C.; Geological Survey of Canada, Memoir 261.

Mulligan, R. (1966): Metallogenic Map, Beryllium in Canada, Geological Survey of Canada, "A" Series Map, 1218A, 1966.

Neufeld, H., Groat, L. and Mortenson, J. (2003): Preliminary investigations of emerald mineralization in the Regal Ridge area, Finlayson Lake District, southeastern Yukon *in* Yukon Exploration and Geology 2002, D.S. Emond and L.L. Lewis (eds.), Exploration and Geological Services Division, Yukon Region, Indian and Northern Affairs Canada, p. 281-284.

Pell, J. and Hora, Z.D. (1990: High-Tech Metals in British Columbia, B.C. Ministry of Energy and Mines, Information Circular 1990-19, 27p.

Pezzotta, F. and Simmons, W.B. editors (2001): Field Course on the Rare Element Pegmatites of Madagascar, Technical Program and Field Trip Guidebook, Mineralogical Society of America,

www.minsocam.org/MSA/Special/Pig/PIG_articles/Madagascar_txt.pdf

Plint, H.E. Metamorphism, deformation, uplift and their tectonic implications in the Horseranch Range, north-central British Columbia; unpublished Ph.D. thesis, University of Alberta, Edmonton, Alberta.

Reesor, J.E. (1996): Geology, Kootenay Lake, British Columbia; Geological Survey of Canada, Map 1864A.

Schroeter, T. (1978): West-Central and Northwest British Columbia; in Geological Fieldwork 1977, Open File 1979-1, p 8,9.

Schwarz, D. and Guilani, G. (2001): Emerald Deposits - a Review; The Australian Gemologist, v. 21, p. 17-23.

Siems, Peter L. (1984): Hydrothermal Alteration for Mineral Exploration Workshop, Lecture Manual, Department of Geology, College of Mines and Earth Resources, University of Idaho, 580 p.

Simandl, G.J. (1999): Schist-hosted Emeralds; in Selected British Columbia Mineral Deposit Profiles, Volume 3, Industrial Mineral Minerals, G.J. Simandl, Z.D. Hora and D.V. Lefebure, Editors, British Columbia Ministry of Energy and Mines, Open File 1999-10.

Simandl, G.J, Payie, G. and Wilson, B. (1998): Blue Beryl/Aquamarine Occurrences in the Horseranch Range, North Central British Columbia (NTS 104P07, 10), Geological Fieldwork 1997, Paper 1998-1, p 25-1 to 25-9.

Soloviev, Serguei (2001): Diamond Drilling Report, Peg Property; B.C. Ministry of Energy and Mines, Mineral assessment report 26701.

Walton, L. (1996): Exploration Criteria for Gemstone Deposits and their Application to Yukon Geology; Indian and Northern Affairs, Open File 1996-2.

White, G. (1987): Hellroaring Creek Pegmatite, B.C. Ministry of Energy and Mines, Exploration in B.C. 1987, pp B109-B116.

Wilson, B.W. (1997): Gemstone occurrences in British Columbia, Canadian Gemmologist, 18(3), p. 74-86.

Wilson, Bradley S. (1998): Report on the Exploration of MRX Property, B.C. Ministry of Energy and Mines, Mineral assessment report 25453.

Wengzynowski, W.A. (1999): Report on the Northern Dancer Claim, B.C. Ministry of Energy and Mines, Mineral assessment report 25933.

THE MID-CRETACEOUS ROCKY RIDGE FORMATION – IMPORTANT HOST ROCKS FOR VMS AND RELATED DEPOSITS IN CENTRAL BRITISH COLUMBIA

D.G. MacIntyre[1], R.H. McMillan[1] and M.E. Villeneuve[2]

KEYWORDS

Skeena Arch, Skeena Group, Rocky Ridge Formation, volcanogenic massive sulphide, Eskay Creek, shallow marine, rhyolite domes, geochronology, lithogeochemistry, U/Pb age-dating, Ar/Ar age-dating, Rocks to Riches program

INTRODUCTION

The recognition of remnants of large cauldron subsidence complexes along the trend of the Skeena Arch first occurred in the Tahtsa Lake area (MacIntyre, 1985). In subsequent years, evidence for other large subsidence complexes was documented in the Rocher DeBoule, Babine Mountains, Buck Creek and Babine Lake areas (MacIntyre, 2001; Church and Barakso, 1990). Originally all of these structures were believed to be Late Cretaceous in age based on the ages of nearby plutonic bodies. However, recent isotopic age-dating in the Babine Lake area suggests that the evolution of these subsidence structures began in the mid-Cretaceous with eruption of the Rocky Ridge volcanics and that this volcanism was at least in part submarine in nature (MacIntyre, 2001).

The importance of the Rocky Ridge volcanic succession of the Lower Cretaceous Skeena Group as potential host rocks for volcanogenic massive sulphide (VMS) deposits was first recognized while conducting regional mapping and geochronologic dating as part of the Nechako NATMAP project (MacIntyre and Struik, 1999; MacIntyre and Villeneuve, 2001). This work was followed up in the 2000 field season with additional lithogeochemistry and collection of samples for Ar-Ar and U-Pb isotopic age-dating from a number of key sites along the Skeena Arch (Figure 1). Unfortunately, due to budget constraints many of the samples collected for age-dating could not be processed and remained in storage at the Geological Survey of Canada's Ottawa geochronology lab. In 2003, a proposal was submitted to the Rocks to Riches program for funding to process these samples and to collect additional samples from the study area. The project was approved and $30,000 was provided to cover the analytical and field-related costs of the project. This report summarizes the work completed in 2003. Additional background information on the project is covered in MacIntyre (2001).

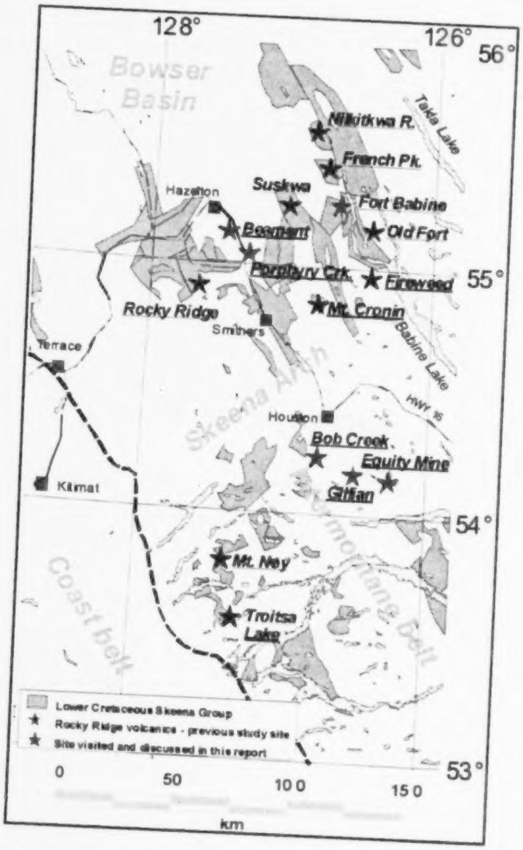
128°
126°
56°
55°
54°
53°
Bowser Basin
Nilkitkwa R.
Takla Lake
French Pk.
Hazelton
Suskwa
Fort Babine
Old Fort
Porphyry Crk.
Fireweed
Rocky Ridge
Smithers
Mt. Cronin
Terrace
Babine Lake
Skeena Arch
HWY 16
Houston
Bob Creek
Equity Mine
Kitimat
Gilfan
Mt. Ney
Coast belt
Troitsa Lake
Intermontane Belt
Lower Cretaceous Skeena Group
Rocky Ridge volcanics - previous study site
Site visited and discussed in this report
0
50
100
150
km

Figure 1. Map showing the areal extent of the Skeena Group (solid pattern) in west central British Columbia relative to major tectonic elements. Stars mark sites where Rocky Ridge volcanic rocks of the Skeena Group were sampled as part of this study.

1- consulting geologist, Victoria B.C.; 2 - Geological Survey of Canada, Ottawa, Ont

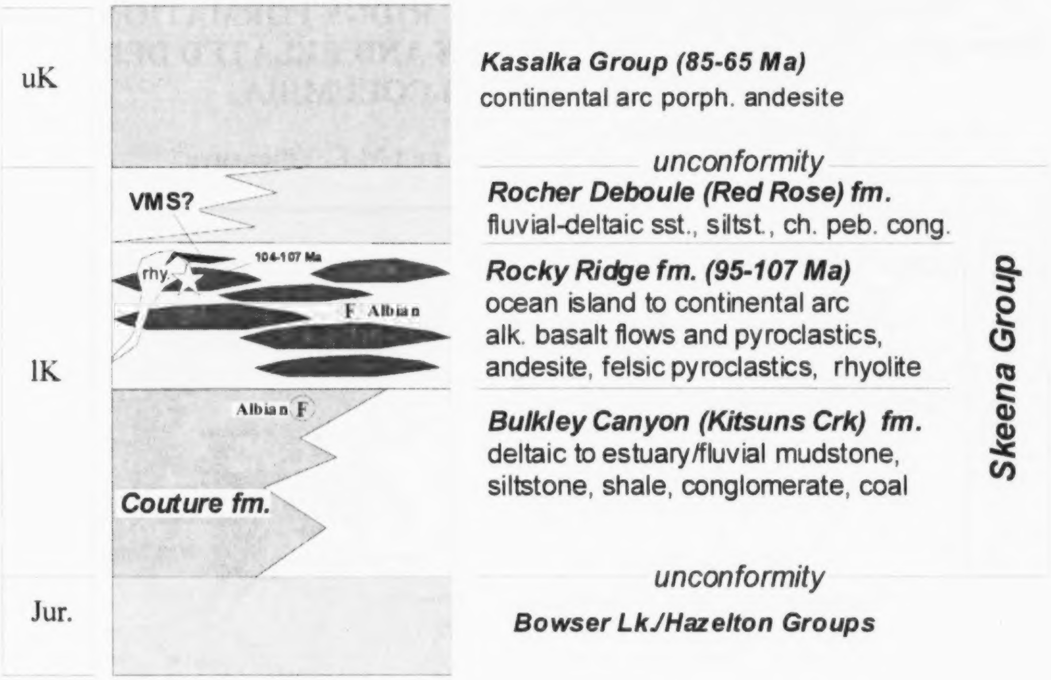
uK
lK
Jur.
Kasalka Group (85-65 Ma)
continental arc porph. andesite
unconformity
VMS?
Rocher Deboule (Red Rose) fm.
fluvial-deltaic sst., siltst., ch. peb. cong.
104-107 Ma
rhy.
F Albian
Rocky Ridge fm. (95-107 Ma)
ocean island to continental arc
alk. basalt flows and pyroclastics,
andesite, felsic pyroclastics, rhyolite
Albian F
Bulkley Canyon (Kitsuns Crk) fm.
deltaic to estuary/fluvial mudstone,
siltstone, shale, conglomerate, coal
Couture fm.
Skeena Group
unconformity
Bowser Lk./Hazelton Groups

Figure 2. Schematic stratigraphy for the Skeena Group showing stratigraphic position of rhyolite domes and Rocky Ridge volcanic rocks discussed in this report. Stratigraphic nomenclature after Bassett and Kleinspehn, 1996). Stratigraphic units of Richards (1990) are shown in brackets.

The main objective of the current project is to define areas underlain by the Rocky Ridge volcanic succession which may have potential for the discovery of additional volcanogenic massive sulphide and related deposits. In order to demonstrate the occurrence of favourable volcanic stratigraphy and associated vein and massive sulphide mineralization within the Rocky Ridge Formation, several key areas were visited and sampled in the 2000 field season. These included Nilkitkwa River, French Peak, Fort Babine, Fireweed, Suskwa River, Mt. Cronin, Beament, Rocky Ridge, Mt. Ney and Troitsa Lake (Figure 1). Samples for geochronology and lithogeochemistry were collected at all of these sites. Follow-up work in 2003, supported by funding from the Rocks to Riches program concentrated on the Fort Babine, Beament, Equity Silver mine, and Bob Creek areas. Dr. Neil Church generously provided additional material for lithogeochemistry from the Gillian and Equity Silver mine properties from his personal mineral property collection.

GEOLOGIC SETTING

The study area is within the Stikine Terrane of the Intermontane geomorphological belt (Figure 1) which is well-exposed along the Skeena Arch, a northeast-trending uplift that forms the southern margin of the Bowser Basin. The core of the uplift exposes volcanic arc assemblages of the Early Permian Asitka, Late Triassic Takla and Early to Middle Jurassic Hazelton groups. Coeval plutonic rocks include the Late Triassic to Early Jurassic Topley and the newly recognized Early to Middle Jurassic Spike Peak intrusive suites (MacIntyre *et al.*, 2001). North of the Skeena Arch, the older volcanic arc rocks are onlapped by marine to non-marine sedimentary strata of the Late Jurassic Bowser Lake and Early Cretaceous Skeena groups; to the south the arch is covered by Tertiary volcanic rocks.

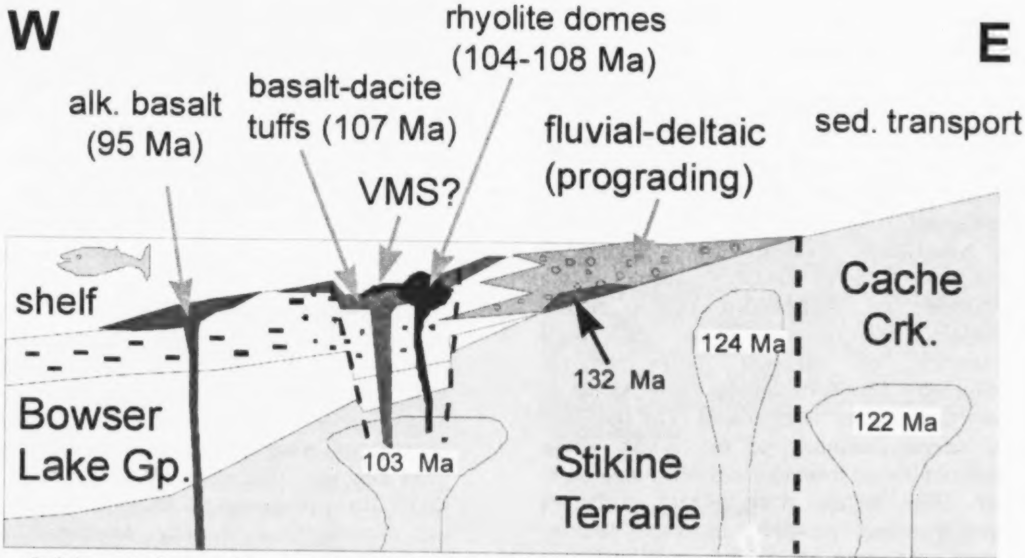

Figure 3. Schematic diagram illustrating the postulated depositional environment for the Skeena Group as suggested by Bassett and Kleinspehn (1996). Also shown are geochronologic controls determined during the Nechako Natmap and Rocky Ridge projects.

SKEENA GROUP STRATIGRAPHY

The Skeena Group is comprised of marine and non-marine sedimentary rocks that overlap Jurassic and older rocks along the southern margin of the Bowser Basin. Although the base of the Skeena Group is rarely seen, where it is exposed it is an angular unconformity with the underlying Hazelton or Bowser Lake group. The Skeena Group is unconformably overlain by continental volcanic arc rocks of the Late Cretaceous Kasalka and Early Eocene Ootsa Lake groups. In general the lower Skeena Group is fluvial to fluvial-deltaic mudstone, siltstone, and sandstone. Higher in the stratigraphy are the volcanic rocks of the Rocky Ridge Formation (Figure 2) as first recognized by Tipper and Richards (1976). Overlying these rocks, and in part interbedded with them, are chert-quartz bearing conglomerates, quartzo-feldspathic wackes and siltstones that were deposited in a fluvial-deltaic environment (Tipper and Richards, 1976; Richards, 1980; 1990; Bassett 1991).

The main Skeena lithologies are dark grey shaly siltstone, greywacke, carbonaceous mudstone and chert-pebble conglomerate. These sedimentary rocks were deposited in a fluviodeltaic, near-shore to shallow marine environment (Basset, 1991). Although fossils are rare, the Skeena Group appears to range from Hauterivian to late Albian or early Cenomanian in age. Paleocurrent measurements indicate north, west and southwest sediment transport with the source area located in the Omineca belt to the east. Bassett and Kleinspehn (1996) suggest that this belt was the main axis of a mid-Cretaceous continental arc and that the Skeena Group is a forearc succession (Figure 3). The Skeena rocks were folded, uplifted and eroded during a mid to late Cretaceous contractional event related to evolution of the Skeena Fold Belt (Evenchick, 1999).

In a recent paper, Bassett and Kleinspehn (1996) proposed a new stratigraphic nomenclature based on lithofacies. In their stratigraphy the lowest unit of the Skeena Group succession is the predominantly deltaic Bulkley Canyon Formation which includes, in the east, the fluvial Kitsuns Creek Member and to the west the subtidal, turbiditic Couture Formation. Locally these rocks are overlain by and in part interbedded with the volcanic arc rocks of the Rocky Ridge Formation, the main subject of this paper. The fluvial to deltaic Rocher Deboule Formation which would include the former Red Rose Formation and Hanawald conglomerate comprises the upper part of the Skeena Group succession.

Rocky Ridge Formation

The Rocky Ridge Formation is comprised of submarine alkali basalt flows, breccias, and lapilli tuffs that were erupted along the southern margin of the Bowser Basin (Bassett and Kleinspehn, 1996) as part of a nascent volcanic arc assemblage. Evidence for a submarine depositional environment includes the occurrence of inter-bedded marine shales, siltstones and conglomerates and local occurrence of pillowed flows. Marine sedimentary inter-beds contain Early Albian to Early Cenomanian macrofossils. The thickness and lateral continuity of the Rocky Ridge Formation varies from thin and discontinuous to over 1000 metres thick. These variations probably reflect proximity to major eruptive centers. At least 5 major mid-Cretaceous volcanic centers have been recognized in central British Columbia. These are located in the vicinity of Old Fort Mountain at Babine Lake, Mt. Cronin in the Babine Range, the Rocher Deboule Range and the Buck Creek and Tahtsa Lake areas. In all of these areas the Rocky Ridge formation is thick, bimodal (basalt-rhyolite), has inter-bedded marine sedimentary beds and displays rapid facies changes consistent with mass movement on unstable escarpments. Numerous base and precious metal mineral occurrences are spatially associated with these suspected cauldron subsidence complexes including classical vein, subvolcanic epithermal and volcanogenic massive sulphide.

One of the key results of the geochronologic dating completed as part of the Nechako NATMAP project was the recognition of mid-Cretaceous rhyolite domes in the Rocky Ridge succession (MacIntyre and Villeneuve, 2001). These domes may be the remnants of submarine cauldron subsidence complexes (MacIntyre, 2001; Tackaberry, 1998). The rhyolite domes were previously mapped as part of the Eocene Babine intrusions (Richards, 1990), but are now mapped as Rocky Ridge Formation because they yield U/Pb and Ar/Ar isotopic ages between 104 and 108 Ma (MacIntyre and Villeneuve, 2001). These ages suggest eruption of the domes occurred during Albian time. Marine sedimentary rocks that are intruded by the rhyolite domes contain Albian macrofossils and abundant angular rhyolite clasts suggesting the domes and sedimentary rocks are coeval. Important epithermal and VMS type mineralization is spatially and most likely temporally associated with development of these felsic volcanic centers.

CURRENT STUDY AREAS

The main focus of this study is to identify the location of Rocky Ridge volcanic centers that may have potential for the discovery of Au-Ag rich volcanogenic massive sulphide and related vein deposits (Figure 1). A preliminary assessment of this area identified several areas with high potential for this type of deposit (Massey, 1999; Massey *et al.*, 1999) and three occurrences were subsequently classified as VMS deposits - Fireweed, Mt. Cronin and the Knoll. These properties all have massive Pb-Zn-Ag mineralization spatially associated with rhyolitic intrusions that are emplaced into marine sedimentary strata of the Lower Cretaceous Skeena Group. The rhyolitic intrusions were previously mapped as Eocene or Late Cretaceous but detailed mapping and isotopic age-dating of rhyolite domes in the Babine Lake area has shown that these rhyolites are part of the mid-Cretaceous Rocky Ridge Formation of the Skeena Group (MacIntyre and Villeneuve, 2001) and are therefore coeval with surrounding sedimentary rocks.

In 2000, the geology and mineral occurrences of the areas shown on Figure 1 were discussed. As part of the current project the Fort Babine, Beament, Bob Creek and Equity Silver mine areas were visited. These areas are underlain by volcanic rocks that are believed to be correlative with the Rocky Ridge Formation. These areas are discussed briefly in this report.

Fort Babine

An east trending, steeply-dipping, fault-bounded panel of Rocky Ridge volcanic rocks is sporadically exposed in clearcuts west of the northern tip of Babine Lake, near Fort Babine (Figure 1). Mapping in this area in 1997 and 1998 suggests a number of rhyolite domes and rhyolite breccia bodies occur within a mixed mafic volcanic and marine sedimentary succession (Richards, 1980, 1990; MacIntyre, 2001a). As at Old Fort Mountain, further to the south, these rocks are believed to be related to formation of a large cauldron subsidence complex in mid-Cretaceous time. Although there are no isotopic age dates available for the Fort Babine section, black shales and siltstones interbedded with mafic and felsic volcanic rocks reportedly contain Albian macrofossils. Based on these fossil ages, the volcanic rocks are mapped as part of the Rocky Ridge Formation.

Due to time and weather constraints, only one day was spent examining exposures in the Fort Babine area. Although there are no known mineral occurrences associated with the Rocky Ridge volcanic rocks at this locality, the occurrence of a felsic component within the volcanic succession is considered evidence for a favourable environment for VMS type deposits. A sample of a porphyritic andesite, typical of exposures in the area was collected and submitted for lithogeochemical analysis (No.2, Table 2). Further prospecting in this area combined with soil and silt sampling might result in new targets for further exploration.

Beament

A south-dipping section of feldspar phyric mafic volcanic rocks that overlie and are in part interbedded with quartzo-feldspathic wacke and chert-bearing heterolithic conglomerate is exposed in a 2 kilometre long road cut north of Beament station on Highway 16 (Photo 1a). The volcanic rocks have been mapped as Late Cretaceous Kasalka Group (Richards 1980, 1990) but are lithologically identical to mid-Cretaceous Rocky Ridge volcanic rocks elsewhere in the area. Sedimentary strata exposed at the north end of the road cut dip to the south and have been mapped as Lower Cretaceous Skeena Group (Photo 1b). The contact with the overlying volcanic rocks appears to be conformable. Although no rhyolitic domes occur in the volcanic succession as they do elsewhere, debris flows underlying the mafic volcanic rocks contain angular rhyolite clasts (Photo 1c), a common lithology found near rhyolite domes in the Babine Lake, Suskwa River and Mt. Cronin localities (MacIntyre, 2001). This is indirect evidence for explosive rhyolitic volcanism in the area prior to eruption of thick piles of alkali basalt flows. This inferred bimodal volcanic succession suggests rocks in the vicinity of Beament may have potential for VMS deposits associated with emplacement of rhyolitic flow domes.

As part of the current study, five samples were collected from strongly altered volcanic rocks exposed along Highway 16 between Porphyry Creek and Beament (Nos. 3-7, Table 2). Additional samples were collected east of the Bulkley River (Nos. 8-9, Table 2). These samples were submitted for lithogeochemical analysis. Although there is an extensive zone of intense phyllic and argillic alteration exposed along the highway and at river level, the age of this mineralization is not certain. Although host rocks are most likely Rocky Ridge volcanic rocks, mineralization may be related to a younger intrusive event. More detailed work is required to resolve the age and genesis of mineralization.

Equity Silver Mine

One of the areas selected for study as part of the current project was the area around the now defunct Equity silver mine. Previous studies suggested that the host rocks at Equity might be correlative with the Skeena Group (Wojdak and Sinclair, 1984; Church and Barakso, 1990). Also of interest is the idea put forth by Church and Barakso (1990) that Equity and other occurrences in the area are within the Buck Creek basin, interpreted to represent an area of volcanic subsidence (cauldron subsidence complex?). In this area, as observed elsewhere along the Skeena Arch, the history of subsidence and associated volcanic activity may have begun in the mid-Cretaceous with eruption of the bimodal, Rocky Ridge volcanic rocks and emplacement of rhyolite flow domes in a shallow, submarine environment.

The Equity silver-copper-gold-antimony deposit is located 38 kilometers southeast of Houston B.C. (Figure 1). Equity Silver Mines Ltd. ceased milling in January 1994, after thirteen years of open pit and underground production. Production was mainly from the Main Zone and Southern Tail open pits and totaled 2,219,480 kilograms of silver, 15,802 kilograms of gold and 84,086 kilograms of copper, from over 33.8 million tonnes mined at an average grade of 0.4 per cent copper, 64.9 grams per tonne silver and 0.46 gram per tonne gold. The Equity Silver mine was British Columbia's largest producing silver mine (Minfile 93L 001).

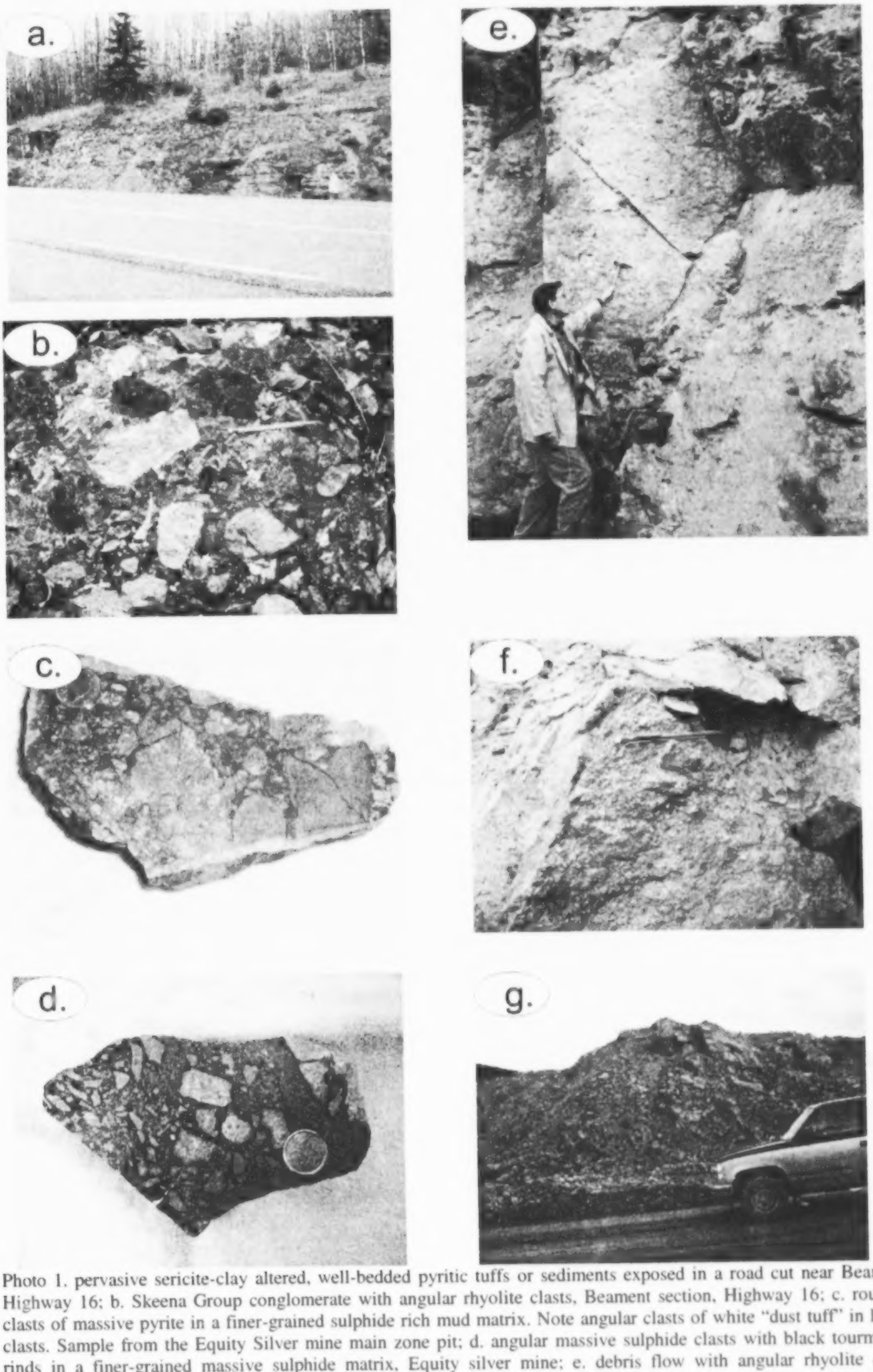

Photo 1. pervasive sericite-clay altered, well-bedded pyritic tuffs or sediments exposed in a road cut near Beament, Highway 16; b. Skeena Group conglomerate with angular rhyolite clasts, Beament section, Highway 16; c. rounded clasts of massive pyrite in a finer-grained sulphide rich mud matrix. Note angular clasts of white "dust tuff" in larger clasts. Sample from the Equity Silver mine main zone pit; d. angular massive sulphide clasts with black tourmaline rinds in a finer-grained massive sulphide matrix, Equity silver mine; e. debris flow with angular rhyolite clasts underlying massive alkali basalt flows, north end of Beament section, Highway 16; f. lense of fragmental massive sulphide (grey) in contact with felsic lapilli tuff, Equity Silver mine, Main Zone pit, west ramp area;g. outcrop off felsic lapilli tuff that was sampled for U-Pb age dating, western ramp, Main Zone pit, Equity Silver mine.

The chief sulphides at the Equity Silver mine are pyrite, chalcopyrite, pyrrhotite and tetrahedrite with minor amounts of galena, sphalerite, argentite, minor pyrargyrite and other silver sulphosalts. The mineralization is generally restricted to tabular, concordant zones comprised of veins, disseminations and massive, coarse-grained fragmental sulphide lenses (Photos 1c, 1d, 1f). Alteration assemblages are characterized by advanced argillic clay minerals, chlorite, specularite and locally sericite, pyrophyllite, andalusite, tourmaline and minor amounts of scorzalite, corundum and dumortierite. Other zones of mineralization include copper-and molybdenum in a quartz stockwork in and adjacent to the quartz monzonite stock and a large zone of tourmaline-pyrite breccia located to the west and northwest of the Main zone. For a more complete description of the Equity deposit go to Cyr *et al.*, (1984) and Wojdak and Sinclair, (1984).

The Equity orebodies are located within a west-dipping panel of tuffaceous sedimentary, dacitic pyroclastic and andesitic flow rocks that have been variably correlated with the Lower Cretaceous Skeena Group (Wojdak and Sinclair, 1984) and the Upper Cretaceous Kasalka Group (Cyr *et al.*, 1984). Three major stratigraphic units have been recognized. A lower clastic division is composed of basal conglomerate, chert pebble conglomerate and argillite typical of the Lower Cretaceous Skeena Group. Conformably overlying and in part inter-bedded with the lower clastic division is a middle pyroclastic division which consists of a heterogeneous sequence of fine-grained tuff or mudstone ("dust tuff"), felsic, locally welded lapilli tuff and breccia and reworked felsic pyroclastic debris, all of which are typical of the Rocky Ridge Formation. This division hosts the main mineral deposits. The middle division grades conformably upward into an upper sedimentary-volcanic division which consists of tuff, sandstone and conglomerate also typical of the Lower Cretaceous Skeena Group.

The west-dipping panel that hosts the Equity deposit is sandwiched between two younger intrusive bodies. The oldest of these is a small, weakly mineralized quartz monzonite intrusion that has given K-Ar ages ranging from 61.1 to 56.2±2.3 Ma on biotite (Cyr *et al.*, 1984). On the east side, and in part cutting the ore zone, is an unmineralized gabbro-monzonite intrusion that gives Eocene ages around 48 Ma (Cyr *et al.*, 1984).

Bob Creek

The Bob Creek area is located some 20 kilometers due south of the town of Houston. Here, andesitic to rhyolitic tuffs, flows and breccia crop out near the junction of Bob and Buck creeks. The most common unit is a massive tuff breccia with thin intercalations of accretionary lapilli tuff and siltstone. Although these rocks have previously been mapped as Jurassic Hazelton Group, they may actually be correlative with the younger Rocky Ridge Formation.

The main exploration target is a belt of strongly pyritic, intensely sericite-clay altered rocks that are exposed over a distance of 600 metres in the Bob Creek canyon (Minfile 93L 009). Although the intensity of alteration makes it difficult to determine original rock compositions, locally the rocks exposed in the canyon show angular rhyolite clasts suggesting they are mainly volcanic breccias 'and lapilli tuffs. These volcanics are crosscut by quartz-feldspar porphyry dikes and breccias that give Late Cretaceous K-Ar ages. A small Late Cretaceous stock intrudes the volcanics south of the canyon.

One day was spent examining outcrops along the banks of Bob Creek. Although the occurrence of felsic clasts in the volcanic units is reminiscent of units in the Rocky Ridge Formation, there is insufficient information to make a definitive correlation. The age of mineralization is also difficult to determine but could well be Late Cretaceous as suggested by previous workers. The lack of rhyolite domes and marine sedimentary strata would suggest that overall it is unlikely that the Bob Creek occurrence is related to Rocky Ridge volcanism.

GEOCHRONOLOGY

U/Pb and ^{40}Ar/^{39}Ar isotopic-dating in the Babine Lake area of central British Columbia documents a distinct magmatic event at 107-104 Ma (MacIntyre and Villeneuve, 2001). This event involved emplacement of rhyolite domes into submarine volcanic and sedimentary rocks of the Rocky Ridge Formation. The volcanic rocks have yielded a U/Pb age of 107.9±0.2 Ma and an ^{40}Ar/^{39}Ar age of 104.8±1.2 Ma. Several samples of rhyolite were also dated but these did not give publishable ages. However, the data that was obtained is consistent with isotopic ages in the 104-108 Ma range (Mike Villeneuve, personal communication). The rhyolites, which were previously mapped as Eocene, are re-interpreted to be part of a previously unrecognized mid-Cretaceous cauldron subsidence complex (MacIntyre, 2001)

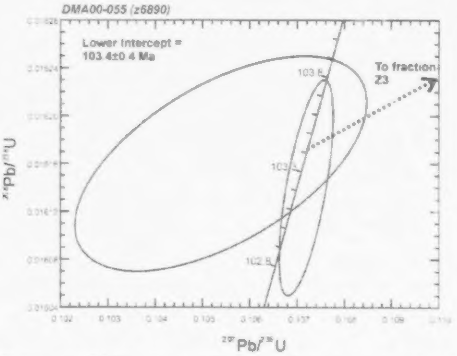

Figure 4. U-Pb concordia plot for zircons extracted from a rhyolite (Sample DMA00-055) intersected in drilling at the Fireweed Property (Minfile 93M 151).

In 2000, samples of rhyolite were collected from the Cronin Mine in the Babine Range and drill core from the Fireweed property at Babine Lake (Malott, 1988; MacIntyre, 2001). These samples were submitted to the GSC geochronology laboratory in Ottawa for U-Pb dating. The sample from the Cronin Mine did not contain sufficient zircons to determine a U-Pb date. However, the Fireweed sample did contain a small number of zircons and these were sufficient to give a lower intercept U-Pb date of 103.4±0.4 Ma (Figure 4). This age indicates that the rhyolite is the same age as marine sedimentary rocks of the Skeena Group, which are the same rocks that are believed to host the massive sulphide lenses on the Fireweed property. Pb-Zn-Ag stockwork veins that cut the rhyolite may be feeders for the massive sulphide lenses. If this interpretation is correct, then the Fireweed deposit can be classified as a typical Kuroko type volcanogenic massive sulphide deposit with a similar geologic setting to the older Eskay Creek deposit (Alldrick, 1995; Hannington, 1999; Roth 2002). As has been documented elsewhere in the Babine Lake area, emplacement of rhyolite domes and dikes occurred during formation of the mid-Cretaceous Old Fort Mountain cauldron subsidence complex (MacIntyre, 2001).

Samples of rhyolite from the Knoll, Rocky Ridge and Troitsa Lake localities were also collected for U/Pb geochronology in 2000 but could not be processed at that time. These samples are currently being processed as part of

TABLE 1. U/PB SAMPLES CURRENTLY BEING PROCESSED AT GSC, OTTAWA

No.	Station	Map	Easting	Northing	Area	Lithology	Comment
1	DMA00-017	93M7	618251	6125954	Suskwa River	rhyolite	dates rhyolite dome at the Knoll property; may be mid-Cretaceous
2	DMA00-050	93L13	596691	6090754	Rocky Ridge	rhyolite	dates large rhyolite intrusion south of Rocky Ridge; may be ring dike to caldera
3	DMA00-042	93E11	607034	5935011	Troitsa Lake	rhyolite	dates rhyolite dike on north shore of Troitsa Lake; may be ring dike to caldera
4	DMA00-043	93E11	612347	5943798	Swing Peak	feldspar phyric andesite	dates Kasalka Group volcanic rocks in the type area of the Kasalka Group; constrains age of underlying Rocky Ridge volcanic rocks
5	DMA03-002	93L1	678330	6008423	Equity Silver mine, Main Zone pit, east ramp	felsic lapilli tuff	dates host rocks at the Equity Silver mine

Notes: UTM zone 9; NAD 83 datum

the current project. This work is being done at the GSC geochronology laboratory in Ottawa, Ontario, Canada under the supervision of Dr. Mike Villeneuve. Results are expected in early 2004. Table 1 lists the samples currently being processed at the GSC Ottawa geochronology lab.

The copper-silver-gold mineralization at Equity has previously been interpreted as epigenetic in origin, possibly related to emplacement of a nearby quartz monzonite stock of Early Tertiary age. This conclusion was based on coincident K-Ar age dates for the quartz monzonite and sericitized tuffs hosting the deposit, all of which give early Tertiary ages around 58 Ma (Cyr *et al.*, 1984). However, given that the host rocks at Equity are more likely correlative with the Rocky Ridge Formation of the Skeena Group one needs to consider the possibility that the K-Ar whole rock isotopic ages determined for the Equity host rocks might be thermally reset. In order to address this issue, a sample of felsic lapilli tuff from the haulage ramp on the west side of the Main Zone pit (Photo 1g) was collected and submitted for U-Pb isotopic age-dating. Results are not expected until early 2004.

LITHOGEOCHEMISTRY

A total of 19 samples were collected for major oxide, trace and rare earth element analyses in 2000 (MacIntyre, 2001). An additional 14 samples were analyzed as part of the current project (Table 2). The analytical results are given in Table 3. All of the samples are from suspected outcrops of Rocky Ridge volcanics in the Fort Babine, Beament, Equity Silver Mine and Bob Creek areas (Figure 1). Two samples from the Gillian prospect and one sample from the Equity Southern Tail zone were generously provided by Dr. Neil Church. Analytical results for these samples (nos. 12-14) are included in Table 3.

Previous major oxide analyses indicate that mid-Cretaceous rhyolites have SiO2 values ranging from 70.61 to 76.5 weight percent (Table 3). By contrast interbedded Rocky Ridge basaltic flows contain between 47.74 to 54.61 weight percent SiO2 and 0.56 to 0.89 weight percent TiO2. Kasalka Group volcanics are more intermediate in composition with SiO2 values ranging from 59.5 to 62.18 weight percent. A standard AFM ternary plot (Figure 5a) shows the bimodal, calc-alkaline nature of Rocky Ridge basalts and coeval rhyolite domes. On an alkali-silica plot these samples range from alkaline to subalkaline in composition (Figure 5b) and plot in the rhyolite and sub-alkaline basalt to andesite fields of a Zr/TiO2 versus SiO2 diagram (Figure 5c). Of the samples analyzed in 2003, only the samples from the Southern Tail zone at Equity (No. 12, Table 3) and a sample from the Gillian prospect (No.14, Table 3) are compositionally rhyolites.

Of the mafic volcanic samples analyzed in 2003, the relatively fresh, massive flow rocks from the Fort Babine and Beament areas all have chemical signatures similar to those previously determined for Rocky Ridge basalts (Figure 5) by MacIntyre, 2001, Tackaberry, 1998 and Bassett and Kleinspehn (1996). This supports the field-based interpretation that all of these rocks are part of the Rocky Ridge Formation.

Highly altered felsic lapilli tuffs collected from the Beament and Bob Creek sections are compositionally dacite or rhyodacite (Figure 5c). This reflects the presence of rhyolitic clasts in these pyroclastic rocks. These rocks might also be correlative with the Rocky Ridge Formation, with the rhyolite clasts derived by explosive felsic volcanism or erosion of unstable rhyolite flow domes.

Rhyolite that hosts Ag-Zn-Pb veins at the Cronin, Knoll and Fireweed properties are strongly altered with nearly total removal of Na and Ca (MacIntyre, 2001). Altered rhyolites can also have anomalous concentrations of Pb, Zn, Ag and As (MacIntyre 2001). A plot of K2O versus Na2O (Figure 5d) clearly distinguishes altered from unaltered rhyolite, with altered samples having very low Na2O and relatively high K2O values. K enrichment is interpreted to reflect the presence of sericitic alteration at the expense of Na-rich plagioclase feldspar. Of the samples analyzed as part of the current project, only two samples display this type of alteration signature, the rhyolite from the Southern Tail zone (No. 12, Table 3) and a sample of strongly altered felsic lapilli tuff from Bob Creek (No. 10, Table 3)

Rare earth element concentrations for basalt and rhyolite were also determined as part of the current study. Chondrite normalized values are plotted in Figure 5e as are those previously determined by Tackaberry (1998) and MacIntyre (2001). Both basalts and rhyolites, regardless of their degree of alteration, have light rare earth element enrichment whereas rhyolites are also moderately to strongly enriched in heavy rare

TABLE 2. LITHOGEOCHEMICAL SAMPLES COLLECTED IN 2003

No.	Station	UTM Easting	UTM Northing	Location	Unit	Description
1	DMA03-001	678305	6008085	Equity Mine - Main Zone	IKSRv	dust tuff or tuffaceous mudstone
2	DMA03-003	649220	6128422	Ft. Babine	IKSRv	andesite, feldspar phyric
3	DMA03-004	603095	6112545	Beament	IKSRv	basalt
4	DMA03-005a	603090	6113131	Beament	IKSRv	andesite
5	DMA03-005b	603090	6113131	Beament	IKSRv?	lahar
6	DMA03-006a	603061	6113583	Beament	IKSRv?	bedded tuff or sediment?
7	DMA03-006b	603061	6113583	Beament	IKSRv?	bedded tuff or sediment?
8	DMA03-007	602811	6115362	Beament	IKSRv	basalt
9	DMA03-008	603497	6114919	Beament	IKSRv	basalt
10	DMA03-010	654500	6020178	Bob Creek	IKSRv?	felsic lapilli tuff
11	DMA03-011	654240	6020315	Bob Creek	IKSRv?	felsic lapilli tuff
12	DMA03-013	678000	6007000	Equity Mine - S. Tail	IKSRv	rhyolite
13	Gil 28-225	668369	6003653	Gillian	IKSRv	andesite
14	Gil 30-949	668369	6003653	Gillian	IKSRv	dacite

Notes: NAD83 datum; UTM zone 9; IKSRv = Rocky Ridge Fm.

earth elements relative to the basalts. A notable exception is the rhyolite from Cronin which has a much lower level of light rare earths compared to other rhyolites in this study.The significance of this difference is not known. All of the rhyolites, including the Cronin sample, have moderate to strong Eu depletion consistent with plagioclase fractionation (Tackaberry 1998). The rare earth patterns determined for Rocky Ridge basalts in this study are very similar to those presented in Bassett and Kleinspehn (1996) for compositionally similar rocks. One sample from the current study that has an unusual REE pattern is the "dust tuff" from the Equity main Zone pit (No. 1, Table 3). This light-coloured, aphanitic rock is probably not a volcanic per se but rather an altered, tuffaceous mudstone. This conclusion is supported by remnant graded bedding observed at the sample site. If this interpretation is correct then it suggests that some, if not all, of the "dust tuff" that hosts the Equity ore bodies is also sedimentary in origin.

DISCUSSION

The search for VMS deposits in central British Columbia has been strongly influenced by the discovery and subsequent development of the Eskay Creek property. This property, which is located 80 km north of Stewart, includes several deposits of precious metal bearing polymetallic sulphide and sulphosalt mineralization as both exhalative massive sulphides and discordant veins. The deposits are hosted by marine mudstone and rhyolite flow domes of late Lower to early Middle Jurassic age. These deposits are economically important because of their precious metal contents and polymetallic nature. As of December 31, 1998, Eskay Creek had proven and probable reserves of 1.9 Mt grading 60.2 g/t Au and 2652 g/t Ag, 3.2% Pb, 5.2% Zn and 0.7%Cu (Sherlock *et al.*, 1999).

The Eskay Creek deposit is described as an unusual precious metal rich, volcanogenic massive sulphide and sulphosalt deposit with epithermal geochemical signatures (Roth, 2002) and as a subaqueous hot spring deposit (Alldrick, 1995), representing an important new class of mineral deposit that has only recently been recognized in modern geological environments (Hannington, 1999). Although beautifully banded massive sulphide does occur, a large portion of the deposit is comprised of partially replaced clastic sulphides that probably represent collapsed, transported and reworked sulphide mounds and chimneys (Roth, 2002). Massive sulphide lenses are hosted by marine argillites that stratigraphically overlie massive, flow banded rhyolites interpreted to be flow domes. Mafic flows overlie the main sulphide horizons. Extensive stockwork mineralization and

TABLE 3. LITHOGEOCHEMICAL RESULTS

Elem.	Units	Limit	Meth.	1	2	3	4	5	6	7
SiO_2	%	0.02	1	61.20	57.60	53.60	61.50	62.70	68.60	57.80
TiO_2	%	0.01	1	1.16	1.06	0.84	0.60	0.64	0.15	0.69
Al_2O_3	%	0.03	1	22.90	18.20	17.10	15.80	16.70	12.80	14.40
Fe_2O_3	%	0.04	1	2.52	8.81	7.75	3.97	2.02	4.35	8.71
MnO	%	0.01	1	0.01	0.16	0.11	0.09	0.05	0.10	0.07
MgO	%	0.01	1	0.56	1.13	1.58	1.38	1.10	0.98	2.07
CaO	%	0.01	1	0.09	0.85	4.56	3.14	3.54	1.78	2.26
Na_2O	%	0.01	1	0.67	8.65	3.20	1.69	1.97	0.39	0.80
K_2O	%	0.04	1	5.33	0.46	2.08	2.92	3.26	3.32	3.77
P_2O_5	%	0.01	1	0.13	0.50	0.49	0.18	0.15	0.05	0.08
Cr_2O_3	%	0.001	1	0.01	0.01	0.01	0.01	0.02	0.01	0.01
LOI	%	0.1	1	3.93	2.86	6.39	7.49	6.13	6.40	7.87
Total	%	--	--	98.51	100.29	97.71	98.77	98.28	98.93	98.53
Ag	ppb	2	2	2413	17	75	89	33	12	40
As	ppm	0.1	2	20.9	0.8	5.6	3.6	3.1	33.1	10.4
Au	ppb	0.2	2	13.7	0.9	0.4	1.2	0.5	0.5	1.2
B	ppm	1	2	1	1	1	1	2	1	1
Ba	ppm	0.5	2	121.7	133.8	66.3	53.0	136.0	85.7	40.3
Bi	ppm	0.02	2	2.61	0.06	0.02	0.40	1.39	0.07	0.37
Cd	ppm	0.01	2	1.63	0.12	0.18	0.63	0.08	0.01	0.01
Co	ppm	0.1	2	17.3	6.0	11.3	9.9	6.7	20.0	44.3
Cr	ppm	0.5	2	0.7	2.5	2.9	3.9	2.2	1.1	4.2
Cu	ppm	0.01	2	47.92	11.87	11.28	50.24	27.58	12.39	22.87
Mo	ppm	0.01	2	1.77	0.3	1.79	1.89	8.01	0.97	1.71
Ni	ppm	0.1	2	3.8	2.0	1.1	18.8	7.9	43.5	83.3
Pb	ppm	0.01	2	10.83	1.79	5.18	17.07	15.13	2.98	3.28
Sb	ppm	0.02	2	17.79	0.07	0.09	0.54	0.51	2.15	1.20
Sc	ppm	0.1	2	0.5	4.8	3.1	2.1	1.4	0.7	1.2
Sr	ppm	0.5	2	6.2	8.1	61.4	79.0	57.4	53.2	77.4
Th	ppm	0.1	2	0.7	0.5	1.1	4.3	3.6	6.0	2.7
Tl	ppm	0.02	2	0.19	0.02	0.11	0.16	0.15	0.13	0.18
U	ppm	0.1	2	0.1	0.2	0.2	0.9	0.2	0.6	0.2
V	ppm	2	2	2	10	50	9	6	7	8
W	ppm	0.1	2	0.4	0.1	0.1	0.1	0.1	0.1	0.3
Zn	ppm	0.1	2	15.3	73.9	87.5	90.3	10.6	10.4	3.7
Be	ppm	1	3	2	2	1	1	2	2	1
Cs	ppm	0.1	3	6.1	0.1	2.9	5.9	4.0	4.2	5.2
Hf	ppm	0.02	3	0.46	2.69	2.97	0.77	1.85	1.1	0.55
Li	ppm	0.1	3	2.9	11.2	9.5	19.4	8.8	11.8	11.2
Nb	ppm	0.04	3	3.23	10.62	8.42	4.64	5.21	10.49	9.98
Rb	ppm	0.1	3	268.7	1.2	39.6	82.0	114.3	140.7	186.5
Sn	ppm	0.1	3	3.5	2.0	1.1	1.2	0.9	1.7	2.4
Ta	ppm	0.1	3	0.3	0.9	0.6	0.5	0.5	1.0	0.8
Y	ppm	0.1	3	2.9	17.6	13.6	8.1	9.3	11.1	18.0
Zr	ppm	0.2	3	14.9	76.9	106.3	22.3	59.0	26.5	18.0
La	ppm	0.1	3	0.5	21.5	17.0	11.2	15.7	12.2	7.7
Ce	ppm	0.02	3	5.38	24.0	30.85	31.48	41.35	48.23	41.28
Pr	ppm	0.1	3	0.6	3.1	3.8	3.3	4.2	4.9	5.8
Nd	ppm	0.1	3	2.7	13.5	16.9	12.3	16.6	17.5	25.0
Sm	ppm	0.1	3	0.6	3.6	3.9	2.5	3.3	3.5	5.9
Eu	ppm	0.1	3	0.1	1.1	0.9	0.6	0.7	0.7	1.2
Gd	ppm	0.1	3	0.6	3.4	3.6	2.0	2.5	3.0	4.8
Tb	ppm	0.1	3	0.1	0.5	0.5	0.2	0.3	0.4	0.7
Dy	ppm	0.1	3	0.6	3.8	2.7	1.5	1.8	1.9	3.8
Ho	ppm	0.1	3	0.1	0.7	0.4	0.3	0.3	0.3	0.6
Er	ppm	0.1	3	0.4	2.4	1.5	0.7	1.0	1.1	1.8
Tm	ppm	0.1	3	0.1	0.3	0.2	0.1	0.1	0.1	0.2
Yb	ppm	0.1	3	0.5	1.9	1.2	0.7	0.9	1.1	1.5
Lu	ppm	0.1	3	0.1	0.2	0.1	0.1	0.1	0.1	0.2

Notes: See Table 2 for sample descriptions and location information.
All analyses done at Acme Analytical Laboratories, Vancouver, B.C.
ppm = parts per million; ppb = parts per billion
1 - LiBO2 fusion followed by XRF analysis for major oxides and LOI (Group 4X).
2 - ICP Mass Spectrometer analysis after aqua regia digestion (Group IF-MS Basic).
3 - ICP Mass Spectrometer analysis of a 4-acid digestion (Group IT-MS).

TABLE 3 (CONTINUED)

Elem.	Units	Limit	Meth.	8	9	10	11	12	13	14
SiO_2	%	0.02	1	54.70	53.70	63.60	68.40	81.10	60.20	67.80
TiO_2	%	0.01	1	0.97	1.18	0.46	0.79	0.75	0.47	0.36
$A_{l2}O_3$	%	0.03	1	19.10	17.60	14.20	14.50	11.30	13.10	15.30
Fe_2O_3	%	0.04	1	7.66	9.38	6.28	5.02	0.66	5.76	3.86
MnO	%	0.01	1	0.27	0.06	0.55	0.08	0.01	0.04	0.04
MgO	%	0.01	1	2.64	2.22	1.03	0.13	0.18	2.50	2.02
CaO	%	0.01	1	3.97	4.87	1.49	0.89	0.04	3.76	1.14
Na_2O	%	0.01	1	6.61	2.99	0.09	5.83	0.17	0.86	3.74
K_2O	%	0.04	1	1.06	3.45	5.31	1.87	3.16	1.18	1.50
P_2O_5	%	0.01	1	0.48	0.44	0.25	0.20	0.01	0.07	0.09
Cr_2O_3	%	0.001	1	0.01	0.01	0.01	0.01	0.05	0.02	0.01
LOI	%	0.1	1	2.61	3.36	6.01	1.93	1.94	9.83	3.93
Total	%	--	--	100.08	99.26	99.28	99.65	99.37	97.79	99.79
Ag	ppb	2	2	48	27	849	56	379	118	31
As	ppm	0.1	2	3.3	4.7	95.4	5.1	3.6	26.8	0.5
Au	ppb	0.2	2	0.2	1.3	48.9	1.0	7.3	1.1	0.4
B	ppm	1	2	3	4	3	3	1	3	5
Ba	ppm	0.5	2	27.2	235.9	19.7	122.3	49.6	54.0	106.1
Bi	ppm	0.02	2	0.02	0.11	1.08	0.02	0.97	0.14	0.17
Cd	ppm	0.01	2	0.28	0.02	6.71	0.38	0.04	0.14	0.03
Co	ppm	0.1	2	18.3	23.9	1.6	3.3	0.5	12.6	8.4
Cr	ppm	0.5	2	1.9	13.7	0.8	4.2	7.7	11.6	7.9
Cu	ppm	0.01	2	11.49	46.84	85.56	2.32	4.39	34.51	18.70
Mo	ppm	0.01	2	0.25	1.55	3.71	0.74	0.45	1.93	1.21
Ni	ppm	0.1	2	6.1	16.0	2.4	1.1	1.5	76.3	7.7
Pb	ppm	0.01	2	2.89	1.65	24.07	8.43	3.14	20.66	9.47
Sb	ppm	0.02	2	0.51	2.58	2.29	1.28	2.53	0.19	0.05
Sc	ppm	0.1	2	3.3	9.1	1.0	6.2	0.3	3.3	2.9
Sr	ppm	0.5	2	34.0	92.4	6.4	7.7	9.4	93.2	74.5
Th	ppm	0.1	2	1.4	0.9	1.2	1.3	1.1	3.2	4.9
Tl	ppm	0.02	2	0.02	0.12	0.34	0.08	0.08	0.13	0.03
U	ppm	0.1	2	0.3	0.1	0.7	0.1	0.1	1.2	1.0
V	ppm	2	2	76	132	8	28	5	19	28
W	ppm	0.1	2	0.1	0.3	0.2	1.6	0.4	0.1	0.1
Zn	ppm	0.1	2	89.2	20.7	915.5	123.2	8.1	88.0	38.2
Be	ppm	1	3	2	1	1	1	1	1	1
Cs	ppm	0.1	3	3.1	12.5	7.8	2.6	3.3	1.0	1.4
Hf	ppm	0.02	3	0.91	1.87	1.7	2.0	0.58	2.03	3.93
Li	ppm	0.1	3	30.1	29.7	8.4	6.7	1.7	39.0	31.9
Nb	ppm	0.04	3	13.65	13.41	4.4	5.29	2.29	2.62	5.83
Rb	ppm	0.1	3	18.4	58.7	212.5	58.4	159.9	30.4	31.8
Sn	ppm	0.1	3	1.0	1.1	1.4	0.5	4.4	1.3	1.1
Ta	ppm	0.1	3	1.1	1.2	0.3	0.4	0.2	0.2	0.9
Y	ppm	0.1	3	14.6	15.3	9.2	17.6	5.3	22.0	15.0
Zr	ppm	0.2	3	25.0	54.2	52.1	66.4	19.0	58.3	121.1
La	ppm	0.1	3	9.2	6.5	4.0	18.9	8.4	1.8	13.6
Ce	ppm	0.02	3	42.9	39.53	27.6	45.94	41.21	34.58	25.07
Pr	ppm	0.1	3	5.1	5.0	3.4	6.1	5.1	4.1	2.9
Nd	ppm	0.1	3	21.8	21.0	14.0	26.9	20.8	16.3	11.6
Sm	ppm	0.1	3	5.1	4.8	3.2	5.9	4.4	3.9	2.9
Eu	ppm	0.1	3	1.4	1.4	0.8	1.1	1.0	0.8	0.5
Gd	ppm	0.1	3	4.1	4.6	2.5	4.7	2.3	3.8	2.5
Tb	ppm	0.1	3	0.6	0.6	0.3	0.5	0.2	0.5	0.4
Dy	ppm	0.1	3	3.4	3.4	1.8	3.3	1.1	3.8	2.6
Ho	ppm	0.1	3	0.5	0.6	0.3	0.6	0.2	0.7	0.5
Er	ppm	0.1	3	1.7	1.7	0.8	2.1	0.6	2.6	1.8
Tm	ppm	0.1	3	0.2	0.2	0.1	0.3	0.1	0.4	0.2
Yb	ppm	0.1	3	1.2	1.5	0.9	2.2	0.6	2.4	2.1
Lu	ppm	0.1	3	0.1	0.2	0.1	0.3	0.1	0.3	0.3

Notes: See Table 2 for sample descriptions and location information.
All analyses done at Acme Analytical Laboratories, Vancouver, B.C.
ppm = parts per million; ppb = parts per billion
1 - LiBO2 fusion followed by XRF analysis for major oxides and LOI (Group 4X).
2 - ICP Mass Spectrometer analysis after aqua regia digestion (Group IF-MS Basic).
3 - ICP Mass Spectrometer analysis of a 4-acid digestion (Group IT-MS).

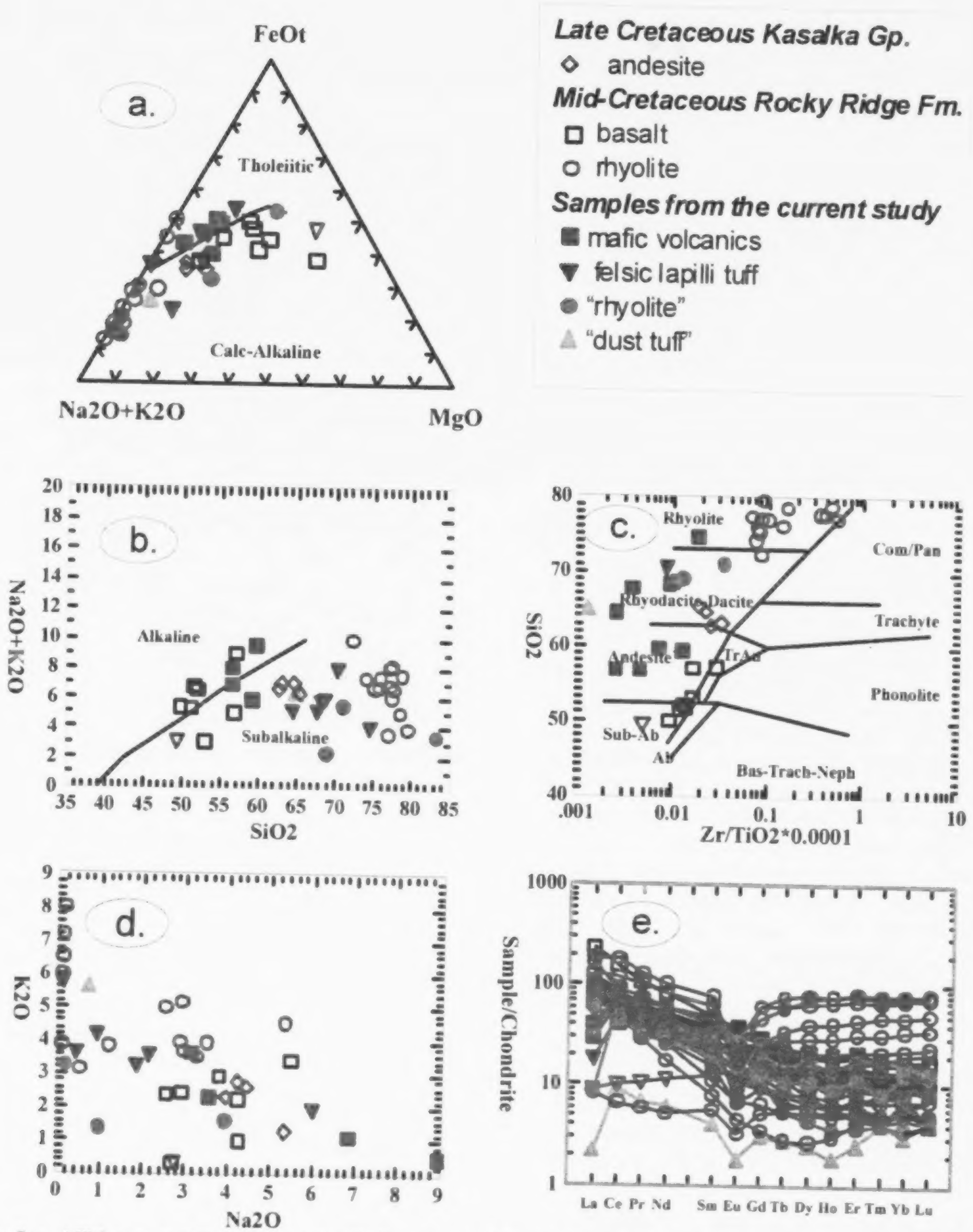

Figure 5. a. AFM ternary plot showing calc-alkaline nature of Rocky Ridge and Kasalka volcanic rocks; b. alkali-silica plot showing subalkaline to alkaline compositional trend; c. SiO2 versus Zr/TiO2 plot showing compositional range and classification of Rocky Ridge volcanic rocks and rhyolite domes; d. K20 versus Na2O plot showing Na depletion of altered rhyolite samples; e. plot of chondrite normalized rare earth element abundances for Rocky Ridge basalts and rhyolites.

pervasive chlorite-sericite alteration occur in the footwall rhyolites. The Eskay Creek deposit shares mineralogical, geochemical and other characteristics of both subaerial epithermal Au-Ag hot spring deposits and deeper water Kuroko and Besshi type volcanogenic massive sulphide deposits (Roth, 2002). Many deposits appear to be associated with bimodal (basalt-rhyolite) submarine volcanic centers, including sea-flooded, breached calderas in an active volcanic arc setting. Given the inferred shallow submarine

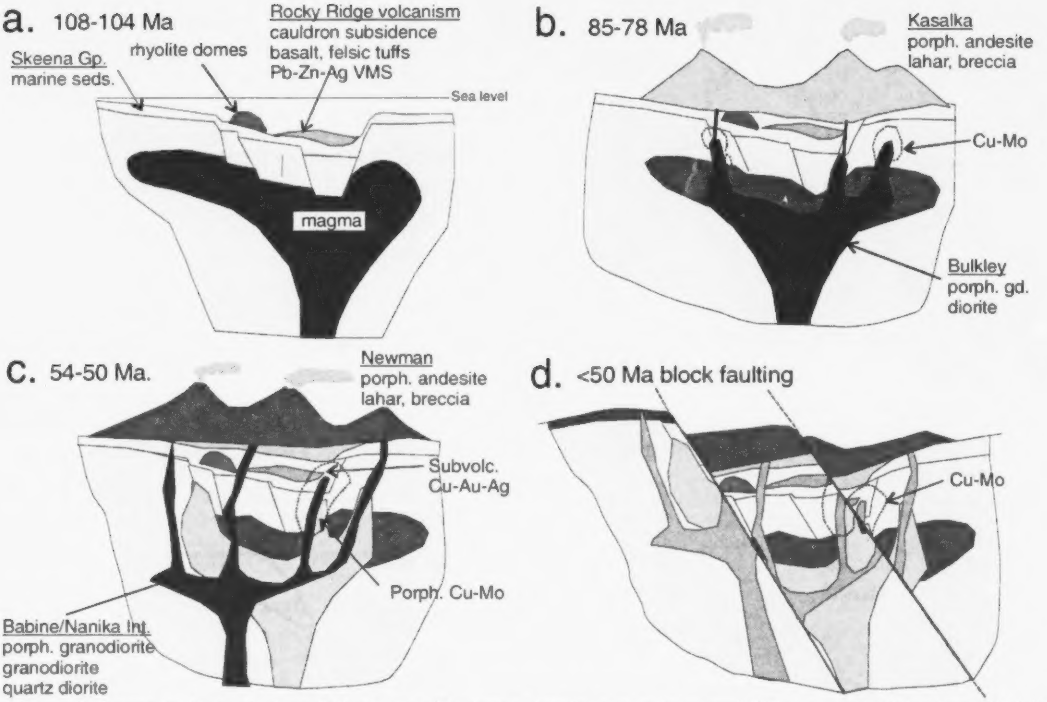
a. 108-104 Ma
Skeena Gp.
marine seds.
rhyolite domes
Rocky Ridge volcanism
cauldron subsidence
basalt, felsic tuffs
Pb-Zn-Ag VMS
Sea level
magma
b. 85-78 Ma
Kasalka
porph. andesite
lahar, breccia
Cu-Mo
Bulkley
porph. gd.
diorite
c. 54-50 Ma.
Newman
porph. andesite
lahar, breccia
Subvolc.
Cu-Au-Ag
Porph. Cu-Mo
Babine/Nanika Int.
porph. granodiorite
granodiorite
quartz diorite
d. <50 Ma block faulting
Cu-Mo

Figure 6. Stages in the evolution of Cretaceous-Tertiary volcanic centers in central BC.; a. nascent island arc (108-104 Ma); b. Late Cretaceous continental arc (85-78 Ma); c. Eocene continental arc; d. post Eocene extension and block faulting.

setting, bimodal composition and apparent spatial association of precious metal rich massive sulphide and vein deposits, the Rocky Ridge Formation is considered to be a favourable host for Eskay Creek type deposits.

The focus of the current study was to demonstrate that rhyolite domes similar to those dated in the Babine Lake area occur elsewhere in the Rocky Ridge succession and that these represent local, felsic volcanic centers in a bimodal, submarine volcanic environment that is favourable for the formation of VMS and/or Eskay Creek type deposits. Based on the presence of strong alteration in the host rhyolites as determined by lithogeochemical analyses and the presence of known mineral occurrences, the most favourable areas identified in a previous study are at the Fireweed, Cronin and Knoll properties. Other, less well-explored areas such as south of Rocky Ridge and at Troitsa Lake may also prove to be favourable. In all of these areas the rhyolite intrusions appear to be emplaced along ring structures related to the development of large submarine cauldron subsidence complexes. Isotopic dating of the rhyolitic intrusions will help constrain the timing of cauldron subsidence and thus demonstrate or repudiate correlation with Rocky Ridge volcanic rocks elsewhere in the study area.

Mineralization and alteration at Beament, Bob Creek and Equity Silver mine suggests a subvolcanic, epithermal environment probably associated with emplacement of nearby intrusions as postulated by previous workers (Cyr *et al.*, 1984). This is the Subvolcanic Cu-Au-Ag (As-Sb) deposit model described by Panteleyev (1995). However, in the authors opinion, some ore at Equity is a fragmental massive sulphide with similarities to Eskay creek and other classical VMS deposits. If this interpretation is correct and the host rocks at Equity prove to be mid-Cretaceous Rocky Ridge Formation then at least some of the massive sulphide at Equity is also this age. Early Tertiary whole rock K-Ar ages determined for sericitized volcanic rocks (Cyr *et al.*, 1984) at Equity might reflect either overprinting of a younger sericite-clay alteration or thermal resetting related to emplacement of nearby Early Tertiary intrusions. A younger Early Tertiary hydrothermal event is appealing as it could explain both the younger ages for sericitized rocks and the replacement textures observed in fragmental massive sulphide beds.

It seems likely that both the mid-Cretaceous Pb-Zn-Ag mineralization at the Knoll, Cronin and Fireweed prospects and possible younger Late Cretaceous or Early Tertiary mineralization at Equity, Beamont and Bob Creek are related to the evolution of major volcanic centers that were periodically active from the mid-Cretaceous to Eocene time. Earliest stages of volcanism, as represented by the Rocky Ridge formation, involved cauldron subsidence in a nascent island arc setting with attendant Pb-Zn-Ag VMS and related epithermal mineralization associated with shallow, submarine eruption of rhyolite flow domes. Younger, Late Cretaceous or Early Tertiary magmatic events resulted in building of stratovolcanoes in an Andean continental arc setting with attendant subvolcanic Cu-Au-Ag and porphyry Cu-Mo type mineralization. A genetic model depicting these evolutionary stages is presented in Figure 6.

CONCLUSIONS

1. Precious metal rich, massive sulphide occurrences at the Fireweed, Knoll and Cronin properties appear to be related to submarine rhyolite flow domes that were emplaced along rifts that formed during mid-Cretaceous cauldron subsidence. This was followed by eruption of thick piles of alkali basalt. The inferred geologic setting (nascent arc, bimodal, submarine, rift related) is similar to that proposed for classical Kuroko and Eskay Creek-type VMS deposits and therefore, areas of Rocky Ridge volcanics in central British Columbia are interpreted to be highly prospective for these types of deposits.
2. Rocks at the Fort Babine, Beament and Bob Creek localities are compositionally and lithologically similar to the Rocky Ridge Formation and a tentative correlation is suggested. Isotopic age-dating is needed to further confirm this correlation.
3. Felsic pyroclastic rocks at Beament, Bob Creek and Equity are strongly pyritic, have elevated base and precious metal concentrations and are pervasively altered to sericite and clay. This style of alteration and mineralization is characteristic of subvolcanic epithermal systems associated with emplacement of porphyritic intrusions. The age of this hydrothermal activity is not known but it is likely younger than, and therefore unrelated to, the Rocky Ridge host rocks.
4. The authors believe that a least some of the fragmental massive sulphide at the Equity mine is syngenetic and may be hosted by mid-Cretaceous Rocky Ridge Formation. A sample of felsic lapilli tuff from Equity has been submitted for U-Pb dating and this may help to confirm or repudiate this correlation.

ACKNOWLEDGMENTS

The authors wish to thank the Rocks to Riches management committee for providing financial support to continue this study. Mike Villeneuve, Geological Survey of Canada, Ottawa has provided invaluable assistance to this project by providing technical and interpretive assistance with U/Pb and Ar/Ar age-dating. Dr. Neil Church generously provided information and samples from the Equity Silver Mine area and Mike Assiz of Placer Dome provided valuable assistance in acquiring samples at the Equity mine site. Assistance in researching information and viewing type collections for properties in the area was kindly provided by Paul Wojdak in the Ministry of Energy and Mines Smithers office

REFERENCES

Alldrick, D.J. (1995): Subaqueous hot spring Au-Ag; *in* Selected British Columbia mineral deposit profiles, Volume 1 - metallics and coal, Lefebure, D.V. and Ray, G.E., Editors, *British Columbia Ministry of Employment and Investment*, Open File 1995-20, pages 55-58.

Bassett, K.N. (1991): Preliminary Results of the Sedimentology of the Skeena Group in West-central British Columbia; *in* Current Research, Part A, *Geological Survey of Canada*, Paper 91-1A, pages 131-141.

Bassett, K.N. and Kleinspehn, K.L, (1996): Mid-Cretaceous transtension in the Canadian Cordillera: evidence from the Rocky Ridge volcanics of the Skeena Group; *Tectonics*, Volume 15, pages 727-746.

Church, B.N. and Barakso, J.J. (1990): Geology, lithogeochemistry and mineralization in the Buck Creek area, British Columbia; *British Columbia Ministry of Energy, Mines and Petroleum Resources*, Paper 1990-2, 95 pages.

Cyr, J.B., Pease, R.B. and Schroeter, T.G. (1984): Geology and mineralization at Equity Silver Mine; *Economic Geology*, Volume 79, pages 947-968.

Evenchick, C. A. (1999): Depositional and structural histories of the northern two-thirds of the Bowser Basin/Skeena Fold Belt, northern British Columbia: records of terrane interactions; *in* Terrane Paths 99, Circum-Pacific Terrane Conference, Abstracts and Program, C.A. Evenchick, G.J. Woodsworth, and R. Jongens, editors; *Geological Survey of Canada/Geological Association of Canada*, pages 30-32.

Hannington, M.D. (1999): Submarine epithermal deposits and the VMS-epithermal transition: a new exploration target; *in* Short Course Proceedings, *Prospectors and Developers Association of Canada*, Toronto, March 1999, pages 101-123.

Krogh, T. E. (1982): Improved accuracy of U-Pb zircon ages by the creation of more concordant systems using an air abrasion technique. *Geochimica et Cosmochimica Acta*, Volume 46, pages 637-649.

MacIntyre, D.G. (1985): Geology and mineral deposits of the Tahtsa Lake District, west central British Columbia; *British Columbia Ministry of Energy, Mines and Petroleum Resources*, Bulletin 75.

MacIntyre, D.G. (2001): The Mid-Cretaceous Rocky Ridge Formation – A new target for subaqueous hot-spring deposits (Eskay Creek-type) in Central British Columbia, in Geological Fieldwork 2000, *B.C. Ministry of Energy and Mines*, Paper 2001-1, pages 253-268.

MacIntyre, D.G. (2001a): Geological compilation of the Babine Porphyry Copper district, *B.C. Ministry of Energy and Mines*, Open File Map 2001-3.

MacIntyre, D.G. and Struik, L.C. (1999): Nechako NATMAP Project, central British Columbia, 1998 Overview; *in* Geological Fieldwork 1998, *British Columbia Ministry of Energy and Mines*, Paper 1999-1, pages1-14.

MacIntyre, D.G. and Villeneuve, M.E. (2001): Geochronology and tectonic setting of mid-Cretaceous to Eocene magmatism, Babine porphyry copper district, central British Columbia; *Canadian Journal of Earth Sciences*, Volume 38, pages 639-655.

MacIntyre, D.G., Villeneuve, M.E., and Schiarizza, P. (2001): Timing and tectonic setting of Stikine Terrane magmatism, Babine-Takla lakes area, central British Columbia. *Canadian Journal of Earth Sciences*, Volume 38, pages 579-601.

Malott, M.L. (1988): Fireweed (093M151); B.C. *in* Exploration in British Columbia 1988, *B.C. Ministry of Energy, Mines and Petroleum Resources*, pages B127-131.

Massey, N.W.D. (1999): Volcanogenic Massive Sulphide Deposits in British Columbia; *B.C. Ministry of Energy and Mines*, Open File 1999-2.

Massey, N.W.D., Alldrick, D.J. and Lefebure, D.V.L. (1999): Potential for subaqueous hot-spring (Eskay Creek) deposits in British Columbia; *B.C. Ministry of Energy and Mines*, Open File 1999-14.

Panteleyev, A. (1995): Subvolcanic Cu-Au-Ag (As-Sb); *in* Selected British Columbia mineral deposit profiles, Volume 1 - metallics and coal, Lefebure, D.V. and Ray, G.E., Editors, *British Columbia Ministry of Employment and Investment*, Open File 1995-20, pages 79-82.

Parrish, R. R., Roddick, J. C., Loveridge, W. D. and Sullivan, R. W. (1987): Uranium-lead analytical techniques at the Geochronology Laboratory, Geological Survey of Canada. *In*: Radiogenic age and isotopic studies. Report 1. *Geological Survey of Canada*, Paper 87-2.

Richards, T.A. (1980): Geology of the Hazelton Map Area (93M); *Geological Survey of Canada*, Open File 720.

Richards, T.A. (1990): Geology of the Hazelton Map Area (93M); *Geological Survey of Canada*, Open File 2322.

Roddick, J. C., Loveridge, W. D. and Parrish, R.R. (1987): Precise U/Pb dating of zircon at the sub-nanogram Pb level; *Chemical Geology*, Volume 66, 111-121.

Roth, T. (2002): Physical and chemical constraints on mineralization in the Eskay Creek deposit, northwestern British Columbia: evidence from petrography, mineral chemistry and sulfur isotopes: unpublished Ph.D. thesis, *University of British Columbia*, 384 pages.

Sherlock, R.L., Roth, T., Spooner, E.T.C. and Bray, C.J. (1999): Origin of the Eskay Creek precious metal-rich volcanogenic massive sulfide deposit: fluid inclusion and stable isotope evidence; *Economic Geology*, Volume 94, pages 803-824.

Tackaberry, D.M. (1998): Petrography, lithogeochemistry and VMS potential of Mid-Cretaceous Rocky Ridge volcanics, Babine Lake area, Central British Columbia, Unpublished honours B.Sc. thesis, *University of Victoria*.

Tipper, H.W. and Richards, T.A. (1976): Geology of the Smithers Area; *Geological Survey of Canada*, Open File Map 351.

Wojdak, P.J. and Sinclair, A.J. (1984): Equity Silver silver-copper-gold deposit: alteration and fluid inclusion studies: Economic Geology, Volume 79, pages 969-990.

Wojdak, P.J., Ethier, D. and Hanson, D. (1999): Knoll (093M 100); *in* Exploration in B.C. 1999, *B.C. Ministry of Energy and Mines*

Woodsworth, J.G. (1980): Geology of the Whitesail Lake (93E) map-area, *Geological Survey of Canada*, Open file Map 708.

York, D. 1969. Least squares fitting of a straight line with correlated errors. *Earth and Planetary Science Letters*, Volume 5, pages 320-324.

APPENDIX A. U/PB ISOTOPIC AGE-DATING METHODOLOGY

Following the separation of heavy minerals using heavy liquids, samples were passed through a Frantz LB-1™ magnetic separator to purify zircon and titanite. Zircon crystals were selected for analysis based on criteria that optimised for their clarity, lack of cloudiness and colour, and lack of fractures. All zircons were abraded prior to analysis to increase concordance by removing the outer portions of the grains where much of the Pb-loss and alteration take place (Krogh, 1982).

Following abrasion, photography, and final mineral selection, mineral fractions were analysed according to methods summarised in Parrish *et al.* (1987). Data have been reduced and errors have been propagated using software written by J. C. Roddick; error propagation was done by numerical methods (Roddick *et al.* 1987; Parrish *et al.*, 1987). Error ellipses on concordia diagrams are shown at the 2-sigma (95% confidence) level of uncertainty. Linear regressions on discordant arrays of data use a modified York (1969) method that takes into account the scatter of the points about the line (see a discussion in Parrish *et al.* 1987).

REGIONAL STUDIES OF ESKAY CREEK-TYPE AND OTHER VOLCANOGENIC MASSIVE SULPHIDE MINERALIZATION IN THE UPPER HAZELTON GROUP IN STIKINIA: PRELIMINARY RESULTS

J.K. Mortensen[1], S.M. Gordee[1], J. B. Mahoney[2] and R.M Tosdal[1]

KEYWORDS: *Volcanogenic massive sulphide deposits, Eskay Creek, Hazelton Group, Stikinia, Early Jurassic, Bella Coola area, Whitesail Lake area, Rocks to Riches program*

INTRODUCTION

Eskay Creek type (ECT) volcanogenic massive sulphide (VMS) deposits represent an attractive exploration target because of their substantial tonnage potential and high precious metal content. Despite numerous geological and geochemical studies of Eskay Creek and years of exploration for ECT deposits in the northern Stikinia terrane, however, deposits in the immediate area of Eskay Creek are still the only significant deposits of this type that have been discovered in British Columbia. New exploration criteria must be developed in order to improve the likelihood of success in future exploration endeavors.

The British Columbia Geological Survey Branch recently completed two major syntheses that provide an excellent basis on which to build a new research project focused on developing new exploration strategies for ECT deposits. Massey (1999) compiled a summary of all known VMS deposits in B.C. and subdivided those associated with felsic volcanic rocks into Kuroko-type and Eskay Creek-type. Massey et al. (1999) undertook a detailed assessment of the potential for ECT deposits throughout British Columbia. Their report summarizes the main geological and geochemical characteristics of ECT deposits and provides brief descriptions of numerous mineral occurrences in the province that share at least some of the key characteristics of ECT deposits. Eight individual occurrences were identified that are considered to be ECT deposits, and several additional prospects were described that have potential to be ECT.

A new two-year research project was initiated by the Mineral Deposit Research Unit at UBC in 2003 aimed at better understanding the geological setting in which Eskay Creek type (ECT) deposits and occurrences formed, and devising better exploration strategies for this much sought after style of mineralization. Funding for the project derives in part from the Rocks to Riches Program, which is administered by the BC & Yukon Chamber of Mines, and by a consortium of mining and exploration companies.

Initial field work carried out during the 2003 field season had two main goals. First, we began a mapping based study of upper Hazelton Group strata in the southern Whitesail Lake area (and northernmost Bella Coola area) in southern Stikinia, aimed at refining our understanding of Hazelton Group stratigraphy in this region, constraining the environment(s) of deposition, and investigating the geological setting of ECT occurrences known to occur in the southern part of the area (Diakow et al., 2002; Haggart et al., 2003). Approximately five weeks of mapping was carried out in the southern Whitesail Lake area. Second, we began regional investigations of ECT occurrences in several other parts of Stikinia, including the Eskay Creek area itself, as well as the geological setting of other VMS occurrences hosted in older portions of the Hazelton Group to compare and contrast with the setting in which ECT mineralization is known to have formed. Approximately two weeks of regional reconnaissance work was directed towards this part of the study. The new research builds on previous work completed by the Mineral Deposit Research Unit (MDRU) at UBC under the auspices of the Iskut Project (results compiled in Lewis and Tosdal, 2000) and the Volcanogenic Massive Sulfide Deposits of the Cordillera Project (most results summarized in Juras and Spooner, 1996; and Roth, 2002).

---

1 - Mineral Deposit Research Unit, Earth & Ocean Sciences, UBC, Vancouver, B.C.; 2 - Department of Geology, University of Wisconsin, Eau Claire, Wisconsin, U.S.A.

CHARACTERISTICS OF ECT DEPOSITS IN STIKINIA AND OUTSTANDING QUESTIONS

ECT deposits are polymetallic VMS deposits characterized by high precious metal contents and highly anomalous levels of "epithermal suite elements", especially Hg, Sb and As (Roth et al., 1999). Several lines of evidence indicate that the Eskay Creek deposit formed at shallow water depths (see summary in Barrett and Sherlock, 1996), although depths as great as 1500 m are permitted by the data (Ross Sherlock, oral communication, 2002). Fluid inclusion data suggest that the mineralizing fluids were relatively low temperatures (120-210°C) and that boiling occurred. Microfossil studies of sedimentary rocks that are the immediate host to ore at Eskay Creek are also consistent with shallow water depths (Nadaraju, 1993), although precise depths cannot be constrained. The high precious metal contents of the ore are considered to be typical of VMS deposits formed in shallow water settings (e.g., Hannington et al., 1999).

The Eskay Creek deposit is associated with a distinctive bimodal basalt-rhyolite volcanic package (the Eskay Creek member of the Salmon River Formation; Lewis and Tosdal, 2000). The host rocks are both slightly younger (172-178 Ma vs. >181 Ma) and compositionally distinct (tholeiitic vs. mainly calc-alkaline) from volcanic rocks that comprise the rest of the Hazelton Group. Rhyolitic rocks associated with the Eskay Creek deposit are characterized by low TiO_2 values, which distinguish them from felsic volcanic units elsewhere in the Hazelton Group. Their Nd isotopic compositions lie in a restricted range with ε_{Nd} between +4 and +5.5, whereas felsic rocks of the rest of the Hazelton Group appear to have a much broader range of isotopic compositions and extend to ε_{Nd} as low as +2 (Childe, 1996, 1997).

A number of polymetallic Kuroko-type VMS deposits and prospects that do not share the ECT characteristics also occur within Early and Middle Jurassic sequences of Stikinia in British Columbia (Massey, 1999). Hydrothermal systems capable of generating VMS deposits were therefore active in a number of areas and at more than one time within Stikinia during the development of the Hazelton arc, and a key question is what specific factors determine which systems will produce an ECT deposit rather than a more typical polymetallic Kuroko-type VMS deposit. Resolution of this question is critical for developing exploration strategies specific to ECT deposits. Factors that may be important include (but are not limited to) the following: 1) water depth; 2) specific composition of associated volcanic rocks; 3) nature and/or depth of associated subvolcanic intrusions; 4) temperature of the associated magmas; 5) seafloor topography; and 6) nature of structural conduits controlling fluid flow in the subsurface.

The new research addresses the relative importance of these and other factors with the ultimate goal of devising more effective exploration criteria for ECT deposits in Stikinia and elsewhere in the world. A broad range of investigative tools is being brought to bear on the problem, including geological mapping, petrography, micropaleontology, lithogeochemistry, U-Pb and Ar-Ar geochronology and Pb and Nd isotopic studies. Specific goals of the study include: 1) comparing the lithogeochemistry of volcanic units associated with other VMS occurrences (both Kuroko-type and ECT) elsewhere in Stikinia with those at Eskay Creek to determine if systematic differences occur that may be used to target areas of high ECT deposit potential; 2) assessing the magmatic temperatures of volcanic units associated with ECT and other VMS occurrences in Stikinia using zircon geothermometry to determine whether ECT deposits are associated with anomalously high temperature magmas; 3) evaluating the water depth in which each of the known VMS occurrences formed using micropaleontology of associated clastic sedimentary units; 4) carrying out a detailed Pb isotopic study of sulphides and host rocks from both ECT and Kuroko-type VMS deposits in Stikinia to determine whether there are systematic differences in metal sources between the two styles of mineralization, and to eliminate occurrences in which the "epithermal geochemical signature" may be related to overprinting by Tertiary epithermal vein systems rather than the primary VMS mineralization itself; and 5) undertaking a 1:50,000 scale mapping study and stratigraphic analysis of a portion of southern Stikinia northeast of Bella Coola (southern Whitesail Lake and northernmost Bella Coola map areas). Here, previously unrecognized upper Hazelton Group stratigraphy have recently been shown to be age equivalent to the Eskay Creek member (Ray et

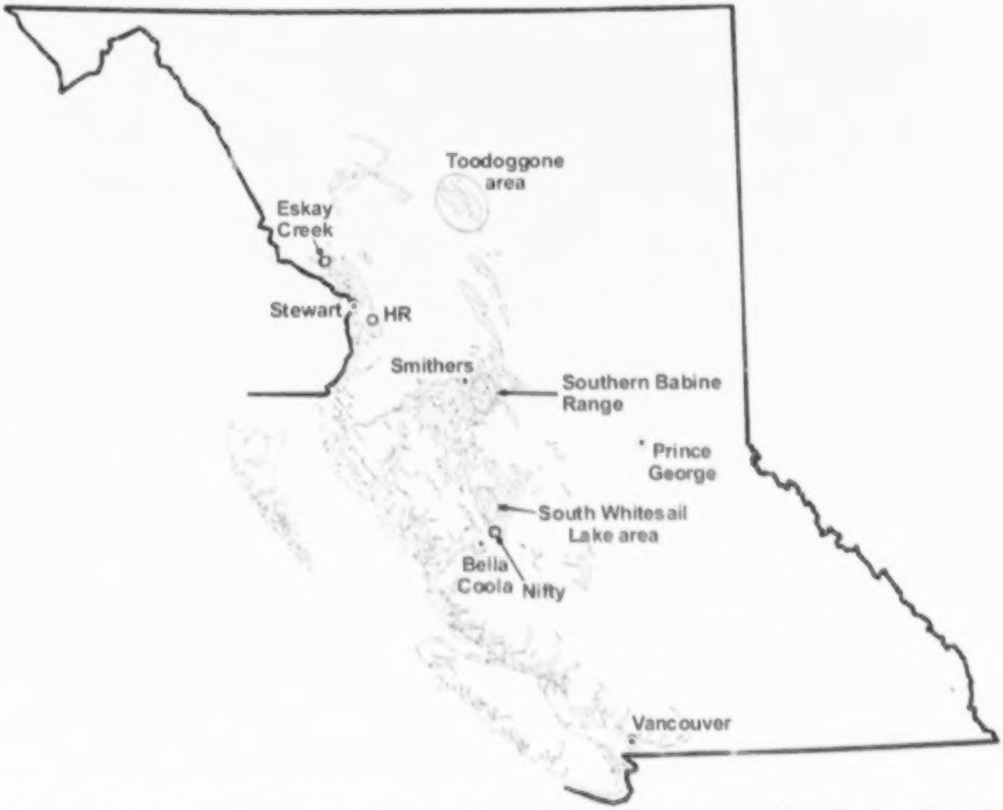

Figure 1. Distribution of Early and Middle Jurassic volcanic and sedimentary strata of the Hazelton Group (in grey) within the Stikine Terrane of British Columbia, showing specific localities referred to in the text.

al., 1998; Diakow et al., 2002). Furthermore, these rocks host both ECT-like and Kuroko-type VMS occurrences, including the Nifty occurrence in northern Bella Coola map area (BC MINFILE 093D 006)) and the Smaby occurrence in southern Whitesail Lake area (BC MINFILE 093E 025). This work is aimed at establishing a stratigraphic, geochronological and lithogeochemical framework for the upper Hazelton Group in southern Stikinia, and the position of ECT and other VMS mineralization within that framework.

MAPPING STUDIES IN THE SOUTHERN WHITESAIL LAKE MAP AREA

The first of two field seasons of mapping in the southern Whitesail Lake area focused on the area between Jumble Mountain in the south and Mount Preston in the north (Figures 1, 2). Hazelton Group volcanic and sedimentary rocks that are very well exposed in this area represent a northwestern continuation of the package of mainly felsic volcanic strata that host the Nifty VMS occurrence in northern Bella Coola map area (Ray et al., 1998; Diakow et al., 2002), approximately 45 km southeast of Jumble Mountain. U-Pb dating of volcanic rocks that host the Nifty occurrence (Ray et al., 1998) indicates an age of 164.2 ± 4.4 Ma. A felsic tuff horizon on the southeast side of Jumble Mountain has given a U-Pb zircon age of 176.6 ± 0.7 Ma (R.M. Friedman, unpublished data). Late Toarcian to Early Aalenian fossils have also been recovered from this locality. Together, these data confirm that the Jumble Mountain section and correlative rocks exposed between Jumble Mountain and Mount Preston, 30 km to the northwest, are roughly age equivalent to host rocks for the Eskay Creek deposit.

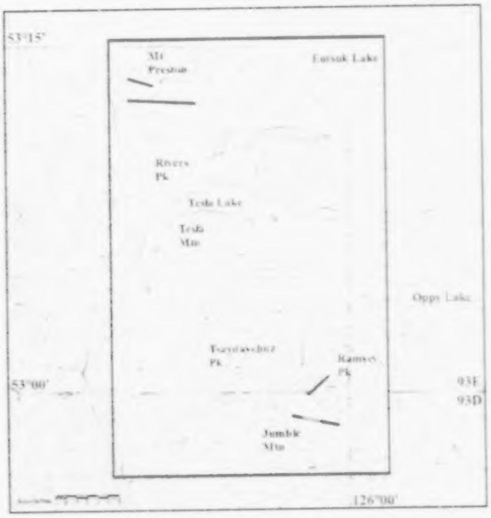

Figure 2. Regional map of the southeast Whitesail Lake and northern Bella Coola map areas. Box shows the outline of the study area and bold lines indicate measured stratigraphic sections, which are named after adjacent mountains.

Several very well exposed stratigraphic sections of Hazelton Group strata between Jumble Mountain and Mount Preston were examined in detail during the 2003 field season, and measured sections were completed in both the northern and southern parts of the study area. U-Pb dating of felsic volcanic units in these sections are in progress to provide firm temporal correlations.

The area between Jumble Mountain and Ramsey Peak (Figure 2) contains three-dimensional exposures of Hazelton Group strata within an area of approximately 50 km^2. Layered rocks in this area trend approximately east/west and dip shallowly to the north and northeast, with very minor structural disruption. The main Jumble Mountain massif itself has superb exposures of shallowly dipping volcanogenic strata that are unfortunately largely inaccessible due to very steep topography and glacial cover. This area will be spot-checked and sampled for U-Pb dating during the 2004 field season.

The base of the measured section in the Jumble Mountain area is exposed on the northeast flanks of the mountain (Figures 2, 3). The base of the section is dominated by coarse-grained, rhyolitic to dacitic fragmental rocks interbedded with massive, volcanogenic granule to pebble conglomerate, which comprises Unit A of this section (Figure 3). Conglomeratic beds generally decrease in abundance up section, becoming intercalated with finer-grained, well-bedded feldspathic-lithic wacke which forms Unit B (Figure 3). Wackes in this unit are fossiliferous, containing articulate and broken bivalves and less abundant gastropods. Ammonites recovered from this unit during previous summers have been identified as Late Toarcian to Early Aalenian (J.W. Haggart, personal communication, 2003), and a U-Pb age of 176.6 ± 0.7 Ma was obtained from a dacitic to rhyolitic crystal-lithic tuff from within this unit (R.M. Friedman, unpublished data). Fossil assemblages and sedimentary structures suggest a relatively shallow-water depositional environment. Unit C of this section is characterized by well-bedded, fine-grained tuffaceous beds intercalated with bioclastic lag deposits and less abundant feldspathic-lithic wacke (Figure 3). This unit is overlain by huge thicknesses of massive, volcanogenic, granule to boulder conglomerate. The entire measured section is intruded by a set of sparsely plagioclase-phyric to aphyric dacitic sills and dykes, which appear to be related to an aphanitic dacitic plug that intrudes the upper part of the section (Figure 3).

Exposures between the Jumble Mountain section and the Ramsey Peak area have not yet been measured or examined in detail but generally comprise large thicknesses of well-bedded, feldspathic-lithic wacke and granule to pebble mudstone, which are overlain by crowded plagioclase-phyric to aphyric, amygduloidal basaltic andesite flows(?).

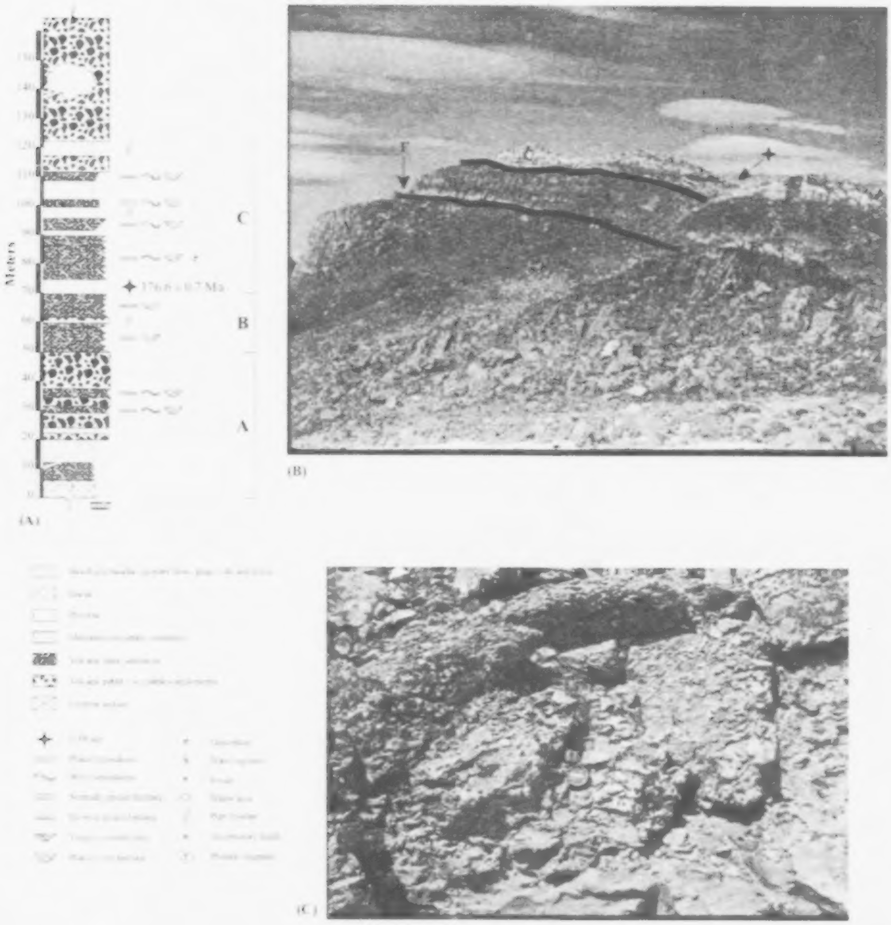

Figure 3. Measured section from the Jumble Mountain study area, showing (a) the location of section shown in Figure 2, (b) a view to the southeast across well-exposed strata northeast of Jumble Mountain, and (c) an outcrop photograph of a bioclastic lag deposit within the lower Jumble Mountain section. Units A, B, and C correspond with the vertical scale beside the measured section. Late Toarcian to Early Aalenian ammonoids have been identified at the indicated fossil site, stratigraphically below a crystal-lithic lapilli tuff which has yielded a U-Pb age of 176.6 ± 0.7 Ma.

Further to the north, volcanic stratigraphy in the Ramsey Peak area is dominated by three distinct groups of lithologies (Figure 4). The base of this section, which is presumed to overlie basaltic flows north of the Jumble Mountain section, is comprised of enormous thicknesses of massive, volcanogenic cobble to boulder conglomerate intercalated with very minor feldspathic-lithic wacke and thin tuffaceous beds. This comprises Unit A in the measured Ramsey Peak section (Figure 4). Overlying the massive conglomerates are moderately to poorly welded lapilli tuff and tuff breccia of felsic to intermediate composition and lesser volcanogenic wacke and mudstone (Unit B, Figure 4). The uppermost unit of measured section in the Ramsey Peak area, Unit C, comprises very thick, very densely welded, rhyolitic crystal-vitric tuff. Abundant plagioclase-phyric to aphyric basaltic dykes cut this section and are presumably related to a poorly exposed, plug-like basaltic intrusion that intrudes the conglomerates at the base of this section. Strata in this area continue northward from Ramsey Peak into the Oppy Lake basin, and will be examined during the 2004 field season.

Stratigraphic units in the Jumble Mountain and Ramsay Peak area extend northward along strike past Tsaydaychuz Peak, which has been mapped by Woodsworth (1980) as the Early Jurassic Telkwa Formation, to the Mount Preston

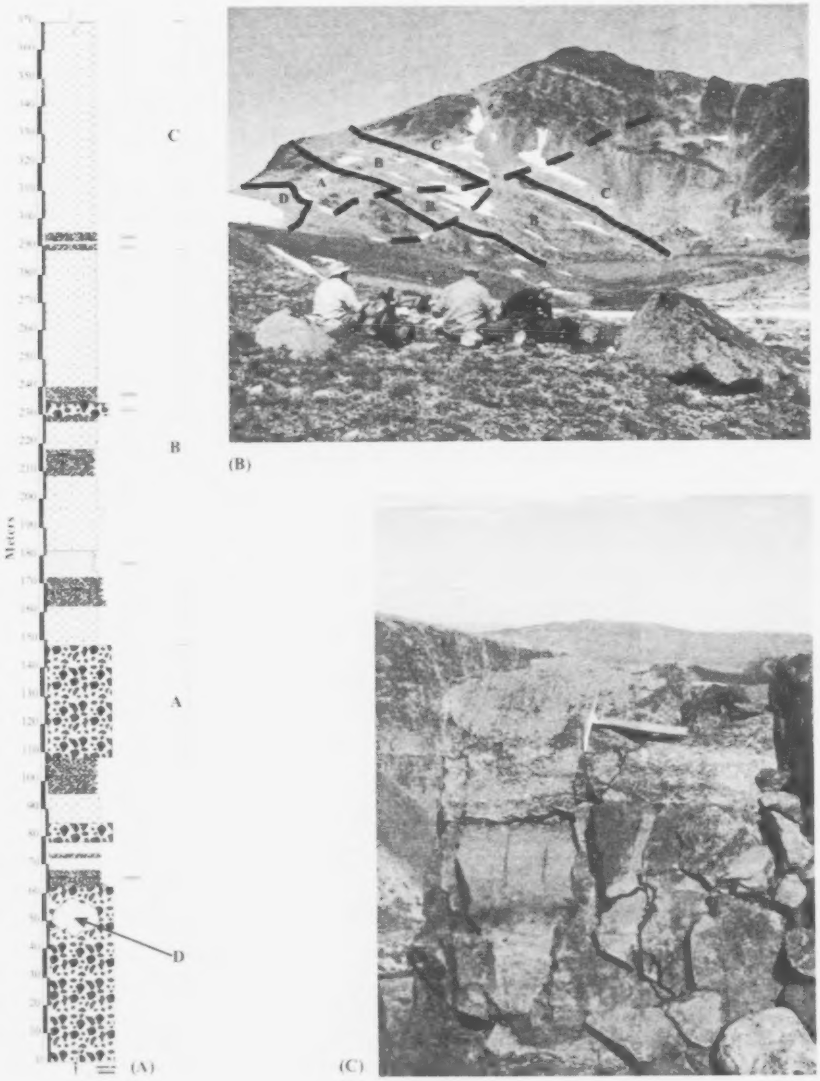

Figure 4. Measured section from the Ramsey Peak study area, showing (a) the location of section shown in Figure 2, (b) a view to the north at southern flank of Ramsey Peak, and (c) a view to the southeast across Sigutlat Lake towards the Nechako Plateau. Units A, B, C, and D correspond with the vertical scale beside the measured section. The outcrop in Figure 4c displays a sharp contact between fine-grained mudstone and densely welded, columnar jointed crystal-vitric tuff within Unit B of the Ramsey Peak section (see above).

area (Figure 2), where several measured sections were completed during the 2003 field season. Exposures in the Mount Preston area mainly consist of approximately northeast/southwest trending, shallowly-dipping volcaniclastic and sedimentary strata.

The base of the measured section in the Mount Preston area is dominated by very fine-grained feldspathic-lithic wacke to mudstone interbedded with less abundant, chloritized, densely welded, quartz-eye bearing rhyolitic crystal-vitric tuff (Figure 5). These units are overlain by a series of plagioclase-phyric to aphyric, variably amygdaloidal basalt to basaltic andesite flows, pillow lavas and broken pillow breccia (Units A and B; Figure 5). Mafic flows are overlain by large thicknesses of feldspathic-lithic wacke and mudstone of variable bedding thickness and grain size, comprising unit C in this area (Figure 5). Interbedded within the

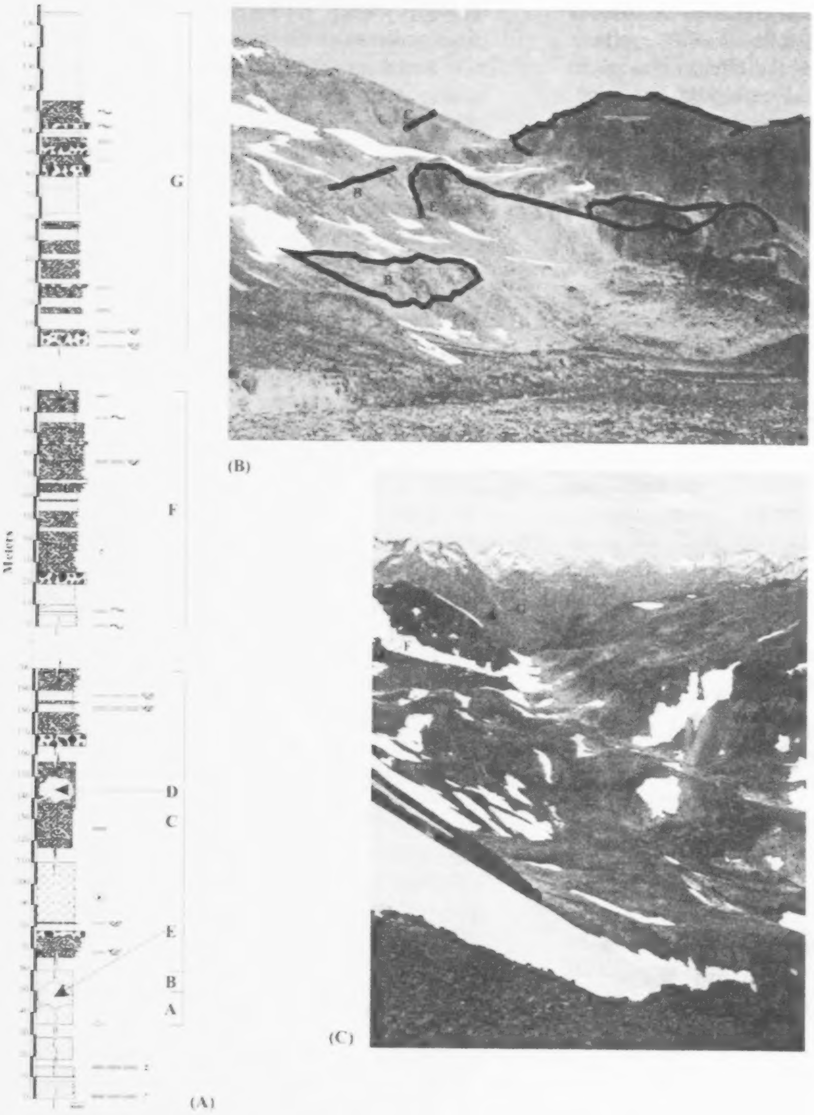

Figure 5. Measured sections from the Mount Preston study area, showing (a) locations of sections shown in Figure 2, (b) a view to the west towards Mount Preston (not visible), and (c) a view to the west into the cirque immediately south of Mount Preston. The cirque wall displays pillow basalts and broken pillow breccia (A), basaltic andesite flows (B), fine-grained volcanogenic mudstone (C), a basaltic plug (D), and a rhyolite dome (E). F and G correspond with the vertical scale beside respective measured sections.

clastic sediments is a densely welded, dacitic vitric-crystal tuff which locally contains distinctive felsic plutonic clasts. These volcanic and sedimentary strata are intruded by an aphanitic basaltic plug, Unit D, which has a distinctly triangular-shaped cross section (Figure 5). The basaltic pillow lavas that form part of the base of this section are intruded by a rhyolite to rhyodacite flow-dome complex, with a well developed carapace breccia (Unit E; Figure 5). Overlying strata in measured sections F and G (Figure 5) consist of a clastic-dominated section, with abundant planar and trough cross-laminae and mudcracks (section F; Figure 5), and a more tuffaceous-dominated section (section G; Figure 5), with variably welded, rhyolitic to dacitic lapilli tuff intercalated with less abundant clastic material.

Preliminary petrographic studies of igneous and sedimentary rock units in the southern Whitesail Lake area show the effects of weak to locally stong chlorite and carbonate alteration. Mafic minerals present within mafic flows and intrusive bodies are pervasively altered to chlorite, and amygdules, where present, are filled with epidote, calcite, and/or quartz. Plagioclase phenocrysts are euhedral and unaltered in porphyritic samples, and groundmass material typically consists of microcrystalline plagioclase that forms a trachytic texture around phenocrysts. Felsic to intermediate composition tuffaceous rocks commonly contain euhedral and broken plagioclase phenocrysts. Welded material is partially or wholly devitrified. Plutonic lithic fragments, where present, appear to be syenitic in composition with distinctive myrmekitic textures. Samples from the rhyolite to rhyodacite flow-dome complex south of Mount Preston are generally aphyric, and contain locally abundant quartz-filled vesicles. Clasts in sedimentary units consist of broken plagioclase grains, fine grained basalt, and welded tuffaceous material. Ongoing petrographic and textural studies of rocks from this region will help further refine rock-unit designations and provide additional information related to the depth of water in which the various units were deposited.

Mineral occurrences present within the southern Whitesail Lake study area include large and impressive gossans developed south of Mount Preston (Pond/Rivers Peak occurrence; BC MINFILE 093E 058) that are likely associated with porphyry-type systems related to small Late Cretaceous (?) porphyry intrusions. However copper mineralization in the form of small, mineralized quartz vein breccias were also noted in this area and this may represent older, possibly Hazelton-age, epigenetic mineralization. Several samples of the Cu-bearing breccias were collected for Pb isotope analysis to test this hypothesis. Numerous other mineral occurrences are also recorded in the BC MINFILE in the Mount Preston area (e.g., the Ron occurrences; BC MINFILE 093E 065, 079, 080, 081, 082); these are mainly narrow stringers, small pods and disseminations of chalcopyrite, pyrite, bornite and hematite in Hazelton Group volcanic rocks.

REGIONAL STUDIES

Regional studies during the 2003 field season included extensive sampling at the RDN (GOZ) property approximately 40 km northeast of Eskay Creek (BC MINFILE 104G 144; Figure 1), which is currently being explored as part of a joint venture between Barrick Gold Corporation and Rimfire Minerals Corporation. Samples were collected for U-Pb zircon dating of some of the main host rocks for mineralization on the property, and to geochemically characterize both the felsic host rocks and the intermediate(?) to mafic volcanic rocks in the area. These data will permit a comparison between the age(s) and geochemistry of volcanic rocks on the RDN property and those at Eskay Creek, and will establish the paleotectonic environment in which the Early and Middle Jurassic rocks in the area formed. Drill core from a deep drill hole on "Pillow Basalt Ridge" between the Iskut River and Forest Kerr Creek approximately 12 km northeast of Eskay Creek was also examined and sampled for lithogeochemical and dating studies. Pillow Basalt Ridge is underlain by a very thick (>1.8 km) pile of mafic volcanic rocks (and minor interlayered argillite) that is thought to be correlative with the hangingwall basalts at Eskay Creek. If this correlation is correct, the section at Pillow Basalt Ridge represents a much thicker and more extensive accumulation of presumably rift-related mafic volcanics than are preserved in the immediate Eskay Creek area. This would have important implications for the geometry and extent of Eskay Creek-age rifting in this area.

The Homestake Ridge property southeast of Stewart (Figure 1) was briefly visited together of personnel from the Bravo Ventures Group Inc., who are currently exploring the area. Samples of several of the main volcanic lithologies present in the Homestake Ridge area, as well as an extensive suite of sulphide samples, were collected for U-Pb dating, lithogeochemical and Pb isotopic studies to better constrain the nature and age of mineralization in the area.

Several mineral occurrences hosted by Hazelton Group volcanic rocks in the southern Babine Range (Figure 1) have been interpreted by Wojdak (1998) to be potentially syngenetic in origin. Volcanic and sedimentary strata in this area have been assigned to the Telkwa and Nilkitkwa formations by MacIntyre (1989) based on lithology and fossil age constraints, which indicate an age of Late Sinemurian to earliest

Toarcian for the immediate host rocks to mineralization. Syngenetic (?) mineralization in the area is therefore somewhat older than that at Eskay Creek. One of these occurrences (Harry Davis; BC MINFILE 093I 203, 204, 205 and 214), near the summit of Mt. Harry Davis north of Houston, was briefly examined and sampled for lithogeochemical analysis, Pb isotopic studies and U-Pb dating. In this area a thick section of flow-banded, quartz- and feldspar-phyric rhyolite is associated with bedded red and maroon lapilli tuffs which locally contain accretionary lapilli. Stratabound, possibly syngenetic, mineralization occurs in the form of sphalerite layers in thinly laminated chert, and epigenetic quartz-calcite-sphalerite(± fluorite) veins are also present in the area (Wojdak, 1998).

GEOCHEMICAL STUDIES – PRELIMINARY RESULTS

Geochemical studies of igneous rock units from the southern Whitesail Lake area and a regional sample suite are underway to characterize the geochemical affinity of each of the units and place constraints on the paleotectonic setting in which they were emplaced. Complete major, trace and rare earth element analyses have been obtained from 40 representative samples of intrusive and extrusive rock units from the southern Whitesail Lake study area and 29 samples of Hazelton Group rocks collected during regional investigations elsewhere in Stikinia. Preliminary interpretations of the data are presented in Figures 6 and 7, and discussed briefly below. Work thus far has focused on geochemically characterizing the various rock suites; detailed comparisons with volcanic host rocks for the Eskay Creek deposit have not yet been done.

Data from the southern Whitesail Lake study area, together with reconnaissance data from host volcanic rocks at the Nifty VMS occurrence in the northern Bella Coola map area (from Ray et al., 1998) are shown on various geochemical discriminant plots in Figure 6. The following main observations arise from the data. Volcanic and subvolcanic rock units in southern Whitesail Lake map area geochemically closely resemble the broadly age equivalent early Middle Jurassic host volcanic rocks at the Nifty occurrence which on strike to the southeast. They are broadly bimodal in composition (mainly basalt to basaltic andesitic and dacitic to rhyodacitic). The felsic units are all subalkaline; however the mafic units include both subalkaline and alkaline compositions. Although on an AFM diagram the Whitesail Lake samples fall mainly in the calc-alkaline field (as do the Nifty samples), immobile trace element plots such as Y vs. Zr (Figure 6) indicates that they are predominantly tholeiitic to transitional in composition. A plot of Rb vs. Y+Nb suggests that all of the volcanic rocks formed in a volcanic arc setting; however immobile trace element plots such as V vs. TiO_2 (Figure 6) indicate that the mafic volcanic and subvolcanic units include both island arc tholeiites and back-arc tholeiites. These mixed volcanic arc/back arc geochemical signatures are very similar to those described by Barrett and Sherlock (1996) at Eskay Creek, and is consistent with an overall rifted arc (intra-arc or back-arc) setting.

Most of the samples collected during regional investigations during the 2003 field season were from the general vicinity of known mineralization, hence most of them show evidence of moderate to strong hydrothermal alteration. Because of this, some major and trace elements have been mobilized and cannot be used to characterize the original geochemical composition and petrotectonic affinity of the samples. Data from three of the areas examined during the regional study (Pillow Basalt Ridge north of Eskay Creek), Homestake Ridge, and the southern Babine Range) are discussed briefly here, focusing mainly on immobile trace elements.

Pillow Basalt Ridge northeast of Eskay Creek comprises a thick section of basaltic flows and less abundant hyaloclastites, locally with thin interbeds of argillite. The volcanic rocks and a 28 m thick medium-grained gabbro sill that intrudes the section and is presumed to be synvolcanic range from basalt to basaltic andesite in composition. On AFM and Y vs. Zr plots the Pillow Basalt Ridge samples all fall in the tholeiitic field (Figure 7), and V vs. TiO_2 and Rb vs. Y+Nb plots indicate both island arc tholeiitic and back-arc affinities (Figure 7). These geochemical characteristics are similar to those for the hangingwall basalt at Eskay Creek and support a correlation between these two volcanic packages.

Two flow-banded felsic domes have been recognized at Homestake Ridge (R. MacDonald, personal communication, 2003). These domes were emplaced into a sequence of mainly intermediate(?) composition volcanic breccias

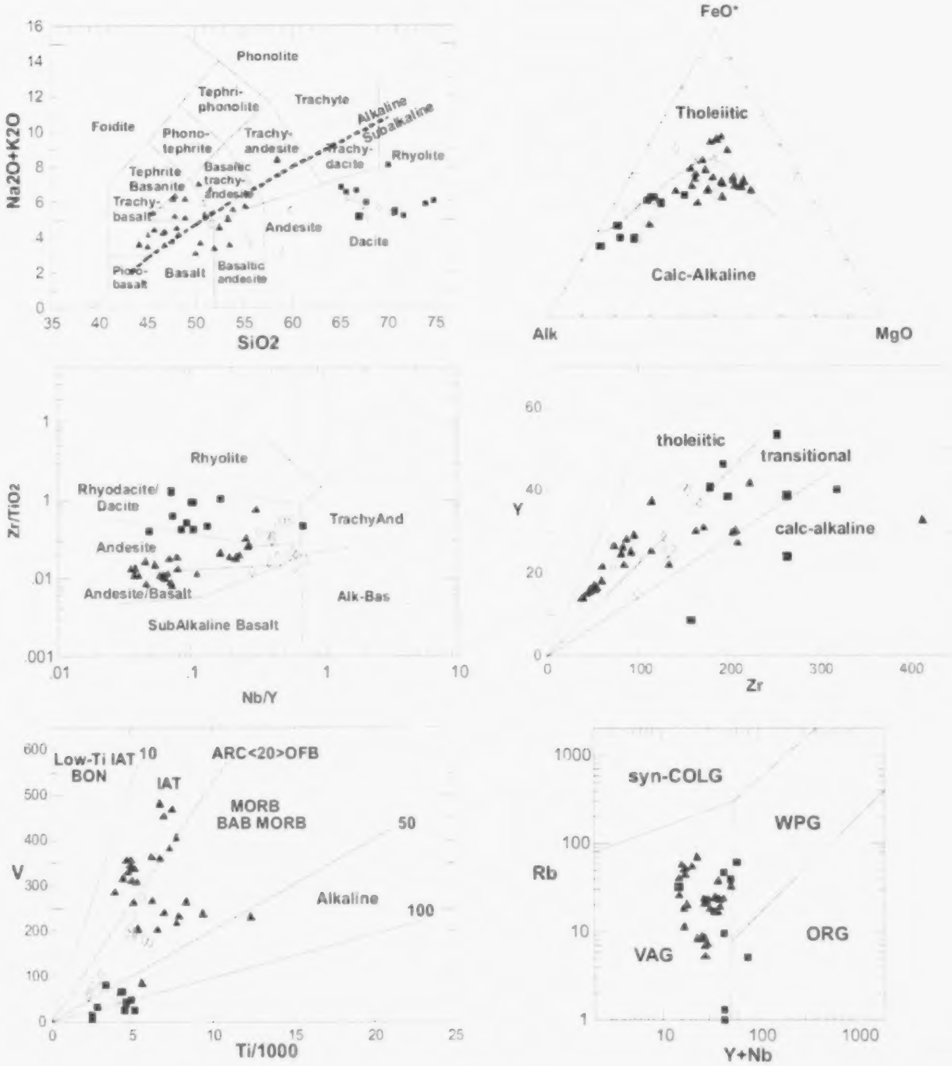

Figure 6. Geochemical discriminant diagrams for volcanic and shallow intrusive rocks in the southern Whitesail Lake study area. Closed squares indicate felsic tuffaceous and intrusive units and closed triangles indicate mafic intrusive and extrusive units. Open diamonds are analyses of felsic and mafic samples from the vicinity of the Nifty prospect (data from Ray et al., 1998).

and argillite. Several bodies of plagioclase-hornblende (± biotite) porphyry also intrude the volcaniclastic and argillite package. The felsic domes and feldspar-hornblende porphyry intrusions are similar in composition (scatter on the total alkalies vs. SiO_2 and AFM diagrams likely reflects major element mobility during the strong hydrothermal alteration that has affected all of the units in the area). They are all calc-alkaline, subalkaline and range from dacite to rhyolite in composition. On a Rb vs. Y+Nb plot all of the Homestake Ridge samples fall well within the volcanic arc field; however on a V vs. TiO_2 plot their compositions are consistent with eruption in a rifted arc setting.

A single sample from a flow-banded, sparsely quartz- and feldspar-phyric rhyolite sampled immediately south of the summit of Mt. Harry Davis in the southern Babine Range yields a calc-alkaline rhyolitic composition with a volcanic arc affinity.

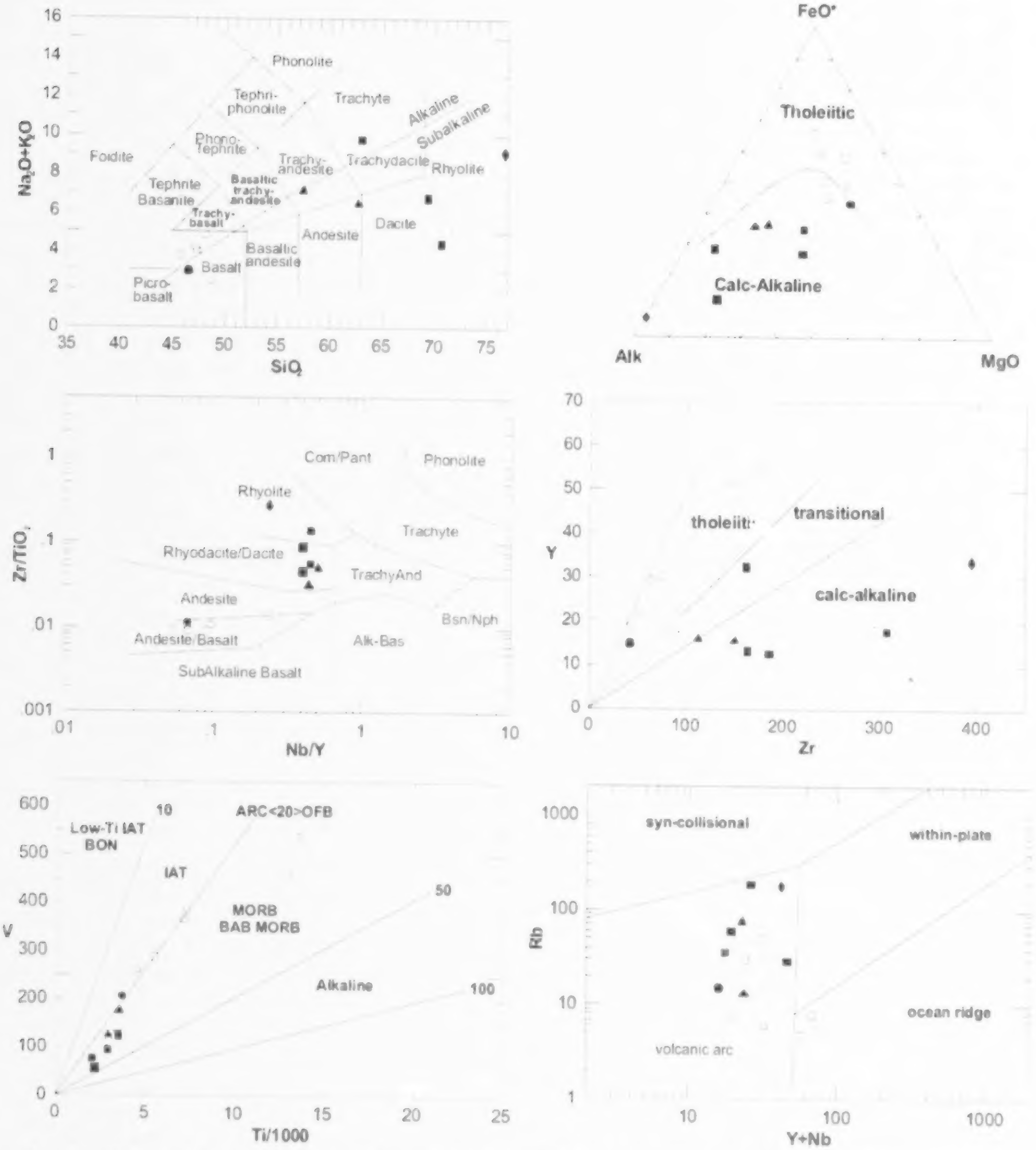

Figure 7. Geochemical discrimination diagrams for volcanic and shallow intrusive rocks from regional investigations of the upper Hazelton Group. Open circles are basalts from Pillow Basalt Ridge and the single closed circle is a gabbro body that intrudes the basalts. Closed squares and closed triangles are flow-banded rhyolite and plagioclase (± hornblende) porphyry bodies at Homestake Ridge. Closed diamond is a flow-banded rhyolite ata the HD prospect on Mt. Harry Davis in the southern Babine Range.

GEOCHRONOLOGY AND LEAD ISOTOPIC STUDIES

A number of samples are presently being processed for U-Pb zircon dating, including several felsic tuff and flow dome samples from the southern Whitesail Lake area, several samples from the RDN and Homestake Ridge properties, an intrusive diorite/gabbro from the Pillow Basalt Ridge section, and a single rhyolite unit from the southern Babine Range. An extensive suite of sulphide samples from all of the studied areas is also being prepared for Pb isotopic analysis.

DISCUSSION AND PRELIMINARY CONCLUSIONS

Although still at an early stage of a projected two-year project, our results thus far provide some new insights into the nature of upper Hazelton Group magmatism in several parts of Stikinia and the regional potential for additional ECT deposits. Mapping in the southern Whitesail Lake area has shown that the host stratigraphy for the Nifty VMS occurrence, which has been shown to be age equivalent to host rocks at Eskay Creek, extends at least another 75 km to the northwest. Furthermore facies analyses of these strata indicate predominantly shallow water deposition, and suggest formation in a rifted arc setting at the termination of Hazelton arc magmatism. Both of these characteristics, together with the presence of subaqueous felsic flow domes, are highly prospective for formation of ECT mineralization, similar to that at the Nifty occurrence. Several VMS prospects are known to occur farther along strike to the northwest in southwestern Whitesail Lake map area; these will be examined during the 2004 field season.

Preliminary work at Pillow Basalt Ridge north of Eskay Creek supports the suggestion that these basalts are stratigraphically equivalent to the hangingwall basalt at Eskay Creek. The great thickness of basalts present on Pillow Basalt Ridge (nearly 2 km), however, indicates that the latest stage of Hazelton Group magmatism in this area occurred during much more extensive rifting and associated subsidence than was manifest at Eskay Creek. The implications of this for ECT potential in the area are still uncertain.

Field examinations, preliminary geochemical studies, and discussions with industry geologists suggest that the Homestake Ridge mineralization occurs within a somewhat older portion of the Hazelton Group than Eskay Creek. In particular the plagioclase (± hornblende) porphyry bodies that intrude the section lithologically and geochemically resemble ~197-202 Ma intrusive units at the Red Mountain and Silbak Premier deposits to the northwest. Since these porphyry bodies intrude the felsic domes, intermediate volcaniclastic units and argillites that underlie much of the Homestake Ridge property, it appears unlikely that Eskay Creek stratigraphic equivalents are present in the area. U-Pb dating is underway to test this. A number of small VMS occurrences are known to be present within Betty Creek Formation-equivalent rocks of the Hazelton Group in the Kisault River valley to the south (e.g., Pinsent, 2001), however; thus the potential for syngenetic mineralization on Homestake Ridge cannot be ruled out.

Work carried out at the RDN property north of Eskay Creek was done as part of the industry-funded portion of this project, and results from that work are subject to a one-year confidentiality agreement.

Reconnaissance examinations of volcanic sections in the southern Babine Range and a single geochemical analysis of a flow-banded rhyolite unit in the area support the suggestion by Wojdak (1998) that these strata are somewhat older than the host rocks at Eskay Creek. U-Pb geochronology and Pb isotopic work is underway to more precisely constrain the age of the host rocks to possible syngenetic mineralization in this area and test whether the mineralization in this area is indeed syngenetic, or is epigenetic and unrelated to Hazelton Group magmatism.

FUTURE WORK

A considerably more extensive field season is planned for 2004, including approximately 6-8 weeks of mapping to complete the Whitesail Lake mapping project, and examination and sampling of a number of VMS (?) occurrences throughout the Hazelton Group. This regional work will be done in conjunction with industry geologists as well as BC Geological Survey

Branch and Geological Survey of Canada personnel.

ACKNOWLEDGMENTS

Danny Hodson of Rainbow West Helicopters and Richard LaPointe of West Coast Helicopters provided outstanding helicopter support during the 2003 field season. We thank Jim Haggart and the Geological Survey of Canada for providing logistical support for the mapping project, Lori Snyder for assistance and insights in the field, and Larry Diakow for valuable on-going discussions about Hazelton Group stratigraphy in the Bella Coola and Whitesail Lake areas and throughout Stikinia. Casey Bowe provided cheerful assistance in the field. We also thank Ian Dunlop and Aletha Buschman of Barrick Gold for guidance and discussions during field work in the Eskay Creek area, Rob MacDonald of Bravo Ventures Group for guidance during a visit to the Homestake Ridge property, Paul Wojdak of the BC Geological Survey Branch for valuable discussions concerning VMS occurrences in the southern Babine Range, and Paul McGuigan of Cambria Geosciences for insights into the regional VMS potential in Stikinia. Funding for this project was provided by the Rocks to Riches Program, which is administered through the BC & Yukon Chamber of Mines, as well as four mining companies (Barrick Gold Corp., Heritage Exploration Inc., Kenrich-Eskay Mining Corp. and Placer Dome Inc.). Richard Friedman is thanked for critically reading the manuscript.

REFERENCES

Barrett, T.J. and Sherlock, R.L. (1996): Geology, lithogeochemistry and volcanic setting of the Eskay Creek Au-Ag-Cu-Zn deposit, northwestern British Columbia; *Exploration and Mining Geology*, Volume 5, pages 339-368.

Childe, F. (1996): U-Pb geochronology and Nd and Pb isotope characteristics of the Au-Ag-rich Eskay Creek volcanogenic massive sulfide deposit, British Columbia; *Economic Geology*, Volume 91, pages 1209-1224.

Childe, F. (1997): Timing and tectonic setting of volcanogenic massive sulphide deposits in British Columbia: constraints from U-Pb geochronology, radiogenic isotopes and geochemistry; *University of British Columbia*, Unpublished Ph.D. thesis, 557 pages.

Diakow, L.J., Mahoney, J.B., Gleeson, T.G., Hrudey, M.G., Struik, L.C. and Johnson, A.D. (2002): Middle Jurassic stratigraphy hosting volcanogenic massive sulphide mineralization in eastern Bella Coola map area (NTS 093/D), southwest British Columbia; *B.C. Ministry of Energy, Mines and Petroleum Resources*, Geological Fieldwork 2001, Paper 2002-1, pages 119-134.

Haggart, J.W., Mahoney, J.B., Diakow, L.J., Woodsworth, G.J., Gordee, S.M., Snyder, L.D., Poulton, T.P., Friedman, R.M. and Villeneuve, M.E. (2003): Geological setting fo the eastern Bella Coola map area, west-central British Columbia; *Geological Survey of Canada*, Current Research 2003-A4, 9 pages.

Hannington, M.D., Poulsen, K.H., Thompson, J.F.H., and Sillitoe, R.H. (1999): Volcanogenic gold and epithermal-style mineralization in the VMS environment; *In* Barrie, C.T., and Hannington, M.D., Volcanic-Associated Massive Sulfide Deposits: Processes and Examples in Modern and Ancient Settings: *Reviews in Economic Geology*, Volume 8, pages 325-356.

Juras, S.J. and Spooner, E.T.C., *eds.* (1996): Volcanogenic Massive Sulfide Deposits of the Cordillera. *Exploration and Mining Geology*, Volume 5, Number 4, pages 281-458.

Lewis, P.D. and Tosdal, R.M. (2000): Metallogenesis of the Iskut River area, northwestern British Columbia; *Mineral Deposit Research Unit*, Special Publication No. 1, 337 pages.

MacIntyre, D.G., Desjardins, P. and Tercier, P. (1989): Jurassic stratigraphic relationships in the Babine and Telkwa ranges (93L/10, 11, 14,15); *B.C. Ministry of Energy, Mines and Petroleum Resources*, Geological Fieldwork 1988, Paper 1989-1, pages 195-208.

Massey, N.W.D. (1999): Volcanogenic massive sulphide deposits in British Columbia; *B.C. Ministry of Energy and Mines*, Open File 1999-2.

Massey, N.W.D., Alldrick, D.J. and Lefebure, D.V. (1999): Potential for subaqueous hot-spring (Eskay Creek) deposits in British Columbia; *B.C. Ministry of Energy and Mines*, Open File 1999-14.

Nadaraju, G.D. (1993): Triassic-Jurassic biochronology of the Iskut River map area, northwestern British Columbia; *University of British Columbia*, Unpublished M.Sc. thesis, 268 pages.

Pinsent, R.H. (2001): Mineral deposits of the Upper Kitsault River area, British Columbia (103P/W); *B.C. Ministry of Energy, Mines and Petroleum Resources*, Geological Fieldwork 2000, Paper 2001-1, pages 313-326.

Ray, G.E., Brown, J.A. and Friedman, R.M. (1998): Geology of the Nifty Zn-Pb-Ba prospect, Bella Coola district, British Columbia; *B.C. Ministry* *of Energy, Mines and Petroleum Resources*, Geological Fieldwork 1997, Paper 1998-1, pages 20-1 – 20-28.

Roth, T., Thompson, J.F.H. and Barrett, T.J. (1999): The precious metal-rich Eskay Creek deposit, northwestern British Columbia; *In* Barrie, C.T., and Hannington, M.D., Volcanic-Associated Massive Sulfide Deposits: Processes and Examples in Modern and Ancient Settings: *Reviews in Economic Geology*, Volume 8, pages 357-373.

Roth, T. (2002): Physical and chemical constraints on mineralization in the Eskay Creek deposit, northwestern British Columbia: Evidence from petrography, mineral chemistry, and sulfur isotopes: *University of British Columbia*, Unpublished Ph.D. thesis, 401 pages.

Wojdak, P. (1998): Volcanogenic massive sulphide deposits in the Hazelton Group, Babine Range, B.C.; *B.C. Ministry of Energy, Mines and Petroleum Resources*, Exploration and Mining in British Columbia 1998, pages C1–C13.

Woodsworth, G.J. (1980): Geology of Whitesail Lake (93E) map area, British Columbia; *Geological Survey of Canada*, Open File 708, 1:250 000.

PLATINUM-GROUP ELEMENTS IN THE AFTON CU-AU PORPHYRY DEPOSIT, SOUTHERN BRITISH COLUMBIA

By Graham T. Nixon[1]

KEYWORDS: Cu-Au porphyry, alkaline, Iron Mask Batholith, platinum-group elements, copper-iron sulphides, geology, geochemistry, Afton, picrite

INTRODUCTION

Alkaline intrusive complexes associated with Cu-Au porphyry deposits in British Columbia (Barr *et al.*, 1976) are currently the focus of investigations funded by the "Rocks to Riches" Program, B. C. and Yukon Chamber of Mines, to determine the potential of these magmatic-hydrothermal systems for platinum-group elements (PGE). Although there are reports of trace amounts of PGE, specifically palladium, in smelter concentrates from Cu-Au porphyry deposits in the province, very little is known about actual abundances in the mineralized rocks and ores being mined. To address this deficiency, data pertaining to PGE mineralization in alkaline complexes has recently been published by Nixon and Carbno (2001), Dunn *et al.* (2001), Nixon (2001, 2002, 2003) and Nixon and Peatfield (2003); and PGE occurrences pertaining to these and other geological environments in the province have been compiled by Hulbert (2001).

A new exploration initiative by DRC Resources Corporation at the Afton mine near Kamloops provided an opportunity to sample core carrying Cu-Au-Ag-PGE mineralization encountered during deep-drilling beneath and beyond the open pit. The core recovered and assayed by DRC Resources allowed a small suite of samples to be collected from PGE-enriched intervals for mineralogical study and multi-element analysis using different analytical techniques. This report presents quantitative data for the PGE and other metals in mineralized drill core from Afton, and petrographic observations of the host rocks, ore minerals and alteration assemblages. These new data, albeit from a small sample suite, allow for a preliminary assessment of the nature and origin of the PGE-bearing sulphide mineralization.

GEOLOGICAL SETTING

The Afton mining camp near Kamloops contains a number of important copper-gold deposits, including past-producing open pit operations at Afton, the most important deposit, Ajax East, Ajax West, Pothook and Crescent, as well as orebodies with published reserves such as Big Onion, DM and Python-Macaoo (Figs. 1 and 2). Grade and tonnage data for these and other deposits and prospects in the district are tabulated by Kwong (1987) and Ross *et al.* (1995). The most significant mineral occurrences are hosted by the Iron Mask Batholith, a northwesterly-trending composite body which intrudes volcanic, volcaniclastic and minor sedimentary rocks of the Late Triassic Nicola Group (Figs. 1 and 2). The batholith is unconformably overlain by, or in fault contact with, volcanic and sedimentary rocks of the Tertiary (Eocene) Kamloops Group (Ewing, 1981).

The geology of the Iron Mask Batholith and its ore deposits have been described by Cockfield (1948), Carr (1956), Carr and Reed (1976), Preto (1967, 1972), Northcote (1974, 1976, 1977), Hoiles (1978), Kwong (1982, 1987), Kwong *et al.* (1982), Snyder (1994), Lang and Stanley (1995), Ross *et. al.* (1995) and Snyder and Russell (1993, 1995). In brief, the batholith comprises two distinct intrusive bodies, the Cherry Creek pluton, exposed around the shores of Kamloops Lake in the north, and the larger Iron Mask pluton to the south (Fig. 1). The Iron Mask Pluton comprises four major intrusive phases: the biotite-clinopyroxene-bearing Pothook diorite and related xenolith-rich, locally hornblende-bearing Hybrid unit, the Cherry Creek diorite-monzonite(-syenite) and the hornblende-phyric Sugarloaf diorite (Snyder and Russell, 1995; Fig. 2). The xenolith-bearing Hybrid unit is subdivided into several phases based on textures and clast abundance: an intrusive, xenolith-rich, heterolithic breccia (Type 1) occurring at contacts with the Nicola Group; a similar breccia with a variegated matrix in which some clasts have reacted with their host (Type 2); and a xenolith-poor breccia with a locally pegmatitic matrix containing recrystallized and digested clasts (Type 3). The Hybrid subtypes exhibit gradational contacts among themselves and with Pothook diorite which has ambiguous relationships with the Cherry Creek phase. All three units were likely emplaced penecontemporaneously, whereas the Sugarloaf diorite is considered to be marginally younger (Snyder and Russell 1995). According to U-Pb zircon dating of the Pothook, Hybrid and Cherry Creek units, the age of the Iron Mask Batholith is approximately 204.5 ± 3 Ma (Mortensen *et al.*, 1995), or latest Triassic according to the time scale of

---

[1] *British Columbia Ministry of Energy and Mines*

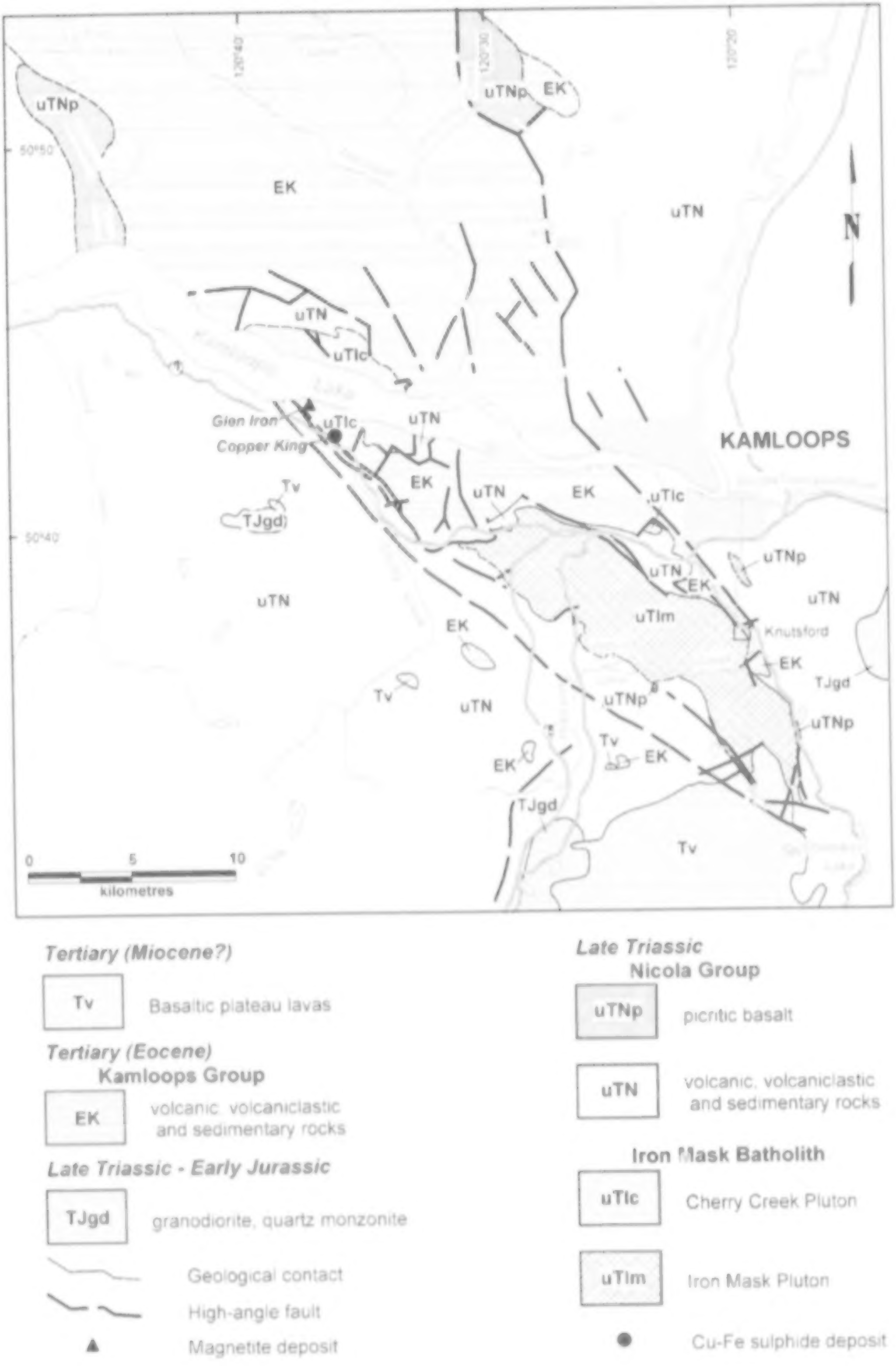
120°40'
120°30'
120°20'
50°50'
50°40'
N
uTNp
EK
uTN
uTlc
Glen Iron
Copper King
Tv
TJgd
KAMLOOPS
uTlm
Knutsford
0
5
10
kilometres
Tertiary (Miocene?)
Tv
Basaltic plateau lavas
Tertiary (Eocene)
Kamloops Group
EK
volcanic, volcaniclastic and sedimentary rocks
Late Triassic - Early Jurassic
TJgd
granodiorite, quartz monzonite
Geological contact
High-angle fault
Magnetite deposit
Late Triassic
Nicola Group
uTNp
picritic basalt
uTN
volcanic, volcaniclastic and sedimentary rocks
Iron Mask Batholith
uTlc
Cherry Creek Pluton
uTlm
Iron Mask Pluton
Cu-Fe sulphide deposit

Figure 1. Regional geological setting of the Iron Mask Batholith (modified after Kwong 1987; Snyder and Russell, 1993, 1995; Snyder 1994).

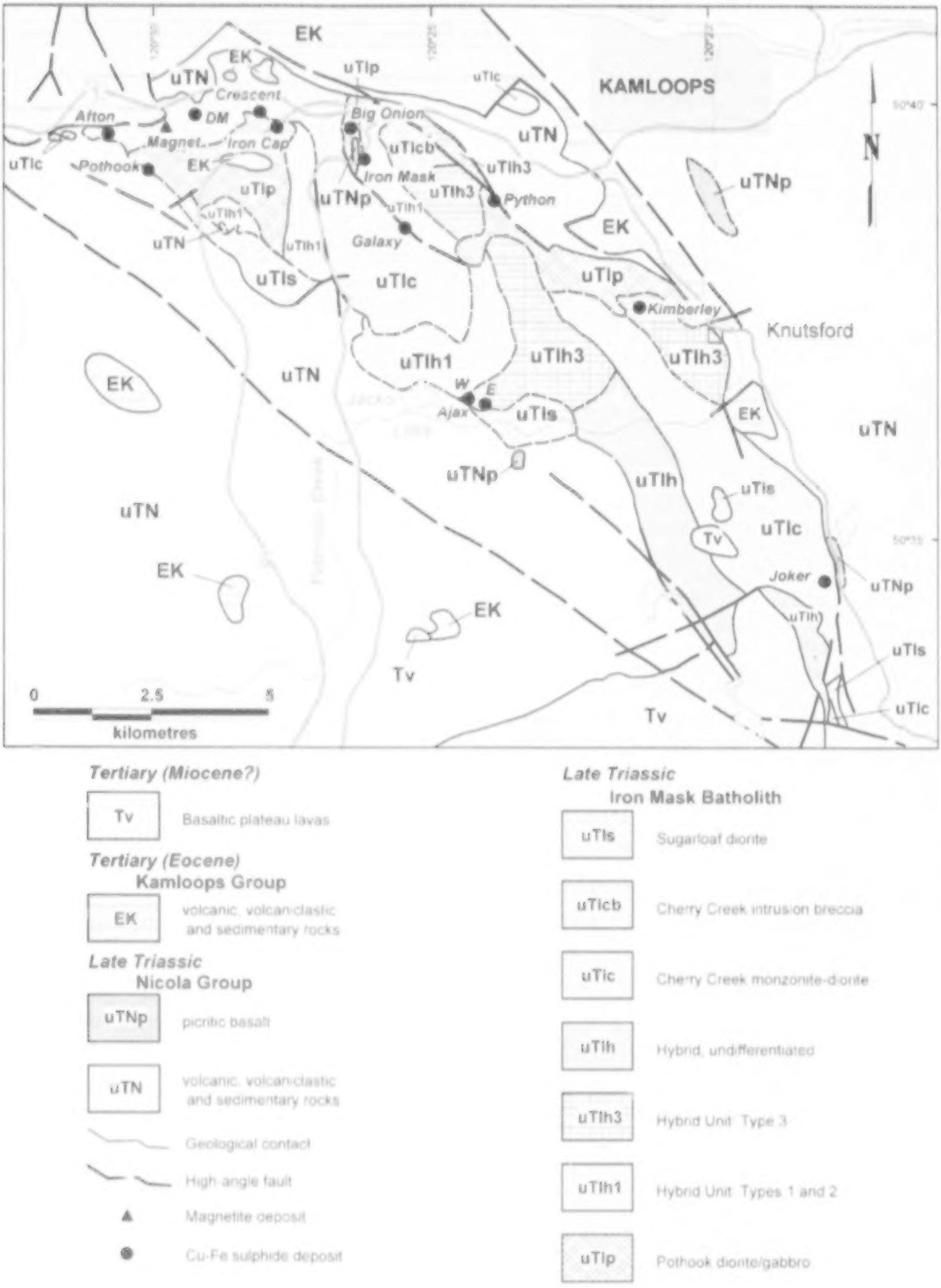
120°30'
120°25'
120°20'
50°40'
50°35'
N
KAMLOOPS
Knutsford
Afton
Magnet
DM
Crescent
Iron Cap
Pothook
Big Onion
Iron Mask
Python
Galaxy
Kimberley
Ajax
W
E
Joker
EK
uTN
uTlc
uTlp
uTlcb
uTlh3
uTNp
uTlh1
uTls
uTlh
Tv
0
2.5
5
kilometres
Tertiary (Miocene?)
Tv Basaltic plateau lavas
Tertiary (Eocene)
Kamloops Group
EK volcanic, volcaniclastic and sedimentary rocks
Late Triassic
Nicola Group
uTNp picritic basalt
uTN volcanic, volcaniclastic and sedimentary rocks
Geological contact
High angle fault
Magnetite deposit
Cu-Fe sulphide deposit
Late Triassic
Iron Mask Batholith
uTls Sugarloaf diorite
uTlcb Cherry Creek intrusion breccia
uTlc Cherry Creek monzonite-diorite
uTlh Hybrid, undifferentiated
uTlh3 Hybrid Unit: Type 3
uTlh1 Hybrid Unit: Types 1 and 2
uTlp Pothook diorite/gabbro

Figure 2. Geology of the southern part of the Iron Mask Batholith showing the main intrusive phases and location of selected Cu-Au porphyry deposits and past-producing mines (modified after Kwong, 1987; Snyder 1994).

Palfy *et al.* (2000).

Within the Kamloops region, the Nicola Group contains picritic basalts which are particularly well exposed at Watching and Carabine creeks (Fig. 1). The most recent studies of these picrites have concluded that they represent volcanic stratigraphy conformably overlying the Nicola Group, and though locally incorporated in the Iron Mask Batholith as serpentinized xenoliths and fault slivers, are genetically unrelated to the plutonic rocks (Snyder and Russell, 1995). In this report, the picritic basalts are included within the Nicola Group.

MINERALIZATION

Carr and Reed (1976) and Kwong (1987), among others, have pointed out that the Afton deposit appears to be unique in the Canadian Cordillera in that it is distinguished by a thick zone of supergene alteration that extends to considerable depth (up to 500 m) due to the wet climate and highly faulted and fractured nature of the orebody. These authors further noted that despite such alteration, the average grade of copper in the supergene zone is nearly equivalent to that in the hypogene zone. Although the Afton deposit generally lacks well-defined hydrothermal alteration zoning, Carr and Reed (1976) did distinguish both pyritic and magnetite-rich zones (Fig. 3). Based on detailed mineralogical observations, Kwong (1987) divided the Afton pit into a northeastern part characterized by potassium feldspar, epidote, hematite and magnetite (and minor clinopyroxene); and a southwestern portion dominated by ankeritic alteration and/or amphibole and pyrite.

The main copper-bearing minerals in the supergene zone are native copper and a sooty variety of chalcocite (in a 2:1 ratio) accompanied by minor cuprite, malachite and azurite. Hypogene sulphides are typically bornite and chalcopyrite with lesser chalcocite, and occur in veins and disseminations. To date, there are no published accounts of platinum-group minerals in the Afton deposit and little data concerning the abundance and distribution of the PGE.

THE AFTON MINE

Prior to the start of mining operations in 1977 by Afton Mines Limited, proven reserves for the Afton orebody, the largest in the district, totalled 30.84 million tonnes grading 1.0 % Cu, 0.58 g/t Au and 4.19 g/t Ag at a cutoff grade of 0.25 % Cu (Carr and Reed, 1976). Although complex in detail, the shape of the orebody, as defined by the 0.25 % Cu cut-off grade, could be generalized as planar, striking N70°W with an average dip of 55°S and tapering downward to form a triangular-shaped zone when viewed in section from the south (Fig. 3). The upper part of the orebody prior to stripping formed a thick supergene zone, estimated to represent approximately 80% of the mineable ore (Carr and Reed, 1976), underlain by hypogene ore (Fig. 3). The open pit resource was depleted in July 1987 after extraction of 22.1 million tonnes of ore grading 0.91 % Cu and 0.67 g/t Au (Ross *et al.*, 1995). Teck-Cominco allowed the claims to lapse in 1999 leaving a known underground mineral resource of approximately 9.5 million tonnes grading 1.5 % Cu and 1.1 g/t Au (Ross *et al.*, 1995).

Subsequently, DRC Resources Corporation acquired the ground and began a deep-drilling program in 2000 in order to evaluate the potential of the underground mineral resource beneath the open pit. By April 2002, 23,800 m of drilling had outlined a steeply dipping, southwesterly-plunging, tabular deposit passing through the southwestern corner, and extending beyond the limits, of the open pit (Fig. 4). According to a recent scoping study (October 2003), the Afton "Main Zone", as the principal orebody is known, measures 90 m in width by at least 800 m in length, and has a measured mineral resource of 9.54 million tonnes grading 1.29 % Cu, 0.94 g/t Au, 3.44 g/t Ag and 0.12 g/t Pd at a 0.7 % Cu *equivalent* cut-off grade; and an indicated resource of 59.16 million tonnes grading 1.05 % Cu, 0.83 g/t Au, 2.49 g/t Ag and 0.12 g/t Pd at the same cut-off. The main zone of mineralization remains open to the southwest and appears to narrow at depth and towards the surface. Further drilling is currently underway to better delineate the mineralization.

Potential Significance of the Picrite

As previously noted by Carr and Reed (1976), picrites are spatially associated with (and commonly within 300 metres of) some of the largest Cu-Au deposits in the Iron Mask Batholith, notably at Afton (Fig. 4) and Ajax (Ross *et al.* 1995).

In the southwestern quadrant of the Afton pit, Kwong (1987) noted the development of an intense, pre-supergene ankeritic alteration associated with the copper mineralization. He proposed that carbonatization occurred during second boiling of a magmatic volatile phase rich in CO_2, and that early ankeritic alteration could be used to identify potentially mineralized zones of magmatic-hydrothermal activity. Given the generally low CO_2 contents of arc magmas, a more plausible source for CO_2 may be the Nicola Group, where contact metamorphism and circulation of hot acidic solutions would promote the breakdown of calcium carbonate in marine sedimentary and volcaniclastic rocks. As argued by Kwong (1987), interaction of CO_2-enriched, magmatic-hydrothermal fluids with highly magnesian picrite would serve to increase the pH of the fluid leading to the precipitation of Cu-Fe sulphides. This could explain the proximity of this style of alteration and mineralization to the picrite contact in the Afton pit. Moreover, the extensions of the faults that control the distribution of the picrite would also be attractive exploration targets (Fig. 4).

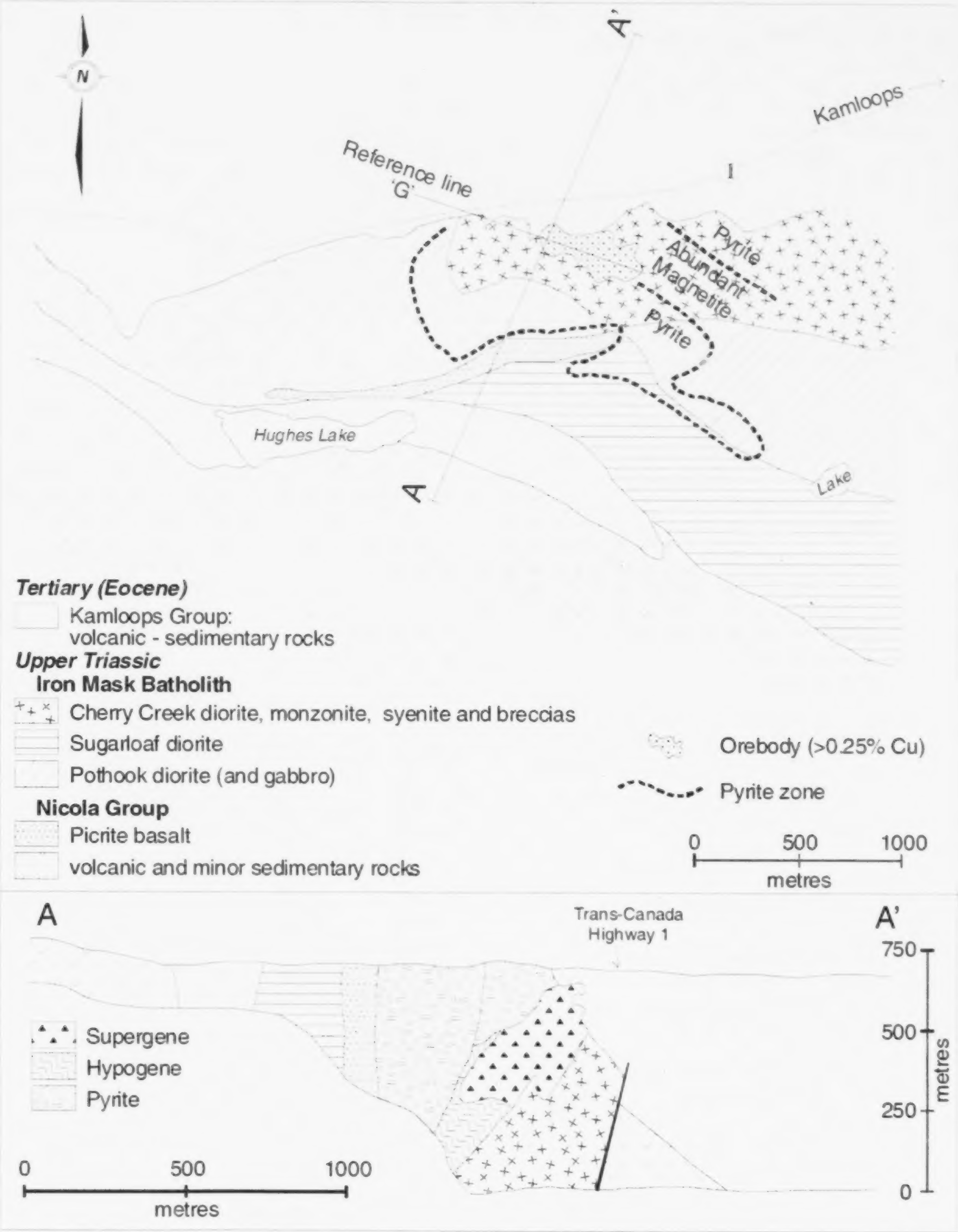
N
A'
Kamloops
Reference line 'G'
I
Pyrite
Abundant Magnetite
Pyrite
Hughes Lake
Lake
A
Tertiary (Eocene)
Kamloops Group: volcanic - sedimentary rocks
Upper Triassic
Iron Mask Batholith
Cherry Creek diorite, monzonite, syenite and breccias
Sugarloaf diorite
Pothook diorite (and gabbro)
Nicola Group
Picrite basalt
volcanic and minor sedimentary rocks
Orebody (>0.25% Cu)
Pyrite zone
0
500
1000
metres
A
Trans-Canada Highway 1
A'
750
500
250
0
metres
Supergene
Hypogene
Pyrite
0
500
1000
metres

Figure 3. Simplified geological map and cross-section of the Afton property prior to mining (modified from Carr and Reed 1976).

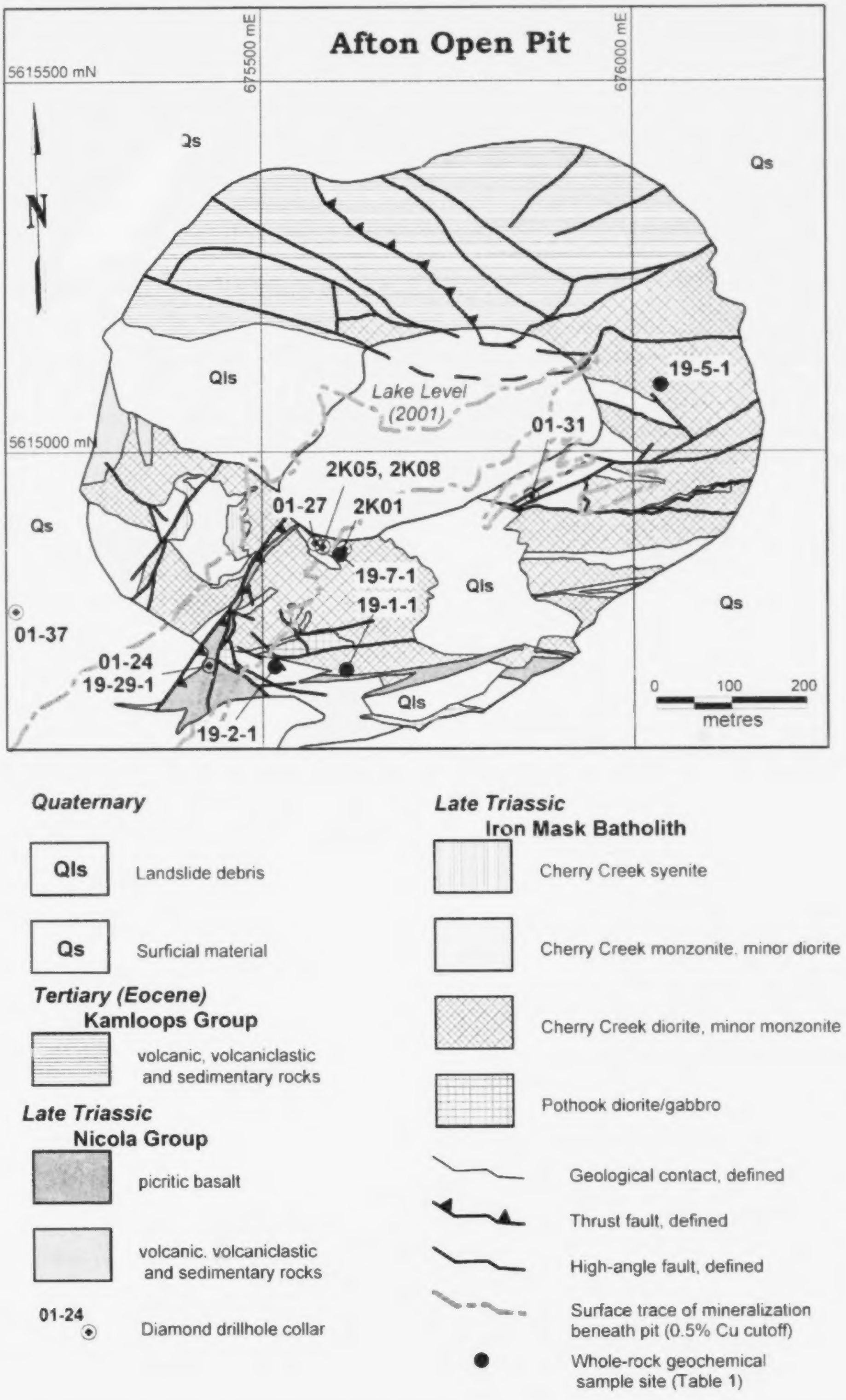
Afton Open Pit
5615500 mN
675500 mE
676000 mE
N
Qs
Qs
Qls
Lake Level (2001)
19-5-1
01-31
5615000 mN
2K05, 2K08
01-27
2K01
Qs
19-7-1
Qls
19-1-1
Qs
01-37
01-24
19-29-1
Qls
19-2-1
0
100
200
metres
Quaternary
Qls
Landslide debris
Qs
Surficial material
Tertiary (Eocene)
Kamloops Group
volcanic, volcaniclastic and sedimentary rocks
Late Triassic
Nicola Group
picritic basalt
volcanic, volcaniclastic and sedimentary rocks
01-24
Diamond drillhole collar
Late Triassic
Iron Mask Batholith
Cherry Creek syenite
Cherry Creek monzonite, minor diorite
Cherry Creek diorite, minor monzonite
Pothook diorite/gabbro
Geological contact, defined
Thrust fault, defined
High-angle fault, defined
Surface trace of mineralization beneath pit (0.5% Cu cutoff)
Whole-rock geochemical sample site (Table 1)

Figure 4. Geological map of the Afton open pit showing surface projection of zones of Cu-Au mineralization intersected in deep drilling and locations of samples collected from the pit and drill core (modified from a figure entitled "Afton Pit Geology Map", DRC Resources website; geology by Chris Sebert and Marek Mroczek).

The anomalously high K_2O concentrations (~3 wt. %; Kwong, 1987) of picrite in the Afton pit compared to picrites in the surrounding region (~1 wt. % or less; Kwong, 1987; Snyder, 1994) indicates that the Afton picrite has experienced potassium metasomatism. The mineralogical evidence for this is represented by trace amounts of phlogopite noted in thin section by Kwong (1987). Although a minor amount of pyrite is typically present in Nicola Group rocks (including the picrite), Cu-Fe sulphides rarely penetrate more than a few centimetres into the picrite. This emphasizes the potential importance of this lithology to serve as a "chemical buffer" for the mineralizing fluids. In certain cases, therefore, the picrites may be important in localizing the site of ore deposition, but are not necessarily the only controls on sulphide mineralization.

WHOLE-ROCK GEOCHEMISTRY

A small suite of intrusive rocks from the walls of the open pit and drill core were analyzed for major elements by x-ray fluorescence spectrometry in the Teck-Cominco Laboratories, Vancouver. The results and details of analytical methods, accuracy and precision are given in Table 1, and sample locations are shown in Figure 4.

Sample Descriptions

The whole-rock suite includes variably altered samples of Cherry Creek diorite, syenite and leuco-monzonite dikes from the pit, and fresh hornblende monzonite from drill core (Fig. 4). The diorite is a dark greyish green, fine grained, inequigranular to microporphyritic rock containing trace amounts of sulphide and relict ferromagnesian minerals altered to chlorite and opaque oxides. The rock contains disseminated carbonate and is cut by orange-brown weathering veinlets of ankeritic carbonate. Two pale pink to greenish pink, fine-grained, leucocratic syenite dikes (~5 vol. % mafic pseudomorphs) cut Cherry Creek diorite and are themselves cut by thin carbonate veins. The syenites are partially altered to epidote-chlorite assemblages, and the dike in the eastern wall of the pit (01GNX19-5-1, Fig. 4) is clearly cut by late, northerly trending magnetite veins and dikes (<1 m in width) with epidotized envelopes. A greenish grey leuco-monzonite dike intruding Cherry Creek diorite is cut by potassium feldspar veins and traversed by fractures lined with finely crystalline pyrite. The hornblende monzonite is a pinkish grey, equigranular, medium-grained rock that is virtually unaltered.

Results

The compositions of samples collected in the walls of the open pit have been modified to varying degrees by secondary alteration processes. For example, the extremely high loss loss on ignition (10.3-15.1 wt. %) for Cherry Creek diorite and a syenite dike (01GNX19-2-1) in the southern wall of the pit, proximal to the surface trace of the "Main Zone" of mineralization (Fig. 4), primarily reflects loss of CO_2 due to intense carbonate alteration. These samples also have anomalously low silica, alumina and alkalis. Mobility of alkalis is also evident in the leuco-monzonite dike (Na_2O/K_2O = 7), which is exposed at the same locality.

The CIPW-normative compositions of rocks from the Afton pit and Iron Mask Batholith in general are plotted in the IUGS classification scheme in Figure 5. This

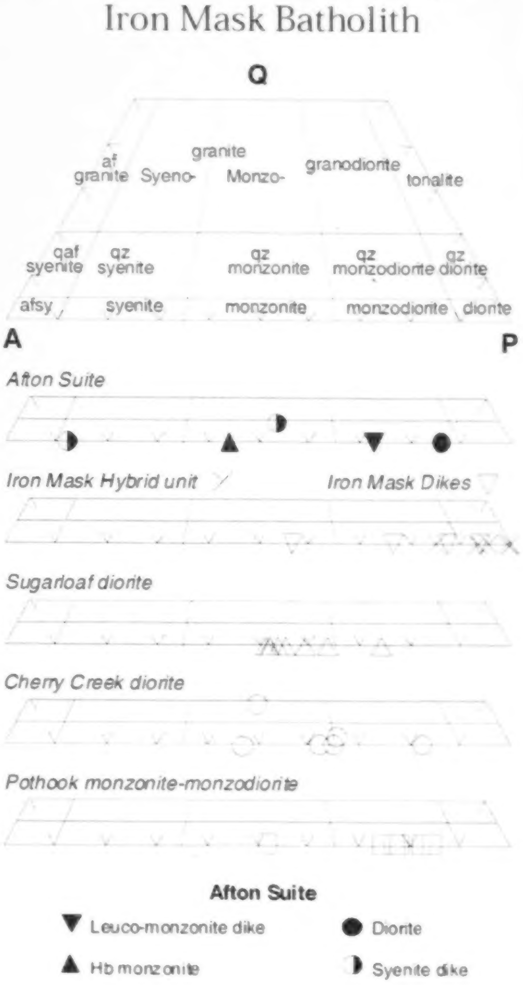

Figure 5. CIPW-normative compositions (wt. %) of the Afton pit suite and plutonic rocks from the Iron Mask Batholith (Snyder 1994) plotted in the QAP classification scheme of Le Maitre (1989) using the projection parameters of Le Maitre (1976).

TABLE 1: MAJOR ELEMENT WHOLE-ROCK ANALYSES OF SELECTED PLUTONIC ROCKS, AFTON PIT

		UTM Zone 10 (NAD 83)		wt. %												
Sample	Rock Type	Easting	Northing	SiO_2	TiO_2	Al_2O_3	Fe_2O_3	FeO	MnO	MgO	CaO	Na_2O	K_2O	P_2O_5	LOI	Sum
01GNX19-1-1	Diorite	675614	5614714	40.65	0.64	9.71	5.43	6.35	0.25	15.15	7.92	1.01	0.55	0.21	10.30	98.17
01GNX19-2-1	Syenite dike	675517	5614714	47.48	0.70	11.60	1.88	2.82	0.07	5.80	8.68	2.58	2.03	0.76	15.14	99.52
01GNX19-5-1	Syenite dike	676037	5615089	58.13	0.40	17.04	2.05	0.31	0.10	1.47	4.34	3.07	8.63	0.18	3.37	99.08
01GNX19-7-1	leuco-monzonite dike	675605	5614875	56.77	0.55	18.20	1.22	1.89	0.07	3.60	4.44	7.05	0.97	0.23	4.66	99.65
01GNX19-29-1	Hornblende monzonite (DDH01-24 352.2m)	675429	5614712	52.55	0.62	18.43	4.31	2.38	0.09	2.83	7.13	3.78	4.36	0.44	2.42	99.35
Quality Control																
Std SY 4 *				49.77	0.28	20.60	3.14	2.70	0.10	0.51	8.02	7.03	1.64	0.12	5.07	98.99
CANMET SY 4**				49.90	0.29	20.69	2.86	3.45	0.11	0.54	8.05	7.10	1.66	0.13	4.56	99.34
% Difference				0.3	2.5	0.4	9.5	24.2	7.7	5.7	0.4	1.0	1.2	8.8	10.5	
01GNX10-4-1				56.93	0.87	14.92	2.72	3.01	0.07	3.85	3.94	3.17	4.19	0.51	4.96	99.15
01GNX10-4-1D				56.90	0.87	15.05	2.69	2.99	0.07	3.92	3.78	3.22	4.19	0.51	4.90	99.09
% Difference				0.1	0.0	0.9	1.1	0.9	0.0	1.8	4.1	1.6	0.0	0.0	1.3	

Samples were jaw crushed (steel) and pulverized in a tungsten carbide swing mill and analyzed by x-ray fluorescence at Teck-Cominco Laboratories using a lithium tetraborate fused bead for major elements (Norrish and Hutton, 1969). Loss on ignition (LOI) was measured gravimetrically at 1100 °C.

D, duplicate analysis; * hidden standard % Difference = ABS ((x1-x2)/(x1+x2)/2)x100

** CANMET recommended value (anhydrous basis; Bowman, 1995). FeO determined by titration and Fe_2O_3 by difference from total Fe as Fe_2O_3

projection permits a direct comparison between modal and normative classification schemes since rocks containing normative feldspathoids plot on the A-P join. Small amounts of feldspathoids do occur in the CIPW norms of some of the least altered batholithic rocks (0-5% normative *ne* and 0-3% *lc* assuming Fe_2O_3 = 0.15 total Fe as FeO) and samples from the Afton pit (0-3.5% *ne*). To date, however, feldspathoids have not been identified in thin section. Modal quartz (<3 vol. %) that appears to be primary in origin is comparatively rare but has been detected locally (Snyder, 1994), and normative *qz* is typically lacking except in altered samples. An altered syenite dike from the Afton pit, for example, contains 2.5% *qz*.

As shown in the QAP plot (Fig. 5), most rocks comprising the Iron Mask Batholith are monzonites, monzodiorites and diorites. The Pothook phase is predominantly dioritic whereas the younger Sugarloaf "diorite" shows a bias towards monzonite. The two least altered rocks in the Afton pit suite fall in the monzonite and syenite fields in accordance with their mineralogy. It is not clear from either its major element chemistry or mineralogy whether the hornblende monzonite encountered in drill core belongs to the Cherry Creek or Sugarloaf suites.

In an alkalis *vs* silica diagram (Fig. 6), the Iron Mask suite forms a linear compositional trend that lies just within the alkaline field. Very few rock compositions plot on the subalkaline side of the discriminant, and these include the highly altered samples from the Afton pit. In terms of the classification of Lang *et al.* (1994, 1995), the suite shows a distinct affinity towards the silica-saturated subclass of plutonic rocks associated with Cu-Au porphyry deposits.

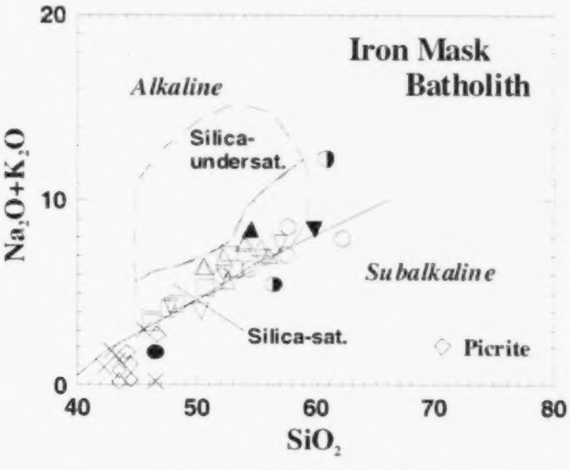

Figure 6. Alkalis vs silica (wt. %) plot for the Afton pit suite, Iron Mask Batholith and picritic basalts (Snyder 1994) showing the discriminant of Irvine and Baragar (1971) between subalkaline and alkaline rock types. Also shown are the fields of Lang *et al.* (1994, 1995) for silica-saturated and silica-undersaturated intrusions associated with alkaline Cu-Au porphyry deposits. Symbols as for Fig. 5. All rock compositions are plotted on an anhydrous basis normalized to 100 wt. % with total iron as FeO.

An alkalis-FeO-MgO (AFM) plot (Fig. 7) shows the strong iron-enrichment of the Iron Mask suite and a marked enrichment in alkalis with differentiation. Altered rocks from the Afton pit lie below this trend with the exception of the least altered syenite dike which is more enriched in alkalis than the rest of the suite (cf. Fig 6).

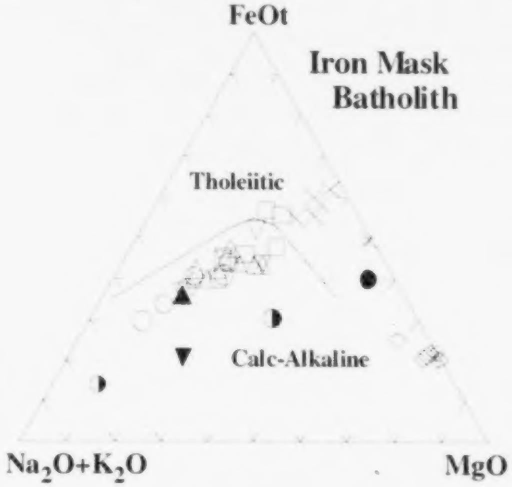

Figure 7. Alkalis-total iron-magnesia (AFM) plot (wt. %) for rocks of the Afton pit suite, Iron Mask Batholith and picritic basalts (Snyder 1994) showing the discriminant of Irvine and Baragar (1971) between the calc-alkaline and tholeiitic fields for subalkaline rocks. The discriminant is shown for reference only, not for classification purposes. Symbols as for Fig. 5. All rock compositions are plotted on a normalized anhydrous basis with total iron as FeO.

PGE MINERALIZATION

A suite of 12 samples of well-mineralized drill core, collected within intervals previously determined by DRC Resources staff to carry anomalously high abundances of Pd and/or Pt, was selected for petrographic study and PGE analysis using both conventional fire assay and multi-element acid digestion methods with an ICP-ES/MS finish. Prior to the most recent phase of exploration at Afton, abundances of PGE in the Cu-Fe sulphide ores were poorly known. For example, Kwong (1987) reported detectable abundances of palladium (0.10-0.15 ppm Pd by emission spectrographic analysis) in mineralized samples from the Afton pit, and a single highly anomalous specimen of fine-grained, carbonate-altered diorite with veins of chalcopyrite returned 0.34 ppm Pd (0.34 g/tonne). The ppb to sub-ppb levels of detection for the PGE combined with the high precision of modern analytical techniques permits the concentrations of PGE in the mineralized rocks to be accurately determined and enables a preliminary assessment of potential "pathfinder" elements in PGE-enriched Cu-Au porphyry systems.

Sample Descriptions

Mineralized samples examined in this study primarily represent drill core from the Cherry Creek unit; however, samples of a pyrite-bearing picritic basalt and a massive magnetite vein are also included. Their principal textural and mineralogical features are described below. More detailed descriptions are given in the Appendix and drillhole locations are shown in Figure 4.

The main host of mineralization in the sample suite is a diorite or leuco-diorite with microporphyritic to inequigranular textures (Photos 1 and 2). Euhedral to subhedral, turbid plagioclase, locally preserving albite twins, forms subequant to lath-like phenocrysts (0.8-3 mm) that rarely exhibit a primary magmatic flow alignment. Relict mafic minerals (amphibole?) are generally sparse (<5 vol. %) and typically pseudomorphed by a fine-grained intergrowth of chlorite/biotite, opaques oxides and leucoxene. Minor quartz forms anhedral crystals in the groundmass that may exhibit subgrain mosaic boundaries; most quartz does not appear to be of primary origin. Due to the extent of potassic alteration in these rocks (discussed below), the amount of primary potassium feldspar, which is confined to the groundmass, is difficult to estimate. Mineralogically, the original rock composition appears to be best described as leuco-diorite or monzodiorite.

Secondary minerals include biotite, chlorite, sericite, epidote, quartz, carbonate (calcite-dolomite-ankerite), apatite, magnetite, hematite, limonite and clay minerals. The principal alteration assemblage is represented by an early potassic or (calcic)-potassic alteration involving biotite-sericite-alkali feldspar-quartz accompanied by minor epidote (Photos 3 and 4). Secondary biotite typically forms tiny (<0.1 mm), deep reddish brown crystals that may be partially altered to pale green, weakly pleochroic chlorite. Fine-grained sericite accompanied by clay minerals preferentially replaces plagioclase. Apatite is not a common accessory phase, but in one sample of magnetite-apatite-carbonate-sulphide breccia it locally forms monomineralic aggregates of large grains (<0.8 mm) with abundant opaque inclusions. Late veins of carbonate-quartz+/-sulphide cut this early potassic alteration, and carbonatization may locally be pervasive.

The principal sulphide minerals in the sample suite are chalcopyrite, bornite, chalcocite, native copper and pyrite. Two core specimens collected one metre apart in the same drillhole (224-225m, drillhole 2K08, Fig. 4) contain disseminations and veins of native copper and chalcocite, respectively (01GNX19-10-1 and 19-9-1; *see* Appendix), and attest to the depth reached (locally) by supergene alteration processes (>400 m below the rim of the pit). The remaining sulphide samples are characterized by hypogene assemblages involving mainly chalcopyrite and bornite accompanied by minor chalcocite and pyrite. These copper sulphides locally show incipient alteration to covellite, ?digenite, malachite and azurite.

Pyrite enclosed by silicates is generally euhedral to subhedral, but typically assumes rounded to embayed habits against Cu-Fe sulphides, which locally occupy fracture fillings (Photos 5 and 6). These textures are indicative of replacement of early pyrite by Cu-Fe sulphide mineralization, and may account for the apparent rarity of pyrite at depth relative to near surface environments (Fig. 3). Both chalcopyrite- and bornite-dominant ores exist, as well as ores with subequal proportions of each where both sulphides apparently crystallized in equilibrium with quartz (Photo 7). Traces of chalcopyrite enclosed in silicates within bornite-dominant ores possibly reflect an earlier chalcopyrite mineralization event (Photo 8).

Textural relationships between secondary silicate assemblages and Cu-Fe sulphides indicate that mineralization accompanied potassic or (calcic)-potassic alteration. For example, faceted crystals of neocrystic alkali feldspar, quartz, biotite, and, to a lesser extent, epidote, locally line replacement cavities or occur as inclusions within, and intergrowths with, the sulphides (Photos 3, 4 and 7). Although both chalcopyrite and bornite are found in veins, their most prevalent mode of occurrence is one of irregular, patchy replacements, fine disseminations and blebs. The sulphides preferentially replace the fine-grained groundmass of microporphyritic diorites (rarely plagoclase phenocrysts) and thus superficially impart a "pseudo-magmatic" interstitial texture to the rock (Photos 1 and 2). However, the intricate nature of sulphide-silicate contacts, and the presence of intimately associated, potassic and (calcic)-potassic alteration assemblages, serve to distinguish these textures from those characteristic of orthomagmatic sulphide deposits. Kwong (1987) also noted that the disseminated sulphides are commonly accompanied by biotite and described them as interconnected impregnations rather than "isolated globules".

A massive to semi-massive magnetite vein (0.5 m wide) cutting Cherry Creek diorite was sampled in the eastern wall of the pit approximately 15 metres north of the syenite dike locality (01GNX19-5-1, Fig. 4). In thin section, the magnetite is locally intergrown with granular epidote and minor to trace amounts of chlorite and apatite, and no sulphides were observed. The presence of finely interlaced and branching magnetite veinlets at the margins of this body within a distinct envelope of epidote(-chlorite) alteration are features consistent with a hydrothermal origin.

A dark grey-green serpentinized and variably oxidized picritic basalt is exposed in the southwestern corner of the Afton pit where it is in fault contact with Cherry Creek rocks along steep northeasterly trending structures (Fig. 4). Weathering appears responsible for the locally nodular outcrop character noted by Kwong (1987). In thin section, faceted to rounded phenocrysts (<3 mm)

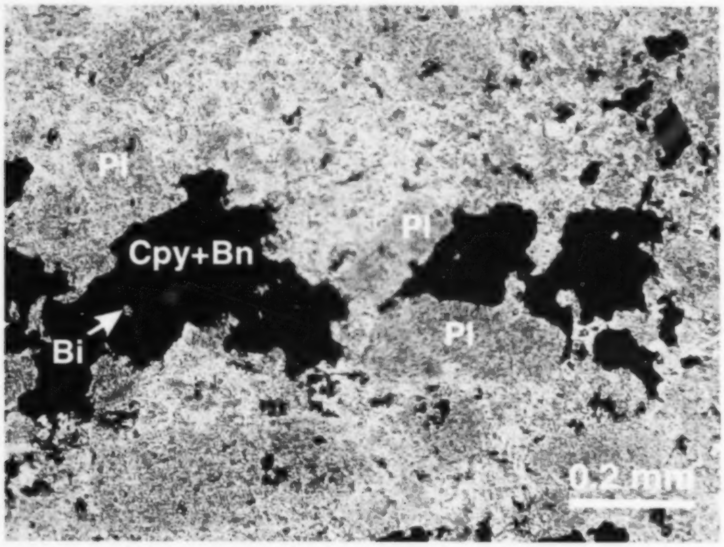

Photo 1. Disseminated chalcopyrite (Cpy) and bornite (Bn) preferentially replacing the groundmass in microporphyritic diorite. Plagioclase (Pl) phenocrysts are partially altered to clay-sericite. Note minute brown biotite (Bi) enclosed in sulfide. (Plane-polarized light; 01GNX19-11-1).

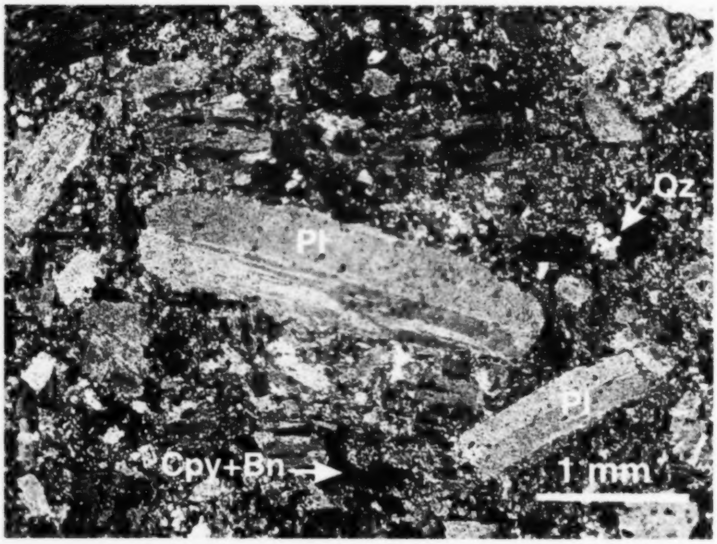

Photo 2. Disseminated chalcopyrite (Cpy) and Bornite (Bn) preferentially replacing the groundmass in microporphyritic diorite. Plagioclase (Pl) phenocrysts are partially altered to clay-sericite. Note tiny quartz (Qz) crystals locally associated with sulfide. (Crossed nicols; 01GNX19-11-1).

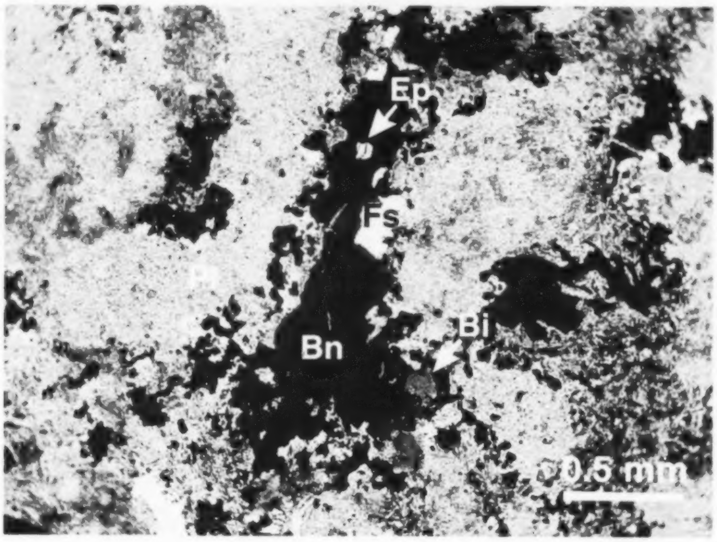

Photo 3. Bornite (Bn) in irregular veins and patchy replacements associated with alkali feldspar (Fs), reddish-brown biotite (Bi) and trace amounts of epidote (Ep). Potassic-altered diorite with sericitized plagioclase (Pl). (Plane-polarized light; 01GNX19-15-1).

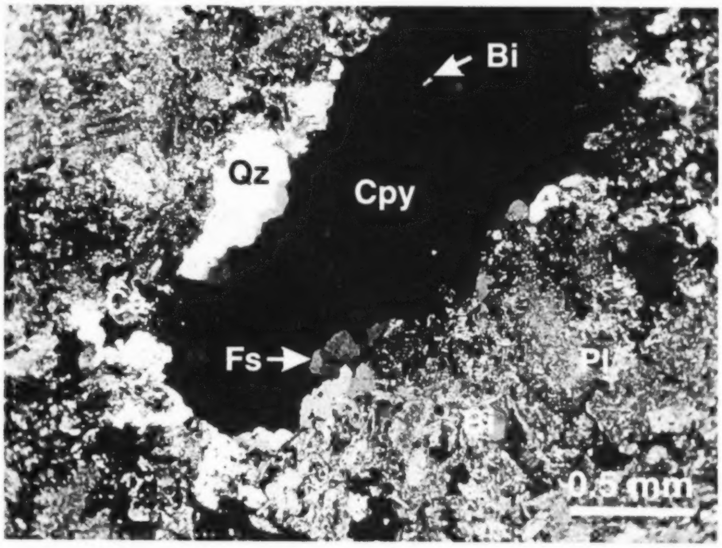

Photo 4. Irregular veins and disseminations of chalcopyrite (Cpy) intergrown with quartz (Qz), biotite-chlorite and minor carbonate (Ca). Plagioclase (Pl) in the diorite host has been partially altered to biotite (Bi) and lesser sericite. (Crossed nicols; 01GNX19-21-1).

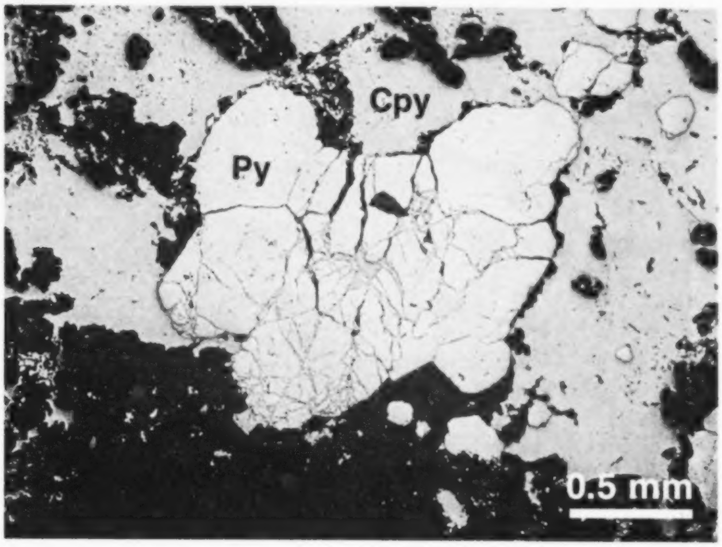

Photo 5. Crystals of pyrite (Py) veined by chalcopyrite (Cpy) and secondary silicates (biotite, alkali feldspar and quartz), calcite and minor apatite. (Reflected plane-polarized light; 01GNX19-21-1).

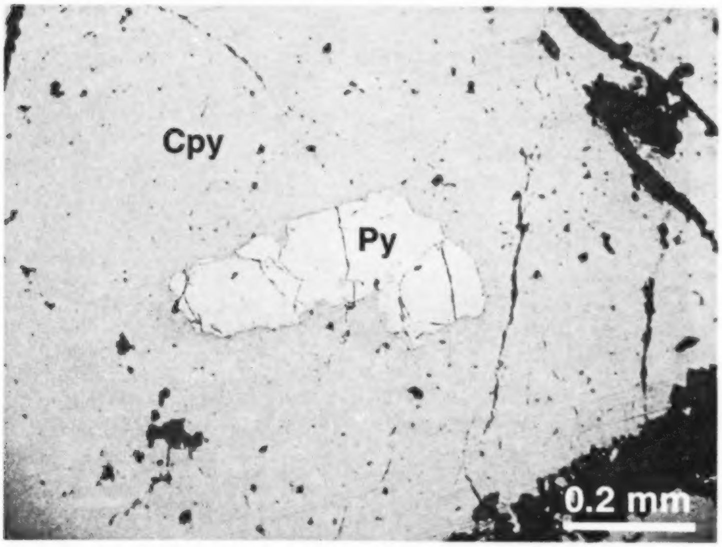

Photo 6. Intricately resorbed pyrite (Py) enclosed in chalcopyrite (Cpy) within sulphide bleb in magnetite-carbonate-sulphide-apatite vein breccia cutting diorite/monzonite. (Reflected plane-polarized light; 01GNX19-26-1).

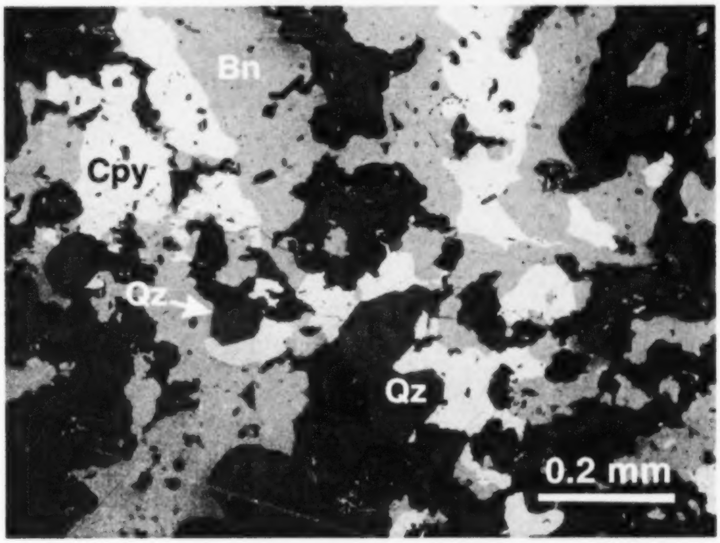

Photo 7. Disseminated chalcopyrite (Cpy) and bornite (Bn) in the groundmass of microporphyritic diorite. Note euhedral quartz (Qz) crystals intergrown with sulfide. (Reflected plane-polarized light; 01GNX19-11-1).

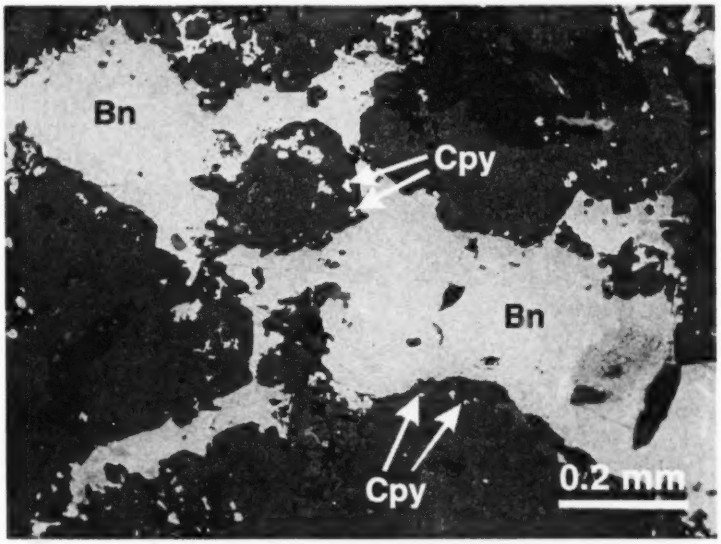

Photo 8. Veins and disseminations of bornite (Bn) associated with variably chloritized, reddish-brown biotite (Bi), alkali feldspar and trace epidote and chalcopyrite (Cpy). Potassic-altered microdiorite. (Plane-polarized light; 01GNX19-15-1).

of fresh clinopyroxene and altered olivine are enclosed in a fine-grained groundmass of feldspar, opaque oxides and secondary alteration products. Olivine is completely pseudomorphed by a felted mixture of magnetite, serpentine and tremolite-actinolite; the latter mineral is also common in the groundmass. A core sample containing small amounts of euhedral to subhedral pyrite (<1 vol. %) was collected for analysis (01GNX19-4-1, drillhole 2K01, Appendix and Fig. 4). The presence of tremolite-actinolite alteration indicates that the picrite is older than the mineralization event, consistent with observations made at the Ajax pits and elswhere in the Iron Mask Batholith (Ross *et al.*, 1995; Lang and Stanley, 1995).

Lithogeochemical Assays

The results of lithogeochemical analyses for the PGE and other elements are presented in Table 2 which includes descriptions of the host rock, mineralization and alteration assemblages. All samples were crushed in a hardened-steel jaw crusher and powdered in a tungsten carbide swing mill. A quartz wash was done between samples to avoid cross-contamination. Splits of the rock powders were analyzed by Acme Laboratories, Vancouver, using conventional fire assay and aqua regia digestion with an ICP-ES/MS finish. Accuracy and precision were monitored by including hidden duplicates and international and in-house reference materials in the run (*see* Table 2).

A comparison of the analytical techniques for Pt, Pd and Au is shown in Figure 8. There is good reproducibility for Pd between the two methods whereas Pt abundances are systematically under-reported by aqua regia digestion. A similar discrepancy was noted previously for mineralized samples from the Sappho property which attain much higher platinum concentrations (up to 8500 ppb Pt; Nixon, 2002). The results for gold exhibit a near-normal distribution about the 1:1 line of perfect agreement between the analytical methods. The scatter is attributed to a "nugget" effect caused by the presence of finely crystalline native gold.

The abundances of Pd, Pt and Au in the sample suite range 5-3833 ppb, 0.2-143 ppb (fire assay) and <1-13905 ppb, respectively (Table 2). Note the large differences that exist in gold determinations on the same sample which, as noted above, is considered to reflect sample inhomogeneity. The determination of Rh by the fire assay technique is only semi-quantitative due to partial loss by volatilization; therefore, Rh values given in Table 2 are probably best regarded as minimum abundances.

Samples enriched in Cu-bearing minerals have the following range of abundances: 19-3833 ppb Pd, <3-143 ppb Pt and 1226-13905 ppb Au. Palladium approaches or exceeds 1 g/t in four samples; the three most Pd-rich contain chalcopyrite in disseminations and veinlets, and the fourth carries bornite (Table 2). All these highly anomalous samples are from the hypogene zone. Given that the average grade for the measured and indicated mineral resource at Afton is approximately 0.12 g/t Pd, it is apparent that zones anomalously enriched in palladium exist within the ore body. Pt abundances are generally low yielding high Pd/Pt ratios in the PGE-enriched zones. Gold is uniformly high, as expected, reaching 13.9 g/t. Copper abundances range from 1.1 to 7.9 wt. %, and all

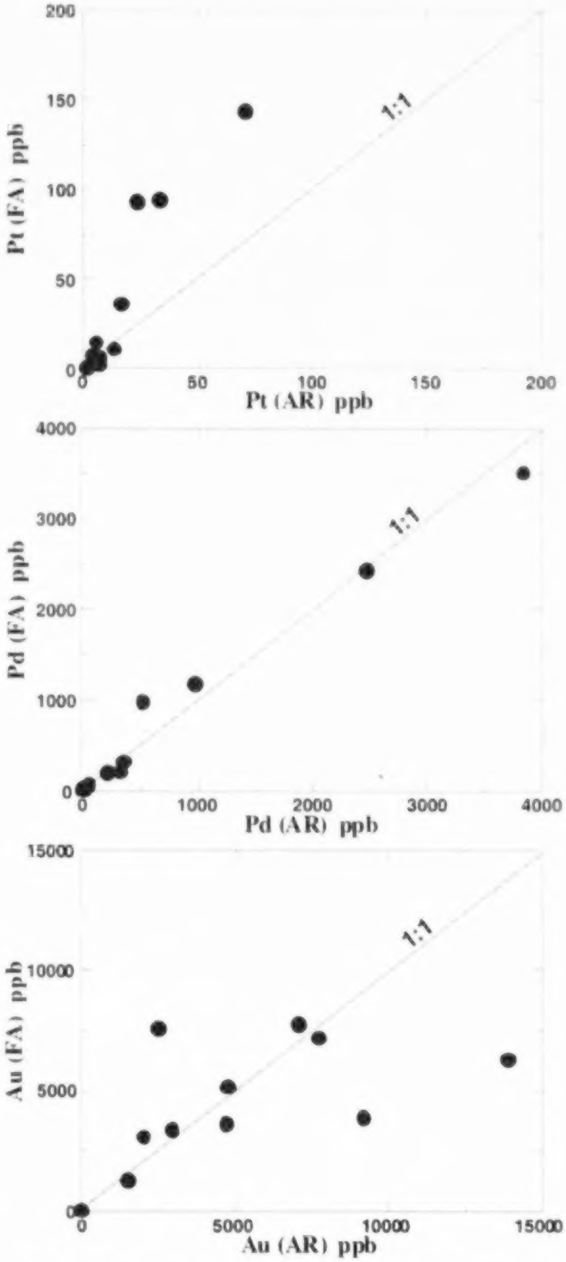

Figure 8. Comparison of analytical methods for platinum-group elements and gold. FA, fire assay; AR, aqua regia digestion. Note the systematic bias towards lower Pt values returned by the aqua regia digestion method.

TABLE 2: LITHOGEOCHEMICAL ASSAYS OF MINERALIZED ROCKS, AFTON MINE

					wt. %								
Sample	DDH (Box)	Depth (m)	Rock Type	Mineralization/Alteration	Ti	Al	Fe	Mg	Ca	Na	K	P	S
01GNX 19-6-1***	Afton pit	outcrop	massive Mt vein	Mt vein (Ep+Chl+Ap)	0.07	0.48	34.45	0.88	0.63	0.02	0.01	0.01	0.02
01GNX 19-4-1	2K01(25)	23.35	Ol-Cpx-phyric basalt (Picrite)	(dissem Py); Tr-Act (Sp)	0.12	3.17	3.41	6.03	1.00	0.09	3.12	0.21	< .01
01GNX 19-10-1	2K05(37)	224.20	microporphyritic Qz-bearing diorite	sparse native Cu+Hm; clay (Ser)	0.00	0.79	1.49	0.11	0.30	0.10	0.37	0.14	< .01
01GNX 19-9-1	2K05(37)	225.20	inequigranular (leuco)diorite	Cc dissem & veinlets; clay+Ca (Ser)	0.00	0.78	2.00	1.42	3.24	0.08	0.35	0.10	1.29
01GNX 19-36-1	2K08(19)	142.50	inequigranular (leuco)diorite	Bn (Cpy+Cov+?Dg); Ser+clay+Ca	0.00	0.74	2.11	2.84	7.12	0.06	0.16	0.71	1.13
01GNX 19-26-1	01-24(62)	349.80	diorite	Cpy (Py) blebs; Mt+Ca (Fs+Ap)	0.01	0.68	21.09	1.67	4.66	0.02	0.01	2.01	3.98
01GNX 19-32-1	01-27(44)	334.30	microporphyritic diorite	dissem Cpy (Mt); Ser+Bi+Fs+Chl	0.07	1.66	7.50	2.29	3.06	0.06	0.50	0.19	3.81
01GNX 19-14-1	01-27(45)	241.80	microporphyritic diorite	Cpy dissem & fractures; Ser+Ca (Hm+Chl+Ap)	0.00	1.46	3.62	1.95	1.82	0.11	0.19	0.18	1.35
01GNX 19-15-1	01-31(06)	33.80	inequigranular diorite	dissem Bn; Ser+Bi (Fs+clay+Ep+Chl)	0.12	1.39	2.55	1.55	1.49	0.13	0.19	0.13	2.48
01GNX 19-22-1	01-37(73)	411.40	microporphyritic diorite	dissem Cpy (+Cc); Ser+Ca (Fs+Bi)	0.02	0.98	3.24	2.34	4.06	0.08	0.41	0.14	0.91
01GNX 19-21-1	01-37(73)	413.50	inequigranular (leuco)diorite	Cpy (Py) dissem & veinlets; Ser+Bi (Ca)	0.08	1.19	4.87	2.70	4.24	0.05	0.44	0.19	2.18
01GNX 19-31-1	01-37(74)	419.50	microporphyritic diorite/monzonite	Cpy dissem & veinlets; Ser+Bi (Fs+Chl+Ca+Ap+clay)	0.06	1.44	4.68	2.30	1.21	0.06	0.25	0.13	2.72
Quality Control													
01GNX 19-9-1					0.00	0.78	2.00	1.42	3.24	0.08	0.35	0.10	1.29
01GNX 19-9-1D					0.00	0.83	2.02	1.45	3.29	0.09	0.33	0.11	1.24
% Difference						6	1	2	2	7	6	12	4
01GNX 12-2-5					0.06	0.81	29.20	0.22	3.76	0.02	0.37	1.81	25.94
01GNX 12-2-5D					0.07	0.85	28.16	0.21	3.77	0.02	0.33	1.65	21.57
% Difference					8	5	4	5	0	0	11	10	18
GSB Std. OC-80					0.09	1.39	4.43	1.35	0.84	0.02	0.13	0.15	0.01
GSB Std. OC-80					0.09	1.71	4.80	1.45	0.90	0.02	0.17	0.18	0.02
% Difference					1	21	8	7	7	6	27	18	67
Std WMG-1					0.13	2.73	7.55	2.60	2.12	0.01	0.02	0.06	2.91
Std WMG-1						4.40	11.89	7.15	10.70				
% Difference						47	45	93	134				

TABLE 2. CONTINUED

	ppm																						
Sample	B	Sr	Ba	Th	U	La	Mn	Sc	V	Cr	Ni	Co	Cu	Mo	Pb	Zn	As	Sb	Bi	Tl	Ga	Cd	Se	Te
01GNX 19-6-1***	< 1	30	41	0.5	0.1	1.0	1845	1.1	1032	11	126	90	968	0.71	0.70	110	9	0.25	< .02	< .02	9.0	0.02	0.1	< .02
01GNX 19-4-1	< 1	47	202	0.6	0.2	2.6	361	1.5	82	820	526	18	9	0.95	0.01	20	3	< .02	< .02	0.26	6.8	< .01	0.2	0.03
01GNX 19-10-1	< 1	98	275	0.3	0.2	1.1	108	9.8	29	23	8	2	43815	0.53	6.9	99	75	64	0.46	< .02	2.2	0.11	7.1	0.46
01GNX 19-9-1	< 1	61	49	0.5	0.5	4.0	3558	12.3	105	21	24	17	58400	4.33	28.97	443	333	222.9	0.76	< .02	3.1	3.39	23.5	0.40
01GNX 19-36-1	< 1	98	78	1.3	0.8	12.5	1401	3.8	134	18	23	5	41527	3.25	12	56	14	0.66	1.22	< .02	3.3	0.81	34.5	0.65
01GNX 19-26-1	< 1	39	37	1.3	0.5	8.3	2325	2.6	954	21	204	45	72641	6.36	29.04	180	504	31.04	7.22	0.17	8.5	0.98	39.8	0.14
01GNX 19-32-1	< 1	56	42	0.8	0.1	4.6	1045	12.4	109	11	70	19	41568	25.7	2.64	70	48	6.77	0.29	< .02	7.4	0.13	21.1	0.31
01GNX 19-14-1	3	33	31	0.6	0.2	3.0	1629	7.1	103	70	51	16	16292	9.81	1.7	90	109	5.46	0.15	0.02	7.8	0.03	16.6	0.13
01GNX 19-15-1	< 1	109	53	0.4	0.5	3.1	692	5.4	114	21	43	9	79322	46.36	212.4	99	1	0.53	0.97	< .02	6.5	11.23	18.0	0.28
01GNX 19-22-1	10	64	62	1.1	0.1	9.0	772	13.0	107	31	141	29	10830	1.38	4.0	38	97	3.44	0.18	0.03	4.5	0.19	9.0	0.05
01GNX 19-21-1	4	57	78	0.7	< .1	4.7	869	15.8	166	41	185	29	23117	2.03	3.6	55	73	1.85	0.52	0.03	6.7	0.22	22.2	0.09
01GNX 19-31-1	2	23	54	0.5	< .1	2.1	565	8.1	126	58	233	66	28142	1.81	1.8	47	76	1.58	0.39	0.02	8.9	0.20	18.0	0.12
Quality Control																								
01GNX 19-9-1	< 1	61	49	0.5	0.5	4.0	3558	12.3	105	21	24	17	58400	4.33	28.97	443	333	222.9	0.76	< .02	3.1	3.39	23.5	0.40
01GNX 19-9-1D	< 1	63	45	0.5	0.5	3.6	3600	10.8	92	18	24	16	59271	3.92	30	452	317	202	0.91	< .02	2.8	3.17	22.8	0.41
% Difference		3	9	0	0	11	1	13	13	14	0	5	1	10	3	2	5	10	18		10	7	3	2
01GNX 12-2-5	-1	673	18	28.8	2.5	337.3	456	-0.1	55	20	330	477	76480	18.71	13.68	2634	31.6	2.93	2.86	0.09	2.4	64.64	120	0.62
01GNX 12-2-5D	-1	616	17	24.4	2.2	276.1	504	-0.1	51	25	298	441	71339	16.68	12.54	2521	25.2	2.64	2.42	0.08	2.3	50.81	96.9	0.58
% Difference	0	9	8	17	13	20	10	0	8	21	10	8	7	11	9	4	23	10	17	12	4	24	21	7
GSB Std. OC-80	1	49	67	1	0	7	743	4	136	72	38	23	59	1	3	51	5	1	0	0	5	0	0	0
GSB Std. OC-80	<1	55	67	1.1	0.3	8.1	813	4.4	142	86	42	25	59	0.54	3.97	57	5.6	0.41	0.04	0.04	5.3	0.14	0.3	0.02
% Difference		11	0	9.524	40	13.16	8.997	7.059	4.317	18	10	9	0	7.692	19.03	11	9.346	25.53	0	28.57	9.901	15.38	40	0
Std WMG-1	90	16	10	0.6	0.2	3.3	271	1.2	45	293	2276	182	6150	0.84	11.62	68	5.7	0.96	0.28	0.03	6.9	0.64	14.8	1.08
Std WMG-1		41	114	1	1		1170		149	770	2700	200	5900	1	15	110	7	2				1		
% Difference		86	167	58.82	105.9		124.8		107.2	90	17	10	4	50	25.39	47	20.47	60.87	200	200	200	52.87	200	200

TABLE 2, CONTINUED

	ppb							ppb**			
Sample	Re	Hg*	Ag	Au	Pt	Pd	Os	Au	Pt	Pd	Rh
01GNX 19-6-1***	1	7	111	0.9	< 2	< 10	< 1	< 1	0.2	4.9	< .05
01GNX 19-4-1	< 1	5	19	0.4	5	< 10	< 1	< 1	7.1	18.4	0.30
01GNX 19-10-1	< 1	>99999	8863	7693	6	209	< 1	7218	14.7	207.9	0.17
01GNX 19-9-1	15	26270	20563	13905	7	224	< 1	6276	2.6	192.5	0.16
01GNX 19-36-1	17	404	17391	1997	5	353	6	3074	2.9	313.4	0.12
01GNX 19-26-1	13	2901	16489	4751	71	2468	< 1	5176	143.3	2424	< .05
01GNX 19-32-1	7	615	3446	7023	24	3833	< 1	7764	92.2	3507	0.35
01GNX 19-14-1	9	411	2400	9182	6	318	< 1	3874	4.5	203.9	0.23
01GNX 19-15-1	24	1234	15013	2527	34	522	7	7564	93.8	983.4	0.12
01GNX 19-22-1	18	198	2199	1492	7	< 10	< 1	1226	6.2	19.3	0.14
01GNX 19-21-1	13	251	4849	2931	14	56	< 1	3336	11.1	53.9	0.22
01GNX 19-31-1	13	494	3388	4672	17	968	1	3608	36.3	1179	0.27
Quality Control											
01GNX 19-9-1	15	26270	20563	13905	7	224	< 1	6276	2.6	192.5	0.16
01GNX 19-9-1D	31	25289	20563	11466	6	231	< 1	6364	2.5	202.8	0.06
% Difference	70	4	0	19	15	3		1	4	5	91
01GNX 12-2-5	3	446	>99999	705	1842	1080	9	641	8507	1519	2.98
01GNX 12-2-5D	6	276	>99999	611	882	859	26	618	3078	1397	3.00
% Difference	67	47		14	70	23	97	4	94	8	1
GSB Std. OC-80	<1	115	53	5.5	<2	<10	<1	2	5.5	7.7	<0.1
GSB Std. OC-80	2	48	52	2.1	8	<10	<1	1	4.3	8.8	<0.1
% Difference		82	2	89				67	24	13	
Std WMG-1	20	137	2266	169	293	447	54	127	867	393.1	11.77
Std WMG-1			2700	110	731	382		110	731	382	26.0
% Difference	200	200	17	42	86	16	200	14	17	3	75

Analyses done by Acme Analytical Laboratories Ltd., Vancouver; aqua regia digestion of 1g sample (-150 mesh; steel mill; quartz wash) and ICP-MS/ES finish

* Maximum concentration of method = 99999 ppb

** Fire assay using Pb collector (15-30g sample) with ICP finish

% Difference = Abs((x1-x2)/((x1+x2)/2))*100

*** Sample located on the 548.6m Bench ~15m north of sample 01GNX19-5-1 (Fig. 4).

wt %, weight percent; ppm, parts per million; ppb, parts per billion; D, duplicate analysis

Mineral abbreviations: Mt, magnetite; Hm, hematite; Cu, native copper; Cpy, chalcopyrite; Py, pyrite; Cc, chalcocite; Bn, bornite; Ca, carbonate (calcite/dolomite/ankerite); Qz, quartz; Chl, chlorite; Ep, epidote/zoisite/clinozoisite; Fs, alkali feldspar; Kspar, potassium feldspar; Tr-Act, tremolite-actinolite; Ap, apatite; Ser, sericite; Bi, biotite; Sp, serpentine; Cpx, clinopyroxene; Ol, olivine. Minerals in parentheses are present in minor to trace amounts.

these samples are markedly enriched in silver (2200 to >22500 ppb Ag). As with most alkaline Cu-Au porphyry deposits, molybdenum is typically low (<26 ppm Mo) along with lead (generally <30 ppm Pb) except for one anomalous sample (212 ppm Pb) which also has high molybdenum (46 ppm Mo). Locally anomalous molybdenum abundances are perhaps not unexpected since Kwong (1987) noted isolated occurrences of chalcopyrite and molybdenite just below the southern rim of the pit. The abundances of zinc are generally less than 100 ppm with one anomalous sample containing 443 ppm Zn.

It is interesting to note that the two samples from the supergene alteration zone contain extremely high levels of mercury (26 and >100 ppm Hg, Table 2). The chalcocite-bearing sample also has anomalously high Au, Ag, As and Sb, indicative of an epithermal signature. The PGE in this sample do not appear to be particularly enriched or depleted, and this may be due to the chalcocite being of hypogene origin. The sample containing native copper carries the highest mercury and has appreciable abundances of PGE (up to 15 ppb Pt and >200 ppb Pd). This raises the possibility that PGE are incorporated via solid solution in the copper alloy. However, the behaviour of PGE during supergene alteration processes is currently not well understood.

Although the aqua regia leach is only partial for iron oxides, the sample of massive magnetite is clearly a vanadiferous variety (>1000 ppm V) and contains cobalt (90 ppm Co). Trace amounts of sulphides, not detected in thin section, also appear to be present judging from the abundances of copper (968 ppm Cu) and sulphur (0.02 wt. % S). The abundances of Pt (0.2 ppb), Pd (5 ppb) and Au (<1 ppb) are near or below detection levels. As anticipated, the picrite yields the highest abundances of Ni and Cr but the lowest concentrations of base and precious metals (9 ppm Cu, 7 ppb Pt, ~18 ppb Pd and <1 ppb Au).

Inter-Element Correlations

In order to investigate inter-element variations, a correlation matrix was established for the Afton sample suite. Selected plots showing Pearson correlation coefficients are presented in Figures 9 to 11. The treatment specifically focuses on correlations among sulphide-rich samples, and excludes the picrite, magnetite vein and magnetite-carbonate-sulphide breccia (01GNX19-26-1, Appendix). Distinctions were also maintained between abundances determined by the aqua regia and fire assay methods. Some preliminary observations appear worthwhile, notwithstanding the small size of the sample population.

Moderate correlations exist between Pt, Pd and S, but not between PGE and Cu or Au, possibly due to the limited number of samples analyzed (Fig. 9). The positive correlation observed in the Cu *vs* Au plot parallels observations at other deposits hosted by the Iron Mask Batholith, and has been interpreted to reflect co-precipitation of these metals during a single hydrothermal event (*e.g.* Lang and Stanley, 1995). Correlations are also evident between PGE and Fe, and the Rh *vs* Fe regression is particularly striking, especially in view of the semi-quantitative determination of rhodium (Fig. 10). Of further note are positive correlations (not shown) between Pt-Ti (R=0.93 using Pt determined by aqua regia) and Pt-Mo (R=0.88). The significance of these latter correlations is not presently understood.

A moderate positive correlation is apparent between Ag and Cu but not between Ag and Au, which may reflect contrasting behaviour of these metals in hydrothermal fluids. However, marked correlations are observed between Ag, Bi and U which would appear to imply that hydrothermal fluids were capable of transporting both low-field-strength and high-field-strength elements to sites of mineralization.

Scattergrams of La and Th *vs* Ca (Fig. 11) and La and Th *vs* P (not shown; R=0.73-0.79) show strong to moderate correlations. This may primarily reflect the ability of apatite to incorporate high-field-strength elements within its structure, since a positive correlation is also evident between Ca and P (R=0.68). However, an epidote-group mineral may also play a subsidiary role. The marked covariance between K and Sc (Fig. 11) may likewise reflect the presence of hydrothermal biotite in these rocks. However, despite the intimate petrographic association between potassic alteration and mineralization, no significant correlations are evident between these elements and the precious or base metals.

SUMMARY AND CONCLUSIONS

A small suite of PGE-enriched, Cu-Fe-sulphide-bearing samples collected from core obtained during deep drilling beneath the Afton pit has been examined petrographically and analyzed by fire assay and aqua regia digestion ICP-ES/MS. The principal observations are as follows:

1. Mineralization is hosted by a microporphyritic diorite-monzodiorite-monzonite(-syenite) phase of the Iron Mask batholith that appears to be part of the Cherry Creek unit. The host rocks belong to the silica-saturated subclass of alkaline intrusions associated with Cu-Au porphyry deposits as defined by Lang *et al.* (1994, 1995). Samples examined in this study are microporhyritic diorite or leuco-diorite that appear to belong to the Cherry Creek unit.
2. There is good petrographic evidence for an intimate association between a potassic- or (calcic)-potassic-style of alteration and sulphide mineralization. Potassic alteration typically comprises a fine-grained assemblage of biotite-

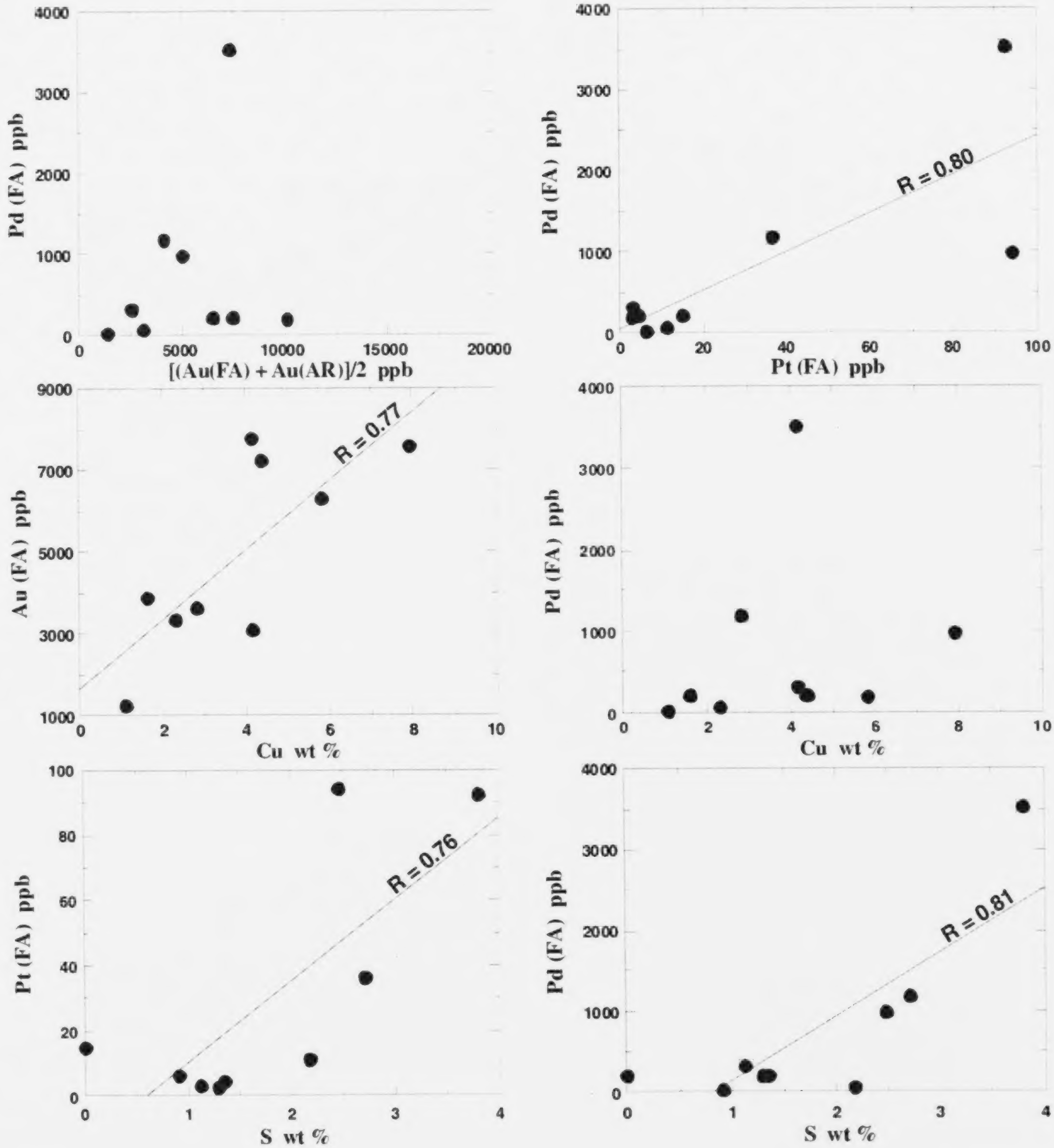

Figure 9. Scatterplots of PGE, Au, Cu and S showing Pearson correlation coefficients.

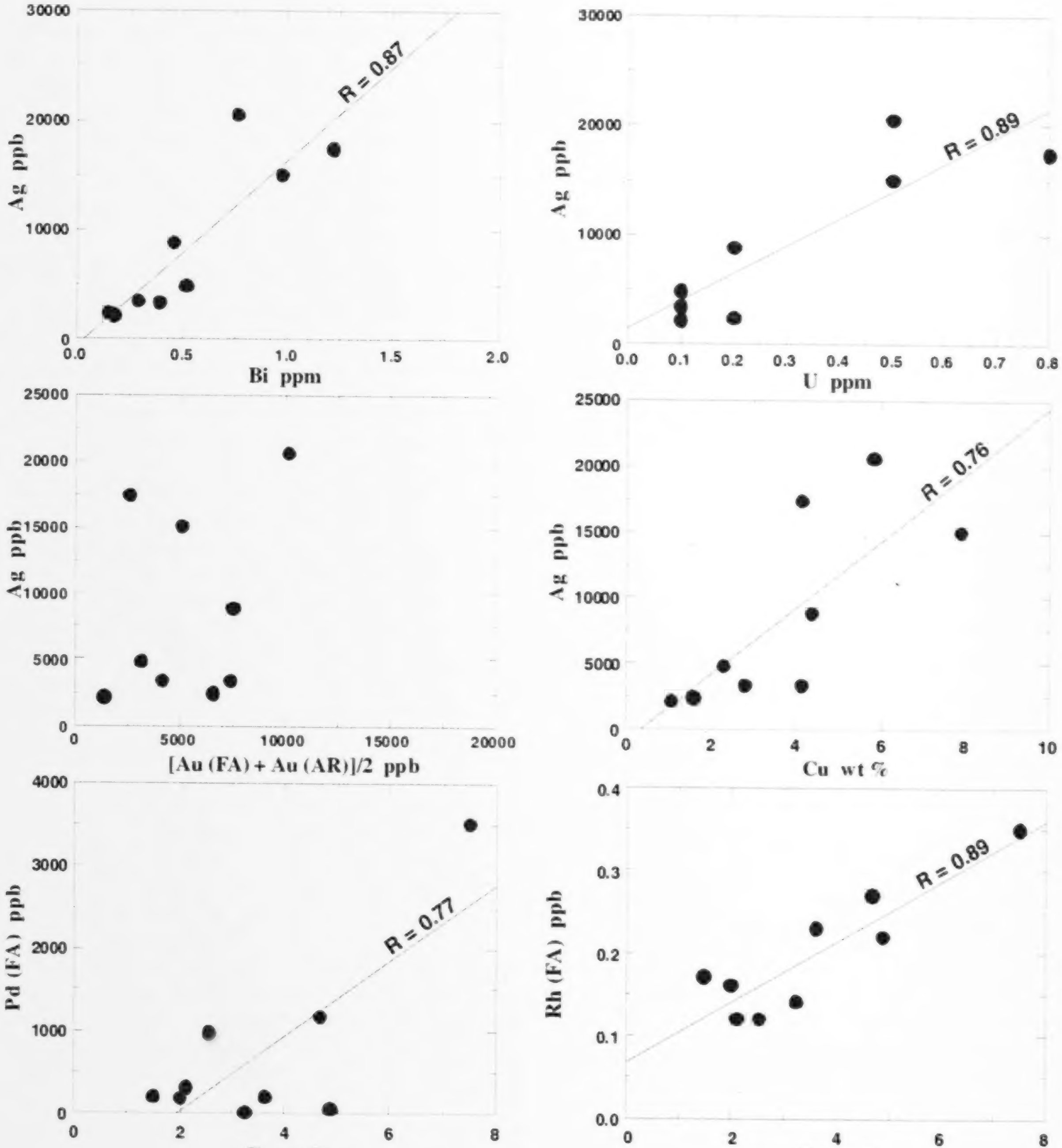

Figure 10. Scatterplots of PGE, Au, Ag, Cu, Fe, Bi and U showing Pearson correlation coefficients.

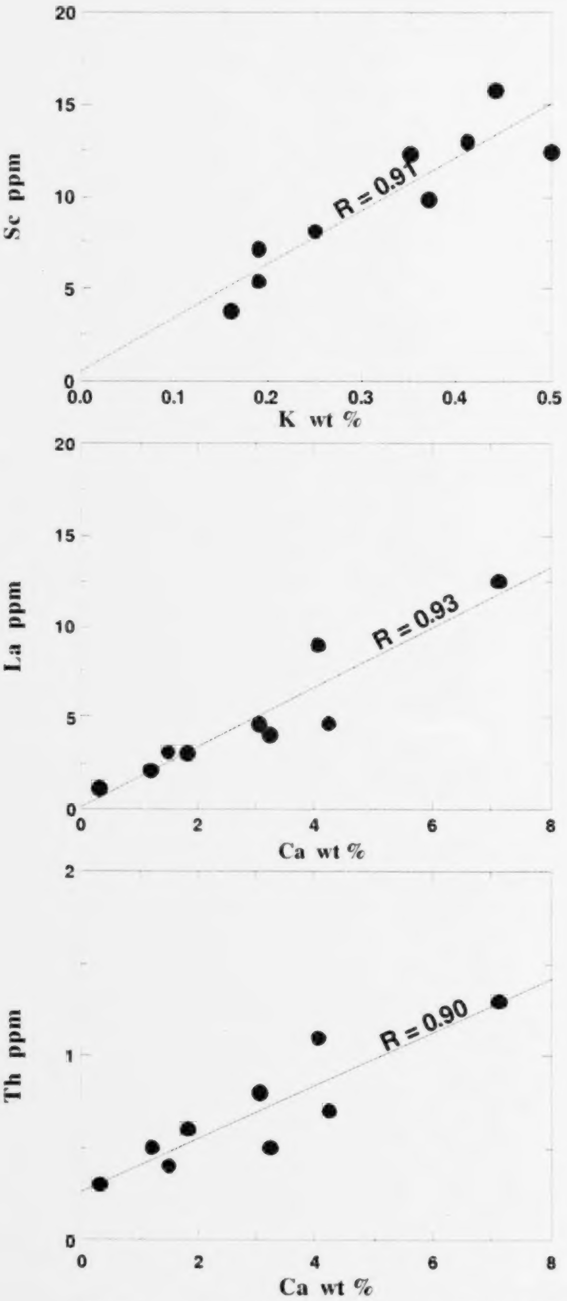

Figure 11. Scatterplots of selected non-metals showing Pearson correlation coefficients.

alkali feldspar-sericite-(minor)epidote +/- magnetite-apatite. Superimposed on this early potassic event is a locally pervasive carbonate (calcite-dolomite-ankerite) alteration and late veins of carbonate+/-quartz. Kwong (1987) notes that carbonate alteration *rarely* appears to be coincident with sulphide mineralization.

3. The principal hypogene ore minerals in the samples examined are chalcopyrite and bornite, locally altered in part to covellite, ?digenite and secondary copper carbonates. Minor amounts of pyrite and chalcocite are present in several samples. Pyrite forms an early component of the mineralization and, where preserved, is partially replaced by Cu-Fe sulphides. Supergene minerals include chalcocite and native copper.
4. The hypogene sulphides commonly form fine to heavy disseminations and blebs which preferentially replace the fine-grained groundmass of their microporhyritic host, reflecting the efficient exploitation of grain boundaries by mineralizing hydrothermal fluids. These sulphides also occur in veins and fracture fillings.
5. The maximum abundances of PGE and associated precious metals in analyzed samples are: 3833 ppb Pd; 143 ppb Pt; 13905 ppb Au; and 20563 ppb Ag. The PGE are intimately associated with chalcopyrite and bornite, but further work is needed to characterize their exact mode of occurrence (*i.e.* solid solution in Cu-Fe sulphides or discrete platinum-group minerals). Two supergene-altered samples carrying native copper and (?hypogene) chalcocite show no obvious depletion or enrichment of PGE.
6. Pd abundances are highly anomalous in 8 out of 10 samples with greater than 1 wt. % Cu, and four samples have 0.98 to 3.8 g/t Pd.
7. Correlations between PGE and elements that may serve as potential geochemical "pathfinders" are generally poor. A moderate positive correlation is statistically evident between PGE and sulphur, but not between PGE and Cu or Au in this small sample suite. The significance of a relatively good covariance between Rh and Fe is not currently understood.
8. The aqua regia digestion method for PGE appears to provide a reliable indication of Pd abundances when compared to fire assay results. However, the former method systematically underestimates Pt abundances in these Cu-Fe-sulphide-bearing samples.

This study is part of an ongoing investigation of alkaline Cu-Au porphyry deposits in British Columbia which is attempting to provide baseline geochemical and mineralogical data for the PGE in these alkaline-associated hydrothermal systems.

ACKNOWLEDGMENTS

The staff of DRC Resources Corporation are thanked for permission to sample core and for providing geological information on the Afton deposit, in particular John Kruzick, John Ball and Marek Mroczek; and Chris Sebert kindly provided a geological tour of the pit. Consulting geologist J. J. McDougall is thanked for lively discussions concerning the Afton deposit; and Mike Cathro shared his knowledge of the regional geology and organized a fieldtrip to the Iron Mask Batholith for participants of the 2003 GAC-MAC Annual General Meeting held last May in Vancouver. Jack Ebbels and Ron Smyth first suggested the Afton study, Brian Grant provided logistical support, Mike Fournier drafted Figure 3, Dave Lefebure kindly provided editorial comments, and Garry Payie prepared the final manuscript for publication.

REFERENCES

Barr, D. A., Fox, P. E., Northcote, K. E. and Preto, V. A. (1976): The alkaline suite porphyry deposits - a summary; *in* Porphyry Deposits of the Canadian Cordillera, Sutherland Brown, A., Editor, *Canadian Institute of Mining and Metallurgy*, Special Volume 15, pages 359-367.

Carr, J. M. (1956): Copper deposits associated with the eastern part of the Iron Mask Batholith near Kamloops; *B. C. Minister of Mines Annual Report*, 1956, pages 47-69.

Carr, J. M. and Reed, A. J. (1976): Afton: a supergene copper deposit; *In* Porphyry Deposits of the Canadian Cordillera, A. Sutherland Brown (Editor), *Canadian Institute of Mining and Metallurgy*, Special Volume 15, pages 376-387.

Cockfield, W. E. (1948): Geology and mineral deposits of Nicola map area, British Columbia; *Geological Survey of Canada*, Memoir 249, 164 pages.

Dunn, C. E., Hall, G. E. M. and Nixon, G. (2001): Orientation study of surface geochemical methods to assist in the exploration for platinum-group metals in the Whiterocks Mountain alkalic complex, near Kelowna, British Columbia (82L/4); *in* Geological Fieldwork 2000, *B. C. Ministry of Energy and Mines*, Paper 2001-1, pages 223-230.

Ewing, T. E. (1981): Regional stratigraphy and structural setting of the Kamloops Group, south-central British Columbia; *Canadian Journal of Earth Sciences*, Volume 18, pages 1464-1477.

Hoiles, H. H. K. (1978): Nature and genesis of the Afton copper deposit, Kamloops, British Columbia; Unpublished M.Sc. Thesis, *The University of Alberta*, Edmonton, Alberta, 186 pages.

Hulbert, L. J. (2001): Digital map and database of mafic-ultramafic hosted Ni, Ni-Cu, Cr +/- PGE occurrences and mafic-ultramafic bodies in British Columbia; *B. C. Ministry of Energy and Mines*, Geoscience Map 2001-2.

Irvine, T. N. and Baragar, W. R. A. (1971): A guide to the chemical classification of the common volcanic rocks; *Canadian Journal of Earth Sciences*, Volume 8, pages 523-548.

Kwong, Y. T. J. (1982): A new look at the Afton copper mine in the light of mineral distributions, host rock geochemistry and irreversible mineral-solution interactions; Unpublished Ph.D. thesis, *The University of British Columbia*, 121 pages.

Kwong, Y. T. J. (1987): Evolution of the Iron Mask Batholith and its associated copper mineralization; *B. C. Ministry of Energy, Mines and Petroleum Resources*, Bulletin 77, 55 pages.

Kwong, Y. T. J., Greenwood, H. J. and Brown, T. H. (1982): A thermodynamic approach to the understanding of the supergene alteration at the Afton copper mine, south-cenral British Columbia; *Canadian Journal of Earth Sciences*, Volume 19, pages 2378-2386.

Lang, J. R. and Stanley, C. R. (1995): Contrasting styles of alkalic porphyry copper-gold deposits in the northern Iron Mask Batholith, Kamloops, British Columbia; in Porphyry deposits of the Northwestern Cordillera of North America, T. G. Schroeter (Editor), *Canadian Institute of Mining, Metallurgy and Petroleum*, Special Volume 46, pages.

Lang, J. R., Stanley, C. R. and Thompson, J. F. H. (1994): Porphyry copper deposits related to alkalic igneous rocks in the Triassic-Jurassic arc terranes of British Columbia; *in* Bootprints Along the Cordillera, J. G. Bolm and Pierce, F. W. (Editors), *Arizona Geological Society Digest*, Volume 20, pages 219-236.

Lang, J. R., Lueck, B., Mortensen, J. K., Russell, J. K., Stanley, C. R., and Thompson, J. F. H. (1995): Triassic-Jurassic silica-undersaturated and silica-saturated intrusions in the Cordillera of British Columbia: implications for arc magmatism; *Geology*, Volume 23, pages 451-454.

LeMaitre, R. W. (Editor) (1989): A classification of igneous rocks and glossary of terms, *Blackwell Scientific Publications*, Oxford, 193 pages.

LeMaitre, R. W. (1976): Some problems of the projection of chemical data into mineralogical classifications; *Contributions to Mineralogy and Petrology*, Volume 56, pages 181-189.

Mortensen, J. K., Ghosh, D. K. and Ferri, F. (1995): U-Pb geochronology of intrusive rocks associated with copper-gold porphyry deposits in the Canadian Cordillera; *in* Porphyry Deposits of the northwestern Cordillera of North America, T. G. Schroeter (Editor), *Canadian Institute of Mining, Metallurgy and Petroleum*, Special Volume 46, pages 142-158.

Nixon, G. T. (2001): Alkaline-hosted Cu-PGE mineralization in British Columbia: the Whiterocks Mountain plutonic complex, south-central B. C.; *B. C. Ministry of Energy and Mines*, Open File 2001-14.

Nixon, G. T. (2002): Cu-PGE mineralization in alkaline plutonic complexes; *B. C. Ministry of Energy and Mines*, Geofile 2002-2.

Nixon, G. T. (2003): Geological setting of the Lorraine Cu-Au porphyry deposit, Duckling Creek Syenite Complex, north-central British Columbia; *B. C. Ministry of Energy and Mines*, Geofile 2003-5.

Nixon, G. T. and Archibald, D. A. (2002): Age of platinum-group-element mineralization in the Sappho alkaline complex, south-central British Columbia; *in* Geological Fieldwork 2001, *B. C. Ministry of Energy and Mines*, Paper 2002-1, pages 171-176.

Nixon, G. T. and Carbno, B. (2001): Whiterocks Mountain alkaline complex, south-central British Columbia: geology and platinum-group-element mineralization; *in* Geological Fieldwork 2000, *B. C. Ministry of Energy and Mines*, Paper 2001-1, pages 191-222.

Nixon, G. T. and Peatfield, G. R. (2003): Geological setting of the Lorraine Cu-Au porphyry deposit, Duckling Creek Syenite Complex, north-central British Columbia; *B. C. Ministry of Energy and Mines*, Open File 2003-4, 24 pages.

Northcote, K. E. (1974): Geology of the northwest half of the Iron Mask Batholith; *in* Geological Fieldwork 1974, *B. C. Ministry of Energy, Mines and Petroleum Resources*, Paper 1975-1, pages 22-26.

Northcote, K. E. (1976): Geology of the southeast half of the Iron Mask Batholith; *in* Geological Fieldwork 1976, *B. C. Ministry of Energy, Mines and Petroleum Resources*, Paper 1977-1, pages 41-46.

Northcote, K. E. (1977): Preliminary Map No. 26 (Iron Mask Batholith) and accompanying notes; *B. C. Ministry of Energy, Mines and Petroleum Resources*, 8 pages.

Palfy, J., Smith, P. L. and Mortensen, J. K. (2000): A U-Pb and ^{40}Ar-^{39}Ar time scale for the Jurassic; *Canadian Journal of Earth Sciences*, Volume 37, pages 923-944.

Preto, V. A. (1967): Geology of the eastern part of the Iron Mask Batholith; *B. C. Minister of Mines Annual Report*, 1967, pages 137-147.

Preto, V. A. (1972): Report on Afton, Pothook; *B. C. Ministry of Energy, Mines and Petroleum Resources*, Geology, Exploration and Mining 1972, pages 209-220.

Ross, K. V., Godwin, C. I., Bond, L. and Dawson, K. M. (1995): Geology, alteration and mineralization in the Ajax East and Ajax West deposits, southern Iron Mask Batholith, Kamloops, British Columbia; *in* Porphyry Deposits of the northwestern Cordillera of North America, T. G. Schroeter (Editor), *Canadian Institute of Mining, Metallurgy and Petroleum*, Special Volume 46, pages 565-580.

Snyder, L. D. (1994): Petrological studies within the Iron Mask Batholith, south-central British Columbia; Unpublished M.Sc. thesis, *The University of British Columbia*, Vancouver, British Columbia, 192 pages.

Snyder, L. D. and Russell, J. K. (1993): Field constraints on diverse igneous processes in the Iron Mask Batholith (92L/9); *in* Geological Fieldwork 1992, *B. C. Ministry of Energy, Mines and Petroleum Resources*, Paper 1993-1, pages 281-286.

Snyder, L. D. and Russell, J. K. (1995): Petrogeneric relationships and assimilation processes in the alkalic Iron Mask batholith, south-central British Columbia; ; *in* Porphyry Deposits of the northwestern Cordillera of North America, T. G. Schroeter (Editor), *Canadian Institute of Mining, Metallurgy and Petroleum*, Special Volume 46, pages 593-608.

APPENDIX: PETROGRAPHIC DESCRIPTIONS OF MINERALIZED SAMPLES

***Sample:* 01GNX19-6-1**

Location: East wall of Afton pit (548.6 m Bench)
Easting 676031 Northing 5615102 (UTM Zone 10 NAD 83)
Rock Type: Magnetite vein cutting microdiorite
Ore Minerals: Magnetite
Alteration: Epidote-rich envelope with subordinate chlorite

Description: Magnetite is semi-massive or forms granular compact grains rarely showing faceted boundaries against carbonate and silicates; minor patchy alteration of magnetite to hematite is observed in reflected light. Minor amounts of very pale green chlorite and granular, weakly pleochroic to colourless epidote are intergrown with the magnetite. A brownish nearly opaque mixture of goethite/limonite occurs locally and trace amounts of colourless subhedral apatite. No sulfides were observed despite careful examination in reflected light. The rock is cut by thin veinlets of colourless carbonate + minor quartz + trace hematite/limonite.

Comments: Sample was collected from the centre of the vein.

***Sample:* 01GNX19-4-1**

Location: DDH 2K01 Box 25 23.35 m
Easting 675610 Northing 5614869
Rock Type: Porphyritic olivine-clinopyroxene basalt
Ore Minerals: Pyrite (trace)
Alteration: Tremolite-actinolite and secondary Fe oxides

Description: Clinopyroxene occurs as large (<3 mm), virtually unaltered, pale brown (oxidized) to very pale green phenocrysts with mostly euhedral to subhedral outlines. A few crystals are resorbed and some have devitrified and altered glass inclusions. Some phenocrysts preserve core to rim zoning, and several grains are partially altered to tremolite-actinolite. The texture is hiatal with a few euhedral microphenocrysts in the groundmass. Subhedral to rounded phenocrysts of olivine are completely replaced by fibrous tremolite-actinolite and fine-grained Fe oxides +/- minor serpentine. Some olivines form glomeroporphyritic clots. The groundmass is formed by fine-grained tremolite-actinolite, feldspar, pyroxene, and opaques and clay minerals (on feldspar sites). The only sulfide present is disseminated subhedral pyrite (<1%). A few irregular veinlets of altered feldspar and carbonate cut the rock.

Comments: This clinopyroxene-olivine-phyric basalt appears to represent a fault sliver of picrite wallrock. Note the presence of pyrite, lack of Cu-Fe sulfides, and alteration assemblages equivalent to the uppermost greenschist facies.

Sample: **01GNX19-10-1**

Location: DDH 2K05 Box 37 224.2 m
Easting 675581 Northing 5614871
Rock Type: Quartz-bearing microporphyritic diorite/leucodiorite
Ore Minerals: Native Cu
Alteration: Argillic, weak sericitic

Description: Plagioclase occurs as pale brownish euhedral to anhedral laths and subequant crystals (<1.5 mm) with a subparallel magmatic foliation. Most grains are partially altered to clay minerals and minor sericite. Interstitial anhedral quartz grains (<0.8 mm) are locally intergrown with opaque material and it is not clear whether they are magmatic or hydrothermal in origin. Microcrystalline opaques comprise goethite/pitch limonite with interspersed very fine-grained hematite. A few large (1-2 mm) irregular grains of native copper are associated with the fine-grained opaques. Granular hematite +/- quartz is also found in anastomozing narrow veinlets cutting the rock.

Comments: The presence of native Cu indicates the presence of the supergene zone at this depth.

Sample: **01GNX19-9-1**

Location: DDH 2K05 Box 37 225.2m
Easting 675581 Northing 5614871
Rock Type: Carbonatized diorite/leucodiorite
Ore Minerals: Chalcocite
Alteration: Pervasively carbonatized

Description: Pale brown, subhedral relict plagioclase crystals (<1.5 mm) with inequigranular textures have been extensively replaced by clay minerals, fine-grained granular carbonate and sericite flecks; some grains preserve albite twinning; colourless calcite occurs in disseminations and veinlets accompanied by minor quartz and sulfide; no relict mafic minerals can be identified; an anastomozing vein network controls the distribution of chalcocite which is the only sulfide mineral identified.

Comments: Note the lack of pyrite.

Sample: **01GNX19-36-1**

Location: DDH 2K08 Box 19 142.5 m
Easting 675581 Northing 5614871
Rock Type: Carbonatized inequigranular leucodiorite(?)
Ore Minerals: Bornite (-chalcopyrite-covellite-?digenite)
Alteration: Intensely carbonatized with moderate sericite development

Description: Plagioclase occurs as pale brown subhedral to anhedral grains (<1 mm) which locally preserve lamellar twinning, and some crystals have well-developed subgrain mosaic boundaries. The feldspars are extensively altered to microcrystalline granular carbonate, sericite and minor clay minerals. No pseudomorphs after mafic minerals have been identified. The dominant sulfide mineral is bornite which encloses trace amounts of tiny (<20 μm) chalcopyrite blebs and is partially altered to covellite and ?digenite. Rare, minute (<20 μm) grains of brown pleochroic biotite are found as inclusions in the bornite. The sulfides are both disseminated and fracture-controlled. Trace quantities of magnetite and hematite occur as tiny grains dispersed among the silicates. The rock is cut by numerous irregular veinlets of carbonate + quartz + minor apatite + sulfides + trace amounts of chlorite and limonite.

Comments: Textures are similar to sample 01GNX19-9-1 but the rock is more pervasively altered. The distribution and texture of the sulfides, and the presence of tiny inclusions of biotite, are features consistent with a hydrothermal origin.

Sample: **01GNX19-26-1**

Location: DDH 01-24 Box 62 349.8 m
Easting 675429 Northing 5614712
Rock Type: Sulfide bleb in magnetite-carbonate vein/breccia/replacement in diorite
Ore Minerals: Magnetite-chalcopyrite(-pyrite)
Alteration: Magnetite-carbonate-apatite

Description: Magnetite occurs as non-faceted, granular crystals crosscut by irregular carbonate-filled microfractures and is locally intergrown with, or marginal to, the sulfides. Colourless euhedral to subhedral crystals of apatite (<0.8 mm) commonly contain tiny opaque inclusions. Apatite may form monomineralic aggregates or localized integrowths with magnetite, carbonate and sulfide. Anhedral crystals (<1.2 mm) of patchy zoned alkali feldspar are intergrown with magnetite and sulfide, and partially altered to carbonate, sericite and clay minerals. One large sulfide-rich bleb, several centimetres across, was examined in reflected light. Massive to disseminated chalcopyrite, the dominant sulfide, is intensely fractured and veined by carbonate, and contains minor inclusions of subhedral to anhedral and resorbed pyrite crystals. No secondary Cu sulfides have been identified. The rock is cut by narrow irregular veinlets of carbonate and quartz.

Comments: Note the presence of chalcopyrite and pyrite. Textural relationships indicate that pyrite is early and partially resorbed by the Cu-rich hydrothermal fluids which precipitated chalcopyrite.

Sample: **01GNX19-32-1**

Location: DDH 01-27 Box 44 234.3 m
Easting 675571 Northing 5614876
Rock Type: Potassic-altered microporphyritic diorite
Ore Minerals: Chalcopyrite
Alteration: Carbonate-sericite-biotite(-chlorite-potassium feldspar)

Description: Plagioclase occurs as euhedral to subhedral laths and subequant crystals (<1.5 mm) set in a fine-grained, altered feldspathic groundmass. Many crystals preserve lameller twinning and display a subparallel magmatic flow foliation. The feldspars are extensively replaced by microcrystalline carbonate + sericite + reddish brown pleochroic biotite flakes. This secondary biotite is intergrown with sulfides and locally

accompanied by minor potassium feldspar and pale green, weakly pleochroic chlorite (mostly pseudomorphous after biotite). The only sulfide identified is very fine to coarsely disseminated chalcopyrite (5-10 %). The rock also contains minor disseminated magnetite (~1 vol. %) locally altered to hematite +/- ilmenite. Colourless carbonate veinlets cut the potassic alteration and thus are very late.
Comments: The presence of secondary biotite intergrown with chalcopyrite clearly points to a potassic style of hydrothermal alteration accompanying introduction of the sulfides.

***Sample:* 01GNX19-14-1**
Location: DDH 01-27 Box 45 241.8 m
Easting 675571 Northing 5614876
Rock Type: Carbonatized and sericitized microporphyritic diorite
Ore Minerals: Chalcopyrite
Alteration: Carbonate-sericite
Description: Plagioclase occurs as very pale brownish euhedral to anhedral , mostly subequant crystals (<1 mm) set in a fine-grained feldspathic groundmass. Lameller twinning is well preserved in some grains, and no obvious primary flow fabric is evident. Feldspar sites are partially altered to microcrystalline carbonate + sericite + minor clay minerals. Localized intergrowths of carbonate + chlorite + opaque minerals may represent pseudomorphs after a primary mafic mineral (hornblende?). Minor patches of euhedral to subhedral colourless apatite, commonly with oriented inclusions of opaque material, appear to be secondary in origin. The sulfides (~5 %) occur as disseminations and veinlets of finely crystalline chalcopyrite. The rock contains minor chlorite but appears to lack biotite.
Comments: Textures indicate a hydrothermal origin for the sulfides.

***Sample:* 01GNX19-15-1**
Location: DDH 01-31 Box 6 33.8 m
Easting 675864 Northing 5614940
Rock Type: Potassic-altered inequigranular microdiorite
Ore Minerals: Bornite
Alteration: Biotite-sericite(-carbonate-clay-epidote-potassium feldspar)
Description: Euhedral to anhedral laths and subequant crystals (<1.5 mm) of pale brownish plagioclase are partially altered to microcrystalline carbonate + sericite + biotite + opaques +/- minor epidote and clay minerals. Some grains preserve albite twinning. Localized carbonate + opaques +/- epidote +/- potassium feldspar intergrowths may represent pseudomorphs of mafic minerals. Finely disseminated and fracture controlled bornite is very fresh and lacks alteration to secondary copper sulfides. Chalcopyrite appears to be absent. The sulfides are clearly associated with secondary, reddish brown pleochroic biotite and minor very pale green to colourless epidote. Disseminated Fe-Ti oxide grains are locally mottled and may be enclosed by bornite.
Comments: The textural features of sulfides and their association with secondary biotite +/- minor epidote indicate a hydrothermal origin for the mineralization.

***Sample:* 01GNX19-22-1**
Location: DDH 01-37 Box 73 411.4 m
Easting 675166 Northing 5614785
Rock Type: Microporphyritic diorite
Ore Minerals: Chalcopyrite(-chalcocite)
Alteration: Carbonate-sericite(-biotite-feldspar)
Description: Plagioclase forms euhedral to anhedral, subequant crystals (<1 mm) set in an altered feldspathic groundmass. Lamellar twinning is preserved locally and no magmatic foliation is evident. Feldspars are partially altered to very fine grained sericite + colourless carbonate + minor clay minerals. Disseminated, patchy and locally fracture-controlled sulfides are associated with minor albitic feldspar and trace amounts of reddish brown, altered biotite and limonite. The rock is cut by late veins of colourless carbonate.
Comments: This non-polished thin section prevented identification of sulfides in reflected light. From the hand sample and cut block, the sulfides appear to be predominantly chalcopyrite, possibly accompanied by minor chalcocite.

***Sample:* 01GNX19-21-1**
Location: DDH 01-37 Box 73 413.5 m
Easting 675166 Northing 5614785
Rock Type: Potassic-altered inequigranular to microporphyritic leucodiorite
Ore Minerals: Chalcopyrite(-pyrite)
Alteration: Biotite-sericite(-carbonate)
Description: Plagioclase forms pale brownish, euhedral to anhedral subequant crystals (<1 mm) partially altered to fine-grained sericite + biotite + minor colourless carbonate and clay minerals. Minor anhedral potassium feldspar in the groundmass may be primary. Disseminated biotite displays reddish brown pleochroism and is locally altered to green biotite/chlorite. Sulfides are primarily associated with biotite and minor quartz, albitic feldspar and euhedral to subhedral colourless apatite prisms containing oriented opaque inclusions. Minor quartz grains commonly exhibit sweeping extinction and subgrain boundaries. Sulfides, principally chalcopyrite, have a patchy distribution and in part are controlled by anastomozing microfractures. The chalcopyrite lacks any sign of alteration to secondary copper sulfides. Subhedral to fractured and broken and partially resorbed crystals of pyrite form a minor proportion of the sulfide and appear to have formed earlier than the chalcopyrite. Rounded "inclusions" of chalcopyrite in pyrite are interpreted as an artifact of the plane of section and represent re-entrants of chalcopyrite formed during dissolution of the pyrite.
Comments: The sulfides in this rock were deposited during alteration by potassium-rich hydrothermal fluids. The rock contains both pyrite and chalcopyrite. The pyrite

formed early and has been partially replaced by chalcopyrite.

Sample: 01GNX19-31-1

Location: DDH 01-37 Box 74 419.5 m
Easting 675166 Northing 5614785
Rock Type: Potassic-altered microporphyritic diorite/monzonite
Ore Minerals: Chalcopyrite
Alteration: Biotite-sericite(-potassium feldspar?)

Description: Plagioclase in this rock forms pale brownish, subhedral to anhedral subequant crystals (<1.6 mm) set in a finer grained feldspathic groundmass. Lamellar twinning is locally well preserved and most grains are partially altered to microcrystalline sericite + biotite + minor clay minerals. Potassium feldspar in this rock occurs interstitial to the plagioclase and it is difficult to discern if it is primary or introduced. Minor pale green chlorite and colourless carbonate form localized granular patches. Colourless monomineralic apatite concentrations are present locally. Sulfides occur in veinlets and as disseminations, and are associated with minor albitic feldspar, chlorite and biotite. Late veinlets of calcite cut the rock.

Comments: This non-polished thin section prevented identification of sulfides in relected light. From the hand sample and cut block, the sulfides appear to be predominantly chalcopyrite.

ADDITIONAL SAMPLES:

Sample: 01GNX19-30-1/2

Location: DDH 01-37 Box 75 419.9 m (0.4 m below 01GNX19-31-1)
Easting 675166 Northing 5614785
Rock Type: Potassic-altered inequigranular to microporphyritic diorite
Ore Minerals: Chalcopyrite(-pyrite)
Alteration: Biotite-sericite-alkali feldspar-carbonate

Description: Very pale brown euhedral to subhedral plagioclase (<1.2 mm) is lightly dusted by sericite and clay minerals, and is locally replaced by fine-grained intergrowths of pale brown, pleochroic biotite. The larger plagioclase crystals may preserve albite twinning. Ovoid to rectangular areas of fine-grained intergrowths of chlorite+opaque oxides/leucoxene+clay-sericite-altered feldspar may represent pseudomorphs of a primary mafic mineral (?hornblende). The sulfides occur as fine disseminations and blebs, and in veinlets, and show curvilinear to finely crenulated contacts with the silicates. Chalcopyrite (~12 vol. %) contains subhedral to strongly resorbed crystals of pyrite (1-2 vol. %) and is intimately associated with secondary alkali feldspar and biotite. The rock is cut by a few veins of potassium feldspar and chlorite, and later veinlets of colourless carbonate.

Comments: The copper mineralization is demonstrably associated with alkali-rich hydrothermal fluids and postdates the formation of pyrite in this rock.

Sample: 01GNX19-11-1

Location: DDH 2K02 Box 59 374.8 m
Easting 675610 Northing 5614869
Rock Type: Microporphyritic diorite
Ore Minerals: Bornite-chalcopyrite
Alteration: Incipient clay-sericite-chlorite-carbonate

Description: Pale brownish plagioclase (<2 mm) occurs as subhedral phenocrysts which grade serially towards the fine-grained feldspathic groundmass. Phenocryst margins appear weakly corroded; alternatively, this finely crenulated margin may reflect the final stages of growth into the groundmass. The larger feldspars locally preserve lamellar twinning and are lightly dusted by minute sericite flakes, clay minerals and rare carbonate. Groundmass feldspars show similar alteration and are locally intergrown with colourless euhedral to subhedral apatite (<0.2 mm), anhedral chlorite (<0.5 mm), which may be partly pseudomorphous after biotite, and minor leucoxene and ?secondary anhedral quartz (<1 vol. %). Disseminated sulfides are preferentially found in the groundmass and locally appear controlled by phenocryst margins. Bornite (~5 vol. %), which shows incipient alteration to chalcocite and covellite, is intergrown with minor chalcopyrite (~2 %). Sulfide-groundmass contacts are commonly highly irregular and appear corrosive. The sulfides contain inclusions of euhedral quartz and rare minute flakes of pale brown biotite. The rock is cut by narrow veinlets of carbonate +/- quartz.

Comments: The distribution and textures of the sulfides bear some resemblance to those of orthomagmatic sulfides. However, the very finely crenulated sulfide-silicate contacts, and the intimate association of sulfides with quartz and biotite, indicate a hydrothermal origin. The absence of pyrite is noteworthy.

Diamond Potential in British Columbia - Progress Report

by George J. Simandl

INTRODUCTION

This is a progress report covering the first phase of a two-year project, aiming at documenting the diamond potential of British Columbia. This study expands upon the use of well-established exploration methods as described by Fipke *et al.* (1995) which are largely based on the well established "Diamondiferous Mantle Root" model and Clifford's Rule.

CONCEPTS AND REVIEW

British Columbia (BC), is located on the western margin of North America, and has a complex tectonic history. It is commonly described in terms of the margin of the North American continent, adjacent pericratonic and displaced terranes, and accreted superterranes. It remains to be established if basement rocks of a similar age and nature as those which underlie the diamond occurrences in Alberta extend into the northeastern portions of British Columbia.

The main concentration of alkali rocks, such as carbonatites, kimberlites, lamproites, and alkaline complexes and syenite gneises, approximately follow the margin of the North American continent (Pell, 1994).

Diamonds were reported in samples from Jack (Lens Mountain) and Mark (Valenciennes River) diatremes. A single microdiamond was also reported from a poorly described breccia within the Xeno carbonatite complex, which is located within the Kechika area. Macrodiamonds were reported within the Cranbrook cluster, from the Bonus and Ram 5 and 6 diatremes.

The tectonic setting and regional geology of the diamond occurrences in BC does not match that of the classical diamond-producing shield areas such as occur in South Africa and the Northwest Territories. Published analyses of the indicator minerals in BC are scarce and limited to a few pipes. The diamond placer potential of the province was never seriously assessed.

Blue schist and eclogite-facies rocks, interpreted as subduction zone related, and alkali basalts containing mantle xenoliths are also present, however, the mineralogy of these facies (Erdmer *et al.* 1998) and mantle xenoliths, where documented, suggests that Pressure-Temperature (PT) conditions for their source areas lie outside of the diamond stability field.

The diamond potential of the province and the significance of the reported microdiamond occurrences in British Columbia can be defined in terms of the traditional "deep keel model", also called the "diamondiferous Mantel Root Model" as described by Haggerty (1986), Boyd and Gurney (1986), Helmstaed and Gurney (1995, Kirkley *et al.* (1991) and Mitchell (1991), and possibly by the modified version of the "subduction zone diamond model" (ES -model) as described by Baron *et al.* (1994) and Barrows *et al.* (1996). Recent discoveries of potentially economic diamond occurrences in non-traditional lithologies in Ontario and elsewhere (Lefebvre *et al.* 2003; Janse, 1994; Xu *et al.*, 1992; Bai, 1993 and Kytayma *et al.* 2001) indicate that exploration geologists should keep an open mind and be ready to test unconventional hypotheses.

Some of the key concepts highlighted above are already published in an electronic form (Simandl, 2003).

FIELD AND LABORATORY WORK IN PROGRESS

In 2003, the fieldwork was concentrated in three areas: in Fernie region (southeastern BC) that contains a group of garnet-bearing diatremes (Figure 1), Kechika (Northern BC) and Fort St. John, (northeastern BC).

Garnet-bearing diatremes

Most of the alkaline rocks documented in British Columbia do not contain garnets which originated in the man-

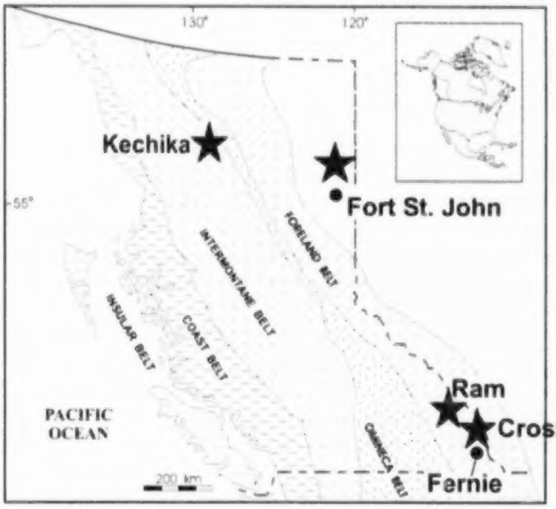

Figure 1: Location of ongoing field and laboratory work in progress. 1) Cross and Ram (pyrop-containing) diatremes, 2) Kechika area, 3) Northeastern British Columbia (east -northeast of Fort St. John).

tle or indicate depths in excess of 50 kilometres. Two garnet-bearing diatremes, Cross and Ram 6, were examined in 2003. The Cross kimberlite was studied by Smith *et al.* (1988) and Hall (1991). Ram 6 diatreme was described by Dr. McCallum in several private, technical reports.

Cross kimberlite

Overall, the field observations are in line with previously published data. Two distinct mantle xenoliths containing olivine, spinel, Cr-diopside, orthopyroxene and deeply colored pyrope garnets were recovered by a University of Victoria student Danae Voormeij. Both xenoliths were studied petrographically and provide textural information that is not available from indicator mineral studies. One of these xenoliths holds promise for pressure and temperature determination. Laboratory work on garnets pyroxenes, spinels and Cr-diopside is in progress.

RAM 6 pipe

Located north of Elkford, the Ram 6 pipe was at least once described as an kimberlite and was reported to be diamondiferous (Allan, 1999 and George Cross News Letter, 1994). The pipe is not well exposed. During the 2003 field season regolith that overlies this pipe was examined in the field and sampled. One sample was washed and pre-concentrated by panning. It contains variety of indicator minerals. Some of the garnets are deeply colored, as is typical of lherzolitic garnets (probably G9 and G8), but no obvious G10 garnets were identified. A number of other garnets recovered are yellow orange or pink-colored and some of these pale garnets may be of eclogitic affinity. Spinel, ilmenite, Cr-diopside, amber-colored mica, orhopyroxene and amphibole were other minerals tentatively identified in the field. Mineral composition will determine if this diatreme can be classified as lamproite, kimberlite or if it belongs to one of the lamprophyre clan lithologies. Assuming equilibrium conditions, "single grain" Cr-diopside geothermobarometry could be also used to determine if this diatreme sampled the diamond stability field.

KECHIKA AREA

Alkaline rocks of the Kechika area were previously described in literature and explored intensively for REE, niobium and tantalum and fluorite. A boulder train along Camp Creek was identified near RAR-5 carbonatite. It contains a variety of green-colored lithologies, including breccias of diatreme facies, tentatively classified in the field as aillikite. These boulders are similar in appearance to a rock from which a diamond was reported by Pacific Ridge Resources (Roberts, 2002), but vary in mineralogy and texture. Some of the boulders are angular, and approach 2 metres in their largest dimension. They contain the following minerals: a bright green mineral in trace concentrations (probably Cr-bearing clinopyroxene), a black pyroxene (probably salite), spinel (possibly Cr-rich), amphibole (?) and some phlogopite/biotite macrocrysts. Garnet was not observed in the field, but it is possible that it will be found in thin sections. The mineralogy needs to be confirmed by microscopic analysis to classify these unusual rocks. Cr-spinel and Cr-mica were previously reported from the RAR-5 diatreme and related rocks. Five stream sediment samples for heavy mineral analyses were collected in the general area. These samples were screened to less than 4 mm, deslimed, and manually pre-concentrated by panning to reduce transportation and processing cost and to permit backpacking. Additional laboratory screening was completed in house. Heavy liquids are used to improve the quality of the concentrate before handpicking.

FORT ST. JOHN AREA

Several stream sediment and glaciofluvial and glaciolacustrine samples were collected in the Fort St. John area, where indicator minerals were previously reported by the industry. For example, the Tyran Transport-Esau Gravel Pit, east of Fort St. John was previously sampled by Stapleton (1997). As is expected throughout most of the northeastern portion of British Columbia, garnets were observed during the sampling. Most of the garnets are probably derived from metamorphic rocks and originated within the Canadian Precambrian Shield. This is in line with the high-pink, granite pebble content of some of the gravel deposits. However, small volcanic pebbles that are similar to Quesnelia rocks were also observed. Eclogitic garnets, if present, may be difficult to distinguish from metamorphic garnets. Where possible, all collected samples for heavy mineral analyses were screened to less than 4 mm, deslimed, and manually pre-concentrated by panning to reduce processing and transportation costs and to permit backpacking. Additional laboratory screaning was completed in house. Heavy liquid separation is contracted out and concentrates will be handpicked in-house.

One of positive byproducts of this fieldwork is identification of visible gold and relatively abundant subrounded to rounded zircons in some of the collected samples. In the past, the area was covered by a large glacial lake (Mathews, 1980) and the related drainage may have some placer gold potential.

ARCHEAN BASEMENT IN NORTHEASTERN BC

The nature and age of the basement under northeastern British Columbia are poorly constrained. Current basement maps are based largely on geological and geophysical extrapolations but suggest that Archean rocks may be present in portions of northeastern British Columbia. They are based on the pioneering work of Hoffman (1988) and Ross *et al.*(1991). Only three basement dates are shown in northeastern BC (Villeneuve *et al.* 1993). Age dating of the basement is needed to establish the diamond potential of this part of the province in terms of the "diamondiferous mantle root" model and Clifford's rule.

Forty-seven oil and gas wells, which are reported to reach the basement in northeastern BC, were selected for preliminary investigations to help clarify the age of the basement in that part of the province. If suitable lithologies have been cut by drilling, ten or more of these holes will be sampled for age dating. The regular zircon dating method is not applicable, because the containers with drill-hole cuttings contain less than 3 cm^3 of sample per 10 metres of borehole. Ion probe U-Pb geochronology on zircons will have to be used. If Archean, or at least Precambrian ages are encountered, the diamond exploration potential of northeastern BC will be greatly enhanced.

ACKNOWLEDGMENT

The research team, for this diamond project, consists of individuals from the British Columbia Ministry of Energy and Mines, the University of Victoria and the Geological Survey of Canada. This ongoing research has received funding from the BC & Chamber of Mines "Rocks to Riches" geoscience program.

REFERENCES

Allan, R.J. (1999): Micro-Diamond Results from Ice Claim Project, B.C.; Skeena Resources Ltd. News Release (August 20, 1999), 2 pages.

Bai, W., Robinson, P.T. and Zhou, M. (1993): Diamond-Bearing Peridotites from Tibetan Ophiolites: Implication for Subduction-Related origin of Diamonds; *in* Kathryn P.E. Dunne and Brian Grant, Editors, Mid-Continental Diamonds; GAC-MAC Symposium Volume, Edmonton, Alberta; Geological Association of Canada, pages 77- 82.

Barron, L.M., Lishmund, S.R., Oakes, G.M. and Barron, B.J. (1994): Subduction Diamonds in New South Wales: Implications for Exploration in Eastern Australia; Geological Survey of New South Wales, Quarterly Notes, Vol 94, pages 1-23.

Barrows, L.M. Lishmunwg, R., Oakes, M., Barron, B.J. and Sutherland , F.L. et al. (1996): Subduction Model for the Origin of some Diamonds in the Phanerozoic of Eastern New South Wales; Australian Journal of Earth Sciences, Vol 43, pages 257-267.

Boyd, F.R. and Gurney, J.J. (1986): Diamonds and the African Lithosphere; Science, Vol 232, pages 472-477.

De Corte, K , Cartigny, P., Shatsky, V.S., De Paepe P, Sobolev, N.V. and Javoy, M. (1999): Characteristics of Microdiamonds from UHPM Rocks of Kokchetav Massif (Kazachstan); Proceedings of the VIIth International Kimberlite Conference, Gurney, J.L. Gurney, M.D. Pascoe and S.H. Richardson, Editors, Volume 1, Red Roof Design, pages 174-182.

Erdmer, P., Ghent, E. D., Archibald, D.A. and Stout, M.Z. (1998): Paleozoic and Mesozoic High Pressure Metamorphism at the Margin of Ancestral North America in Central Yukon; Geological Society of America Bulletin, Vol110, no.5, pages 615-629.

Fipke, C.E., Gurney, J.J. and Moore, K.O. (1995): Diamond Exploration Techniques Emphasizing Indicator Mineral Geochemistry and Canadian Examples; Geological Survey of Canada, Bulletin 423, 85 pages.

George Cross News Letter (1994): BC Diamonds Discovered; Consolidated Ramrod Gold Corporation; No.225 (November 24, 1994).

Hall, D.C.(1991): A Petrological Investigation of the Cross Kimberlite Occurrence, Southeastern British Columbia, Canada; Queen's University, Kingston, Ontario, Unpublished PhD thesis, 460 pages.

Haggerty, S. E. (1986): Diamond Genesis in a Multiply Constrained Model; Nature, Vol 320, pages 34-38.

Helmstaedt, H.H. and Gurney, J.J. (1995): Geotectonic Controls of Primary Diamond Deposits; Implications For Area Selection; Journal of Geochemical Exploration, Vol 53, pages 125-144.

Hoffman, P.F. (1988). United Plates of America: The Birth of the Craton; Annual Reviews in Earth and Planetary Sciences, Vol. 16, pages 543-603.

Janse, A.J.A. (1994b): Review of Supposedly Non-Kimberlitic and Non-Lamproitic Diamond Host Rocks; *in* Henry O.A. Meyer and Othon H. Leonardos, Editors, Kimberlites, Related Rocks and Mantle Xenoliths, Proceedings of the 5th International Kimberlite Conference, Araxa, Volume 2; Companhia de Pesquisa de Recursos Minerais - CPRM, Special Publication 1/B Jan 94, Brasilia, pages 144-159.

Katayama, I., Maruyama, S., Parkinson, C.D., Terada, K. and Sano, Y. (2001): Ion Microprobe U-Pb Zircon Geochronology of Peak and Retrograde Stages of Ultrahigh-Pressure Metamorphic Rocks from the Kokchetav Massif, Northern Kazachstan; Earth and Planetary Science Letters, Vol. 188, pages 185-196.

Kirkley, M.B., Gurney, J.J. and Levinson, A.A. (1991): Age, Origin and Emplacement of Diamonds: Scientific Advances in the Last Decade; Gems & Gemology, Spring 1991, pages 2 -25.

Lefebvre, N., Kopylova, M., Kivi, K, Barnett, R (2003): Diamondiferous Volcaniclastic Debris Flows of Wawa, Ontario, Canada; *in* 8th International Kimberlite Conference, Victoria, BC, Canada, June 22-27th 2003, Extended abstracts, CD ROM, 5 pages.

Lefebvre, N., Kopylova, M., Kivi, K. and Barnett, R. (2003): Diamondiferous Volcaniclastic Debris Flows of Wawa, Ontario, Canada; *in* 8th International Kimberlite Conference, Victoria, BC, Canada, June 22-27th 2003, Extended abstracts, CD ROM, 5 pages.

Mathews, W.H. (1980): Retreat of the last Ice Sheets in Northeastern British Columbia and Adjacent Alberta; Geological Survey of Canada, Bulletin 331, 22 pages.

Mitchell, R.H. (1991): Kimberlites and Lamproites: Primary Sources of Diamonds; Geoscience Canada, Vol 18, pages 1-16.

Pell, J. (1994): Carbonatites, Nepheline Syenites, Kimberlites and Related Rocks in British Columbia; British Columbia Ministry of Energy and Mines, Bulletin 88, 136 pages.

Roberts, W.J. (2002): Diamond Discovery at Xeno; News Release -Wednesday, March 13, 2002, Pacific Ridge Exploration limited, 1 page.

Ross, G.M., Parish, R.R., Villeneuve, M.E., and Bowring, S.A. (1991): Geophysics and Geochronology of the Crystalline Basement of the Alberta Basin, Western Canada, Canadian Journal of Earth Sciences, Vol 28, pages 512-522.

Simandl, G.J. (2003): Diamond Potential in British Columbia, Canada. *in* 8th International Kimberlite Conference, Victoria, BC, Canada, June 22-27th 2003, Extended abstracts, CD ROM, 6 pages.

Smith, C.B., Colgan, E.A., Hawthorne, J.B. and Hutchinson G (1988): Emplacement Age of the Cross Kimberlite, Southeastern British Columbia, by Rb-Sr Phlogopite Method; Canadian Journal of Earth Sciences, Vol 25, pages 790-792.

Stapleton, J. (1997): Moose Creek & Neighbouring Claims Assessment Work Report; BC Ministry of Energy and Mines, Assssment Report 25081, 49 page.

Villeneuve, M.E., Ross, G.M., Thériault, R.J., Miles, W., Parish, R.R and Broome, J. (1993): Tectonic Subdivision and U-Pb geochronology of the Crystalline Basement of the Alberta Basin, western Canada; Geological Survey of Canada, Bulletin 447.

Xu, S., Okay, A.I., Ji, S. Sengor, A.M.C., Su, W., Liu, Y. and Jiang, L. (1992): Diamond from Dabie Shan Metamorphic Rocks and its Implication for Tectonic Setting; Science, Vol 256, pages 80-82.

BRITISH COLUMBIA REGIONAL GEOCHEMICAL CLUSTER ANOMALIES AND BEST MATCHES TO MINERAL DEPOSIT TYPES

By C.P. Smyth[1]

KEYWORDS: Geochemistry, Regional Geochemical Survey, RGS, Mineral Deposit Profiles, Mineral Deposit Models, Exploration, Target Generation, Rocks to Riches, MineMatch Geochemistry, MineMatch.

INTRODUCTION

The "Rocks to Riches" program was inaugurated and funded by the British Columbia government in June 2003 to rekindle mineral investment in the province of British Columbia. It is specifically designed to provide new data or ideas that will attract mineral exploration to BC.

The "MineMatch Geochemistry" project was one of 16 projects approved for funding by the "Rocks to Riches" program in July 2003.

The project's goal was the generation of Internet-accessible, easy-to-validate exploration targets based on a re-evaluation of all the province's 45000 regional geochemistry stream sediment sample (RGS) analyses.

All the project's results have been published on the Internet, and may be freely viewed at www.rockstorichesbc.com.

PROJECT BACKGROUND

Generating high quality exploration targets is a time-consuming and expensive task, particularly when information has to be obtained from multiple sources.

Even in the age of the Internet, integrating this information in a systematic way is a challenge. The MineMatch Geochemistry project seeks to make this integration easier in the context of target generation.

British Columbia's geology hosts many different mineral deposit types. It also has extensive, diverse, and high quality information records pertinent to minerals exploration and target generation - many of them available on the Internet. The MineMatch Geochemistry project capitalizes on these resources to generate a competitive advantage for companies looking for economic mineral deposits in B.C.

But primarily this project recognizes that, given a supportive permitting and fiscal environment, there can be no better way of encouraging exploration in an area than providing prospectors and companies with sound exploration targets which have not yet been tested. Government geological databases and modern software techniques can be combined to cost-effectively generate such new, easily validated, exploration targets for free distribution on the Internet to parties interested in exploring in BC.

PROJECT PURPOSE

The purpose of the project was therefore to provide new evidence of potentially economic mineralization in British Columbia in an easy-to-use format, obtained by applying new evaluation methods to the broad coverage of geochemical data existing for the province.

The Internet-accessible maps and supporting documentation delivered by the project are intended to be of immediate value to exploration licence-holders in BC, as well as those seeking to stake new claims in the province.

The project is therefore an example to explorers and potential explorers in BC of how, by investing in a province with an unsurpassed wealth of high-quality, well-maintained base geological data sets, they can gain maximum leverage on their exploration dollars.

PROJECT METHODS

Geochemical Analysis

The project has evaluated the majority of RGS stream sediment sample analyses in the British Columbia Geological Survey (BCGS) RGS database, in conjunction with the sample's primary-associated rock-types, as derived from the almost-complete integrated 1:250 000 geological map of British Columbia (Massey *et al.*, 2003). Approximately 75% of BC is covered by RGS surveys, as shown in Figure 1. Moss-mat samples were excluded from the project on the basis of their being a different medium from conventional stream sediments.

Geochemical anomaly selection for the study was based on choosing values that exceed the 99th percentile for any specific lithology. Percentile-based threshold selection is widely recognized as the best automated anomaly-picking method in exploration geochemistry (Amor, 2000). A high percentile level was chosen to identify truly anomalous samples.

---

[1] *GeoReference Online Ltd, 301-850 West Hastings St. Vancouver, B.C. V6C 1E1*

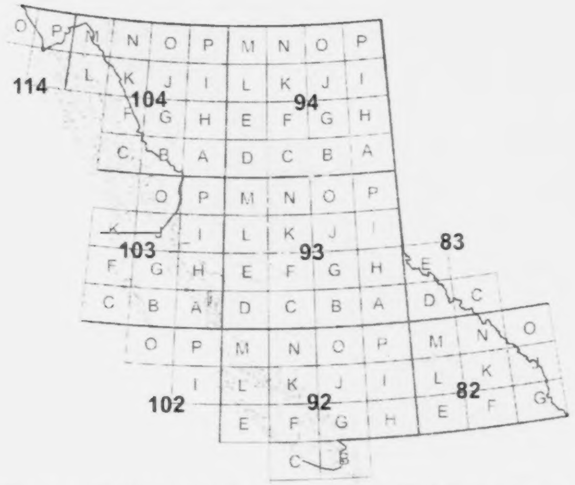

Figure 1. Regional Geochemical Sampling (RGS) coverage of British Columbia. Shaded map sheets have been sampled.

All thresholds have been published on the project web site, together with the number of samples in each lithology-specific population.

Despite its merits, minor problems can arise from this method of anomaly selection when the sample population is too small, or when the population contains no truly anomalous samples, even if it is large. In both cases, non-anomalous levels may be flagged as anomalous.

Since the project web site makes it easy to check the absolute elemental levels in anomalous samples, and the lithology over which the sample was taken, it is quick and easy to disregard anomalies that have arisen because of these effects.

Since large mineral deposits may display zoned anomalous geochemistry over more than 2 kilometres, anomalous samples within a two and a half kilometre radius of any "in-focus" sample site were combined to form an "anomaly cluster". The description of the anomaly cluster prepared for use in MineMatch (see next section) includes all the anomalous elements of all the samples in the cluster, as well as all the lithologies present at each of the included sample sites. Table 1 shows the MineMatch description for Anomaly Cluster 3191, which is derived from two samples. The original sample data, together with relevant statistics for the lithology types over which the samples were taken, are shown in Table 2.

If there are no additional anomalous samples within the search radius, we still call the site an anomaly cluster, but only if it is anomalous in more than one element. Sample sites anomalous in only one element, which are more than 2.5 km from any other anomalous sample, are ignored in this study. They are, however, plotted with a unique symbol (a blue dot) on the project's main output map, and can be included in any target characterization studies by working with MapPlace[5] tools.

Mineral Deposit Matching

MineMatch® is a Windows-based program which assists geologists to document and compare exploration prospects, mineral deposits and mineral deposit models. Built on internationally recognized standard geological vocabularies, it is able to provide similarity rankings between mineral deposits or geochemical anomalies and mineral deposit models. This is a fundamental aspect of target generation.

In this project the geochemical anomalies identified using the techniques described above are matched against a collection of 95 globally recognized mineral deposit types. These include most of the United States Geological Survey (USGS) deposit types (Cox *et al.*, 1986), and 15 deposit types described by the BCGS (Lefebure *et al.*, 1995; Lefebure *et al.*, 1996) in order to produce the following aids to minerals exploration in BC.

(1) Maps showing localities which display similarities with recognized mineral deposit types based on multi-element anomalies and lithologies present in the region sampled;

(2) Similarity rankings for each anomalous locality against each deposit type (Table 3);

(3) Detailed comparisons of the attributes of each locality with the attributes of the two mineral deposit types it most closely matches (example: Table 4). These comparisons provide powerful guidelines for the further exploration of each locality by highlighting what additional information is required to enhance the exploration potential of the site. This aspect of the proposed project caters explicitly for Recommendation 2 of the "Geochemistry and Geophysics" section of the 2001 BCGS "Five Year Plan" (BC Geological Survey, 2001).

The evaluations were carried out using a combination of ESRI's ArcView® 8.3 geographic information system[2] and GeoReference Online Ltd's MineMatch® software system[3].

ArcView® 8.3 was used to:

(1) Group samples according to lithology before determining anomaly thresholds;

(2) Identify and flag anomalous samples;

(3) Identify anomalous sample clusters comprised of closely spaced anomalous samples (using GIS buffering techniques); and

---

[2] *As described at www.esri.com*

[3] *As described at www.minematch.com*

TABLE 1

MINEMATCH DESCRIPTION OF ANOMALY CLUSTER NO 3191

Cluster 3191's MineMatch Description	Comment
ElementEnhanced - Au	From Sample 93N831386
ElementEnhanced - Na	*From Sample 93N831385*
ElementEnhanced - Ta	*From Sample 93N831385*
ElementEnhanced - U	*From Sample 93N831385*
RockHost - alkali-feldspar-granite*	From Sample 93N831386
RockHost - granite*	From Sample 93N831386
RockHost - fine-grained-normal-crystalline-rock*	*From Sample 93N831385*
RockHost - volcaniclastic-igneous-rock*	*From Sample 93N831385*
* These are the standard rock names taken from the British Geological Survey Rock Classification Scheme (Gillespie *et al*., 1999) which most closely match the lithologies shown to be present at the sample sites on the BC 1: 250 000 geological map.	

TABLE 2

SAMPLE DATA FOR CLUSTER NO 3191, WITH SAMPLE POPULATION SIZE AND 99TH PERCENTILE VALUE FOR THE LITHOLOGY TYPES OVER WHICH ITS CONSTITUENT SAMPLES WERE TAKEN

ClusterNo	SampleID	ANOMS	U_INAA	AU1_INAA	NA_INAA	TA_INAA	LITHOLOGY_TYPE
3191	93N831386	1	10	**110**	2.9	2	granite, alkali feldspar granite intrusive rocks
99th Percentile for Lithology Type			200	94	3.9	20	
No of Samples for Lithology Type			1784	1784	1784	1784	
3191	93N831385	3	**18**	6	**3.7**	**2.7**	undivided volcanic rocks
99th Percentile for Lithology Type			18	164	3.4	2.7	
No of Samples for Lithology Type			1328	1328	1328	1328	

TABLE 3

SIMILARITY RANKING FOR ANOMALY CLUSTER 3191, SHOWING ONLY THE BEST SIX MATCHES

Deposit Type	Similarity Ranking
Subvolcanic Cu-Au-Ag (As-Sb)	1
Porphyry Cu + Mo + Au	2
Hot-spring Au-Ag	3
Porphyry Cu-Au Alkalic	4
Sn Greisen Deposits	5
Gold on flat faults	6
… etcetera	

TABLE 4

EXTRACT FROM THE DETAILED COMPARISON GENERATED BY MINEMATCH OF THE ATTRIBUTES OF ANOMALY CLUSTER 3191 TO THE ATTRIBUTES OF THE BCGS VERSION OF THE PORPHYRY CU/MO/AU DEPOSIT TYPE. THE UNMATCHED DEPOSIT TYPE ATTRIBUTES, MANY OF WHICH DO NOT APPEAR IN THIS EXTRACT, PROVIDE A CHECKLIST OF ATTRIBUTES TO LOOK FOR IN THE VICINITY OF THE ANOMALY CLUSTER

Cluster 3191: Attributes	Cluster 3191's Value	Cluster 3191: Present or Absent	Porphyry Cu + Mo + Au Deposit Type: Attribute	Porphyry Cu + Mo + Au Deposit Type's Value	Deposit Type: Expected Frequency of Attribute Value	Match Type	Porphyry Cu + Mo + Au's Comment
			Alteration	altAssemblage 1	sometimes		Na-Ca silicate alteration, dominated by albite. Sometimes classed as 'propylitic' alteration
ElementEnhanced	Ta	present					
ElementEnhanced	Au	present	ElementEnhancedToOre	Au	sometimes	maAKOca	Inherited
ElementEnhanced	U	present					
ElementEnhanced	Na	present					
			FormDepositHost	breccia	sometimes		Hydrothermal origin
			FormDepositHost	contact zone	sometimes		Intrusive contact
			FormDepositHost	pluton	usually		Commonly small, multiphase stocks. Deposits referred to as 'classic' or 'southwest U.S.A. type' porphyry coppers
			RockHost	quartz-monzonite	sometimes		Most common intrusive hostrock for mineralization in Canadian Cordillera
RockHost	granite	present	RockHost	granite, porphyritic	sometimes	maybeAKO	
RockHost	fine-grained-normal crystalline-rock	present	RockHost	porphyry	usually	maybeAKO	Commonly granitic plutonic rocks and dykes in intrusive-hydrothermal complex
			RockHost	quartz feldspar porphyry	sometimes		
			RockHost	granodiorite	sometimes		
			RockHost	hornfels	usually		
RockHost	volcaniclastic-igneous-rock	present	RockHost	volcaniclastic-igneous-rock	usually	exact	Commonly andesitic rocks, volcanic flow rocks are locally dominant
RockHost	alkali-feldspar-granite	present	RockHost	<any value>	always	exact	

(4) Combine lithological information with anomalous cluster characteristics (using spatial joins of sample points with the lithology of the geological polygons within which they lie),

MineMatch® was used to:

(1) Represent information characterizing 95 mineral deposit models;

(2) Compare anomaly clusters with deposit model descriptions, and publish their similarity rankings; and

(3) Publish referenced comparison reports (see "Referencing" below) for the best and second-best matching model for each anomaly cluster.

PROJECT OUTPUTS

All project maps, as well as the data used to generate them, are available from the www.rockstorichesbc.com web site.

Geochemical Anomaly Cluster Maps

Figure 2 illustrates the main map output from the project, in which all identified anomaly clusters are shown. These clusters are highly anomalous[4], as their values exceed 99% of the values for the lithology over which they occur. The clusters are plotted, together with 1:250 000 geology outlines, sample positions, mineral occurrences, and mineral claims boundaries, as they were portrayed on MapPlace in October 2003[6].

Approximately 85% of the anomaly clusters identified have centroids which lie over free ground, as determined from the mineral claims boundaries mentioned above.

A second way of viewing the project outputs is as maps of anomalous clusters matching different deposit types. Figure 3 shows the distribution of anomalous clusters best matching Copper Porphyry, Eskay Creek Gold, and Zinc-Lead Skarn deposit types.

Reports and References

For each anomaly cluster, the model similarity ranking, best, and second-best match reports are accessed by clicking in the map on the cluster of interest, and then clicking on the desired link in the link-list that appears below the map on the computer screen. See Tables 3 and 4 for examples of these reports.

The best and second-best matching models are hyperlinked to detailed Internet-accessible descriptions of the models on either USGS or BCGS web sites.

Documented mineral occurrences falling within the anomaly cluster boundaries are listed and hyperlinked to their entries in the BCGS MINFILE database.

All anomaly clusters are linked to the MapPlace web site[5], where custom maps of the samples comprising the anomaly clusters can be dynamically created in a web browser without the need for proprietary software.

Geochemical Sample Statistics

In the course of calculating anomaly thresholds, informative statistical plots were produced, which have value beyond the scope of this project.

For example, bedrock mappers will be interested in the extent to which the statistics validate lumping and splitting of rock types into different mappable lithological units at a scale of 1:250 000. The statistics are also important to environmental studies interested in the background values, and maximum and minimum expected values, of metals in streams in different geological settings. They may also be important to the selection of analytical techniques for future sampling programs.

Consequently all statistical plots produced by the project have been published on the project website, in the "Geochemical Statistics" area.

The statistical plots fall into three categories:

(a) Box and Whisker plots to summarize compositional distributions for each lithology type;

(b) Histograms to provide greater detail of compositional distributions for each lithology type; and

(c) Scatter plots of duplicate analyses.

Figure 4 shows box and whisker plots for cobalt in 31 of the 62 lithologies present on the BC 1:250 000 geology map. These results show how the mean and range of geochemical values change as a function of surrounding lithology-type.

---

[4] *Bearing in mind the qualifications made in the section entitled "Geochemical Analysis" above*

[5] *A BCGS map portal, accessible at www.em.gov.bc.ca/Mining/Geolsurv/MapPlace/*

[6] *Some of these claim boundaries might have been up to one year out of date in October 2003. An online titles administration system, scheduled for release in 2004, will remove these backlogs. See the following web site for current titles information www.em.gov.bc.ca/Mining/Titles/TitlesSearch/mguideInfo.htm*

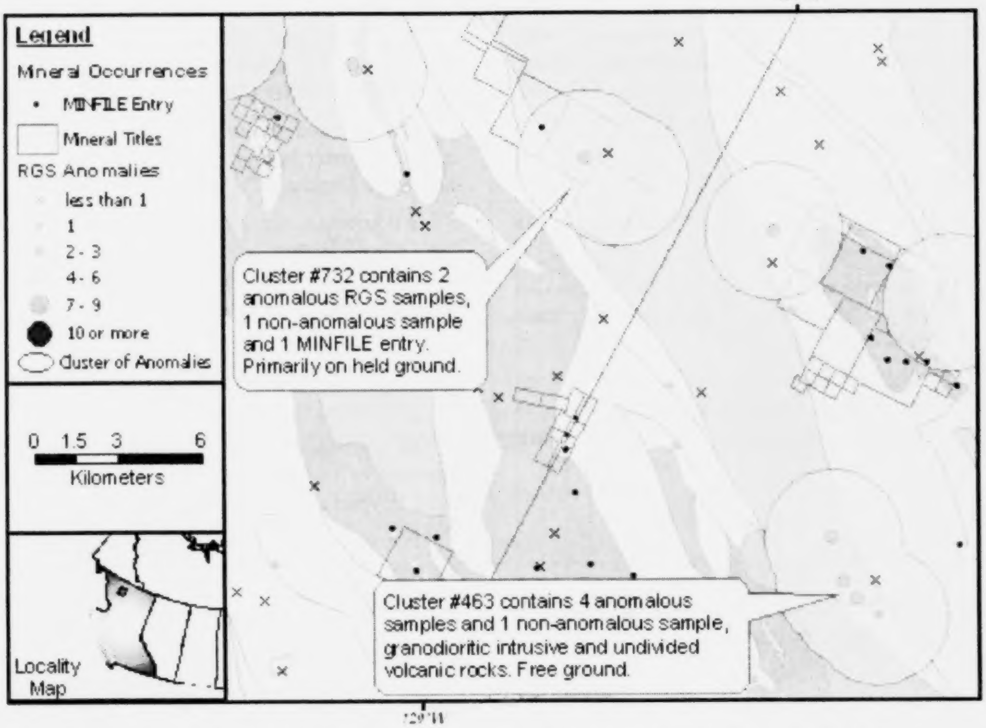
Legend
Mineral Occurrences
• MINFILE Entry
Mineral Titles
RGS Anomalies
less than 1
1
2 - 3
4 - 6
7 - 9
10 or more
Cluster of Anomalies
0 1.5 3 6
Kilometers
Locality Map

Cluster #732 contains 2 anomalous RGS samples, 1 non-anomalous sample and 1 MINFILE entry. Primarily on held ground.

Cluster #463 contains 4 anomalous samples and 1 non-anomalous sample, granodioritic intrusive and undivided volcanic rocks. Free ground.

Figure 2. Detail from a MineMatch Geochemistry Anomaly Cluster map, showing 2.5 km buffers around anomaly clusters (some may be "clusters" of only one sample), geology polygons, non-anomalous RGS sample points, MINFILE mineral occurrences, and claim outlines. Note that only mineral occurrences within cluster boundaries are referenced in the MineMatch cluster reports.

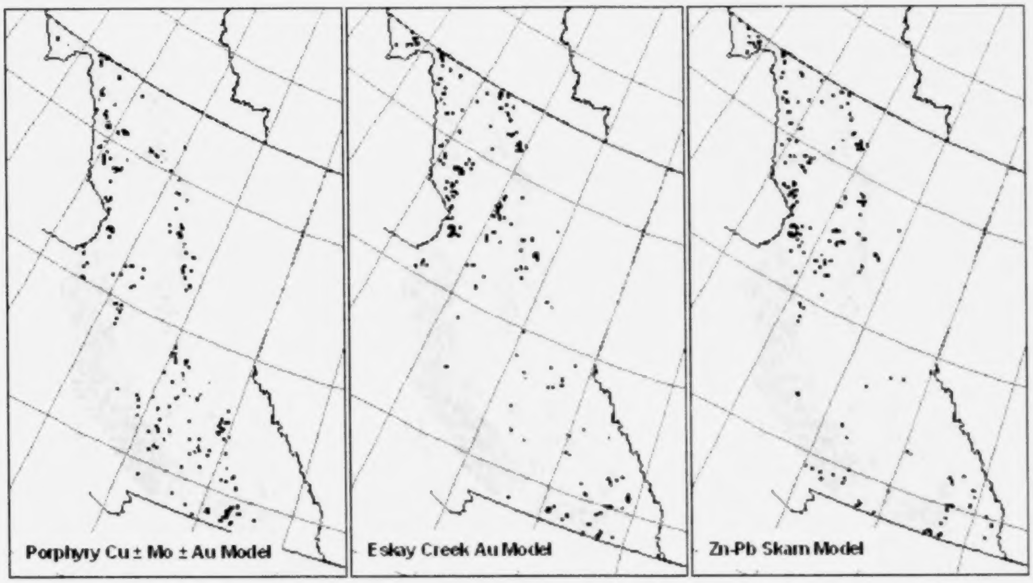

Porphyry Cu ± Mo ± Au Model

Eskay Creek Au Model

Zn-Pb Skarn Model

Figure 3. Distribution of anomaly cluster best-matches, according to deposit type. From left to right: Zn-Pb Skarn, Iron Oxide Copper Gold, and Polymetallic Replacement deposit types.

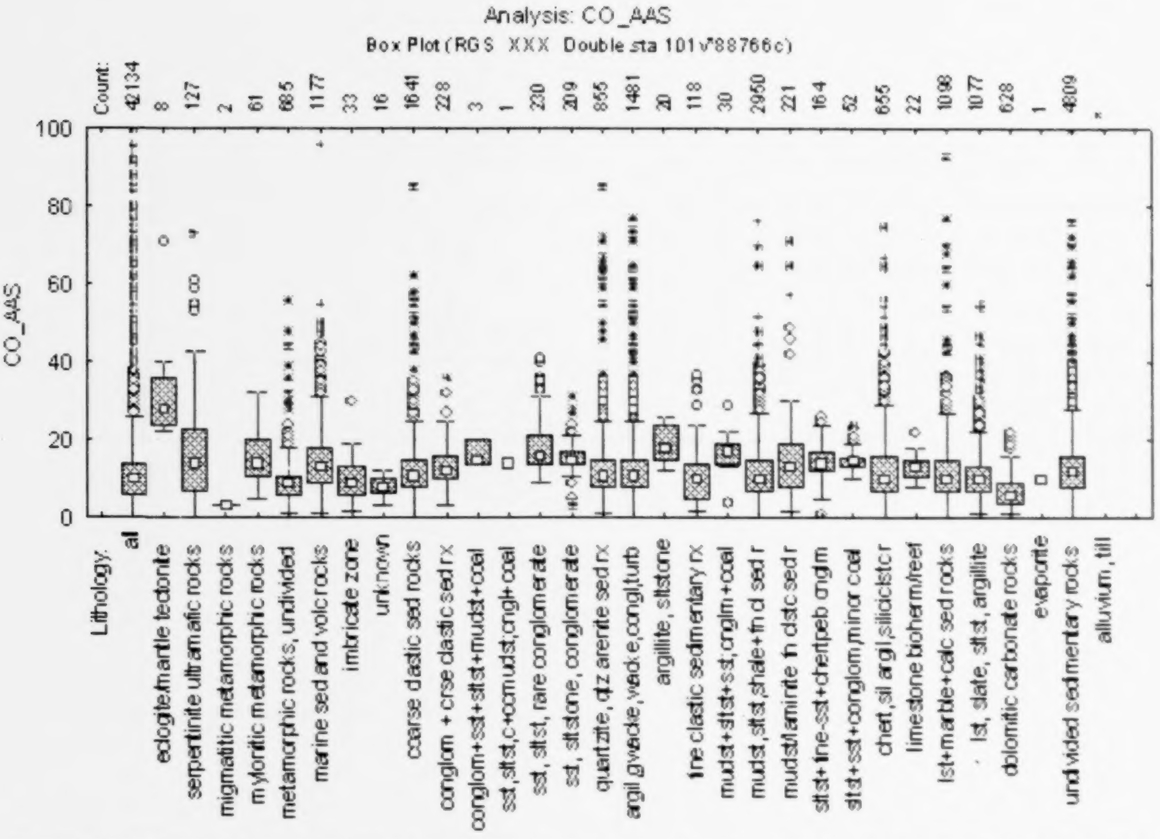

Figure 4. Box and whisker plots showing the distribution of cobalt levels, as determined by AAS, in 31 of the 62 lithology types appearing on the 1:250000 geology map of British Columbia.

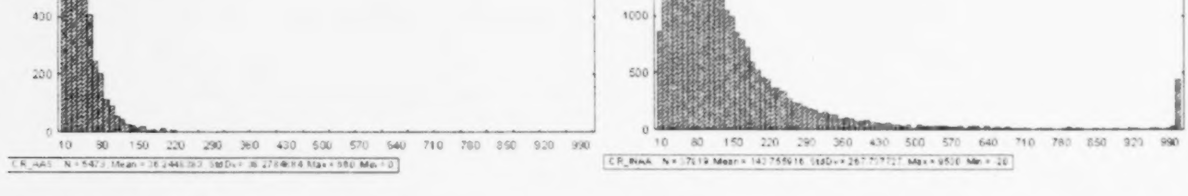

Figure 5. Histograms of chromium levels as determined by Atomic Absorption Spectrometry (left) and Neutron Activation Analysis (right)respectively. All available determinations from the RGS stream sediment database have been plotted. The lower levels in the AA results probably result from only partial extraction of chromium into the solution analysed in the AA spectrometer.

Figure 5 shows histograms of chromium levels as determined by Atomic Absorption Spectrometry and Neutron Activation Analysis respectively. The higher levels in the neutron activation results are almost certainly because of the method's ability to see all the chromium in the sample, while the atomic absorption technique is effectively a partial analysis for chromium.

In addition, scatter plots of all duplicate analyses were generated to assist in anomaly evaluation. A detailed discussion of anomaly evaluation techniques is beyond the scope of this report. However, the importance of these plots may be seen in the differences between the Au (INAA) and V (AAS) duplicates scatter plots in Figures 6a and 6b. Clearly, using the sample medium analysed in the British Columbia RGS program, the absence of an anomalous level of gold in the gold analytical result does not un-equivocally establish that elevated levels of gold are not present in the sampled stream. This issue has long been recognized in the BCGS, and as a result for many years the BCGS did not analyse for gold because the small samples available were known to be unreliable for gold analysis in many locations because of the nugget effect (Matysek *et al.*, 1988). As with all geochemical surveys, prospectors and geologists should be aware that there can be numerous reasons why an RGS sample can be downstream of a major mineral occurrence, but not show anomalous values.

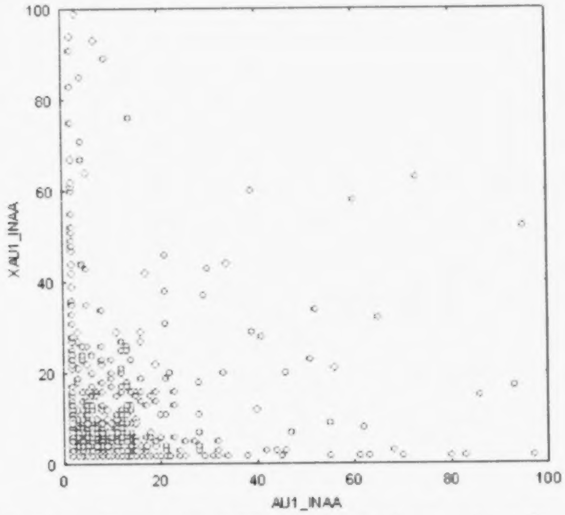

Figure 6a. Scatter plot of RGS sample duplicate analyses for gold by Neutron Activation.

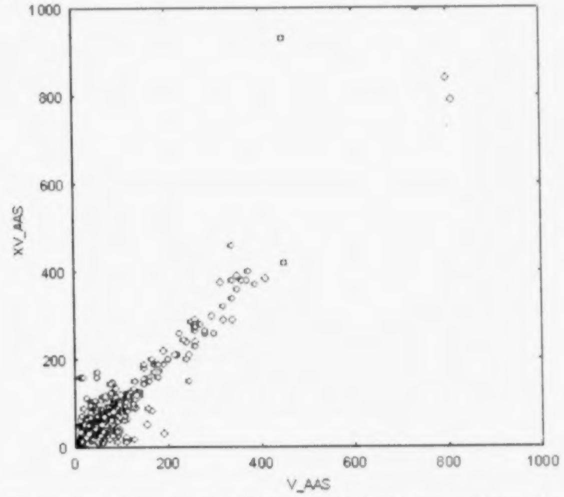

Figure 6b. Scatter plot of RGS sample duplicate analyses for vanadium by Atomic Absorption Spectrometry.

On the other hand, vanadium analysis of the stream sediments, as measured by AA, which may be reporting only a partial extraction, yields highly reproducible results, as shown in Figure 6b.

CONCLUSION

British Columbia's high quality geological databases and mineral exploration records have been combined with state-of-the-art computer technology to yield a large number of new exploration targets in the province.

These targets have been made available free-of-charge to the world's minerals exploration community, with the purpose of encouraging investment in exploration in British Columbia.

If only one of the new targets leads to an economic discovery, the "Rocks to Riches" program will have paid its sponsors, the taxpayers of British Columbia, a handsome dividend.

ACKNOWLEDGMENTS

Project funding from the Government of British Columbia's "Rocks to Riches" program is gratefully acknowledged.

The author would also like to thank Larry Jones, Nick Massey, Ray Lett and Dave Lefebure, all of the British Columbia Geological Survey, for their assistance in this project.

REFERENCES

Amor, S. (2000): "Data Presentation and Interpretation Requirements for Geochemical Exploration" in Exploration Geochemistry in Today's World: Notes for Professional Development Workshop held at Queen's University, March 11-17, 2000, Part 9, 37 pages.

British Columbia Geological Survey (2001): Five Year Minerals Geoscience Plan for British Columbia, Information Circular 2001-2.

Cox, D. P. and Singer, D. A., Editors (1986): Mineral Deposit Models; U. S. Geological Survey, Bulletin 1693, 379 pages.

Gillespie, M. R. and Styles, M. T. (1999): BGS Rock Classification Scheme, Volume 1, Classification of Igneous Rocks; British Geological Survey Research Report, (2nd Edition), RR 99-06, 51 pages.

Lefebure, D. V. and Hoy, T., Editors (1996): Selected British Columbia Mineral Deposit Profiles, Volume 2; B.C. Ministry of Employment and Investment, Open File 1996-13, 172 pages.

Lefebure, D. V. and Ray, G. E., Editors (1995): Selected British Columbia Mineral Deposit Profiles, Volume 1; B.C. Ministry of Energy, Mines and Petroleum Resources, Open File 1995-20, 135 pages.

Massey, N.W.D., MacIntyre, D.G. and Desjardins, P.J. (2003): Digital Geology Map of British Columbia: Tile NN10 Central B.C., B.C. Ministry of Energy and Mines, Geofile 2003-21.

Matysek, P.F. and Day, S.J. (1988): Geochemical Orientation Surveys: Northern Vancouver Island, Fieldwork and preliminary results; B.C. Ministry of Energy, Mines and Petroleum Resources, Geological Fieldwork 1987, Paper 1988-1, pages 493-502.

Queen's Printer for British Columbia©
Victoria

QP412128